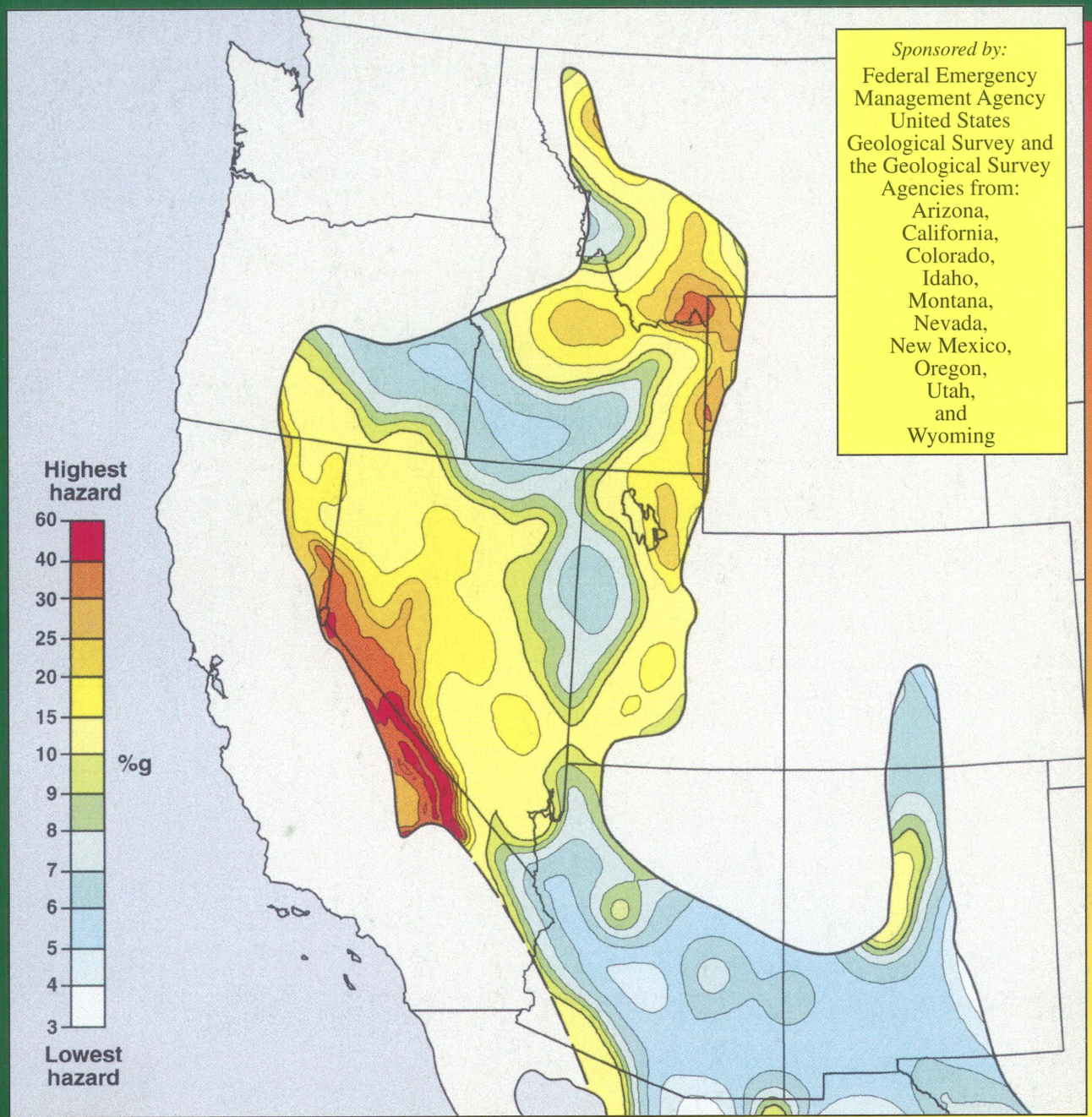


WESTERN STATES SEISMIC POLICY COUNCIL

PROCEEDINGS VOLUME BASIN AND RANGE PROVINCE SEISMIC-HAZARDS SUMMIT

Edited by William R. Lund



1998

WESTERN
STATES
SEISMIC
POLICY
COUNCIL



MISCELLANEOUS PUBLICATION 98-2
UTAH GEOLOGICAL SURVEY
a division of
UTAH DEPARTMENT OF NATURAL RESOURCES



WESTERN STATES SEISMIC POLICY COUNCIL

PROCEEDINGS VOLUME BASIN AND RANGE PROVINCE SEISMIC-HAZARDS SUMMIT

Edited by
William R. Lund
Utah Geological Survey

Sponsored by:
Federal Emergency
Management Agency
United States
Geological Survey and
the Geological Survey
Agencies from:
Arizona,
California,
Colorado,
Idaho,
Montana,
Nevada,
New Mexico,
Oregon,
Utah,
and
Wyoming

Hosted by:



The Miscellaneous Publication series of publications from the Utah Geological Survey provides non-UGS authors with a high-quality format for papers concerning Utah geology. Although reviews have been incorporated, this publication does not necessarily conform to UGS technical, policy, or editorial standards.

Design and layout by Sharon Hamre
Cover: Peak horizontal accelerations (%g) having 10% probability of being exceeded in 50 years.

1998



MISCELLANEOUS PUBLICATION 98-2
UTAH GEOLOGICAL SURVEY
a division of
UTAH DEPARTMENT OF NATURAL RESOURCES

STATE OF UTAH

Michael O. Leavitt, Governor

DEPARTMENT OF NATURAL RESOURCES

Kathleen Clarke, Executive Director

UTAH GEOLOGICAL SURVEY

M. Lee Allison, Director

UGS Board

Member	Representing
Russell C. Babcock, Jr. (Chairman)	Mineral Industry
D. Cary Smith	Mineral Industry
Craig Nelson	Civil Engineering
E.H. Deedee O'Brien	Public-at-Large
C. William Berge	Mineral Industry
Jerry Golden	Mineral Industry
Richard R. Kennedy	Economics-Business/Scientific
David Terry, Director, Trust Lands Administration	Ex officio member

UTAH GEOLOGICAL SURVEY

The **UTAH GEOLOGICAL SURVEY** is organized into five geologic programs with Administration, Editorial, and Computer Resources providing necessary support to the programs. The **ECONOMIC GEOLOGY PROGRAM** undertakes studies to identify coal, geothermal, uranium, hydrocarbon, and industrial and metallic resources; initiates detailed studies of these resources including mining district and field studies; develops computerized resource data bases, to answer state, federal, and industry requests for information; and encourages the prudent development of Utah's geologic resources. The **APPLIED GEOLOGY PROGRAM** responds to requests from local and state governmental entities for engineering-geologic investigations; and identifies, documents, and interprets Utah's geologic hazards. The **GEOLOGIC MAPPING PROGRAM** maps the bedrock and surficial geology of the state at a regional scale by county and at a more detailed scale by quadrangle. The **GEOLOGIC EXTENSION SERVICE** answers inquiries from the public and provides information about Utah's geology in a non-technical format. The **ENVIRONMENTAL SCIENCES PROGRAM** maintains and publishes records of Utah's fossil resources, provides paleontological and archeological recovery services to state and local governments, conducts studies of environmental change to aid resource management, and evaluates the quantity and quality of Utah's ground-water resources.

The UGS Library is open to the public and contains many reference works on Utah geology and many unpublished documents on aspects of Utah geology by UGS staff and others. The UGS has several computer data bases with information on mineral and energy resources, geologic hazards, stratigraphic sections, and bibliographic references. Most files may be viewed by using the UGS Library. The UGS also manages a sample library which contains core, cuttings, and soil samples from mineral and petroleum drill holes and engineering geology investigations. Samples may be viewed at the Sample Library or requested as a loan for outside study.

The UGS publishes the results of its investigations in the form of maps, reports, and compilations of data that are accessible to the public. For information on UGS publications, contact the Natural Resources Map/Bookstore, 1594 W. North Temple, Salt Lake City, Utah 84116, (801) 537-3320 or 1-888-UTAH MAP. E-mail: nrugs.geostore@state.ut.us and visit our web site at <http://www.ugs.state.ut.us>.

UGS Editorial Staff

J. Stringfellow	Editor
Vicky Clarke, Sharon Hamre	Graphic Artists
Patricia H. Speranza, James W. Parker, Lori Douglas	Cartographers

The Utah Department of Natural Resources receives federal aid and prohibits discrimination on the basis of race, color, sex, age, national origin, or disability. For information or complaints regarding discrimination, contact Executive Director, Utah Department of Natural Resources, 1594 West North Temple #3710, Box 145610, Salt Lake City, UT 84116-5610 or Equal Employment Opportunity Commission, 1801 L Street, NW, Washington DC 20507.



Printed on recycled paper

10/98

CONTENTS

INTRODUCTION	1
DEDICATION	3
PROGRAM SCHEDULE	4
POSTER TOPICS	9
ABSTRACTS	
PRESENTER ABSTRACTS	12
POSTER SESSION ABSTRACTS	35
PAPERS	50
1997 UNIFORM BUILDING CODE GROUND-SHAKING CRITERIA <i>by Robert Bachman, Fluor Daniel, Inc</i>	51
WHAT EMERGENCY MANAGERS NEED FROM GEOSCIENTISTS <i>by Stephen Weiser, Idaho Bureau of Disaster Services</i>	59
CHALLENGES OF CHARACTERIZING SEISMIC HAZARDS IN THE BASIN AND RANGE PROVINCE <i>by Clarence R. Allen, Seismological Laboratory, California Institute of Technology</i>	61
SURFACE-FAULTING HAZARD AND LAND-USE PLANNING IN UTAH <i>by Gary E. Christenson, Utah Geological Survey, and Brian A. Bryant, Salt Lake County Planning Department</i>	63
AGE CRITERIA FOR ACTIVE FAULTS IN THE BASIN AND RANGE PROVINCE <i>by Craig M. dePolo, Nevada Bureau of Mines and Geology, and D. Burton Slemmons, University of Nevada, Reno</i>	74
CONTRASTS BETWEEN SHORT- AND LONG-TERM RECORDS OF SEISMICITY IN THE RIO GRANDE RIFT - IMPORTANT IMPLICATIONS FOR SEISMIC-HAZARD ASSESSMENTS IN AREAS OF SLOW EXTENSION <i>by Michael N. Machette, U.S. Geological Survey</i>	84
THE CHARACTERISTICS AND QUANTIFICATION OF NEAR-FAULT GROUND MOTION, WITH IMPLICATIONS FOR THE BASIN AND RANGE PROVINCE <i>by Paul Somerville, Woodward-Clyde</i>	96
SEISMIC HAZARDS IN THE BASIN AND RANGE PROVINCE: PERSPECTIVES FROM PROBABILISTIC ANALYSIS <i>by Ivan G. Wong and Susan S. Olig, Woodward-Clyde Federal Services</i>	110
POTENTIAL FOR TECTONICALLY INDUCED TILTING AND FLOODING BY THE GREAT SALT LAKE, UTAH FROM LARGE EARTHQUAKES ON THE WASATCH FAULT <i>by Wu-Lung Chang and Robert B. Smith, University of Utah</i>	128
SHALLOW GEOPHYSICAL CONSTRAINTS ON DISPLACEMENT AND SEGMENTATION OF THE PAHRUMP VALLEY FAULT ZONE, CALIFORNIA-NEVADA BORDER <i>by John Louie, Gordon Shields, Gene Ichinose, Michael Hasting, Gabriel Plank, and Steve Bowman, University of Nevada, Reno</i>	139
NONLINEAR AMPLIFICATION STUDIES OF DEEP DEPOSITS IN RENO, NEVADA <i>by Raj V. Siddharthan, Shen-Der Ni, and John G. Anderson, University of Nevada, Reno</i>	147
MAGMA INTRUSIONS AND SEISMIC-HAZARDS ASSESSMENT IN THE BASIN AND RANGE PROVINCE <i>by R.P. Smith and S.M. Jackson, Idaho Engineering and Environmental Laboratory, and W.R. Hackett, WRH Associates</i>	155
RELATION OF GRAVITATIONALLY DRIVEN LITHOSPHERIC EXTENSION TO LOW SLIP-RATE FAULTS AND REGIONAL SEISMIC HAZARDS IN THE WESTERN UNITED STATES <i>by Jeffrey R. Unruh, William Lettis and Associates, Inc., Leslie J. Sonder, Dartmouth College, and Craig H. Jones, University of Colorado</i>	167
STATE SEISMICITY AND PROBABILISTIC MAPS	180
AUTHOR INDEX	202

THE BASIN AND RANGE SEISMIC-HAZARDS SUMMIT

The Western States Seismic Policy Council (WSSPC) and the Nevada Bureau of Mines and Geology (NBMG) hosted the Basin and Range Province (BRP) Seismic-Hazards Summit in Reno, Nevada, May 13-15, 1997, to review important technical issues in characterizing seismic hazards in the BRP and consider their public-policy implications. The purpose of the summit, and of the WSSPC BRP committee, is to accurately and effectively characterize seismic hazards in the province and identify policies and means of communication that will effectively reduce the loss of life and property.

Seismic-hazard characterization in the BRP poses several distinct challenges. This extensional, intraplate tectonic setting has hundreds to thousands of potentially active faults, most of which have average earthquake recurrence intervals ranging from thousands to hundreds of thousands of years. The long recurrence intervals can greatly complicate paleoseismic assessments and predictions of which faults are likely to generate strong earthquakes in the near future. Most potentially active faults in the province have predominantly normal slip or normal-slip components, which are believed by some to produce distinctly less bedrock ground motion than strike-slip or reverse faults. However, most communities within the province are located within alluviated basins, where issues for ground motion consideration include response of low-rigidity sediments to shaking and focusing of seismic waves due to basin geometry and/or other effects. Input for probabilistic analyses includes several data sets that can be used independently or collectively, but these are by nature statistically unsatisfying due to the sparse historical earthquake record and/or non-unique interpretations. Some historical earthquake sequences, such as the 1954 Rainbow Mountain-Fairview Peak-Dixie Valley sequence in Nevada, indicate that major earthquakes can be highly variable, with significant spatial and/or temporal clustering. A key question is whether this kind of earthquake behavior is a characteristic of the province that can be expected to be repeated or whether this was a chance happening.

As a framework for discussion, the conference presented an overview of important issues involved in characterizing seismic hazards in the BRP. Participants included a broad range of researchers and scientists, as well as users. A conference-long poster session presented seismic-hazards maps of each of the WSSPC BRP states and results of recent scientific research.

This conference provided a vehicle by which we can advocate a firm scientific foundation for seismic policy. WSSPC had recently defined "seismic policy" as related to the concept of "government policy," which is the philosophical basis for laws and regulations adopted by government. Thus "seismic policy" is government policy that relates to earthquake hazards and earthquake mitigation. As examples, seismic policy encompasses such items as funding for research at the federal level, guidelines for evaluating and mitigating seismic hazards, and recommendations for changes in building codes adopted by local governments.

The earthquake characteristics of the BRP are not necessarily unique, but have some distinctions, warranted in seismic-policy considerations. Each day of the summit ended with a discussion to develop policy recommendations to be presented to the WSSPC Board of Directors for consideration for formal adoption as WSSPC policy.

The opening session of the summit highlighted user's perspectives on information needs and how seismic-hazards information is being put to practical use. One example is the new seismic provisions in the 1997 Uniform Building Code, which now include factors to address near-source effects and a new method to address site effects. Speakers addressed issues related to the trend toward performance-based building codes and problems caused by making changes to the codes, particularly seismic-zone boundary changes. Loss estimation is becoming increasingly important, and issues related to characterizing seismic sources and information needs for the new FEMA HAZUS loss-estimation software were highlighted. Finally, to set the stage for subsequent technical discussions, Clarence Allen spotlighted the uniqueness of the BRP and the challenges in characterizing its earthquake hazards.

The initial technical discussion centered on difficulties in characterizing "active" faults and the issue of defining which faults should be considered active for what purposes in seismic-hazards assessments. Typical BRP faults have relatively low slip rates and long, irregular recurrence intervals, although faults covering a wide range of activity levels are found in the BRP. Talks centered on whether a Holocene or late Pleistocene definition of active faults is more appropriate in the BRP, how to characterize the hazard from BRP faults, what types of recurrence models should be used, and how the actual hazard of surface faulting is handled in various BRP states.

The second day of the summit concentrated on characterizing strong ground motions in BRP normal-faulting earthquakes, given the current lack of strong-motion data for such earthquakes. Some data indicate that ground motions in extensional regimes are somewhat less than those of similar-magnitude earthquakes in compressional regimes, and this is supported by new field evidence documenting the preservation of semi-precarious rocks near BRP normal faults. New BRP attenuation relations are being developed, chiefly as a result of work for the Yucca Mountain Nuclear Waste Repository in Nevada. Researchers noted spatial variations in shaking intensity in a normal-faulting earthquake in Turkey, where damage statistics indicated larger ground motions on the downthrown block. Near-fault rupture pulses are well documented in strike-slip and reverse-faulting earthquakes, but laboratory models indicate that such pulses may not be as important in normal-faulting earthquakes. Computer modeling and instrumental monitoring of seismic-wave amplification in deep BRP basins indicate that the basins significantly amplify and increase the duration of longer period ground motions, particularly in deeper parts of the basins.

The final day of the summit addressed probabilistic

seismic-hazards analyses (PSHAs) and their application in the BRP. One theme of the session was the need to standardize historical earthquake catalogs and collect additional fault slip-rate data. Because of the irregularities in earthquake recurrence and uncertainties in BRP recurrence models, PSHAs are particularly well-suited for assessing seismic hazards in the BRP. PSHAs can be improved as more becomes known about: 1) modern strain rates from GPS measurements, 2) distributed faulting (displacement on multiple faults in one earthquake), 3) earthquakes on one fault causing seismic "loading" on adjacent faults, 4) magnitude-frequency distribution of earthquakes regionally and on individual faults, and 5) causes and likelihood of temporal clustering of earthquakes.

As a result of the BRP Seismic-Hazards Summit, the following motions were adopted at the WSSPC Annual Business Meeting on November 7, 1997, during the Annual Conference. Before these became WSSPC Policy Recommendations, they were approved by the participants at the BRP Seismic-Hazards Summit, then by the WSSPC Board of Directors, and then by the full membership of WSSPC.

WSSPC PR97-1: Active Fault Definition Categories for the Basin and Range Province

WSSPC recommends that the following guidelines be used in defining active faults in the Basin and Range physiographic province. Active faults can be categorized as follows, recognizing that all degrees of fault activity exist and that it is the prerogative of the user to decide the degree of anticipated risk and what degree of fault activity is considered "dangerous":

Holocene Active Fault - a fault that has moved within the past 10,000 years.

Late Quaternary Active Fault - a fault that has moved within the past 130,000 years.

Quaternary Active Fault - a fault that has moved within the past 1,600,000 years.

It should be emphasized that more than half of the historic magnitude 6.5 or greater earthquakes in the Basin and Range Province have occurred on faults that did not have Holocene activity, furthermore, earthquakes in the province will occur on faults in all three categories.

WSSPC PR97-2: Developing Guidelines for Fault Trace Setbacks

WSSPC encourages individual state workshops to develop guidelines for local jurisdictions to establish consistent criteria for setbacks from surface traces of one or more categories of active faults, such as those defined in WSSPC PR-1. In several western states, policy for the regulation of setbacks from active surface fault traces is established at the local level. WSSPC encourages individual jurisdictions that are traversed by the same active fault to have consistent setback requirements. Note that setbacks deal with surface fault ruptures from earthquakes, but do not address the broader, more significant hazards of ground shaking and other effects, such as ground-motion amplification, liquefaction, rock falls, and

landslides.

WSSPC PR97-3: Development of National Earthquake-Hazard Risk Mitigation Priorities

WSSPC proposes to take the initiative to coordinate a process with the federal NEHRP agencies and regional earthquake consortia to establish national earthquake-hazard risk mitigation priorities. This may be accomplished by WSSPC facilitating dialog among the states and presentation of consensus to the federal government.

WSSPC PR97-4: Seismic Monitoring Networks

Because seismic monitoring networks are vital for earthquake-hazard characterization and because there is an insufficiency in available data, WSSPC advocates the continuation and expansion of seismic monitoring networks, including strong-motion instrumentation, by support from state and federal agencies. WSSPC further recommends existing networks be interconnected by compatible hardware and software.

WSSPC is a regional organization that includes the emergency management directors and state geologists or provincial or territorial lead geoscience agency heads of thirteen states, three U.S. territories, one Canadian province, and one Canadian territory. WSSPC's mission is to provide a forum to advance earthquake-hazard reduction programs throughout the western United States and to develop, recommend, and present seismic policies and programs through information exchange, research, and education.

ACKNOWLEDGMENTS

The WSSPC Basin and Range Province Seismic-Hazards Summit was developed and convened through the efforts of many people. All of them cannot be mentioned here, but a handful of individuals should be recognized for their diligent work. Particular appreciation goes to the WSSPC Basin and Range Province Committee, which organized the summit under the leadership of Craig de Polo (NBMG). The Committee also recognizes the WSSPC Board of Directors for their support in convening this event. Board members Jonathan Price and James Davis deserve special recognition for their work in developing the seismic policy aspect for this event.

The United States Geological Survey and the Federal Emergency Management Agency gave tremendous support to allow this event to grow and develop. The staff of WSSPC, Steven Ganz and Andrea James, are recognized for their innumerable hours of hard work in coordinating this event, and Terri Garside (NBMG) is acknowledged for her diligent work and patience. Thank you to Alan Ramelli (NBMG) for coordinating the poster session, and a special thank you to the speakers, poster participants, and all of the summit attendees for coming together in Reno, Nevada to characterize seismic hazards in the Basin and Range Province.

Finally, thank you to the authors of papers in this proceedings volume and to William Lund and the Utah Geological Survey for editing and publishing the volume.

DEDICATION

David Burton Slemmons

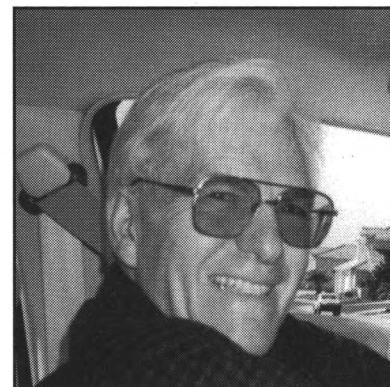
The Western States Seismic Policy Council dedicates this volume to Dr. David Burton Slemmons in recognition of his pioneering efforts in seismic-hazard analyses in the Basin and Range Province.

Burt received his Bachelor of Science degree in geology from the University of California, Berkeley in 1947 and his doctoral degree in geology from Berkeley in 1953. In 1952 he joined the faculty at the University of Nevada, Reno where he conducted research for nearly 40 years. He almost immediately began neotectonic research through his observations of the 1954 Fairview Peak-Dixie Valley, Nevada earthquake sequence. Burt quickly recognized the importance of documenting historical earthquakes and the value of these events in interpreting paleoseismic scarps, and over the following decades he conducted systematic studies of historical earthquakes, not only in the Basin and Range Province but throughout the world. He pioneered ways to analyze the earthquake potential of faults, including the use of low-sun-angle photography to identify small scarps that are usually missed by traditional photography, and was an early promoter of paleoseismic and earthquake research. In his pursuit of the latter goal, he established the University of Nevada, Reno Seismological Laboratory at the beginning of his career, and the Center for Neotectonic Studies at the University of Nevada, Reno shortly before retiring from the University.

Burt supervised over two dozen theses while at the University of Nevada, and students such as James Brune, Thomas Rockwell, and Gary Carver have continued the earthquake research inspired by Burt and have built outstanding programs and reputations on their own. Burt's research and analytical skills are regarded so highly that he has served as an expert for the U.S. Nuclear Regulatory Commission for over 25 years and, since 1984, in the same capacity for the International Atomic Energy Commission on nuclear power plant sites in Armenia, Brazil, Croatia, and Indonesia. He currently serves on the expert panel evaluating the seismic hazard for the proposed high-level nuclear waste repository at the Yucca Mountain site in Nevada.

Burt's research interests are reflected in the papers he has written and the volumes he has helped edit. His classic 1957 paper on "Geological effects of the Dixie Valley-Fairview Peak, Nevada earthquakes of December 16, 1954" includes a map of the surface ruptures with offset descriptions annotated along the fault; this is a prototype of contemporary maps that detail earthquake ruptures. Slemmons (1967), in an address given in Japan, explained the neotectonic research he and his students conducted in the Great Basin. This work, "Pliocene and Quaternary crustal movements of the Basin and Range Province, USA," had involved a systematic review of 1:60,000 scale photography throughout Nevada wherein faults were investigated for relative geomorphic expression and evidence of most recent activity. This was the first time Nevada faults were studied on a regional basis, and many of the general patterns he recognized and observations he made have held up to more detailed, later examination. His 1977 paper, "Faults and earthquake magnitude," is a classic in engineering-geology studies. Burt long ago recognized that academic research needed to be relevant to society, and involved himself and his students in industry during their academic tenure. His classes always emphasized the utility and application of geology. The 1977 "state-of-the-art paper" showed how to characterize the earthquake potential of faults and described the geomorphic features associated with strike-, normal-, and reverse-slip faults in detail that has not been rivaled, much less surpassed, since. Burt's research through the 1980s included papers such as "Determination of design earthquake magnitudes for microzonation," which in 1982 updated his pioneering work in magnitude versus surface-rupture relations. Burt has continued his work since retiring from the University of Nevada, recently (1995) writing "Complications in making paleoseismic evaluations in the Basin and Range Province, western United States." Burt has co-edited several important volumes on seismic-hazard studies, including the Geological Society of America's "Neotectonics in engineering evaluations" (1990), the DNAG volume on the "Neotectonics of North America" (1991), and the "Seismotectonics of the central California Coast Ranges" (1994), and the Association of Engineering Geologists recent volume on "Perspectives in paleoseismology" (1995). He continues his public service commitment by serving as a charter member of the Nevada Earthquake Safety Council.

Burt's accomplishments are legion: he developed many of the earthquake evaluation procedures that are routinely applied today; he instilled in his students the importance of conducting detailed characterization of earthquake sources, and a thirst for new approaches for solving seismotectonic problems; and he began much of the research on faults in Nevada and elsewhere that is continuing today. In appreciation of his outstanding work and enthusiasm, this volume is dedicated to Burt Slemmons.



Selected Bibliography

- Slemmons, D.B., 1957, Geological effects of the Dixie Valley-Fairview Peak, Nevada earthquakes of December 16, 1954: Bulletin of the Seismological Society of America, v. 47, p. 353-375.
- Slemmons, D.B., 1967, Pliocene and Quaternary crustal movements of the Basin and Range Province, USA: Osaka City University, Journal of Geoscience, v. 10, p. 91-103.
- Slemmons, D.B., 1977, Faults and earthquake magnitude: U.S. Army Engineer Waterways Experiment Station, State-of-the-art for assessing earthquake hazards in the United States, Report 6, Miscellaneous Paper S-73-1, 166 p.
- Slemmons, D.B., 1982, Determination of design earthquake magnitudes for microzonation, in Third International Earthquake Microzonation Conference Proceedings, Seattle, Washington, v. 1, p. 119-130.
- Slemmons, D.B., 1995, Complications in making paleoseismic evaluations in the Basin and Range Province, western United States, in Serva, L., and Slemmons, D.B., editors, Perspectives in paleoseismology: Association of Engineering Geologists, Special Publication 6, p. 19-33.

PROGRAM SCHEDULE

TIME	PROGRAM	PRESENTER	ROOM
Monday, May 12, 1997			
3:00 p.m.	Poster Set-up		Expo B
	Registration		Expo B
6:00 p.m.	Poster Display/Social		Expo B
Tuesday, May 13, 1997			
7:00 a.m.	Breakfast		Expo B
	Registration (continues)		Expo B
8:00 a.m.	Conference Opening		Expo C
8:30 a.m. - 11:30 a.m.	Perspectives and User Needs		Expo C
8:30 a.m.	1997 Uniform Building Code	Bob Bachman Fluor Daniel, Inc. Mike Blakely Blakely, Johnson & Ghusn Structural Engineers, Ltd. Ronald T. Eguchi Vice President EQE International	
	Ground-Shaking Criteria		
9:00 a.m.	Engineering/Infrastructure Needs		
9:30 a.m.	Sensitivity of Loss Estimates to Different Source-Zone Maps and Parameters		
10:00 a.m.	Break		Expo B
10:30 a.m.	Perspectives and User Needs (cont.) Emergency Management Needs in the Basin and Range Province	Stephen Weiser Mitigation Officer, Idaho Military Division, Bureau of Disaster Services Robert Redden New Mexico, Office of Emer- gency Planning & Coordination Gil Jamieson Branch Chief Federal Emergency Management Agency	Expo C
11:00 a.m.	HAZUS: The FEMA Tool for Estimating Earthquake Losses		
11:30 a.m.	Challenges of Characterizing Seismic Hazards in the Basin and Range Province		
12:00 p.m.	Lunch	Clarence R. Allen Prof. Emeritus California Institute of Technology, Seismological Lab	Expo B
1:15 p.m. - 4:15 p.m.	Active Fault Characterization		Expo C
1:15 p.m.	Surface-Faulting Hazards and Land-Use Planning in Utah	Gary Christenson Manager, Applied Geology Utah Geological Survey Craig M. dePolo Nevada Bureau of Mines and Geology Ron Lynn Assistant Director, Clark Co., Nevada Building Dept.	
1:45 p.m.	130,000 Year vs. 10,000 Year (Holocene) Classification of "Active" Faults in the Basin and Range Province		
2:15 p.m.	A Practical Approach to Implementing Fault Criteria in Community Planning		
2:45 p.m.	Break		Expo B

TIME	PROGRAM	PRESENTER	ROOM
3:15 p.m.	Active Fault Characterization (cont.) Contrasts Between Short- and Long-term Records of Seismicity in the Rio Grande Rift-Important Implications for Seismic- Hazards Analysis	Michael N. Machette Research Geologist U.S. Geological Survey	Expo C
3:45 p.m.	Earthquake Recurrence Models	David P. Schwartz U.S. Geological Survey	
4:15 p.m.	Technical Discussion with Speakers		Expo C
5:15 p.m.	Policy Discussion	Jonathan G. Price State Geologist Nevada Bureau of Mines and Geology	Expo C
6:00 p.m.	Poster Session and Social		Expo B

Wednesday, May 14, 1997

7:00 a.m.	Breakfast		Expo B
8:00 a.m.	Day's Overview		Expo C
8:15 a.m. - 11:45 a.m.	Strong Ground Motion Characterization		Expo C
8:15 a.m.	Earthquake Ground Motions in Extensional Tectonic Regimes	Paul Spudich Geophysicist U.S. Geological Survey	
8:45 a.m.	Yucca Mountain Ground-Motion Panel	Norman Abrahamson Seismologist Pacific Gas & Electric, Geoscience Department	
9:15 a.m.	Analysis of the Strong-Motion Data Associated with the 1995 Dinar (Turkey) Earthquake	Eser Durukal Professor Bogazici University, Turkey	
9:45 a.m.	Break		Expo B
10:15 a.m.	Strong Ground Motion Characterization (cont.) Rupture Directivity Effects and Strong Fault-Normal Pulses Near Normal Faults	Paul G. Somerville Senior Associate Woodward-Clyde Federal Services	Expo C
10:45 a.m.	Strong Ground Motion Expected from Large Normal-Fault Earthquakes Based on Evidence from Precarious Rocks and Source Modeling	James N. Brune Director Seismological Lab, Mackay School of Mines, Univ. NV	
11:15 a.m.	Attenuation and Site Effects in Northern and Southern Nevada from Three-Component Digital Seismograms	Ken Smith Research Asst. Prof. Seismological Lab, Univ. NV	
11:45 a.m.	Lunch		Expo B
1:15 p.m. - 2:45 p.m.	Basin Effects on Ground Motion		Expo C
1:15 p.m.	Numerical Prediction of Seismic-Wave Amplification in the Salt Lake Basin, Utah	Xu Ji University of Utah Geology/Geophysics Depart.	
1:45 p.m.	Site Effects on Strong Motion in Las Vegas	Feng Su Research Assistant Professor Seismological Lab, Univ. NV	

TIME	PROGRAM	PRESENTER	ROOM
2:15 p.m.	Characterizing Basin Effects	Jacobo Bielak Professor, Carnegie Mellon University, PA	
2:45 p.m.	Break		Expo B
3:15 p.m.	Technical Discussion with Speakers		Expo C
4:30 p.m.	Policy Discussion	Jonathan G. Price State Geologist Nevada Bureau of Mines and Geology	Expo C
5:30 p.m.	Dinner (on own)		
7:30 p.m.	Earthquake Clearinghouse Discussion	Jonathan G. Price State Geologist Nevada Bureau of Mines and Geology	Brew Brothers

Thursday, May 15, 1997

7:00 a.m.	Breakfast		Expo B
8:00 a.m.	Day's Overview		Expo C
8:15 a.m. - 2:00 p.m.	Probabilistic Seismic-Hazard Analysis		Expo C
8:15 a.m.	Earthquake Database Issues for Seismic-Hazard Analysis in the Utah Region	Walter J. Arabasz Director University of Utah Seismograph Stations Ted Barnhard Geologist U.S. Geological Survey	
8:45 a.m.	Quaternary Faults Used for the 1996 National Seismic-Hazard Maps		
9:15 a.m.	Impact of Distributed Faulting to Seismic-Hazard Assessments in the Basin and Range Province--Examples from Yucca Mountain, Nevada	Silvio Pezzopane U.S. Geological Survey	
9:45 a.m.	Break		Expo B
	Probabilistic Seismic-Hazard Analysis (cont.)		Expo C
10:15 a.m.	Earthquake-Risk Assessment for Seismically Dormant Normal Faults: An Example from the Wasatch Front, Utah, Using GPS Measurements, Quaternary Faults, and Seismicity.	Robert B. Smith Professor University of Utah	
10:45 a.m.	Shape of the Magnitude-Frequency Distribution for Individual Faults	Mark W. Stirling Mackay School of Mines, University of Nevada	
11:15 a.m.	New Seismic-Hazard Maps for the Western U.S.	Art Frankel Geophysicist U.S. Geological Survey	
12:00 p.m.	Lunch (on own)		
1:15 p.m.	Seismic Hazards in the Basin and Range Province: Perspectives from Probabilistic Analyses	Ivan G. Wong Vice President, Woodward-Clyde	
1:45 p.m.	Natural Limits on PSHAs	John G. Anderson Professor, University of Nevada	

TIME	PROGRAM	PRESENTER	ROOM
2:15 p.m.	Sensitivities of Probabilistic Seismic-Hazard Analyses to Earthquake Recurrence Along Faults in the Basin and Range Province	David M. Perkins Geophysicist, U.S. Geological Survey	
2:45 p.m.	Break		Expo B
3:15 p.m.	Technical Discussion with Speakers		Expo C
4:15 p.m.	Policy Discussion & Review of Conference	Jonathan G. Price State Geologist Nevada Bureau of Mines and Geology James Davis State Geologist California Divisions of Mines and Geology	Expo C
5:30 p.m.	Conference Adjournment		Expo C
	Poster Breakdown		Expo B
7:30 p.m.	WSSPC Basin & Range Province Committee Meeting	Craig M. dePolo Nevada Bureau of Mines and Geology	Platinum Salon

POSTER TOPICS

DETACHMENT FAULTS: SUPERSTARS OR BIT PLAYERS IN SEISMIC HAZARDS OF THE GREAT BASIN

ANDERSON, R. Ernest, and Sharon F. Diehl, U. S. Geological Survey, MS 966, Federal Center, Denver
CO 80225-0046 (anderson@gldvxa.cr.usgs.gov)

PROBABILISTIC GROUND-MOTION MAPS FOR NEVADA BY TREND SURFACE ANALYSIS

BELL, John W., Raj Siddharthan, John Anderson, Craig dePolo, and Ron Hess, Nevada Bureau of Mines and
Geology/MS178, University of Nevada, Reno, NV 89557

PALEOSEISMOLOGY FROM LUMINESCENCE DATING: TESTS AND APPLICATION NEAR LANDERS, CALIFORNIA

BERGER, Glenn W., Desert Research Institute, P.O. Box 60220, Reno, NV 89506-0220 (gwberger@maxey
.dri.edu) T.K. Rockwell, Geological Sciences, San Diego State Univ., San Diego, CA 92182; D.J. Huntley,
Dept. Physics, Simon Fraser Univ., Burnaby, B.C., V5A 1S6, Canada

EARTHQUAKE HAZARD ON THE WASATCH FRONT, UTAH, FROM FAULT INTERACTION AND TECTONIC INDUCED FLOOD INUNDATION ASSOCIATED WITH THE WASATCH FAULT

CHANG, Wu-Lung, R. B. Smith, Department of Geology and Geophysics; University of Utah, Salt Lake City, UT,
84112 (wchang@mines.utah.gov) (rbsmith@mines.utah.edu); R. W. Simpson Jr., (USGS, 345 Middlefield Road,
Menlo Park, CA, 94025

PLANNING SCENARIO FOR A MAJOR EARTHQUAKE IN WESTERN NEVADA

dePOLO, Craig M., Jim G Rigby, Gary L. Johnson, and Steven L. Jacobson, Nevada Bureau of Mines and
Geology, University of Nevada, Reno; John G. Anderson, Seismological Laboratory, University of Nevada,
Mail Stop 178, Reno, NV 89557-0088, (cdepolo@nbmg.unr.edu) and Thomas J. Wythes, WESTEC

HISTORICAL EARTHQUAKES, AND PATTERNS AND BEHAVIOR OF SEISMICITY IN WESTERN NEVADA AND EASTERN CALIFORNIA

dePOLO, Diane M., Ken D. Smith, and John G. Anderson, Seismological Laboratory, University of Nevada,
Reno, MS 174, Reno, NV 89557 (diane@seismo.unr.edu); Craig M. dePolo, Nevada Bureau of Mines and
Geology, University of Nevada, Reno, MS 178, Reno, NV 89557 (cdepolo@nbmg.unr.edu)

GEOLOGIC INPUT FOR SEISMIC-HAZARDS MAPS - - EXAMPLES FROM THE DATABASE OF QUATERNARY FAULTS IN MONTANA

HALLER, Kathleen M., U.S. Geological Survey, Central Region Geologic Hazards Team, Denver, Colorado,
P.O. Box 25046, Mail Stop 966, Denver Federal Center, Denver, CO 80225 (haller@gldvxa.cr.usgs.gov)

THE SEISMOTECTONICS AND SOURCE PARAMETERS OF RECENT EARTHQUAKES NEAR RENO, NEVADA

ICHINOSE, Gene A., Kenneth D. Smith, John G. Anderson, and James N. Brune, University of Nevada Reno
Seismological Laboratory, Mail Stop 178, Reno, NV 89557-0088 (ichinose@seismo.unr.edu)

IMPLICATIONS OF VARIABLE LATE QUATERNARY RECURRENCE INTERVALS FOR PROBABILISTIC SEISMIC-HAZARD ASSESSMENTS; EXAMPLES FROM UTAH AND WEST TEXAS

KEATON, Jeffrey R., AGRA Earth & Environmental, Inc., 130 Yucca Drive, Sedona, AZ 86336-3222
(72560.1510@CompuServe.COM)

RECOGNITION OF ACTIVE BUT NON-SEISMOGENIC SALT-RELATED DEFORMATION WITHIN AN EXTENSIONAL ENVIRONMENT, WEST-CENTRAL COLORADO

KIRKHAM, Robert M., and Randall K. Streufert, Colorado Geological Survey, PO Box 172, Montevista,
CO 81144

GEOPHYSICAL CHARACTERIZATION OF ACTIVE FAULTS IN THE BASIN AND RANGE, AND THE EARTHQUAKE HAZARD OF THE PAHRUMP VALLEY FAULT ZONE

LOUIE, John, Gordon Shields, Gene Ichinose, Michael Hasting, Gabriel Plank, and Steve Bowman, Associate
Professor of Seismology, Seismological Lab (174) The University of Nevada, Reno, Reno, NV 89557-0141
(louie@seismo.unr.edu)

CHARACTER OF FAULTING ALONG THE HUNTER MOUNTAIN FAULT ZONE AND EVIDENCE FOR ACTIVE DEXTRAL SLIP TRANSFER ACROSS SALINE VALLEY RHOMBOCHASM, EASTERN CALIFORNIA

OSWALD, John A., and S. G. Wesnousky, Center for Neotectonic Studies, m/s 169, University of Nevada, Reno,
NV 89557-0135 (johnno@seismo.unr.edu SteveW@seismo.unr.edu)

RECENT LARGE-MAGNITUDE EVENTS ALONG THE CARSON RANGE FAULT SYSTEM, A PRINCIPAL FRONTAL FAULT OF THE NORTHERN SIERRA NEVADA

RAMELLI, Alan R., Craig M. dePolo, and John W. Bell, Nevada Bureau of Mines and Geology/MS178, University of Nevada, Reno, NV 89557, (ramelli@nbmg.unr.edu)

HOLOCENE PALEOSEISMICITY, SEGMENTATION, AND SEISMIC POTENTIAL OF THE FISH LAKE VALLEY FAULT ZONE, NEVADA AND CALIFORNIA

SAWYER, T.L., Consultant, 10455 San Fernando Rd. Reno, NV 89506 (103253.1322@compuserve.com); M.C. Reheis, U.S. Geological Survey, MS 980, Federal Center, P.O. Box 25046, Lakewood, CO 80225 (mreheis@usgs.gov)

NONLINEAR AMPLIFICATION STUDIES ON DEEP SOIL DEPOSITS IN RENO, NEVADA

SIDDHARTHAN, Raj V., Professor of Civil Engineering, University of Nevada, Reno, NV 89557. (siddhart@unr.edu) Ni Shean-Der, Graduate Student, and John G. Anderson, Professor of Seismology

MAGMA INTRUSION AND SEISMIC-HAZARDS ASSESSMENT IN THE BASIN AND RANGE PROVINCE

SMITH, Richard P., and S.M. Jackson, Idaho National Engineering and Environmental Laboratory, P.O. Box 1625, Idaho Falls, ID 83415-2107, (rps3@inel.gov); W.R. Hackett, WRH Associates, 2880 E. Naniloa Circle, Salt Lake City, UT 84117

DEFINITION OF FAULT SEGMENTS ON YOUNG NORMAL FAULTS: GEOMETRY, OFFSET, AND SCARPS OF THE HURRICANE FAULT, UTAH AND HIKO FAULT, NEVADA

TAYLOR, Wanda J., Douglas D. Switzer, and K. Jill Hammond, Dept. of Geoscience, University of Nevada, 4505 Maryland Parkway, Las Vegas, NV 89154-4010 (wjt@nevada.edu)

RELATION OF GRAVITATIONALLY DRIVEN LITHOSPHERIC EXTENSION TO LOW SLIP-RATE FAULTS AND REGIONAL SEISMIC HAZARDS IN THE WESTERN U.S.

UNRUH, J.R., Lettis & Associates, William Lettis & As., 1777 Botelho Dr., #262, Walnut Creek, CA 94596 (unruh@lettis.com); C.H. Jones, CIRES, University of Colorado, Boulder; L.J. Sonder Dartmouth College, Hanover, NH

SEISMICITY IN THE SGB: WHAT DO EARTHQUAKE CATALOGS ACCURATELY INDICATE?

VON SEGGERN, D. H., and J. N. Brune, Seismological Laboratory, MS 174, University of Nevada-Reno, MS 174, Reno, NV 89557 (vonseg@seismo.unr.edu)

THE SEISMO-WATCH WEEKLY EARTHQUAKE REPORT, A WEEKLY BROADCAST OF GLOBAL AND REGIONAL EARTHQUAKE INFORMATION ON COMMUNITY ACCESS TELEVISION

WATSON, Charles P., Advanced Geologic Exploration, Reno, NV (watson@seismo-watch.com)

CHARACTER OF LATE QUATERNARY LOW-ANGLE(?) NORMAL FAULTING ON THE NORTHWESTERN SIDE OF THE RUBY MOUNTAINS / EAST HUMBOLDT RANGE, NORTHEASTERN NEVADA

WILLOUGHBY, C.H., and S.G. Wesnousky, Center for Neotectonic Studies, MS 169, University of Nevada, Reno, NV 89557, (chrisw@seismo.unr.edu steview@seismo.unr.edu)

RECENT MICROSEISMICITY IN THE WESTERN SNAKE RIVER PLAIN, IDAHO, AND TRENCH EVIDENCE FOR RECURRENT LATE QUATERNARY FAULTING NEAR THE WSRP SOUTHERN MARGIN

ZOLLWEG, J. E., G. S. Beukelman, and C. J. Waag, Dept of Geosciences, Boise State University, Boise, ID 83725 (zollweg@sisyphus.idbsu.edu)

PRESENTER ABSTRACTS
(in chronological order by presentation time)

1997 UNIFORM BUILDING CODE GROUND-SHAKING CRITERIA

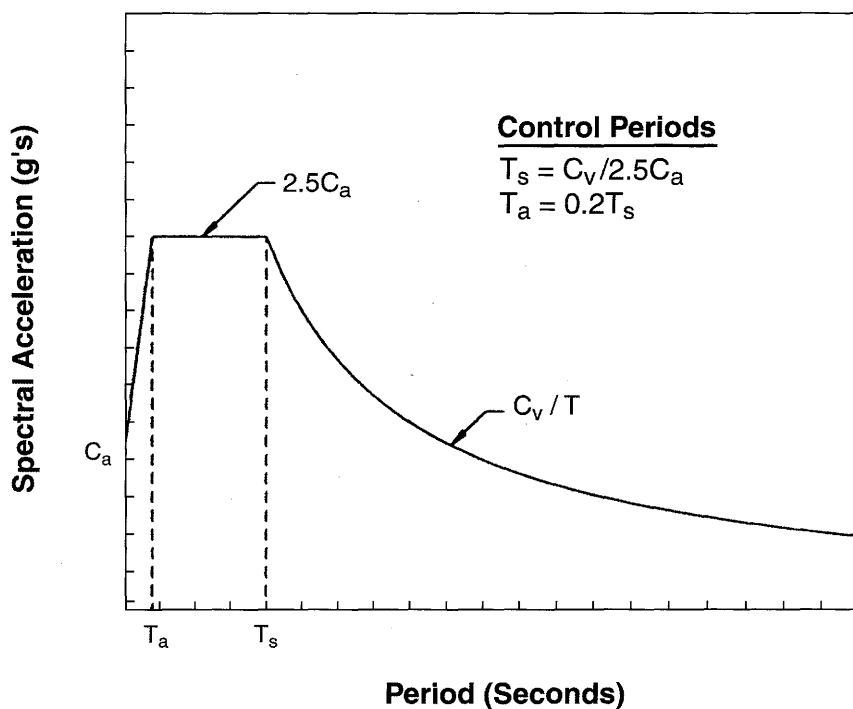
BACHMAN, Robert E., Structural Engineer, Fluor Daniel, Inc., 3353 Michelson Dr., Irvine, CA 92730

The recently published 1997 Uniform Building Code incorporates two significant changes to the ground-shaking criteria which apply to all structures. The first change is a revision to soil types and soil-amplification factors. The second change is the incorporation of near-source factors in UBC seismic zone 4. Together these changes result in the largest increases in code ground-shaking criteria which has occurred in the past 30 years. Records obtained from the Strong-Motion Instrumentation Program (SMIP) along with U.S. Geological Survey (USGS) records were the primary sources of data used to justify these code changes.

Soil Types and Soil-Amplification Factors

The ground shaking basis for code design is reflected in the 5 percent damped elastic response spectra shown in figure 1 (UBC figure 16-3). The response spectra is defined in terms of two site seismic coefficients C_a and C_v . The site seismic coefficients are determined as a function of seismic zone, soil type, and in zone 4 near source factors. The soil profiles are subdivided into six types based on the average soil properties in the top 100 feet of the soil profile. The types are identified as S_A through S_F and are defined in accordance with Table 16-J (attached). The types are based on consensus deliberations from the USGS/NCEER/SEAOC workshop held at USC in 1992. These are identical to soil-profile types that are found in 1994 NEHRP Provisions.

The site seismic coefficients C_a and C_v are determined from tables 16-S and table 16-T (attached) based upon the soil-profile type, seismic zone, and in UBC seismic zone 4 the near-source factors N_a and N_v . It should be noted that the value of the soil factors depart significantly from previous codes in that both short-period and long-period structures are affected by soil effects and that the amplifications increase significantly at lower ground-acceleration levels. In previous codes, soil effects were only considered for long-period structures. The amplification factors are consistent with the consensus from the previously referenced USC workshop and are identical to those found in the 1994 NEHRP provisions. These effects are consistent with observations in the Mexico City and the Loma Prieta earthquakes.



Near-Source Factors

The near-source factors were developed by the Ad Hoc Ground-Motion Committee of the SEAOC Seismology Committee to account for the effects of ground motions near the source of seismic events. The factors are a refinement of what was developed for seismically isolated structures included initially in the 1991 UBC. Near-source ground-motion records and observed damage from Northridge and Kobe have provided convincing evidence of significantly more intense ground shaking near the fault rupture than had been previously accounted for.

In order to establish the near-source factors, the first step is to identify and locate known active faults in UBC zone 4 and classify them into one of three source types based on maximum moment magnitude and slip rate in accordance with table 16-U (attached). Faults are classified based on their maximum magnitude M and slip rate R . Type A sources are faults that have a moment-magnitude potential of $M \geq 7.0$ and a slip rate SR equal to or greater than 5 mm/year. These types of faults are considered to be active and capable of producing large-magnitude events. Most segments of the San Andreas fault would be classified as a Type A fault. Type C sources are faults that have a moment-magnitude potential of $M < 6.5$ and a slip rate of $SR \leq 2$ mm/year. Type C faults are considered to be sufficiently inactive and not capable of producing large-magnitude events such that potential near-source ground-shaking effects can be ignored. Most faults outside of California are Type C. Type B sources are all faults that are not either Type A or Type C and include most of the active faults in California. The 1997 UBC requires that the locations and characteristics of these faults be established based on approved

Figure 1. Design response spectra.

geotechnical data from reputable sources such as the California Division of Mines and Geology (CDMG) and the USGS.

Once faults are located relative to a site and the source type is established, the near-source factors N_a and N_v are determined in accordance with table 16-S and 16-T (attached). These factors were established by the Ad Hoc Ground-Motion Committee and are based on the average increase, measured in the near field from Northridge and other earthquakes. The near source factors apply to both strike-slip and reverse-slip (thrust) fault mechanism although reverse-slip faults produce about 20 percent greater shaking on the average. The short-period (acceleration domain) near-source factor (N_a) is based on response at 0.3 seconds and long-period (velocity-domain) near-source factor (N_v) is based on 1.0 second response. Values of N_v are bumped upward by about 20 percent to account for the increase in average response in the fault-normal direction above that predicted by the attenuation function for the random component of horizontal ground shaking (Somerville, 1996, 7th US/Japan Workshop, Lessons learned from Kobe and Northridge). The commentary to the SEAOC bluebook notes ground shaking at "forward directivity" sites is likely to be 1.25 times the C_v and C_a coefficients based on average fault-normal response. The values of N_a and N_v are used in tables 16-S and 16-T to determine the values of C_a and C_v in UBC seismic zone 4 ($Z = 0.40$).

Table 16-J. Soil Profile Types

Soil Profile Type	Soil Profile Name/Generic Description	Average Soil Properties for Top 100 Feet (30 480 mm) of Soil Profile		
		Shear Wave Velocity, \bar{v}_s feet/second (m/s)	Standard Penetration Test, \bar{N} (or \bar{N}_{ch} for cohesionless soil layers) (blows/foot)	Undrained Shear Strength, \bar{S}_u psf (kPa)
S_A	Hard rock	>5000 (1500)		
S_B	Rock	2,500 to 5,000 (760 to 1500)		
S_C	Very dense soil and soft rock	1,200 to 2,500 (360 to 760)	>50	>2,000 (100)
S_D	Stiff soil profile	600 to 1,200 (180 to 360)	15 to 50	1,000 to 2,000 (50 to 100)
S_E^1	Soft soil profile	<600 (180)	<15	<1,000 (50)
S_F	Soil requiring site-specific evaluation. See Section 1644.3.1			

¹ Soil profile Type S_E also includes any soil profile with more than 10 ft (3048 mm) of soft clay defined as a soil with a plasticity index, $PI > 20$, $w_{mc} > 40$ percent and $\bar{S}_u < 500$ psf (25 kPa). The Plasticity Index, PI , the moisture content, w_{mc} , shall be determined in accordance with approved national standards.

Table 16-Q. Seismic Coefficient C_a

Soil Profile Type	Seismic-Zone Factor, Z				
	Z = 0.075	Z = 0.15	Z = 0.2	Z = 0.3	Z = 0.4
S _A	0.06	0.12	0.16	0.24	0.32N _a
S _B	0.08	0.15	0.20	0.30	0.40N _a
S _C	0.09	0.18	0.24	0.33	0.40N _a
S _D	0.12	0.22	0.28	0.36	0.44N _a
S _E	0.19	0.30	0.34	0.36	0.36N _a
S _F	See Footnote 1				

- ¹ Site-specific geotechnical investigation and dynamic site response analysis shall be performed to determine seismic coefficients for Soil Profile Type S_F.

Table 16-R. Seismic Coefficient C_v

Soil Profile Type	Seismic-Zone Factor, Z				
	Z = 0.075	Z = 0.15	Z = 0.2	Z = 0.3	Z = 0.4
S _A	0.06	0.12	0.16	0.24	0.32N _v
S _B	0.08	0.15	0.20	0.30	0.40N _v
S _C	0.13	0.25	0.32	0.45	0.56N _v
S _D	0.18	0.32	0.40	0.54	0.64N _v
S _E	0.26	0.50	0.64	0.84	0.96N _v
S _F	See Footnote 1				

- ¹ Site-specific geotechnical investigation and dynamic site response analysis shall be performed to determine seismic coefficients for Soil Profile Type S_F.

Table 16-U. Seismic-Source Type¹

Seismic Source Type	Seismic Source Description	Seismic-Source Definition	
		Maximum Moment Magnitude, M	Slip Rate, SR (mm/year)
A	Faults that are capable of producing large magnitude events and which have a high rate of seismic activity	M ≥ 7.0 and	SR ≥ 5
B	All faults other than Types A and C		
C	Faults which are not capable of producing large magnitude earthquakes and which have a relatively low rate of seismic activity	M < 6.5 and	SR ≤ 2

- ¹ Subduction sources shall be evaluated on a site-specific basis.

Table 16-S. Near-Source Factor N_a ¹

Seismic Source Type	Closest Distance to Known Seismic Source ^{2,3}		
	≤ 2 km	5 km	10 km
A	1.5	1.2	1.0
B	1.3	1.0	1.0
C	1.0	1.0	1.0

- ¹ The near-source factor may be based on the linear interpolation of values for distances other than those shown in the table.
- ² The location and type of seismic sources to be used for design shall be established based on approved geotechnical data (e.g. most recent mapping of active faults by the United States Geological Survey or the California Division of Mines and Geology).
- ³ The closest distance to seismic source shall be taken as the minimum distance between the site and the area described by the vertical projection of the source on the surface (i.e., surface projection of fault plane). The surface projection need not include portions of the source at depths of 10 km, or greater. The largest value of the near-source factor considering all sources shall be used for design.

Table 16-T. Near-Source Factor N_v ¹

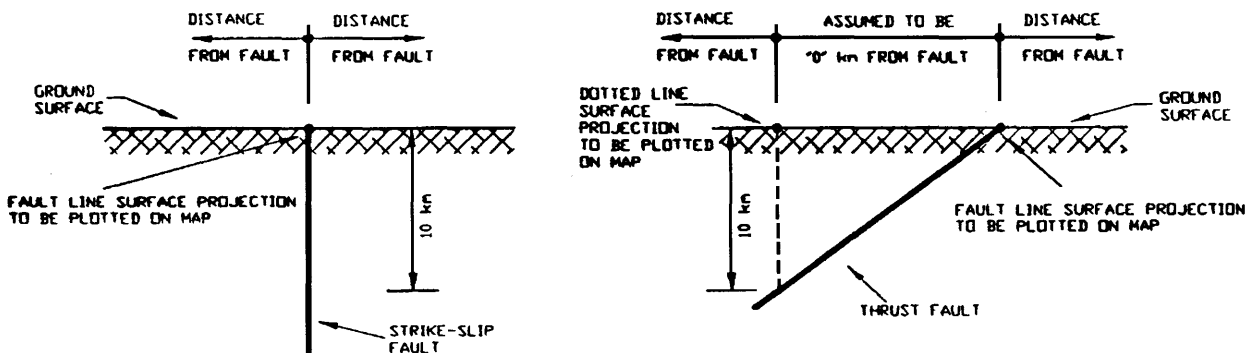
Seismic Source Type	Closest Distance to Known Seismic Source ^{2,3}			
	≤ 2 km	5 km	10 km	15 km
A	2.0	1.6	1.2	1.0
B	1.6	1.2	1.0	1.0
C	1.0	1.0	1.0	1.0

- ¹ The near-source factor may be based on the linear interpolation of values for distances other than those shown in the table.
- ² The location and type of seismic sources to be used for design shall be established based on approved geotechnical data (e.g. most recent mapping of active faults by the United States Geological Survey or the California Division of Mines and Geology).
- ³ The closest distance to seismic source shall be taken as the minimum distance between the site and the area described by the vertical projection of the source on the surface (i.e., surface projection of fault plane). The surface projection need not include portions of the source at depths of 10 km, or greater. The largest value of the near-source factor considering all sources shall be used for design.

Distance from Faults and Fault Maps

The rules for measuring distance from a fault were also established by the Ad Hoc Ground-Motion Committee and are found in the code. The rules are illustrated in figure 2 for a variety of fault types and depths. It is interesting to note that for non-vertical faults, a zero distance fault zone has been established as illustrated. The distance from a fault is measured from this zero distance fault zone.

1997 UBC NEAR SOURCE FACTOR RULES FOR DETERMINING PLOTTED FAULT LOCATION AND DISTANCE FROM FAULT



ACTIVE A & B SEISMIC SOURCES WHOSE FAULT PLANE EXTENDS TO SURFACE

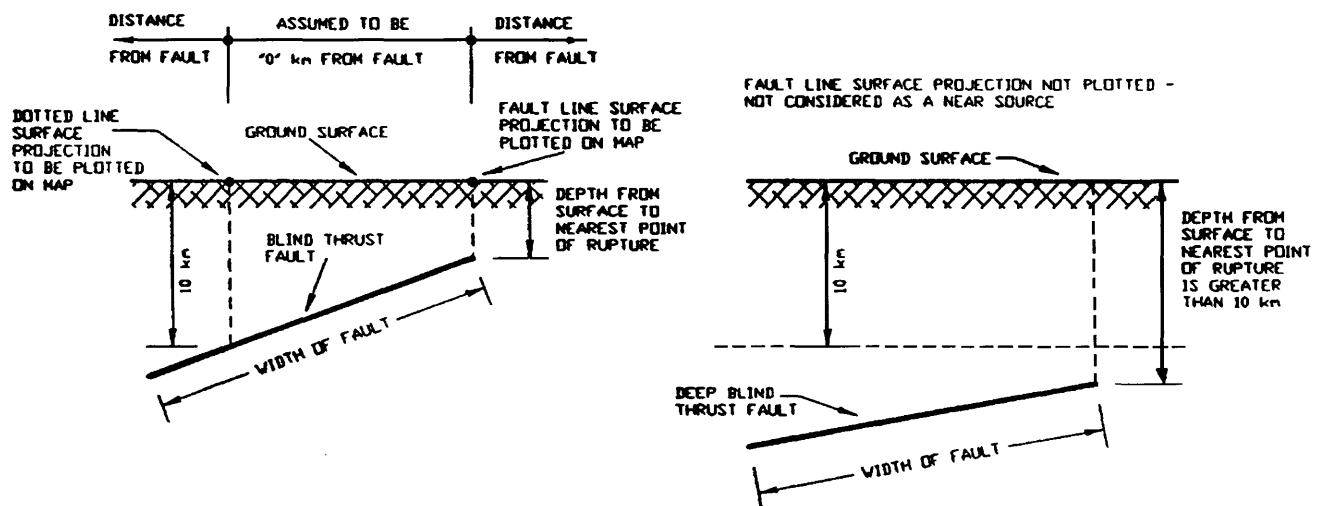
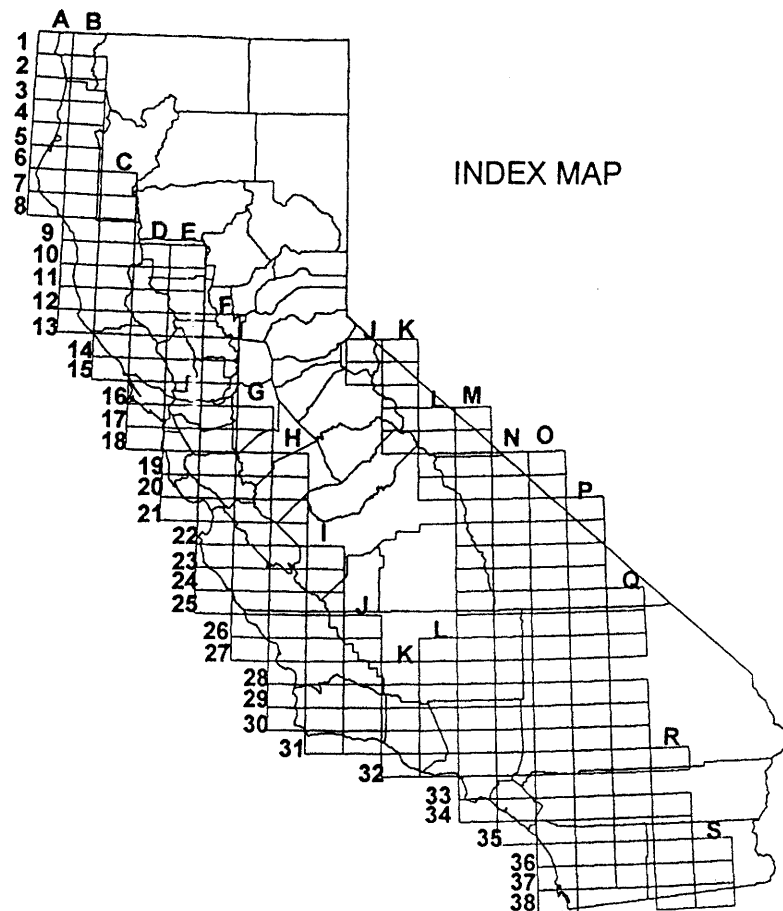


Figure 2. 1997 UBC near-source factor, rules for determining plotted fault location and distance from fault.

Active fault near-field maps are currently being developed for California seismic zone 4 by the CDMG. The form of the maps will be like a Thomas Guide and will be at a scale of 1:150,000. The background will include street maps and freeways. An individual will be able to find their house on the maps. The USGS is providing fault information developed for Project 97 for maps outside of California and the maps will be developed by donated private sources. The maps will be published for sale by ICBO in fall of 1997. Examples of the legend sheet are shown in figure 3 and examples of expected near-field maps are shown in figures 4 and 5.

Conclusion

In conclusion, the inclusion of soil- and near-field effects in the 1997 UBC represent one of the most state-of-the-art, meaningful, and impactful changes in the code by the geoscience community in the history of seismic codes. The effects will continue to be improved in the new International Building Code which replaces the UBC beginning in the year 2000.



EXPANDED LEGEND

The maps are intended for use with the 1997 Uniform Building Code (UBC), Tables 16-S and 16-T, to determine near fault seismic factors N_a and N_v .

The shaded areas are near field zones of active faults where the near source factors are maximum (within 2 km of "zero" fault width zones).

Active faults are classified as A or B in accordance with Table 16-u of 1997 UBC.

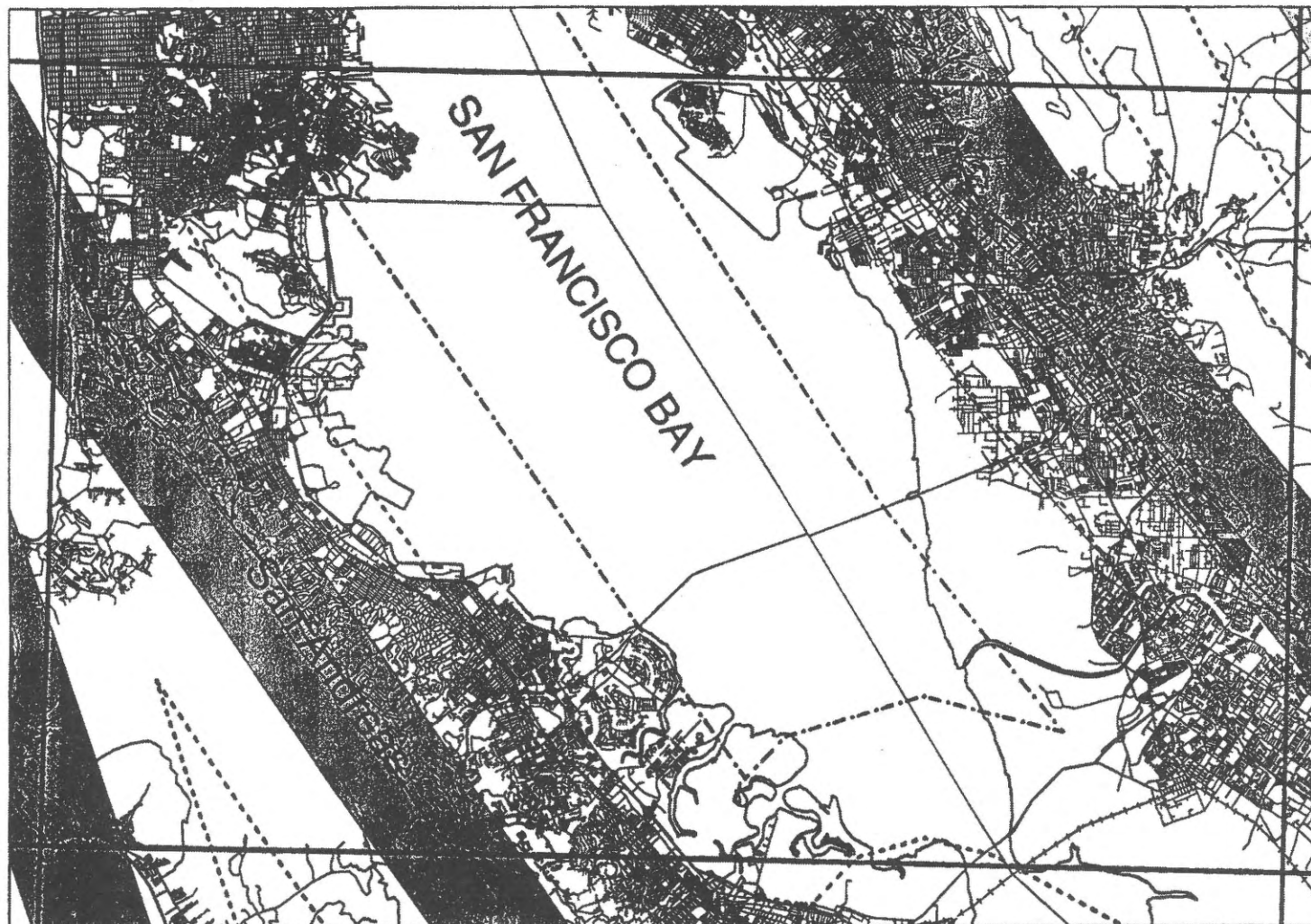
The dotted lines indicate distances of 5, 10, and 15 km from the "zero" fault width zones.

Figure 3. Example legend page for near-field fault maps.

X-15

Active Fault Near Field Zones

This map is intended to be used in conjunction with the 1997 Uniform Building Code, Tables 16-S and 16-T



X-15

Department of Conservation
Division of Mines and Geology



LEGEND

See expanded legend and index map

Shaded areas are within 2 km of active zero width zone.



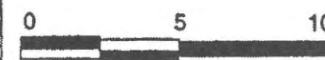
A fault



B fault

Contours of closest distance to fault zero width zone

- 5 km
- 10 km
- 15 km



Kilometers

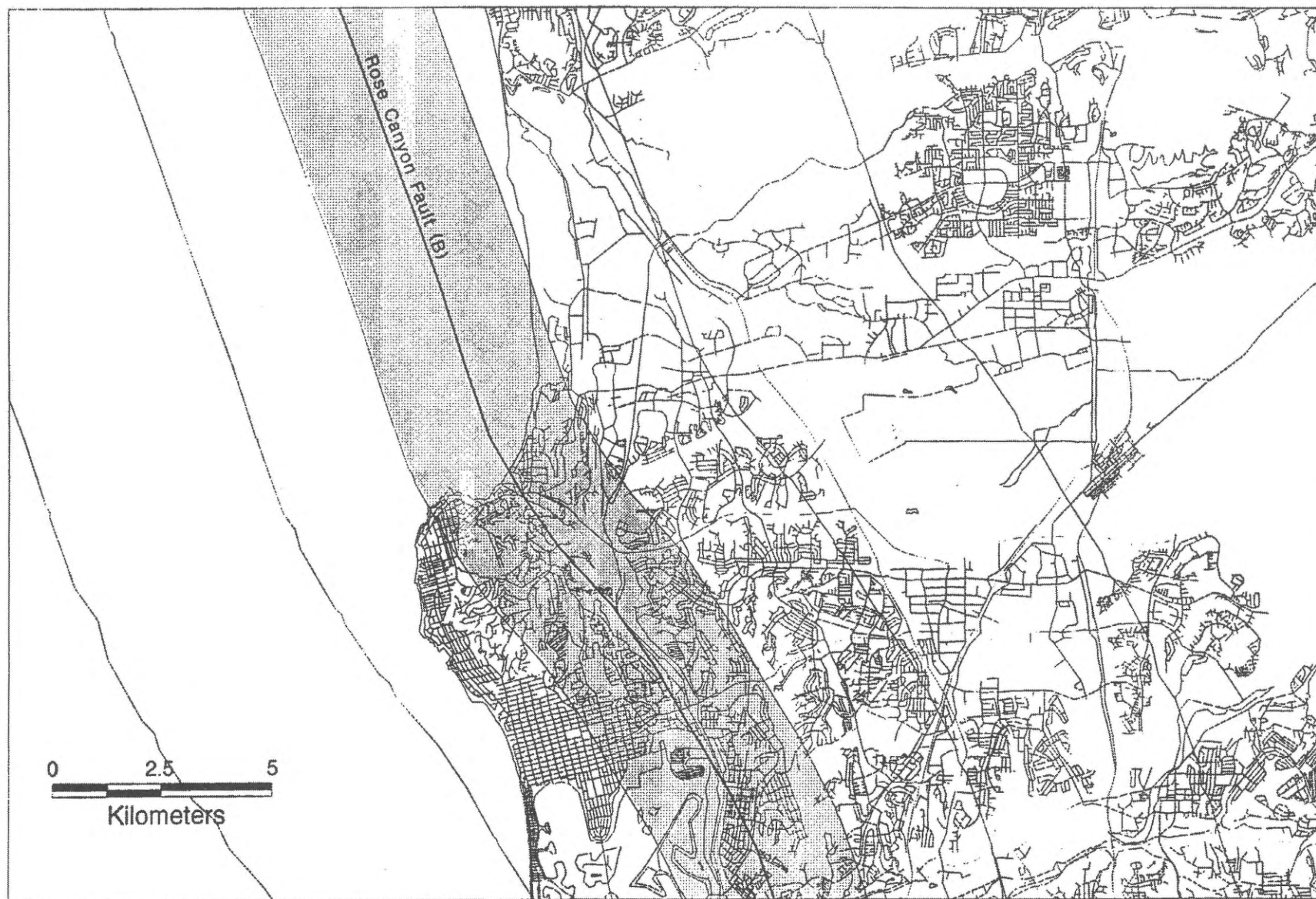
1/4" is approximately equal to 1 km

August, 1997

Figure 4. Example of active fault near-field map for San Francisco Bay area.



CALIFORNIA DEPARTMENT OF CONSERVATION
DIVISION OF MINES AND GEOLOGY



Near fault zones, La Jolla, City of San Diego. (Scale 1: approx. 98,000)

Figure 5. Example of active fault near-field map for La Jolla, City of San Diego.

ENGINEERING INFRASTRUCTURE NEEDS

BLAKELY, Mike D., Structural Engineer, Blakely, Johnson & Ghush Structural Engineers, Ltd., 100 W. Grove St. #475, Reno, NV 89509

Current and future seismic-design methods for structures are compared. The current technique using static design with public life safety as the performance criteria is compared to more progressive techniques which more closely predict various levels of structural performance based on earthquakes magnitudes.

Needs for site-specific ground motions with different magnitudes and recurrence periods are discussed as they relate to various levels of structural performance.

The needs of owners, insurers, and the public to understand structure performance under various earthquake magnitudes and recurrence periods are discussed.

Problems and contradictions in seismic-design criteria are discussed. Included are moving seismic-zonation lines, setting lines through the center of cities, comparing accelerations and frequency on the San Andreas to the Basin and Range, solving poor design and construction methods by increasing design forces, and ground-motion predictions based on detailed analysis of limited data.

SENSITIVITY OF LOSS ESTIMATES TO DIFFERENT SOURCE-ZONE MAPS AND PARAMETERS

EGUCHI, Ronald T., Center for Advanced Planning and Research, EQE International, Inc. 18101 Von Karma, Suite 400, Irvine, CA 92715

The purpose of this presentation is to discuss how changes in seismic-source parameters for the southern California area affect the calculation of expected annual losses to building stock. It is common, for insurance purposes, to estimate the seismic risk to a portfolio of buildings or facilities by calculating expected losses over a specified time period, e.g., one year, 50 years, etc. In most cases, seismic hazards are described by the frequency of earthquakes on selected faults and the distribution of earthquake magnitudes that are possible on these faults. In the southern California region, there are about 100 faults or source zones that can contribute to the seismic hazard throughout the Los Angeles basin.

In order to demonstrate the sensitivity of building-loss estimates to differences in seismic-source models or parameters, two seismic-source models were used: the 1982 U.S. Geological Survey model that incorporates roughly 80 source zones, and the 1995 Southern California Earthquake Center (SCEC) model which includes 96 zones. Some of the key differences between these two models include; different zonation boundaries, earthquake occurrence rate differences, maximum-magnitude differences, and in the case of the SCEC model, the inclusion of conditional probabilities of occurrence for selected faults. These latter probabilities involve the estimation of the probability of the next earthquake based on past earthquake occurrence data, geological information, and the time since the last major event. In order to keep the calculations of earthquake ground motions consistent between the two models, the same ground-motion attenuation function for a rock site condition was used (Sadigh and others, 1993). The final products from this calculation were annual probabilities of exceedance of various levels of peak ground acceleration (PGA). These were transformed into occurrence probabilities, and PGAs were converted to modified Mercalli intensities (MMI). MMIs were calculated in order to be consistent with available damage functions for California buildings.

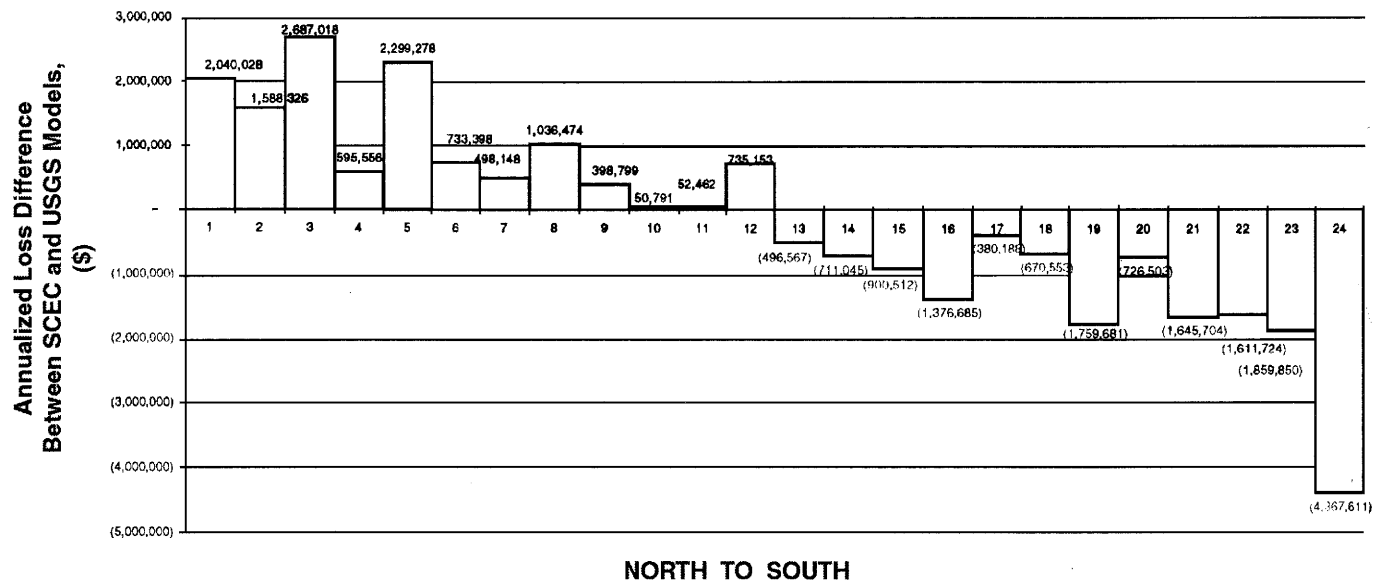
The area of interest for this cursory study was Los Angeles County. To represent exposed building population, summary information from the Los Angeles County Assessor's office was used. In general, the following information is available for most taxable properties in the county: building location (in terms of zip code), structural type, number of stories, building use, and building age. Building information was aggregated for selected zip codes within Los Angeles County. Time did not permit a complete evaluation of the effects of these different seismic-source models on the entire county. In total, 24 zip codes were strategically selected within Los Angeles County to represent a limited sample of buildings exposed in this area. In general, these zip codes were selected based on total replacement value of buildings exposed and relative location to major fault zones. Total number of buildings and replacement values ranged from roughly 5,000 building with a value of \$1 billion, to close to 20,000 buildings and a replacement value of roughly \$3 billion. The total value exposed for the 24 zip codes used in the study is about \$32 billion. Note that these are estimated replacement values for the building structure only (i.e., contents, and other indirect effects are not addressed here). The large majority of the buildings are of wood-frame construction and were built prior to the 1960s.

The results of the analysis show that using the SCEC source maps increases the seismic-hazard potential for the Los Angeles basin in the San Fernando Valley and the Ventura region, and decreases the hazard in the central Los Angeles basin, relative to the U.S. Geological Survey (USGS) maps. Resulting loss estimates reflect higher estimates of annualized loss in the San Fernando Valley and Ventura, and lower estimates in Los Angeles. Figure 1 shows the difference in annualized loss between SCEC and the USGS models, as one views zip codes starting at the north and proceeding to the south. As is evident from the figure, there is a clear impact on expected losses depending on which seismic-source model is used. It is interesting to note, however, that the difference in total annualized loss for the 24 zip codes used in this study only amounts to \$4 million on an annual basis. Some caveats are appropriate here however. It must be recognized that only a small sample of zip codes were used in this analysis and that some buildings may be missing from the database; therefore, actual trends or differences may vary with a full analysis of all zip codes in Los Angeles County. Also, since rock conditions were used in the analysis, sites located on soils (particularly soft soils) may reflect higher losses, thus the distribution

of losses by subarea or zip code may vary.

In spite of these caveats, it is interesting to note that on a large regional scale, the differences in loss estimates using the two different source-zone maps may not be significant. On a local scale, that is comparing loss estimates for different cities or areas within the Los Angeles basin, the differences can be important.

**Annualized Loss Difference Between SCEC and USGS Models,
From Northern to Southern Los Angeles County**



HAZUS: THE FEMA TOOL FOR ESTIMATING EARTHQUAKE LOSSES

JAMIESON, Gil, Federal Emergency Management Agency, Federal Center Plaza, 500 C Street, S.W., Washington, D.C. 20472
(gil.jamieson@fema.gov)

The Federal Emergency Management Agency through a cooperative agreement with the National Institute of Building Science (NIBS) has developed a nationally applicable standardized methodology for estimating potential earthquake losses. The primary purpose of this multi-year project is to develop guidelines and procedures for making earthquake loss estimates at the regional or local scale. These loss estimates can be used by local, state and regional officials to plan and stimulate efforts to reduce risks from earthquakes and to prepare for emergency response and recovery. A secondary purpose of this project is to provide FEMA with a basis for assessing nationwide risk of earthquake losses.

The methodology development and implementation into a GIS-based computer program is being completed by a consortium of natural-hazard loss experts composed of earth scientists, engineers, architects, economists, emergency planners, social scientists, and software developers. Technical direction and review of methodology development is provided by the 8-member Project Working Group (PWG) with guidance from the Project Oversight Committee (POC), a group representing user interests in the earthquake-engineering and emergency-planning community.

The first task of this project was to assess the state-of-the-art in earthquake loss estimation. The study (FEMA 249.1994) was conducted as a joint effort between the California Universities for Research in Earthquake Engineering (CUREE) and Risk Management Solutions, Inc. It revealed that although numerous regional earthquake loss studies have been carried out in the past two decades, potential users of these studies, such as emergency-response planners and local governments, found them to be less useful than they had hoped. The report identifies a variety of reasons for this, including but not limited to, the inability of a single study to meet the very different needs of users at different levels of government, the costs of collecting inventory and performing the studies, the stagnant nature of the results when they are in a report form, and the technical nature in which results have been presented. In addition, the final reports rarely contained any documentation of the inventory used, and the output was often provided in a tabular format that provided little insight about the geographical distribution of the damage and losses.

With these concerns in mind, the PWG focused the project goal on developing a useful tool for local, state and regional officials to estimate losses on a regional scale. With this tool, loss estimates can be generated which provide a basis for the planning of emergency response and recovery and for stimulating efforts to mitigate risks from earthquakes. With input from a panel of potential users (POC), the PWG established a set of criteria to best accomplish the project goal.

CHALLENGES OF CHARACTERIZING SEISMIC HAZARDS IN THE BASIN AND RANGE PROVINCE

ALLEN, Clarence R., Seismological Laboratory, California Institute of Technology, Pasadena, CA 91125 (allen@gps.caltech.edu)

Active extensional faulting such as that which characterizes the Basin and Range Province is by no means unique, but the very large area of the province and the remarkable symmetry of the fault patterns are virtually unduplicated worldwide. The Basin and Range Province presents a number of intriguing challenges-as well as opportunities-in characterizing and assessing seismic hazards: How is the province tectonically and seismically similar to and different from other worldwide areas of normal faulting? What is its plate-tectonic setting? How can the sizes of maximum earthquakes be evaluated? How does one realistically assess hazards and risks for earthquakes with long recurrence intervals, such as those that characterize large parts of the province? To what degree have recent Basin and Range earthquakes been "surprises to geoscientists? Do normal faults have different ground-shaking characteristics from those of thrust and strike-slip faults that dominate in other parts of the U.S.? Do buried detachment faults constitute a real seismic hazard in the province? And what are the most promising research areas to pursue in gaining a better understanding the Basin and Range Province's seismic hazards?

SURFACE-FAULTING HAZARDS AND LAND-USE PLANNING, UTAH

CHRISTENSON, Gary E., Utah Geological Survey, P.O. Box 146100, Salt Lake City, UT 84114-6100 (nrugs.gchriste@state.ut.us); Brian A. Bryant, Salt Lake County, 2001 S. State St., # N3700, Salt Lake City, UT 84190-4200 (BBRYANT@PW.co.slc.ut.us)

In the Wasatch Front of Utah, as elsewhere in the Basin and Range Province, active faults trend through major urban areas. The amount of surface displacement that is expected in a Basin and Range surface-faulting earthquake is sufficient to cause severe damage to structures and threaten life safety. Although little damage has occurred historically from surface faulting, the hazard is significant and its impact may be minimized with appropriate land-use regulation.

The probability of surface faulting, which indicates the severity of the hazard, depends on the activity of the fault. In Utah, most local governments define "active" faults for purposes of urban land-use planning as those with evidence for rupture in Holocene time. Requirements for detailed studies may vary according to the type of land use and proposed facility, and the level of risk acceptable to the regulatory authority.

Assessing the surface-fault-rupture hazard of a fault requires information on its recurrence interval, time of most recent event, and/or slip rate. The Quaternary fault map of Utah classifies faults according to the time of the most recent event, with the youngest fault class being younger than the initial rise of Lake Bonneville about 30,000 years ago. A derivative

surface-fault-rupture-hazard map has been developed for Utah in which faults in this youngest class have been further subdivided into those with evidence for multiple Holocene events and average recurrence intervals of several thousand years (high hazard), multiple post-30,000-year-old events and average recurrence intervals on the order of 10,000 years (moderate to high hazard), and single Holocene or post-30,000-year-old events and average recurrence intervals of tens of thousands of years (moderate hazard). Older, pre-Bonneville faults have a moderate to low surface-faulting hazard. These classes give an indication of fault activity and potential for surface fault rupture to help determine which faults are important for a particular need.

The principal technique used to reduce surface-faulting hazards is to set structures back from faults. Because surface fault ruptures occur repeatedly on the same traces, studies to address surface-faulting hazards focus on mapping these traces. In addition, these studies must evaluate whether a fault meets criteria to be considered “active” as defined in the applicable regulations and, where possible, estimate the displacement per event.

For land-use regulation along faults in the Wasatch Front, special-study zones extending 500 feet on the downthrown side and 250 feet (or more, depending on scarp height) on the upthrown side delineate the area where more detailed studies are required prior to development. Detailed studies usually include surficial geologic mapping and subsurface investigations including trenches, boreholes, and/or geophysical surveys. At sites with limited options for structure locations, trenches are typically oriented perpendicular to fault trends, covering and extending beyond the proposed building footprint, to determine if faults are present. At sites where structures may be placed to avoid faults, such as residential subdivisions, trenches are located to identify faults, map them across the property, define the widths of zones of deformation, and determine setbacks. Final setback distances are based on site-specific conditions. In areas where deep fill, thick late Holocene (post-most-recent-event) deposits, shallow ground water, or heavy urbanization make trenching inconclusive or impractical, boreholes and geophysical techniques may be needed to locate faults.

EMERGENCY MANAGEMENT NEEDS IN THE BASIN AND RANGE PROVINCE

WEISER, Stephen, Military Division, Bureau of Disaster Services, 4040 Guard St., Boise, ID 83705- 5004 (sweiser@bds.state.id.us)

In the earthquake arena, emergency managers and geoscientists have a mutually supportive relationship. When selling preparedness and mitigation to a “show-me” public, we emergency managers need “scientific evidence” for our claims of death and destruction.

REDDEN, Robert, New Mexico Department of Public Safety, Office of Emergency Planning and Coordination, P.O. Box 1628, Santa Fe, NM 87504-1628

The seismic hazard within the Basin and Range Province is particularly challenging to state Emergency Managers due to the incertitude of the seismic risk in many parts of the Province. The threat of a damaging earthquake in the eyes of many public officials, and private citizens, seems remote because of long recurrence intervals, little or no historical experience, and in many cases because of the lack of scientific data on seismic resources. The needs of the emergency management and scientific communities should compliment each other. Geological, seismological, geophysical, and geotechnical studies as well as close cooperation between the emergency-management and technical communities are fundamental to these ends. Only when emergency managers have the necessary technical data will they be able to address the seismic hazards within their states and be able to develop awareness and mitigation programs that accurately portray seismic risk. Specific products that are useful to the emergency manager as well as local planners, engineers, building officials, government agencies, and others include identification and characterization of seismic-source zones; deterministic and probabilistic ground-shaking maps; ground-failure susceptibility studies, i.e. subsidence, landslide, and liquefaction; paleoseismic studies of young faults to determine numbers and relative timing of young fault events; and analysis of background seismicity not associated with young faults, are but a few examples. Equally important to the emergency manager is the need for standardized criteria for defining the hazard/risk that is appropriate for a specific area of interest.

130,000 YEAR VS. 10,000 YEAR (HOLOCENE) CLASSIFICATION OF “ACTIVE” FAULTS IN THE BASIN AND RANGE PROVINCE

dePOLO, Craig M., Nevada Bureau of Mines and Geology, University of Nevada, Reno, NV 89557 (cdepolo@nbmg.unr.edu); D. Burton Slemmons, Professor Emeritus, Center for Neotectonic Studies, University of Nevada, Reno (retired at P.O. Box 81050, Las Vegas, NV 89180)

In the Basin and Range Province (BRP), a Holocene criterion is commonly used to discriminate “active” faults. This “time since the last event” criterion is commonly used to discern hazardous faults for considering setback distances and moderate risks (similar to usage in California). Observations from the BRP, however, suggest a longer time period for this criterion may be more appropriate, especially since most (but certainly not all) average earthquake recurrence intervals appear to exceed 10,000 years. We advocate that a latest Pleistocene age criterion, specifically 130,000 years, be used for a general active-fault classification in the province. A 130,000-year activity criterion is appropriate for the BRP because: 1) it better encompasses typical recurrence intervals for faults in the BRP, 2) it helps account for temporal clustering of the earthquake activity along a fault by capturing most intercluster periods, 3) it is practical to use because it is linked with the

beginning of a climatic episode, Oxygen Isotope Stage 5, a strong interglacial period when distinct soils were formed (Sangamonian-age soils), and 4) 64 percent of the historical earthquakes in the Basin and Range Province with primary surface faulting occurred along faults that lack Holocene faulting. Another practical aspect of using a 130,000-year activity criterion is that it would allow most hazardous faults to have at least a few events and create discernible geomorphic expression, aiding in their identification and delineation. In Nevada this latest Quaternary fault classification would include most significant faults that define the contemporary seismotectonic pattern.

A PRACTICAL APPROACH TO IMPLEMENTING FAULT CRITERIA IN COMMUNITY PLANNING

LYNN, Ron L., Assistant Director, Clark County Building Department, 5051 Paradise Rd., Las Vegas, NV 89119

Myopic points of view from academia, engineers, building officials, and politicians often result in the lack of established setback criteria for identified faults. This continued phenomena severely hinders effective earthquake planning and increases the potential for repercussions to life and property.

Active development of stake-holder coalitions made up of diverse elements of a community, combined with realistic economic approaches, often result in a meaningful consensus and workable standards being implemented.

The process involves diverse input, advance awareness of intent to constituent groups, realistic and accurate assessment of hazards, and the dedication to a workable end result with established procedures for effective enforcement.

CONTRASTS BETWEEN SHORT- AND LONG-TERM RECORDS OF SEISMICITY IN THE RIO GRANDE RIFT - IMPORTANT IMPLICATIONS FOR SEISMIC-HAZARDS ANALYSIS

MACHETTE, Michael N., Geologic Hazards Team-Central Region, U.S. Geological Survey, MS 966, Box 25046, Federal City., Denver, CO 80225-0046 (machette@gldvxa.cr.usgs.gov)

In extensional domains of the Western U.S., fault slip rates are typically $<1\text{--}2$ mm/year and recurrence intervals for surface-rupturing faults are as short as several 10^3 yr. (Wasatch fault zone) or as long as 10^4 yr. (the typical Basin and Range fault) to 10^5 yr. (some faults in the Rio Grande rift). Obviously, the 150- to 300-year-long record of historical seismicity can only portray a small fraction of the potentially active faults in these regions.

In the Rio Grande rift, the record of historical seismicity is relatively short and unimpressive: instrumental data exist from the mid-1960s but felt reports go back to the 16th century in specific locations (i.e., Santa Fe). Although the paleoseismic record reveals evidence of abundant late Pleistocene (10-130 kyr) and Holocene (<10 kyr) faulting, we have no evidence of historic surface ruptures. Thus, a striking paradox exists between the short-term and long-term records of seismicity that has important implications for seismic-hazards analyses based primarily on modern seismicity.

Quaternary faults are widespread in the Rio Grande rift, but young activity is restricted primarily to major range-bounding faults, such as those along the Sangre de Cristo, Jemez, Socorro, Magdalena, Caballo, San Andres, Organ, and Franklin Mountains. The paleoseismic record of faulting in the rift is poor, mainly because there have been few detailed studies and partly because many of the faults have long recurrence intervals (e.g., $10^4\text{--}10^5$ years), which makes dating them difficult by radiocarbon methods alone. Based on preliminary studies of fault age and distribution, I previously suggested a composite recurrence interval (CRI) of about 750 ± 250 years for a major surface-rupturing earthquake in the New Mexico part of the Rio Grande rift. Our new compilation of data for the rift suggests Holocene movement on 19 faults. Several of these faults (Sangre de Cristo, La Jencia, Organ Mountains) have evidence for multiple movements in the Holocene; thus, one should consider that at least 22 large earthquakes of probable $M > 6.25$ were associated with surface ruptures during the Holocene. These data suggest a CRI of 450 years, which is approaching the length of time that the Rio Grande Valley has been occupied by non-native Americans. Because historical surface faulting is absent and the level of seismicity of the Rio Grande rift is generally low, the populace believes that earthquakes do not pose a significant threat to them. Conversely, the paleoseismic record clearly demonstrates that potentially large and devastating earthquakes may occur as frequently as every 450 years somewhere in the region. From a geologic viewpoint, it seems obvious that modern seismic-hazards assessments for regions like the Rio Grande rift must use not only catalogs of modern seismicity, but also integrate data from a comprehensive inventory of Quaternary faults, especially those structures showing evidence of movement in the past 100,000 years. By doing so, the geologic data will portray the true potential for surface-rupturing earthquakes on a time frame equivalent to the average earthquake cycle ($10^4\text{--}10^5$ year recurrence intervals). Once accomplished, the probability of occurrence of large earthquakes on individual structures may prove to be extremely low, but the position of these strong-ground-motion generating structures will be known in relation to urban areas and critical facilities. In addition, the hazard posed by numerous low-slip-rate faults within a given radius (i.e. 50-100 km) of a town, city, or critical facility results in a composite recurrence interval (CRI) that can be just a fraction (i.e., 1/10th) of each individual fault. A myopic view of earthquake hazards posed by individual structures (i.e., recurrence intervals of 10^4 years or more) can lead to a complacent attitude that strengthens a perception of low seismic potential. This attitude can be manifested in construction styles, building codes, land-use policies, and the siting (or relocation) of important or critical facilities.

EARTHQUAKE RECURRENCE MODELS

SCHWARTZ, David P., United States Geological Survey, 345 Middlefield Rd., MS 977, Menlo Park, CA 94025 (dschwartz@usgs.gov)

Paleoearthquake dates, fault slip rates, and historical seismicity define a spectrum of recurrence behavior that ranges from relatively uniform to highly variable. High slip rate (5mm/yr or more) master segments of major plate-boundary faults, where repeat times of large displacement events are measured in hundreds of years, tend to exhibit quasi-periodic behavior (a coefficient of variation of about 0.25 to 0.45). These are exemplified by segments of faults such as the San Andreas with radiocarbon dated intervals between successive earthquakes that are similar to average recurrence calculated from independently derived slip per event observations and late Holocene slip rates. Such quasi-periodic recurrence, which is a conceptual underpinning of many seismic-hazard analyses, does not appear to be common.

Faults in intraplate and stable continental regions typically have low slip rates (1mm/yr or less) and repeat times measured in thousands (or even tens of thousands) of years. Recurrence intervals for these are frequently highly variable or clustered. Earthquake clustering occurs in all settings and takes a variety of forms including: (1) the complete rupture of long, multi-segmented fault zones in a few decades (North Anatolia fault, 1939-1968) or several hundred years (Wasatch fault, between about 300-1,200 yr B.P.), (2) long periods of quiescence (many tens of thousands of years) followed by an active cycle with interevent times of a few thousand years (Lost River fault, Meers fault), (3) closely timed repeated slip on low displacement segments of large ruptures (northern Imperial fault in 1940 and 1979), and (4) closely timed events on a set of regional faults (Nevada seismic zone 1915-1954; western Mongolia-northern China M8s in 1905, 1931, 1957). While some regional clusters appear to repeat (1992 Landers rupture segments and associated faults in the western Mojave at about 6-9 kyr and again between about 1.5 kyr-present), fault segments of the Nevada sequence exhibit large differences in the ages of paleoearthquakes.

Paleoseismicity data, in the form of timing and size of past earthquakes, provide earth scientists with a window into the driving mechanism of the earthquake engine - the cycle of stress build-up and release. For intraplate environments in general, and the Basin and Range in particular, they challenge us to understand the driving process and model the hazard associated with complex and variable earthquake recurrence.

EARTHQUAKE GROUND MOTIONS IN EXTENSIONAL TECTONIC REGIMES

SPUDICH, P., J.B. Fletcher, M. Hellweg, J. Boatwright, W.B. Joyner, T.C. Hanks, D.M. Boore, A. McGarr, L.M. Baker, and A.G. Lindh: U.S. Geological Survey, MS 977, 345 Middlefield Road, Menlo Park, CA 94025 (spudich@samoa.wr.usgs.gov)

We compare several existing empirical relations that predict earthquake response spectra, peak acceleration, and peak velocity, given magnitude, distance, and site conditions, with a set of observed strong-motion seismograms recorded in extensional regions around the world. In addition, we present a new predictive relation, SEA96 for horizontal peak ground acceleration and 5 percent damped pseudo-velocity response spectrum derived from this data set. For all relations considered, we calculate the residuals between predicted and observed motions, and from these residuals we develop various correction factors that can be used to make each relation consistent with our observed data set. Our data set consists of seismograms from earthquakes having moment magnitude between 5.0 and 7.0 recorded at distances less than 105 kilometers. Extensional regimes are characterized by both normal faulting and strike-slip faulting events, both of which we used. We rejected records from structures of more than two stories height, from deeply embedded basements, or records that triggered during the S wave. For each earthquake we retained records recorded at distances greater than the "cutoff distance," the distance beyond the first untriggered accelerograph. Recording sites were classified into several geologic categories including hard and soft rock, and shallow and deep soil. We use the source-receiver distance metric of Joyner and Boore (1981, 1988), the shortest distance from the receiver to the surface projection of the boundary of the fault rupture area. In developing our new relation, we adopt the magnitude dependent coefficients determined from a larger data set by Boore and others (1993, 1994) and we use our extensional regime data set to constrain the distance and site dependent coefficients. Our new relation does not depend on earthquake mechanism. However, there is some evidence that normal-faulting earthquakes may have motions slightly lower than strike-slip events. Also, in general ground motions in extensional regimes are slightly lower than those for equivalent moment events in other tectonic regimes.

YUCCA MOUNTAIN GROUND-MOTION PANEL

ABRAHAMSON, Norman, Pacific Gas & Electric, GeoScience Dept., P.O. Box 770000, Mail Code N4C, San Francisco, CA 94177
(nabraham@holonet.net)

The ground-motion attenuation at Yucca Mountain is being characterized by seven ground-motion experts using the SSHAC methodology. The experts are John Anderson (UNR), Dave Boore (USGS), Ken Campbell (EQE), Art McGarr (USGS), Walt Silva (Pacific Engineering), Paul Somerville (Woodward-Clyde), and Marianne Walck (Sandia).

The experts are evaluating the ground-motion predictions from various proponent models. These proponent models include eight empirical attenuation relations, four numerical simulation procedures, and one underground nuclear explosion model. Since the empirical models are primarily based on California data, scaling relations are also provided to account for differences in the source, path, and site effects between Yucca Mountain and California.

Key differences between ground motions at Yucca Mountain and California are due to lower kappa values (less damping in the shallow rock) at Yucca Mountain and lower stress drops for earthquakes in extensional regimes. Since these ground motion models are site-specific for Yucca Mountain, they may not be directly applicable to other rock sites in the Basin and Range.

Attenuation relations are being developed for the average horizontal component and the vertical component for peak acceleration, peak velocity, and 5 percent damped spectral acceleration at seven spectral periods: 0.05, 0.1, 0.2, 0.5, 1.0, 2.0, and 3.0 seconds. The reference site condition is a hard rock site ($V_s=1900$ m/s) which corresponds to "outcrop" motion from the repository level (300 m below the surface). Attenuation relations are being developed for vertical strike-slip faults and 60-degree-dipping normal faults. These ground-motion models will be finalized by the end of May, 1997.

ANALYSIS OF THE STRONG-MOTION DATA ASSOCIATED WITH THE 1995 DINAR (TURKEY) EARTHQUAKE

ERDIK, Mustafa, and E. Durukal, Dept. of Earthquake Engineering, Bogazici University, 81220 Cengelkoy, Kandilli Observation/EQ Resource Inst., Istanbul, Turkey 81220 (erdik@hamlin.cc.boun.edu.tr)

An earthquake of magnitude M_w 6.0 (GS) occurred on October 1, 1995, causing casualties and physical damage in Dinar, Turkey. Strong-motion data associated with the main shock and aftershocks of the 1995 Dinar earthquake have been analyzed to investigate the source, attenuation, and site-response parameters.

Dinar is located in the "Region of Lakes" of the Western Anatolia's extensional province. This region is dissected by a multitude of NE-SW trending faults of predominantly normal-slip motions. Dinar town is located at the foot of a hill with variable geological and geotechnical conditions varying from limestones on the hill to soft alluvium on the plain. The earthquake is associated with a NW-SE trending fault and the focus was directly underneath the town. Rupture mechanism determinations, based on p-wave inversions, indicate two 8s separated ruptures with 2.5s rise time for each rupture. The fault-mechanism solutions indicate predominantly normal faulting with a strike of 130° , dip of 41° , and slip of -76° . The total seismic moment is reported as 1.3×10^{25} N.m (GS). Field evidence obtained from a 135° trending fresh fault scarp indicates oblique normal faulting (western block down) with about 30 centimeters vertical and 5 centimeters right-lateral maximum offsets. The earthquake was recorded by a strong-motion station in Dinar and by three other distant stations. Peak horizontal ground acceleration at Dinar is 0.33g. Immediately after the earthquake a five-station strong motion array was formed within the city and several aftershocks with magnitudes about M_b 4 have been recorded.

The strong-motion data were base-line corrected to yield the ground velocity and displacements. We were able to recover some permanent vertical displacements using a hybrid base-line processing scheme. The dual rupture fault mechanism manifests itself as two partially merged shocks in the Dinar strong-motion record. The local magnitudes of the main earthquake and the aftershocks are computed on the basis of synthetic Wood-Anderson seismometer response. The main earthquake has an overall local magnitude of M_L 5.9.

S-wave spectra of the horizontal ground acceleration were fitted with the omega-square source model for the assessment of the anelastic attenuation parameter (kappa), seismic moment (M_0), and the corner frequency (f_c). The anelastic attenuation parameter was computed by estimating the decay in the semi-log plot of the Fourier Amplitude Spectrum of ground acceleration versus frequency, within a specified high frequency band. Average kappa value associated with the main shock was found to be 7.7×10^{-2} s. For the aftershocks, it exhibits a site-specific variance between 6.1 and 9.1×10^{-2} s. We have not observed a systematic site-specific variation of kappa values with the amplitude of ground motion.

Velocity and displacement spectra, calculated from the attenuation-corrected acceleration spectrum, was used for the estimation of the corner frequency (f_c) following the Andrews (1986) procedure. The corner frequency estimated for the main shock varies between 0.8 and 1.3 Hz. Aftershocks are associated with higher corner frequencies. With known values of kappa and f_c , a single-parameter least-square inversion scheme was utilized to yield the seismic moments (M_0). The overall seismic moment estimated from the accelerogram of the main shock recorded at Dinar has an average value of 2×10^{25} N.m.

Data obtained from the field investigations, source inversions and spectral studies of the Dinar earthquake regarding its source processes were used to model the low-frequency ground motion in a deterministic manner. The discrete wave-num-

ber technique was used to propagate waves due to the rupture of an extended seismic source through a 3-D, viscoelastic, layered half-space. Time histories of seismic ground motion are calculated inclusive of permanent ground deformation. The source is described deterministically by Haskell's model and by the Barrier model. Different rupture pattern scenarios were modeled to simulate the strong-motion recordings in the low frequency range (typically <1 Hz).

For the assessment of site-response transfer functions between different sites, Nakamura's procedure (i.e. the site-specific ratio of horizontal to vertical spectrum) was utilized. We have found out that the spectral response ratio between soft- and stiff-soil sites, located in the downthrown block, is in the order of 2-3 within the frequency range 0.5 and 3 Hz. The spatial extent of the strong-motion data does not allow for any quantitative assessment of the ground motion differences between the downthrown and the footwall blocks arising from radiation pattern. However, the structural damage statistics clearly indicate much larger motions on the downthrown block.

RUPTURE-DIRECTIVITY EFFECTS AND STRONG FAULT-NORMAL PULSES NEAR NORMAL FAULTS

SOMERVILLE, Paul, Woodward-Clyde Federal Services, 566 El Dorado St., Pasadena, CA 91101 (pgsomer0@wcc.com)

Forward rupture-directivity effects occur when two conditions are met: the rupture front propagates toward the site, and the direction of slip on the fault is aligned with the site. The propagation of rupture toward a site at a velocity that is almost as large as the shear-wave velocity causes most of the seismic energy from the rupture to arrive in a single large pulse of motion which occurs at the beginning of the record. This pulse of motion represents the cumulative effect of almost all of the seismic radiation from the fault. The radiation pattern of the shear dislocation on the fault causes this large pulse of motion to be oriented in the direction perpendicular to the fault. The resulting strike-normal ground motions are systematically larger than the strike-parallel motions at periods longer than 0.5 second. The conditions required for forward directivity are met in normal faulting when the rupture direction and the slip direction are both aligned up the fault plane. These conditions produce rupture-directivity effects at sites located around the surface exposure of the fault. There are few strong-motion recordings close to large normal-faulting earthquakes, but those that exist show evidence of the rupture-directivity effect. Geometrically, rupture-directivity effects for normal faulting should be identical to those for reverse faulting (with the exception of a change in ground-motion polarity), so the empirical rupture-directivity model for dip-slip faulting derived by Somerville and others. (1997) should be applicable to normal-faulting earthquakes. However, if differences in the fault dynamics between normal and reverse faulting exist, this may cause differences in the ground-motion characteristics between these two kinds of faults.

To account for large ground-motion levels caused by rupture-directivity effects, the 1997 revision of the UBC includes a near-fault factor N which applies to sites located within 15 kilometers of major active faults in seismic zone 4. The near-source factor depends on the slip rate of the fault and the maximum magnitude of the earthquake that the fault can generate. If the slip rate of the fault is less than 2 mm/yr., which is the case for most faults in the Basin and Range, then the near-source factor does not apply. Also, with the exception of western Nevada and the Yellowstone region, the Basin and Range lies in seismic zones lower than 4 and the near-source factor does not apply. The intent of the code revision was to address near-fault ground motions only near the most active faults. However, this avoided the issue of how to address near-fault ground motions close to less active faults and close to smaller faults, which is particularly relevant in the Basin and Range. The 1997 NEHRP probabilistic ground-motion maps and design include the effects of proximity to faults, and thus address the issue of near-fault ground motions in the Basin and Range in a more specific way. However, they do not account for the increased level of long-period ground motions close to faults caused by rupture-directivity effects. To date, none of the code approaches addresses the issue of larger ground motions in the strike-normal than in the strike-parallel direction. However, for sites located close to major normal faults in the Basin and Range whose strike directions are known, this difference can be quantified in a straightforward way using the empirical model of Somerville and other. (1997).

STRONG GROUND MOTION EXPECTED FROM LARGE NORMAL-FAULT EARTHQUAKES BASED ON EVIDENCE FROM PRECARIOUS ROCKS AND SOURCE MODELING

BRUNE, James N., and Abdolrasool Anooshehpour, Seismological Laboratory, Mackay School of Mines, University of NV, MS 174, Reno, NV 89557 (brune@seismo.unr.edu)

There are essentially no instrumental strong-motion data from rock sites very near large normal faults. Standard dislocation modeling does not provide a clear basis for predicting differences in expected ground motion for strike-slip, thrust, and normal faulting, since the source-time function is specified, not determined from the source physics. There are obviously great geometrical differences in dynamic wave propagation near the rupture outcrop for strike-slip, thrust, and normal faulting, but these differences have not generally been taken into account.

We have constructed a foam rubber model of normal-fault dynamics. The strong motion near the fault outcrop is much less than that observed for strike-slip motions in the model. We interpret the difference to be due to two factors: (1) dynamic and geometrical effects of the normal-fault rupture intersecting the surface at an angle of 60 degrees, and the strike-slip rupture intersecting the surface at an angle of 90 degrees, and (2) the low stresses (normal and shear) at the tip of the normal fault, as compared to stresses in the strike-slip model. These differences should apply to real-earth condi-

tions also, and thus from the modeling we might expect lower near-source ground accelerations for normal faults, as compared to strike-slip faults.

Although there are no near-source instrumental acceleration data from normal faults in the Basin and Range, there is field evidence from semi-precarious rocks near large normal-faulting earthquakes that suggests relatively low ground motions. Earthquakes for which we have such data are: (1) the 1915 Pleasant Valley earthquake, (2) a subfault of the 1954 Fairview peak earthquake, and (3) a 500-600 year old earthquake near Genoa, Nevada. All the data are for the hard-rock footwall of the faults. The data indicate that at these sites, the hard-rock ground motions on the footwall of these earthquakes did not exceed about 0.25 g. This acceleration level is considerably less than indicated in some dislocation models, and also less than regression results based primarily on strike-slip earthquakes.

ATTENUATION AND SITE EFFECTS IN NORTHERN AND SOUTHERN NEVADA FROM THREE-COMPONENT DIGITAL SEISMOGRAMS

SMITH, Kenneth D., and Glenn P. Biasi, *Seismological Laboratory, Mackay School of Mines, University of Nevada-Reno, Reno, NV 89557 (ken@seismo.unr.edu)*

Since mid-1995, the University of Nevada Reno Seismological Laboratory has been operating a high-dynamic range, three-component digital seismic network in Nevada. Twenty-four instruments are in the region around the potential high-level nuclear waste storage site at Yucca Mountain and four are in northern Nevada in the Reno-Carson City area. The aperture of the array in southern Nevada is about 50 kilometers and this net is configured to record local earthquake activity for seismic-hazard analysis for the Yucca Mountain Project. The data set for the southern Nevada array is more extensive than for the northern array, with most of the earthquake sources in the aftershock zone of the 1992 Little Skull Mountain earthquake. The network in northern Nevada has only been in operation for several months, but activity north of Reno provides an initial data set to generate some preliminary results for limited path coverage.

Robust estimates of body-wave $Q(f)$ and site effects can be developed because of the sensitivity of the network and station siting at low-noise locations. The magnitude detection threshold for the network in southern Nevada is as low as $M = -1.0$ in some locations and is generally about $M = 1.0$ for the entire 50-kilometer area. Because of this, we are able to select several thousand records that represent earthquakes that are large enough to trigger most stations in a regional array and also small enough that their corner frequencies are higher than the frequencies of interest in this study. This allows us to assume that the displacement spectra is flat at all frequencies, stabilizes the Q determination for weak motion, and reduces the source-dependent term to just the seismic moment. Site effects resulting from local structure, topographic relief, and sediment thickness are obvious in the time series records at many sites. Also, strong attenuation is observed along ray paths through Mt. Rose in the Reno area that is most likely associated with geothermal activity; these regions may be more accurately defined with further study. There has been some controversy with regard to the attenuation estimates in the southern Great Basin. The Rogers and others, (1987) study indicated a low attenuation in the southern Great Basin relative to California, but recent studies have contradicted these results. Preliminary results for this analysis indicate a $Q(f)$ similar to that in California.

NUMERICAL PREDICTION OF SEISMIC-WAVE AMPLIFICATION IN THE SALT LAKE BASIN, UTAH

Ji, Xu, Kim B. Olsen, Jinlong Xu, Gerard T. Schuster, and James C. Pechmann, *Department of Geology and Geophysics, University of Utah, Salt Lake City, UT 84112 (jxu@mines.utah.edu)*

We have carried out a research program to investigate the major causes of ground-motion amplification in the Salt Lake Valley, Utah. This work involved (1) finite difference simulations of 2-D, and 3-D elastic and viscoelastic wave propagation through models of the sedimentary basin underlying the valley, and (2) comparisons between synthetic seismograms from these simulations and recordings of a teleseism and open-pit mining blasts obtained with a temporary seismograph network.

In approximate order of importance, this study shows that the primary mechanisms influencing 0.2-1.2 Hz ground motion in the Salt Lake Valley are the following:

- (1) Multiple reflections and resonances in the basin, especially in the shallow, low-velocity, unconsolidated sediments, which trap energy near the surface to produce large-amplitude, long-duration shaking,
- (2) Anelastic attenuation in the sediments, which plays a dominant role in reducing the strength and duration of the later arrivals, including surface waves,
- (3) P-to-S wave conversions at strong velocity/density contrasts, which can contribute significantly to the strength and duration of the shaking,
- (4) Surface-wave generation at the edges of the basin,
- (5) Impedance effects, which in our models can approximately double body-wave amplitudes during propagation from bedrock into unconsolidated sediments,
- (6) Topographic scattering from the mountains bordering the basin, which increases shaking durations in the valley as well as in the mountains, and

(7) Seismic focusing by the curved walls of the basin.

Synthetic seismograms for the teleseism and the blasts do not match the observed seismograms on a wiggle-for-wiggle basis. However, there is fair agreement between simulated and observed measures of ground-motion amplification in the basin relative to the surrounding rock, such as ratios of spectral magnitudes, peak velocities, and cumulative kinetic energies. These results suggest the possibility that computer modeling can predict earthquake ground motions in the Salt Lake Valley. However, a more accurate knowledge of the subsurface velocity/density/attenuation structure of the basin, especially at shallow depths, is needed for more accurate prediction of these ground motions.

SITE EFFECTS ON STRONG MOTION IN LAS VEGAS

SU, Feng, and John G. Anderson, Seismological Laboratory, Mackay School of Mines, University of Nevada, Reno, NV, 89557, (feng@seismo.unr.edu)

The June 29, 1992 Little Skull Mountain earthquake (ML=5.6) was recorded at 9 strong-motion stations in Las Vegas. The epicenter is located more than a hundred kilometers away. Several of the strong-motion seismograms recorded in the Las Vegas Valley show a remarkable long duration of shaking. To study the site effect and basin response on ground motion in Las Vegas Valley, we used a new method we developed recently to calculate S-wave site amplification relative to a regional layered crust model. In this method, the site-response function is defined as a ratio of ground response of empirical Green's function to synthetic Green's function. To apply this method, we first computed the synthetic Green's function in a layered elastic model using an improved reflectivity method of Luco and Apsel (1983) with a Brune's rise-time function (1970, 1971) at all the recording sites. Then we took the ratio of the observed acceleration data to the synthetics we calculated at the same site, with proper adjustment of the earthquake size and corner frequency. The logarithm of the ratio is defined as the site amplification function at that site. Our result shows more than a factor of 10 difference in site amplification for some sediment stations compared to a rock station at frequencies below 2 Hz. These site amplifications are much greater than those previously observed by Murphy and Hewlett (1975) because there is a strong site effect at the station they used for a reference. The strong site amplifications in Las Vegas Valley thus appear to have a great impact to the earthquake-hazard prospect in this area, especially to those buildings of five stories or higher. Large earthquakes at moderate distances, which would excite strong long-period waves are a particular concern. For example, the Death Valley fault system, which is the largest and potentially most active seismic source in the Basin and Range, is just 150 kilometers west of Las Vegas. To display the possible consequences of a large earthquake on the Death Valley fault system, we used the composite source model to generate a scenario ground motion from an assumed earthquake, including site amplification.

CHARACTERIZING BASIN EFFECTS

BAO, Hesheng, Jacobo Bielak, Omar Ghattas, Loukas Kallivokast, and Jifeng Xu, Computational Mechanics Laboratory, Department of Civil and Environmental Engineering, Carnegie Mellon University, Pittsburgh PA 15213

The importance of site effects on seismic ground motion has been dramatically underscored by several recent large earthquakes, such as the 1985 Michoacan, Mexico; the 1987 Valparaiso, Chile; the 1989 Loma Prieta, California, and the 1994 Northridge, California, earthquakes. In all four instances it was observed that surface ground motion at various locations within sedimentary valleys exceeded by factors of five or greater the corresponding motion on rock. In addition, these earthquakes also illustrate that surface ground motion can vary rapidly over short distances, as observed at sites in Santa Cruz and the San Fernando Valley, where different levels of shaking were detected by seismometers located as close as 50 meters from each other.

In order to gain a better understanding of basin effects on ground motion we have conducted parametric studies by computer simulation of the response to earthquake excitation of several basin models, ranging in size from a small 500 meter valley in Kirovakan, Armenia to the entire San Fernando Valley in Southern California. One reason for considering the small valley is that available summaries of the building-damage statistics during the 1988 Armenia earthquake make it possible to compare the simulated behavior of the structures against their actual performance. In addition to evaluating the ground motion and structural response, attention is given to examining whether there is a correlation between the spatial distribution of ground motion and the modal properties of the valley, separate from the particular characteristics of the seismic excitation. Using the small Kirovakan valley as background, we then examine the synthetic ground motion of the San Fernando Valley to the main shock and several aftershocks of the 1994 Northridge earthquake. Results of the simulations indicate that (1) the duration of the surface ground motion is longest atop the deeper parts of the valley, (2) constructive interference of surface and trapped body waves in the shallower regions of the valley is responsible for the strong-motion amplification observed on the surface overlying these two regions, (3) strong response is also concentrated near interfaces where surficial material properties change abruptly, and (4) rapid spatial variation of ground motion may be associated with higher modal contributions of the valley response. Overall, these results indicate that simulations, combined with available observations from actual earthquakes, can significantly facilitate the task of seismic zonation in basins.

EARTHQUAKE DATABASE ISSUES FOR SEISMIC-HAZARD ANALYSIS IN THE UTAH REGION

ARABASZ, Walter J., and James C. Pechmann, Department of Geology and Geophysics, University of Utah, Salt Lake City, UT 84112 (arabasz@uuss.seis.utah.edu)

Earthquake catalogs are critically important in seismic-hazard analysis, especially in cases where historical seismicity "drives the hazard" e.g., for relatively short exposure periods or for areas far removed from known active faults. Most earthquake catalogs, however, are fundamentally heterogeneous because of evolutionary changes in seismographic monitoring and data analysis. Thus, it is necessary to recognize and account for inhomogeneities in the earthquake database, lest systematic errors propagate through the seismic-hazard analysis. Key issues include uniformity of earthquake size estimates, the relationship of these size estimates to moment magnitude (which is important for ground-motion modeling), the effective discrimination of main and secondary events for recurrence modeling, and the space-time completeness of the catalog. The accuracy of the results of national, regional, and local seismic-hazard analyses demands careful attention to these data-base issues.

We examine the earthquake for what we term the "Utah region" (lat. 36.75° - 42.5° N, long. 108.75° - 114.25° W), with primary focus on the University of Utah's instrumental earthquake catalog from July 1962 through 1996. In order to address the issues outlined above, we compare the results of different approaches to "declustering" or differentiating the catalog into independent main shocks and secondary events (foreshocks, aftershocks, swarm earthquakes). We use the interactive software package ZMAP (see Wiemer and Wyss, 1994, BSSA, 84, 900) to systematically identify space-time changes in network sensitivity and inadvertent changes in magnitude estimation. We also address the challenge of arriving at uniform moment magnitude. Finally, using a maximum-likelihood algorithm for modeling recurrence with a truncated exponential relationship, we tabulate representative recurrence parameters for spatial subsets of the Utah region as a guide for regional and local seismic-hazard analyses.

QUATERNARY FAULTS USED FOR THE 1996 NATIONAL SEISMIC-HAZARD MAPS

BARNHARD, Ted, Geologic Hazards Team - Central Region, U.S. Geological Survey, P.O. Box 25046, MS 966, Denver, CO 80225 (barnhard@gldvxa.cr.usgs.gov)

The 1996 National Seismic-Hazard Maps, produced by the U.S. Geological Survey, used Quaternary faults with slip rates, along with seismicity and background zones, to determine probabilistic seismic hazards for the United States. Four hundred and forty-eight faults with slip rates, from 28 publications or personal communications, were used in the hazards calculations. Almost all of these faults are in the western United States (west of the eastern edge of the Colorado Plateau). The surficial fault traces were digitized, dip directions and amounts were tabulated, fault lengths calculated, segmentation information incorporated if available, and the slip rates for each fault were used as input into the hazard calculations.

The 448 faults were divided into two types, A and B. A-type faults are faults with sufficient studies to produce models of fault segmentation. In California, the A-type faults are: San Andreas, San Jacinto, Elsinore, Hayward, Rodgers Creek, and Imperial. The only fault outside of California that we classified as A-type is the Wasatch fault in Utah.

For California, we followed the rupture scenarios specified by Petersen, Cramer, and Bryant of CDMG, with input from Lienkaemper of USGS for northern California. We assumed single-segment, characteristic rupture for the San Jacinto and Elsinore faults. For the San Andreas fault, multiple-segment ruptures were included in the hazard calculation, including repeats of the 1906 and 1857 rupture zones, and a scenario with the southern San Andreas fault rupturing from San Bernardino through the Coachella segment. Both single-segment and double-segment ruptures of the Hayward fault were included.

For California faults, we used characteristic magnitudes derived by CDMG from the fault area using the relations in Wells and Coppersmith (1994). For the remainder of the western U.S., we determined characteristic magnitude from the fault length using the relations of Wells and Coppersmith (1994) appropriate for that fault type.

For the B-type faults, we felt there were insufficient studies to warrant specific segmentation boundaries. For these faults, we used both characteristic and Gutenberg-Richter (G-R; exponential) models of earthquake occurrence. These recurrence models were weighted equally. The G-R model basically accounts for the possibility that a fault is segmented and may rupture only part of its length. We assume that the G-R distribution applies from a minimum moment magnitude of 6.5 up to a moment magnitude corresponding to rupture of the entire fault length. In the Pasadena workshop, we showed that without the $M = 6.5$ minimum, Southern California faults would produce far too many $M = 4-5$ events compared to the historic record. For this comparison we determined the predicted rates of $M = 4-5$ events using fault slip rates and the equation for a -values.

Fault widths (except for California) were determined by assuming a seismogenic depth of 15 kilometers and then using the dip, so that the width equaled 15 kilometers divided by the sine of the dip. For most normal faults we assumed a dip of 60°. Dip directions were taken from the literature. For the Wasatch, Lost River, Beaverhead, Lemhi, and Hebgen Lake faults, the dip angles were taken from the literature. Strike-slip faults were assigned a dip of 90°. Reverse faults ranged in dip from 15° to 45°. For California faults, widths were often defined using the depth of seismicity. Fault length was calculated from the total length of the digitized fault trace.

Wells, D.L., and K.J. Coppersmith (1994), *New empirical relationships among magnitude, rupture length, rupture width, and surface displacement*, *Bulletin of the Seismological Society of America*, v. 84, p. 974-1002.

IMPACT OF DISTRIBUTED FAULTING TO SEISMIC-HAZARD ASSESSMENTS IN THE BASIN AND RANGE PROVINCE - EXAMPLES FROM YUCCA MOUNTAIN, NEVADA

PEZZOPANE, Silvio K., and John W. Whitney U.S. Geological Survey, MS 425 Federal Center Box 25046, Denver, CO 80225
(spezzo@ympbnwis1.cr.usgs.gov)

Results of paleoseismic studies on late Quaternary faults within 15 kilometers of Yucca Mountain, Nevada, are used to model paleoearthquake magnitude and recurrence relations for ground-motion and fault-displacement hazard assessments at the nation's first potential nuclear waste repository in the southern Great Basin of the Basin and Range Province. Almost all Yucca Mountain Quaternary faults strike approximately north, dip moderately to steeply west, have mapped lengths less than 25 km, and are commonly spaced only a few kilometers apart. Paleoseismic studies there interpret cracking, fracturing (no measurable offset), and (or) displacement of late Quaternary deposits across faults as evidence of possible paleoearthquakes (referred to here as paleoevents), and that fracturing paleoevents are nearly as common as displacement events. These interpretations have led to inferences that the fracturing events interpreted from trenches are either the record of relatively frequent, small- to moderate-magnitude earthquakes ($M_w < 6$) that commonly do not produce measurable displacements at the surface, or they are a record of distributed fracturing and faulting produced by rarer, larger magnitude, surface-rupturing earthquakes on any one of several closely spaced nearby faults in the Yucca Mountain site area.

Paleoevent data from two to six exploratory trenches or natural exposures on each of the seven to eight principal normal faults in the Yucca Mountain site area are modeled in three different ways to provide two end-member models and a preferred recurrence model. End-member models consider that the paleoevents from fault to fault do not correlate in time. The preferred model correlates the paleoevents in time using stratigraphic and geochronological constraints from the trench studies to produce paleoearthquake rupture scenarios for Yucca Mountain faults. Using geological constraints to aggregate the probability density functions of paleoevent ages and their uncertainties indicates that most fracturing and small displacement paleoevents correlate with relatively larger displacement paleoevents. Comparing the impact of end-member models with the preferred model indicates that accounting for possible distributed faulting can lengthen interevent return times by as much as a factor of 4 and increase maximum magnitudes 0.1-0.3 moment magnitude units for cases where the distributed single-event displacements must be summed across two or more adjacent parallel faults. Surface-rupturing paleoearthquakes at the site likely produced distributed faulting on two to four nearby faults. Distributed faulting is probably common at sites having several closely spaced faults, and as a result, for relatively short time periods of engineering significance, ground motion and especially fault-displacement-hazard levels are lower because distributed faulting makes for larger magnitude events that occur less frequently. Over longer time periods, however, hazard levels are higher as a result of distributed faulting.

EARTHQUAKE-RISK ASSESSMENT FOR SEISMICALLY DORMANT NORMAL FAULTS: AN EXAMPLE FROM THE WASATCH FRONT, UTAH, USING GPS MEASUREMENTS, QUATERNARY FAULTS, AND SEISMICITY

SMITH, Robert B., W. L. Chang, and C. M. Meertens, Department of Geology and Geophysics, University of Utah, Salt Lake City, UT 84112, (rbsmith@mines.utah.edu)

Eighty percent of Utah's two million population lives along or near the 370-km-long, seismically dormant Wasatch fault that is considered the main contributor to its seismic risk. Because of its low historical seismicity, corresponding to displacements from cumulative moment release of 0.1 to 0.04 mm/yr., traditional methods of assessing seismic risk are most heavily weighed by the late Quaternary fault record with fault slip rates of up to ~2 mm/yr. We will discuss the concept of using the rate of deformation of the crustal deformational field across the entire Wasatch fault zone using precise GPS (Global Positioning System) measurements, from 1992 to 1995, with comparisons of older geodetic observations, <1940, that reveal consistent rates of E-W extension of ~2.7 mm/yr. These rates are much larger than that for the Late Quaternary fault slip rates and many times larger than that implied by historical seismicity. An implication for this unexpected high rate, if concentrated on the Wasatch fault modeled as a 60°, west-dipping, planar normal fault, is a very high ~5 mm/yr. fault slip rate. Assuming that this deformation is related to loading of the Wasatch fault, it increases the probabilistic estimate of the predicted PGA (peak ground accelerations) by 25 percent compared to using traditional data, historic earthquake, and Quaternary fault displacements. Another factor to consider is a recently completed PGA attenuation study for earthquakes in extensional regimes (Spudich and others, 1997) that predicts a reduction in ground accelerations for such areas as the Wasatch Front by 10 to 15 percent compared to attenuation models from strike-slip and compressional regimes. Alternate models for the observed high contemporary strain rate include loading of "hidden" faults beneath and surrounding the valleys of the Wasatch Front, as well as uniform extension of the entire Basin Range-Rocky Mountain transition. To accomplish time-dependent deformational monitoring of the Wasatch fault zone, the University of Utah in conjunction with the California Institute of Technology, the Smithsonian Institution, and Harvard University (funded by the USGS and NSF), is in the process of installing an array of up to 8 permanent GPS stations across the central Wasatch fault zone that will be monitored in real time. Data from these sites will be interpreted much like traditional earthquake data by time and spatial comparisons with historical seismicity, faults, etc. While we do not yet know the balance between aseismic loading versus fault-specific loading, this type of earthquake monitoring provides further information for assessments

of earthquake risk incorporating the full measurement of fault budget-the key to a complete earthquake-hazards assessment.

SHAPE OF THE MAGNITUDE-FREQUENCY DISTRIBUTION FOR INDIVIDUAL FAULTS

STIRLING, Mark W., and Steven G. Wesnousky, Center for Neotectonic Studies and Department of Geological Sciences, University of Nevada, Reno, NV, 89557 (stirling@seismo.unr.edu)

We examine whether the shape of the magnitude-frequency distribution for individual faults is described by the Gutenberg-Richter relationship ($\log(n)=a-bM$) or the characteristic earthquake model, by analyzing a global data set of faults. For faults within regional seismic networks, curves of the form $\log(n/yr.) = a-bM$ are fit to the instrumental record of seismicity, and geological data are used to estimate the size and recurrence rate of the largest earthquakes that would rupture the total fault length. Extrapolation of instrumentally derived curves to larger magnitudes agrees with the geological recurrence rates for only four of the 22 faults, and significantly underestimates the geological recurrence rates in the remaining cases. Also, if we predict the seismicity of the faults as a function of fault length and slip rate, and the predicted seismicity is distributed in accord with the Gutenberg-Richter relationship, we find the predicted recurrence rate to be greater than the observed recurrence rates of smaller earthquakes along most faults. If individual fault zones satisfy the Gutenberg-Richter relationship over the long term, our observations imply that, during the recurrence interval of the largest earthquakes, the recurrence of lesser sized events is strongly clustered in time. However, if the instrumental records provide an estimate of the long-term rate of small to moderate earthquakes along the faults, our observations imply that the faults generally exhibit a magnitude-frequency distribution consistent with the characteristic earthquake model. Also, we observe that the four faults that are consistent with the Gutenberg-Richter relationship are among those characterized by the least amount of cumulative slip. We therefore suggest that the ratio of the recurrence rate of small to large earthquakes along a fault zone may decrease as slip accumulates on a fault.

NEW SEISMIC-HAZARD MAPS FOR THE WESTERN U.S.

FRANKEL, A., C. Mueller, T. Barnhard, S. Harmsen, E. Leyendecker, D. Perkins, N. Dickman, and S. Hanson, U.S. Geological Survey, MS 966, Box 25046, Denver Federal Center, Denver, CO 80225 (afrankel@usgs.gov)

We have recently completed new probabilistic seismic-hazard maps for the contiguous United States. These maps will be the basis for seismic-design maps in the 1997 edition of the NEHRP Recommended Provisions for Seismic Regulations for New Buildings, which is a resource document for model building codes prepared by the Building Seismic Safety Council and published by FEMA. The new maps are the result of a 3-year process consisting of six regional workshops where the methodology was presented and revised based on feedback from participants. The California portion of the maps was produced jointly with the California Division of Mines and Geology. The maps were generally constructed using three components of hazard: 1) spatially smoothed historic seismicity, 2) background source zones to quantify hazard in areas with little historic seismicity, and 3) specific fault sources. Recurrence times for faults were determined from geologic slip rates and/or paleoseismic event chronologies. Hazard estimates for approximately 500 Quaternary faults in the western U.S. were used in the new maps. We used geodetic information to constrain the expected seismicity rates in shear zones in western Nevada and northeastern California. The maps display peak ground acceleration and spectral response at 0.2, 0.3, and 1.0 sec with 10 percent, 5 percent, and 2 percent probabilities of exceedance. We have also calculated hazard at 0.1, 0.5, and 2.0 sec and have produced uniform hazard spectra. The maps are based on hazard curves calculated at about 100,000 sites in the U.S. For several cities in the western U.S. we have deaggregated the hazard to assess the contribution as a function of magnitude and distance. We are estimating uncertainties in the hazard curves by using Monte Carlo simulations. We varied seismicity parameters, recurrence rates, and magnitudes to estimate uncertainties at selected sites. The maps and the gridded values used to make the maps are available for viewing and downloading from our Internet website (<http://geohazards.cr.usgs.gov/eq/>).

SEISMIC HAZARDS IN THE BASIN AND RANGE PROVINCE: PERSPECTIVES FROM PROBABILISTIC ANALYSES

WONG, Ivan, and Susan S. Olig, Woodward-Clyde Federal Services, 500 12th Street, Suite 200, Oakland, CA 94607 (IGWONGX0@wcc.com)

Much of the Basin and Range Province, particularly along its boundaries, is characterized by numerous major late Quaternary normal faults, which are capable of generating moment magnitude (M_w) 6 and greater earthquakes. Such events are, however, relatively infrequent on individual structures due to long recurrence intervals which range from a few thousand years for the most active faults to more than 100,000 years.

We have evaluated the seismic hazard at seven sites located throughout the Basin and Range Province and neighboring extensional tectonic regimes in the western U.S. These sites include Yucca Mountain, Nevada; eastern Snake River Plain, eastern Idaho; Salt Lake Valley, Utah; northern Rio Grande rift, central Colorado; central Rio Grande rift, northern New

Mexico; Paradox Basin, Utah in the Colorado Plateau; and Sierra Nevada foothills, eastern California. These analyses emphasize the importance of several aspects of seismic sources which can significantly influence the probabilistic hazard at a given site including: (1) fault segmentation, particularly the potential for multiple segment ruptures, (2) temporal clustering, which can result in inter-event times that vary by more than an order of magnitude and the question of whether the fault is presently within an intercluster or intracluster period, (3) the rate of recurrence of background seismicity and the issue of nonstationarity, and (4) the possibility of low dynamic stress drops in extensional regimes, which can lead to lower ground motions than in compressional regimes. Path and site factors in the Basin and Range Province are also critical to deterministic as well as probabilistic hazard because many urban areas are situated in alluvial basins bounded by major normal faults. These factors include elevated ground motions in the hanging wall of normal faults, possible basin amplification of long-period ground motions, and site amplification due to the presence of near-surface, low-velocity, unconsolidated sediments. The lack of strong-motion records in the Basin and Range Province has also limited our understanding of crustal attenuation and in particular, whether it differs from California.

Because of the range of interpretations and the associated uncertainties in addressing the above issues, probabilistic analysis is ideally suited for evaluating seismic hazards. Probabilistic seismic-hazard analysis also provides the best approach in assessing the seismic risk in regions where large but infrequent earthquakes can occur such as the Basin and Range Province. In this paper, we provide our perspectives on seismic hazards in the Basin and Range Province and the issues involved in evaluating such hazards based on the above case histories.

POSTER SESSION ABSTRACTS

(in alphabetical order by main author)

DETACHMENT FAULTS: SUPERSTARS OR BIT PLAYERS IN SEISMIC HAZARDS OF THE GREAT BASIN

ANDERSON, R. Ernest, and, Sharon F. Diehl, U. S. Geological Survey, MS 966, Federal Center, Denver, CO 80225-0046 (ander-son@gldvxa)

In highly extended parts of the Great Basin, low-angle normal faults (LANFs) or detachment faults are among the youngest structures known and, as such, are reasonable candidates for involvement in neotectonic deformation. Much uncertainty exists, however, as to their seismotectonic significance. To assess the likelihood that LANFs generate large (>M7.5) earthquakes, we evaluate the geometry, total displacement, tectonic setting, petrofabrics, and the stable-isotope properties of the damage zones of selected dormant examples including three major ones in the Nevada, Utah, Arizona tri-corner area, the Castle Cliff, Tule Springs, and Mormon Mountains faults.

In theory, LANFs are efficient structures on which to accomplish extensional deformation. For them to generate large earthquakes requires down-dip widths and strike-parallel lengths ranging to 50 to 70 kilometers. Detachment-fault geometry in some well-exposed, highly extended areas reveals a conspicuous lack of fault continuity, interconnectedness, or planarity over such dimensions. Geologic maps typically reveal strong differential uplift at widely varying scales and a resultant lumpy structural pattern. Only by postulating buried LANFs beneath the conspicuously lumpy structural pattern of the uppermost crust can the dimensions of large earthquakes be achieved. Assessing the seismic hazards of such postulated features can be an engaging process that tests the limits of the imagination.

Part of the allure leading to considerations of LANFs as generators of major earthquakes stems from conclusions that they are primarily responsible for enormous simple-shear extension (ca. 200% or 55 km in the tricorn area) and that they have played important roles in long-range tectonic transport of blocks such as Frenchman Mountain in the Lake Mead area (65 km). In the tricorn area, we show that total extension is less by about an order of magnitude and that fluid-flow-driven dissolution creep formed many of the features previously interpreted as formed in simple shear. For the large extension in the Lake Mead area, we suggest that a fundamentally "aseismic" process such as tectonic rafting on an asthenosphere-like ductile substrate is preferable over simple-shear detachment faulting. We do not suggest that the lumpy discontinuous geometry or the involvement of dissolution creep or tectonic rafting portend truly aseismic deformation, only that they greatly diminish the opportunity for large earthquakes on LANFs and that evaluation of some geometry and processes may have province-wide application to seismic-hazard assessment.

PALEOSEISMOLOGY FROM LUMINESCENCE DATING: TESTS AND APPLICATION NEAR LANDERS, CALIFORNIA

BERGER, Glenn W., Desert Research Institute, P.O. Box 60220, Reno, NV 89506-0220 (gwberger@maxey.dri.edu); T.K. Rockwell, Geological Sciences, San Diego State Univ., San Diego, CA 9218; D.J. Huntley, Dept. Physics, Simon Fraser Univ., Burnaby, B.C., V5A 1S6, Canada

The magnitude 7.5 1992 event at Landers stimulated controversy. Some workers considered this as manifesting a young, previously unrecognized fault. Others considered that old fault slips may go unrecognized because of the difficulty of dating slip. The paucity of charcoal for ^{14}C dating in trenches across the 1992 rupture trace led us to employ luminescence sediment-dating techniques (e.g., Berger, 1995), using detrital feldspars for measuring the time since the last exposure to daylight (the burial time), to determine the history of past ruptures.

Because the depositional environment was apparently different from that of previous thermoluminescence (TL) studies of paleo-earthquakes (e.g., Forman and others., 1991), we chose to make some site-specific tests of the main assumptions of the luminescence techniques. To test the assumption of negligible post-depositional translocation of fine-silt (4-11 μm diameter) grains in the sandy deposits, we compared fine-silt TL age estimates with ages from optical dating using infrared (IR at ~ 880 nm wavelengths) stimulation (IR-OSL) on sand-size (~ 200 μm diameter) feldspar grains from the same samples. The TL and IR-OSL ages are statistically similar, from which we deduce there to be no measured grain-size effect. This implies that fine silt grains could be used reliably for such dating in similar environments, obviating the need for mineral separation and special dose-rate measurements.

To test the zeroing assumption, we chose sediment from active turbation features on the surface (an ant hill and a ground-squirrel nest), as well as the upper few centimeters of the A horizon ruptured by the 1992 event. Relict or residual ages obtained were $\sim 500 \pm 100$ yr. for squirrel-nest feldspars, ~ 300 yr. for the upper 1 centimeter from the ant hill, $\sim 50 \pm 10$ yr. (from IROSL) for the upper 1.5 centimeters from the surface A horizon, and 600-1,000 yr. for grains 4-5 centimeters below the surface within this A horizon. Other tests strongly suggest that each of these samples is a mixture of well-zeroed grains and poorly zeroed grains. These bulk-sample tests thus indicate a residual luminescence age of about 500 yr. at this site, less than the analytical error for samples older than 5-10 kyr.

Samples from a trench across the Landers fault gave ages ranging from 4-5 kyr near the surface to ~ 25 kyr at ~ 2.5 meter depth. Thus before 1992, this fault last ruptured at 4-5 kyr. Reconstruction of vertical displacement of other dated horizons in the trench suggests 3-4 1992-sized events since ~ 17 kyr, and 5-6 events in the past ~ 25 kyr. These data therefore suggest a ~ 5 kyr recurrence interval for large slip events along this fault.

References

- Berger, G.W., 1995, Progress in luminescence dating methods for Quaternary sediments, *in* Dating methods for Quaternary deposits. (Rutter, N.W., and Catto, N., editors). Geological Association of Canada, GEOText no. 2, 81-103.
- Forman, S.L., Nelson, A.R., and McCalpin, J.P., 1991, Thermoluminescence dating of fault-scarp-derived colluvium: Deciphering the timing of paleoearthquakes on the Weber Segment of the Wasatch Fault Zone, north-central Utah: *Journal of Geophysical Research*, v. 96, p. 595-605.

EARTHQUAKE HAZARD ON THE WASATCH FRONT, UTAH, FROM FAULT INTERACTION AND TECTONIC INDUCED FLOOD INUNDATION ASSOCIATED WITH THE WASATCH FAULT

CHANG, Wu-Lung, and R. B. Smith, *Department of Geology and Geophysics; University of Utah, Salt Lake City, UT, 84112* (wchang@mines.utah.gov); R. W. Jr., Simpson (USGS, 345 Middlefield Road, Menlo Park, CA 94025) (rbsmith@mines.utah.edu)

To evaluate the earthquake risk on the Wasatch Front from fault-related hazards, we have studied models of the interaction amongst individual segments of the 370-km-long, Wasatch fault using its paleoseismic record. Fault interaction and accompanying stress changes are often cited as evidence for systematic space-time variations in aftershock distributions. Changes in stress accompanying an earthquake can in turn affect loading or unloading of adjacent faults, changing their potential for future rupture. We studied this effect by examining the space-time behavior of events from 6,000 yr. to 475 yr. old, including more than a dozen $6.7 < M_w < 7.1$ paleoearthquakes on the Wasatch fault. We employed a 3-D elastic, boundary element code (Simpson, 1994) to examine how stress on a specific fault was perturbed by rupture on a nearby fault. These results revealed how prehistoric earthquakes may affect the current state of stress on the Wasatch fault. We also analyzed an unusual earthquake hazard for the Wasatch Front due to possible flooding by tectonically induced inundation by the Great Salt Lake accompanying large normal-faulting earthquakes on the Wasatch fault. We first developed a high-resolution topographic data set, digitized at 500-foot horizontal intervals and at a 2-foot vertical interval, then applied the boundary element modeling method to calculate vertical displacements for scenario normal-faulting earthquakes. Differences between the undeformed and deformed topography reveals where water could flow into the hanging-wall subsidence basin. We also used the observed ground deformation of the maximum credible earthquake for the Intermountain region, the Ms 7.5, 1959 Hebgen Lake, Montana, event as a scenario earthquake. Because of the close proximity of the Great Salt Lake to Salt Lake City, we will demonstrate that this unappreciated hazard is very important depending upon the lake level and the location and size of the scenario earthquake. We are also examining another hazard related to hanging-wall deformation due to backtilt of sewer lines that could malfunction with sediment settling given sufficiently large changes in gradient.

PLANNING SCENARIO FOR A MAJOR EARTHQUAKE IN WESTERN NEVADA

dePOLO, Craig M., Jim G Rigby, Gary L. Johnson, and Steven L. Jacobson, *Nevada Bureau of Mines and Geology, University of Nevada, Reno; John G. Anderson, Seismological Laboratory, University of Nevada, Mail Stop 178, Reno, NV 89557-0088* (cdepolo@nbgm.unr.edu) and Thomas J. Wythes, WESTEC

The western Nevada earthquake planning scenario was created to aid in understanding what a large local earthquake could be like. The goals of the scenario are to intensify the understanding of the earthquake hazards in western Nevada, to explain potential consequences from a major earthquake, to encourage local preparedness and mitigation measures, and to enhance disaster-response planning.

A magnitude 7.1 earthquake along the northern Carson Range fault system is used as the scenario event. Earthquake effects presented are modified Mercalli earthquake intensity, surface faulting, liquefaction, and landsliding. The resulting map of intensity from the scenario event indicates very intense and potentially damaging shaking (intensity IX) in the Reno, Washoe Valley, and Carson City areas. The surrounding mountains have intensities of VII to VIII. A zone of normal-slip surface faulting 32 kilometers long and up to 33 meters wide extends from Washoe Valley, along the base of the Carson Range, and into southwest Reno. The ground is offset 2 meters vertically over much of this distance, with a localized maximum of 4 meters, and the rupture decreases to 0.5 meters and less in Reno. High and moderate liquefaction susceptibility areas are scattered throughout the urban corridor, and localized damage from liquefaction would be anticipated from the scenario event. Areas of major rockslide and landslide hazards pose threats mostly to transportation routes, with a few communities and utilities threatened as well.

The second part of the scenario describes some of the general consequences and impacts to lifeline utilities from the scenario event. These include general descriptions of the most hazardous types of buildings (e.g., unreinforced masonry buildings); impacts on the school system and the number of children at risk; potential impacts on medical systems, fire, police, and emergency facilities (including decision-making facilities, such as city halls, emergency operating centers, and emergency information dispatch centers); and generalizations of hazardous materials incidents. The impact on the transportation system (principally roads and airports) is described by hours or days out of service, and specifications for airports (e.g., runway length, wheel-bearing load capacity) are given for emergency planning involving large transport planes.

Impacts to communication systems, electric power, natural gas, water systems, wastewater systems, and petroleum are described with input from the local utilities. Local input helps assure accuracy, but more importantly, helps obtain local "buy in" and "ownership" of the scenario, increasing its ultimate usage.

The consequences described are a combination of general impacts that likely would result from a large earthquake, and some specific, hypothetical information for illustration. Nonstructural mitigation is emphasized throughout the text. The scenario earthquake strongly shakes western Nevada and poses many serious geologic hazards, engineering risks, and potential impacts on important lifeline systems. Preparation for an event of this severity would, in general, be adequate for any earthquake that could affect the region.

HISTORICAL EARTHQUAKES, AND PATTERNS AND BEHAVIOR OF SEISMICITY IN WESTERN NEVADA AND EASTERN CALIFORNIA

dePOLO, Diane M., Ken D. Smith, and John G. Anderson, Seismological Laboratory, University of Nevada, Reno, MS 174, Reno, NV 89557 (diane@seismo.unr.edu); Craig M. dePolo, Nevada Bureau of Mines and Geology, University of Nevada, Reno, MS 178, Reno, NV 89557 (cdepolo@nbgm.unr.edu)

Western Nevada has a notable earthquake history, and high levels of background seismicity are warning signs of future strong earthquakes. The region is part of the belt of seismicity that occurs in the western Great Basin and along the eastern Sierra Nevada, referred to as the Eastern California seismic belt. Although distinct earthquakes and earthquake sequences occur along the eastern Sierra Nevada front, the seismicity of western Nevada might better be described as part of a higher level of seismicity that occurs in the Walker Lane belt of the western Basin and Range Province. Thirteen historical earthquakes of magnitude 6 have occurred in the western Nevada region, many of which occurred early in the Nevada's history. In the past 30 years, only one earthquake of magnitude 6 has occurred, a contrast to the earlier history. The University of Nevada, Reno Seismological Laboratory (UNRSL) operates a seismic network in western Nevada and eastern California, and has recorded and located earthquakes for the past 27 years. Nearly 6,000 earthquakes have been recorded by this network in the Reno-Carson City region confirming the active earthquake character of the area.

A detailed study of a subset of these earthquakes (1980 -1996) reveals the distribution and character of this seismicity. Phase data from UNRSL and Northern California Seismic Network were merged and the events relocated. Different velocity models were tested against a series of quality criteria. Seismicity in the area tends to cluster at the intersections and ends of faults and, in some cases, appears to outline faults. Northwest and northeast trends to the seismicity, mimicking local fault patterns, are common. Focal mechanisms are dominated by strike-slip and oblique strike-slip, with fewer normal-slip mechanisms, consistent with translational activity in the Walker Lane belt. Although, relatively aseismic, the Sierra Nevada block has had earthquakes of up to magnitude 5.2 within it, such as the 1980 Soda Springs earthquake. The depth of seismicity increases into the Sierra Nevada block from the Basin and Range Province, reflecting the thermal structure. Ninety percent of the earthquakes locate at depths of 10 kilometers or shallower in the Basin and Range Province, with this depth increasing to 18 kilometers in the Soda Springs area within the Sierra Nevada block. The change in depth appears to occur gradually over 30 to 40 kilometers, whereas the transition between the seismically active Walker Lane belt and the aseismic Sierra Nevada occurs over a more abrupt 10 to 20 kilometer transition.

GEOLOGIC INPUT FOR SEISMIC-HAZARDS MAPS - EXAMPLES FROM THE DATABASE OF QUATERNARY FAULTS IN MONTANA

HALLER, Kathleen M., U.S. Geological Survey, Central Region Geologic Hazards Team, Denver, Colorado, P.O. Box 25046, Mail Stop 966, Denver Federal Center, Denver, CO 80225 (haller@gldvxa.cr.usgs.gov)

Seismic-hazards analyses based primarily on historical seismic record can be improved by incorporating Quaternary fault data, particularly in regions characterized by low slip rates. Geologic data on faults expand the time frame considered from less than a few hundreds of years for the historical record to hundreds of thousands of years for the paleoseismic record. The detailed paleoseismic and historical data that we compiled on Quaternary faults in Montana not only augments seismicity for seismic-hazards analyses, but also displays the current level of understanding of the Quaternary history of large-magnitude earthquakes and, thus, surface faulting in Montana.

Our compilation provides digital fault data, as well as paleoseismologic data that characterize the history of the faults. The former include the location, sense of movement, and length; paleoseismic data include timing of most recent movement and slip rate that are portrayed graphically by color and line thickness, respectively. The graphical fault data are compiled digitally, and from that data, fault length can be computed, which provides some constraint on maximum magnitude. Timing of the most recent movement are constrained to five age categories, which include Historic, post-latest Pleistocene (<15 kyr), late Quaternary (<130 kyr), late and middle Quaternary (<750 kyr), and Quaternary (<1.6 myr). These age categories define the maximum time of the most recent movement and thus allow some latitude in age assignment. We define four ranges of slip rate for this project: <0.2 mm/yr., 0.2-1 mm/yr., 1-5 mm/yr., and >5 mm/yr.; however, published data indicate that all of the faults in Montana fall into the two lower ranges.

We compiled data on 68 Quaternary faults in Montana; the 1996 National Seismic-Hazards Maps incorporate data on 15 of those faults. Future iterations of the national maps will be able to incorporate the paleoseismic data in this compila-

tion, and the other state compilations that follow. The data we present are compiled in a consistent manner; this will provide the same level of consistency in the data used to produce future national maps. Paleoseismological studies and recent geologic studies are given preferential citation in the compilation. In general, most of the faults in Montana are not well studied; data are lacking in some critical piece of information. The timing of most recent events on many of the faults is poorly constrained and is inferred primarily from morphologic studies and surficial geologic relations; there are few cases where faulting events are constrained by numerical age determinations. Fewer than 20 percent of the faults are characterized by published recurrence intervals; only one of these is well constrained, where the timing of the two most recent events is known. Slip rates are published for about 10 percent of the faults and, of those, half are highly suspect. Even though specific timing, recurrence interval, and slip-rate parameters may not be complete, data are presented in the compilation that allows the user to determine permissive values in the absence of published parameters. Clearly, additional studies are needed to better characterize the histories of these faults and, thus, better define the seismic hazards of the region.

THE SEISMOTECTONICS AND SOURCE PARAMETERS OF RECENT EARTHQUAKES NEAR RENO, NEVADA

ICHINOSE, Gene A., Kenneth D. Smith, John G. Anderson, and James N. Brune, University of Nevada Reno Seismological Laboratory, Mail Stop 178, Reno, NV 89557-0088 (ichinose@seismo.unr.edu)

We examine recent earthquake sequences in western Nevada since 1994 using broadband networks and portable digital recorders. The mechanisms of these earthquakes provide constraints on the strain transfer through the Walker Lane belt and eastern Sierras in northern Nevada, and earthquake stress drops and site effects can be used to estimate the high frequency ground motion for potentially damaging earthquakes in the Reno-Carson City metropolitan area.

The September 12, 1994 Mw 5.9 Double Spring Flat (DSF) earthquake has been followed by an unusual aftershock period for western Basin and Range sequences. The mainshock initiated at the intersection of a northeast and northwest striking set of conjugate faults; rupture progressed on the northeast striking fault plane (dePolo and others, 1994). Eight days after the mainshock, the activity migrated from the mainshock fault plane to the northwest striking high-angle, right-lateral structure. Over the next two years the focus of activity moved southward, primarily into the footwall block of the Antelope Valley fault zone. This sequence has produced a total of 18 $M = 4$ to 5.9 events. The focal mechanisms of $M > 4$ events were estimated from moment tensor inversion (Dreger and others, 1993) using broadband regional data. There are a variety of faulting mechanisms. The T-axis (minimum stress direction) is oriented east-west (N80E to N140E) for the sequence. The style of focal mechanisms and the east-west oriented T-axis is commonly observed along the Eastern Sierran front in northern Nevada. The estimated static stress drop for the mainshock, using an average slip of 54 centimeters, and a seismic moment of 5.7×10^{24} dyne-cm is 15 bars. We have calculated about the stress drops of about 200 aftershocks.

The 15 November 1995, Mw 4.5 Border Town, Nevada, earthquake sequence occurred near the California-Nevada border approximately 20 kilometers northwest of Reno, Nevada (Ichinose and others, 1997). The mainshock occurred on a steeply west-dipping fault at a depth of 14 kilometers, and showed a normal-oblique slip mechanism. The projection of the preferred fault plane to the surface coincides with the trace of a suspected Quaternary fault. We infer that the more prominent through going Last Chance fault, to the west, is also a high-angle fault most likely accommodating strike-slip motion. The mainshock static stress drop is 65 bars estimated from spectral inversion of waveforms recorded at an intermediate period station at Washoe City, Nevada. The December 2, 1996, $M = 4.3$ Sutcliffe, Nevada, earthquake occurred in the Pyramid Lake fault zone at a depth of 13.5 kilometers. A high-angle, strike-slip mechanism and seismic moment of 2.2×10^{22} dyne-cm has been estimated from the moment tensor inversion. Using a spectra inversion method from data recorded at a local broadband station we estimate a static stress drop of 10 bars for the Sutcliffe event.

IMPLICATIONS OF VARIABLE LATE QUATERNARY RECURRENCE INTERVALS FOR PROBABILISTIC SEISMIC-HAZARD ASSESSMENTS; EXAMPLES FROM UTAH AND WEST TEXAS

KEATON, Jeffrey R., AGRA Earth & Environmental, Inc., 130 Yucca Drive, Sedona, AZ 86336-3222 (72560.1510@CompuServe.COM)

Probabilistic seismic-hazard assessments are based in part on recurrence intervals of future earthquakes generated by all possible sources. Future recurrence intervals are based on historical and paleoseismic data. Average recurrence intervals of major earthquakes traditionally are represented as uniform with time. Episodic or variable recurrence of surface-faulting earthquakes has been found for some faults. The present abstract summarizes such evidence for two normal faults in the Basin & Range Province: the West Valley fault zone (WVFZ) near Salt Lake City, Utah, and the East Franklin Mountains fault zone (EFMFZ) near El Paso, Texas. The WVFZ consists of two subparallel traces, the western Granger fault and the eastern Taylorsville fault, with east-facing scarps as high as 6.1 meters in late Pleistocene Lake Bonneville sediments. It displays increasing slip rate over the past 140 kyr with clear evidence for tectonic quiescence during deposition of Lake Bonneville sediments (27 to 12 kyr in the elevation range of the WVFZ). Boring cores and sediment ages estimated from TL and amino acid racemization methods indicate that the top of the 140-kyr Little Valley Alloformation has a vertical separation of 17.4 to 18.9 meters across the Granger fault (slip rate >0.12 to >0.14 m/kyr). The top of the 60-kyr Cutler Dam Alloformation has a vertical separation of 12.8 to 14.3 meters across the Granger fault (slip rate >0.21 to >0.24 m/kyr).

The top of the 12-kyr Lake Bonneville Alloformation has a vertical separation of 5.2 to 6.7 meters across the Granger fault (slip rate >0.43 to >0.56 m/kyr). Post-Bonneville sediments (<12 kyr) are displaced or warped 1.2 to 1.5 meters across the Taylorsville fault (deformation rate >0.10 to >0.13 m/kyr). Slip rates for the WVFZ are shown on figure 1. Previously published drill-hole data suggests that buried 1.8-Myr late Pliocene pediment surfaces are offset 64 to 77 meters across the WVFZ (average Quaternary slip rate of 0.03 to 0.04 m/kyr). The Taylorsville fault displays 2 flexure-displacement events in post-Gilbert (<10.3 kyr) littoral and lagoonal sediments (Holocene recurrence rate of 5.15 kyr). The southern part of the Granger fault displays 2 normal-slip events in post-Bonneville (<12 kyr) lacustrine sediments, and 3 normal-slip events in post-Gilbert paleochannels of the Jordan River and other geomorphic features (Holocene recurrence rate of 2.4 kyr). A combined Holocene recurrence rate of 1.7 kyr would result if the events on the Taylorsville fault were independent of those on the Granger fault.

The north-trending EFMFZ is one of many Quaternary faults in the Rio Grande rift area of west Texas and New Mexico. It is the southern part of the 182-kilometer-long San Andres-Organ-East Franklin Mountains fault system. The EFMFZ obviously offsets Quaternary units by as much as 125 meters in a non-urbanized area north of El Paso. Using units correlative to those established for the Desert Project in southern New Mexico, geologic mapping indicated faulting of Jornada II-age calcrete units (150 to 25 kyr) and older. No younger units displayed conclusive evidence of offset. It remains unclear if Isaack's Ranch-age units (15 to 8 kyr) exist in the area; however, younger Organ units (<8 kyr) are clearly unfaulted. Drill-hole data reveals more than 48.3 meters of vertical separation of the top of 250 to 400-kyr Camp Rice Formation (Jornada I surface). Trenching of a 10.7-meter-high scarp revealed multiple post-Jornada II displacements (4 to 6 events) with approximately 1.8 to 3.5 meters of offset per event. Interpretations of slip rate for the EFMFZ are based on two radiometric dates from colluvial-wedge sediments and speculations regarding time for soil carbonate development and ages of alluvial units and geomorphic surfaces. The most recent colluvial wedge on the EFMFZ yielded a soil carbonate date of approximately 10.9 kyr, whereas the penultimate colluvial wedge yielded a soil carbonate date of approximately 15.6 kyr. Substantial periods of seismic quiescence must have occurred to allow multiple stage IV calcretes to develop. The variability in time between surface-faulting earthquakes on the EFMFZ may be episodic. A slip rate of 0.1 m/kyr for the past 500 kyr appears reasonable, as shown on figure 2; however, a slip rate of 0.3 m/kyr is justified by the two most recent surface-faulting events. The faulted stratigraphy along the WVFZ indicates that the Holocene slip rate is an order of magnitude greater than the early Quaternary slip rate. Paleoseismic quiescence occurred during the Bonneville deep-lake cycle. The relationship of the WVFZ to the nearby Wasatch fault and the potential independence of the WVFZ as a generator of seismicity in the Salt Lake Valley remain unresolved. Assessment of earthquake hazards in the El Paso area depends on a judgment about the frequency of future earthquakes: Is the EFMFZ still in a episode of relatively frequent surface-faulting earthquakes, or has it entered another episode of seismic quiescence? Issues such as these contribute to uncertainty in the results of probabilistic seismic-hazard assessments.

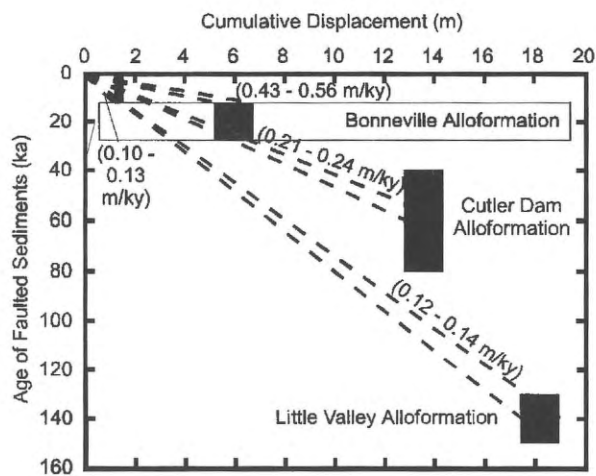


Figure 1. Summary of slip-rate data for the West Valley fault zone, Utah.

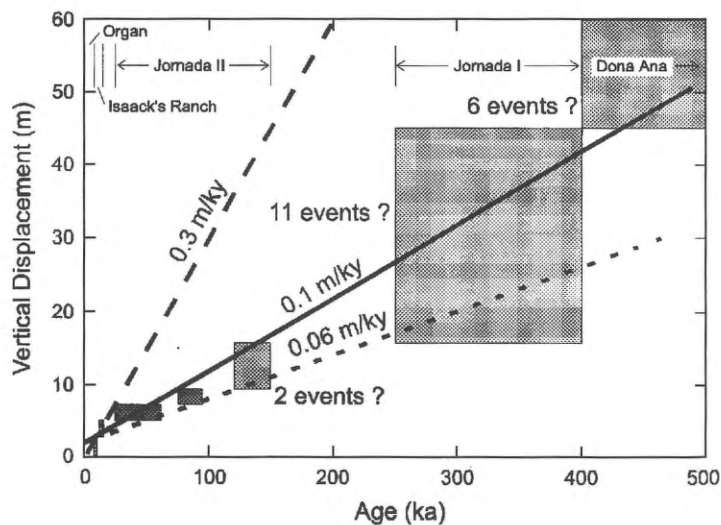


Figure 2. Summary of slip-rate data for the East Franklin Mountains fault zone, Texas.

RECOGNITION OF ACTIVE BUT NON-SEISMOGENIC SALT-RELATED DEFORMATION WITHIN AN EXTENSIONAL ENVIRONMENT, WEST-CENTRAL COLORADO

KIRKHAM, Robert M., and Randall K. Streufert, Colorado Geological Survey, PO Box 172, Montevista, CO 81144

During the past five years the Colorado Geological Survey has mapped the geology of six 7.5-minute quadrangles in the Glenwood Springs-Carbondale-Dotsero area of west-central Colorado, which lies about 45 kilometers west of the northern end of the Rio Grande rift. This region contains widespread late Cenozoic volcanic rocks, including the 4,150-year-old Dotsero volcano, it has experienced a moderate level of historic seismicity, and several previous investigators had reported evidence of late Tertiary and Quaternary extensional deformation. During the initial phases of our project we discovered several geologically young structures which could be interpreted as evidence of significant paleoseismicity, suggesting this area had potential for large future earthquakes.

As geologic mapping progressed, we encountered many more young structures but began to realize that these were unusual types of structures unlike those typically found in extensional environments. They included diapiric valley anticlines which fold late Pleistocene terraces, synclinal sags, ductily folded, yet brittle volcanic flows, intrusive contacts between evaporitic and clastic formations, large topographic troughs in outwash terraces, and extensive deposits of broken and rubbly rock. These unusual structural features lie within a 650 kilometer area where Pennsylvanian evaporitic rocks occur at or near the ground surface. Late Tertiary volcanic rocks are downropped up to 1,300 meters within this collapsed block. Deformation along the boundaries of the collapse block include monoclinical folding of late Tertiary volcanic flows and relaxation or unfolding of the Laramide Grand Hogback monocline.

We now interpret this widespread, geologically young structural deformation as resulting from regional and localized collapse due to flowage, dissolution, and diapirism of underlying evaporitic rocks. This interpretation greatly affects the seismogenic potential of these structures. If these features were related to crustal extension, they could be capable of generating potentially damaging earthquakes of magnitude 6.5 to 7.0. If, as we suspect, they are shallow structures resultant from predominantly plastic deformation in the underlying evaporitic rocks or from subsidence or collapse into dissolution cavities in the evaporite, then their seismic potential is much lower.

GEOPHYSICAL CHARACTERIZATION OF ACTIVE FAULTS IN THE BASIN AND RANGE, AND THE EARTHQUAKE HAZARD OF THE PAHRUMP VALLEY FAULT ZONE

LOUIE, John, Gordon Shields, Gene Ichinose, Michael Hasting, Gabriel Plank, and Steve Bowman, Associate Professor of Seismology, Seismological Lab (174) The University of Nevada, Reno, Reno, NV 89557-0141 (louie@seismo.unr.edu)

We employ the seismic-reflection, gravity, magnetic, and electromagnetic geophysical techniques to examine the subsurface geometry of seismogenic structures such as the Pahrump Valley fault zone (PVFZ), 50 to 100 kilometers west of Las Vegas. Geophysical techniques can provide clues to segmentation and rates of activity in advance of detailed trench studies, and can uncover deeper and older displacements. On the PVFZ we can locate fault strands near eroded fault-line scarps from pronounced magnetic and soil conductivity anomalies. We also observe truncations and limit the vertical offsets of reflective ash beds in shallow seismic profiles. The sharpness of the magnetic and soil conductivity anomalies appears to correlate with the relative geomorphic youth of the scarps. These three geophysical techniques in combination can locate faults that lack clear surface expressions. PVFZ strands in southern Stewart Valley show clear evidence for more than 18 meters of Holocene dextral displacement in a 3-D seismic survey, but without any vertical component of displacement. The Pahrump Valley fault zone appears to have little potential for segmentation, suggesting ruptures as long as 100 kilometers. The 18 meter minimum displacement of Wisconsin and pre-Wisconsin age lacustrine formations likely results from a Holocene dextral slip rate above 0.1 mm/yr.; the rate is certainly larger than 0.03 mm/yr., and probably less than 2 mm/yr. Having a slip rate above that of other faults in southern Nevada, and more typical of Great Basin faults in general, the PVFZ may be able to produce a magnitude 7 event only 50 kilometers from the Las Vegas metropolitan area.

CHARACTER OF FAULTING ALONG THE HUNTER MOUNTAIN FAULT ZONE AND EVIDENCE FOR ACTIVE DEXTRAL SLIP TRANSFER ACROSS SALINE VALLEY RHOMBOCHASM, EASTERN CALIFORNIA

OSWALD, John A., and S. G. Wesnousky, Center for Neotectonic Studies, m/s 169, University of Nevada, Reno, NV, 89557-0135 (johnno@seismo.unr.edu SteveW@seismo.unr.edu)

The Hunter Mountain fault zone is a 46-kilometer-long, northwest trending, right-lateral fault zone that links the northern end of the Panamint Valley fault zone to the southern end of the Saline Valley fault. When combined, the three faults total approximately 160 kilometers of nearly continuous fault scarps, and fault-related features. The Panamint Valley-Hunter Mountain-Saline Valley fault zone is one of three major fault zones that distribute approximately 8 mm/yr. of dextral slip from the Mojave Desert northward into the Walker Lane belt. Dextral slip on the Hunter Mountain fault zone accommodates the opening of Saline Valley and northern Panamint Valley, forming near perfect rhombochasm.

Our observations show that the pass between Panamint Valley and Saline Valley exhibits a clear history of dextral off-

set in preserved geomorphic features. In southern Saline Valley, in addition to faulting along the Inyo Mountains range front, there exist several normal faults that splay northward off the main trace and trend toward Eureka Valley. Scarps along the normal faults within Saline Valley display a morphology and offset units that we interpret to represent a Holocene event.

A single event scarp, east of Daisy Canyon and on the Hunter Mountain fault zone, shows a 2:1 ratio of dextral to normal separation of a channel levee. The youthful appearance of the scarp, and the surficial characteristics of the offset unit suggest 2 meters of right-lateral separation at this location in the Holocene. The discrepancy in the style of offset between the two sites can be explained by one of two scenarios: (1) two separate events within the Holocene, a dextral event on the Hunter Mountain fault, and a normal event on the Saline Valley fault, or (2) a single event that produced spatial variations in the dextral and normal component of offset due to variations in fault strike.

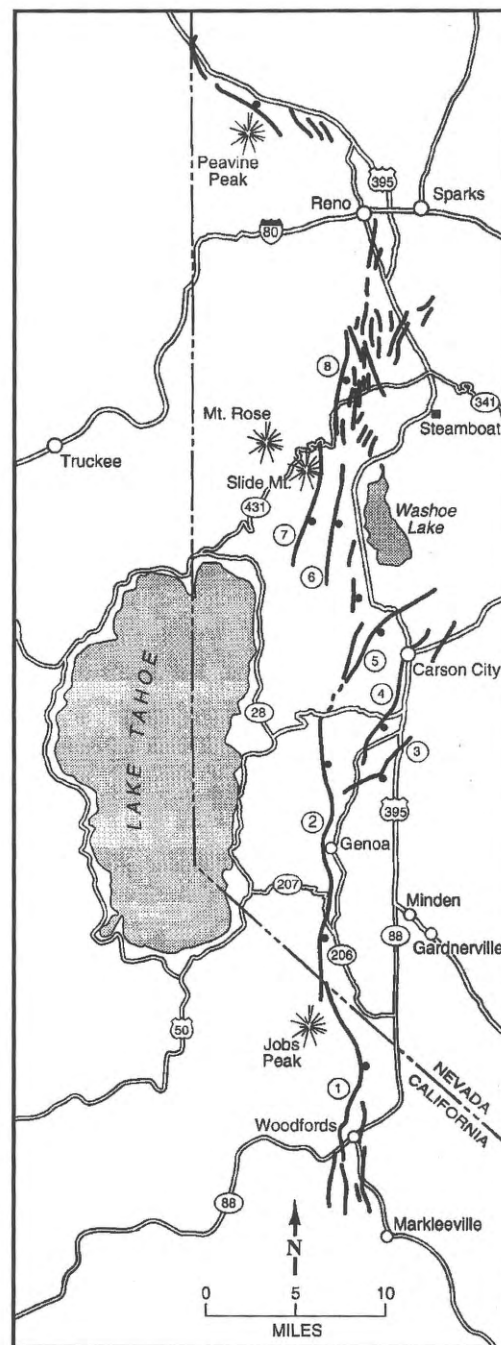
RECENT LARGE-MAGNITUDE EVENTS ALONG THE CARSON RANGE FAULT SYSTEM, A PRINCIPAL FRONTAL FAULT OF THE NORTHERN SIERRA NEVADA

RAMELLI, Alan R., Craig M. dePolo, and John W. Bell, Nevada Bureau of Mines and Geology/MS178, University of Nevada, Reno, NV 89557 (ramelli@nbmg.unr.edu)

The Carson Range fault system (CRFS) bounds the eastern sides of the urbanized basins of western Nevada and poses the primary seismic hazard to the Reno/Carson City area, the second most populated area in the state. The CRFS, one of the most active faults in the west-central Basin and Range Province, has generated multiple large-magnitude earthquakes within the past few thousand years.

The southern CRFS, commonly referred to as the Genoa fault, displays a conspicuous paleoseismic scarp indicating at least one recent surface-rupturing event. Three exploratory trenches excavated across the main stretch of the Genoa fault revealed evidence of two late Holocene events with normal surface displacements of 3 to 5.5 meters per event. Such offsets are comparable to the largest historical Basin and Range Province earthquakes (e.g., 1915 Pleasant Valley, NV and 1959 Hebgen Lake, MT) and suggest earthquakes of about magnitude 7.5. Based on ^{14}C ages derived from stratified charcoal in two trenches, the most recent and penultimate events on this part of the Genoa fault appear to have occurred during ranges of 500-650 yr B.P., and 2,000-2,200 yr B.P., respectively. The southern Genoa fault lacks a prominent paleoseismic scarp, and bedrock outcrops and mid-Pleistocene alluvial fans present on the downthrown side indicate a significantly lower rate of activity. Nonetheless, latest Pleistocene glacial outwash terraces along the West Carson River at Woodfords are displaced vertically by at least 10 meters.

From Carson City to Reno, constraints on recent activity of the CRFS are not as good as for the Genoa fault, but what data exist suggest similar timing and smaller offsets. One or more of three northeast-striking faults in the Carson City area (Kings Canyon, Carson City, and Indian Hill faults) may rupture with the Genoa fault. A left step and bedrock high separate the Kings Canyon and Washoe Valley faults, reflecting a probable earthquake segment boundary. Trenching in Washoe Valley similarly indicates two events within the past 2 kyr (about 2 m offset per event), but stratigraphic constraints were insufficient to bracket the timing of individual events. Near Reno, the CRFS is a highly distributed zone, with several subparallel, nested grabens cutting the Pleistocene Mt. Rose outwash fan. Timing constraints are poor in this area due to a paucity of Holocene alluvial surfaces, but a ^{14}C age from organic material within a fissure along the range-front trace about 1 kilometer north of Nevada Highway 431, suggests an event within the past several hundred years.



Generalized strip map of the Carson Range fault system (CRFS), a principal frontal fault of the northern Sierra Nevada and the primary seismic hazard to the Reno/Carson City urban corridor. Sections of the CRFS include: 1) southern Genoa fault; 2) main section of the Genoa fault; 3) Indian Hill fault; 4) Carson City fault; 5) Kings Canyon fault zone; 6) Washoe Valley fault; 7) Little Valley fault; and 8) Mt. Rose frontal fault.

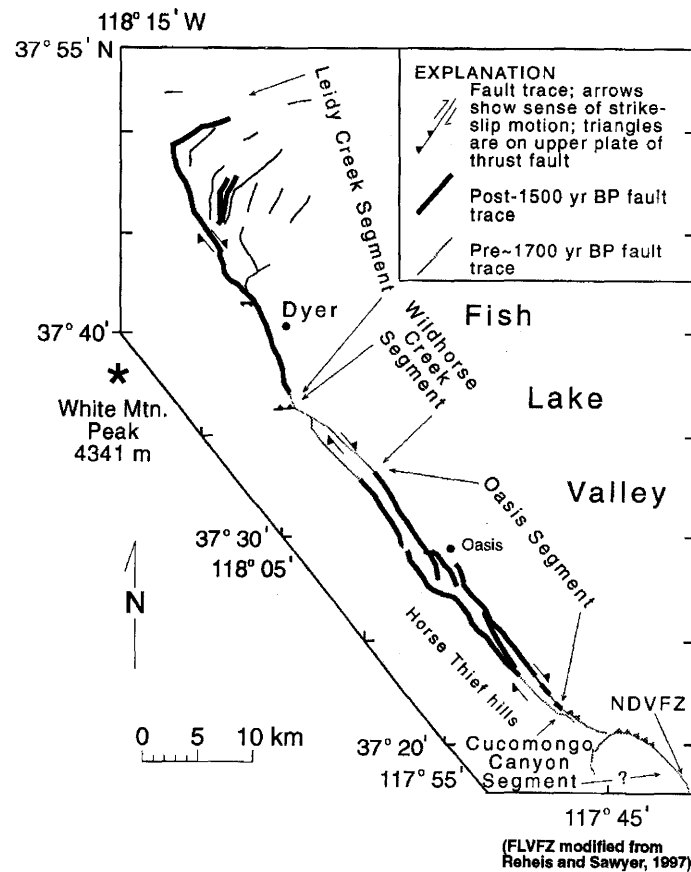
HOLOCENE PALEOSEISMICITY, SEGMENTATION, AND SEISMIC POTENTIAL OF THE FISH LAKE VALLEY FAULT ZONE, NEVADA AND CALIFORNIA

SAWYER, T.L., Consultant, 10455 San Fernando Rd. Reno, NV 89506 (103253.1322@compuserve.com); M.C. Reheis, U.S. Geological Survey, MS 980, Federal Center, P.O. Box 25046, Lakewood, CO 80225 (mreheis@usgs.gov)

The ~70-km-long, right-oblique Fish Lake Valley fault zone (FLVFZ) is the northern part of the Furnace Creek fault zone; the adjacent section is the Northern Death Valley fault zone (NDVFZ). We conducted detailed mapping of this major fault zone and a well-dated sequence of surficial deposits, and interpreted trench exposures at six sites to assess the Holocene fault behavior and seismic potential of the FLVFZ. Our results indicate that the FLVFZ has produced several moderate to large earthquakes in the past 5,000 years.

We propose that the fault zone includes four earthquake-rupture segments, from north to south: Leidy Creek, Wildhorse Creek, Oasis, and Cucomongo Canyon segments (see figure). These segments differ somewhat from the sections defined by Reheis and Sawyer (1977, GSA Bull., v. 109). The en echelon, N25° - 40° W-striking Leidy Creek segment, Oasis segment, and NDFVZ form two approximately 4-kilometer-wide left (i.e., restraining) steps, in which the N50° W to east-west-striking Wildhorse Creek and Cucomongo Canyon segments are located. The Leidy Creek and Oasis segments are characterized by right-oblique-normal slip, have ruptured in the past 700 to 1,500 years, and have average recurrence intervals of approximately 500 to 1,000 years. In contrast, the Wildhorse Creek and Cucomongo Canyon segments are characterized by right-oblique-reverse slip, have not ruptured in the past 1,700 years, and probably have recurrence intervals <1,700 years. Thus, adjacent rupture segments different in sense of dip-slip and are separated by, or occupy, large (~4-km-wide) releasing or restraining steps. Smaller releasing and restraining steps on the Leidy Creek segment appear to have had no effect on the rupture associated with the most recent event (MRE).

Recent comparisons of geodetic and geologic slip rates help constrain the seismic potential of the FLVFZ. The FLVFZ and NDFVZ account for about half the rate of 10-12 mm/yr of Pacific-North American plate-boundary shear accommodated in the Basin and Range Province between about lat. 36° 30' and 38° N (Klinger and Piety, 1996, USBR report 96-10; Reheis and Sawyer, 1997). Our trench and mapping data combined with these slip rates indicate the following: (1) the MRE on each of the four proposed segments is distinct in time and space, (2) roughly >7 meters of right-lateral strain has accumulated on both the Wildhorse Creek and Cucomongo Canyon segments, if strain accumulates at our preferred late Pleistocene rate of 4 mm/yr on the FLVFZ, (3) empirical relations suggest characteristic earthquakes on the Leidy Creek and Oasis segments of M_w 6.7 to 6.8 and on the Wildhorse Creek and Cucomongo Canyon segments of about M_w 6.2 to 6.3. Thus, either (a) these right-oblique-reverse-slip segments should have ruptured more than 30 times in the past 1,700 years, which has not occurred; or (b) we suspect that some earthquakes nucleating on the Wildhorse Creek and Cucomongo Canyon segments may rupture the entire FLVFZ producing M_w 7 or greater maximum earthquakes, which suggests a complex "nested" segmentation model, (4) recurrence intervals range from 500 to $\geq 1,700$ years and are longest where the dip-slip component is reverse, rather than normal, (5) elapsed times since the MRE on the Leidy Creek and Oasis segments equal or exceed their recurrence intervals, suggesting that the FLVFZ is a prime candidate for producing an earthquake within the White Mountain seismic gap, and (6) restraining steps ≥ 4 kilometers wide along strike-slip faults should be considered as potential segment boundaries or as containing obliquely oriented, nested(?) rupture segments.



Earthquake-rupture segmentation model of the Fish Lake Valley fault zone, Nevada and California.

NONLINEAR AMPLIFICATION STUDIES ON DEEP SOIL DEPOSITS IN RENO, NEVADA

SIDDHARTHAN, Raj V., *Professor of Civil Engineering, University of Nevada, Reno, NV 89557 (siddhart@unr.edu)* Ni Shean-Der, *Graduate Student, John G. Anderson, Professor of Seismology*

Many field investigations of past earthquake damage have clearly revealed the role of the foundation soil on the damage to structures founded in soil. The contribution of foundation soil may be viewed as from (1) wave-passage effects, and (2) soil-structure interaction effects. The wave-passage effect is due to the fact that the seismic waves have to travel through the foundation soil to reach the structure. A realistic evaluation of the wave-passage effects using the free-field typically is the first step in the study of the seismic-risk evaluation of a superstructure.

There is clear evidence (Lotung SMART1 array data, Loma Prieta, Kobe and other earthquakes) that soil exhibits nonlinear characteristics above an acceleration level of 0.1g or so. Thus soil nonlinearity can play a significant role in many of the seismic designs of structures such as bridges and buildings. The soil nonlinearity can influence characteristics of the motion (amplitude, frequency, and duration) that reaches the foundation level.

A modified version of DESRA2 dynamic response model for saturated soil has been applied to study the nonlinear seismic response, including liquefaction of a typical soil deposit found in Reno-Sparks area. This deposit is deep (over 120 m in depth) with water table near the surface. Soil properties needed to use in the model were obtained from in-situ seismic-velocity measurements and from the recent design guidelines proposed for the dynamic soil properties by EPRI. These EPRI guidelines recommend that the dynamic soil properties (shear modulus ratio and damping) be characterized as a function of depth (or stress level). The influence of important parameters such as the excitation strength and residual porewater pressure on the response of the deep soil column are presented in the paper. The base excitation used with the DESRA2 model was developed based on the recently completed work on Reno Scenario Earthquake.

The study reveals that (1) there is substantial deamplification in the surface motion as the strength of the base excitation increased, (2) influence of generation of porewater pressure is important in higher excitation levels, and (3) response predicted from conventionally used stress-independent soil properties (e.g., SHAKE) is unconservative.

MAGMA INTRUSION AND SEISMIC-HAZARDS ASSESSMENT IN THE BASIN AND RANGE PROVINCE

SMITH, Richard P., and S.M. Jackson, *Idaho National Engineering and Environmental Laboratory, P.O. Box 1625, Idaho Falls, ID 83415-2107, (rps3@inel.gov); W.R. Hackett, WRH Associates, 2880 E. Naniloa Circle, Salt Lake City, UT 84117*

In Basin and Range Province seismic-hazards assessments it is often appropriate to consider the influence of magmatic processes on tectonic faulting. Magma intrusion into the seismogenic crust tends to supplant single, large tectonic earthquakes with swarms of low to moderate magnitude earthquakes. If magma intrusion is not considered, both maximum magnitude and frequency of large earthquakes can be overestimated.

Magma intrusion and normal faulting are fundamental processes of crustal extension. In areas with sufficient magma output rates, extension is accommodated in the upper crust by intrusion of vertical dikes perpendicular to the extension direction and tectonic normal faulting is suppressed or replaced. This is because the dike intrusion process prevents differential stresses from building to levels necessary for normal faulting. Dike intrusion commonly induces surface deformation in extensional volcanic terrains. Surface deformation includes open fissures, monoclines, normal faults, and graben. They are caused by extensional stresses above and ahead of dikes propagating in the shallow subsurface.

The mechanism of dike intrusion and the nature of co-intrusive seismicity have important implications for determination of the maximum magnitude and recurrence of earthquakes. Observational seismicity from volcanic rift zones worldwide suggests the maximum magnitudes of dike-induced earthquakes are 3.8 ± 0.8 . Earthquakes are generally small to moderate because downdip extents of dike-induced faults and fissures are controlled by the depth to the top of the associated dike (usually <5 km), permitting only small rupture areas. Also, rupture and displacement on faults and fissures migrate incrementally at about the velocity of propagating dikes (0.5 m/s) as dike dilation stresses the zone above and ahead of the dike. Earthquake recurrence is tied to recurrence of volcanic cycles based on the geochronology of the associated volcanic materials. The volcanic recurrence data must be interpreted as representing recurring periods of co-intrusive seismicity, not the recurrence of individual earthquakes as are typically used for estimating slip rates in normal faults.

Areas where magmatism has affected the activity of Basin and Range normal faults include the eastern Snake River Plain (ESRP) of Idaho, the Mono Basin of eastern California, the Northern Nevada rift in the central Great Basin, and possibly the Yucca Mountain area of southern Nevada and the Modoc Plateau-Lassen volcanic highland of northern California. The distribution of Quaternary igneous rocks in the Basin and Range Province shows that magma intrusion may be important over large areas of southwestern Nevada and southwestern Utah.

In the ESRP (Smith and others, 1996, JGR, 101, 6277-6292), Quaternary basaltic magmatism has completely replaced normal faulting as the primary extension mechanism. Northwest-trending volcanic rift zones with both volcanoes and dike-induced extensional structures are the surficial manifestations of magmatic accommodation of northeast-directed extension. In the Mono Basin (Bursik and Sieh, 1989, JGR, 94, 15587-15609), volcanism and dike intrusion in the Mono Craters and Inyo Domes, beginning at about 40 kyr, caused shutdown of normal-fault slip on the adjacent portions of the Sierra Nevada range-front normal fault. Recognition of magma intrusion as the source of seismicity in place of large, normal-faulting earthquakes can greatly affect seismic-hazards assessments. Because of low magnitudes and long recurrence intervals, the seismic hazard associated with magma intrusion is commonly less than that posed by background (non-surface rupturing) tectonic seismicity.

DEFINITION OF FAULT SEGMENTS ON YOUNG NORMAL FAULTS: GEOMETRY, OFFSET, AND SCARPS OF THE HURRICANE FAULT, UTAH AND HIKO FAULT, NEVADA

TAYLOR, Wanda J., Douglas D. Switzer, and K. Jill Hammond, Dept. of Geoscience, University of Nevada, 4505 Maryland Parkway, Las Vegas, NV 89154-4010 (wjt@nevada.edu)

Segmented faults have distinct sections that may rupture during a single earthquake. Thus, it is important to define segments on individual faults and to evaluate the seismic risk associated with the entire fault as well as with each segment.

In cases where high-quality seismic data are not available, it is more straightforward to define fault segment boundaries rather than the fault segments. Segment boundaries, the connecting zones between segments, may be geometric or behavioral (cf., dePolo and others, 1991, *Journal of Structural Geology*). Geometric boundaries are relatively large bends that are convex toward a normal-fault hanging wall; the fault strike and dip change across a geometric boundary. Geometric boundaries and segments can be simply defined based on marked changes in strike and dip along the trace of a fault. Behavioral boundaries are locations of rupture initiation or termination. Therefore, behavioral boundaries are directly related to earthquakes. A significant issue, then, is whether or not geometric boundaries correspond to behavioral boundaries, and thus, are important to defining seismic hazards.

Along the ~250-kilometer-long, generally north-striking Hurricane fault in southwestern Utah five geometric boundaries are evident. All of these boundaries are marked bends that are convex toward the hanging wall. We suggest that at least two of these geometric bends are also behavioral bends. One of these bends lies near Toquerville, Utah, and the other lies about 15 kilometers south of the Utah-Arizona state line. At each bend (1) the total stratigraphic separation along the fault markedly decreases at the bend suggesting that the numbers or sizes of earthquakes that crossed the bend are different from those that occurred north and south of the bend, and (2) the scarps north of the bend are larger or younger suggesting that the last earthquake on each of the bends were of different ages or sizes. In addition, on the boundary near Toquerville, the number of fault strands south of the boundary is larger than north of the boundary (cf., Stewart and Taylor, 1996, *Journal of Structural Geology*).

Along the ~45-kilometer-long, generally north-striking Hiko fault in southeastern Nevada one geometric boundary is evident. The boundary is broad bend (~8-kilometers-long) and convex toward the hanging wall. This bend is both a geometric and a structural boundary. The fault changes geometry across the bend; specifically the strike changes from north-northeast to north-northwest. This bend also is a structural boundary because the location of the bend is controlled by the location of older northeast- to east-striking oblique-slip faults. The older faults crop out near the north and south edges of the geometric barrier. These faults are presently cut by various strands of the Hiko fault. North of the bend the fault has one to four strands, whereas, south of the bend the fault has six to eight strands. The difference in the number of strands suggests that the number or distribution of earthquakes is different north and south of the bend.

RELATION OF GRAVITATIONALLY DRIVEN LITHOSPHERIC EXTENSION TO LOW SLIP-RATE FAULTS AND REGIONAL SEISMIC HAZARDS IN THE WESTERN U.S.

UNRUH, J.R., Lettis & Associates, William Lettis & As., 1777 Botelho Dr., #262, Walnut Creek, CA 94596 (unruh@lettis.com); C.H. Jones, CIRES, University of Colorado, Boulder; L.J. Sonder Dartmouth College, Hanover, NH

Quaternary normal faults with very low slip rates and long recurrence intervals for surface-rupturing events are well documented in the interior of the western Cordillera. In contrast to plate boundary structures (e.g., the San Andreas fault system in western California) and zones of localized deformation in the interior of the Cordillera (e.g. the Wasatch fault system in Utah), where active faults exhibit slip rates on the order of mm/yr. to tens of mm/yr., low slip-rate faults in mountainous regions of the western U.S. typically move at rates of 10^{-2} to 10^{-4} mm/yr. These structures are best documented in the Sierra Nevada of California, but examples also are present in the Basin and Range and southern Rocky Mountains. Locally, these faults are recognized as potentially significant seismic sources for engineered and critical facilities. To date, however, low slip-rate normal faults have not been the subject of focused research to place them in a regional tectonic context, or to evaluate quantitatively the forces responsible for active (but very slow) extensional deformation of the Cordilleran interior.

We propose that low slip-rate normal faults in areas of high elevation like the Sierra Nevada primarily accommodate slow extension driven by gradients in gravitational potential energy (PE) in the lithosphere. Our previous work (Jones and others, 1996, *Nature*, v. 381, p. 37-41) has shown that PE values over much of the southwestern United States are capable of driving extensional strain rates of 10^{-16} /s to 10^{-15} /s, similar to those measured in the Basin and Range by geodetic and geologic techniques. The Sierra Nevada is characterized by values of gravitational potential energy similar to those in the Basin and Range, which should give rise to similar horizontal tensile deviatoric stresses. Indeed, analysis of seismic focal mechanisms from the Sierra Nevada consistently show evidence for horizontal extension, distinct from strike-slip deformation in the Walker Lane belt to the east. Based on our preliminary analyses using estimates of the average strength of the Sierran lithosphere, we find that the PE available to drive extensional deformation in the northern Sierra Nevada is sufficient to produce average extension rates of 10^{-18} /s to 10^{-17} /s. These extension rates are at least an order of magnitude slower than the average extension rates across the Basin and Range. Total dip-slip displacement of late Miocene volcanic flows along an 70 kilometer NE-SW transect across the northern Sierra Nevada (Page and others, 1995) suggests an aver-

age integrated late Cenozoic extensional velocity of approximately 10-1 mm/yr. The corresponding extensional strain rate is approximately 10^{-17} /s, consistent at the order-of-magnitude level with our predictions derived from PE estimates. Additional work is needed to further evaluate the relations between PE and low slip-rate faults in the Sierra Nevada and other regions of the Cordillera.

The PE-based approach has implications for seismic-hazard assessment in large areas of the western United States. Evaluating hazards associated with low slip-rate faults is problematic using classic deterministic methods because the low rates of activity imply very long return periods between large events. The contribution to total hazard posed by these faults probably is better evaluated using probabilistic techniques. Our approach provides a theoretical basis for confidently assigning very low rates of activity to normal faults outside of well-defined zones of active tectonism. Our method also provides a means of estimating maximum regional strain rates in continental interiors due to PE gradients. Although large uncertainties are attached to the method, it may be useful for assessing the possibility that high-hazard faults (i.e., long rupture segments; high slip rates) have been overlooked by reconnaissance investigations.

SEISMICITY IN THE SGB: WHAT DO EARTHQUAKE CATALOGS ACCURATELY INDICATE?

VON SEGGERN, D. H., and J. N. Brune, *Seismological Laboratory, MS 174, University of Nevada-Reno, MS 174, Reno, NV 89557* (vonseg@seismo.unr.edu)

The Great Basin has not been adequately instrumented for many aspects of seismicity studies, even to the current time. The southern Great Basin is an exception due to issues related to weapons testing and nuclear waste storage. But even here, the duration of the well-determined seismic catalog is short, only starting in the 1960s. The earliest seismic catalog entry is for 1868; this, and most entries until 1932 are based on felt reports. Due to the extremely sparse population of this area, the epicenters are very poorly determined from the felt data and the intensity estimates. Beginning in 1932, earthquakes of reasonable size ($M > 3.5$) in the southern Great Basin were reported by Pasadena and Berkeley. However, the locations were of poor quality, with nominal depths and large epicenter uncertainties. The installation of seismic-monitoring instruments in the 1960s for weapons' tests at the Nevada Test Site improved earthquake catalog quality in the southern Great Basin, but these installations were usually temporary and not utilized specifically for earthquake monitoring. In 1978, the USGS started operation of a network in southern Nevada in support of the Yucca Mountain site characterization program. This network provided continuous coverage of the southern Great Basin through 1995. In late 1995, a network of digital, 3-component instruments was put into operation by the UNR Seismological Laboratory. Although covering a lesser area, this latest network has returned exceptional data quality.

This paper traces the data quality aspects of the seismic catalogs in the southern Great Basin from the felt earthquakes of the late 1800s through the currently detected microearthquakes at Yucca Mountain, as small as -1.0 in magnitude. The limitations of the reported data are discussed, along with estimates of the reliability. Three cases illustrate the problems with seismic-catalog data in the Great Basin. One, a large earthquake in the Death Valley area in 1916 ($M \sim 6$) has a location which changes by up to 100 kilometers, depending on the interpretation of key recordings. Another case, a $M = 3.6$ earthquake originally located within 10 kilometers of Yucca Mountain by Pasadena, was found to lie significantly farther south after a careful re-examination of available seismograms. The last case is the Non-Proliferation Experiment (NPE) of 1993. In spite of excellent first-arrival times and many stations well spaced in azimuth and distance, the epicentral error was 2 kilometers. Other aspects of the southern Great Basin catalogs which hinder unqualified use, are the large number of presumably induced earthquakes in the areas of underground nuclear tests and a significant number of probably falsely identified earthquakes whose signals arise from cultural sources.

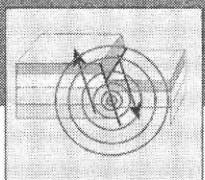
Although the seismic catalog in the southern Great Basin has steadily improved over time, the lack of instrumental locations until just 60 years ago and the cultural component make the earthquake record since the late 1800s somewhat difficult to interpret. Moreover, the relatively slow deformation of the southern Great Basin makes prehistoric measures of seismic activity, such as provided by trenching or precarious rocks, less certain.

THE SEISMO-WATCH WEEKLY EARTHQUAKE REPORT, A WEEKLY BROADCAST OF GLOBAL AND REGIONAL EARTHQUAKE INFORMATION ON COMMUNITY ACCESS TELEVISION

WATSON, Charles P., *Advanced Geologic Exploration, Reno, NV* (watson@seismo-watch.com)

Since November 1996, Advanced Geologic Exploration has featured the television series, "The Seismo-Watch Weekly Earthquake Report" on Sierra Nevada Community Access Television (SNCAT), in Reno, Nevada. The television series consists of a sequence of 7 to 12 non-audio earthquake graphic panels shown on an electronic community message billboard. The panels are nested in a stack of community service messages and are updated on a weekly basis with new information about global and regional earthquake activity. The billboard operates about 70 percent of a 24 hour broadcast schedule and cycles through the message stack about two or three times per hour. This indicates the Seismo-Watch Weekly Earthquake Report is potentially shown from 30-50 times a day, or 200 to 400 times per week per network channel. SNCAT operates a pair of community access channels on two of the primary cable television networks (TCI and Continental Television) in the Reno/Sparks metropolitan area, with a combined potential viewership of 221,000 people from 65,000 homes.

The Seismo-Watch Earthquake Report is built around two panel-sets: two global-activity panels, and two regional-



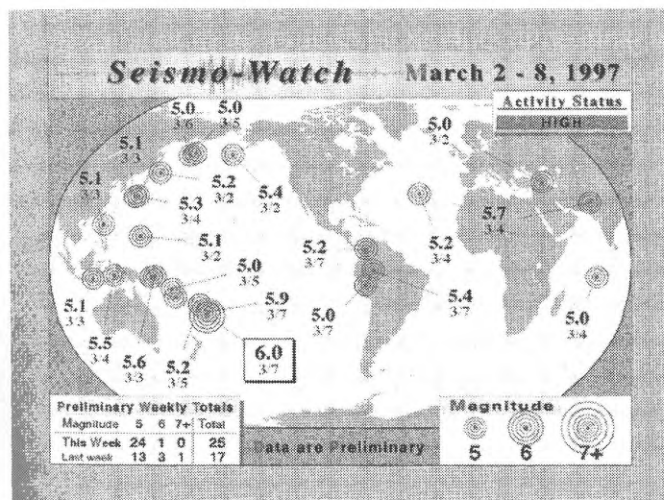
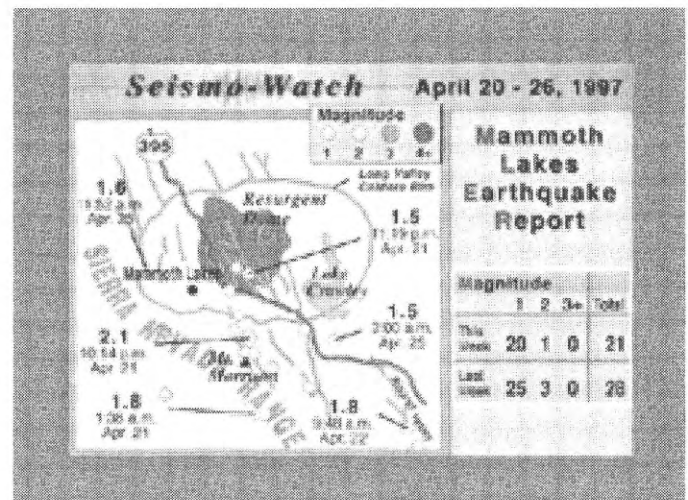
Seismo-Watch

Earthquake
Information Services

The premier source for
earthquake information
presents:

The Seismo-Watch
Weekly Earthquake Report

Produced By:
Advanced Geologic Exploration
Reno, Nevada

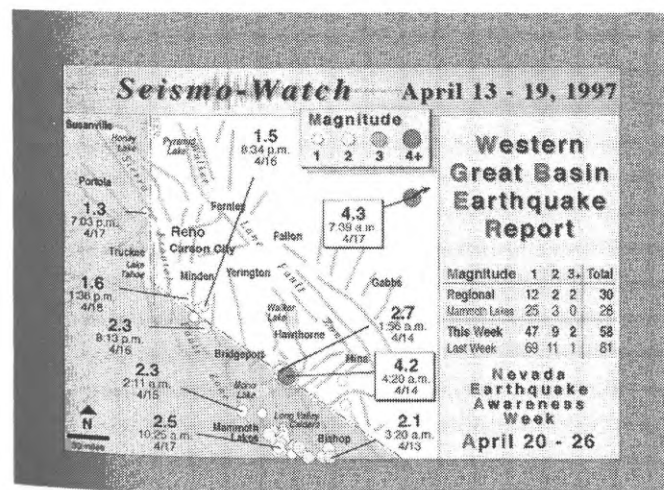
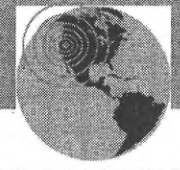


"Get Earthquake Safe"



NEVADA EARTHQUAKE AWARENESS AND MITIGATION WEEK APRIL 20 - 27

Seismo-Watch

Support for The Seismo-Watch Weekly Earthquake Report is provided in part by:

INETworld, Inc.
Reno, Nevada
An Internet Service Provider
for the Reno/Carson area
324-1211

Your Name Here
Reno, Nevada
A one to two line statement describing your excellent products or services provided by your company.

activity panels. Each panel-set includes an earthquake activity base map and a discussion panel, or Seismic Summary, which highlights significant or notable earthquake activity during the week using bullet text form. Earthquake activity base maps feature magnitude, time, and date annotations for epicenters plotted on well-designed and colorful base maps. Earthquake magnitude totals are summarized for the current week as well as for the previous week. The global map presents M5+ earthquake activity and the regional map features M+1.0 seismicity for the California/Nevada border region, including the very active Mammoth Lakes region and Long Valley caldera. Data sources include the National Earthquake Information Center, U. S. Geological Survey, and the Seismological Laboratory at University of Nevada, Reno.

These foundation panel-sets are preceded by an Introduction panel which highlights the sequence content, and followed by three panels: (1) a Source panel presenting the data and information sources, (2) a Preparedness panel which presents earthquake safety tips and emergency preparedness procedures, and (3) an Exit panel showing the Advanced Geologic Exploration contact number for more earthquake and preparedness information. Special Earthquake Report panels are also inserted in the sequence to show information about notable earthquake activity from outside the region. Program underwriters are acknowledged with a one-line organization or company slogan in a format similar to the Public Broadcasting System. Underwriting panel(s) are inserted after the Introduction panel and/or before the Exit panel.

The weekly television series of the Seismo-Watch Earthquake Report begins a new era of transferring earthquake information from the seismic-monitoring networks to the public at large via an effective media – television. With its excellent graphic presentation, high broadcast frequency, and its relatively economical format, Seismo-Watch Earthquake Report provides the people of the Reno/Sparks metropolitan area with increased awareness to earthquake activity of their region. The community message billboard is a common feature for Community Access Television stations throughout the United States, and similar broadcasts for these networks are being explored.

CHARACTER OF LATE QUATERNARY LOW-ANGLE(?) NORMAL FAULTING ON THE NORTH-WESTERN SIDE OF THE RUBY MOUNTAINS / EAST HUMBOLDT RANGE, NORTHEASTERN NEVADA

WILLOUGHBY, C.H., and S.G. Wesnousky, *Center for Neotectonic Studies, MS 169, University of Nevada, Reno, NV 89557, (chrisw@seismo.unr.edu, stevew@seismo.unr.edu)*

Triangular facets on the range front and fault scarps of varying height in Quaternary glacial and alluvial deposits indicate the presence of an active normal fault along the northwestern side of the Ruby Mountains and East Humboldt Range. We are currently examining the neotectonic character of the fault within an area ~10 kilometers west of Ruby Dome in the south, to an area near the small town of Welcome on Interstate 80 in the north.

The fault trace exists either as an active range-front trace, or as an active piedmont trace ~5 kilometers outboard from a less active range-front trace. The active trace of the fault consists of three major overlapping en echelon traces each separated by a ~5 kilometer left-step. Slopes are less steep and triangular facets are less developed where faulting exists outboard of the range front. The fault forms grabens ~50 to 200 meters wide at many localities.

Interpretations of a seismic profile line in Lamoille Valley by previous workers suggest that a 15 to 20 degree dipping fault zone projects up to scarps in Quaternary deposits at the range front of the northern Ruby Mountains. In addition, the slope of triangular facets from apex to fault trace is 14 to 23 degrees throughout the study area. Hence, the fault zone in this study possibly dips at a low angle.

Previous workers recognize two ages of glacial deposits: the older more extensive Lamoille (early Wisconsin), and the younger Angel Lake (late Wisconsin). At the mouth of Lamoille, Seitz, and Hennen Canyons, the fault offsets glacial moraines and glacial outwash surfaces. Offset Lamoille moraine crests at Seitz Canyon indicate the displacement on the fault is principally dip-slip. Measurements of an offset Lamoille glacial moraine crest constrain a slip-rate of 0.1 to 1.0 mm/yr. The smallest vertical separations on Angel Lake and correlative surfaces are 1 to 2 meters along the southern 32 kilometers, and 2 to 3 meters along the northern 41 kilometers of the fault zone. Assuming the scarp measurements represent a single event that ruptured the entire fault zone, a M_w 7.2 or greater earthquake occurred sometime in the past 13 to 20 kyr.

RECENT MICROSEISMICITY IN THE WESTERN SNAKE RIVER PLAIN, IDAHO, AND TRENCH EVIDENCE FOR RECURRENT LATE QUATERNARY FAULTING NEAR THE WSRP SOUTHERN MARGIN

ZOLLWEG, J. E., G. S. Beukelman, and C. J. Waag, *Dept of Geosciences, Boise State University, Boise, ID 83725 (zollweg@sisyphus.idbsu.edu)*

The Western Snake River Plain (WSRP) of southwestern Idaho is a large northwest-trending graben bounded by complex late Cenozoic normal-fault zones. The age of most recent faulting related to WSRP development has been commonly accepted to be in excess of 100 kyr. Historically, the WSRP and its margins have been an area of extremely low seismicity, although until recently location thresholds have been limited to $M = 4+$ events. A small number of recent earthquakes in the $M = 1-2$ range demonstrate the WSRP is seismically active at the microearthquake level, with epicenters located in the interior and near both margins of the WSRP.

Scarp slope/height characteristics indicate Holocene surface rupture occurred on the Halfway Gulch fault at the WSRP southern margin, and on the Water Tank fault located about 8 kilometers into the WSRP. Trenching of a late Quaternary fan deposit offset by the Water Tank fault revealed a sequence of five complete and one partial colluvial wedges, suggesting a minimum of 6 earthquakes have occurred in the late Pleistocene and Holocene. Colluvial-wedge thicknesses were used to estimate moment magnitudes of approximately 6.5 to 6.7 for the five most recent events. Pedogenic carbonate analysis of wedge deposits indicates the five most recent events occurred within approximately the past 30 kyr, and that the most recent event occurred about 3 kyr. The recurrent fault motion and the observed microseismicity are evidence that portions of the WSRP are tectonically active. The majority of Idaho's population resides within the WSRP, and this study indicates that seismic hazard in the Boise-Mountain Home area may be greater than was previously thought.

PAPERS

1997 UNIFORM BUILDING CODE GROUND-SHAKING CRITERIA

Robert E. Bachman, S.E.
Fluor Daniel, Inc., 3353 Michelson Drive
Irvine, California 92698

ABSTRACT

The recently published 1997 Uniform Building Code (UBC) incorporates two significant changes to the ground-shaking criteria which apply to all structures. The first change is a revision to soil types and soil-amplification factors. The second change is the incorporation of near-source factors in UBC seismic zone 4. Together these changes result in the largest increases in code ground-shaking criteria in the past 30 years. Records obtained from the Strong Motion Instrumentation Program (SMIP) along with U.S. Geological Survey (USGS) records were the primary sources of data used to justify these code changes.

SOIL TYPES AND SOIL-AMPLIFICATION FACTORS

The ground shaking basis for code design is reflected in the 5 percent damped elastic response spectra shown in figure 1 (UBC figure 16-3). The response spectra is defined in terms of two site seismic coefficients C_a and C_v . The site seismic coefficients are determined as a function of seismic zone; soil type; and in zone 4, near-source factors. The soil profiles are subdivided into six types based on the average soil properties in the top 100 feet of the soil profile. The types are identified as S_A through S_F and are defined in accordance with table 16-J (attached) from the 1997 UBC. The types are based on consensus deliberations from the USGS/National Center for Earthquake Engineering Research (NCEER)/Structural Engineers Association of California (SEAOC) workshop held at the University Southern California (USC) in 1992. These are identical to the soil-profile types found in 1994 National Earthquake Hazards Reduction Program (NEHRP) Provisions.

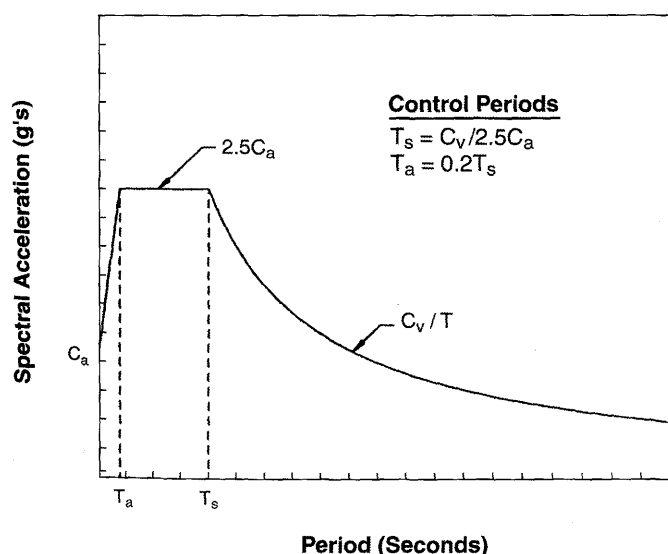


Figure 1. Design response spectra.

The site seismic coefficients C_a and C_v are determined from tables 16-Q and table 16-R (attached) based upon the soil-profile type; seismic zone; and in UBC zone 4, the near source factors N_a and N_v . It should be noted that the value of the soil factors depart significantly from previous codes in that both short-period and long-period structures are affected by soil effects and that the amplifications increase significantly at lower ground-acceleration levels. In previous codes soil effects were only considered for long-period structures. The amplification factors are consistent with the consensus from the previously referenced USC workshop and are identical to those found in the 1994 NEHRP provisions. These effects are consistent with observations in the Mexico City and the Loma Prieta earthquakes.

NEAR-SOURCE FACTORS

The near-source factors were developed by the Ground-Motion Ad Hoc Committee of the SEAOC Seismology Committee to account for the effects of ground motions near the source of seismic events. The factors are a refinement of what was developed for seismically isolated structures included initially in the 1991 UBC. Near-source ground-motion records and observed damage from Northridge and Kobe have provided convincing evidence of significantly more intense ground shaking near the fault rupture than had been previously accounted for.

In order to establish the near-source factors, the first step is to identify and locate known active faults in UBC zone 4 and classify them into one of three source types based on maximum moment magnitude and slip rate in accordance with table 16-U (attached). Faults are classified based on their maximum magnitude M , and slip rate, R . Type A sources are faults that have a moment magnitude potential of $M \geq 7.0$ and a slip rate of $R \geq 5$ mm/year. These types of faults are considered to be active and capable of producing large magnitude events. Most segments of the San Andreas fault would be classified as a Type A fault. Type C sources are faults that have a moment magnitude potential of M less than 6.5 and a slip rate of R less than or equal to 2 mm/year. Type C faults are

Table 16-J. Soil Profile Types

Soil Profile Type	Soil Profile Name/Generic Description	Average Soil Properties for Top 100 Feet (30 480 mm) of Soil Profile		
		Shear Wave Velocity, \bar{v}_s feet/second (m/s)	Standard Penetration Test, \bar{N} (or \bar{N}_{ch} for cohesionless soil layers) (blows/foot)	Undrained Shear Strength, \bar{S}_u psf (kPa)
S _A	Hard rock	>5000 (1500)		
S _B	Rock	2,500 to 5,000 (760 to 1500)		
S _C	Very dense soil and soft rock	1,200 to 2,500 (360 to 760)	>50	>2,000 (100)
S _D	Stiff soil profile	600 to 1,200 (180 to 360)	15 to 50	1,000 to 2,000 (50 to 100)
S _E ¹	Soft soil profile	<600 (180)	<15	<1,000 (50)
S _F	Soil requiring site-specific evaluation. See Section 1644.3.1			

¹ Soil profile Type S_E also includes any soil profile with more than 10 ft (3048 mm) of soft clay defined as a soil with a plasticity index, $PI > 20$, $w_{mc} > 40$ percent and $\bar{S}_u < 500$ psf (25 kPa). The Plasticity Index, PI , the moisture content, w_{mc} , shall be determined in accordance with approved national standards.

Table 16-Q. Seismic Coefficient C_a

Soil Profile Type	Seismic Zone Factor, Z				
	Z = 0.075	Z = 0.15	Z = 0.2	Z = 0.3	Z = 0.4
S _A	0.06	0.12	0.16	0.24	0.32N _a
S _B	0.08	0.15	0.20	0.30	0.40N _a
S _C	0.09	0.18	0.24	0.33	0.40N _a
S _D	0.12	0.22	0.28	0.36	0.44N _a
S _E	0.19	0.30	0.34	0.36	0.36N _a
S _F	See Footnote 1				

¹ Site-specific geotechnical investigation and dynamic site response analysis shall be performed to determine seismic coefficients for Soil Profile Type S_F.

Table 16-R. Seismic Coefficient C_v

Soil Profile Type	Seismic Zone Factor, Z				
	Z = 0.075	Z = 0.15	Z = 0.2	Z = 0.3	Z = 0.4
S _A	0.06	0.12	0.16	0.24	0.32N _v
S _B	0.08	0.15	0.20	0.30	0.40N _v
S _C	0.13	0.25	0.32	0.45	0.56N _v
S _D	0.18	0.32	0.40	0.54	0.64N _v
S _E	0.26	0.50	0.64	0.84	0.96N _v
S _F	See Footnote 1				

¹ Site-specific geotechnical investigation and dynamic site response analysis shall be performed to determine seismic coefficients for Soil Profile Type S_F.

considered to be sufficiently inactive and not capable of producing large magnitude events such that potential near-source ground-shaking effects can be ignored. Most faults outside of California are Type C. Type B sources are all faults that are not either Type A or Type C and include most of the active faults in California. The 1997 UBC requires that the locations and characteristics of these faults be established based on geotechnical data from reputable sources such as the California Division of Mines and Geology (CDMG) and the USGS.

Once faults are located relative to a site and the source type is established, the near source factors N_a and N_v are determined in accordance with tables 16-S and 16-T (attached). These factors were established by the Ground-Motion Ad Hoc Committee and are based on the average increase, measured in the near field from Northridge and other earthquakes. The near-source factors apply to both

strike-slip and reverse-slip (thrust) fault mechanism although reverse-slip faults produce about 20 percent greater shaking on average. The short period (acceleration domain) near-source factor (N_a) is based on response at 0.3 seconds and long-period (velocity-domain) near-source factor (N_v) based on a 1.0 second response. Values of N_v are bumped upward by about 20 percent to account for the increase in average response in the fault-normal direction above that predicted by the attenuation function for the random component of horizontal ground shaking (ref. Somerville, 1996 7th US/Japan Workshop, Lessons learned from Kobe and Northridge). The commentary to the SEAOC bluebook notes ground shaking at "forward directivity" sites is likely to be 1.25 times the C_v and C_a coefficients based on average fault-normal response. The values of N_a and N_v are used in tables 16-S and 16-T to determine the values of C_a and C_v in UBC Zone 4 ($Z = 0.40$).

Table 16-U. Seismic Source Type¹

Seismic-Source Type	Seismic Source Description	Seismic Source Definition	
		Maximum Moment Magnitude, M	Slip Rate, SR (mm/year)
A	Faults that are capable of producing large magnitude events and which have a high rate of seismic activity	$M \geq 7.0$ and	$SR \geq 5$
B	All faults other than Types A and C		
C	Faults which are not capable of producing large magnitude earthquakes and which have a relatively low rate of seismic activity	$M < 6.5$ and	$SR \leq 2$

¹ Subduction sources shall be evaluated on a site specific basis.

Table 16-S. Near-Source Factor N_a ¹

Seismic-Source Type	Closest Distance to Known Seismic Source ^{2,3}		
	≤ 2 km	5 km	10 km
A	1.5	1.2	1.0
B	1.3	1.0	1.0
C	1.0	1.0	1.0

¹ The near-source factor may be based on the linear interpolation of values for distances other than those shown in the table.

² The location and type of seismic sources to be used for design shall be established based on approved geotechnical data (e.g. most recent mapping of active faults by the United States Geological Survey or the California Division of Mines and Geology).

³ The closest distance to seismic source shall be taken as the minimum distance between the site and the area described by the vertical projection of the source on the surface (i.e., surface projection of fault plane). The surface projection need not include portions of the source at depths of 10 km, or greater. The largest value of the near-source factor considering all sources shall be used for design.

Table 16-T. Near-Source Factor N_v ¹

Seismic-Source Type	Closest Distance to Known Seismic Source ^{2,3}			
	≤ 2 km	5 km	10 km	15 km
A	2.0	1.6	1.2	1.0
B	1.6	1.2	1.0	1.0
C	1.0	1.0	1.0	1.0

- ¹ The near-source factor may be based on the linear interpolation of values for distances other than those shown in the table.
- ² The location and type of seismic sources to be used for design shall be established based on approved geotechnical data (e.g. most recent mapping of active faults by the United States Geological Survey or the California Division of Mines and Geology).
- ³ The closest distance to seismic source shall be taken as the minimum distance between the site and the area described by the vertical projection of the source on the surface (i.e., surface projection of fault plane). The surface projection need not include portions of the source at depths of 10 km, or greater. The largest value of the near-source factor considering all sources shall be used for design.

DISTANCE FROM FAULTS AND FAULT MAPS

The rules for measuring distance from a fault were also established by the Ground-Motion Ad Hoc Committee and are found in the code. The rules are illustrated in figure 2 for a variety of fault types and depths. It is interesting to note that for non-vertical faults, a zero distance fault zone has been established as illustrated. The distance from a fault is measured from this zero distance fault zone.

Active fault near-field maps are currently being devel-

oped for California zone 4 by the CDMG. The form of the maps will be like a Thomas Guide and will be at a scale of 1:150,000. The background will include street maps and freeways. An individual will be able to find their house on the maps. The USGS is providing fault information developed for the 1997 NEHRP Provisions ground-motion maps for areas outside of California. The maps will be published for sale by International Conference of Building Officials in fall of this year. Examples of the legend sheet are shown in figure 3 and examples of expected near-field maps are shown in figures 4 and 5.

1997 UBC NEAR SOURCE FACTOR RULES FOR DETERMINING PLOTTED FAULT LOCATION AND DISTANCE FROM FAULT

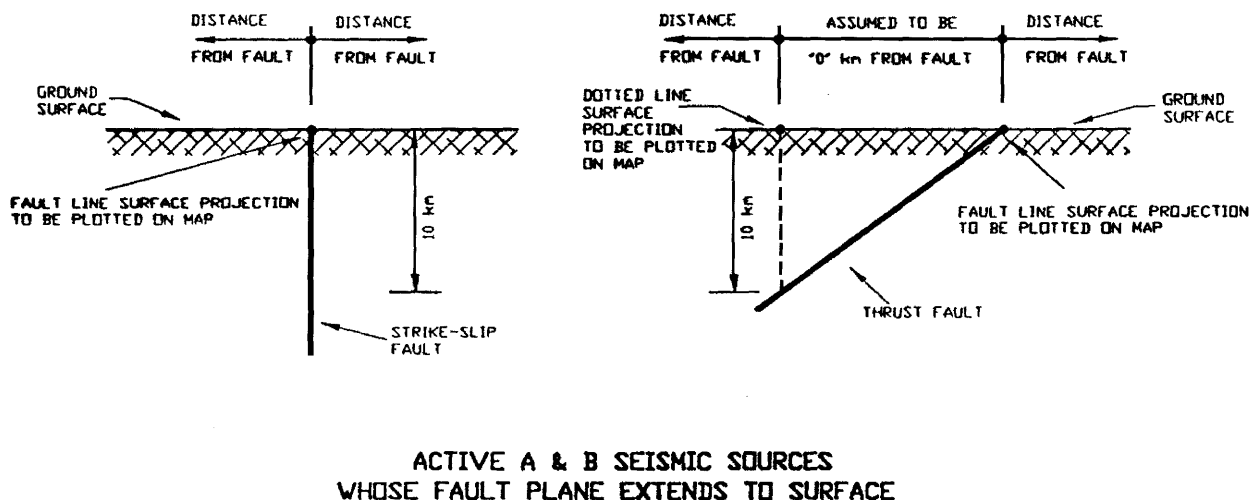


Figure 2. 1997 UBC near-source factor, rules for determining plotted fault location and distance from fault.

Figure 2 (continued)

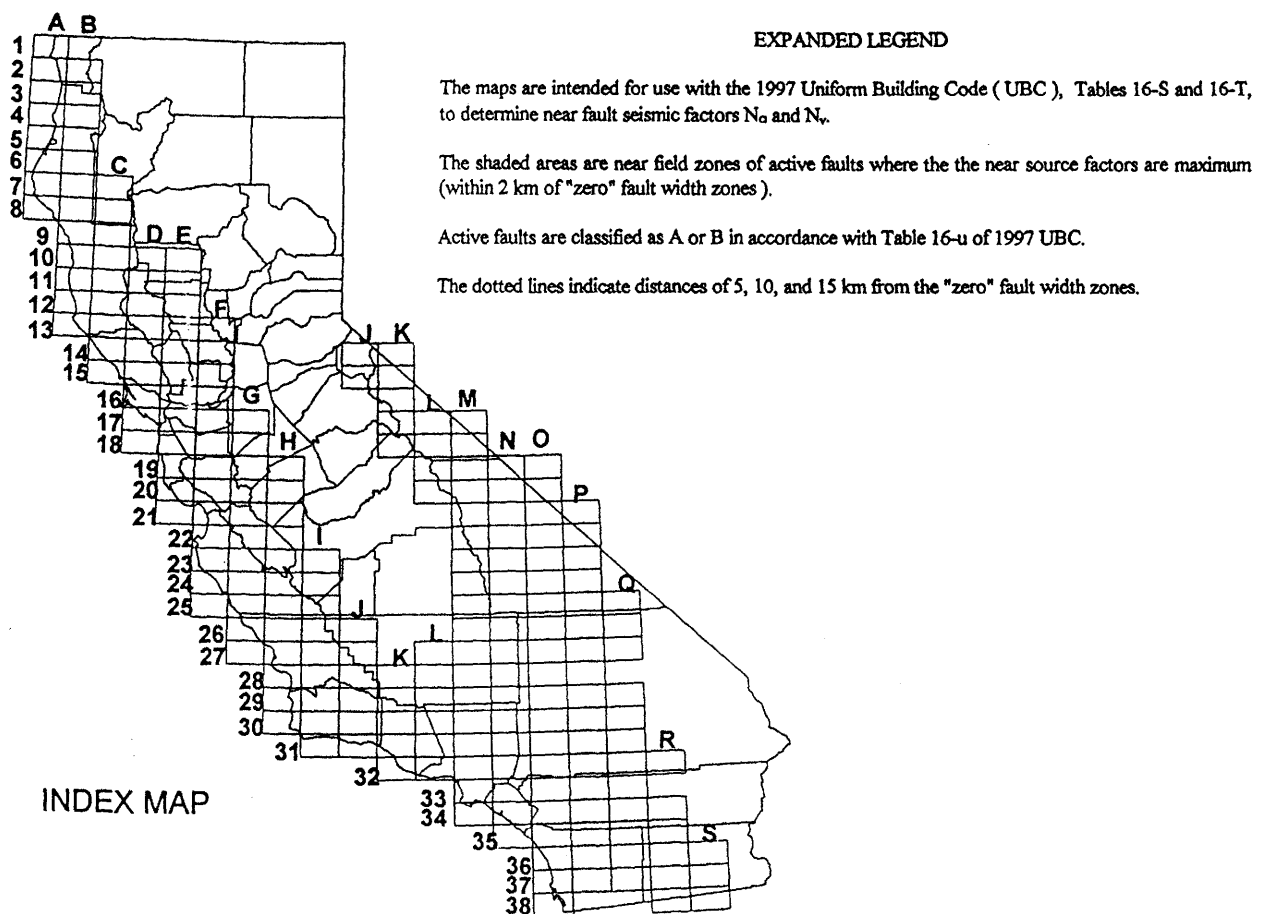
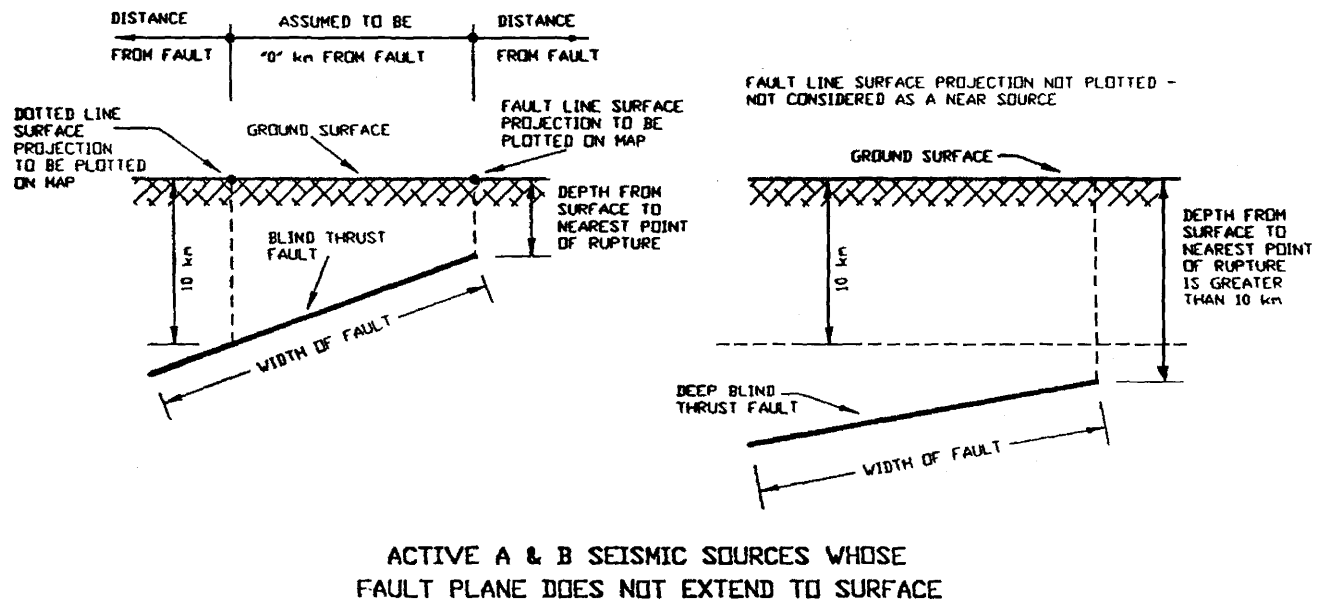
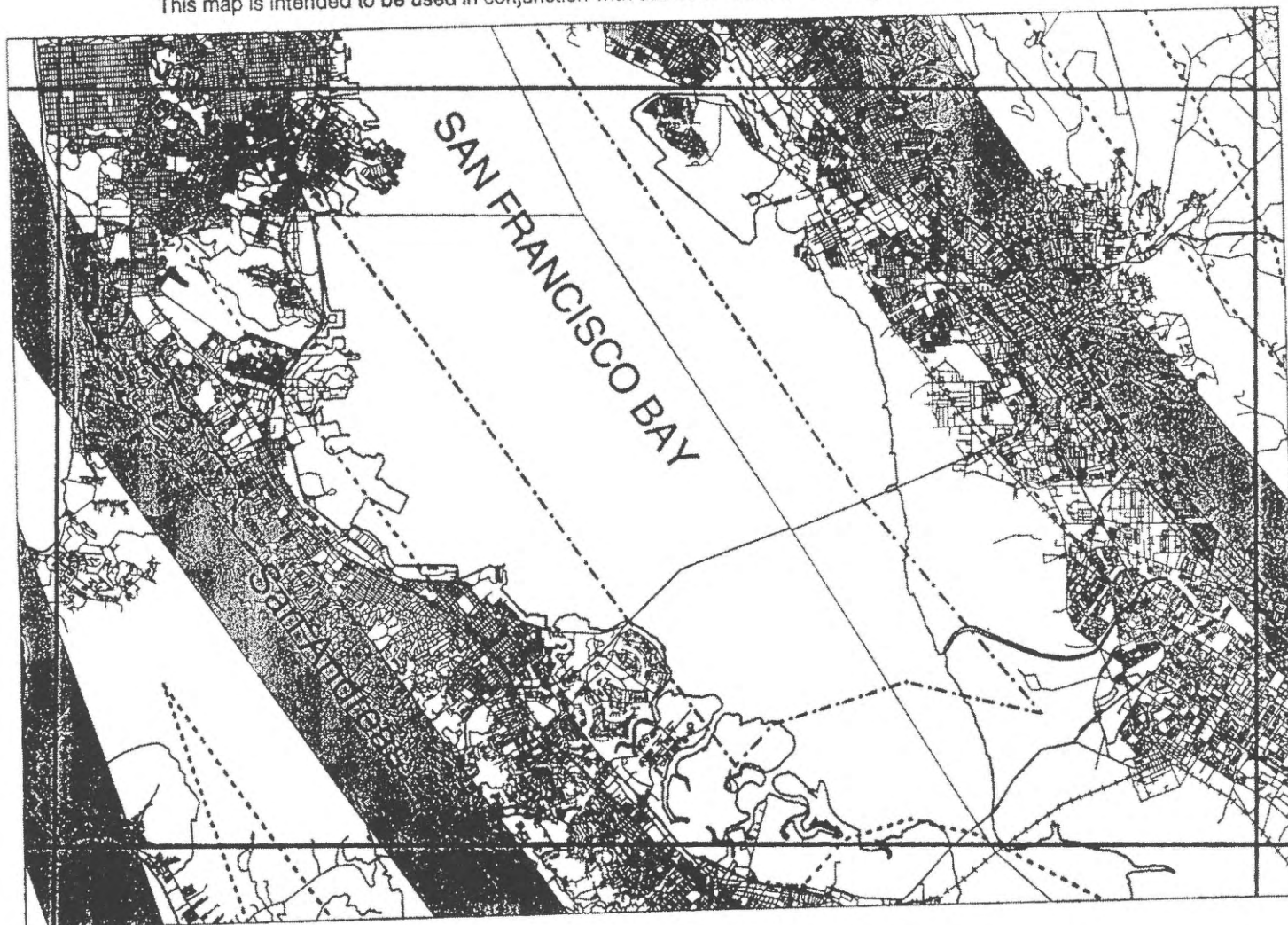


Figure 3. Example legend page for near-field fault maps.

X-15

Active Fault Near Field Zones

This map is intended to be used in conjunction with the 1997 Uniform Building Code, Tables 16-S and 16-T



X-15

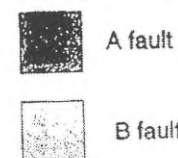
Department of Conservation
Division of Mines and Geology



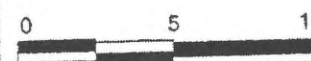
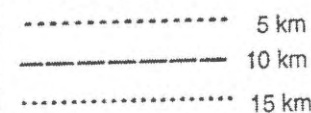
LEGEND

See expanded legend and index map

Shaded areas are within 2 km of active zero width zone.



Contours of closest distance to fault zero width zone



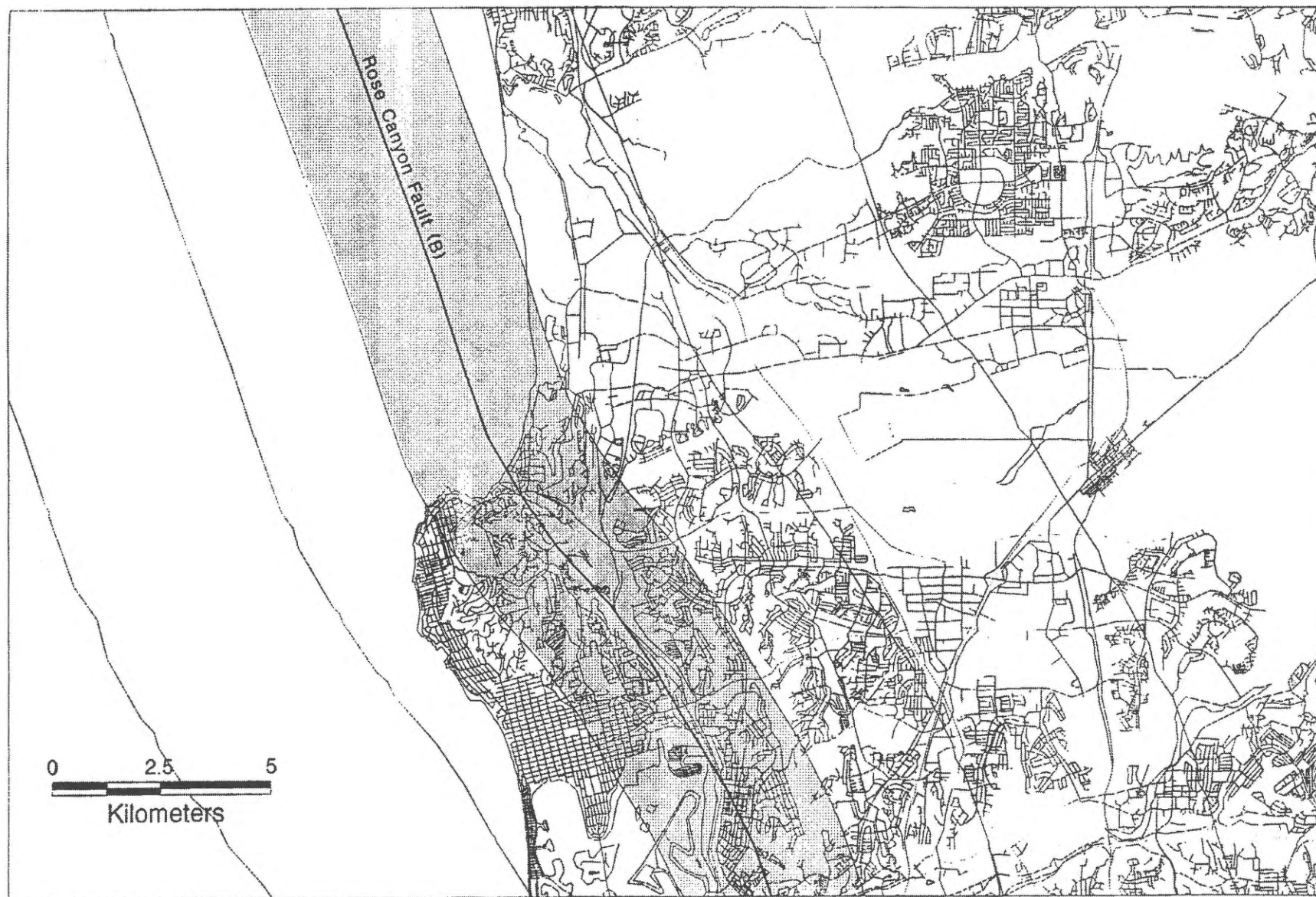
Kilometers
1/4" is approximately equal to 1 km

August, 1997

Figure 4 Example of active fault near-field map for San Francisco Bay area.



CALIFORNIA DEPARTMENT OF CONSERVATION
DIVISION OF MINES AND GEOLOGY



Near fault zones, La Jolla, City of San Diego. (Scale 1: approx. 98,000)

Figure 5. Example of active fault near-field map for La Jolla, City of San Diego.

CONCLUSION

The inclusion of soil and near-field effects in the 1997 UBC represent one of the most state-of-the-art, meaningful, and impactful changes in the code by the geoscience community in the history of seismic codes. The effects will continue to be improved in the new International Building Code which replaces the UBC beginning in the year 2000.

REFERENCES

- dePolo, Craig M., 1997, Written communication (Data from an advanced chapter of dePolo's dissertation).
- Euge, K. M., and Schell, R.G., 1992, Development of Seismic Maps for Arizona, Final Report: Prepared for the Arizona Department of Transportation, Report Number; FHWA-AZ92-344.
- Geomatrix Consultants, 1995, Seismic design mapping state of Oregon, Personal Services Contract 11688: Report prepared for the Oregon Department of Transportation and many faults from Pezopane, S.K., 1993, Active faults and earthquake ground motions in Oregon, Ph.D. dissertation, 208 pp., University of Oregon, Eugene.
- Haller K. M., and Dart, R.L., 1995, Digital map and database of Quaternary faults in Montana: Geological Society of America Abstracts with Programs, v. 27, no. 4 p. 13.
- Hecker, S., 1993, Quaternary tectonics of Utah with emphasis on earthquake-hazard characterization: Utah Geological Survey Bulletin 127, 157 p., 6 pl.
- Kirkham, R. M., and Rogers, W. P., 1981, Earthquake potential in Colorado: Colorado Geological Survey Bulletin 43, 171 p.
- Machette, M. M., Unpublished data.
- Machette, M.N., 1987a, Preliminary assessment of paleoseismicity at White Sands Missile Range, southern new Mexico--Evidence for recency of faulting, fault segmentation, and repeat intervals for major earthquakes in the region: U.S. Geological Survey Open-File Report 87-0444, 46 p.
- 1987b, Preliminary assessment of Quaternary faulting near Truth or Consequences, New Mexico: U.S. Geological Survey Open-File Report 87-652, 40 p.
- McCrary, P.A., 1995, Fault-hazard evaluation in the Humboldt area, northwestern California: Submitted as a U.S. Geological Survey Open-File Report, 76 p.
- Petersen, M. D., Cramer, Chris, and Bryant, William, 1995, Written communication. Many references found in Petersen, Mark D. and Wesnousky, Steven G., 1994, Fault slip rates and earthquake histories for active faults in Southern California; Bulletin of the Seismological Society of America, v. 84, no. 5, pp 1608-1649.
- Wesnousky, S. G., 1986, Earthquakes, Quaternary faults and seismic hazard in California, Journal of Geophysical Research, v. 91, p. 12,587-12,631.
- Ostenaar, D., Manley, W., Gilbert, J., LaForge, R., Wood, C., and Weisenberg, C.W., 1990, Flathead Reservation regional seismotectonic study--An evaluation for dam safety: U.S. Bureau of Reclamation Seismotectonic Report 90-8, 161 p., 7 pl.

WHAT EMERGENCY MANAGERS NEED FROM GEOSCIENTISTS

Stephen Weiser

Idaho Bureau of Disaster Services
4040 Guard Street Boise, Idaho 83705
sweiser@bds.state.id.us

With all the sophisticated maps on display at this conference, it's easy to forget that for some emergency managers, the most important map in our portfolio is the Seismic Zonation map of the Uniform Building Code (UBC). For a number of states in the Basin and Range Province, the essential task still is to convince government-wary populaces that building codes are useful, important, and ultimately cost-beneficial. Idaho, for instance, does not have a state-wide building code, so we have a wide range of enforcement—from the current edition of the UBC to the 1973 edition to none at all. Not surprisingly to us, none at all includes a county that is partly zone 4. Luckily, all our major urban areas enforce a current edition of the code, which will have a positive impact on a rapidly growing new building stock. And many cities are also adopting or at least applying the Uniform Code for Building Conservation, which will strengthen unreinforced masonry buildings when they are renovated to trendy restaurants, upscale offices, and boutiques. We're making progress, but it's a real challenge to convince 44 counties and a score of towns that earthquakes are something to prepare for.

After the UBC map, my next most-used map is one of historic epicenters in and near Idaho to get people's attention, and then a map of faults with Plio-Pleistocene to Holocene offsets to remind them why our scenic mountains are scenic. Plio-Pleistocene may be cheating, but with long recurrence intervals for our earthquakes, I need convincing that it is truly dishonest. I also use a lot of isoseismic maps to show people that earthquakes don't need to be close to be dangerous. Isoseismic maps of course report on the perception of physical phenomena, but by people who have no idea of the difference between ML and MB, and are therefore inherently non-scientific.

Modified Mercalli, an extended concept of "active fault," and straight peak-ground-acceleration maps are not very sophisticated in comparison with what we see next door. But for emergency management in Idaho, shaking is shaking, and shaking is what knocks down chimneys, buildings, and bridges. As soon as we have a significant awareness of seismic safety and a conscious, state-wide application of measures to increase it, then we can invest in the concepts that drive the maps next door.

So what do we need from scientists? We have your embarrassingly old stuff and we use it in grossly unprofessional ways to accomplish devious goals. So what else could we possibly want from you?

Cooperation—several kinds of cooperation. At the most obvious and most crassly opportunistic level, there is good reason for emergency managers and geoscientists to talk to each other. Just as your science can lend credibility to our efforts, our needs can fund science. As an example, a 1991 study by Breckeridge and Sprengle, *Seismic Inten-*

sities in Idaho, was funded partly by the Idaho Bureau of Disaster Services as a foundation for a study of seismic exposure of Idaho public school buildings by the University of Idaho School of Engineering. Seismic Intensities is a probabilistic assessment for the state on a regional basis, and, because of limited historical records, the region around Pocatello in southeast Idaho indicates a surprisingly low hazard from shaking, given its proximity to major active fault systems. Such a low hazard doesn't appear consistent with the message we're delivering to the rest of the state.

To get another perspective, we have worked on a multi-year project with the Idaho Geological Survey to characterize the alluvial soils of the valley in which Pocatello is located and to assess amplification potential using two deterministic events, a near-field "background" quake and a distant large-magnitude event. The results of this study are useful to emergency management in discussing seismic-safety issues in Pocatello. And IGS was able to combine our grant with other funds to support its urban mapping, soil characterization, acquisition of modeling software, and a doctoral dissertation.

We also need a model for basin-and-range earthquakes, including a definition for "active" faults. For instance, Idaho's local land-use planning act requires counties to assess the impact of surface ruptures and shaking, but gives no further guidance. California's ten-thousand year rule appears arbitrarily in various places, such as EPA's regulations for siting of landfills, and is commonly applied as a definition of "active," but few people know why. We talk to folks about long recurrences tempered by segmentation, but it would be useful to point to a Respected Name - citing authority being an important tool for convincing people of things hard to believe. A more regionally defined set of parameters like attenuation and recurrence would be useful for modeling and evaluating urban hazard to complement the current risk-assessment program, HAZUS, being used by us in mitigating seismic risk in Idaho.

And we need your cooperation when the press calls. There is usually a reason for their calling - an event or anniversary, something that makes a story. So when the press shows up, recognize it as an opportunity to advance both our causes.

Realistic scenarios would be helpful to our cause. Hardly anyone reacts to worst-case projections of death and destruction. While extreme visions hold a fascination for many of us - and certainly emergency managers are among the most gleeful - they frustrate attempts to promote mitigation. People's reaction is, not unreasonably, if we are going to experience a catastrophic event that can be mitigated only by infusion of gigabucks for rebuilding our cities and towns, we'll just have to live with the threat.

But if we prepare for less-than-catastrophic events, not only are the fixes less costly, but reducing recurrence intervals to something less than the span of human civilization makes selling the fixes a lot easier. And of course, if we are prepared for moderate events, we are better prepared for large ones.

Next, no hobby horses. Reporters are looking for a story, you can confuse them by giving them stories that they don't know how to deal with. Help them to focus on the one they came to get. This is not the time to espouse pet theories or attack colleagues. Even though it catches in your throat, say "Most seismologists think that . . ."

And finally, consistent stories are essential to dealing with skeptical publics. Everybody is guilty of inconsistency. When we discuss seismic hazards, we often mix in risk without any definitions - a hazard puts people "at risk," but this is a different kind of risk than potential dollar losses. And again, worst-case scenarios do little to convince people of mitigation or reasoned approaches to preparedness.

And then, with respect to consistent stories, I return to maps. FEMA publishes colored maps that picture Idaho

entirely red like California, and at the same time they publish maps that make most of the state look like an aseismic paradise. Neither version resembles UBC maps. Likewise, USGS maps, NEHRP maps, and state maps all have their own flavor that, because they all seem to speak with equal authority, cloud the issue for the people we are trying to convince. And how about the map that graces the cover of this conference? I'm here because I'm convinced that basin-and-range seismicity has a direct impact on Boise. And what kind of support do I get from this map?

So after cooperation at that most important level of funding and technical support, what we want from you is another kind of cooperation - a recognition that emergency management is not another scientific forum. Instead, it is a sober, narrow, prosaic institution - one that provides all of us an opportunity to reinforce a sober, narrow, prosaic message: *Natural hazards surround us, and we can neither predict nor prevent them. But, as wise and prudent creatures, we can take wise and prudent measures to lessen their effect on our infrastructure, our communities, and our lives.*

CHALLENGES OF CHARACTERIZING SEISMIC HAZARDS IN THE BASIN AND RANGE PROVINCE

Clarence R. Allen, Seismological Laboratory, California Institute of Technology, Pasadena, CA 91125

I am somewhat embarrassed to be standing here today speaking on this topic, because at least half of the audience knows more about the subject than I do! But I've been asked to "set the stage" for the conference, at least in a geological and seismological context, and that I'll try to do - particularly for those of you who are not geologists or seismologists. And I have the great advantage in this role, as compared to subsequent speakers, of being permitted to ask questions that I cannot answer!

The first and foremost question for this conference is whether, from the seismic-hazard point of view, the Basin and Range Province is unusual. That is, is it worthy of a special conference or "summit" devoted to this subject alone? I think the answer is "yes," and let me explain why.

The Basin and Range Province is certainly not the only area in the world of active normal faulting. But before I go further, let me explain to the non-earth scientists that the word "normal" in this context is geological jargon that might perhaps be easily misunderstood. Are all faults divided into two categories, "normal" and "abnormal"? In fact, in the minds of early coal miners in England, this was indeed the case. The usual or "normal" situation was to encounter in the mine faces steeply slanted faults whose displacements of the coal-bearing strata reflected horizontal extension, and thus the word "normal" came to be associated with this particular style of faulting. Only subsequently have geologists learned that the coal mines of England are, in fact not typical of the rest of the world. Particularly for large, damaging earthquakes, causative faults associated with horizontal compression (i.e., thrust and reverse faults) are far more numerous than those associated with crustal extension. But the word "normal fault" has nevertheless remained in the geological jargon as describing extensional faulting such as that characteristic of the Basin and Range Province.

The astute listener might ask, parenthetically, whether, if compressional faults outnumber extensional faults worldwide, should not the Earth be getting smaller with time? The fact is, we now think that the bulk of the extension is going on beneath the ocean floor - in the regions of the mid-oceanic ridges - where the newly generated crustal materials are sufficiently hot so that large earthquakes do not typically occur, despite the large extensional strains. Thus, we think that worldwide extension really is roughly equal to worldwide compression, although large earthquakes in themselves do not manifest this equality.

But to return to the question of the uniqueness of the Basin and Range Province, there are, in fact, a number of other worldwide areas on the continents that are also typified by normal faults. But none of these areas has either the great areal extent or the high degree of seismic activity as that of the Basin and Range Province. The east African rift valleys, for example, cover an area about as long as that of the Basin and Range Province (from Montana to Sonora - some 2,000 kilometers), but not as wide nor nearly as active; only one earthquake exceeding magni-

tude 6.4 has occurred in this part of east Africa within the historical record. Thus, the Basin and Range Province really is some-what unusual, and it really does have some aspects of seismic-hazard assessment that deserve special study and discussion.

Because most large, damaging earthquakes worldwide are associated with thrust and reverse faults, we sometimes forget that areas of normal faulting can also be associated with disastrous earthquakes. In fact, seven normal fault earthquakes of magnitude 7.2 or greater have occurred in the Basin and Range Province within the historical record, and this represents a very short period of only about 150 years. In this context, one should note that both the 1989 Loma Prieta and 1994 Northridge earthquakes in California were of lesser magnitude than any of these seven Basin and Range earthquakes.

What is the largest worldwide normal-fault earthquake of record? Insofar as I am aware, it is the 1933 Sanriku earthquake off the coast of Japan, which well exceeded magnitude 8. But this earthquake was associated with bending of the brittle oceanic plate as it starts to be subducted beneath the adjacent tectonic plate underlying Japan, and it is of little relevance to typical Basin and Range earthquakes. That is, it didn't represent regional extension. On the other hand, many of you may not appreciate that the most disastrous earthquake in recorded human history was the normal-fault event of 1556 near Xian, China, involving the well-documented loss of more than 800,000 lives. And this particular area is geologically very similar to the Basin and Range Province. Satellite images reveal, for example, steep serrated mountain fronts in the Xian region that are remarkably reminiscent of similar features on satellite images of the Wasatch Range front in Utah. A primary contributor to the great loss of life in 1556 was the high population density in the Xian region, but we must recognize that the population of the Wasatch region - Ogden, Salt Lake City, Provo, and other cities - is also increasing very rapidly.

Turning to the challenges of earthquake hazard assessment in the Basin and Range Province, let me discuss specific historic earthquakes. Each of these events, of course, displayed a variety of relevant geological and seismological phenomena, but let me pick out, in each case, one particular subject representing a challenge to our understanding of regional seismic hazard.

The 1872 Owens Valley (California) earthquake, of estimated magnitude 7.6, was associated with both horizontal and vertical displacements along a 100-km-long fault trace near the east base of the Sierra Nevada. Several investigators have pointed out that the vertical displacements that occurred in 1872 account for only about a third of the total height of the late Quaternary scarp, and if one had visited the area in the years prior to 1872, one would have seen a relatively fresh scarp extending along much of the same trace that subsequently broke in 1872. Thus, one must conclude that the 1872 rupture was essentially a re-

peat of what had happened in two earlier events. But how is this possible? The entire Sierra Nevada front is much longer than the segment that broke in 1872 and its predecessor earthquakes, yet similar fresh scarps do not occur north and south of this segment. Why does one particular segment break several times repeatedly, during which time other adjoining segments do not? In this light, how does one evaluate the overall seismic hazard? Typically, one assumes that in a long, active fault system, individual segments will break - either randomly or systematically - until the entire zone has ruptured, and then the process will start over again. Will the next large earthquake along the eastern Sierra front simply be a repeat of 1872, or will another segment break?

The 1915 Pleasant Valley (Nevada) earthquake, also of estimated magnitude 7.6, is the northernmost historic large earthquake within the Central Nevada Seismic Zone, and most - but not all - of this extensive zone has now broken in association with the 1915 and subsequent large earthquakes at other localities along the zone (e.g., 1932, 1934, 1954.) Once the entire zone has broken, will earthquakes recur within the same zone, or will activity shift to another fault system somewhere else within the Basin and Range Province? Other zones have been active at earlier times within the Quaternary Epoch - zones which are now relatively quiescent - but how often do such major changes take place in the locations of areas of activity? Is Pleasant Valley, for example, now a likely or an unlikely place for a large earthquake similar to that of 1915, as compared to other areas of Quaternary faulting in the Basin and Range Province?

The 1954 Fairview Peak-Dixie Valley (Nevada) earthquake, of magnitude 7.2, occurred in a relatively remote area, but one of the most widely printed photographs of a fresh scarp - taken by Karl Steinbrugge - shows an essentially undamaged cabin situated only a few meters away from the base of the spectacular 4-meter-high scarp. And anecdotal reports indicate that unbroken cups and bottles remained on the shelves within the cabin. Was the ground shaking as intense as one would normally have thought during an earthquake of this size and this close to the fault - well within the "near field"? Do normal-fault earthquakes have different ground-motion parameters from those of thrust, reverse, and strike-slip faults? There is some evidence to suggest that this may, in fact, be the case, and James Brune and Paul Spudich will be reporting on some of this research later in the conference. It's clearly a very critical subject for seismic-hazard assessment in the Basin and Range Province.

The 1959 Hebgen Lake or West Yellowstone (Montana) earthquake, also of magnitude 7.6, was characterized by a very complex surface fault pattern involving several individual faults and a very complicated tectonic environment - perhaps affected here by the proximity to the Yellowstone volcanic area. Although earlier Quaternary scarps had been identified along some of the same faults that broke in 1959, would anyone have thought that all of these would break together in an earthquake as large as magnitude 7.6? How would geologists have segmented these faults prior to 1959? Other Basin and Range earthquakes have also been characterized by multiple fault rup-

tures, such as at Cedar Mountain in 1932 ($M = 7.2$), and this type of scenario is being proposed by a number of scientists at the proposed high-level nuclear-waste repository at Yucca Mountain, Nevada. The 1959 Hebgen Lake earthquake, along with the 1992 Landers earthquake in California, calls into question the present capability of geologists to predict how many adjacent and adjoining faults will "get their act together" in a single large earthquake.

The 1983 Borah Peak (Idaho) earthquake, of magnitude 7.3, was much more intensively monitored geophysically than any earlier large Basin and Range event. Aftershock hypocenters clearly delineate the fault plane, which was remarkably planar, dipping about 50° , to the depth of the deepest aftershocks near 16 kilometers. This was surprising to many scientists, who instead expected that the fault would have been listric, that is, displaying a curved cross section flattening with depth, perhaps approaching horizontality. Indeed, many near-horizontal normal faults, known as detachments, have been imaged by seismic reflection surveys at various localities in the Basin and Range Province, and a number of very old, deformed, and eroded detachment surfaces are exposed in the province at the earth's surface. Yet the 1983 fault plane extended in perfectly planar fashion to a depth well below that of many imaged detachments in the region. Is the 1983 earthquake unique, or are detachment surfaces simply not currently seismogenic - that is, "active" - in the Basin and Range Province? Ongoing controversy exists among investigators as to whether any detachments in this region - or even elsewhere in the world - are active at the present time, and the subject remains an important challenge to our understanding of Basin and Range tectonics, as well as to its seismic hazard. If detachments are not, in fact, now active in the province, how was the tectonic environment in which they originated different?

The multitudes of small earthquakes currently occurring in the Basin and Range Province are concentrated near the western and eastern borders of the province. But is the ongoing regional tectonic strain across the province similarly divided? That is, is the bulk of the current extensional strain concentrated near the borders? This has been the subject of some discussion for many years, but we now finally have a tool that may give us the answer quickly. The Global Positioning System (GPS) offers unprecedented opportunities for understanding rapidly and relatively cheaply the details of ongoing tectonic deformation. A vigorous program of GPS surveys across the Basin and Range Province is currently underway, and we will hear some initial results of the project during this conference.

Let me conclude by asking and answering two questions that hark back to the title of this presentation: First, do significant challenges remain in the understanding of the seismotectonics of the Basin and Range Province? My simple answer is: "You bet they do!" Second, are the resolution of these challenges relevant to seismic-hazard assessment in the Basin and Range Province. And my simple answer is: "You bet they are!"

Thus, I hope I have helped to "set the stage" for the research papers that will follow.

SURFACE-FAULTING HAZARDS AND LAND-USE PLANNING IN UTAH

Gary E. Christenson
Utah Geological Survey
1594 W. North Temple
Salt Lake City, UT 84116

Brian A. Bryant*
Salt Lake County Planning
Rm N3700, 2001 S. State Street
Salt Lake City, UT 84190

*Present address: Antelope Valley High School, Lancaster, California

ABSTRACT

In the Wasatch Front of Utah, as elsewhere in the Basin and Range Province, active faults trend through major urban areas. The amount of surface displacement expected in a basin-and-range surface-faulting earthquake is sufficient to cause severe damage to structures and threaten life safety. Although little damage has occurred historically from surface faulting, the hazard is significant and its impact may be minimized with appropriate land use.

The likelihood of surface faulting depends on the activity of the fault. In Utah, most local governments define "active" faults for purposes of urban land-use planning as those with evidence for surface rupture in Holocene time. Requirements for detailed studies and hazard reduction may vary according to the type of land use and proposed facility, and the level of risk acceptable to society and the regulatory authority.

Assessing the surface-rupture hazard of a fault requires information on its activity, including recurrence interval, time of most recent event, and/or slip rate. The Quaternary fault map of Utah classifies faults according to the time of the most recent surface-faulting event, with the youngest fault class being younger than the initial rise of Lake Bonneville about 30,000 years ago. This age is used because Lake Bonneville deposits provide a useful, regional datum to assess fault activity. A derivative surface fault-rupture hazard map for Utah subdivides faults in this youngest class into those with evidence for:

- (1) multiple Holocene events, average recurrence intervals of several thousand years, and slip rates of 1 millimeter (0.04 in)/year or more (high hazard);
- (2) multiple post-30,000-year-old events, average recurrence intervals on the order of 10,000 years, and slip rates from 0.1-1 millimeter (0.004-0.04 in)/year (moderate to high hazard); and
- (3) a single post-30,000-year-old event, average recurrence intervals of tens of thousands of years, and slip rates less than 0.1 millimeter (0.004 in)/year (moderate hazard).

Older, pre-Bonneville faults have a lower surface-faulting hazard. These classes give a direct indication of fault activity and resulting potential for surface fault rupture so that users may determine which faults are important for their particular needs.

The principal technique used to reduce surface-faulting hazards is to set structures back from faults. Because surface fault ruptures occur repeatedly on the same traces, studies to address surface-faulting hazards focus on mapping these traces. In addition, these studies must evaluate whether a fault meets criteria to be considered "active" as defined in the applicable regulations and, where possible, estimate the displacement per event.

For land-use regulation along faults in the Wasatch Front, special-study areas extending 500 feet (152 m) on the down-thrown side and 250 feet (76 m) (or more, depending on scarp height) on the upthrown side delineate the area where site-specific studies may be required prior to development. These studies usually include surficial geologic mapping and subsurface investigations including trenches, boreholes, and/or geophysical surveys. At sites with predetermined structure locations, trenches are typically oriented perpendicular to fault trends, covering and extending beyond the proposed building footprint, to determine if faults are present. At sites where structures may be located to avoid faults, such as residential subdivisions, trenches are located to identify faults, map them across the property, and define the widths of zones of deformation. Fault setback distances are based on these site-specific conditions. In areas where deep fill, thick late Holocene (post-most-recent-event) deposits, shallow ground water, or heavy urbanization make trenching inconclusive or impractical, boreholes and geophysical techniques may be needed to identify faults.

INTRODUCTION

Fault scarps are perhaps the most visible reminders of the earthquake threat in the Basin and Range Province of the western United States. Future surface ruptures in large earthquakes are expected along known faults, and the likelihood of the hazard is directly related to the activity of the fault. The purpose of this paper is to examine how the hazard from surface fault rupture along normal faults is considered in land-use regulation in Utah as an example of an earthquake-hazard-reduction technique in the Basin and Range Province.

The Alquist-Priolo Earthquake Fault Zoning Act of 1972 in California represents the most significant attempt in the western states to deal with surface fault-rupture hazards in land-use regulation (Hart, 1994). The act defines "active" faults as those with Holocene (younger than 11,000 years) displacement and tasks the state to delineate "earthquake-fault" zones along "active" faults. Local governments are required to regulate land use within these zones to reduce risk from surface faulting. The state provides regulatory guidelines to assist local government with this mandate.

Similar regulations specific to Basin and Range normal faults have been adopted by many local governments in Utah. Administratively, all land-use regulation in Utah is performed by local governments. No state statutes exist such as California's Alquist-Priolo Act, and the state only provides technical advice to local governments regarding land use and earthquake hazards.

Historically, land use near recognized active faults in Utah has proceeded without systematic consideration for reducing the risk. Dense, high-rise development (figure 1), commercial buildings, less dense residential development (figure 2), and open space (figure 3) are found near and within active fault zones. Regulations regarding development in fault zones have varied with time, and the specific language addressing surface fault-rupture hazards in ordinances varies among local governments. However, most local governments now take a similar approach and address surface fault-rupture hazards in subdivision, sensitive-area, hillside-protection, or natural-hazards ordinances (Christenson, 1987). This is particularly true along the Wasatch Front, where the 1985-88 Wasatch Front

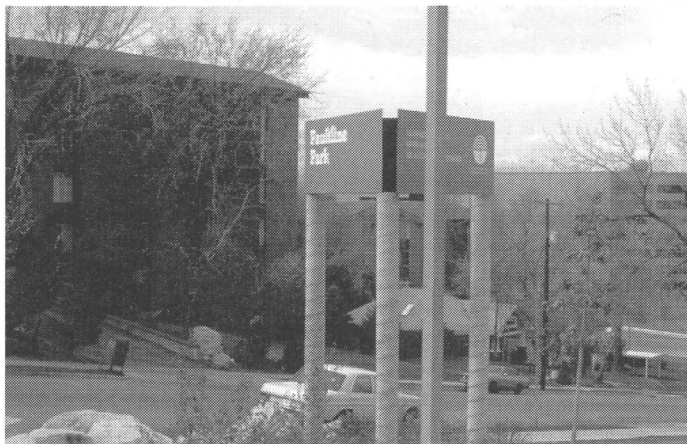


Figure 1. High-rise structures in the Wasatch fault zone in Salt Lake City.

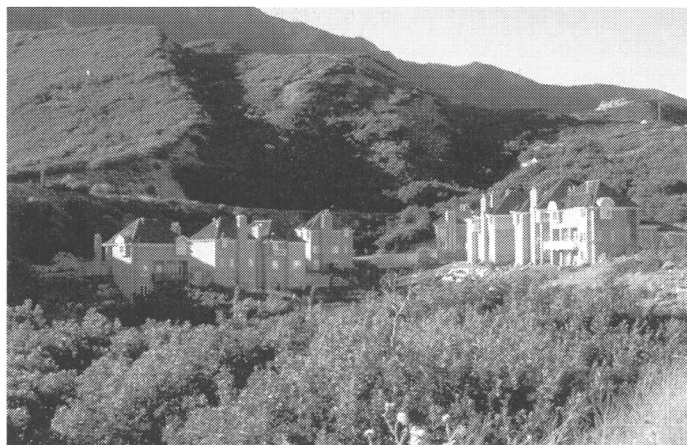


Figure 2. Subdivision in the Wasatch fault zone at the mouth of Little Cottonwood Canyon in Salt Lake County.



Figure 3. City park along the Wasatch fault zone in Salt Lake City across the street from figure 1.

County Hazards Geologist Program (Christenson, 1993) promoted such a uniform approach to earthquake and other geologic hazards. Presently, only Salt Lake County employs a permanent, full-time geologist to assist in implementing these and other geologic-hazard regulations. The Utah Geological Survey (UGS) assists other cities and counties with enforcement, and has published guidelines for surface fault-rupture hazard studies (Utah Section of the Association of Engineering Geologists, 1987; Nelson and Christenson, 1992).

SURFACE FAULTING

Effects

Surface faulting occurs in an earthquake when the rupture at depth propagates to the surface, and commonly occurs in Basin and Range earthquakes larger than magnitude 6.5 (Smith and Arabasz, 1991; dePolo, 1994). Studies along the Wasatch fault and other normal faults in Utah indicate that "characteristic" surface-faulting earthquakes on these faults may displace the ground 1 meter (3 ft) or more (Schwartz and Coppersmith, 1984; McCalpin, 1987,

1994; Jackson, 1991; Lund and others, 1991; Machette and others, 1991, 1992; McCalpin and Foreman, 1994; McCalpin and others, 1994; Olig and others, 1995; Black and others, 1996). In a survey of surface-faulting events throughout the Basin and Range Province, dePolo and others (1991) and dePolo (1994) also showed that primary surface rupture in such events typically exceeds 1 meter (3 ft). The result is formation of a near-vertical scarp and a zone of associated deformation perhaps hundreds of meters wide (figure 4). Hazards associated with such surface faulting include ground displacement, tilting, cracking, and erosional raveling and slope instability in resulting scarps.



Figure 4. View of the fault scarp and zone of deformation from the 1983 Borah Peak, Idaho earthquake illustrating the type of effects to be expected from typical basin-and-range surface faulting.

In a study of the effects of ground displacements in earthquakes, Youd (1980) found that damage was related to displacement as shown in table 1. Although his measured displacements were caused by liquefaction-induced ground failure, the resulting damages would presumably be the same for displacements from other causes such as faulting. As shown in table 1, the typical displacement expected in a basin-and-range surface-faulting event of more than 1 meter (3 feet) is generally large enough to cause severe damage and perhaps collapse of a structure. To date, losses from surface faulting in historical earth-

quakes have been relatively low compared to losses from other earthquake hazards such as ground shaking and liquefaction. This is partly because of the relatively small areas affected by surface faulting, and partly because few surface fault ruptures have occurred in urban areas. However, many faults in Utah and, in particular the Wasatch fault, traverse heavily urbanized areas and thus have the potential for causing significant damage (figure 5). Loss estimates by the Applied Technology Council (Stephanie King, written communication, 1997) indicate that over \$600 million in damage may result in the Salt Lake City area from surface faulting in a large Wasatch fault earthquake.



Figure 5. Eastward view of the East Bench fault (Salt Lake City segment, Wasatch fault zone; shown by arrows) trending through the central Salt Lake City metropolitan area.

Hazard Areas

The area affected in a typical Basin and Range normal-faulting earthquake is along a pre-existing fault trace in generally long, narrow corridors along a fault-bounded mountain front. Much work has shown that such ruptures occur repeatedly along the same traces (Yeats and others, 1997), even when ruptures are propagating upward through unconsolidated deposits of varying thicknesses. Bonilla (1970) surveyed historical normal fault ruptures and found that nearly all major displacements followed pre-existing faults for all or nearly all of their extent. The scarp of the 1983 Borah Peak, Idaho earthquake followed

Table 1. Relation between ground displacement and damage to structures (Youd, 1980).

GROUND DISPLACEMENT	LEVEL OF EXPECTED DAMAGE
Less than 4 inches (0.1 m)	Little damage, repairable
4 inches (0.1 m) to 1 foot (0.3 m)	Severe damage, repairable
1 foot (0.3 m) to 2 feet (0.6 m)	Severe damage, non-repairable
More than 2 feet (0.6 m)	Collapse, non-repairable

pre-existing scarps for much of its length (Crone and Machette, 1984; McCalpin, 1987). Trenching along the Wasatch fault and other Basin and Range normal faults documents repeated displacements along the same or closely related traces (McCalpin, 1987, 1994; Jackson, 1991; Lund and others, 1991; Machette and others, 1991, 1992; McCalpin and Foreman, 1994; McCalpin and others, 1994; Olig and others, 1995; Black and others, 1996). However, in some cases normal-faulting has extended beyond mapped traces into previously unfaulted material, as in the 1959 Hebgen Lake earthquake (Myers and Hamilton, 1964).

Repeated faulting along existing traces is also evident along minor and antithetic faults within the zone of deformation of a major fault. Remapping of a pre-1983 Borah Peak earthquake trench at Doublespring Pass indicated that nearly all pre-existing faults in the graben were similarly displaced in 1983 (Schwartz and Crone, 1985). However, not all events evident on main traces displace all minor faults in a zone of deformation in every event. Likewise, in a fault zone which consists of many subparallel main traces, rupture does not occur on every trace in every earthquake (Black and others, 1996).

In a study of the fault-rupture history of a 400-meter (1,200-ft)-wide fault zone consisting of six main fault traces, Black and others (1996) found that ruptures occur on different traces in different events (figure 6), and that a

lack of rupture in one event does not indicate that rupture would not occur again in subsequent events. Thus, in dealing with surface fault-rupture hazards, we must assume that any existing fault may be reactivated in subsequent earthquakes, and recognize that new faults may form as well.

FAULT CLASSIFICATION

Fault Activity and Acceptable Risk

The hazard due to surface faulting is directly related to the activity of a fault; that is, how often the fault ruptures the ground surface and how likely it is to rupture in the future. Determining the level of activity that is acceptable involves making both scientific decisions regarding uncertainty in our understanding of faulting, and societal decisions regarding what levels of risk and uncertainty are acceptable.

Scientific decisions relate principally to assessing fault activity and the likelihood of surface faulting, which depends on the model used to characterize earthquake occurrence. Using a Poisson model, earthquake occurrence is considered random and the likelihood of a surface-faulting earthquake is related only to past average recurrence. The shorter the average recurrence, the higher the likelihood, and the likelihood does not change with time. In a

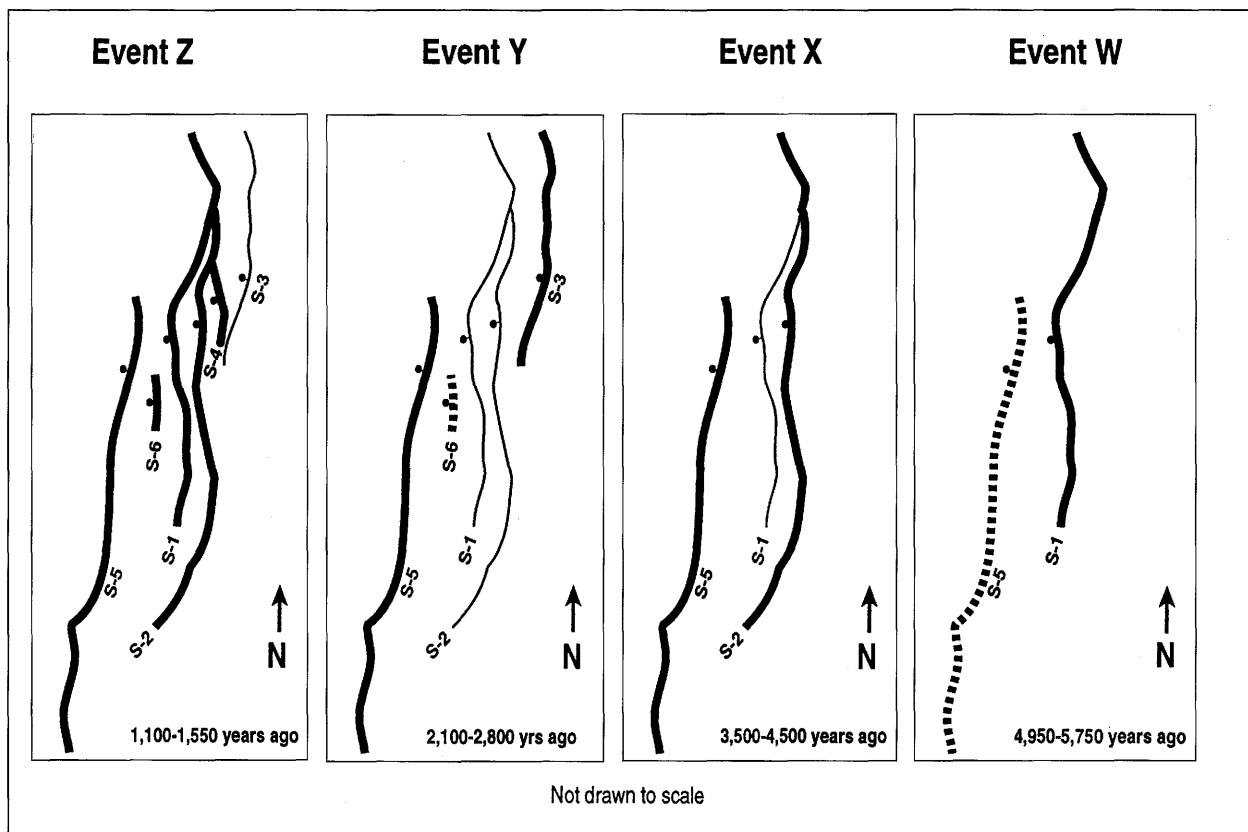


Figure 6. Pattern of surface faulting in a section of the Salt Lake City segment of the Wasatch fault zone. Main scarps (S-1 through S-6) known to be active during individual surface-faulting earthquakes are shown by heavy solid lines; scarps possibly active are shown by heavy dotted lines (Black and others, 1996).

time-dependent model, the likelihood of faulting increases as the time since the most recent event (MRE) approaches the average recurrence (Working Group on California Earthquake Probabilities, 1990; McCalpin and Nishenko, 1996). Although a Poisson model is generally applied to Basin and Range normal faults (McCalpin and Nishenko, 1996), other models may apply. The most appropriate model remains uncertain.

To assess the potential for surface fault rupture in Utah, we consider the average recurrence and the time of the MRE. Where average recurrence information is available, a Poisson model is used and faults with evidence for repeated Holocene displacements and shorter average recurrence intervals are considered to have a relatively higher hazard than faults with either single or no Holocene events. Where only the timing of the MRE is known, the time since the MRE is considered a minimum recurrence interval and is used to estimate the relative rupture probability. Large uncertainties exist in assessing rupture probabilities on Basin and Range faults because of their generally irregular recurrence, the lack of paleoseismic data, and the possibility of shorter term temporal clustering (Wallace, 1987; Yeats and others, 1997).

Slip rates are another useful secondary parameter for assessing surface-faulting hazards when recurrence and MRE timing data are lacking. However, slip rates not only reflect the frequency of surface faulting but also the amount of displacement per event. In assessing surface-faulting hazards, we need to know, for instance, whether a 1 millimeter (0.04 in)/year slip-rate fault generates five 2-meter (6-ft) displacements or ten 1-meter (3-ft) displacements every 10,000 years. Because displacements on Basin and Range normal faults are capable of causing life-threatening damage, all surface-faulting events on main faults are considered significant from a surface fault-rupture hazard standpoint and the actual amount of displacement is of secondary importance.

Few paleoseismic studies have been able to bracket more than one or two recurrence intervals on a given fault. For the more active faults such as the Wasatch fault, multiple bracketed intervals on each of the five central segments indicate a bimodal regularity, with a relatively regular recurrence of about 1,200 years on some segments and 2,600 years on others (McCalpin and Nishenko, 1996). Calculated 50-year probabilities assuming various recurrence models are given in table 2. To derive the two different time-dependent (renewal) models,

McCalpin and Nishenko (1996) empirically fit the paleoseismic data to two different families of recurrence-time distributions (lognormal and Weibull). In both of these time-dependent models, the higher probability for the Salt Lake City segment reflects the relatively long time since the MRE in comparison to the average recurrence. For faults with longer recurrence intervals than the central Wasatch fault zone, we commonly can only estimate the minimum recurrence, or time since the MRE.

Dealing with surface-faulting hazards requires making societal decisions regarding risk tolerance. This involves defining "active" faults; a definition that varies depending on facility type and land use. For example, "active" faults for siting of a dam are generally less active than those for siting single-family dwellings. This is because, from a societal standpoint, the level of acceptable risk is generally less for a critical facility such as a dam than for a single-family dwelling, so less "active" faults are considered in the hazard analysis. Society's risk tolerance appears to be decreasing in light of the many natural disasters in the 1990s. Present seismic provisions in the 1997 Uniform Building Code (UBC; International Conference of Building Officials, 1997) require minimum design for ground-shaking levels with a return period of 475 years (10 percent probability of exceedance in 50 years). Provisions in the draft International Building Code, proposed to replace the UBC in 2000, use the ground-shaking levels with a return period of 2,500 years (2 percent probability of exceedance in 50 years) in its "maximum considered earthquake ground motion" maps. A 2,500-year return period approximates the average recurrence for surface faulting at a given location on the more active Basin and Range faults such as the Wasatch fault (table 2), but is shorter than the return period for many less active Basin and Range faults.

For regulation of standard residential and commercial development in fault zones, cities and counties in Utah have adopted a definition of "active" faults similar to that used in the Alquist-Priolo Act in California. Any fault with evidence for displacement during Holocene time (defined as the past 10,000 years), or any fault closely associated with a fault having evidence for Holocene displacement, is considered "active." This definition includes some faults with a single Holocene displacement and relatively long recurrence intervals, sometimes more than 10,000 years. This recurrence period is longer than that considered for some other hazards (for example, 100-year

Table 2. Probabilities of surface faulting (percent) in 50 years on three central segments of the Wasatch fault zone (McCalpin and Nishenko, 1996).

Recurrence Model	Segment		
	Weber	Salt Lake City	Provo
Poisson	2.6	3.5	2.6
Time-dependent (renewal)			
Lognormal	3.2	5.4	0.2
Weibull	1.4	25.2	0.0

floods or 475/2,500-year ground shaking, as discussed above). One reason to consider longer return times for surface faulting than for ground shaking is the severity of the consequences to structures subjected to both faulting and ground shaking over that from ground shaking alone. A second reason is that individual buildings are considered to have a 50- to 100-year life span, so ground-shaking requirements in building codes are meant to prevent collapse of a specific building for a specific time period. Land use, however, is more permanent, and once an area is urbanized it is likely to remain urbanized for the foreseeable future.

Evaluating surface fault-rupture hazards must in some cases include consideration of minimum displacements per event. Main fault traces typically generate large, destructive, single-event displacements. The amount of displacement becomes an issue when considering antithetic faults, secondary faults, fissures, or folds within the zone of deformation where displacements can be small. Faults with minimum displacements of 1 foot (0.3 m) or more can cause life-threatening damage and collapse (table 1), and faults with 4-12 inches (0.1-0.3 m) of displacement can cause severe damage. Thus, in Salt Lake County, any Holocene fault with evidence for 4 inches (0.1 m) or more of displacement must be avoided. However, developers are encouraged not to build across any Holocene fault, even those with small displacements.

Surface Fault-Rupture Hazard Map

Utah's surface fault-rupture hazard map is derived from the Quaternary tectonics map of Hecker (1993). She depicted faults based on the time of the MRE using the following subdivisions:

- Holocene to latest Pleistocene** (0-30,000 years ago)
- Late Pleistocene** (10,000-130,000 years ago)
- Middle to late Pleistocene** (10,000-750,000 years ago)
- Early to middle Pleistocene** (130,000-1,650,000 years ago)
- Quaternary (?)** (less than 1,650,000 years ago).

The Holocene-latest Pleistocene definition for the youngest faults is based on a natural geologic datum present over most of northern Utah. Lake Bonneville expanded to cover much of the area (figure 7) beginning around 30,000 years ago, and had contracted to a level below the present Great Salt Lake by early Holocene time (Oviatt and others, 1992). Deposits of Lake Bonneville cover the floors of the basins in northern Utah where urban development is occurring, and most of the preserved Lake Bonneville geomorphic features and the shallow stratigraphic units commonly exposed in trenches date from the later stages of the lake. These Lake Bonneville beds form a natural datum for assessing fault activity and calculating slip rates. Although Hecker's (1993) post-30,000-year definition does not correspond to the Holocene definition used in Wasatch Front ordinances, for practical purposes, any fault which cuts late-stage Lake Bonneville deposits is considered active unless overlain by uncut early Holocene deposits. Outside of the Bonneville basin, other techniques, chiefly involving dating of

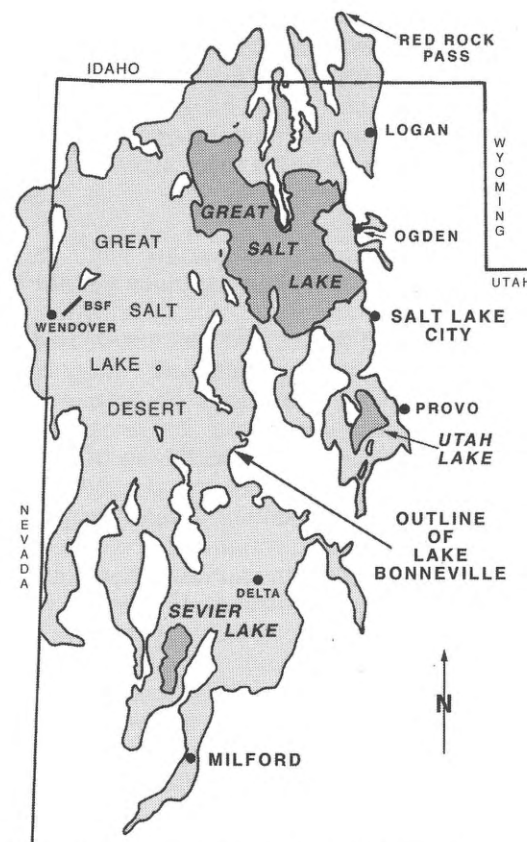


Figure 7. Maximum extent of Lake Bonneville in Utah.

fault scarps and displaced units in unconsolidated deposits, are used to estimate ages of faulting.

Hecker (1993) also compiled recurrence and slip-rate data which Christenson (in preparation) used in conjunction with the timing of the MRE to categorize Utah faults with respect to potential for surface fault rupture (figure 8). This classification divides faults relative to the near-term (for example, the next few hundred years) likelihood of surface fault rupture. Slip rate is used as a principal factor only where data on recurrence and time of the MRE are lacking. The surface fault-rupture hazard classification is as follows:

High - multiple Holocene events, average recurrence intervals of several thousand years, and slip rates of 1 millimeter (0.04 in)/year or more.

Moderate to high - multiple post-30,000-year-old events, average recurrence intervals on the order of 10,000 years, and slip rates from 0.1-1 millimeter (0.004-0.04 in)/year.

Moderate - single post-30,000-year-old event, average recurrence intervals of tens of thousands of years, and slip rates less than 0.1 millimeter (0.004 in)/year.

Moderate to low - no Holocene events, last rupture during the late Pleistocene; average recurrence intervals of many tens of thousands of years, and slip rates much less than 0.1 millimeter (0.004 in)/year.

Low - last rupture probably early to middle Pleistocene; average recurrence intervals of many tens to hundreds of thousands of years.

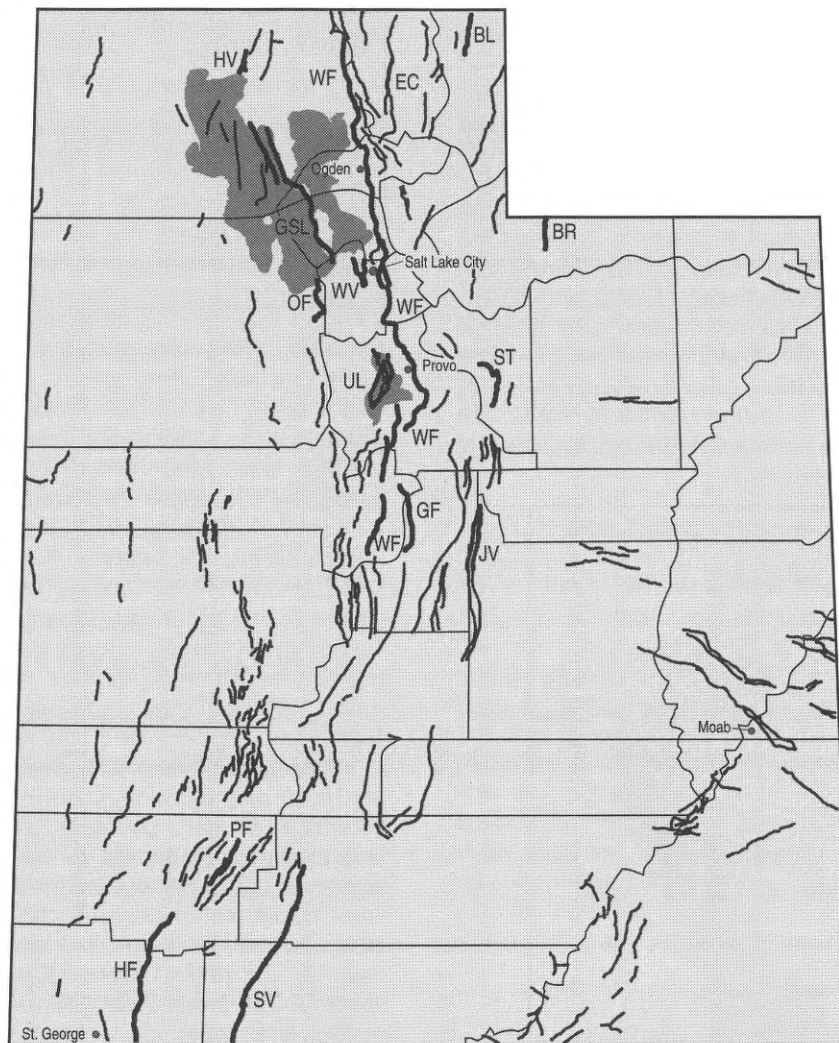


Figure 8. Quaternary faults in Utah; heavy lines indicate faults with high and moderate to high surface fault-rupture hazard (faults: W, Wasatch; BR, Bear River; EC, East Cache; BL, East Bear Lake; HV, Hansel Valley; O, Oquirrh; WV, West Valley; GSL, East Great Salt Lake; UL, Utah Lake; H, Hurricane; P, Paragonah; SV, Sevier; ST, Strawberry; JV, Joes Valley; G, Gunnison).

Hecker's (1993) youngest fault grouping of post-30,000-year faults is subdivided into the moderate, moderate to high, and high surface fault-rupture hazard ratings. Older pre-Bonneville faults in Utah, where in general the only evidence for recurrence is the minimum obtained from the timing of the MRE, are generally included in the low and moderate to low classes.

This classification system provides a breakdown of relative fault activity based on practical geologic constraints, and represents the relative hazard posed by the faults. All faults in the high, moderate to high, and moderate categories must be considered "active" for purposes of local government land-use regulation and landfill siting (which consider active faults to be Holocene age), as well as for seismic evaluations of dams and nuclear facilities (which consider active faults to be those with displace-

ment less than 35,000 years old). These regulatory definitions are practical to apply in geologic studies, particularly in northern Utah, because of the widespread and readily identifiable datum provided by Lake Bonneville deposits. Many older faults are probably buried by Lake Bonneville deposits. Where found, older faults in the low and moderate to low categories lack evidence for post-30,000-year surface faulting, but detailed paleoseismic studies have generally not been performed on these faults and further investigation is needed. Based on the level of acceptable risk for the proposed land use, regulators can choose which fault classes they wish to consider in their ordinances or other regulatory functions. In doing so, regulators must keep in mind that surface fault-rupture hazard classes are based on relative likelihood, and that rupture may occur on any fault at any time.

LAND-USE REGULATION

Approach

Local government ordinances require that "active" faults be identified and avoided using appropriate setbacks (Lowe and others, 1991). These ordinances typically adopt 1:24,000- or larger-scale fault maps, where available, and define special-study areas (SSA) along faults within which surface fault-rupture hazard studies must be performed (figure 9). Because the zone of deformation along normal faults is typically wider on the downthrown than upthrown sides, the SSA extends 500 feet (152 m) from mapped traces on the downthrown side, and 250 feet (76 m) on the upthrown side. These distances are taken not just from the main trace but from the outermost traces mapped in the fault zone, including antithetic faults. In areas of steep, high scarps where the top of the scarp is

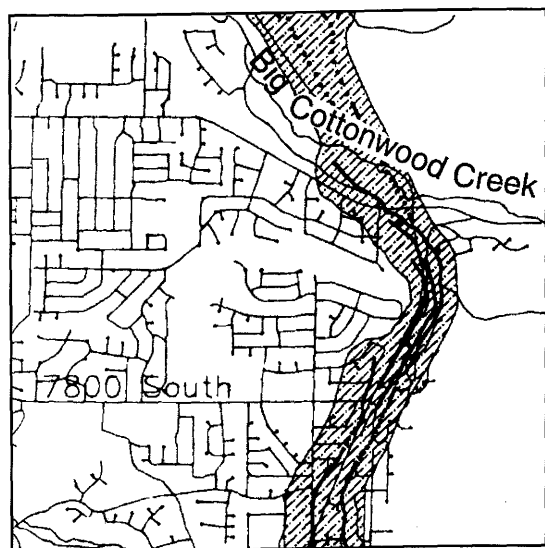


Figure 9. Special-study area (cross-hatched) surrounding mapped traces of the Wasatch fault (heavy lines) near Big Cottonwood Canyon in Salt Lake County.

more than 250 feet (76 m) from the mapped trace, the SSA is increased to 500 feet (152 m) on the upthrown side to include the entire scarp. The width of the SSA is based qualitatively on a typical maximum width of the zone of deformation from previous trenching studies, maximum scarp heights, and the scale of original fault maps (generally 1:24,000) used to draw the SSA in the ordinance.

Within the SSA, the developer must map scarps, define faults and zones of deformation (back-tilting, grabens), and recommend setbacks for structures. This typically involves detailed Quaternary geologic mapping and trenching by a consulting engineering geologist. Ordinances may vary their special-study requirements according to the type of proposed structure. A matrix is typically included in the ordinance outlining the special-study requirements according to proposed land use. Table 3 shows the general special-study recommendations by

Table 3. Special-study recommendations for surface faulting in Utah. Disclosure recommended for all structures in SSAs.

"Active" Fault	Critical Facilities	Commercial and Residential Facilities
Holocene	Yes*	Yes*
Pre-Holocene	Yes	No**
*setback required		
**only disclosure required		

the UGS. Once site-specific investigations have been performed, a report is submitted to the local government and either reviewed by the county geologist or by the UGS (Nelson and Christenson, 1992). This review is an essential part of the process to ensure the adequacy of the study. The following section discusses implementation of surface fault-rupture hazard regulations in the unincorporated areas of Salt Lake County as an example of typical methods used in Utah.

UNINCORPORATED SALT LAKE COUNTY

Site-Specific Studies

Salt Lake County's Natural Hazards Ordinance (chapter 19.75 of the county's zoning ordinance) defines SSAs in which, prior to any development, certain natural hazards must be evaluated to identify risks to "the health, safety and general welfare of the citizens of the county." The ordinance is presently limited to three natural hazards; surface fault rupture, liquefaction, and avalanches. The surface fault-rupture SSA is associated with known faults in Salt Lake County which have had surface rupture in the Holocene. If a proposed development site lies within a surface fault-rupture SSA, a fault investigation is required. Trenching perpendicular to the known fault trace is the preferred means of investigation (McCalpin, 1996), but if near-surface ground water is present or relatively young alluvial soils or fill are too thick for trenching, various borehole and/or geophysical techniques may be substituted (Benson and Baer, 1987; Stephenson and others, 1993; Benson and Mustoe, 1995; Benson and others, 1995).

The purpose of the investigation is to determine if active faults exist on the site and, if present, to make recommendations concerning setbacks and possible design specifications for structures. Trenching precisely locates mapped faults and identifies unmapped faults and secondary features which are no longer recognizable at the surface due to natural erosion or deposition, or cover by urbanization. On smaller sites such as single lots, and on sites with predetermined structure locations, the fault trench is typically cut perpendicular to the fault trend covering and extending beyond the proposed building footprint. The distance investigated beyond the limits of the structure would be the largest setback distance anticipated for the general area or to the limits of the property. On

subdivisions or large commercial projects with flexibility in site layout, the whole site may be investigated, faults and setbacks designated, and non-buildable areas delineated. Areas with faults can be designated roadways, parking, or open space. In practice, because most of the Salt Lake County urbanized area is underlain by Lake Bonneville or post-Bonneville deposits, all faults in the SSAs are considered active unless compelling geologic evidence suggests otherwise.

For single-family dwellings, a site reconnaissance and aerial-photograph analysis is first performed to determine if a fault may pass beneath the proposed house. If a fault is suspected beneath a house, a subsurface investigation is required. If not, at least a disclosure document must be completed by the owners acknowledging that they are aware the house is in the surface fault-rupture SSA. If an investigation shows that a fault is present, setback recommendations must be presented. The process may become very controversial because discovery of a fault requires avoidance, which may limit the size of houses that can be built or, in rare cases, eliminate development.

When Lake Bonneville sediments are exposed during an investigation, fault identification and vertical separation of displaced beds is generally straightforward due to the layering of the lacustrine sediments. However, in some massive or chaotic coarse deposits along the Wasatch Front, fault identification is more difficult. Lacking evidence to suggest multiple events such as colluvial wedges, vertical separation is considered to represent a single event.

Ideally, trenches will extend into Pleistocene sediments, usually Lake Bonneville deposits, to confirm that the entire Holocene section is being observed for possible faulting. In some cases this is not possible, however, and a report will conclude that no faulting was observed, even though buried Holocene faulting may be present. In such cases, borehole or geophysical techniques may be required.

Setbacks

McCalpin (1987) performed a statistical analysis of fault-related parameters important in defining setbacks using data from trenches on the Wasatch and other normal faults. He found that a main fault is commonly located at or slightly below the midpoint of its scarp, and that in areas lacking grabens or other related wide zones of deformation, that the mean width of deformation from the main fault on the downthrown side was about 13 meters (43 ft) and on the upthrown side about 2 meters (6 ft).

In addition to the extent of faulting, McCalpin (1987) also considered the final stable slope configuration following a typical scarp-forming event. Assuming this to be an angle-of-repose slope forming from a free-face height varying from 2 to 4 meters (6-12 ft), he calculated setbacks from faults in newly faulted material (no existing scarp) to be 40 feet (12 m) on the upthrown side and 50 feet (15 m) on the downthrown side. On existing scarps with a stable slope angle, he found these setbacks to be somewhat less.

in California under the Alquist-Priolo Act. In practice, however, site modifications and uncertainty in fault locations typically require subsurface investigations, and actual setbacks are then based on the results of these site-specific investigations.

Salt Lake County's Natural Hazards Ordinance states that no habitable structures "shall be built astride an active fault." The distance a structure is set back from a fault is determined on a case-by-case basis. Generally, the greater the expected vertical separation during a single faulting event, the greater the setback distance. Setbacks are designed to keep the structure off the fault, allow for inaccuracies in fault trace mapping across the property, and allow for a setback away from any created vertical face if surface rupture should occur. For structures with deep foundations, the dip of the fault must be considered when determining setbacks.

Disclosure

Salt Lake County requires that a disclosure form be completed if a development lies within a natural-hazards SSA. Three different disclosure forms are used: (1) an Acknowledgment and Disclosure form indicating only that the site lies within a SSA; (2) an Acknowledgment and Disclosure form indicating that the natural hazard has been evaluated by a qualified professional and the submitted report or letter is available for review in the county planning division; and (3) an Acknowledgment, Disclosure and Agreement form which indicates that the natural hazard has been evaluated and that specific recommendations must be followed during development of the site. All forms are recorded and attached to the deeds of the parcels so that subsequent property owners will be informed of any natural hazard risk potential on the site.

SUMMARY

Along the Wasatch Front in Utah and in other urban areas in the Basin and Range Province, "active" faults are a hazard. Displacements typical of Basin and Range surface-faulting earthquakes are sufficient to damage structures and cause life-threatening collapse. The probability of the hazard, and resulting loss, depends on the relative activity of the fault. In Utah, local governments define active faults as those with evidence for movement in the Holocene. Ruptures occur repeatedly on the same fault traces, although not on all traces in every earthquake.

Assessing the relative hazard from surface fault rupture requires information on recurrence and time of the MRE, or slip-rate data where the former are lacking. The Quaternary fault map of Utah classifies faults according to the time of the MRE, with the youngest fault class post-dating the onset of Lake Bonneville, or younger than 30,000 years. For purposes of assessing relative surface fault-rupture hazards, faults in this class have been further subdivided into those with evidence for multiple Holocene (high hazard), multiple post-30,000-year-old (mod-

generally have a lower hazard. When considering surface fault rupture as a geologic hazard, the fault class(es) appropriate to the level of acceptable risk for the proposed land use can be chosen.

For land-use regulation along faults in the Wasatch Front, SSAs extending 500 feet (152 m) on the downthrown side and 250 feet (76 m) (or more, depending on scarp height) on the upthrown side delineate the area where detailed studies are required prior to development. Detailed studies usually include geologic mapping of surficial deposits and subsurface investigations, usually trenches, but may include boreholes and/or geophysical surveys. At sites with predetermined structure locations, trenches are typically oriented perpendicular to fault trends, covering and extending beyond the proposed building footprint, to determine if faults are present. At sites where structures may be located to avoid faults, such as residential subdivisions or large commercial developments, trenches are located to identify faults, map them across the property, define the widths of zones of deformation, and determine setbacks. Final setback distances are based on these site-specific conditions.

REFERENCES

- Benson, A.K., and Baer, J.L., 1987, Close-order gravity surveys -- A means of fault definition in valley fill sediments, *in* McCalpin, J.P., editor, *Proceedings of the 23rd Symposium on Engineering Geology and Soils Engineering*: Boise, Idaho, Idaho Department of Transportation, p. 219-240.
- Benson, A.K., and Mustoe, N.B., 1995, An integrated geophysical analysis of shallow faulting in the Wasatch fault zone near Springville, Utah County, Utah, *in* Lund, W.R., editor, *Environmental and engineering geology of the Wasatch Front region*: Utah Geological Association Publication 24, p. 51-64.
- Benson, A.K., Mustoe, N.B., and Carver, J.N., 1995, Integrating geophysical and trench data to analyze shallow faulting in the Wasatch fault zone near Provo, Utah County, Utah, *in* Lund, W.R., editor, *Environmental and engineering geology of the Wasatch Front region*: Utah Geological Association Publication 24, p. 65-76.
- Black, B.D., Lund, W.R., Schwartz, D.P., Gill, H.E., and Mayes, B.H., 1996, Paleoseismic investigation of the Salt Lake City segment of the Wasatch fault zone at the South Fork Dry Creek and Dry Gulch sites, Salt Lake County, Utah: Utah Geological Survey Special Study 92, 22 p.
- Bonilla, M.G., 1970, Surface faulting and related effects, *in* Wiegel, R.L., editor, *Earthquake engineering*: Englewood Cliffs, N.J., Prentice-Hall Inc., p. 47-74.
- Christenson, G.E., 1987, Suggested approach to geologic hazards ordinances in Utah: Utah Geological and Mineral Survey Circular 79, 16 p.
- Christenson, G.E., 1993, Wasatch Front County Hazards Geologist Program, *in* Gori, P.L., editor, *Applications of research from the U.S. Geological Survey program, Assessment of regional earthquake hazards and risk along the Wasatch Front*, Utah: U.S. Geological Survey Professional Paper 1519, p. 114-120.
- Christenson, G.E., in preparation, *Earthquake hazards in Utah*: Utah Geological Survey Map.
- Crone, A.J., and Machette, M.N., 1984, Surface faulting accompanying the Borah Peak earthquake, central Idaho: *Geology*, v. 12, no. 11, p. 664-667.
- dePolo, C.M., 1994, The maximum background earthquake for the Basin and Range Province, western North America: *Bulletin of the Seismological Society of America*, v. 84, no. 2, p. 466-472.
- dePolo, C.M., Clark, D.G., Slemmons, D.B., and Ramelli, A.R., 1991, Historical surface faulting in the Basin and Range Province, western North America--Implications for fault segmentation: *Journal of Structural Geology*, v. 13, p. 123-136.
- Hart, E.W., 1994, Fault-rupture hazard zones in California: California Division of Mines and Geology Special Publication 42, 34 p.
- Hecker, Suzanne, 1993, Quaternary tectonics of Utah with emphasis on earthquake-hazard characterization: Utah Geological Survey Bulletin 127, 37 p., scale 1:500,000.
- International Conference of Building Officials, 1997, Uniform building code: Wittier, California, International Conference of Building Officials, 3 volumes, variously paginated.
- Jackson, Michael, 1991, The number and timing of paleoseismic events on the Nephi and Levan segments, Wasatch fault zone, Utah: Utah Geological Survey Special Study 78, 23 p.
- Lowe, Mike, Christenson, G.E., Nelson, C.V., Robison, R.M., and Tingey, Jim, 1991, Basic strategies for loss reduction, *in* Arabasz, W.J., editor, *A guide to reducing losses from future earthquakes in Utah, "Consensus Document"*: Utah Geological and Mineral Survey Miscellaneous Publication 91-1, p. 3-5.
- Lund, W.R., Schwartz, D.P., Mulvey, W.E., Budding, K.E., and Black, B.D., 1991, Fault behavior and earthquake recurrence on the Provo segment of the Wasatch fault zone at Mapleton, Utah County, Utah: Utah Geological Survey Special Study 75, 41 p.
- Machette, M.N., Personius, S.F., and Nelson, A.R., 1992, Paleoseismology of the Wasatch fault zone -- A summary of recent investigations, interpretations, and conclusions, *in* Hays, W.W., and Gori, P.L., editors, *Assessment of regional earthquake hazards and risk along the Wasatch Front*, Utah: U.S. Geological Survey Professional Paper 1500-A-J, p. A1-A71.
- Machette, M.N., Personius, S.F., Nelson, A.R., Schwartz, D.P., and Lund, W.R., 1991, The Wasatch fault zone, Utah -- Segmentation and history of Holocene earthquakes: *Journal of Structural Geology*, v. 13, no. 2, p. 137-149.
- McCalpin, J.P., 1987, Recommended setbacks from active normal faults, *in* McCalpin, J.P., editor, *Proceedings of the 23rd Symposium on Engineering Geology and Soils Engineering*: Boise, Idaho, Idaho Department of Transportation, p. 35-56.
- McCalpin, J.P., 1994, Neotectonic deformation along the east Cache fault zone, Cache County, Utah: Utah Geological Survey Special Study 83, 37 p.
- McCalpin, J.P., 1996, *Paleoseismology*: San Diego, Academic Press, 588 p.
- McCalpin, J.P., and Forman, S.L., 1994, Assessing the paleoseismic activity of the Brigham City segment, Wasatch fault zone, Utah; site of the next major earthquake on the Wasatch Front?: Logan, Utah State University, unpublished Final Technical Report to the U.S. Geological Survey, 19 p.
- McCalpin, J.P., Forman, S.L., and Lowe, Mike, 1994, Re-evaluation of Holocene faulting at the Kaysville site, Weber segment of the Wasatch fault zone, Utah: *Tectonics*, v. 13, no. 1, p. 1-16.
- McCalpin, J.P., and Nishenko, S.P., 1996, Holocene paleoseismicity,

- temporal clustering, and probabilities of future large ($M > 7$) earthquakes on the Wasatch fault zone, Utah: *Journal of Geophysical Research*, v. 101, no. B3, p. 6233-6253.
- Myers, W.B., and Hamilton, Warren, 1964, Deformation accompanying the Hebgen Lake earthquake of August 17, 1959: U.S. Geological Survey Professional Paper 435, p. 55-98.
- Nelson, C.V., and Christenson, G.E., 1992, Establishing guidelines for surface fault rupture hazard investigations - Salt Lake County, Utah: Association of Engineering Geologists 35th Annual Meeting Proceedings, p. 242-249.
- Olig, S.S., Lund, W.R., Black, B.D., and Mayes, B.H., 1995, Paleoseismic investigation of the Oquirrh fault zone, Tooele County, Utah, *in* Lund, W.R., editor, The Oquirrh fault zone, Tooele County, Utah -- Surficial geology and paleoseismicity: Utah Geological Survey Special Study 88, p. 22-64.
- Oviatt, C.G., Currey, D.R., and Sack, Dorothy, 1992, Radiocarbon chronology of Lake Bonneville, eastern Great Basin, USA: *Palaeogeography, Palaeoclimatology, Palaeoecology*, v. 99, p. 225-241.
- Robison, R.M., 1993, Surface fault rupture -- A guide for land-use planning, Utah and Juab Counties, Utah, *in* Gori, P.L., editor, Applications of research from the U.S. Geological Survey program, Assessment of regional earthquake hazards and risk along the Wasatch Front, Utah: U.S. Geological Survey Professional Paper 1519, p. 121-128.
- Schwartz, D.P., and Coppersmith, K.J., 1984, Fault behavior and characteristic earthquakes -- Examples from the Wasatch and San Andreas fault zones: *Journal of Geophysical Research*, v. 89, no. B7, p. 5681-5698.
- Schwartz, D.P., and Crone, A.J., 1985, The 1983 Borah Peak earthquake -- A calibration event for quantifying earthquake recurrence and fault behavior on Great Basin normal faults, *in* Stein, R.S., and Buchnam, R.C., editors, Proceedings of Workshop XXVIII on the Borah Peak, Idaho earthquake, Vol. A: U.S. Geological Survey Open-File Report 85-290, p. 153-160.
- Smith, R.B., and Arabasz, W.J., 1991, Seismicity of the Intermountain seismic belt, *in* Slemmons, D.B., Engdahl, I.R., Zoback, M.L., and Blackwell, D., editors, Neotectonics of North America: Boulder, Colorado, Geological Society of America, Decade Map Volume 1, p. 185-228.
- Stephenson, W.J., Smith, R.B., and Pelton, J.R., 1993, A high-resolution seismic reflection and gravity survey of Quaternary deformation across the Wasatch fault, Utah: *Journal of Geophysical Research*, v. 98, no. B5, p. 8211-8223.
- Utah Section of the Association of Engineering Geologists, 1987, Guidelines for evaluating surface fault rupture hazards in Utah: Utah Geological and Mineral Survey Miscellaneous Publication N, 2 p.
- Wallace, R.E., 1987, Grouping and migration of surface faulting and variations in slip rates on faults in the Great Basin province: *Bulletin of the Seismological Society of America*, v. 77, no. 3, p. 868-876.
- Working Group on California Earthquake Probabilities, 1990, Probabilities of large earthquakes in the San Francisco Bay region, California: U.S. Geological Survey Circular 1053, 51 p.
- Yeats, R.S., Sieh, Kerry, and Allen, C.R., 1997, The geology of earthquakes: New York, Oxford University Press, 568 p.
- Youd, T.L., 1980, Ground failure displacement and earthquake damage to buildings: American Society of Civil Engineers 2nd conference on Civil Engineering and Nuclear Power, Knoxville, Tenn., v. 2, p. 7-6-2 to 7-6-26.

AGE CRITERIA FOR ACTIVE FAULTS IN THE BASIN AND RANGE PROVINCE

Craig M. dePolo
Nevada Bureau of Mines and Geology
University of Nevada, Reno, Nevada 89557

D. Burton Slemmons
Professor Emeritus
Center for Neotectonic Studies, University of Nevada, Reno
@P.O. Box 81050, Las Vegas, Nevada 89180

ABSTRACT

A Holocene (10,000 year) criterion is commonly used to discriminate "active" faults in the Basin and Range Province. This "time-since-the-last-event" definition is used to define faults that could move during future earthquakes, for avoiding building structures across them, and for estimating potential earthquake ground motion. However, observations from the Basin and Range Province suggest that a longer time period is appropriate for this criterion, especially since most (but by no means all) earthquake recurrence intervals exceed 10,000 years. We advocate the use of a latest Pleistocene age criterion, specifically 130,000 years, for active fault classification in the province. A 130,000-year activity criterion is appropriate for use in the Basin and Range Province because: 1) it encompasses most recurrence intervals for faults in the province, which typically are between a few thousand to a few hundred thousand years; 2) it accounts for temporal clustering of the earthquake activity along a fault by capturing most intercluster periods; 3) it is linked with the beginning of a recognizable climatic episode, Oxygen Isotope Stage 5, a strong interglacial period when distinct surfaces and soils were formed (Sangamon-age soils), and 4) at least 50 percent of historical earthquakes of magnitude 6.5 in the province involved fault traces that lacked prior Holocene faulting. Another practical aspect of using a 130,000-year activity criterion is that it is sufficiently long that most hazardous faults have had several surface-rupturing events producing discernable geomorphic expression, to aid in their identification and delineation. In Nevada, this latest Quaternary fault classification would include most significant faults that define the contemporary seismotectonic pattern.

INTRODUCTION

An "active fault" criterion is a set of definitions to distinguish faults that are capable in the future of having earthquakes and potential surface rupture. Most definitions are based on considerations, such as the risk to people and the geological chance of an earthquake occurring along faults having certain characteristics. For risk decisions to be relevant decision makers need the best information available; this includes information about the seismotectonic environment.

In this paper we examine the geological input needed to define an "active fault" for the Basin and Range Province. We evaluate the 10,000-year criterion commonly used and suggest that this definition is inadequate based on historical earthquake data and the general character of earthquake occurrence in the province. We propose that a much longer time frame than Holocene (10,000 years) is needed, and recommend 130,000 years.

ACTIVE FAULT DEFINITIONS

Active-fault definitions present criterion for determining which faults to use in an assessment of earthquake sources for seismic-hazard analyses, or which to consider for evaluating surface-faulting hazard. Examples of surface-faulting hazards and avoidance are illustrated in figures 1 through 4. Another use of active-fault definitions is in the review of the seismic safety of dams. The Utah Division of Dam Safety and the California Division of

Safety of Dams both employ a 35,000-year active-fault criterion for consideration of ground shaking and surface-displacement hazards. In the Basin and Range Province, a 10,000-year criterion is used for fault set-backs in urban areas (e.g., Robison, 1993, Alquist-Priolo Special Studies Zones [technically this is an 11,000-year criterion] Hart, 1994, and Nevada Association of Engineering Geologists, 1996), for the consideration of faults to include in a seismic-hazard analysis, such as for the seismic design of mine tailings dams. In the near future, the 10,000-year criterion is proposed for use in new building codes (Bachman, 1997).

Although we endorse a late Pleistocene "active fault" criterion for use in the Basin and Range Province, we acknowledge that there are shortcomings to a simple time-since-the-last-event active-fault definition. Some of these ideas are presented in the "Overview and Recommendations" of the National Research Council's book on "Active Tectonics" (National Research Council, 1986). The overview states that the historical lack of agreement on an active-fault definitions has "caused confusion and attendant engineering, social, and legal difficulties." The overview further notes that, "Many of the definitions inappropriately have mixed elements including criteria for identifying faults, criteria for estimating degree of activity, and value judgements about the level of activity that constitutes acceptable risk to mankind." This issue is addressed in this paper by focusing on the geological input to the decision. At the 1997 Basin and Range Province Seismic-Hazard Summit, an anonymous written comment suggest-

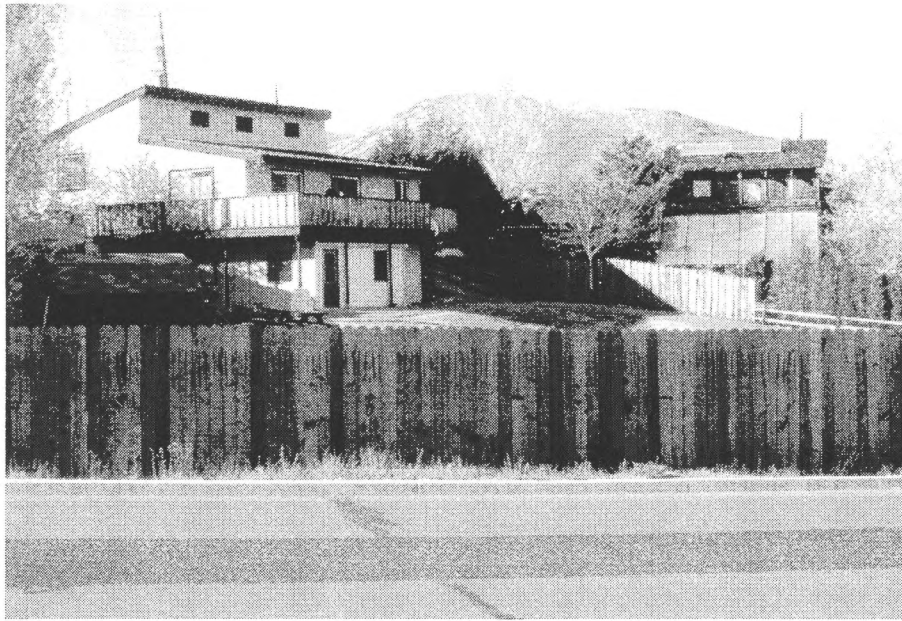


Figure 1. House on the left is built across a fault scarp. The upper part of the house, just to the right of the telephone pole, is built on the upper offset surface and the lower part is built on the lower offset surface. The fault in this area likely lies midslope on the scarp or beneath the middle of the house. The house on the right is built immediately adjacent to the toe of scarp and would likely be subject to secondary faulting if an earthquake ruptured the surface along this fault. (Photograph by C. dePolo)



Figure 2. House built across fault scarp in a rural Basin and Range Province setting. There is little developmental pressure here and the house could have easily been offset from the fault had the owner known it was an active fault. (Photograph by C. Willoughby)



Figure 3. Barn that crossed the Red Canyon fault and was offset during the 1959 Hebgen Lake, Montana, earthquake. The back wall of the barn is crushed and the whole structure is disrupted. (Photograph by K. Steinbrugge)

ed the term "active" is misleading and should be replaced by the term "earthquake." Labeling faults as active, and by inference, inactive, leads to the expectation of having "good" versus "bad" faults. Good faults don't have earthquakes (at least of any consequences); these are the "inactive" faults. Confusion and a certain distrust from society ensues when good faults suddenly turn bad. A policy recommendation from the Summit notes that earthquakes in the province will occur on faults of different age criteria, including Holocene faults, late Quaternary faults (130,000 years), and Quaternary faults (1.6 million years). It is the prerogative of the user to decide the degree of anticipated risk and what degree of fault activity is considered "dangerous" (from the conference policy recommendation).

There are practical reasons to employ specific active-fault definitions, and current usage is anticipated to continue. Therefore, geoscientists need to be involved in evaluating the input for these decisions. What is incumbent on the users of an active-fault definition is that they clearly understand what the criterion means and doesn't mean, and what input elements were used in making the definition. This helps achieve optimum use of the criterion and the information it represents.

HISTORICAL EARTHQUAKES IN THE BASIN AND RANGE PROVINCE

To gain a perspective on the time criterion applied to faults to determine which are most likely to have future

earthquakes we compare existing criteria with the activity of faults with historical earthquakes. How well can a given criterion predict faults along which historical earthquakes have occurred? To answer this question, we examined earthquakes with magnitudes of 6.5 and greater. Earthquakes of this size are more likely to rupture the surface (dePolo, 1994).

Historical earthquakes with surface faulting in the Basin and Range Province and the activity of the faults and fault traces involved in these events are listed in table 1 (for further discussion of these earthquakes see dePolo and others (1989, 1991). Constraints on earlier fault activity are based on trenching studies, scarp-degradation modeling, identification of offset alluvial surface and soils, and cross-cutting relations with pluvial shorelines and deposits. Six to nine of the eleven fault zones that generated the historical earthquakes had prior Holocene activity along some portion of them, and at least two did not. In contrast, six to eight of these events (>50%) involved significant surface faulting along fault traces that lacked prior Holocene activity.

Ten of the eleven events (91%) occurred along faults that have ruptured since 130,000 years (not including the historical event). Only the Pitaycachi fault, along which the 1887 Sonora, Mexico earthquake occurred, definitely had a pre-130,000 year penultimate event. Thus, a 130,000-year criterion would have been more complete than a 10,000-year criterion at identifying fault zones that generated historical earthquakes, and especially at identifying fault traces involved in historical surface rupture.



Figure 4. Example of avoidance mitigation of surface-faulting hazard along the Hayward fault in California. A major trace of the fault passes from the right of the bus through the gap in the apartment buildings. This gap is the set-back area to avoid the fault; the area was replanned to be a small, open, grassy area and parking spaces. Many communities in the Basin and Range Province have the opportunity to guide planning such that buildings and other structures avoid crossing faults when it is unnecessary. (Photograph by C. dePolo)

Table 1.
Activity of faults that were involved in historical earthquakes in the Basin and Range Province, magnitude 6.5 and greater.

Earthquake	Holocene Activity along the Fault Zone	Fault Traces without Holocene Activity	Reference
1872 Owens Valley Eq.	Yes	No	Bierman and others (1995)
1887 Sonora, Mexico Eq.	No	Yes	Bull and Pearthree (1988)
1915 Pleasant Valley Eq.	No/Yes?	Yes	Pearthree (1990)
1932 Cedar Mountain Eq.	Yes	No	Bell and others (in press)
1934 Hansel Valley Eq.	No?	Yes	McCalpin (1986)
1954 Rainbow Mountain Eq.	Yes	Yes	Bell (1981)
1954 Stillwater Eq.	?	Yes?	Bell (1981)
1954 Fairview Peak Eq.	No	Yes	Pearthree (1990)
1954 Dixie Valley Eq.	Yes	Yes	Bell and Katzer (1990)
1959 Hebgen Lake Eq.	Yes	No?	Noller and others (1996)
1983 Borah Peak Eq.	Yes	No	Hanks and Schwartz (1987)

A 10,000-YEAR CRITERION

A 10,000-year (Holocene) criterion for active faults is widely used in the Basin and Range Province. Selection of the Holocene appears to have come from the gradual adoption of this criterion from California. The significant attribute of the Holocene is that it is defined by the change from a glacial to interglacial environment, which has led to the development of distinctive soils and geomorphic surfaces. It is also within the range of the radiocarbon dating method. In California, particularly west of the Basin and Range Province where the rate of earthquake activity is high, a Holocene criterion encompasses most faults a geologist would be concerned about when assessing seismic hazard. Many of these faults have had multiple Holocene events.

Because most average earthquake recurrence intervals for faults in the Basin and Range Province are longer than 10,000 years, we consider a Holocene time frame inadequate for an active-fault criterion in the Basin and Range Province. Most Quaternary faults in the province appear to lack Holocene activity, and most of the large historical earthquakes in the province occurred along faults that did not show evidence of prior Holocene activity.

A shortcoming of a Holocene activity criterion is that most of the range-bounding faults that are involved in the contemporary deformation of the province would be considered inactive. Fault slip rates in Basin and Range Province range from a few m/kyr (m/kyr are equivalent to mm/yr) to below a thousandth of a m/kyr, with values around a tenth of a m/kyr being common (dePolo, unpublished research). If we consider 1 to 5 meters as a typical range of maximum surface offset during an event, a slip rate of a tenth of a m/kyr yields average earthquake return times of 10 to 50 kiloyears; thus, a 10,000-year criterion only represents a fraction of the recurrence intervals for these faults.

Faults with Holocene activity taken from Dohrenwend and others (1996) are shown in figure 5. Holocene faults include those with the highest rates of activity (a few tenths of a m/kyr or greater) and a subset of the rest of the late Quaternary faults. It is this subset aspect that renders a Holocene activity criterion incomplete. A 1990 reconnaissance study of Quaternary faults in Nevada (Siddarthan and others, 1990) indicates the level of incompleteness. Only 16 percent of known and suspected Quaternary faults were estimated to have earthquake recurrence intervals of 10,000 years or less.

Reiterating, six to eight of the eleven historical earthquakes involved significant surface faulting along fault traces that lacked prior Holocene activity. This observation further casts doubt on the utility of a Holocene criterion. Society expects an active-fault criterion to distinguish fault traces that are the most hazardous and which potentially will rupture in future earthquakes. A Holocene criterion fails this expectation in the Basin and Range Province. Because more faults in the contemporary deformational pattern lack Holocene activity than have it, it is likely that the next large earthquakes in the Basin and Range Province will occur on non-Holocene faults. We conclude that the Holocene is inadequate as an active fault

criterion in the Basin and Range Province.

A 130,000-YEAR CRITERION

We recommend using a 130,000-year criterion for active fault definitions in the Basin and Range province because: (1) it encompasses most recurrence intervals for faults in the province, which typically are between a few thousand to a few hundred thousand years; (2) it accounts for temporal clustering of the earthquake activity along a fault by capturing most intercluster periods; (3) it is linked with the beginning of a recognizable climatic episode, Oxygen Isotope Stage 5, a strong interglacial period when distinct surfaces and soils were formed (Sangamon-age soils), and (4) at least 60 percent of historical earthquakes of magnitude 6 in the province occurred along faults that generally lack Holocene faulting.

To demonstrate the utility of a 130,000-year criterion, we present Dohrenwend and others's (1996) map of faults with this age activity or younger in figure 6. This map includes many more major range-bounding faults than the map highlighting only Holocene activity (figure 5). With respect to Siddarthan and others (1990), 59 percent of the faults had average earthquake recurrence intervals of 130,000 years or less. Using the 1990 study as an indicator, even the 130,000-year criterion is incomplete, but it is three times better than using the Holocene for identifying faults that could have future major earthquakes in Nevada (59% versus 16%).

Temporal clustering of earthquakes along faults in the Basin and Range Province also warrants consideration. As noted by Wallace (1987), earthquakes appear to cluster through time along faults, in contrast to a model of quasi-periodicity (see figure 7). It is unclear to what extent a Holocene criterion would include (and proportionately highlight) faults in periods of clustered behavior, but it would definitely bias against those about to return to a more active phase from dormancy. Although well-dated examples are sparse, 130,000 years appears to be longer than many of these swings between active and less active periods, making it a better indicator of faults that are part of the contemporary deformation in the province.

With respect to historical surface faulting, a 130,000-year criterion does quite well. All but the 1887 Sonora, Mexico earthquake occurred along faults that have ruptured in the past 130,000 years (see table 1).

There are two practical aspects to a 130,000-year criterion: (1) it marks the beginning of a pronounced interglacial period that yielded surfaces and soils that are still recognizable in many places, and (2) it allows sufficient time for multiple earthquakes along many faults, thus creating the geomorphic expression with which to identify them. The 130,000-year boundary is at the beginning of the Sangamon interglacial period, or Oxygen Isotope Stage 5 (Gallup and others, 1994; Ehlers, 1996; see figure 8). Estimates for the age of this boundary have ranged from 128 kiloyears (Morrison, 1991) to 132 kiloyears (Richmond and Fullerton, 1986). Recent estimates are 130 ka (Gallup and others, 1994; Ehlers, 1996) and this value is adopted in this paper. During the Sangamon,

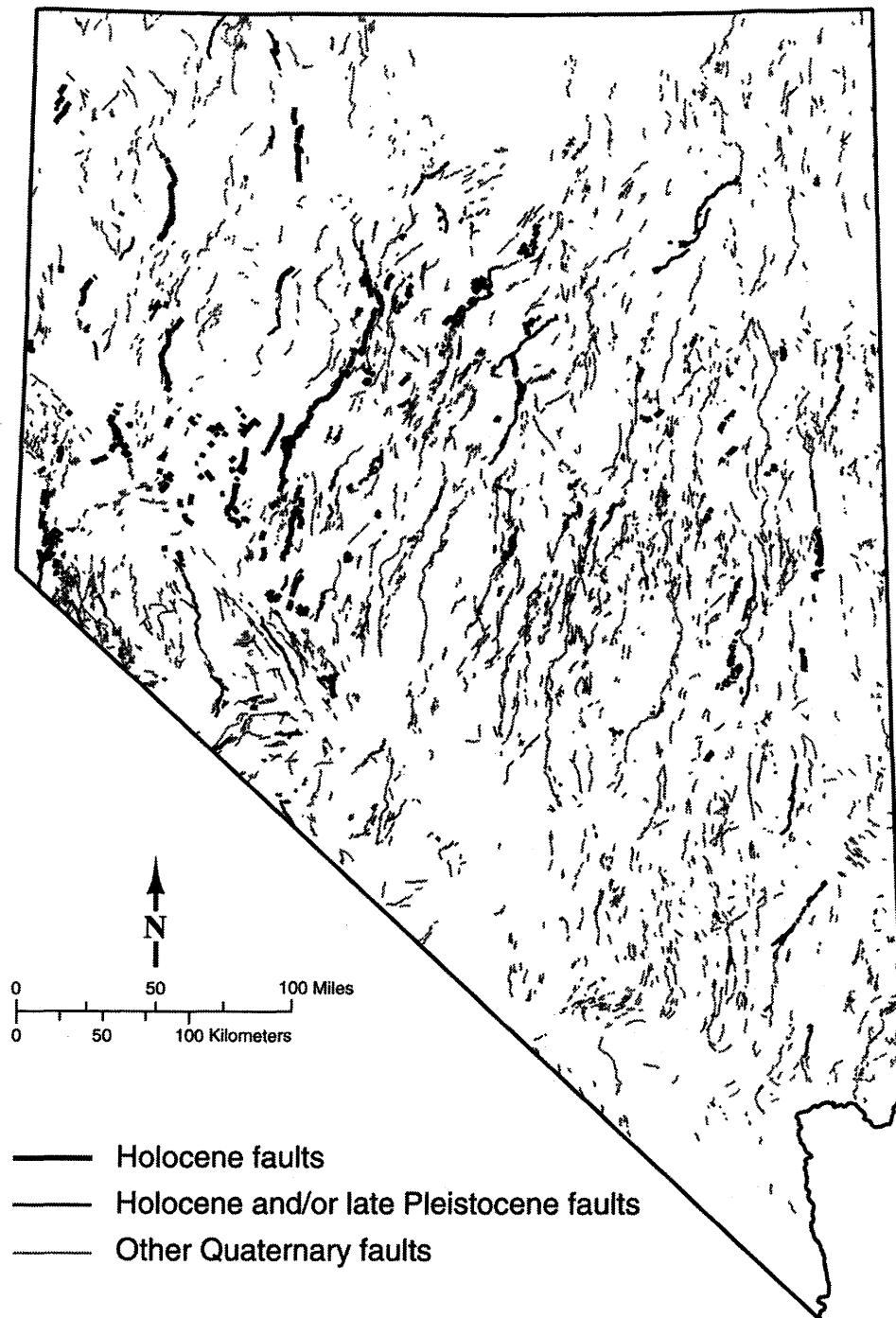


Figure 5. Reconnaissance photogeologic map of Quaternary faults in Nevada, produced by Dohrenwend and others (1996). Holocene and possible Holocene faults are highlighted. This map indicates a relatively small percentage of the faults would be classified as Holocene. Recent studies conducted since this map was made would add some additional Holocene faults, but would not change the overall impression that most faults lack Holocene activity.

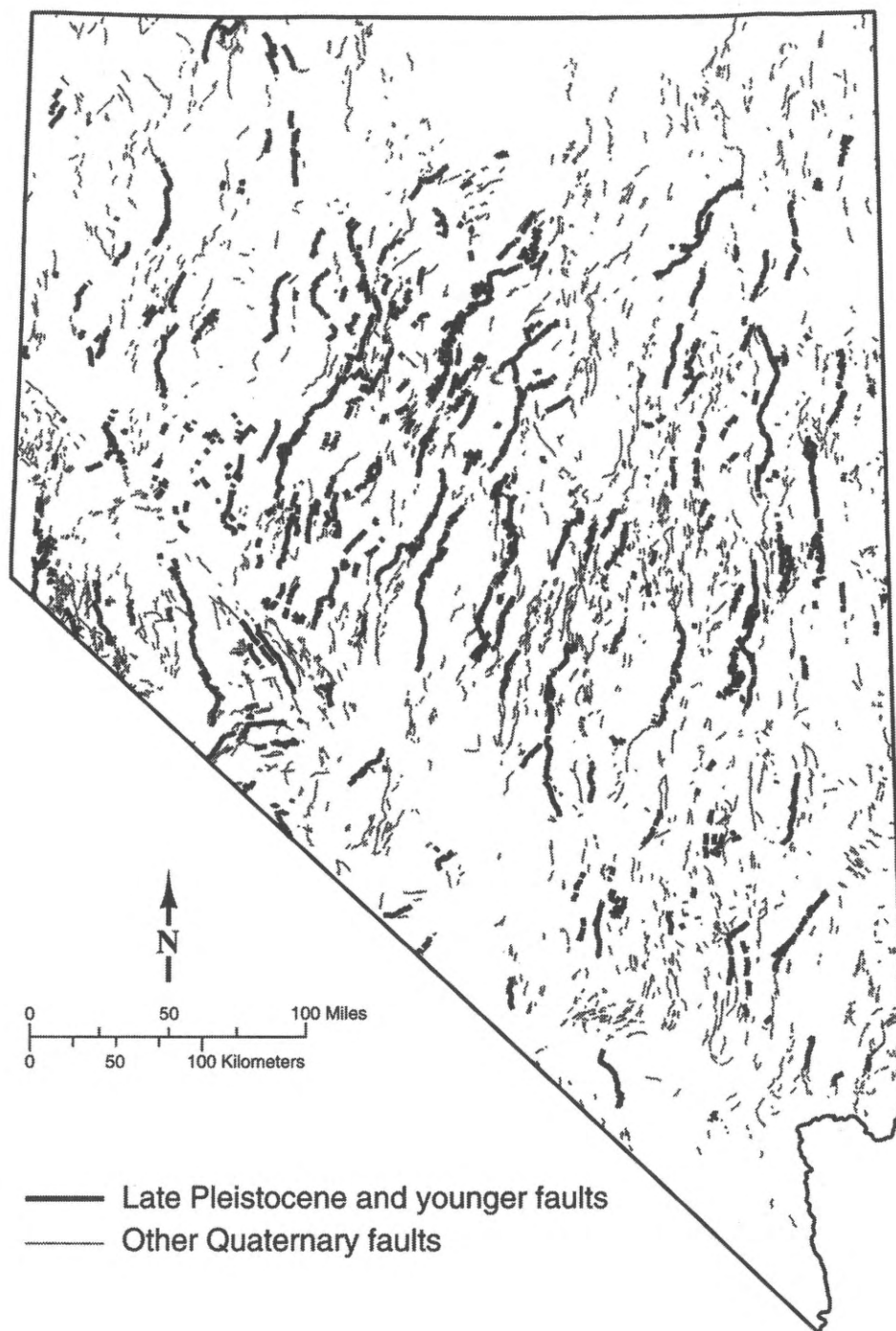


Figure 6. Reconnaissance photogeologic map of Quaternary faults in Nevada, produced by Dohrenwend and others (1996). Faults active in the late Pleistocene (130,000 years) are highlighted. Many more range-front faults are included in the late Pleistocene criterion versus the Holocene criterion (figure 5).

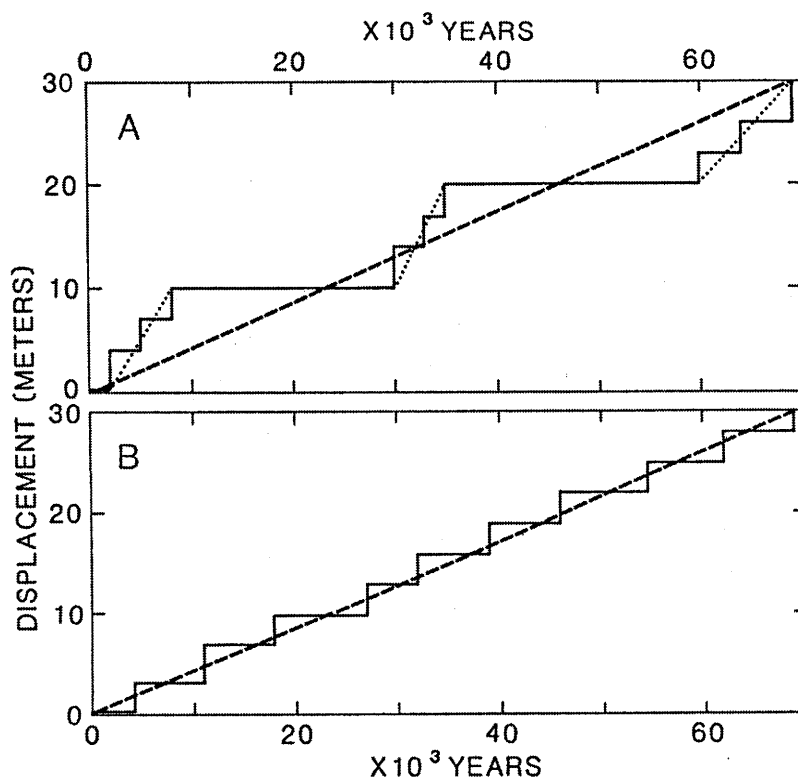


Figure 7. Diagrammatic graphs of two types of fault displacement time histories. (A) Temporal grouping of slip events separated by quiescent periods (solid lines). For a few thousand years during groups of events, the average slip rate (dotted lines) may be several times that of the long-term slip rate averaged over tens of thousands of years (dashed line). (B) More regular recurrence of slip events. Dashed lines show an average displacement rate which is the same in both examples. Wallace suggests that (A) rather than (B) represents more nearly the characteristic time history of individual faults and fault segments in the Basin and Range Province (figure and caption from Wallace, 1987).

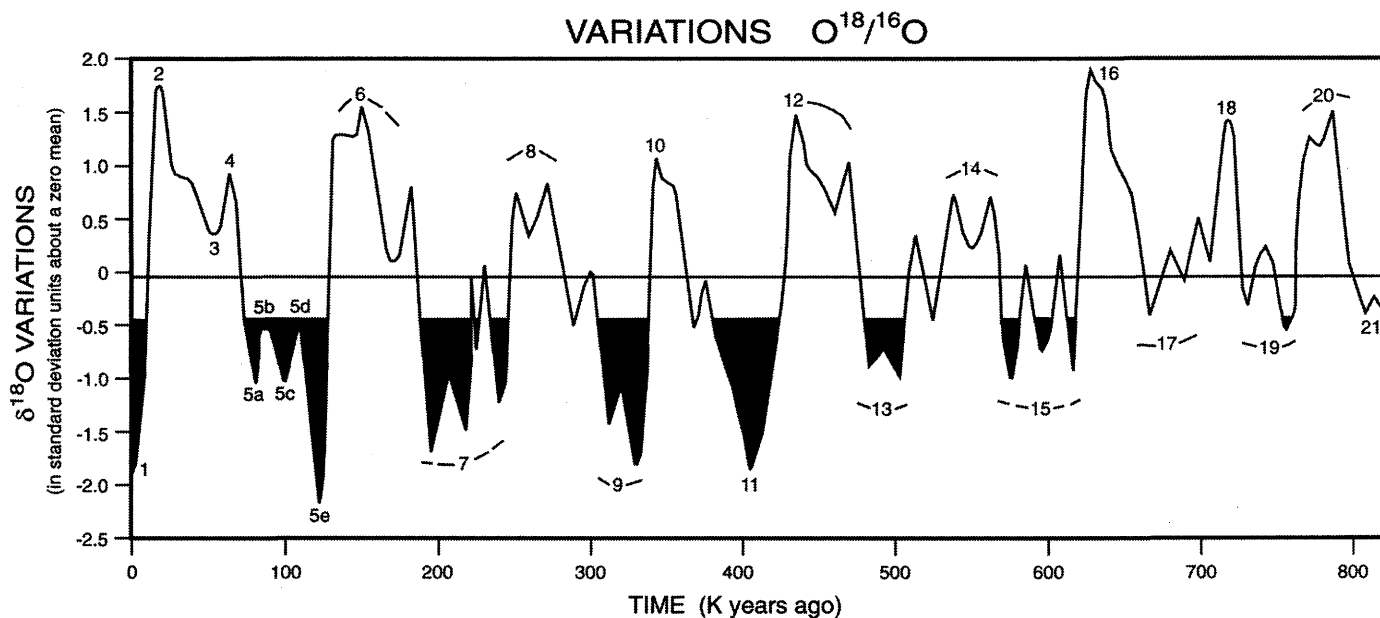


Figure 8. Record of $^{18}\text{O}/^{16}\text{O}$ variations in five deep-sea cores as a function of time, prepared by Morrison (1991). Shaded areas are interglacial episodes, based on a cut-off at -0.5 $\delta^{18}\text{O}$ oxygen-isotope values (equivalent to Holocene interglacial values). The numbers along the graph indicate oxygen-isotope stages: the even-numbered peaks (at top) are glacial maxima, and odd-numbered troughs are interglacial minima. This figure illustrates that Sangamon (Stage 5) is the penultimate interglacial period and that the 130,000-year criterion is at the beginning of the Sangamon.

strong soils were formed that can be identified (e.g., Bell and Pease, 1980). In the arid to semiarid setting of much of the Basin and Range Province, direct dating opportunities are rare, thus soil correlation and age assignment have a particular importance, despite the difficulty often associated with soils.

The estimate of average earthquake occurrence rate in the province is on the order of 10 to 50 kiloyear (as noted earlier). Many faults would therefore have produced several earthquakes in 130,000 years, making them easy to identify and delineate.

PROBABILITY OF EARTHQUAKES IMPLIED BY A 130,000-YEAR CRITERION

An important consideration when defining an active fault is the probability that an individual fault will have an earthquake. If you only know the time since the last event, what are its chances of having an earthquake? Some might infer that if a 130,000-year criterion is used that the chances are 1 in 130,000 in a given year. However, consider the number of historical earthquakes in Nevada that have occurred on faults that have had activity in the past 130,000 years. There are about 300 relatively large faults in Nevada and it would be conservative to consider that they all have been active in the past 130,000 years (see figure 4). Six to nine earthquakes of magnitude 6.5 or greater have occurred among these 300 faults in the past 150 years in Nevada. The range in the number of historical events is due to uncertainty in magnitude values and whether the events are association with faults. There is an implied earthquake recurrence interval for faults that have moved in the past 130,000 years considering these historical earthquakes. The rate of M 6.5 earthquakes in Nevada over the past 150 years is 0.04 to 0.06 events per year among about 300 faults. When normalized to a per fault value (divided by 300), this becomes 0.0001 to 0.0002 events per year per fault. In other words, given the historical record, events might occur along Nevadan late Pleistocene faults once every 5000 to 10,000 years on average. This is not meant to be a rigorous estimate, as much as an illustration. This historical earthquake probability implies that a 130,000-year time criterion for fault activity should be multiplied by a coefficient of less than one when compared to a risk time frame. For example, 10,000 years (on average) = "a" times 130,000 years, where the coefficient "a" is ~ 0.00008 . This example implies that in Nevada, the general probability of an earthquake along a fault, for which all that is known is that it has moved in the last 130,000 years, is significantly less than a 1 in 130,000 chance a year.

DISCUSSION

We acknowledge the practicality and applicability of a simple, single fault activity criterion for seismic-hazard

characterization, but emphasize that for more detailed analyses, a spectrum of time frames is more useful. In the Basin and Range Province, several different time frames of activity have been used, generally the oldest being Quaternary. A better way to characterize hazard is to estimate the earthquake recurrence interval of a fault. Whether earthquakes occur along an individual fault every 1000, 10,000, or 100,000 years makes a big difference in how dangerous a fault might be considered.

The difference in the suggested time criterion for active faulting between the Basin and Range Province and San Andreas plate boundary system (for which Holocene is generally used) is largely related to differences in the style and rates of tectonism. In the plate boundary system, deformation is focused on relatively high slip rate faults, and these dominate the earthquake hazard. In the Basin and Range Province, earthquake return times are longer and deformation is widely distributed among many faults. Thus, a longer time frame is needed to include faults that might have earthquakes in the future.

CONCLUSIONS

If a time-since-the-last-event criterion is to be used to characterize fault activity in the Basin and Range Province, the late Pleistocene is a more appropriate criterion than the Holocene. A Holocene criterion selects only a small percentage of the faults that are likely to produce earthquakes in the future. This is because most earthquake recurrence intervals in the province appear to be longer than 10,000 years. In addition, most large earthquakes in the province have ruptured fault traces that lacked prior Holocene activity. Thus, the Holocene in the Basin and Range Province is a poor indicator of faults that will be involved in large earthquakes in the future. In contrast, a 130,000-year criterion would have identified most of the faults that generated large historical earthquakes and that were involved in surface faulting, and it encompasses typical earthquake recurrence intervals in the province. Furthermore, the 130,000-year criterion is practical to use because it is the beginning of a major interglacial period with distinct surfaces and soils that can be used to constrain fault activity. Also, many faults have produced more than one earthquake during this time period aiding in the identification and delineation of fault traces. Therefore, we believe 130,000 years is an effective and practical active fault criterion for the Basin and Range Province.

ACKNOWLEDGMENTS

This paper benefitted greatly from the comments and insights of Mark Stirling from the Center for Neotectonic Studies and Jon Price and John Bell from the Nevada Bureau of Mines and Geology. The manuscript was also significantly improved with the editing skills of Bill Lund of the Utah Geological Survey.

REFERENCES CITED

- Bachman, R.E., 1997, 1997 Uniform Building Code ground shaking criteria, in Basin and Range Province seismic-hazards summit: Western States Seismic Policy Council, Program and Abstracts, p. 12-20.
- Bell, J.W., 1981, Quaternary fault map of the Reno 1° x 2° quadrangle: U.S. Geological Survey Open-File Report 81-982, scale 1:250,000, 62 p.
- Bell, J.W., and Katzer, T., 1990, Timing of late Quaternary faulting in the 1954 Dixie Valley earthquake area, central Nevada: *Geology*, v. 18, p. 622-625.
- Bell, J.W., and Pease, R.C., 1980, Soil stratigraphy as a technique for fault activity assessment in the Carson City area, Nevada, in *Proceedings of Conference X, Earthquake hazards along the Wasatch, Sierra-Nevada frontal fault zones*: U.S. Geological Survey Open-File Report 80-801, p. 577-600.
- Bell, J.W., dePolo, C.M., Ramelli, A.R., Dorn, R.I., Sarna-Wojcicki, A.M., and Meyer, C.E., in press, Surface faulting and paleoseismic history of the 1932 Cedar Mountain earthquake area, west-central Nevada and implications for modern tectonics of the Walker Lane: submitted to the *Geological Society of America Bulletin*, 58 p.
- Bierman, P.R., Gillespie, A.R., and Caffee, M.W., 1995, Cosmogenic ages for earthquake recurrence intervals and debris flow fan deposition, Owens Valley, California: *Science*, v. 270, p. 447-450.
- Bull, W.B., and Pearthree, P.A., 1988, Frequency and size of Quaternary surface ruptures of the Pitaycachi fault, northeastern Sonora, Mexico: *Bulletin of the Seismological Society of America*, v. 78, p. 956-978.
- dePolo, C.M., 1994, The maximum background earthquake for the Basin and Range Province, western North America: *Bulletin of the Seismological Society of America*, v. 84, p. 466-472.
- dePolo, C. M., Clark, D.G., Slemmons, D.B., and Aymard, W.H., 1989, Historical Basin and Range Province surface faulting and fault segmentation: U.S. Geological Survey Open-File Report 89-315, p. 131-163.
- dePolo, C.M., Clark, D.G., Slemmons, D.B., and Ramelli, A.R., 1991, Historical surface faulting in the Basin and Range Province, western North America: Implications for fault segmentation: *Journal of Structural Geology*, v. 13, p. 123-136.
- Dohrenwend, J.C., Schell, B.A., Menges, C.M., Moring, B.C., and McKittrick, M.A., 1996, Reconnaissance photogeologic map of young (Quaternary and late Tertiary) faults in Nevada, in Singer, D.A., editor: *An analysis of Nevada's metal-bearing mineral resources*, Nevada Bureau of Mines and Geology Open-File Report 96-2, p. 9-1 - 9-11.
- Ehlers, Jürgen, 1996, Quaternary and glacial geology: Chichester, England, John Wiley and Sons, 578 p.
- Gallup, C.D., Edwards, R.L., and Johnson, R.G., 1994, The timing of high sea levels over the past 200,000 years: *Science*, v. 263, p. 796-800.
- Hanks, T.C., and Schwartz, D.P., 1987, Morphologic dating of the pre-1983 fault scarp on the Lost River fault at Doublespring Pass Road, Cluster County, Idaho: *Bulletin of the Seismological Society of America*, v. 77, p. 837-846.
- Hart, E.W., 1994, Fault-rupture hazard zones in California: California Division of Mines and Geology, Special Publication 42, 34 p.
- McCalpin, J., 1986, Thermoluminescence (TL) dating in seismic hazard evaluations: An example from the Bonneville basin, Utah, in *Proceedings of the 22nd Symposium on Engineering Geology and Soils Engineering*: Department of Geology and Geophysics, Boise State University, Boise, Idaho, p. 156-167.
- Morrison, R.B., 1991, Introduction, in Morrison, R.B., editor, Quaternary nonglacial geology; conterminous U.S.: Geological Society of America, *The Geology of North America*, v. K-2, p. 1-12.
- National Research Council, 1986, Active tectonics: National Academy Press, Studies in Geophysics, 266 p.
- Nevada Associations of Engineering Geologists, 1996, Guidelines for fault studies in Nevada: available from the Nevada Bureau of Mines and Geology on line at <http://www.nbmng.unr.edu/guide.html>
- Noller, J.S., Zreda, M.G., and Lettis, W.R., 1996, Use of cosmogenic ³⁶Cl to date late Quaternary activity of the Hebgen Lake fault, Montana: Geological Society of America, Abstracts with Programs, p. A-300.
- Pearthree, P.A., 1990, Geomorphic analysis of young faulting and fault behavior in central Nevada: Tucson, University of Arizona PhD Dissertation, 212 p.
- Richmond, G.M. and Fullerton, D.S., 1986, Quaternary glaciations of the United States of America, in Sibrava, V., Bowen, D.Q., and Richmond, G.M., editors., *Quaternary glaciations in the northern hemisphere*: Oxford, Pergamon Press, p. 3-11.
- Robison, R.M., 1993, Surface-fault rupture: A guide for land-use planning, Utah and Juab Counties, Utah, in *Applications of research from the U.S. Geological Survey program, assessment of regional earthquake hazards and risk along the Wasatch Front*, Utah: U.S. Geological Survey Professional Paper 1519, p. 121-128.
- Siddharthan, R., Bell, J.W., Anderson, J.G., and dePolo, C.M., Peak bedrock acceleration for the State of Nevada (final report to the Nevada Department of Transportation): University of Nevada, Reno, 51 p. (Unpublished report).
- Slemmons, D.B., Steinbrugge, K.V., Tocher, D., Oakeshott, G.B., and Gianella, V.P., 1959, Wonder, Nevada, earthquake of 1903: *Bulletin of the Seismological Society of America*, v. 49, p. 251-265.
- Wallace, R.E., 1987, Grouping and migration of surface faulting and variations in slip rates on faults in the Great Basin Province: *Bulletin of the Seismological Society of America*, v. 77, p. 868-876.

CONTRASTS BETWEEN SHORT- AND LONG-TERM RECORDS OF SEISMICITY IN THE RIO GRANDE RIFT—IMPORTANT IMPLICATIONS FOR SEISMIC- HAZARD ASSESSMENTS IN AREAS OF SLOW EXTENSION

Michael N. Machette
U.S. Geological Survey, MS 966
Geologic Hazards Team—Central Region
Denver, Colorado 80225
(machette@gldvxa.cr.usgs.gov)

ABSTRACT

The Rio Grande rift has a relatively short and unimpressive record of historical seismicity. However, there is abundant evidence of prehistoric (Quaternary) surface faulting associated with large ($M > 6$) earthquakes. This paradox between historical and prehistoric seismicity (paleoseismicity) has important implications for seismic-hazards analyses based primarily on modern seismicity.

The paleoseismic record of faulting in the rift is poorly documented compared to most seismically active regions, mainly because there have been few detailed studies and partly because many of the faults have long recurrence intervals (e.g., 10,000–100,000 years), which makes dating them difficult by radiocarbon methods alone. Nevertheless, a new compilation of Quaternary fault data for the rift suggests Holocene ($< 10,000$ years) movement on at least 20 faults. Several of these faults have evidence for multiple movements; thus, at least 22 large earthquakes of probable $M > 6.25$ were associated with surface ruptures during the past 10,000 years, or one about every 450 years.

Because the level of seismicity of the Rio Grande rift is generally low, the populace (in general) believes that earthquakes do not pose a significant threat to them, whereas the presence of abundant young faults tells a different story. From a geologic viewpoint, it seems obvious that modern seismic-hazards assessments for regions like the Rio Grande rift must use not only catalogs of modern seismicity, but also integrate data from a comprehensive inventory of Quaternary faults, especially those structures showing evidence of movement in the past 100,000 years (a time interval which encompasses a complete earthquake cycle for most all active faults). A myopic view of earthquake hazards posed by individual faults (i.e., having recurrence intervals of 10,000 years or more) can lead to a complacent attitude that strengthens a perception of low seismic potential for the region. Without proper caution, this attitude can be manifested in inappropriate construction styles, building codes, land-use policies, and the siting (or relocation) of important or critical facilities.

INTRODUCTION

Virtually all modern earthquake-hazards assessments are based primarily on historical seismicity coupled with geologic evidence of faulting that is associated with strong ground motion (paleoseismology). The predictive nature of these assessments follows the widely accepted paradigm that "the past is the key to the future." This seismological basis for earthquake-hazards assessments is natural, quantitative, and justified through traditional practice. However, a paradox exists in many recently developed countries with short historical records, such as the United States where the recorded history of seismicity may be only 100–300 years long and the instrumental record may be considerably shorter. The problem lies in the potential disparity between short-term records of strong ground motion reflected by historical seismicity and long-term records of strong ground motion indicated from paleoseismic studies. This paper reflects on these disparities and the reasons they exist.

The U.S. and many other countries have geologically distinct regions that fall into markedly different seismogenic settings. Commonly, these regions are directly associated with tectonic provinces, their seismic activity being

controlled by their proximity to tectonic plate margins, regional geologic setting, and their current state of stress. Although there is probably a continuum between these regions, let us consider that there are three general types of seismogenic settings in the United States. This simple characterization allows us to frame the present and Neogene seismotectonic setting of the Rio Grande rift.

In tectonically active regions, especially those bordering convergent or transpressive plate margins, large ($M > 6$) earthquakes are associated with catastrophic movement on faults having slip rates that are typically tens of mm/year to several cm/year and recurrence intervals of several hundreds (e.g., San Andreas fault) to several thousand years long (e.g., blind thrust faults within the Los Angeles basin). Strike-slip and thrust faults in coastal California and the Cascadia subduction zone fall in this broad category of tectonically active regions. Here, the brief record of felt seismicity (100–150 years) may adequately portray many of the active faults. Nevertheless, even seismicity fails to image some seismogenic structures, such as blind thrusts (e.g., the 1994 Northridge earthquake).

In tectonically less-active regions such as the extensional domains of the Basin and Range Province and Rio Grande rift of the western U.S., fault slip rates are typi-

cally <1-2 mm/year; thus, recurrence intervals for surface rupturing fault are as little as several thousand years (e.g., the Wasatch fault zone) or as long as 10,000 years (e.g., a typical Basin and Range fault) to 100,000 years (e.g., some of the least active Quaternary faults in the Rio Grande rift). Obviously, the 150- to 300-year-long record of felt seismicity only portrays a small fraction of the potentially active faults in these regions.

Finally, in even less tectonically active regions, such as the passive margin of the eastern U.S. and compressional domain of the stable continental interior of the U.S., Canada, and Australia, fault slip rates are probably measured in hundredths of a mm/year, and intervals between surface rupturing events may be extremely long (>100,000 years) or immeasurable. However, these regions also seem prone to clustered earthquake activity—that is, one where seismic structures are recurrently active over relatively short geologic time frames (hundreds to thousands of years), then inactive for long intervals of time (thousands to tens of thousands of years). The New Madrid and Charleston seismic zones (mid-continent and eastern U.S., respectively) and the Cheraw fault (southeastern Colorado) are examples of faults that have evidence of short-term clustering but no geologic evidence of similar long-term tectonic activity.

In extensional domains such as the Rio Grande rift, a situation exists where the record of historical seismicity is relatively short and generally unimpressive. Instrumental data exist from the mid-1960s and felt reports go back to the 1600s in specific locations (e.g., Santa Fe). Although the paleoseismic record reveals evidence of abundant late Pleistocene (i.e., 10,000-130,000 years ago) and Holocene (<10,000 years ago) faulting in the rift, we only have evidence of a single historic surface rupture from an earthquake that occurred a little more than 110 years ago in northern Sonora, Mexico, south of Douglas, Arizona. Within the U.S. portion of the rift, the largest felt or recorded earthquake (M_s 6.3) occurred in 1931 near Valentine, Texas, and although this event did not form a demonstrable surface rupture, it may have had as much as 38 centimeters of slip in the subsurface (Doser, 1987). This earthquake, and similar-size ones in the Basin and Range Province (see Wells and Coppersmith, 1994), suggest that the threshold for surface ruptures is in the lower half of the M 6 range (i.e., M 6.25 \pm 0.25) for normal faults that have earthquakes nucleating at depths of 15 kilometers to perhaps 20 kilometers. Thus, there is an apparent paradox in the Rio Grande rift between the short-term record of seismicity (relatively aseismic, no surface rupture) and the long-term record (abundant evidence of late Quaternary faults and, hence, paleoseismicity). The manner in which this disparity is dealt with has important implications for seismic-hazards analyses.

QUATERNARY FAULTING IN THE RIO GRANDE RIFT

The Rio Grande rift lies within the eastern part of the Basin and Range and the southern part of the Rocky Mountain provinces as defined by Fenneman (1931); it forms a nearly continuous, deep, sediment-filled valley of

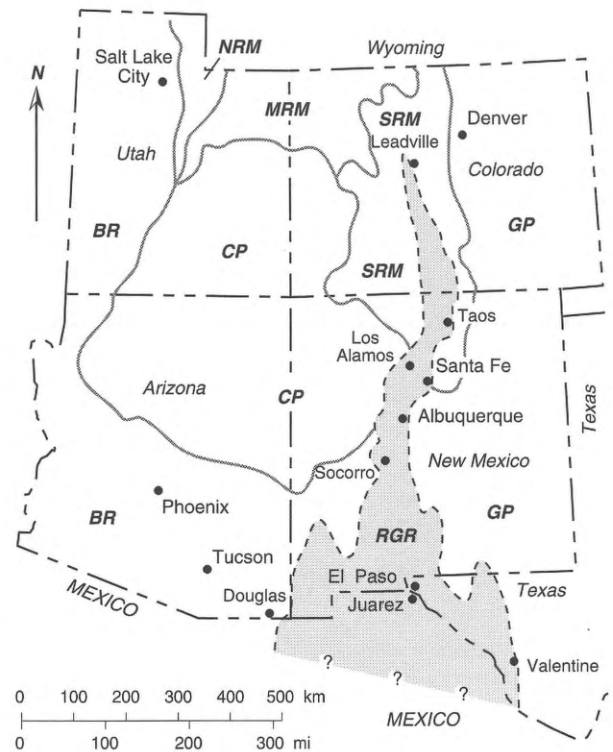


Figure 1. Index map of the Rio Grande rift showing cultural and geographic features mentioned in the text. Physiographic provinces (from Fenneman, 1931) are as follows: BR, Basin and Range; CP, Colorado Plateau; GP, Great Plains; MR, Middle Rocky Mountains (includes Wyoming Basin); RGR, Rio Grande rift subprovince (shaded pattern); and SR, Southern Rocky Mountains. Solid lines show province boundaries; dashed line shows limits of Rio Grande rift as used in this paper.

Neogene age that extends almost 1,000 kilometers from Leadville, Colorado, south into western Texas, southeastern Arizona, and northern Chihuahua and Sonora (northernmost Mexico) (figure 1). The rift widens to the south; it is a singular 30- to 40-kilometer-wide, half-graben north of Taos, New Mexico. The down-to-the-west Sangre de Cristo fault zone (faults 3 and 4, figure 2) is the predominant rift-bounding structure in this area. South from a line between roughly Taos and Los Alamos, New Mexico, the rift widens to 40-60 kilometers, with alternating-polarity half grabens in the Espanola, Santo Domingo, and Albuquerque basins. South of Socorro, the rift becomes even wider (60-150 kilometers) and is comprised of 2 or more half grabens or grabens. The southern part of the Rio Grande rift lies with a southeastern part (extension) of the Basin and Range, the rift's western margin is herein considered to be near the Arizona/New Mexico border; however, some have placed the boundary of the Neogene Rio Grande rift further east near Deming, New Mexico. Nevertheless, at the International Border with Mexico, the rift is on the order of about 400 kilometers wide. On the basis of the north-south orientation and youthfulness of faulting, the Quaternary Rio Grande rift probably extends from the Animas Valley in southwestern New Mexico and San Bernardino Valley in northern Sonora, Mexico (on the west) to the Lobo Valley near Valentine, Texas (on the east) (figure 2).

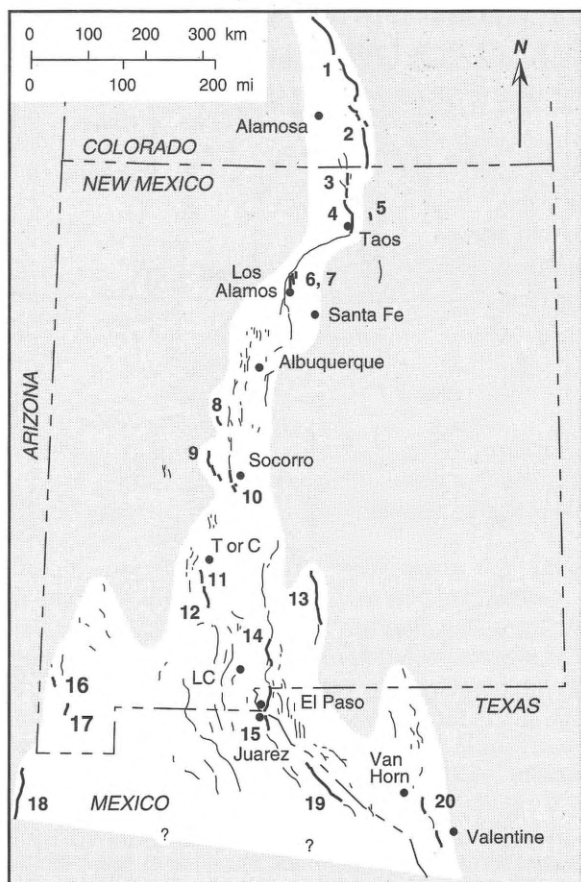


Figure 2. Generalized map of Quaternary faults of the Rio Grande rift in southern Colorado, New Mexico, western Texas, and northern Mexico. Faults of Holocene (and historic) age are numbered and described in table 1.

Quaternary faults are both widespread and common in the Rio Grande rift (Nakata and others, 1982; Machette and others, 1996), but relatively young (<15,000 year old) surface ruptures are restricted primarily to major range-bounding faults (Machette and Hawley, 1996) such as those along the Sangre de Cristo, Jemez, Socorro, Magdalena, Caballo, San Andres, Organ, and Franklin Mountains (see figure 2). The paleoseismic record of faulting in the rift is poorly understood, mainly because there have been few detailed studies and partly because many of the faults have long recurrence intervals (i.e., 10,000-100,000 years), which makes dating times of movement on them difficult by radiocarbon methods. Thus, it is difficult to assess prehistoric levels of seismicity in the rift. However, based on preliminary studies of fault age and distribution, I previously suggested a composite recurrence interval (CRI) of about 750 ± 250 years for a major surface-rupturing earthquake in the New Mexico part of the Rio Grande rift (Machette, 1987a). We now have a compilation of paleoseismic data for the rift in southern Colorado (Sangre de Cristo fault), New Mexico, west Texas and northern Mexico (Collins and others, 1996; Machette and others, 1996; respectively). These data indicate Holocene movement on 20 faults (table 1), including the one historical rupture in northern Mexico. In addition to these 20

earthquake events, the Sangre de Cristo and Organ Mountains faults have evidence for two separate movements in the Holocene; thus, one should consider that there have been at least 22 large ($M > 6.25$) earthquakes associated with surface ruptures in the Rio Grande rift in the past 10,000 years. These data suggest a Holocene composite recurrence interval (CRI) of about 450 years for the above mentioned portion of the rift. Some portions of the rift, especially those settled by Spanish missionaries along the Rio Grande, have been continuously occupied since nearly A.D. 1600, thus the CRI is approaching the time that the region has been occupied by Americans of European origin (i.e. the historical record). The new calculated CRI is considerably less than before (750 years) because I have included faults from a larger area (Texas, Mexico, and southern Colorado) and because there are several newly documented faults in the listing. The most recent movement on the prehistoric faults seems to have been along the Organ Mountains fault about 1,000 years ago (Gile, 1987), whereas the Pitaycachi fault is the only historic surface rupture in the rift (see table 1). Based on past experience, it seems likely that with further paleoseismic studies the number of faults with known Holocene movement will probably increase, and the CRI will decrease somewhat, as it has in many other parts of the Basin and Range. In contrast, the CRI for the rift is roughly equivalent to that of the Wasatch fault zone (5 active segments) in Utah (Machette and others, 1991, table 2), a fault zone which is considerably more active than those typical of the Basin and Range Province.

There are two major urban centers in the relatively sparsely populated Rio Grande rift. The northern center includes Los Alamos, Santa Fe, and Albuquerque, a region where an estimated 50 percent (i.e., 750,000) of New Mexico's population lives (ca. 1.5 million in 1990). This area is close to or includes several Quaternary faults (the Embudo, Parajito, Guaye Mountain, Rendija Canyon, and Hubbell Springs) that have clear evidence for either Holocene or latest Pleistocene movements associated with large earthquakes. New studies of the Parajito fault indicate latest Pleistocene (Kelson and others, 1993) or possibly younger movement (James McCalpin, oral communication 1997), whereas two of its subsidiary faults (the Rendija and Guaye Mountain) are known to be Holocene (Kelson and others, 1993). The Parajito fault has a long history of Quaternary movement—its scarp on 1.1-million-year-old Bandelier Tuff is commonly 120 meters high; more importantly, the fault bounds the west side of the Los Alamos National Laboratory, an important research and defense-related facility. In addition, there are several other critical facilities (Kirkland Air Force Base and Sandia National Laboratory), the State Capital, and Cochiti Reservoir within this region, all of which could be subject to damage from severe ground shaking during large earthquakes on nearby active faults.

At the southern margin of the rift, population is mainly concentrated in the El Paso/Juarez metropolitan area (estimated population of more than 1.8 million), with a smaller urban area at Las Cruces (70 kilometers to the north-northwest). El Paso has nearly 600,000 people living in a relatively small area (El Paso County), whereas

Table 1. Faults with known or suspected Holocene movement in the Rio Grande rift.

(Abbreviations: SM, scarp morphology; ST, stratigraphic relations; S, soils; C14, radiocarbon dating; T, trenching; Mtns., mountains; EQ, earthquake)

Name of fault	Number & general location (see figure 2)	Time of most recent event	Evidence for timing & main reference(s)
Sangre de Cristo (section A)	1. West front of Sangre de Cristo Mtns., NE of Alamosa, Colorado.	Early Holocene	SM, ST, S, C14, & T; McCalpin, 1982.
Sangre de Cristo (section B)	2. West front of Sangre de Cristo Mtns., E of San Luis, Colorado.	2-3(?) events in Holocene	ST & C14; Kirkham & Rogers, 1981.
Sangre de Cristo (section C)	3. West front of Sangre de Cristo Mtns., near Cuesta, New Mexico.	Middle to early Holocene	SM & ST; Menges, 1990.
Sangre de Cristo (section D)	4. West front of Sangre de Cristo Mtns., near Taos, New Mexico.	Early (?) Holocene	SM & ST; Machette & Personius, 1984.
Valle de Vidal	5. East side of Valle Vidal, northern New Mexico.	Late to middle Holocene	SM; Menges & Walker, 1990.
Guaye Mountain	6. West side of Espanola basin, N of Los Alamos, New Mexico.	Middle Holocene	ST, T, & C14; Kelson & others, 1993.
Rendija Canyon	7. West side of Espanola basin, N of Los Alamos, New Mexico.	Early Holocene	ST, T, & C14; Kelson & others, 1993.
Coyote Springs	8. North flank of Ladrone Mtns., central New Mexico.	Early (?) Holocene	SM; Machette & McGimsey, 1983.
La Jencia	9. West side of La Jencia basin, central New Mexico.	1-2(?) events in Holocene	SM, ST, S, & T; Machette, 1988.
Socorro Canyon	10. East side of Socorro Mtns., S of Socorro, New Mexico.	Early (?) Holocene	SM; Machette & McGimsey, 1983.
Caballo (Williamsburg scarp)	11. Northern segment of Caballo fault, S of Truth or Consequences, New Mexico.	Late(?) Holocene	SM, ST, C14, & T; Machette, 1987c, Foley & others, 1988.
Caballo	12. Central segment of Caballo fault, S of Truth or Consequences, New Mexico.	Middle Holocene	SM, ST, & T; Machette, 1987c, Foley & others, 1988.
Alamogordo	13. West flank of Sacramento Mtns, Alamogordo, New Mexico.	Early (?) Holocene	SM & ST; Machette, 1987b.
Organ Mountains	14. East flank of Organ Mtns., southern New Mexico.	2 events in Holocene	SM, S, C14, & T; Gile, 1987; Machette, 1987b.
East Franklin Mountains	15. East flank of Franklin Mtns., north of El Paso, Texas.	Early (?) Holocene	SM & ST; Machette, 1987b.
Washburn (zone)	16. East flank of Pelloncillo Mtns., W. of Animas, New Mexico.	Holocene	SM; Machette & others, 1986.
Gillespie Mtn.	17. West flank of Animas Mtns., Animas Valley, SW New Mexico.	Holocene	SM; Machette & others, 1986.
Pitaycachi (Sonora EQ)	18. East side of San Bernardino Valley, NE Sonora, Mexico	Historic (May 3, 1887)	75 km rupture, scarp height 4 m max., Bull & Pearthree, 1988.
West Lobo Valley	19. West side of Lobo Valley, W of Valentine, Texas.	Holocene (?)	SM; Machette unpubl. data, 1982; Collins & Raney, 1991.
Amargosa	20. Northeast side of Amargosa Mtns., NW Chihuahua, Mexico.	Early (?) Holocene	SM, ST; Collins & Raney, 1991.

Ciudad Juarez just across the Rio Grande has a burgeoning population roughly estimated at 1.2 million in 1990. The largest historical earthquake to affect the El Paso region was a MM VI (cited in Collins and Raney, 1991). However, both El Paso and Juarez would be threatened by movement of the East Franklin Mountains fault, which extends through the heart of both urban areas. The East Franklin Mountains fault is just the southern one-quarter of a 182-kilometer-long fault zone that extends from south of the International Border with Mexico (in the city of Juarez) north through El Paso and Fort Bliss and into New Mexico along the west side of White Sands Missile Range and the Tularosa Basin. This fault zone is one of the longer active normal faults in the Rio Grande rift, exceeded only by the Sangre de Cristo fault zone in northern New Mexico and southern Colorado. The most recent movement on the East Franklin Mountains fault probably was in the latest Pleistocene or early(?) Holocene (J. Keaton and J. Barnes, written communication, 1995), but the fault has a history of recurrent movement as documented by Quaternary scarps as much as 60 meters high. In earlier studies, Machette (1987b) estimated that this entire fault zone is comprised of five discrete parts (fault segments), each having recurrence intervals of 10,000-20,000 years. If this is true, then a major surface-rupturing earthquake may occur, on average, about once every 2,000-4,000 years (CRI) somewhere on the 182-kilometer-long fault zone. This fault system and many others are invisible (not imaged) on seismicity maps of the Rio Grande rift.

SEISMICITY

Seismicity in the rift is relatively diffuse with few meaningful concentrations or associations with active faults (figure 3). About half of the earthquakes shown in figure 3 are within the rift, and the other half are in the Colorado Plateaus Province and, to a lesser extent, the Great Plains Province adjacent to the rift. Much of the felt (but not recorded) seismicity for the period 1849-1961 (Northrup, 1976) was concentrated along the Rio Grande Valley between Albuquerque and Socorro. The historical documentation of these earthquakes probably reflects the concentration of early settlers in towns along the Rio Grande and local sources of low to moderate seismicity. For example, the swarm of earthquakes that occurred at Socorro in 1906 (MM VIII; Sanford and others, 1991) appears likely a result of magma movement at depth. The Socorro area continues to be a focus of small, but numerous earthquakes (figure 3). Conversely, the distribution of $M \geq 2.5$ earthquakes in New Mexico for the period of 1962-86 (figure 5 in Sanford and others, 1991), shows only a weak association with the rift and some of the transverse structures such as the Jemez lineament, which partly control the geometry of the rift (i.e., accommodation zones).

Within New Mexico between 1962 and 1986, there were only six earthquakes larger than M 3.5, and the largest (1966 Ms 4.6-4.9; Sanford and others, 1991) occurred in the Colorado Plateaus province near the bor-

der with Colorado (figure 3). The largest instrumentally recorded earthquakes in the rift have been a M 5 in 1989 near Bernardo (between Socorro and Belen, New Mexico; Sanford and others (1991) and a significantly larger Ms 6.3 earthquake in 1931 near Valentine, Texas (Doser, 1987). Although the Valentine earthquake was not quite large enough to cause surface faulting, the epicentral area has several Quaternary faults that have been active in the Holocene(?) or latest Pleistocene (table 1; Collins and Raney, 1991; Collins and others, 1996). Also, it is interesting to note that on the basis of instrumental data (through 1977), the Great Plains and Colorado Plateaus - two provinces considered to be tectonically stable—had equivalent or greater seismicity than the Rio Grande rift (Sanford and others, 1991). The most recent moderate size earthquake was an M 5.7 shock that struck Alpine, Texas (east of the rift) in April 1995. Thus, modern seismicity within the rift is remarkable only for its subdued level and lack of association with known Quaternary faults.

Even though the rift seems to be a relatively quite seismogenic region, past history shows its potential for large and devastating earthquakes. For example, the great 1887 Sonoran earthquake (Mw 7.4) of northern Mexico

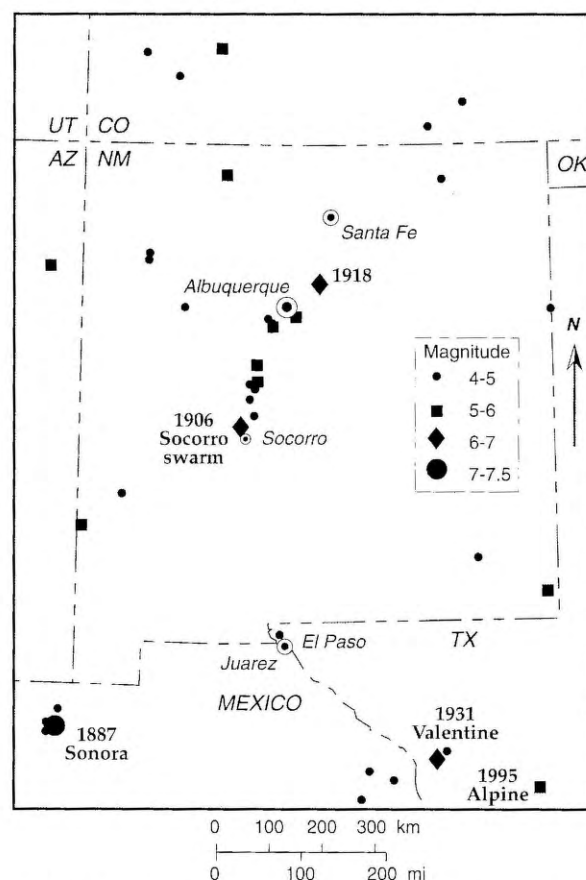


Figure 3. Map showing earthquakes with magnitudes 4.0 and greater in New Mexico and adjacent regions. Earthquakes, keyed to magnitude by symbols, are from the combined catalog used by Frankel and others (1996). The 1887 Sonora, Mexico earthquake (table 1, no. 18) is the largest historic surface-rupturing earthquake to have occurred in the region. Other large earthquakes, such as the 1931 Valentine, Texas earthquake and the 1906 Socorro, New Mexico earthquake (swarm), are discussed in the text.

has not been traditionally associated with the Rio Grande rift because the earthquake occurred in Mexico and the rift has been considered to be a largely U.S. feature. However, many of the rift structures in New Mexico and west Texas continue south into Chihuahua and Sonora. The 1887 Sonoran earthquake occurred along the Pitachyichi fault (Bull and Pearthree, 1988)—a range-bounding, north-south-trending, high-angle normal fault that is a southward continuation of Quaternary faulting in the San Bernardino Valley of southwestern New Mexico (see Machette and others, 1986). As such, this fault should be considered as a modern rift structure. It has the characteristics of a major surface-rupturing rift fault (see for example Pearthree and Calvo, 1987; Machette, 1988) in that it has an extremely low slip rate and long-recurrence interval (Bull and Pearthree, 1988). Although almost forgotten because it occurred about 110 years ago, movement on the Pitachyichi fault formed the longest (75 kilometers) historic surface rupture of a normal fault in North America. Tucson, then a dusty frontier town and now a major urban area of Arizona, was subject to strong ground motion and portions of the intervening countryside experienced both liquefaction and artesian water spouts.

SEISMIC HAZARDS IN THE RIO GRANDE RIFT

The scarcity of historical surface faulting (figure 2) and the general low level of seismicity of the Rio Grande rift (figure 3) has led the populace in that area to believe that earthquakes do not pose a significant threat to the region. In fact, the most recent series of USGS seismic-hazard maps (Frankel and others, 1996) indicate 1) low levels of ground acceleration (≤ 0.1 g) with 10 percent probability of exceedance in 50 years and 2) low to moderate (≤ 0.3 g) levels of ground acceleration with 2 percent probability of exceedance in 50 years (see figure 4a and 4b, respectively). For example, 0.10 g may be an appropriate threshold for damage to older structures (pre-1965 dwellings) or dwellings not made resistant to earthquakes (see Frankel and others, 1996). The seismic-hazard maps shown in figure 4a illustrates the domination of moderate seismicity in areas of slow extension, such as the Rio Grande rift, whereas figure 4b starts to show the affect of faults on the hazard. Thus, the populace's perceptions are well based on what has happened in New Mexico over the past several centuries. The areas of highest map-

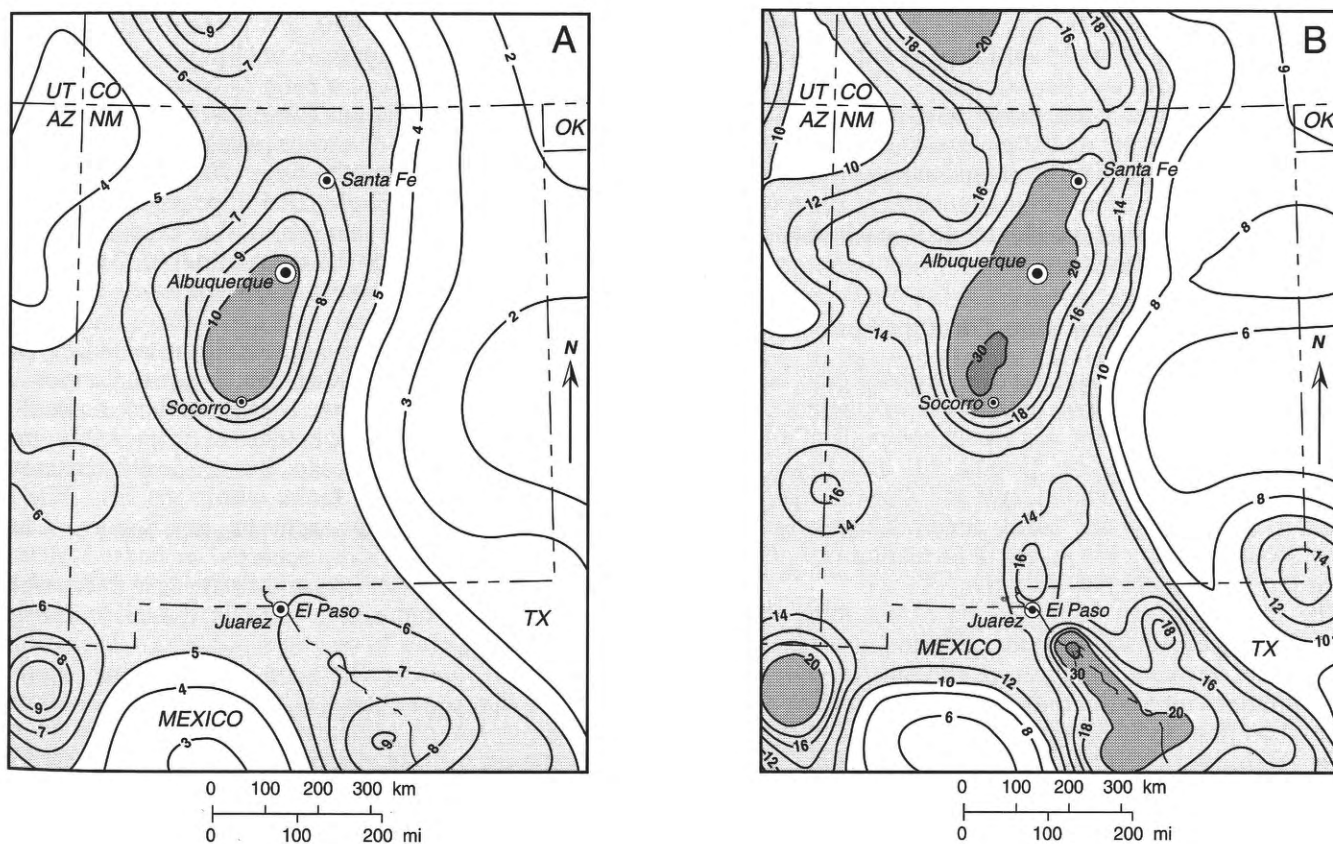


Figure 4. Recent seismic-hazard maps of the New Mexico portion of the Rio Grande rift. Maps show ground-motion hazard (contoured in percent g) at a given level of probability. A) 10 percent probability of exceedance in 50 years. B) 2 percent probability of exceedance in 50 years. Maps based on Frankel and others, 1996. Data downloaded from U.S. Geological Survey web site at <http://gldage.cr.usgs.gov/eq/html/custom.shtml>, which allows you to create custom ground-motion-hazard maps using varying parameters.

ped ground acceleration are centered over areas where $M > 4$ earthquakes have occurred historically (compare figure 3 with figures 4a and 4b). Interestingly, one of the areas of large predicted ground acceleration (≤ 0.2 g, figure 4b) is centered over the 1887 Sonoran M_w 7.4 earthquake partly as a result of continued M 4 earthquakes in the area (which might be aftershocks from 1887 earthquake). Interestingly, the Pitachyichi fault, on which this earthquake occurred, has an estimated recurrence interval of 100,000 years or more (see Bull and Pearthree, 1987) for large surface ruptures. Thus, although the maps indicate potential for moderate ground acceleration associated with a $M < 6$ earthquake in Sonora, Mexico area, paleoseismologic studies predict an extremely long return time for another 1887-like $M > 7$ earthquake.

The paleoseismic record clearly demonstrates that potentially large and devastating earthquakes may occur somewhere in New Mexico as frequently as every 750 years (or less) to as frequently as every 450 years for the rift. On this basis alone, one cannot argue that large earthquakes will not occur on low-slip (long-recurrence) faults. More likely, one might argue that these faults are typically aseismic for long intervals between movements, and that most of the seismicity that is occurring in the rift occurs as minor adjustments on a myriad of non-surface rupturing faults. In a sense, the elephant is snoring. From a geologic perspective, it seems that most major surface-rupturing, normal faults tend to be aseismic (the normal mode), but can move during $M > 6.25$ earthquakes without significant precursory activity (foreshocks). Similarly, the Wasatch fault zone in Utah (a world-class normal fault with a Holocene slip rate of 1-2 mm/year) is currently less seismic than the surrounding basin-and-range blocks, yet it has a proven history of recurrent movement on roughly 400-year intervals during the Holocene (see Machette and others, 1991, 1992a, 1992b).

Variations in Slip Rate Through Time

When geologic data are used in probabilistic hazard assessments, one of the most important parameters is the slip rate (and the associated recurrence interval) of a fault. In regions such as the Rio Grande rift and Basin and Range Province (as a whole), reliable slip-rate data are difficult to obtain. In many cases, one must use long-term slip rates because data for recent deformation (i.e., Holocene or late Pleistocene) do not exist.

The main problem with long-term slip rates (those averaged over several to hundreds of earthquake cycles) is that there can be major variations in slip rate through time. These variations are difficult to document and many times are based on first-order observations such as geomorphology or sedimentation rates. One moderately well documented example exists for the Wasatch fault zone. On this fault, most of the slip-rate data are from faulted deposits of Holocene or latest Pleistocene age (post high stand of Lake Bonneville; 15,000 years ago). These slip rates are typically 1-2 mm/yr, but some data from the interval between 12,000 and 15,000 years ago suggest much higher slip rates, perhaps related to the catastrophic draining and crustal rebound of Lake Bonneville (see Machette

and others, 1992b for a more complete discussion). Conversely, sparse data from older datums (70,000- to 140,000-year-old lake deposits) indicate much slower slip rates (i.e., 0.1-0.2 mm/yr) on the Wasatch and associated faults. Thus, in the span of one complete climatic cycle (e.g., 120,000 years), the Wasatch fault zone may have had a 10-fold variation in slip rate. This example may be somewhat extreme owing to possible lake/rebound affects, but an analysis of slip rates at Socorro, New Mexico suggests a similar potential change through time.

The Socorro Canyon fault zone (fault 10 on table 1 and figure 2) bounds the eastern margin of the Socorro Mountains, a rotated fault block which is composed of Precambrian and Paleozoic rocks and intruded by a mid-Tertiary volcanic caldera. The northern margin of the caldera is spectacularly exposed in cross section within the mountain front escarpment. The range was uplifted during early rift formation (early Miocene time), but by late Miocene time (ca. 9-10 million years ago) the range was covered by playa deposits of the Popotosa Formation. Subsequent rejuvenation of the mountain range by uplift along the Socorro Canyon fault zone has resulted in about 500 meters of local relief and about 750 meters of vertical offset of the 9-million-year-old playa deposits (C, figure 5). Although these ages and offset amounts are relatively crude estimates, they yield a long-term vertical slip rate of 0.08 mm/yr (750 m in 9 million years).

Two additional datums are present across the fault zone for temporal comparison of slip rate: 4.1- to 4.5-million year-old basalts and a early Quaternary (ca. 750,000 years) piedmont surface. These datums have about 200 meters and 25 meters of vertical offset, respectively (see A and B, figure 4). Using the three datums, the slip rate on the Socorro Canyon fault zone appears to have slowed from about 0.18-0.20 mm/yr in the latest Miocene, to about 0.05 mm/yr in the Pliocene, and 0.02-0.04 mm/yr in the past 750,000 years of the Quaternary. As with the Wasatch fault zone, there appears to be a 5- to 10-fold change (decrease in this case) in slip rate and, by inference, seismic activity along the Socorro Canyon fault zone. The youngest slip rate is extremely slow (0.02-0.04 mm/yr) and the recurrence interval is probably on the order of 50,000-100,000 years, but the fault is characteristic of many other major faults within the rift. The most recent surface-rupturing event on the Socorro Canyon fault zone appears to have occurred in latest Pleistocene time (Machette and McGimsey, 1983), and thus would be considered to be an active fault in the seismic-hazards sense.

Hazard versus Recurrence Time

In regions of high seismicity such as the West Coast, many Holocene faults have a record of movement that suggests relatively high rates of slip (> 5 mm/year), short recurrence intervals (hundreds to a thousand years), and are often associated with ongoing seismicity. Thus, these faults pose an obvious hazard and are recognized as such. However, as we know, much of the Rio Grande rift is characterized by faults with low slip rates and long recurrence intervals; they are most often not associated with

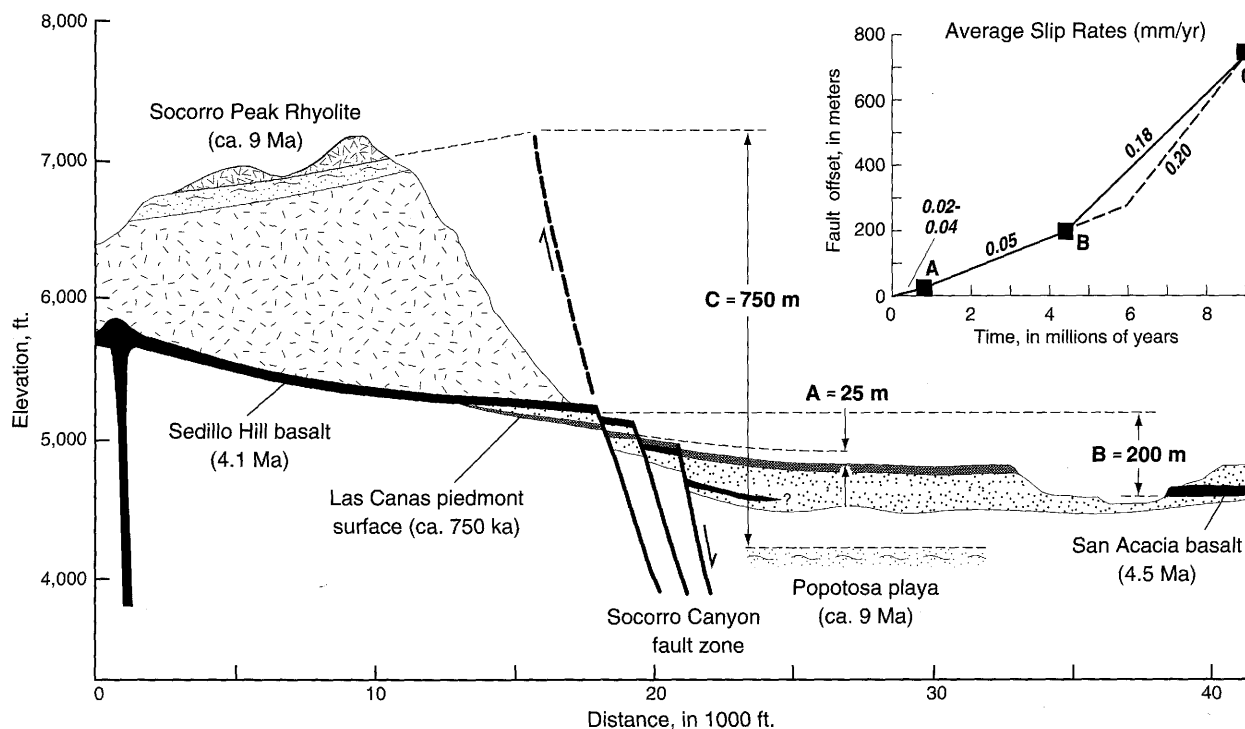


Figure 5. Schematic cross section near Socorro, New Mexico, showing evidence for late Cenozoic and Quaternary slip rates on the Socorro Canyon fault zone. Three age datums exist in the area: playa deposits of the Popotosa Formation (overlain by ca. 9-million-year-old rhyolite of Socorro Peak), early Pliocene basalts (4.1 - 4.5 million years old) that flowed on Rio Grande sediment (Sierra Ladrones Formation), and the uppermost piedmont-slope surface (Las Canas; ca. 750,000 years old) related to an ancient basin floor of the Rio Grande valley. The amounts of offset are estimates based on geologic mapping and stratigraphic relations in the area.

obvious patterns of seismicity and thus appear to be inactive (aseismic). This relation suggests the question of which faults pose more of a seismic hazard in terms of earthquake occurrence: a late Holocene (e.g., 1,000- to 2,000-year-old) fault with a 40,000-year recurrence interval or a 35,000-year-old fault with a 40,000-year recurrence interval? The answer may seem obvious from a geologic (i.e., deterministic) viewpoint, but most probabilistic seismic-hazard assessments, which are driven by patterns and rates of modern seismicity, see the younger fault as the potential hazard and minimize (or ignore) the older fault. Rarely is there adequate fault-timing information to make a meaningful deterministic assessment.

Preservation of Paleoseismic Evidence

Another problem that must be considered in regional analyses of fault activity is the preservation of the geologic record. Detailed analysis of subsurface well-logs, geologic mapping, and geophysical data from the Albuquerque basin by Hawley (1996) reveals a complex pattern of late Cenozoic deformation (figure 6), far more complex than previously determined from reconnaissance mapping of the basin. Although most of the faults in the subsurface strike north-south, there are a large number of subordinate faults that strike northeast-southwest. Previous mapping did not reveal surficial evidence for these cross-basin faults, perhaps because the prevailing paradigm was one of Quaternary north-south faulting related to east-west extension. However, recent surficial geologic mapping and the excellent subsurface work by Hawley

(1996) is starting to reveal relations between the fault patterns shown in figure 6 and the location and lateral extent of young volcanic centers, deep basins, and the Quaternary geology of the basin.

The preservation of surficial evidence of this complex structural pattern is another complication in seismic-hazards analysis for this particular area, and likely for other basins of the rift. For example, large parts of the landscape in the Rio Grande rift are formed by either high-level surfaces related to the early Pleistocene filling of the basins (prior to Rio Grande entrenchment) or are formed by latest Pleistocene (10,000-30,000 year old) sediment in alluvial-fan complexes or in entrenched stream valleys (figure 7). If faults in such basins have average recurrence intervals of 50,000-100,000 years, then virtually all faults would be recorded on the high-level surfaces whereas only some of the faults would be expected to have disturbed surfaces of late Pleistocene or Holocene age. Thus, in regions where faults are characterized by long recurrence intervals (10,000-100,000 years), one must look at a geologic record that is at least one recurrence interval long (or longer) in order to capture spatial and temporal patterns of faulting. Additional research using subsurface methods (high-resolution seismic reflection, geophysical surveys, analysis of water-well data, etc.) are needed to detect potentially active faults in areas of young landscape. One should note that most of the older buildings in the business districts of Albuquerque and El Paso are located close to the Rio Grande on young, low, flood-plain surfaces.

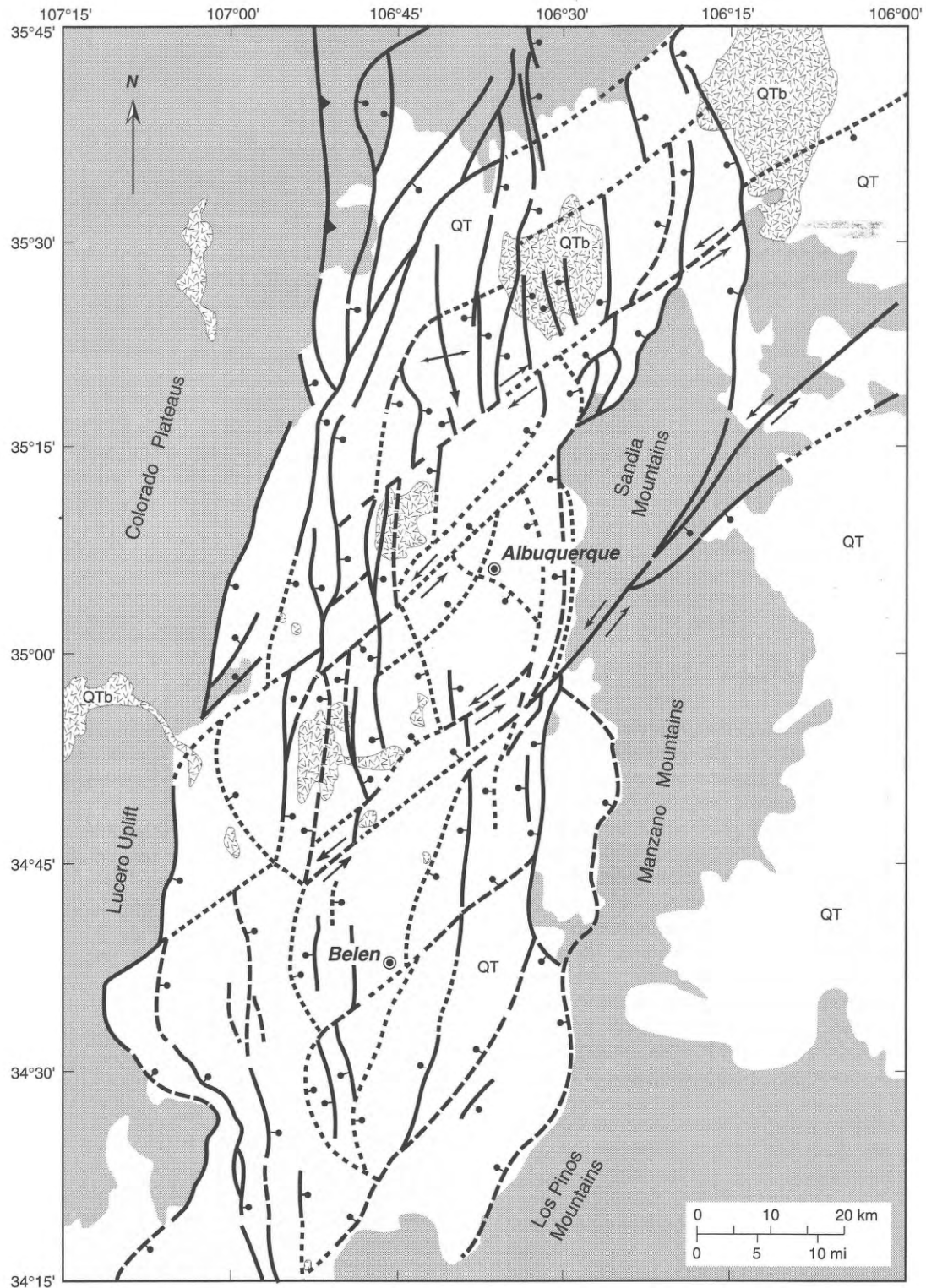


Figure 6. Late Cenozoic (Pliocene and Quaternary) faulting in the Albuquerque basin, middle Rio Grande rift. Fault pattern (simplified here) was determined by Hawley (1996) on the basis of detailed analysis of subsurface wells, geophysical data, and geologic mapping. Note the bimodal distribution of faults: predominately north-south with northeast-trending faults that accommodate disparate basin geometries and/or transfer slip. The basin deposits are shown as QT (undifferentiated Quaternary and upper Cenozoic sediment, light stipple pattern); Pliocene and Pleistocene basalts as QTb (v-pattern), and Tertiary and older bedrock (dark stippled pattern).

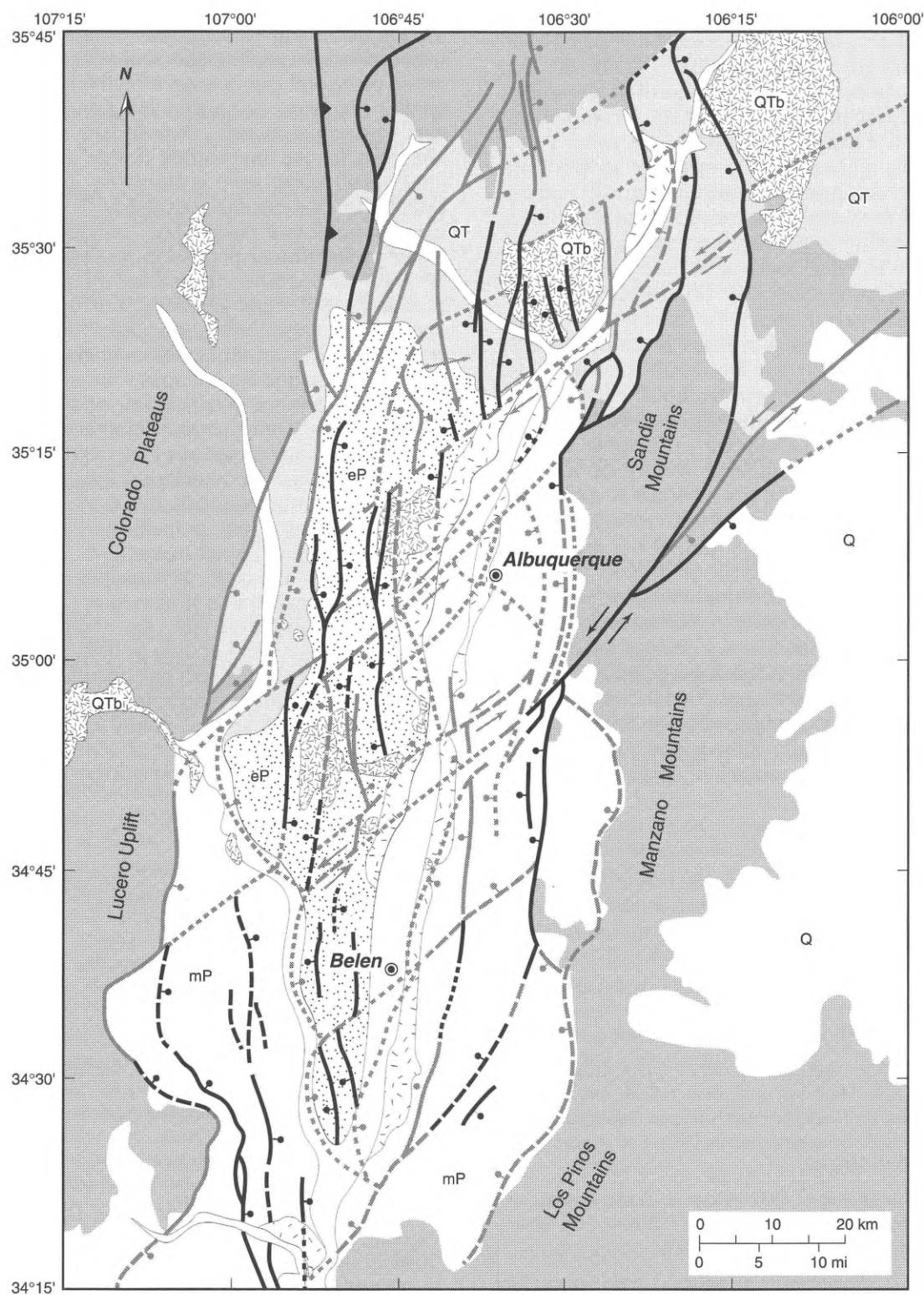


Figure 7. Quaternary faults and generalized geology of the Albuquerque basin, middle Rio Grande rift. Faults with surficial evidence of Quaternary movement are shown in black; those without such evidence are shown in gray (data from unpublished compilation; see Machette and others, 1996). Symbols: QTb, Quaternary and late Cenozoic basalts; QT, undivided basin deposits; eP, early Pleistocene sediment; mP, middle Pleistocene sediment; lP, late Pleistocene sediment; and H, Holocene sediment. Bedrock is shown by the darkest stippled pattern.

A GEOLOGIC PERSPECTIVE

From a geologic viewpoint, it seems obvious that modern seismic-hazard assessments for regions like the Rio Grande rift must use not only catalogs of modern seismicity, but also must integrate data from a comprehensive inventory of Quaternary faults, especially those structures showing evidence of movement in the past 100,000 years. By doing so, the geologic data will portray the true potential for surface-rupturing earthquakes on a time frame equivalent to the average earthquake cycle (10,000- to 100,000- year recurrence intervals). Once accomplished, the probability of occurrence of large earthquakes on individual structures may prove to be extremely low, but the location of these potential, strong-ground-motion-generating structures will be known in relation to urban areas and critical facilities. In addition, the hazard posed by numerous low-slip-rate faults within a given radius (e.g., 50-100 kilometers) of a town, city, or critical facility results in a composite recurrence interval (CRI) that can be just a fraction (i.e., 1/10th) of each individual fault. A myopic approach of not appreciating the potential for earthquake hazards posed by individual structures (i.e., recurrence intervals of 10,000 years or more) can lead to a complacent attitude that strengthens a perception of low seismic potential. Without proper caution, this attitude can be manifested in inappropriate construction styles, building codes, land-use policies, and the siting (or relocation) of important or critical facilities.

Various mitigation strategies require different portrayals of earthquake hazard. Emergency planning and disaster response plans, for example, generally require

information regarding the potential effects of a large earthquake that are possible, but perhaps unlikely to occur. Their intention is to base such plans on a worst-case or near-worst-case earthquake scenario. If response plans are in place and can operate effectively for such an earthquake, response to smaller-magnitude earthquakes can easily be accomplished. Probabilistic ground-motion hazard maps for the engineering design of buildings of standard construction have customarily used a 1/500 annual probability of exceedance (roughly 10 percent in 50 years) as a standard (see figure 4a). In some circumstances, a lower probability (2 percent in 50 years, figure 4b) might be used for facilities of special interest. These ground-motion hazard maps generally will not reflect the influence of the large rare earthquakes in the rift that have recurrence times of thousands of years since the probability of that earthquake occurring in any 50-year period is low. On the other hand, design of important or critical facilities such as nuclear and defense facilities, reservoirs, hospitals, and any structures that should remain in service following a large earthquake are generally engineered to stricter standards and may make use of ground-motion estimates at very low probability levels (i.e., 1/10,000 annual or 5 percent in 500 years). In this case, the occurrence of rare, but large earthquakes on long-recurrence faults is of considerable importance. Thus, as paleoseismological information for the western United States becomes more widely known to user communities and to the public, there likely will be concerns and controversies over what is considered acceptable levels of risk. Clearly, resolution of such seismic-safety issues will require the cooperation and participation of a wide range of users of earthquake-hazard information and the research community.

REFERENCES

- Bull, W.A., and Pearthree, P.A., 1988, Frequency and size of Quaternary surface ruptures of the Pitaycachi fault, northeastern Sonora, Mexico: *Bulletin of the Seismological Society of America*, v. 78, p. 956-978.
- Collins, E.W., and Raney, J.A., 1991, Tertiary and Quaternary structure and paleotectonics of the Hueco basin, trans-Pecos Texas and Chihuahua, Mexico: [Texas] Bureau of Economic Geology Geological Circular 91-2, 44 p.
- Collins, E.W., Raney, J.A., Machette, M.N., Haller, K.M., and Dart, R.L., 1996, Map and data for Quaternary faults in west Texas and adjacent parts of Mexico: U.S. Geological Survey Open-File Report 96-002, 74 p., 1 plate, scale 1:500,000.
- Doser, D.I., 1987, The 16 August 1931 Valentine, Texas, earthquake—Evidence for normal faulting in west Texas: *Bulletin of the Seismological Society of America*, v. 77, p. 2005-2017.
- Fenneman, N.M., 1931, *Physiography of western United States*: New York, McGraw-Hill Book Co., 534 p.
- Gile, L.H., 1987, Late Holocene displacement along the Organ Mountains fault: New Mexico Bureau of Mines and Mineral Resources Bulletin 116, 43 p.
- Foley, L.L., LaForge, R.C., and Piety, L.A., 1988, Seismotectonic study for Elephant Butte and Caballo Dams, Rio Grande project, New Mexico: U.S. Bureau of Reclamation Seismotectonic Report 88-9, 60 p., 3 appendices, 1 pl., scale 1:24,000.
- Frankel, A., Mueller, C., Barnhard, T., Perkins, D., Leyendecker, E.V., Dickman, N., Hanson, S., and Hopper, M., 1996, National Seismic Hazards Maps—Documentation June 1996: U.S. Geological Survey Open-File Report 96-532, 110 p. (see also <http://gldage.cr.usgs.gov/eq/>).
- Hawley, J.W., 1996, Hydrogeologic framework of potential recharge areas in the Albuquerque basin, central Valencia County (Chapter 1), in Whitworth, T.M., and Hawley, J.W., editors, *Hydrogeology of potential recharge and hydrogeochemical modeling of proposed artificial-recharge methods in basin- and valley-fill aquifer systems, Albuquerque Basin, New Mexico*: New Mexico Bureau of Mines and Mineral Resources Open-File Report 402-D, various pagination.
- Kelson, K.I., Hemphill-Haley, M.A., Wong, I.G., Gardner, J.N., and Reneau, S.L., 1993, Paleoseismologic studies of the Parajito fault system, western margin of the Rio Grande rift near Los Alamos: *Geological Society of America Abstracts with Program*, v. 25, no. 5, p. 61-62.
- Kirkham, R.M., and Rogers, W.P., 1981, Earthquake potential in Colorado - A preliminary evaluation: *Colorado Geological Survey Bulletin* 43, 171 p., 3 pls., scale 1:500,000.
- Machette, M.N., 1987a, Neotectonics of the Rio Grande rift, New Mexico: *Geological Society of America Abstracts with Program*, v. 19, no. 7, p. 754.

- 1987b, Preliminary assessment of paleoseismicity at White Sands Missile Range, southern New Mexico - Evidence for recency of faulting, fault segmentation, and repeat intervals for major earthquakes in the region: U.S. Geological Survey Open-File Report 87-444, 46 p.
- 1987c, Preliminary assessment of Quaternary faulting near Truth or Consequences, New Mexico: U.S. Geological Survey Open-File Report 87-652, 40 p.
- 1988, Quaternary tectonic history of the La Jencia fault, central New Mexico: U.S. Geological Survey Professional Paper 1440, 82 p., 25 figs., 23 tables, 2 pls., scale 1:48,000.
- Machette, M.N., and Hawley, J.W., 1996, Neotectonics of the Rio Grande rift, New Mexico: Geological Society of America Abstracts with Program, v. 28, no. 7, p. A-271.
- Machette, M.N., and McGimsey, R.G., 1983, Quaternary and Pliocene faults in the Socorro and western part of the Fort Sumner 1 x 2 quadrangles, central New Mexico: U.S. Geological Survey Miscellaneous Field Studies Map MF-1465-A, 12 p., 1 pl., scale 1:250,000.
- Machette, M.N., and Personius, S.F., 1984, Map showing Quaternary and Pliocene faults in the east part of the Aztec 1 x 2 quadrangle and west part of the Raton 1 x 2 quadrangle, northern New Mexico: U.S. Geological Survey Miscellaneous Field Studies Map MF-1465-B, 14 p., 1 pl., scale 1:250,000.
- Machette, M.N., Personius, S.F., Menges, C.M., and Pearthree, P.A., 1986, Map showing Quaternary and Pliocene faults in the Silver City 1 x 2 quadrangle and the Douglas 1 x 2 quadrangle, southeastern Arizona and southwestern New Mexico: U.S. Geological Survey Miscellaneous Field Studies Map MF-1465-C, 20 p., 1 pl., scale 1:250,000.
- Machette, M.N., Personius, S.F., Kelson, K.I., and Seager, W.R., 1996, New digital map and computer database of Quaternary faults and folds in New Mexico: Geological Society of America Abstracts with Program, v. 28, no. 7, p. A-377.
- Machette, M.N., Personius, S.F., Nelson, A.R., Schwartz, D.P., and Lund, W.R., 1991, The Wasatch fault zone, Utah—Segmentation and history of Holocene earthquakes, in Hancock, P.L., Yeats, R.S., and Sanderson, D.J., editors, Characteristics of active faults (Special Issue): Journal of Structural Geology, v. 13, p. 137-149.
- Machette, M.N., Personius, S.F., Nelson, A.R., 1992a, The Wasatch fault zone, U.S.A.: Annales Tectonicae, v. 6, Supplement, p. 5-39.
- 1992b, Paleoseismology of the Wasatch fault zone—A summary of recent investigations, conclusions, and interpretations, in Gori, P. L., and Hays, W.W., editors, Assessment of regional earthquake hazards and risk along the Wasatch Front, Utah: U.S. Geological Survey Professional Paper 1500-A, p. A1-A71.
- McCalpin, J.P., 1982, Quaternary geology and neotectonics of the west flank of the northern Sangre de Cristo Mountains, south-central Colorado: Colorado School of Mines Quarterly 77, no. 3, 97 p., 1 pl., scale 1:250,000.
- Menges, C.M., 1990, Late Quaternary fault scarps, mountain-front landforms, and Pliocene-Quaternary segmentation on the range-bounding fault zone, Sangre de Cristo Mountains, New Mexico, Chapter 7, in Krinitzsky, E.L., and Slemmons, D.B., editors, Neotectonics in earthquake evaluation: Geological Society of America Reviews in Engineering Geology, v. 8, p. 131-156.
- Menges, C.M., and Walker, J., 1990, Geomorphic analyses of scarps along the eastern border of the Valle Vidal, north-central New Mexico, in Bauer, P.W., Lucas, S.G., Mawer, C.W., and McIntosh, W.C., editors, Tectonic development of the southern Sangre de Cristo Mountains: New Mexico Geological Society Guidebook, 41st Field Conference, p. 431-438.
- Nakata, J.K., Wentworth, C.M., and Machette, M.N., 1982, Quaternary fault map of the Basin and Range and Rio Grande rift provinces, western United States: U.S. Geological Survey Open-File Report 82-579, 2 pls., scale 1:2,500,000.
- Northrup, S.A., 1976, New Mexico's earthquake history, 1849-1975: New Mexico Geological Society Special Publication 6, p. 77-87.
- Pearthree, P.A., and Calvo, S.S., 1987, The Santa Rita fault zone—Evidence for large-magnitude earthquakes with very long recurrence intervals, Basin and Range Province of southeastern Arizona: Bulletin of the Seismological Society of America, v. 77, p. 90-116.
- Sanford, A.R., Jaksha, L.H., and Cash, D.J., 1991, Seismicity of the Rio Grande rift in New Mexico" (Chapter 12), in Slemmons, D.B., Engdahl, E.R., Zoback, M.D., and Blackwell, D.D., editors., Neotectonics of North America: Geological Society of America Decade of North American Geology Map Volume 1, p. 185-228.
- Schwartz, D.P., and Coppersmith, K.J., 1984, Fault behavior and characteristic earthquakes—Examples from the Wasatch and San Andreas fault zones: Journal of Geophysical Research, v. 89, no. B7, p. 5681-5698.
- Wells, D.L., and Coppersmith, K.J., 1994, New empirical relationships among magnitude, rupture length, rupture width, rupture area, and surface displacement: Bulletin of the Seismological Society of America, v. 84, no. 4, p. 974-1002.

THE CHARACTERISTICS AND QUANTIFICATION OF NEAR-FAULT GROUND MOTION, WITH IMPLICATIONS FOR THE BASIN AND RANGE PROVINCE

Paul Somerville

Woodward-Clyde

566 El Dorado Street, Suite 100, Pasadena, CA, 91101-2560

ABSTRACT

This paper explains the effects of rupture directivity on near-fault ground motions, describes an empirical model of these effects, provides guidelines for the specification of response spectra and time histories to represent near-fault ground motions, provides guidelines for the selection of time histories, and describes the adequacy of current building codes in representing near-fault effects in the Basin and Range Province.

INTRODUCTION

An earthquake is a shear dislocation that begins at a point on a fault and spreads at a velocity that is almost as large as the shear wave velocity. The propagation of fault rupture toward a site at a velocity close to the shear wave velocity causes most of the seismic energy from the rupture to arrive in a single, large, long-period pulse of motion that occurs at the beginning of the record (Somerville and Graves, 1993). This pulse of motion, sometimes referred to as "fling," represents the cumulative effect of almost all of the seismic radiation from the fault. The radiation pattern of the shear dislocation on the fault causes this large pulse of motion to be oriented in the direction perpendicular to the fault, causing the strike-normal peak velocity to be larger than the strike-parallel peak velocity. The effect of forward rupture directivity on the response spectrum is to increase the level of the response spectrum of the horizontal component normal to the fault strike at periods longer than 0.5 seconds. This causes the peak response spectral acceleration of the strike-normal component to shift to longer periods, for example from 0.25 seconds to as much as 0.75 seconds. Near-fault effects cannot be adequately described by uniform scaling of a fixed response spectral shape; the shape of the spectrum must become richer in long periods as the level of the spectrum increases. Figure 1 shows these effects of rupture directivity in the time history and response spectrum of the Rinaldi recording of the 1994 Northridge earthquake.

Forward-rupture-directivity effects occur when two conditions are met: the rupture front propagates toward the site, and the direction of slip on the fault is aligned with the site. The conditions for generating forward-rupture-directivity effects are readily met in strike-slip faulting, where the fault slip direction is oriented horizontally in the direction along the strike of the fault, and rupture propagates horizontally along strike either unilaterally or bilaterally. However, not all near-fault locations experience forward-rupture-directivity effects in a given event. Backward-directivity effects, which occur when the rupture propagates away from the site, give rise to the opposite effect: long-duration motions having low amplitudes

at long periods. This is illustrated in figure 2, which shows the directivity effect in strike-slip faulting using the strike-normal components of ground velocity from two near-fault recordings of the magnitude 7.3 Landers earthquake of 1992 (Wald and Heaton, 1994). The Lucerne record, which is located 1.1 kilometers from the surface rupture and 45 kilometers from the epicenter of the Landers earthquake, consists of a large, brief pulse of motion (due to forward-directivity effects), while the Joshua Tree record, located near the epicenter, consists of a long-duration, low amplitude record (due to backward-directivity effects).

The conditions required for forward directivity are also met in dip-slip faulting, including both reverse and normal faults. The alignment of both the rupture direction and the slip direction up the fault plane produces rupture-directivity effects at sites located around the surface exposure of the fault (or its updip projection if it does not break the surface). Consequently, it is generally the case that all sites located near the surface exposure of a dip-slip fault experience forward rupture directivity when an earthquake occurs on that fault. Unlike the case for strike-slip faulting, where forward-rupture-directivity effects are expected to be most concentrated away from the hypocenter, dip-slip faulting produces directivity effects on the ground surface that are most concentrated updip from the hypocenter. Recordings of the 1994 Northridge earthquake from the northern margin of the San Fernando Valley, such as the one at Rinaldi shown in figure 1, contain forward-rupture-directivity effects.

Guidelines for the specification and selection of near-fault strong-motion time histories for use in design are provided at the end of this paper. It is important that the selection of time histories be based on an awareness of the rupture-directivity effects that they contain. The large differences between near-fault recordings that have directivity effects and those that do not are shown in figures 3 and 4. For each of four earthquakes, we show the response spectra of one recording that contains forward directivity and one recording that does not. The recordings that contain forward directivity are characterized by large response spectral displacements in the strike-normal direction at long periods, while those that do not are characterized by much smaller displacements.

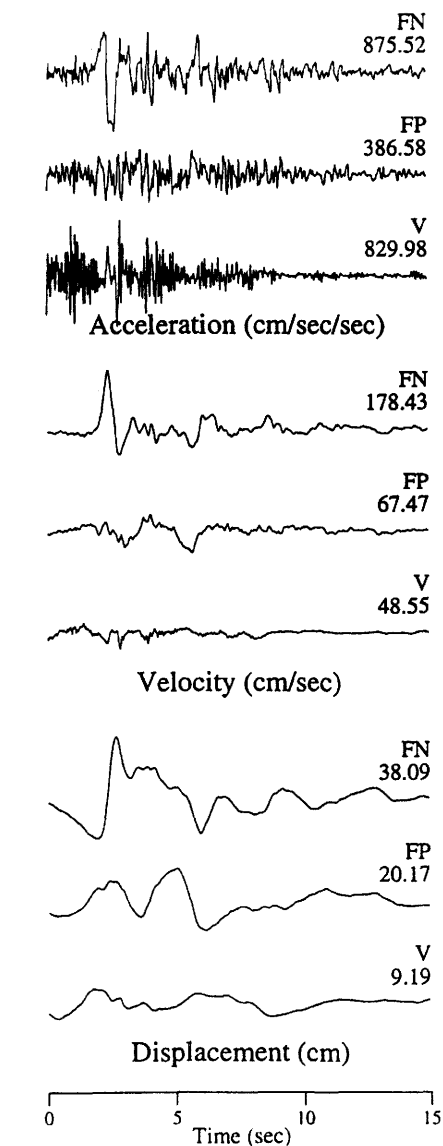


Figure 1. Acceleration and velocity time histories for the strike-normal and strike-parallel horizontal components of ground motion, and their 5 percent damped response spectra, recorded at Rinaldi during the 1994 Northridge earthquake.

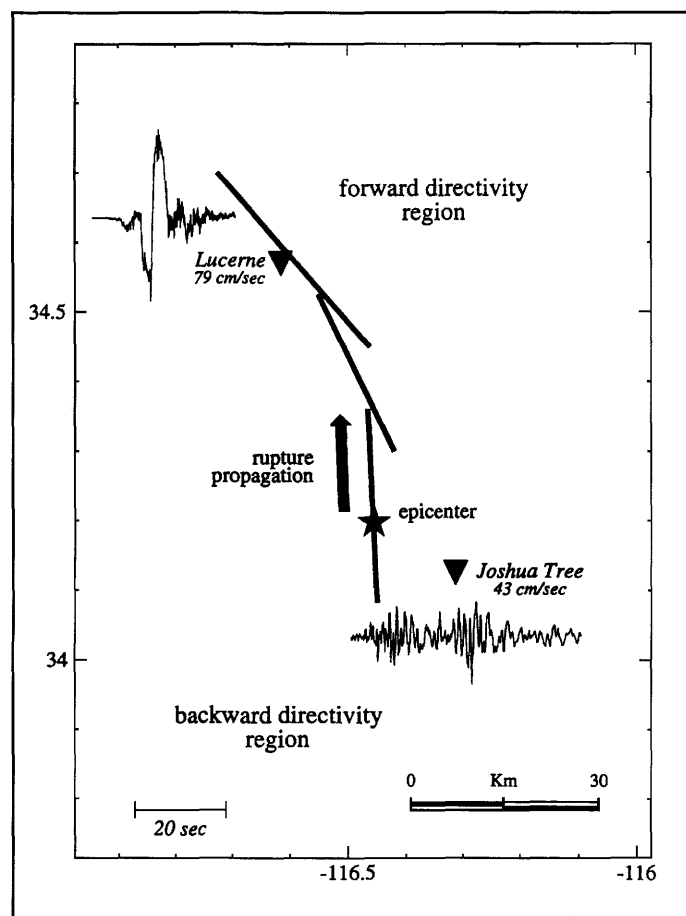


Figure 2. Map of the Landers region showing the location of the rupture of the 1992 Landers earthquake (which occurred in three fault segments), the epicenter, and the recording stations at Lucerne and Joshua Tree. The strike-normal velocity time histories at Lucerne and Joshua Tree exhibit forward and backward-rupture directivity effects respectively.

EMPIRICAL MODEL OF NEAR-FAULT GROUND MOTIONS

Somerville and others (1997a) used a large set of near-fault strong-motion recordings to develop a quantitative model of rupture-directivity effects. The data set contains strong-motion recordings from earthquakes having magnitudes larger than 6. It includes data from strike-slip and reverse-slip earthquakes, but does not contain any strong-motion data from normal faulting earthquakes. The near-fault ground-motion model derived from these recordings includes separate models for strike-slip and reverse faulting. As described in more detail below, the geometrical similarity between reverse and normal faulting suggests that the model for reverse faulting provides a reasonable basis for estimating the near-fault motions from normal faults, after reduction of the reverse-faulting model by 25 percent to account for observed differences between reverse- and normal-faulting earthquakes at larger distances.

The near-fault-ground-motion model derived by Somerville and others (1997a) can be used to modify existing ground-motion attenuation relations to incorporate directivity effects in ground motions used for seismic de-

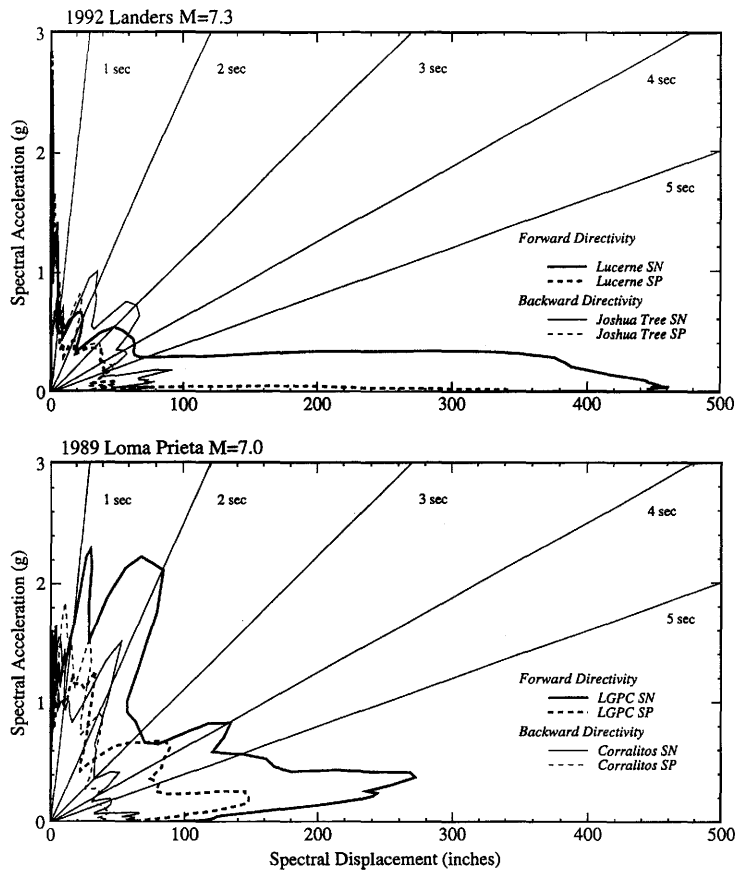
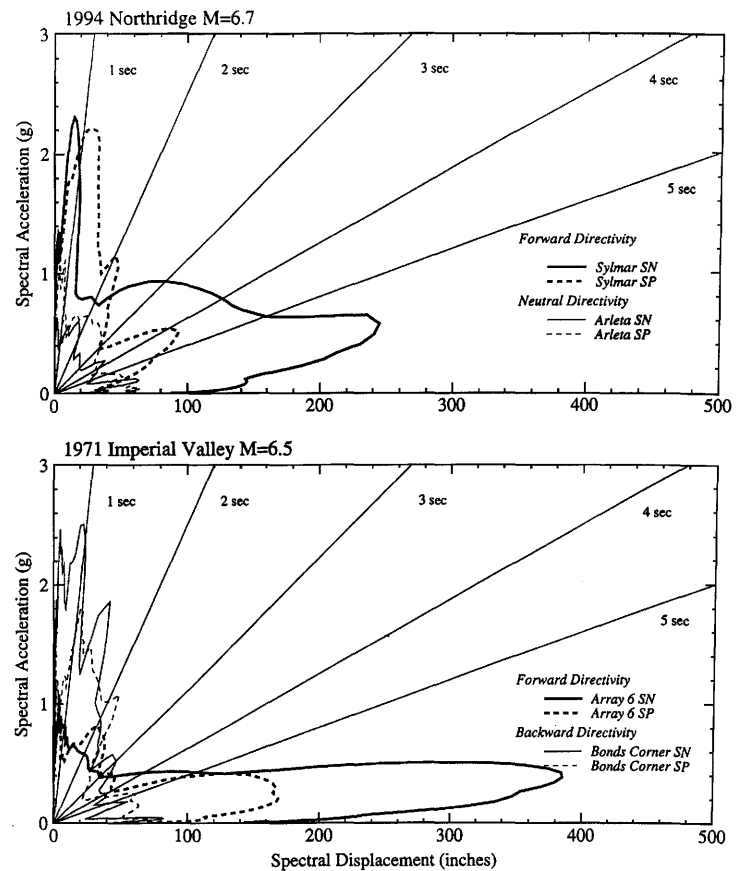


Figure 3. Response spectral acceleration - displacement at 5 percent damping of pairs of near-fault recordings: 1992 Landers and 1989 Loma Prieta earthquakes. For each earthquake, one recording has forward-rupture directivity and the other has backward-rupture directivity. SN: strike-normal; SP: strike-parallel.

Figure 4. Response spectral acceleration - displacement at 5 percent damping of pairs of near-fault recordings: 1994 Northridge and 1979 Imperial Valley earthquakes. For each earthquake, one recording has forward-rupture directivity and the other has backward-rupture directivity. SN: strike-normal; SP: strike-parallel.



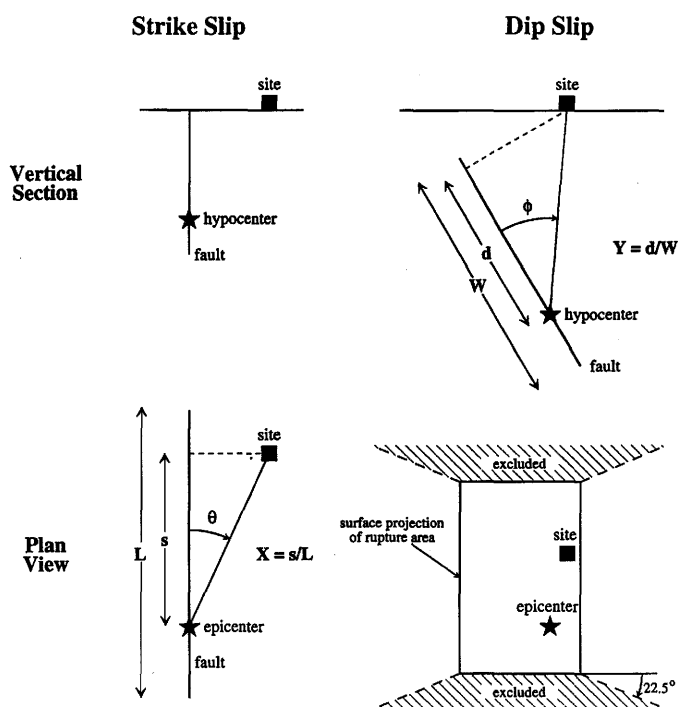


Figure 5. Definition of rupture-directivity parameters θ and X for strike-slip faults, and ϕ and Y for dip-slip faults, and region off the end of dip-slip faults excluded from the model.

sign. The ground-motion parameters that are modified for directivity effects include the average horizontal response spectral acceleration, the average duration of the two horizontal acceleration time histories, and the ratio of strike-normal to strike-parallel spectral acceleration. *Strike-normal* refers to the horizontal component of motion normal to the strike of the fault. *Strike-parallel* refers to the horizontal component of motion parallel to the strike of the fault. Following the method of Husid (1969), duration is defined as the time between 5 percent and 75 percent of the cumulative squared acceleration.

In this model, amplitude variations due to rupture directivity depend on two geometrical parameters. First, the smaller the angle between the direction of rupture propagation and the direction of waves travelling from the fault to the site, the larger the amplitude. Second, the larger the fraction of the fault rupture surface that lies between the hypocenter and the site, the larger the amplitude. The duration of strong motion is modeled using the same two parameters, with an inverse relationship between duration and amplitude. The azimuth and zenith angles and length and width ratios are illustrated for strike-slip and dip-slip faulting in figure 5. For strike-slip faults, the angle θ and length ratio X are measured from the epicenter to the site in the horizontal plane. For dip-slip faults, the angle ϕ and width ratio Y are measured from the hypocenter to the site in the vertical plane oriented normal to the fault.

The effects of rupture directivity on ground-motion amplitudes and duration are modeled using the function $X \cos \theta$ for strike-slip faults and $Y \cos \phi$ for dip-slip faults. For strike-slip faults, the variation of ground-motion parameters with θ is independent of the distance from the rup-

ture, r_{rup} . However, between the ends of a dip-slip fault, the variation of ground-motion parameters with ϕ is indistinguishable from its variation with rupture distance r_{rup} . Since rupture distance is a primary ground-motion parameter already included in attenuation relations, we find more spatial variability of strike-slip motions with $\cos \theta$ than of dip-slip motions with $\cos \phi$. The strike-normal to strike-parallel ratio was modeled using a $\cos 2\xi$ dependence of the strike-normal to strike-parallel ratio, where ξ is θ for strike-slip and ϕ for dip-slip in the range of 0 to 45 degrees.

The dependence of the spectral amplification factor on $X \cos \theta$ for strike-slip faulting and $Y \cos \phi$ for dip-slip faulting is shown in figure 6a. These effects begin at 0.6 seconds period and increase with period. For strike-slip faulting, maximum directivity conditions ($X \cos \theta = 1$) cause an amplitude about 1.8 times larger than average at 2 seconds period, while minimum directivity effects cause an amplitude about 0.6 times average. In the model for dip-slip faulting, which excludes sites off the ends of the fault as shown in figure 5, the effects lie in the range of about 1.2 to 0.8.

The dependence of the duration factor on $X \cos \theta$ for strike-slip faulting and on $Y \cos \phi$ for dip-slip faulting is shown in figure 6b. As expected, there is an inverse correlation between duration residuals and amplitude residuals. For maximum directivity conditions ($X \cos \theta$ or $Y \cos \phi = 1$), the duration is about 0.55 times the average duration for both strike-slip and dip-slip faulting. For minimum directivity conditions, the ground-motion durations are 2.1 and 1.6 times longer than average for dip-slip and strike-slip faulting respectively.

The model of the strike-normal to average horizontal

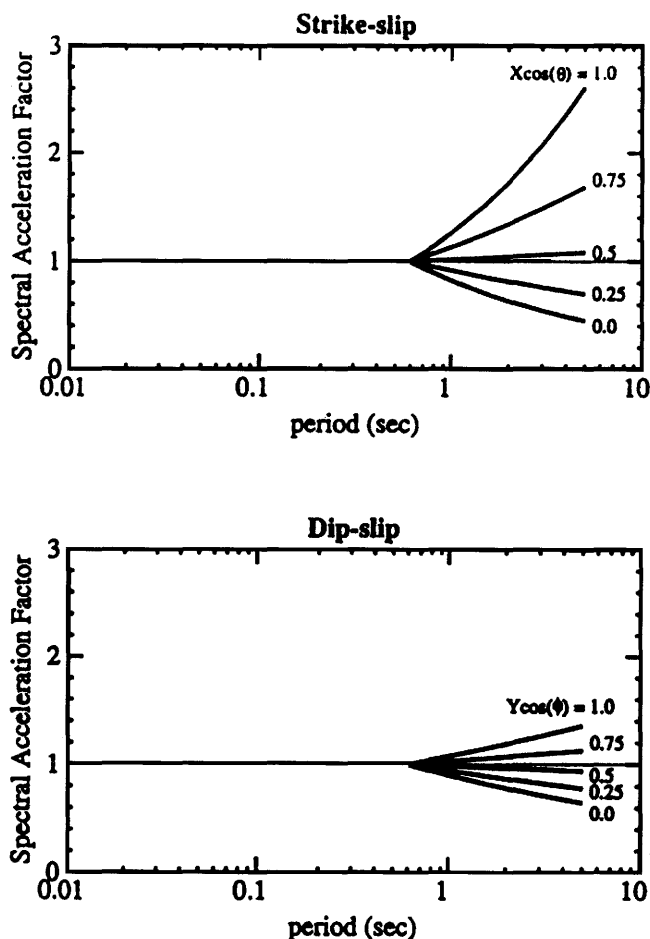


Figure 6a. Empirical model of the response spectral factor, showing its dependence on period and on the directivity function ($X \cos \theta$ for strike-slip; $Y \cos \phi$ for dip-slip).

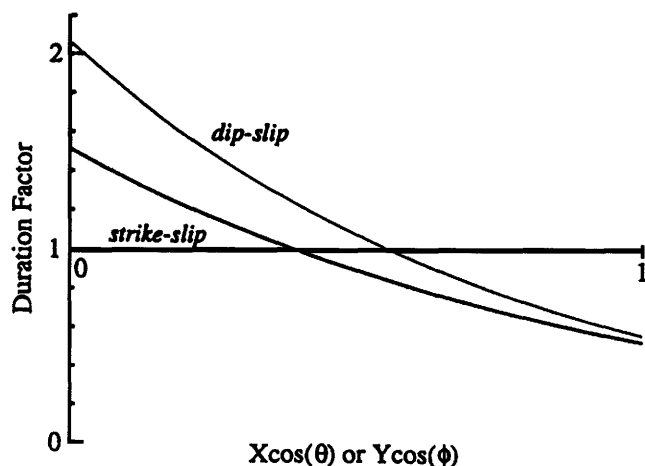


Figure 6b. Empirical model of the duration factor, showing its dependence on period and on the directivity function ($X \cos \theta$ for strike-slip; $Y \cos \phi$ for dip-slip).

ratio, which is independent of faulting mechanism, is displayed in figure 7. The top part of the figure shows the period dependence of the ratio for various magnitudes and distances, and the bottom part of the figure shows the distance dependence of the ratio for various magnitudes and periods, averaged over all values of the angles θ and ϕ . The strike-normal motion is obtained by multiplying the attenuation relation value by the strike-normal to average horizontal ratio, and the strike-parallel motion is obtained by dividing the attenuation relation value by this ratio. The bottom right part of the figure shows the dependence of the ratio on θ or ϕ for $M = 7$ and $r_{rup} = 5$ as a function of period. The period dependence of the ratio indicates a transition, at a period of about 0.6 seconds, from coherent source radiation and wave propagation conditions at long periods to incoherent source radiation and wave propagation conditions at short periods.

NEAR-FAULT GROUND MOTIONS FROM NORMAL-FAULTING EARTHQUAKES

The model for near-fault ground motions described above is based on a strong-motion data set from magnitude 6 and larger earthquakes that does not contain any recordings from normal faults. The recordings in the data set are from either strike-slip or reverse faults, and separate near-fault-ground-motion models were derived for these two categories of earthquake mechanism. However, the conditions required for forward directivity for normal faulting are identical to those for reverse faulting: they occur when the rupture direction and the slip direction are both aligned up the fault plane. Geometrically, rupture-directivity effects for normal faulting should be identical to those for reverse faulting (with the exception of a change in ground-motion polarity), so the empirical rupture-directivity model for dip-slip faulting described above should be applicable to normal-faulting earthquakes. Although there are few strong-motion data close to large normal-faulting earthquakes, it appears overall that the ground motions from reverse faults are 30 percent to 50 percent larger than for normal faults. Moreover, hypothesized differences in the fault dynamics between normal and reverse faulting exist (Shi and others, 1997) which may cause the near-fault ground motions from normal faults to be even lower than this. Given the presently available data, it seems appropriate to assume that near-fault ground motions from normal faults can be approximated by taking 75 percent of the near-fault ground motions predicted for reverse faulting in the model described above.

SPECIFICATION OF RESPONSE SPECTRA FOR NEAR-FAULT GROUND MOTIONS

Scenario Earthquake Approach

The ground motions used in the design or evaluation of a structure are usually specified in the form of a response spectrum or set of response spectra. In some instances, the response spectrum may represent a speci-

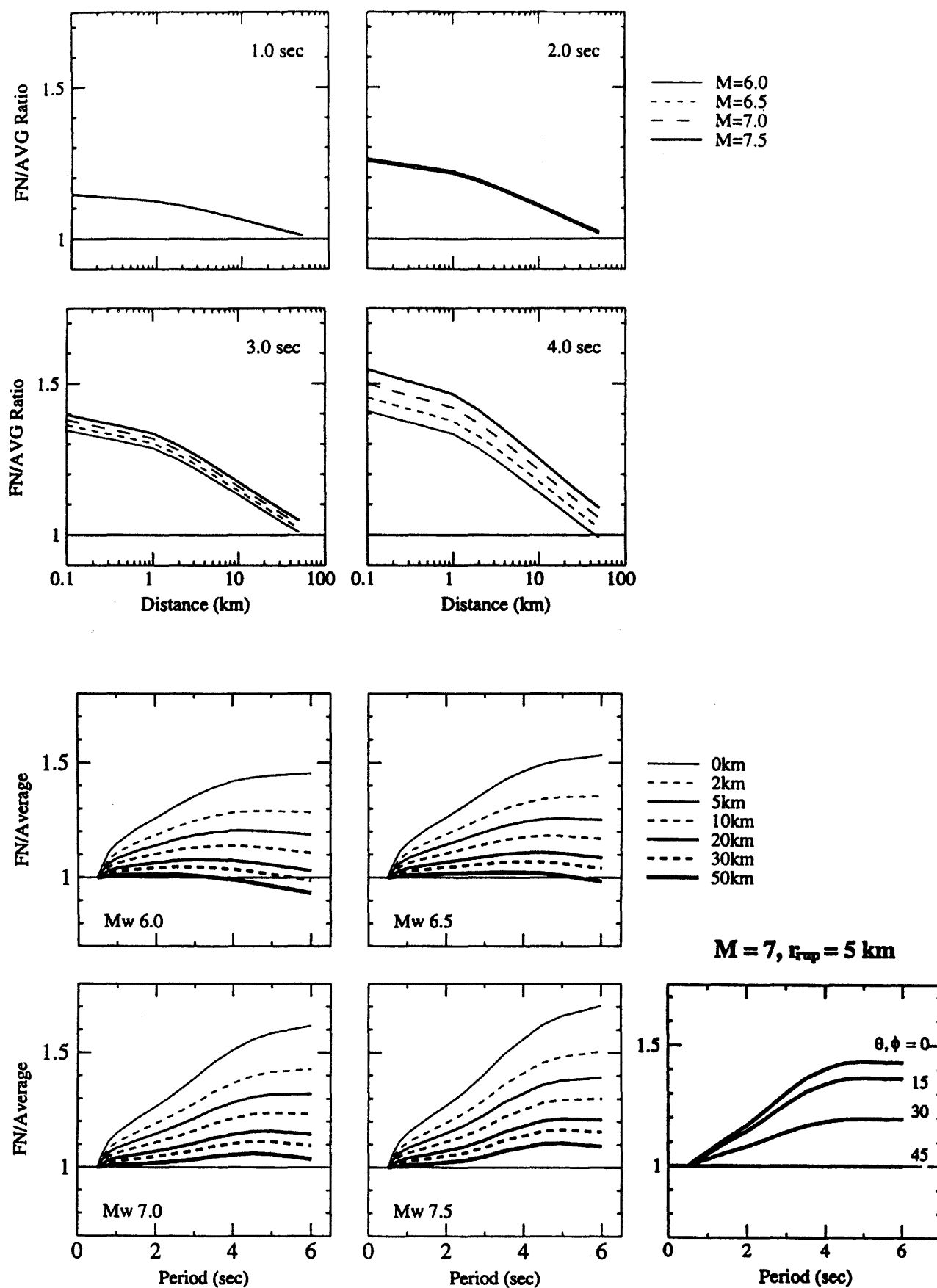


Figure 7. Empirical model of the strike-normal to average horizontal response spectral ratio excluding dependence on the angles θ or ϕ , shown as a function of period for various magnitudes and distances (top), and as function of distance for various magnitudes and periods (bottom). The dependence on angle θ or ϕ for $M = 7$ and $r_{rup} = 5$ kilometers is shown as a function of period on the bottom right.

fied earthquake magnitude and distance. Until recently, the state of practice was to assume that near-fault effects are adequately represented in empirical ground-motion models that are used to estimate the response spectrum for the specified magnitude and distance. The ground motions predicted by these empirical models represent the average of all rupture-directivity conditions: forward, backward, and neutral. However, ground motions influenced by forward rupture directivity are much larger than those for average rupture directivity for periods longer than 0.5 seconds. Since forward directivity has a high likelihood of occurring at any near-fault site, it may be appropriate to include forward rupture directivity as a criterion for the development of ground motions for the maximum credible event. The common practice of using the 84th percentile ground motion instead of the mean may in part accomplish this objective.

During the past 5 years, response spectra for the design of retrofits of Caltrans toll bridges have contained modifications of these empirical models to incorporate near-fault effects. These modifications consist of increasing the response spectrum level of the average horizontal component of ground motion at periods longer than 1 second, and specifying separate response spectra for the strike-normal and strike-parallel components of motion, using models such as that described by Somerville and others (1995a). These modifications provide a response spectrum that is more nearly representative of forward-rupture-directivity effects. To date, Caltrans is the only organization that has adopted the use of different response spectra in the strike-normal and strike-parallel directions.

Modifications to the response spectral level have been included in the Structural Engineers' Association of California (SEAOC) Strength Code Change (SEAOC, 1996) in the form of the near-source factor N . This factor modifies the basic response spectrum using factors N_a and N_v that depend on the distance to the fault, the slip rate of the fault, and the maximum magnitude that the fault can generate. At distances close to major active faults, the design values ("maximum considered") ground-motion map in the 1997 National Earthquake Hazard Reduction Program (NEHRP) Provisions (Building Seismic Safety Council, 1997) incorporates an increase in the 1994 NEHRP response spectrum.

In figures 8 and 9 we compare response spectra for the same earthquake (magnitude 7 strike-slip, distance 5 kilometers, stiff soil conditions) but two different rupture-directivity conditions. The spectra at the top are for average rupture-directivity conditions (sites located randomly around the fault), while the spectra at the bottom are for forward-rupture-directivity conditions (where rupture propagates towards the site). In each case, we show the strike-normal, strike-parallel, and average horizontal response spectra based on the model of Somerville (1996). For comparison, we show proposed 1997 SEAOC code spectra including the near-fault factor for the appropriate source category (B) and site category (S_p). We use the "design basis" spectrum for comparison with average rupture-directivity conditions, and the "maximum capable" spectrum from the base isolation part of the code (a factor of 1.25 higher) for comparison with forward-rupture-

directivity conditions. The modifications for rupture-directivity effects in Somerville (1996) are based not on the general model described above, but on a model derived from ten recordings at close distances to the 1989 Loma Prieta, 1994 Northridge, and 1995 Kobe earthquakes. This model has larger modifications than the general model for periods between 0.5 and 2.0 seconds.

The model for average directivity conditions shown at the top of figures 8 and 9 does not change the average horizontal spectrum given by the empirical model (Abrahamson and Silva, 1997), but gives a strike-normal component that is larger and a strike-parallel component that is smaller. The model for forward-directivity conditions, shown at the bottom of the figures, not only has a larger difference between these two components, but also increases

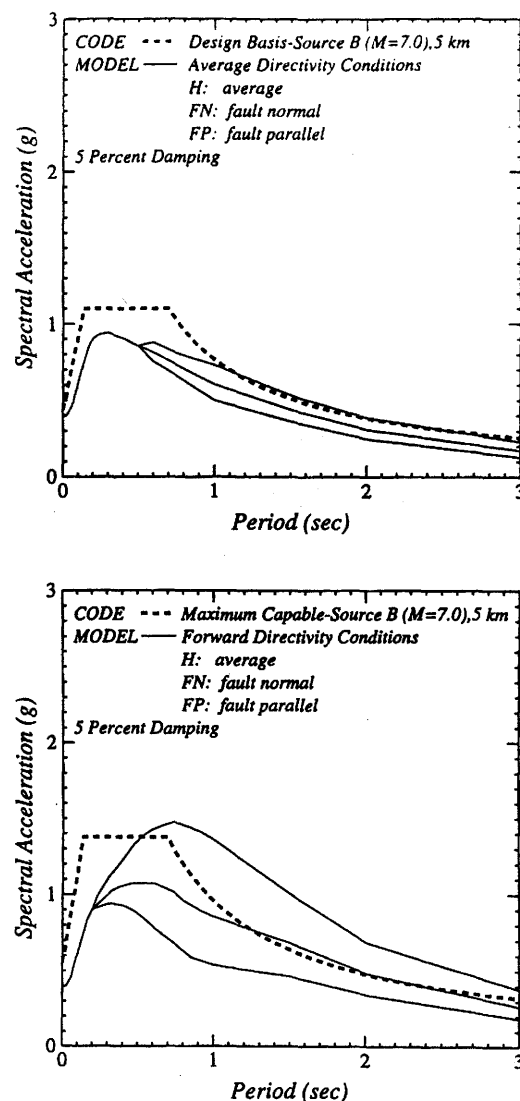


Figure 8. Acceleration response spectra for (top) average rupture-directivity conditions (bottom) and forward-rupture-directivity conditions for a magnitude 7 earthquake at a distance of 5 kilometers on soil. The response spectra are shown for the strike-normal, strike-parallel, and average horizontal components. Also shown for comparison are UBC spectra including the near-fault factor for design basis (top) and maximum capable events (bottom).

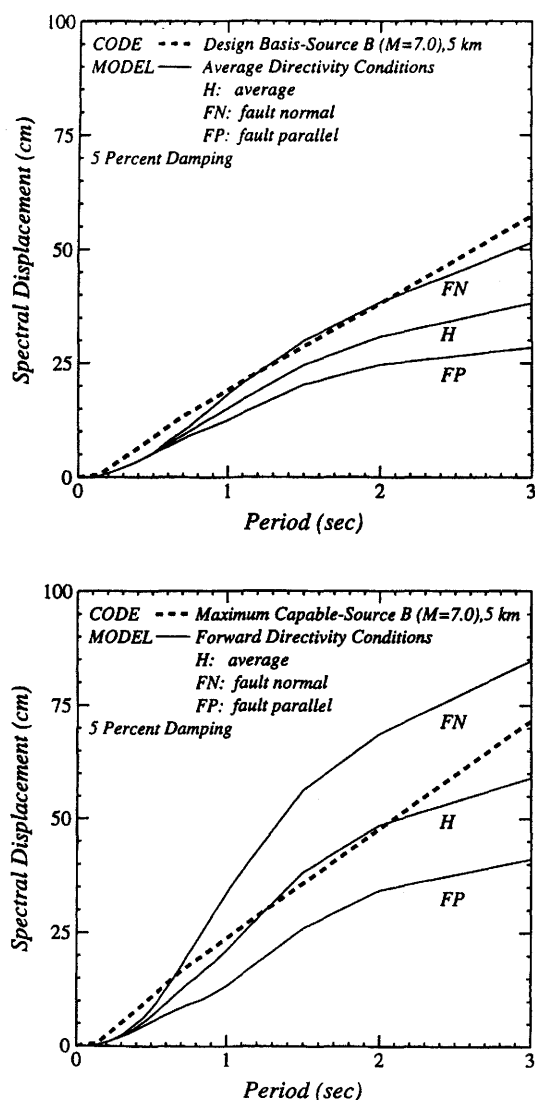


Figure 9. Displacement response spectra for (top) average rupture-directivity conditions and (bottom) forward-rupture-directivity conditions for a magnitude 7 earthquake at a distance of 5 kilometers on soil. The response spectra are shown for the strike-normal, strike-parallel, and average horizontal components. Also shown for comparison are UBC spectra including the near-fault factor for design basis (top) and maximum capable events (bottom).

the average horizontal component above that given by the empirical attenuation relation. The combination of these two modifications for forward-directivity conditions results in the strike-normal motion being about 2 times higher than the average given by the empirical attenuation relation for periods longer than about 0.5 seconds, and the strike-parallel motion being about the same as the average given by the empirical attenuation relation.

Comparing the response spectral models at the top and bottom of figures 8 and 9, we see that the most important effect of forward rupture directivity on the response spectrum is to increase the level of the response spectrum at periods longer than 0.5 seconds. This is manifested in a shift in the peak of response spectral acceleration from 0.3 seconds (which is also the peak for the strike parallel com-

ponent) to 0.5 seconds for the average of the horizontal components and to 0.75 for the strike-normal component. This indicates that near-fault effects cannot be adequately described by uniform scaling of a fixed response spectral shape; the shape of the spectrum must become richer in long periods as the level of the spectrum increases. This has been implemented in the proposed 1997 SEAOC code change by using separate near-fault factors N_a and N_v for the acceleration and velocity parts of the code response spectrum.

The "design basis" spectrum at the top of figures 8 and 9 envelopes both the strike-normal and strike-parallel components of motion for average directivity. However, the "maximum capable" spectrum at the bottom of the figures lies below the strike-normal component for forward-rupture directivity. Should engineers be concerned about the possibility of the strike-normal component exceeding the design criterion? There are two reasons for thinking that the answer is yes. First, recent destructive earthquakes have shown evidence of near-fault damage occurring in preferred directions that correspond to the strike-normal direction (north-south in the 1994 Northridge earthquake; northwest-southeast in the 1995 Kobe earthquake). Second, the difference between strike-normal and average motions is statistically significant close to large earthquakes. For example, in the case shown in the lower part of figures 8 and 9, (forward-rupture directivity at a distance of 5 kilometers from a magnitude 7 earthquake), the strike-normal component is a factor of 1.4 times larger than the average horizontal component at long periods, with a standard error of a factor of 1.28.

In figure 10, we compare the near-fault spectra for average (top) and forward (bottom) directivity conditions with the ground-motion model of Abrahamson and Silva (1997) from which they were modified. For periods longer than about 0.75 seconds, the strike-normal component for forward-rupture directivity is about 25 percent larger than the 84th percentile ground motion for the average of the two horizontal components for average rupture-directivity conditions, as given by the Abrahamson and Silva (1997) model. This indicates that use of the 84th percentile may partly, if not completely, accommodate the ground-motion level in the strike-normal direction for forward-rupture-directivity conditions.

Since fault strike is usually well known close to major faults, it is straightforward to take the difference between the strike-normal and strike-parallel components of motion into account in the evaluation of near-fault ground motions, especially for structures that are sensitive to long-period ground motions. Consideration of these differences may be especially important for the retrofit of existing structures near active faults (e.g., Salah-Mars and others, 1994). For new structures, the stronger ground motion in the strike-normal direction could be accommodated by orienting the structure with its long axis normal to the fault, as shown in figure 11. Even if the specific location and orientation of faults is not known, there may be a high enough level of certainty in the strike of faults in a region (for example, of blind thrust faults in the Los Angeles basin) to warrant consideration of larger strike-normal ground motions.

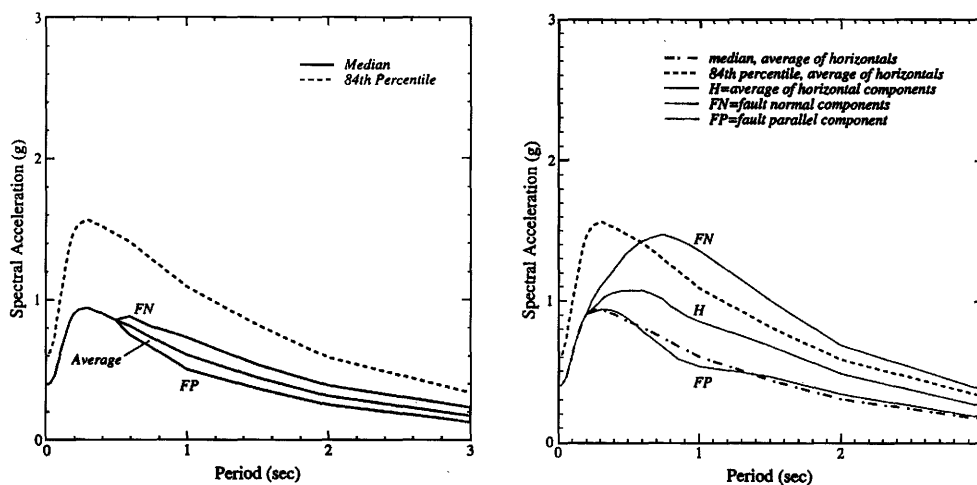


Figure 10. Response spectra for average rupture-directivity (left) and forward-rupture-directivity (right) conditions for a magnitude 7 earthquake at a distance of 5 kilometers on soil. The response spectra are shown for the strike-normal, strike-parallel, and average horizontal components. Also shown for comparison are the median and 84th percentile spectra for the empirical attenuation relation (Abrahamson and Silva, 1997) on which the modifications for near-fault effects are based.

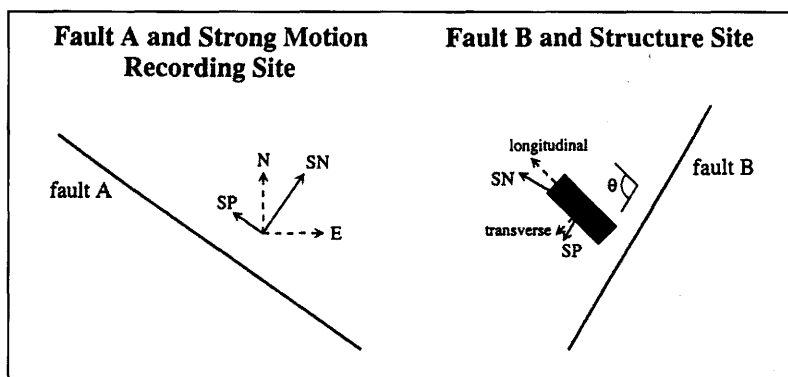


Figure 11. Schematic diagram of the orientation of ground motion at a recording site, its rotation into strike-normal and strike-parallel components, transfer to a structure site in that orientation, and rotation into longitudinal and transverse components of the structure.

Probabilistic Approach

In many instances, the response spectrum is defined probabilistically as that having a specified annual probability of exceedance. A probabilistic response spectrum contains contributions from the entire range of magnitude-distance pairs that affect the site. This is the approach that is used to generate response spectra using the site-specific method prescribed by the Uniform Building Code. It is also the approach used by the United States Geological Survey to generate the National Seismic-Hazard Maps. The "maximum capable" ground motion used in the base isolation code is associated with a specified probability of occurrence (10% in 100 years).

The current state of practice in the development of probabilistic response spectra is to assume that near-fault effects are adequately represented in the empirical ground-motion models that are used to estimate the response spectrum for the specified magnitude and distance. However, the means now exist to incorporate near-fault effects in a more specific way by using the empirical model of Somerville and others (1997a) which is summarized in figures 6 and 7. This model can be implemented

by randomizing the location of the hypocenter on the fault planes of earthquakes having magnitudes larger than 6. The model has not yet been implemented in a probabilistic seismic-hazard analysis. However, the main anticipated effect is a larger strike-normal response spectrum and a smaller strike-parallel response spectrum than the average horizontal spectrum estimated by current methods. At low probabilities, there may also be some increase in the average response spectrum due to the larger variability in ground motions predicted by the model.

SPECIFICATION OF TIME HISTORIES FOR NEAR-FAULT GROUND MOTIONS

Design and analysis of large structures is often done using time histories that are representative of the design response spectrum. The time histories, which may be from recorded earthquakes or from strong-motion simulations of the kind described below, are sometimes spectrally matched to a design response spectrum. The modifications that we have developed to incorporate rupture-directivity effects in the response spectrum are not suffi-

cient to ensure the appropriate incorporation of rupture-directivity effects in time histories that are matched to these spectra. This is because the forward-rupture-directivity effect is manifested in the time domain by a large pulse of long-period ground motion, and the spectral matching process cannot build a rupture-directivity pulse into a record where none is present to begin with. Forward-rupture-directivity effects are present in some but not all near-fault strong-motion recordings. Since the response spectrum developed for design or evaluation of a near-fault site will be influenced by forward-rupture-directivity effects at most sites, it is important to select an appropriate proportion of time histories that include forward-rupture-directivity effects if time histories are being used to represent the response spectrum.

Orientation of Time Histories

If it is desired to fully represent near-fault conditions in the time histories, then it is necessary to initially specify the strike-normal and strike-parallel components of the time histories. If the axis of the structure is aligned at some angle θ to the strike of the fault, then the longitudinal and transverse time histories should then be derived from the strike-normal (SN) and strike-parallel (SP) time histories using the following equation:

$$\begin{aligned} \text{long} &= \text{SP} \cos \theta + \text{SN} \sin \theta \\ \text{trans} &= \text{SP} \sin \theta - \text{SN} \cos \theta \end{aligned}$$

In figure 11, we schematically illustrate the recording of strong motion near fault A on the north and east components, the rotation of the north and east to strike-normal and strike-parallel, the transposition of the strike-normal and strike-parallel components to the structure site near fault B, and the rotation of the strike-normal and strike-parallel components into longitudinal and transverse components at the structure site. We have begun to archive near-fault strong-motion recordings and simulations in their strike-normal and strike-parallel components.

Although near-fault ground displacements contain permanent displacements due to the static displacement field of the earthquake, traditional analog recording systems do not retain these displacements, and in any case they are removed by highpass filtering in traditional processing methods. However, in some cases the permanent ground displacements may be significant for design, and in these cases it is important to specify the correct orientation of the static and dynamic ground displacements. In figure 12, we show the sense of motion of the permanent ground displacement near left-lateral and right-lateral unilateral strike-slip faults for rupture propagation in either direction (that is, for epicenters at either end of the fault). The sense of strike-normal displacement is continuous across the fault, whereas the sense of strike-parallel displacement is discontinuous across the fault (reflecting the displacement on the fault). For a given sense of slip (e.g., strike-slip), the polarity of the strike-parallel displacement is the same for rupture in either direction, but the polarity of the strike-normal displacement is opposite for rupture in opposite directions. Current design procedures assume that the two horizontal components are uncorrelated, and

prescribe interchanging the two horizontal components in structural analyses. This is clearly inappropriate for near-fault ground motions, in which there are systematic differences between the strike-normal and strike-parallel components. Interchanging the components can represent physically unrealizable scenarios given the known orientation of the fault.

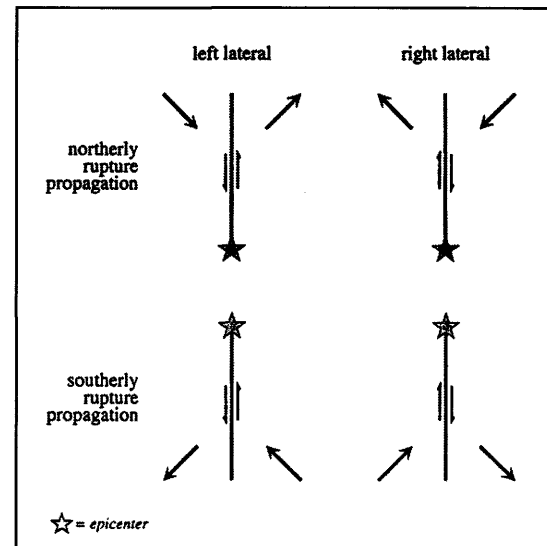


Figure 12. Schematic diagram of the polarity of permanent ground displacement for strike-slip earthquakes. The motions are shown for both left-lateral and right-lateral unilateral faults, and for both northerly and southerly rupture propagation on north-striking faults.

Scenario Earthquake Approach

If the response spectrum is derived from a scenario earthquake, then the magnitude and distance of the earthquake are specified, and time histories representative of that magnitude and distance need to be selected. If the response spectrum is based on the median level ground motion, then it represents average directivity conditions, and it is appropriate to select time histories that span a range of directivity conditions. However, if the response spectrum is based on the mean plus one standard deviation ground-motion level, then it represents forward-directivity conditions, and most if not all of the time histories should be for forward-rupture-directivity conditions. As described in figure 10, the strike-normal ground-motion level for forward-rupture-directivity conditions is about as large as or larger than the 84th percentile response spectrum for average directivity conditions.

With the exception of Caltrans toll bridges noted above, design or analysis response spectra apply to the average of the two horizontal components of ground motion. When scaling a time history to match this spectrum, a scaling factor should be found that matches the average of the two horizontal components of the time history to the design spectrum. This factor should then be applied to each of the two horizontal components in order to leave unchanged the ratio between the two horizontal components. In the case when the response spectra of the strike-

normal and strike-parallel components of motion are separately specified (e.g., for Caltrans toll bridges), then the time histories can be scaled separately to these response spectra.

Probabilistic Approach

A probabilistic seismic-hazard analysis (PSHA) takes into account the ground motions from the full range of earthquake magnitudes that can occur on each fault or source zone that can affect the site. The time histories selected must represent the dominant combinations of magnitude, distance, and ϵ that contribute to the response spectrum. The parameter ϵ is defined as the number of standard deviations above or below the median ground-motion level for that magnitude and distance that is required to match the probabilistic spectrum. The magnitude, distance, and ϵ combinations are identified through deaggregation of the seismic hazard (McGuire, 1995; Silva and Toro, 1996).

If the probabilistic seismic-hazard analysis were to include the near-fault modifications for rupture-directivity effects described above, then the deaggregation could include values of the directivity function $X \cos \theta$ for strike-slip faults and $Y \cos \phi$ for dip-slip faults, and the directivity content of time histories could be selected based on the predominant value of the directivity function. Otherwise, some estimate of the appropriate directivity content of the time histories can be obtained from the parameter ϵ defined above. If the predominant value of ϵ is near zero, then the response spectrum approximately represents average directivity conditions, and it is appropriate to select time histories that span a range of directivity conditions. However, if the predominant value of ϵ is one, then the response spectrum is at the mean plus one standard deviation ground-motion level for that event, representing forward-directivity conditions, and most if not all of the time histories should be for forward-rupture-directivity conditions. For example, in the deaggregation of seismic hazard at 10 percent probability of exceedance in 50 years in Los Angeles and San Francisco, Silva and Toro (1996) found that the ϵ value was approximately one on average for the predominant contribution to the hazard. This indicates the need to select time histories having predominantly forward-rupture-directivity conditions in order to represent the 10 percent in 50 year ground motions in Los Angeles and San Francisco. In the Basin and Range Province, the lower slip rates of faults means that the 10 percent in 50 year ground motions would be represented by average rather than forward-directivity conditions.

SELECTION OF TIME HISTORIES FOR NEAR-FAULT GROUND MOTIONS

If time histories are used in conjunction with the response spectrum, it is important to select time histories which appropriately include rupture-directivity effects because the spectral matching process cannot build a rupture-directivity pulse into a record where none is present to begin with. As a guide to the selection of time histories for use in design and evaluation of structures that are sen-

sitive to long-period ground motions, a set of near-fault strong-motion recordings, indicating the nature of the rupture-directivity effects that they contain, is listed in table 1. It includes those whose closest distance to the fault rupture is 10 kilometers or less in the data set that was used by Somerville and others (1995a, 1997a) to develop an empirical model of directivity effects on strong ground motions. The influence of rupture-directivity effects on each record is indicated, based on the geometrical relations between the recording site, the fault rupture, the epicenter, and the direction of slip on the fault. The table lists the peak horizontal accelerations and velocities of the records in the strike-normal and strike-parallel directions. This table can complement the extensive classification and evaluation of earthquake records using a range of ground-motion parameters provided by Naeim and Anderson (1993, 1996).

The recorded time histories listed in table 1 include a limited number of recordings at close distances to large earthquakes. Broadband simulation techniques which have been validated against recorded strong ground motions can be used to generate time histories for large magnitudes and close distances. For example, broadband time histories for hypothesized magnitude 7 earthquakes on the Elysian Park thrust beneath downtown Los Angeles (Somerville and others, 1995b), and on the predominantly strike-slip Palos Verdes fault in the Long Beach area, were used by Somerville and others (1997b) to complement recorded ground motions in a set of near-fault recordings for use in Phase 2 of the Federal Emergency Management Agency (FEMA) and SAC Joint Venture. SAC is a partnership of the Structural Engineers Association of California (SEAOC), the Applied Technology Council (ATC), and the California Universities for Research in Earthquake Engineering (CUREE) (SAC) Steel Project. Both the recorded and simulated near-fault time histories can be accessed by anonymous ftp to "ftp.csn.net" in the directory wwcllyde/SAC2, file NearFault. They are rotated into strike-normal and strike-parallel components.

In the following sections, some specific guidelines for the selection of appropriate time histories for the representation of near-fault rupture-directivity effects are provided.

Forward Rupture Directivity

Forward directivity occurs when the rupture propagates toward the site and the direction of slip on the fault is also toward the site. Most near-fault strike-slip recordings, and all near-fault reverse-fault recordings, are influenced by forward directivity. Backward directivity occurs when the rupture propagates away from the site. Recordings near the epicenters of strike-slip earthquakes, a relatively small group, fall in the backward-directivity category. None of the reverse faults in our data set ruptured in the downdip direction away from surface stations, so none have backward directivity. Recordings that do not clearly belong in either of these categories are grouped in a neutral category. This category includes sites located fairly close to the epicenters of strike-slip earthquakes, and sites located off the end of the updip projection of reverse faults.

Table 1. Description of rupture-directivity effects in near-fault strong-motion recordings. (See table 8 of Somerville and others, 1997a for a listing that includes directivity parameters X and q for strike-slip faults, and f and Y for dip-slip faults, in place of the general directivity [forward, neutral, backward] provided in this table).

EQK DATE	STAT. NO.	STATION	CLOSEST DISTANCE (km)	SITE CODE ¹	PEAK HORIZONTAL				DIRECTIVITY ³
					ACCEL (g)		VEL (cm/s)		
					FN ²	FP ²	FN ²	FP ²	
400519	117	IMPERIAL VAL IRRIG. DIST, EL CENTRO	10.0	SL	0.21	0.32	32.2	60.1	B
660627	014	CHOLAME, SHANDON, CA ARY 5	3.7	SL	0.33	0.36	26.1	23.6	F
660627	015	CHOLAME, SHANDON, CA ARY 8	8.0	SL	0.24	0.28	11.7	12.2	F
660627	097	TEMBLOR, CA, STATION 2	4.4	HR	0.36	0.25	23.5	12.6	F
671210	9001	KOYNA DAM	3.0	HR	0.51	0.45	32.9	21.9	B
710209	24207	PACOIMA DAM	3.3	HR	1.17	1.08	114.9	59.3	F
760517	9201	KARAKYR POINT, USSR	3.0	SR	0.65	0.67	63.7	59.8	N
780916	9101	TABAS	1.2	SR	0.90	0.98	110.2	106.7	N
791015	6616	AEROPUERTO MEXICALI	0.4	SL	0.28	0.36	27.1	42.7	B
791015	6618	AGRARIAS	0.8	SL	0.24	0.36	38.7	39.7	B
791015	955	EL CENTRO ARY 4, ANDERSON ROAD	7.1	SL	0.36	0.49	77.7	38.0	F
791015	952	EL CENTRO ARY 5, JAMES ROAD	4.1	SL	0.37	0.53	88.1	43.8	F
791015	942	EL CENTRO ARY 6, HUSTON ROAD	1.2	SL	0.43	0.35	106.2	62.9	F
791015	5028	EL CENTRO ARY 7, IMPERIAL VAL COLL.	0.2	SL	0.46	0.33	106.4	44.7	F
791015	958	EL CENTRO ARY 8, CRUICKSHANK RD	3.8	SL	0.47	0.61	50.1	52.7	F
791015	412	EL CENTRO ARY 10, HOSPITAL	9.0	SL	0.18	0.23	44.9	39.9	F
791015	5054	BONDS CORNER, EL CENTRO	2.4	SL	0.79	0.59	48.6	43.8	B
791015	5053	FIRE STATION, CALEXICO	10.1	SL	0.26	0.21	18.3	15.4	N
791015	6619	MEXICALI CASA FLORES	9.7	SL	0.23	0.43	19.3	28.8	B
791015	6622	COMPUERTAS	4.5	SL	0.15	0.15	9.7	13.7	B
791015	9301	EL CENTRO DIFFERENTIAL ARRAY 1	5.5	SL	0.73	0.74	119.8	111.8	F
791015	9302	EL CENTRO DIFFERENTIAL ARRAY 2	5.5	SL	0.62	0.77	121.6	110.4	F
791015	9304	EL CENTRO DIFFERENTIAL ARRAY 3	5.4	SL	0.61	0.68	120.8	109.5	F
791015	9305	EL CENTRO DIFFERENTIAL ARRAY 4	5.2	SL	0.83	0.73	117.9	104.4	F
791015	9306	EL CENTRO DIFFERENTIAL ARRAY 5	5.1	SL	1.19	2.07	131.4	135.7	F
791015	5165	DIFFERENTIAL ARRAY-DOGWOOD ROAD	5.2	SL	0.41	0.45	56.0	49.3	F
791015	5055	POST OFFICE, HOLTVILLE	7.5	SL	0.27	0.23	50.3	42.7	N
791015	335	IMPERIAL COUNTY FF	7.4	SL	0.18	0.22	52.1	41.3	F
840424	1652	ANDERSON DAM, DOWNSTREAM	4.5	SL	0.44	0.28	27.0	28.9	F
840424	57217	COYOTE LAKE DAM, SAN MARTIN	0.01	SR	0.85	0.93	66.5	68.3	F
840424	57191	HALLS VALLEY	2.5	SL	0.31	0.16	39.0	14.2	B
851223	6097	IVERSON, NW TERRITORIES (STA 1)	9.6	HR	1.24	1.20	45.3	44.1	N
851223	6098	SLIDE MOUNTAIN (STA 2)	6.1	HR	0.40	0.42	27.0	37.6	N
860708	5073	CABAZON - POST OFFICE	8.4	SL	0.23	0.20	6.9	16.2	F
860708	12149	DESERT HOT SPRINGS	6.7	SL	0.34	0.29	29.7	22.9	N
860708	5997	DEVERS HILL SUBSTATION	4.1	SL	1.10	0.42	90.0	14.7	F
860708	5070	NORTH PALM SPRINGS POST OFFICE	4.0	SL	0.71	0.60	67.8	32.9	F
860708	12025	PALM SPRINGS AIRPORT	9.6	SL	0.16	0.15	14.7	10.3	F
860708	5072	WHITEWATER CANYON TROUT FARM	5.9	SL	0.50	0.58	39.6	29.9	F
891017	57007	CORRALITOS	3.4	SR	0.47	0.51	45.7	43.9	B
891017	47006	GAVILAN COLLEGE PHYS. SCI. BLDG.	9.5	SL	0.30	0.39	31.9	27.6	N
891017	47379	GILROY #1 - GAVILAN WATER TOWER	9.2	SR	0.42	0.41	39.5	29.8	N
891017	57180	LEXINGTON DAM - LEFT ABUTMENT	6.3	SR	0.45	0.39	118.0	45.6	F
891017		LOS GATOS PRESENTATION CNTR	3.5	HR	0.66	0.44	105.5	57.4	F
891017	58065	SARATOGA - ALOHA AVENUE	8.3	SL	0.37	0.35	57.0	44.8	F
920313	9401	ERZINCAN, TURKEY	2.0	SL	0.43	0.46	120.2	65.4	F
920628	22170	JOSHUA TREE - FIRE STATION	7.4	SL	0.28	0.19	42.7	30.0	B
920628		LUCERNE VALLEY	1.1	SL	0.76	0.73	127.5	95.3	F
940117	655	JENSEN FILTRATION PLANT	6.5	SL	0.38	0.62	45.4	100.1	F
940117	24088	PACOIMA; KAGEL CANYON	8.0	HR	0.53	0.24	55.5	36.8	N
940117	24279	NEWHALL; LA COUNTY FIRE STATION	6.7	SL	0.72	0.65	118.2	49.3	F
940117	24087	ARLETA; NORDHOFF FIRE STATION	9.5	SL	0.24	0.33	26.0	31.4	N
940117	24207	PACOIMA DAM - DOWNSTREAM	7.6	HR	0.50	0.24	48.5	18.9	F
940117	5968	RINALDI RECEIVING STATION - FF	7.5	SL	0.89	0.39	178.4	67.5	F
940117	306	SYLMAR CONVERTER STATION - FF	6.4	SL	0.59	0.80	130.1	89.3	F
940117	6273	SYLMAR CONVERTER STATION E - FF	6.2	SL	0.84	0.49	116.3	75.8	F
940117	637	SEPULVEDA VA HOSPITAL	9.3	SL	0.73	0.79	48.7	76.0	F
940117	24514	SYLMAR; OLIVE VIEW FF	6.2	SL	0.73	0.59	122.2	54.3	F
950117		KOBE UNIVERSITY (CEORKA)	3.8	RK	0.33	0.26	49.1	38.8	F
950117		KOBE (CEORKA)	6.2	SL	0.67	0.54	56.4	38.2	F
950117		KOBE (JMA)	3.4	SL	0.86	0.52	104.3	51.9	F
950117		KOBE PORT ISLAND, SURFACE	6.6	SL	0.43	0.14	95.9	30.3	F
950117		TAKATORI (JR)	4.3	SL	0.81	0.42	174.9	62.7	F

¹HR-HARD ROCK; SR-SEDIMENTARY AND CONGLOMERATE ROCK; SL-SOIL AND ALLUVIUM

²FN-FAULT NORMAL; FP-FAULT PARALLEL

³F-FORWARD; N-NEUTRAL; B-BACKWARD

Recordings Close to Epicenters

It is a common fallacy to assume that recordings close to the epicenters of strike-slip and oblique-slip earthquakes (such as Bond's Corner, 1971 Imperial Valley earthquake; Corralitos, 1987 Loma Prieta earthquake; and Joshua Tree, 1992 Landers earthquake) contain forward-rupture-directivity effects. On the contrary, these records contain neutral or backward-directivity effects, produced when the rupture propagates away from the site, and are characterized by relatively low amplitudes of long-period ground motions. Also, strong-motion recordings above shallow thrust faults, such as the Cape Mendocino and Petrolia recordings of the 1992 Cape Mendocino earthquake, do not contain rupture-directivity effects. The effects of rupture directivity are primarily manifested at the longer periods, so that large peak accelerations in near-fault recordings do not necessarily imply large long-period ground motions.

Faulting Mechanism

If the seismic hazard at a site is dominated by a particular style of faulting (e.g., strike-slip or normal), it is preferable to use time histories from that style of faulting. In the recorded data analyzed by Somerville and others (1997a), it was found that the relation between strike-normal and strike-parallel ground motions is similar for strike-slip and reverse earthquakes. However, differences between strike-slip and reverse faulting were found in the azimuthal variation of duration and response spectral amplification. Also, for larger earthquakes, there may be differences between strike-slip and reverse ground motions because the rupture-directivity effect in reverse faulting builds up over a limited fault width, whereas for strike-slip faulting it can build up over a much larger fault length. There are few strong-motion recordings close to large normal-faulting earthquakes. Given the presently available data, it seems appropriate to assume that near-fault ground-motion time histories from normal faults can be represented by time histories from reverse faults, or from broadband time history simulations for normal faulting. The response spectrum for the normal-faulting time history can be approximated by taking 75 percent of the near-fault ground motions predicted for reverse faulting in the model described above.

Duration

It is a common fallacy to assume that near-fault ground-motion time histories close to large earthquakes should have a long duration. As shown in figure 6b, the stronger the near-fault directivity effect, the shorter the duration. This is because the forward-directivity effect causes nearly all of the seismic radiation from the fault to arrive in a single brief pulse of motion. It does not make sense to sequentially combine several near-fault records containing brief pulses to make up for the short duration that is characteristic of forward-rupture-directivity effects.

ADEQUACY OF 1997 NEHRP AND UBC CODE SPECTRA IN REPRESENTING NEAR-FAULT MOTIONS FROM NORMAL FAULTS

To account for large ground-motion levels caused by rupture-directivity effects, the 1997 revision of the UBC includes a near-fault factor N which applies to sites located within 15 kilometers of major active faults in seismic zone 4. The near-source factor depends on the slip rate of the fault and the maximum magnitude of the earthquake that the fault can generate. If the slip rate of the fault is less than 2 mm/yr, which is the case for most faults in the Basin and Range Province, then the near-source factor does not apply. Also, with the exception of western Nevada and the Yellowstone region, the Basin and Range Province lies in seismic zones lower than 4 and the near-source factor does not apply. The intent of the code revision was to address near-fault ground motions only near the most active faults. However, this avoided the issue of how to address near-fault ground motions close to less active faults and close to smaller faults, which is particularly relevant in the Basin and Range Province.

The 1997 NEHRP probabilistic ground-motion maps and design include the effects of proximity to faults, and thus address the issue of near-fault ground motions in the Basin and Range Province in a more specific way. However, they do not account for the increased level of long-period ground motions close to faults caused by rupture-directivity effects. To date, none of the code approaches addresses the issue of larger ground motions in the strike-normal than in the strike-parallel direction. However, for sites located close to major normal faults in the Basin and Range Province whose strike directions are known, this difference can be quantified in a straightforward way using the empirical model for reverse faults described by Somerville and others (1997b), reduced by 25 percent to account for style of faulting differences.

CONCLUSIONS

The propagation of fault rupture toward a site at a velocity close to the shear wave velocity causes most of the seismic energy from the rupture to arrive in a single large, long-period pulse of motion which occurs at the beginning of the record. This pulse of motion represents the cumulative effect of almost all of the seismic radiation from the fault. The radiation pattern of the shear dislocation on the fault causes this large pulse of motion to be oriented in the direction perpendicular to the fault, causing the strike-normal peak velocity to be larger than the strike-parallel peak velocity.

The effect of forward rupture directivity on the response spectrum is to increase the level of the response spectrum of the horizontal component normal to the fault strike at periods longer than 0.5 seconds. Consequently, near-fault effects cannot be adequately described by uniform scaling of a fixed response spectral shape. A complete representation of the near-fault response spectrum requires the specification of separate horizontal components in the strike-normal and strike-parallel directions.

These components are significantly different within about 15 kilometers of the fault at periods longer than about 0.5 seconds. Since fault strike is usually well known close to major faults, it is straightforward to take the difference between the strike-normal and strike-parallel components of motion into account in the evaluation of near-fault ground motions, especially for structures that are sensitive to long-period ground motions.

If time histories are used in conjunction with the response spectrum, it is important to select time histories that appropriately include forward-rupture-directivity effects. This is true even if time histories are being matched to a design spectrum, because the spectral matching process cannot build a rupture-directivity pulse into a record where none is present to begin with. This indicates the need to identify the ground-motion conditions that control the design spectrum. When the design spectra are based on scenario earthquakes, there may be two levels of design spectra, one based on the median ground-motion level and the other based on the median plus one standard deviation ground-motion level. If the response spectrum is based on the median ground-motion level, then it represents average directivity conditions, and it is appropriate to select time histories that span a range of directivity conditions. However, if the response spectrum is based on the mean plus one standard deviation ground-motion level, then it represents forward-directivity conditions, and most if not all of the time histories should be for forward-rupture-directivity conditions. If the design spectra are based on probabilistic seismic-hazard analysis, then deaggregation of the seismic hazard can be used to identify the degree to which the ground motions that dominate the seismic hazard represent larger than median levels, which in turn provides a basis for selecting the appropriate proportion of recordings containing forward rupture directivity in the suite of time histories used for analysis.

As a guide to the selection of time histories for use in design and evaluation of structures that are sensitive to long-period ground motions, a list of near-fault strong-motion recordings indicating the nature of the rupture-directivity effects that they contain has been prepared. In situations where there are insufficient recorded time histories, strong-motion simulation methods can be used to generate time histories for the required combinations of magnitudes and distances.

REFERENCES

- Abrahamson, N.A., and Silva, W.J., 1997, Empirical response spectral attenuation relations for shallow crustal earthquakes: *Seismological Research Letters*, v. 68, p. 94-127.
- Building Seismic Safety Council, 1997, NEHRP recommended provisions for seismic regulations for new buildings: Washington, D.C.
- Husid, R.L., 1969, Analisis de terremotos: Analisis General, *Revista del IDIEM*, 8, p. 21-42, Santiago, Chile.
- McGuire, R.K., 1995, Probabilistic seismic hazard analysis and design earthquakes: Closing the loop: *Seismological Society of America Bulletin*, v. 86, p. 1275-1284.
- Naeim, F., 1995, On seismic design implications of the 1994 Northridge earthquake records: *Earthquake Spectra* 11, p. 91-110.
- Naeim, F., and Anderson, J.C., 1993, Classification and evaluation of earthquake records for design: *Earthquake Engineering Research Institute*, 287 p.
- Naeim, F., and Anderson, J.C., 1996, Design classification of horizontal and vertical earthquake ground motion: Report to the U.S. Geological Survey by John. A. Martin & Associates, Inc., JAMA Report No. 7738.68-96, 427 p.
- Salah-Mars, S., Mejia, L.H., Somerville, P.G., Green, R.K., Hamburger, R.O., and Cole, C.A., 1994, Ground motions for base isolation seismic retrofit of a building near the Hayward fault: U.S. National Conference on Earthquake Engineering 5th, Chicago, Il., July, 1994 [Proceedings]
- Shi, Baoping, Zeng Y., and Brune, J.N., 1997, Numerical simulations of earthquake ruptures: A comparison between thrust, normal, and contained strike-slip faulting [abs.]: *Seismological Research Letters*, v. 68, p. 333.
- Silva, W., and Toro, G., 1996, Verification of response spectral shapes and anchor points for different site categories for building design codes: SMIP96 Seminar on Seismological and Engineering Implications of Recent Strong Motion Data, p. 37-51.
- Somerville, P.G., Smith, N.F., Graves, R.W., and Abrahamson, N.A., 1997, Modification of empirical strong ground motion attenuation relations to include the amplitude and duration effects of rupture directivity: *Seismological Research Letters*, v. 68, p. 199-222.
- Somerville, P.G., Smith, N.F., Punyamurthula, S., and Sun, J., 1997b, Development of ground motion time histories for Phase 2 of the FEMA/SAC Steel Project: Report No. SAC/BD-97/04.
- Somerville, P.G., 1996, Strong ground motions of the Kobe, Japan earthquake of Jan. 17, 1995, and development of a model of forward rupture directivity effects applicable in California: Western Regional Technical Seminar on Earthquake Engineering for Dams, Association of State Dam Safety Officials, Sacramento, Ca., April 11-12, 1996 [Proceedings]
- Somerville, P.G., Smith, N.F., Graves, R.W., and Abrahamson, N.A., 1995a, Representation of near-fault rupture directivity effects in design ground motions, and application to Caltrans bridges: National Seismic Conference on Bridges and Highways, San Diego, Ca., December 10-13, 1995 [Proceedings]
- Somerville, P.G., Graves, R.W., and Saikia, C.K., 1995b, Characterization of ground motions during the Northridge earthquake of January 17, 1994: Report No. SAC 95-03 of the SAC Joint Venture.
- Somerville, P.G., and Graves, R.W., 1993, Conditions that give rise to unusually large long-period ground motions: The structural design of tall buildings 2, p. 211-232.
- Structural Engineers' Association of California, 1996, 1997 UBC Code Change #178, 1996-095-56A.
- Wald, D.J., and Heaton, T.H., 1994, Spatial and temporal distribution of slip of the 1992 Landers, California earthquake: *Seismological Society of America Bulletin*, v. 84, p. 668-691.

SEISMIC HAZARDS IN THE BASIN AND RANGE PROVINCE: PERSPECTIVES FROM PROBABILISTIC ANALYSES

Ivan G. Wong and Susan S. Olig
Seismic Hazards Branch
Woodward-Clyde Federal Services
500 12th Street, Suite 200
Oakland, CA 94607

ABSTRACT

In this paper, we summarize the results of probabilistic seismic-hazard analyses for seven sites located throughout the Basin and Range Province and neighboring extensional tectonic regimes in the western U.S. The levels of probabilistic hazard at these sites range from one of the highest in the Basin and Range Province, in the seismically active Salt Lake Valley adjacent to the Wasatch fault, to one of the lowest in the Canyonlands area in the Colorado Plateau interior, where seismicity is low and known late Quaternary faults are scarce. Based on these analyses, the dominant contributors to ground shaking in the western U.S. interior are active faults and background earthquakes within a few tens of kilometers of a site. More distant active faults characterized by large maximum earthquakes and high slip rates (>1 mm/yr) can contribute significantly to long-period ground-motion hazard. The probabilistic analyses described in this paper emphasize the importance of several aspects of seismic sources that can significantly influence the probabilistic hazard at a given site, including: (1) fault segmentation and its correlation with recurrence; (2) earthquake recurrence models (truncated exponential or characteristic), and the approach used to characterize recurrence (recurrence intervals or slip rates); (3) temporal clustering, which can result in inter-event times that vary by more than an order of magnitude and the issue of whether the fault is presently within an intercluster or intracluster period; (4) the rate of recurrence of background seismicity and the issue of nonstationarity; and (5) the possibility of low dynamic stress drops in extensional regimes, which can lead to lower ground motions than in compressional settings. Path and site factors in the Basin and Range Province are also critical to probabilistic as well as deterministic hazard because many urban areas are situated in alluvial basins bounded by major normal faults. These factors include site amplification due to the presence of near-surface, low-velocity unconsolidated sediments and possible basin amplification of long-period ground motions.

INTRODUCTION

The Basin and Range Province dominates the interior of the western U.S. both in terms of areal extent and tectonic deformation rates. Extensional tectonic processes operating in the province can also be found in the neighboring but less active Colorado Plateau, Northern and Southern Rocky Mountains, and all western states with the possible exception of Washington. Seismicity rates in these four distinctive tectonic provinces range from low to moderate compared to California. Late Quaternary normal faults, particularly along the boundaries of the Basin and Range Province with the Colorado Plateau and Rocky Mountains, exhibit evidence of past ruptures indicative of large earthquakes of moment magnitude (M_w) $6\frac{3}{4}$ and greater. Such events are, however, infrequent on individual structures, with recurrence intervals ranging from less than a few thousand years for the most active faults to more than 100,000 years for the least active.

Evaluating the seismic hazard in regions like the Basin and Range Province or less active regions such as the Northern or Southern Rocky Mountain provinces poses unique problems compared to active plate boundary regions like California because, although the hazard can be low due to the long fault recurrence times, the risk can be high. Many of the major urban centers in the western U.S. interior are located adjacent to or in the vicinity of major late Quaternary faults including Salt Lake City, Utah, Reno, Nevada, and Albuquerque, New Mexico, re-

sulting in high seismic exposure. In addition, although smaller in size, potentially damaging moderate-sized "background" (non-surface rupturing) earthquakes as large as M_w 6 to $6\frac{1}{2}$ generated by buried, unknown and unmapped faults can occur at much higher rates than large surface-faulting events throughout many areas of the western interior (e.g., Intermountain seismic belt and Rio Grande rift).

The assessment of seismic risk requires an evaluation of the probability of occurrence of specific seismic hazards. Probabilistic seismic-hazard analysis, as first developed by Cornell (1968), has become the approach most suited for quantifying these probabilities in seismic settings such as the Basin and Range Province where there are large uncertainties in characterizing seismic sources and ground-motion attenuation. There are several reasons why these uncertainties are large. For example, active faults in the western U.S. interior have not been studied to as great a degree as in California. The short and incomplete historical seismicity record and the low activity of the faults that have been investigated also make estimation of earthquake recurrence difficult. Thus, because there may be a range of interpretations and large uncertainties in characterizing the rupture geometry and behavior of late Quaternary faults in regions such as the Basin and Range Province, probabilistic seismic-hazard analysis has been and should be used more extensively in quantifying the level of hazards in the western U.S. interior.

In this paper, we briefly describe the results of proba-

bilistic analyses performed at seven sites located throughout the Basin and Range Province and neighboring extensional tectonic regimes. These analyses emphasize the importance of several aspects of seismic source and ground-motion characterization that can significantly impact probabilistic hazard. Several issues are also raised by these analyses that should be addressed in future earth science research in the western U.S. interior.

CASE STUDIES

The seven sites described in this paper are: Yucca Mountain, southern Nevada (YM); an area straddling the boundary between the eastern Snake River Plain (ESRP) and northern Basin and Range (NBR) province, southeastern Idaho (ESRP-NBR); west Salt Lake Valley, northern Utah (WSLV); northern Rio Grande rift, central Colorado (NRGR); southern Rio Grande rift, northern New Mexico (SRGR); Canyonlands, southeastern Utah in the interior of the Colorado Plateau (C); and the Sierra Nevada Foothills, eastern California (SNF) (figure 1).

Yucca Mountain

Wong and others (1997a) performed a preliminary probabilistic analysis of the U.S. Department of Energy's potential high-level nuclear waste repository northwest of Las Vegas in the southern Great Basin to develop criteria for early seismic-design studies. A total of 88 Quaternary faults located within 100 kilometers of the site was considered in the hazard analysis (figure 2a). Fifteen faults exhibiting varying degrees of Quaternary activity occur within 15 kilometers of the site (table 1). Individual faults

are characterized by maximum earthquakes that range from M_w 5.1 to 7.6. Fault slip rates range from a very low 0.00001 mm/yr to as much as 4 mm/yr. Potentially significant faults include, for example, the Paintbrush Canyon, Solitario Canyon, Bare Mountain, Furnace Creek, and Death Valley faults. Wong and others (1997a) used a single areal source zone representing background earthquakes up to M_w $6\frac{1}{4} \pm \frac{1}{4}$ in the analysis. Recurrence rates for these background earthquakes are based on the 1904-1996 historical record, which contains events up to M_w 5.6 in size.

A significant aspect of the analysis was the use of a new attenuation relationship for earthquakes in extensional tectonic regimes (Spudich and others, 1996). This relationship, developed as part of the Yucca Mountain Project, gives significantly lower ground motions than five other predominantly California-based relationships used in the analysis (Wong and others, 1997a).

Eastern Snake River Plain - Northern Basin and Range Province

Woodward-Clyde Federal Services (WCFS) and others (1996) performed a site-specific probabilistic seismic-hazard analysis for seven facility sites at the Idaho National Engineering Laboratory (INEL). The INEL is located within the ESRP but adjacent to and just south of the northern Basin and Range Province. Because of its location within the ESRP volcano-tectonic regime, three types of seismic sources were considered significant to the INEL: (1) three major Basin and Range faults immediately to the north to northwest including the Lost River,

Table 1. Significant nearby faults.

<u>Location</u>	<u>Faults</u>	<u>Shortest Horizontal Distance (km)</u>	<u>Probability of Being Seismogenic</u>	<u>Best Estimate Maximum Magnitude (M_w)</u>	<u>Best Estimate Slip Rate (mm/yr)</u>
Yucca Mountain, NV	9 Local Faults	≤ 10	≥ 0.5	6.2-6.7	0.002-0.02
ESRP-NBR, ID	Lost River/Lemhi	15/20	1.0	7/7	0.05-1
West Salt Lake Valley, UT	East Great Salt Lake/Wasatch	2/12	1.0	7/7 $\frac{1}{4}$	0.3-0.5/1-2
Northern Rio Grande Rift, CO	Mosquito/Williams Fork Mountain	3/2	0.5/1.0	7/6 $\frac{1}{2}$	0.05/0.12
Southern Rio Grande Rift, NM	Pajarito System	≤ 5	1.0	6.9	0.01-0.1
Canyonlands, UT	Moab	0	0.1	6 $\frac{1}{2}$ -7	0.015
Sierran Foothills, CA	Maidu East and Rescue	14	1.0	6 $\frac{1}{4}$	0.004

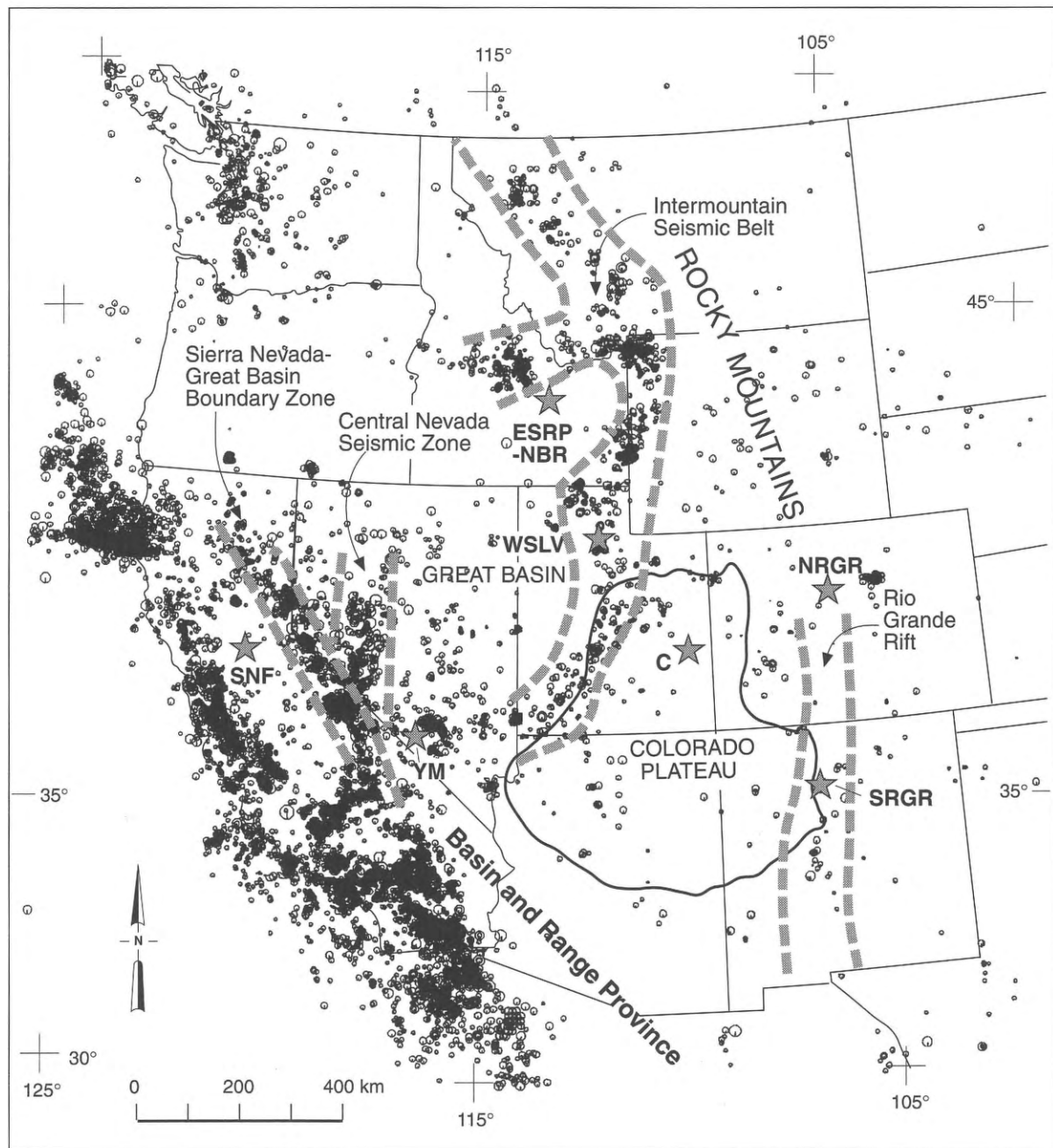


Figure 1. Seismicity ($M \geq 3.0$) of the western U.S. (1808 to 1996), physiographic provinces and major seismic source zones located in or adjacent to the Basin and Range Province. Also shown are locations (stars) of the case studies described in this paper. Abbreviation are: C, Canyonlands; ESRP-NBR, eastern Snake River Plain-northern Basin and Range; NRGR, northern Rio Grande rift; WSLV, west Salt Lake Valley; SNF, Sierra Nevada Foothills; SRGR, southern Rio Grande rift; and YM, Yucca Mountain. Seismicity data are from the USGS National Earthquake Information Center.

Lemhi, and Beaverhead faults (figure 2a and table 1); (2) four volcanic zones within the ESRP including the Arco, Lava Ridge-Hells Half Acre, and Great rift zones and the axial volcanic zone; and (3) areal seismic-source zones, including most significantly, the northern Basin and Range Province and the ESRP. Maximum earthquakes for the various fault segments of the Lost River, Lemhi, and Beaverhead faults ranged from M_w 6.7 to 7.4 and slip rates from 0.02 to 1.0 mm/yr (WCFS and others, 1996). They considered the maximum earthquake for the volcanic rift zones to be a low probability M_w $5\frac{1}{2} \pm \frac{1}{2}$ and the recurrence of such events is based on the estimated recurrence of episodes of dike injection. Maximum earthquakes for the seismic-source zones ranged from M_w $5\frac{1}{2} \pm \frac{1}{2}$ for the ESRP to M_w $7\frac{1}{4} \pm \frac{1}{4}$ for portions of the Intermountain seismic belt where distant Quaternary faults were not specifically included as separate sources. Thus, the source zones for the latter included both faults and background earthquakes.

Woodward Clyde Federal Services and others (1996) modeled ground-motion attenuation and site effects using four empirical western U.S. rock relationships and site-specific relationships developed for each of the facility sites. The latter were calculated using a stochastic point-source numerical modeling technique (Silva, 1992) which incorporated a best estimate range of earthquake stress drops of 50 to 75 bars, magnitude-dependent focal depths, region-specific attenuation with a quality factor of $Q(f) = 200f^{0.44}$, site-specific near-surface attenuation as expressed by the parameter kappa (Anderson and Hough, 1994), which ranged from 0.012 to 0.033 sec, and site-specific shear-wave and density profiles. Typical kappa values for western U.S. rock range from 0.02 to 0.06 sec (Silva and Darragh, 1995). Incorporating the site response at the INEL is especially significant because of the unique sedimentary interbedded nature of the underlying basalt. This volcanic stratigraphy differs significantly from typical western U.S. rock in terms of site effects (WCFS and others, 1996).

West Salt Lake Valley

Wong and others (1995) performed a seismic-hazards evaluation to develop the seismic-design criteria for a tailings impoundment near the town of Magna on the west side of Salt Lake Valley. Late Quaternary faults considered in the probabilistic seismic-hazard analysis included the East Great Salt Lake fault, whose southern end extends to within 1 to 3 kilometers of the site (table 1), the Oquirrh, West Valley, East Cache, Hansel Valley, and Stansbury faults and segments of the Wasatch fault (Wong and others, 1995) (figure 2a). The East Great Salt Lake fault consists of two segments of which the closest, the Antelope Island segment, can generate a maximum earthquake of M_w 7. Its Quaternary slip rate is estimated at 0.4 to 0.7 mm/yr.

The site also lies due west of the Salt Lake City segment of the Wasatch fault (figure 2a). Its estimated maximum earthquake is M_w 7 which occurs on average every $1,350 \pm 500$ years (Black and others, 1995). Wong and others (1995) also included the Brigham City, Weber,

Provo, Nephi, and Levan segments of the Wasatch fault in the hazard analysis. An areal source zone of background earthquakes with a maximum magnitude of M_w $6\frac{1}{4} \pm \frac{1}{4}$ was also incorporated into the probabilistic seismic-hazard analysis. Wong and others (1995) used three empirical attenuation relationships appropriate for deep soil to estimate the ground motions.

Northern Rio Grande Rift

A probabilistic seismic-hazard analysis was performed to evaluate the seismic safety of two tailings dams located north of Leadville in central Colorado (Wong and others, 1996a). Although the sites lie within the Southern Rocky Mountain province, the tectonic setting is similar to the Basin and Range Province in that normal faulting and extensional stresses characterize the earthquake processes in the region. The two sites are in fact located in the vicinity of the northern Rio Grande rift in central Colorado. Unlike the southern portion of the rift, however, seismicity is relatively low level and known late Quaternary faults are relatively few in number (Wong and others, 1996a).

Wong and others (1996a) considered nine late Quaternary faults in the probabilistic analysis with the most significant structures being the Mosquito, Williams Fork Mountain, Frontal, and Skylark faults because of their proximity to the two sites (figure 2a and table 1). Slip rates for these faults ranged from about 0.1 to 0.4 mm/yr. Maximum earthquakes ranged from M_w $6\frac{1}{2}$ to 7 and a single background zone for the Colorado Rocky Mountains was utilized with a maximum magnitude of M_w 6.5 ± 0.3 . Ground-motion attenuation was characterized by three empirical relationships for stiff soil conditions.

Southern Rio Grande Rift

From 1991 to 1995, Wong and others (1996b) performed an extensive seismic-hazard evaluation of the Los Alamos National Laboratory (LANL). As part of this program, a site-specific probabilistic analysis of eight technical areas was carried out to update the seismic-design criteria for the LANL. Seismic sources within the site region included 25 Quaternary faults (figure 2b) and four seismic-source zones; the latter to account for background earthquakes. The source zones included the Rio Grande rift, Colorado Plateau transition zone, Southern Rocky Mountains province, and the Great Plains. The most significant faults were those of the Pajarito fault system (figure 2b and table 1) which consists of the Pajarito, Guaje Mountain, and Rendija Canyon faults. The main 41-kilometers-long Pajarito fault is located along the western margin of the LANL, and has an estimated maximum earthquake of M_w 6.9 ± 0.3 and a long-term slip rate of about 0.1 mm/yr. It is a down-to-the-east normal fault that dips beneath LANL. Both the Rendija Canyon and Guaje Mountain faults are west-dipping faults that are probably antithetic to the main Pajarito fault and transect portions of the LANL.

Wong and others (1996b) addressed crustal attenuation and site response beneath the LANL through numerically modeling-based site-specific attenuation relationships

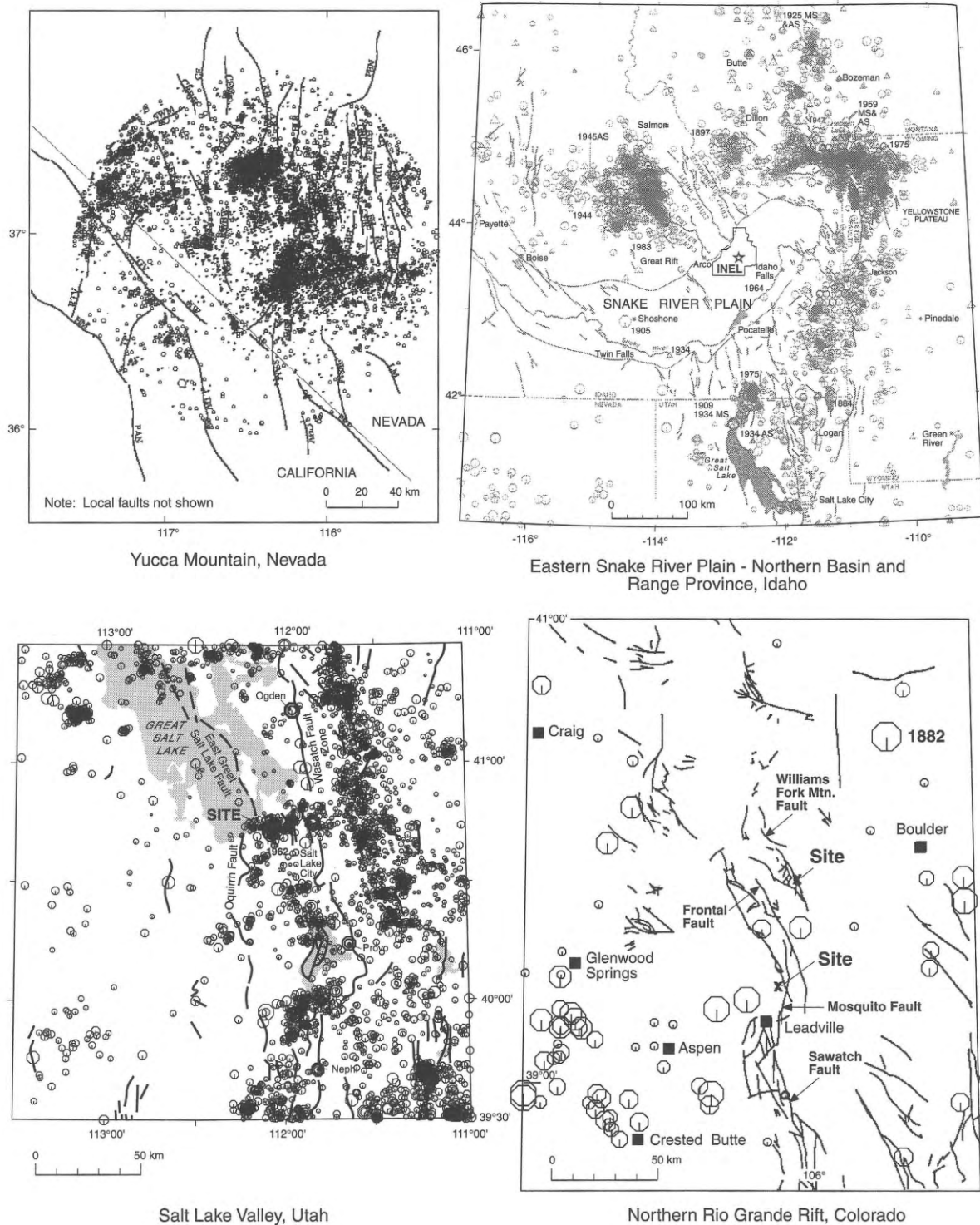
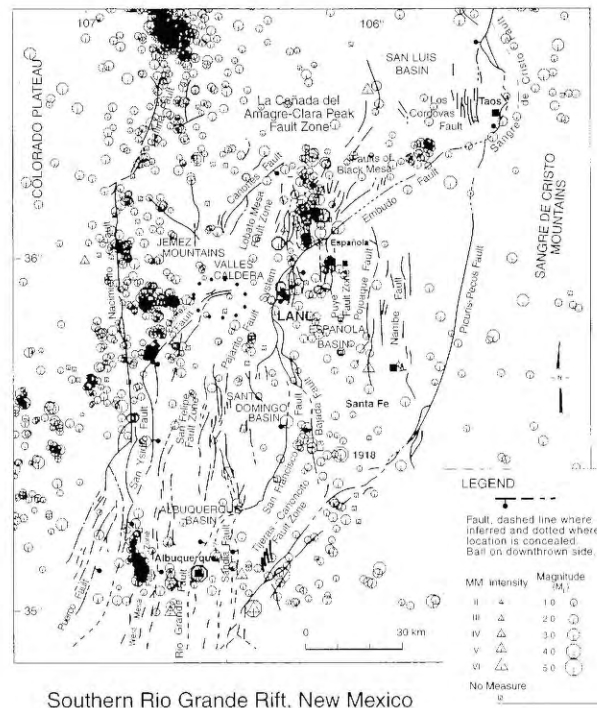
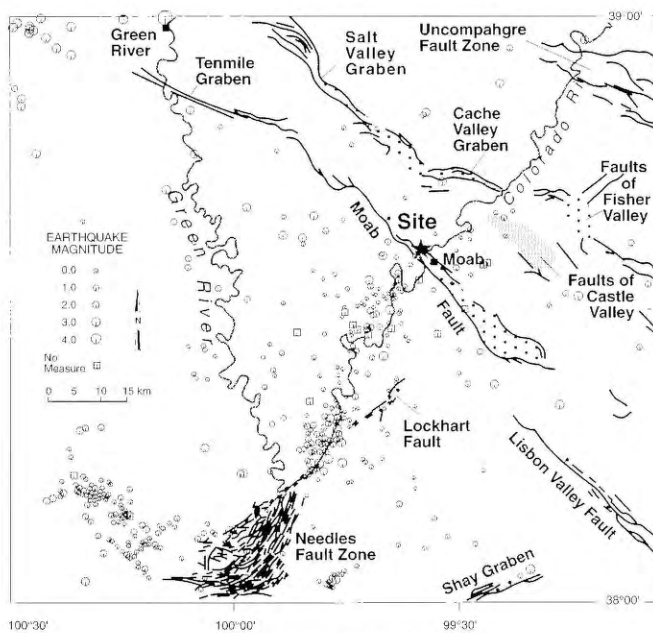


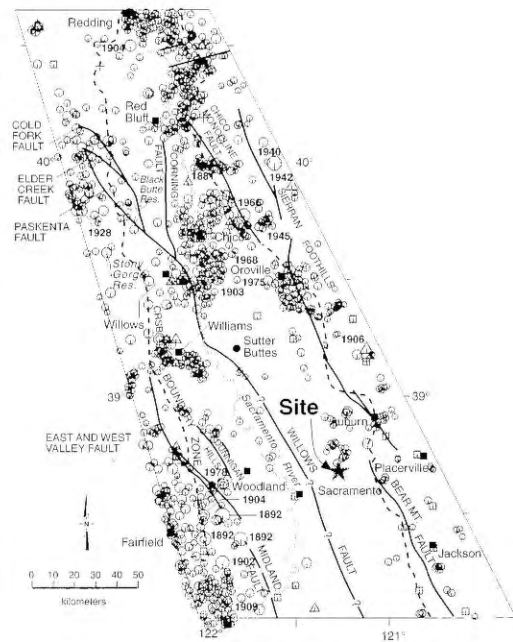
Figure 2a. Active and potentially active faults and historical seismicity surrounding the case study sites. Detailed information on these site maps can be found in the original sources, cited in the text.



Southern Rio Grande Rift, New Mexico



Canyonlands, Utah



Sierra Nevada Foothills, California

Figure 2b. Active and potentially active faults and historical seismicity surrounding the case study sites. Detailed information on these site maps can be found in the original sources, cited in the text.

developed using an approach similar to that used at the INEL and three empirical relationships. They performed a program of drilling, downhole velocity measurements, and dynamic laboratory testing to characterize the material properties of the volcanic stratigraphy beneath the LANL. A site-specific kappa of 0.035 sec was estimated based on an analysis of microearthquakes recorded by the local seismographic network. Although LANL is generally situated on volcanic tuff, the site conditions are most similar to deep soil conditions.

Canyonlands, Colorado Plateau

Wong and others (1996c; 1997b) performed a seismic-hazards evaluation as part of the reclamation of a uranium mills tailings site near Moab, Utah. The site came under regulatory review by the U.S. Nuclear Regulatory Commission (NRC), which typically requires a deterministic specification of the seismic-design criteria. However, because of the large uncertainties regarding active faulting and background earthquakes in the Colorado Plateau interior, a probabilistic seismic-hazard analysis accepted by the NRC was also carried out as an alternative approach to developing seismic-design criteria for on-site disposal.

Potential seismic sources that could affect the site include 11 faults and 2 seismic-source zones (figure 2b). Ten of the faults including the Moab (table 1), Lisbon Valley, Salt Valley, and Paradox Valley faults developed as a result of salt dissolution and are probably not seismogenic (Wong and others, 1996c). To accommodate the remote possibility, however, that these faults could generate earthquakes, Wong and others (1996c) considered them in the seismic-hazard analysis with very low probabilities of being seismogenic. Seismogenic structures included the frontal faults associated with the Uncompahgre uplift.

Although the Colorado Plateau interior is seismically active, few studies have seismicity definitively associated with known faults. Wong and others (1996c) incorporated the contribution to seismic hazard from such background earthquakes into the hazard analysis as the Colorado Plateau interior seismic-source zone. They adopted a maximum earthquake of $M_w 6 \pm \frac{1}{2}$ for this zone. The second seismic-source zone (maximum magnitude $M_w 5\frac{3}{4} \pm \frac{1}{4}$ considered in this analysis was a northeast-trending zone of microseismicity aligned approximately along the

stretch of the Colorado River southwest of Moab. Three soil empirical attenuation relationships were used in the probabilistic analysis to characterize the ground motions.

Sierra Nevada Foothills

Wong and others (1994) performed a probabilistic seismic-hazard analysis to evaluate the existing seismic design of the U.S. Bureau of Reclamation's Mormon Island Auxiliary Dam in the Sierra Nevada Foothills near Folsom, California. The Sierra Nevada Foothills lie within an extensional transitional zone between the compressional regime along the San Andreas plate boundary and the Basin and Range Province whose western boundary is 120 kilometers to the east along the eastern margin of the Sierra Nevada. The region is characterized by a low to moderate level of seismicity and very low slip rate faults including the Foothills fault system.

In the analysis, Wong and others (1994) considered a total of 17 faults within the Sierra Nevada Foothills (figure 2b), five major faults within the San Andreas fault system, the Sierra-Nevada Frontal fault, and the Coast Ranges-Sierran Block boundary zone. The relatively short Foothills faults (e.g., Maidu East and Rescue) generally have estimated maximum earthquakes of $M_w 6\frac{1}{2} \pm \frac{1}{4}$ and slip rates significantly less than 0.01 mm/yr. The closest known faults were at a distance of 14 kilometers (figure 2b and table 1).

A background source zone for the Foothills was characterized by a maximum earthquake of $M_w 6 \pm \frac{1}{4}$ and recurrence rates based on the historical record. Ground-motion attenuation was characterized by four western U.S. empirical relationships believed appropriate for soft rock.

PROBABILISTIC SEISMIC HAZARD

To understand which earthquake sources drive the ground-shaking hazard at these seven sites, we must understand the contributions of both seismogenic faults and background earthquakes to the total probabilistic hazard. Based on probabilistic seismic-hazard analyses performed for each of the seven sites, we summarize in table 2 the calculated peak horizontal accelerations for three return periods of engineering significance: 500, 2,000, and 10,000 years. Note that the ground motions are for both

Table 2. Site-specific probabilistic peak horizontal accelerations (g's).

Location	Return Period		
	500 years	2,000 years	10,000 years
Yucca Mountain, NV	0.16	0.28	0.50
ESRP-NBR, ID	0.06-0.09	0.10-0.18	0.16-0.33
West Salt Lake Valley, UT	0.27	0.43	0.72
Northern Rio Grande Rift, CO	0.09-0.12	0.21-0.25	0.42-0.43
Southern Rio Grande Rift, NM	0.15	0.30	0.55
Canyonlands, UT	0.04	0.10	0.21
Sierran Foothills, CA	0.10	0.23	0.47

Bold values indicate soil sites. Remaining values are for rock sites.

rock and soil sites, although, as we will discuss later, our use of multiple empirical relationships results in very little difference in ground motions for the two types of site conditions. The highest peak horizontal-acceleration hazard occurs in the western Salt Lake Valley, while the lowest is, not surprisingly, in the Canyonlands area in the Colorado Plateau interior. Comparatively moderate hazard is estimated for the southern Rio Grande rift, Yucca Mountain, and somewhat surprisingly, the Sierran Foothills and the northern Rio Grande rift.

In table 1, we summarize the closest and generally most significant faults to the seven sites. Reflecting the varied levels of fault activity rates found in the Basin and Range Province and adjacent extensional regimes, slip rates range from 0.002 mm/yr for the low activity Yucca Mountain faults to 1 to 2 mm/yr for the active Wasatch fault. Maximum magnitudes are as low as $M_w 6\frac{1}{4}$ for the short reactivated faults in the Sierra Nevada Foothills fault system to $M_w 7\frac{1}{4}$ for segments of the Wasatch fault.

Table 3 summarizes the recurrence parameters (a and b) for the background seismic-source zones in which the sites are located, with the exception of the INEL where we cite the parameters for the adjacent northern Basin and Range Province. Both a and b parameters are listed as well as the return periods for $M_w 5$ and 6 and greater earthquakes normalized to an area of 10,000 km² (100 km x 100 km). A truncated exponential form of the recurrence curve (Youngs and Coppersmith, 1985) has been assumed for all background source zones. Yucca Mountain, the northern Basin and Range Province, and Salt Lake Valley exhibit the highest rates of background seismicity with return periods for $M \geq 5$ and $M \geq 6$ earthquakes of less than 50 years and less than about 800 years, respectively. Not surprisingly, the Canyonlands in the interior of the Colorado Plateau and the northern Rio Grande rift in central Colorado are the least seismically active areas considered in our studies (table 3).

To identify the major contributors to the peak horizontal-acceleration hazard at each site, we can deaggregate the hazard by seismic source; the dominant contributors

are listed in table 4. The western side of Salt Lake Valley has the highest hazard of any of the seven sites studied due to the high level of background seismicity (table 3) and the proximity of the nearby and moderate slip rate East Great Salt Lake fault system. (In a very recent analysis of sites within a few kilometers of the Wasatch fault, it is the dominant contributor to hazard at return periods greater than 50 years [Wong and others, 1997c].) Similarly, the southern Rio Grande rift has a moderate hazard level because of the moderate rate of background seismicity (table 3) and the proximity of the moderately active Pajarito fault system (table 1). Although the hazard is somewhat lower due to a lower level of background seismicity, a similar situation exists at the two northern Rio Grande rift sites (table 4).

At both short and long return periods, the moderate levels of background seismicity control the moderate peak-acceleration hazard at Yucca Mountain and the Sierra Nevada Foothills (table 4). Although Quaternary faults exist close to both sites, their low slip rates (table 1) result in small contributions to hazard even up to return periods of 10,000 years. At the INEL, the peak-acceleration hazard is comparatively lower because the distance to the nearest faults, the Lost River and Lemhi faults, is approximately 15 to 20 kilometers and the sites are all located in the adjacent aseismic ESRP. The lowest peak-acceleration hazard exists at the Canyonlands site in the Colorado Plateau interior (table 2) where only the low level of background seismicity contributes to the hazard (table 4).

For low-frequency (long-period ≥ 1 sec) ground shaking, faults rather than background earthquakes are often the major contributors to hazard except at short return periods or in the absence of moderately active Quaternary faults (slip rates ≥ 0.1 mm/yr) in the region. At longer spectral periods, the faults are even more dominant. This is because faults produce the largest events and the larger the rupture area, the greater the amount of long-period ground motions generated.

Table 3. Recurrence of background earthquakes.

<u>Location</u>	<u>b-value</u>	<u>Approximate Return Periods (yrs)</u> <u>(per 10,000 km²)</u>			
		<u>a-value</u> <u>(per km²)</u>	<u>M_{max}</u>	<u>M≥ 5</u>	<u>M≥ 6</u>
Yucca Mountain, NV	0.87	-1.08	6 $\frac{1}{4}$	30	350
Northern Basin and Range, ID	0.81	-1.32	6 $\frac{1}{2}$	25	160
West Salt Lake Valley, UT	0.78	-1.64	6 $\frac{1}{4}$	40	770
Northern Rio Grande Rift, CO	0.90	-2.33	6 $\frac{1}{2}$	670	10,000
Southern Rio Grande Rift, NM	0.75	-2.45	6.3	100	1,000
Canyonlands, UT	0.92	-2.15	6	560	7,000
Sierran Foothills, CA	0.85	-1.53	6	60	500

Table 4. Dominant contributors to peak horizontal acceleration hazard.

<u>Location</u>	<u>Return Period</u>	
	<u>500 years</u>	<u>10,000 years</u>
Yucca Mountain, NV	Background Earthquakes	Background Earthquakes
ESRP-NBR, ID	Lost River Fault	Lost River Fault
West Salt Lake Valley, UT	Background Earthquakes	East Great Salt Lake Fault
Northern Rio Grande Rift, CO	Background Earthquakes	Mosquito & Williams Fork Mountain Faults
Southern Rio Grande Rift, NM	Background Earthquakes	Pajarito Fault System
Canyonlands, UT	Background Earthquakes	Background Earthquakes
Sierran Foothills, CA	Background Earthquakes	Background Earthquakes

OBSERVATIONS AND ISSUES

Based on these case histories, we discuss and summarize the following observations and issues regarding seismic-source and ground-motion characterization and their impacts on probabilistic seismic hazard.

Major Contributors to Hazard

As previously illustrated, probabilistic seismic hazard in the Basin and Range Province and similar extensional regimes in the western U.S. interior is a product of the hazard generated by both late Quaternary (or Quaternary) faults and background seismicity (buried faults). The level of hazard is controlled by the proximity of these faults, their maximum earthquakes and activity rates, and the rate of background seismicity. The most hazardous sites are those adjacent to active faults whose slip rates are greater than 0.1 mm/yr and/or in areas with high levels of background seismicity. Areas such as Salt Lake Valley adjacent to the East Great Salt Lake and Wasatch faults and along the active margins of the southern Rio Grande rift (e.g., LANL) are examples.

Because the rate of background earthquakes (defined as M_w 5, the minimum magnitude considered in most probabilistic-hazard analyses, to about M_w 6½) is much higher than for surface-faulting earthquakes generated by known faults, the probabilistic hazard is usually dominated by background seismicity at short return periods. This situation is exaggerated by the tendency for faults to behave in a characteristic manner (see discussion in next section). The exceptions to the dominance of background seismicity are sites in areas of very low seismicity (e.g., ESRP) or adjacent to very active faults whose slip rates are greater than 1 mm/yr such as along the Wasatch fault (Wong and others, 1997c).

At long return periods, greater than a few thousand years (which begins to approach the recurrence intervals of many faults), faults within a distance of 10 to 20 kilometers will generally be the dominant contributor to high-

frequency hazard (e.g., peak horizontal acceleration). If no such faults exist or if they have low slip rates, the background earthquake will dominate the probabilistic hazard.

Our discussion so far has focused on high-frequency seismic hazard. For most engineered structures, intermediate to high-frequency seismic waves (1 to 10 Hz) are of greatest concern in terms of potential damage. For low-frequency ground-shaking hazard, which is important for tall or long structures such as high-rise buildings and bridges, the dominant contributor will often be faults.

This trade-off between faults and background earthquakes is illustrated in figure 3, which shows the deaggregated peak horizontal acceleration and 1.0 sec spectral-acceleration hazard at Yucca Mountain for the return periods of 2,000 and 10,000 years. At 2,000 years, the peak-acceleration hazard is dominated by background earthquakes of M_w 5 to 6½ at short distances (<20 km) with a small contribution from distant active faults. At a 10,000-year return period, the contribution of the Paintbrush Canyon fault becomes more significant and the dominant magnitude range shifts to slightly higher values (figure 3). For 1.0 sec spectral acceleration, background earthquakes continue to dominate, but the Furnace Creek and Death Valley faults also contribute significantly, particularly at return periods less than about 10,000 years (figure 3).

Earthquake Recurrence Models

In the seven probabilistic seismic-hazard analyses, we have generally adopted the position that faults largely follow the "characteristic" earthquake model. In most cases, we have weighted the model about 0.70 compared to a weight of 0.30 assigned to the truncated exponential model. The specific form of the characteristic model we have adopted in our analyses is taken from Youngs and Coppersmith (1985) and we refer the reader to their paper for a more detailed description of their model. In their model, the magnitude range of the characteristic earthquake is $\pm \frac{1}{4}$ magnitude unit and the interval between the

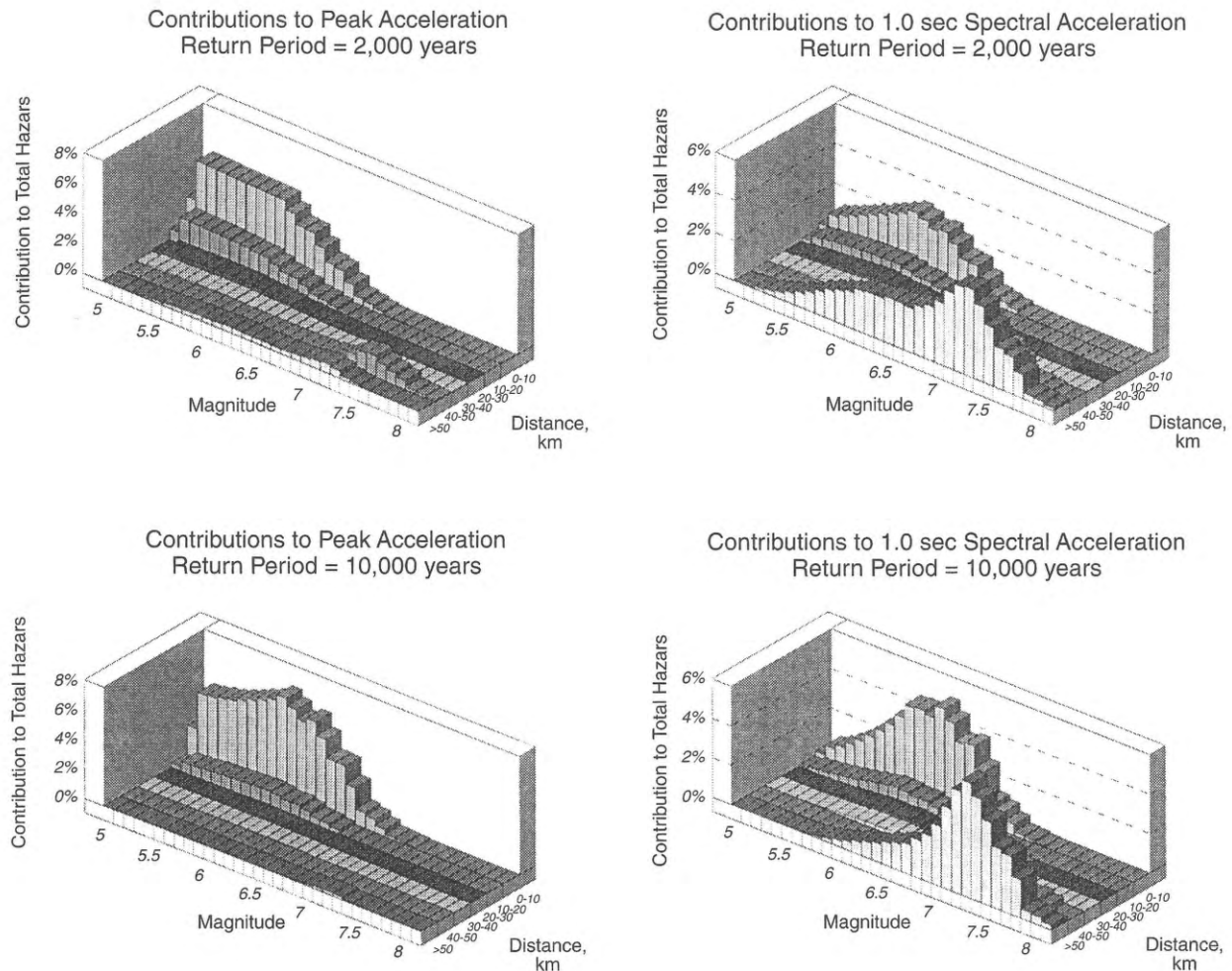


Figure 3. Magnitude and distance contributions to the mean peak horizontal acceleration and 1.0 second spectral acceleration hazard at Yucca Mountain for the return periods of 2,000 and 10,000 years.

minimum characteristic magnitude and the exponential portion of the recurrence curve is about one magnitude unit. As previously mentioned, fewer moderate-sized events in the characteristic model compared to the truncated exponential model can result in lower probabilistic hazard at return periods of most engineering significance. It is thus crucial that sufficient paleoseismic investigations of significant faults be performed to assess their recurrence behavior. The Wasatch fault is possibly the most studied fault in the Basin and Range Province and it clearly exhibits a dominantly characteristic behavior (Schwartz and Coppersmith, 1984; Machette and others, 1992).

Displacement data from paleoseismic studies of the Lost River and Lemhi faults also suggest dominantly characteristic behavior (e.g., Schwartz and Crone, 1985; Olig and others, 1995), however, rupture behavior patterns appear much more complex than the Wasatch fault with some segments exhibiting non-characteristic displacement patterns, non-persistent segment boundaries, and partial

segment ruptures (Crone and others, 1987; Hemphill-Haley and others, 1994; Olig and others, 1995). Incorporating these rupture behavior uncertainties into the probabilistic analyses not only affects recurrence models used but also segmentation models (discussed in the next section).

Earthquake Recurrence Methods

The earthquake recurrence on an individual fault can be expressed in terms of either recurrence intervals or slip rates. Recurrence interval data are not available for most faults in the western U.S. and the use of slip rates is often a "fall-back" approach when faults are poorly understood. Recurrence intervals are used directly to determine the recurrence rates for the maximum earthquakes along a fault. The frequency-magnitude distribution (recurrence curve) of a fault is anchored by the recurrence intervals for the maximum earthquakes and its shape is controlled by the recurrence model(s) assumed

appropriate for that fault. For the slip-rate approach, average net slip rates are first converted to seismic-moment rates (assuming a rupture area and shear modulus), and then events of different sizes are proportioned according to the recurrence models, similar to the recurrence interval approach (see Youngs and Coppersmith, 1985, for further discussion of both methods). Thus, the extra step of converting to moment rates in the slip-rate approach requires introducing a dependence of recurrence rates on fault geometry. This introduced dependence may be undesirable, particularly when fault length and downdip width are poorly constrained or highly variable. It not only somewhat arbitrarily introduces additional uncertainties but can also measurably affect hazard assessments (effects of varying fault length are discussed further in the later section on segmentation). Thus, if adequate recurrence interval data are available, we believe its use is preferable to the slip-rate approach, however, the quality of the available activity rate data should always be a primary consideration in weighting the two approaches. For example, assuming arbitrary displacements per event combined with slip rate to estimate average recurrence values also introduces additional uncertainties and is not necessarily preferable to using slip rates directly.

Another often overlooked aspect of the slip-rate approach is the difficulty and uncertainty of assessing *average* slip rates from typically only a few data points along the fault. Along-strike variations in fault displacement patterns can be significant and often slip-rate data are only available from a few selected sites, typically where the fault is best expressed in the youngest deposits. Whether data from these sites are representative of average rates or are closer to maximum values is difficult to assess. An example of how this could result in overestimating the hazard is illustrated by data on the Pajarito fault in the southern Rio Grande rift, where the average 1.2 million-year slip rate of 0.07 mm/yr (integrated from data at over two dozen sites along strike) is about half the maximum 1.2-million year slip rate of 0.13 mm/yr which was measured near the along-strike midpoint of the fault (Olig and others, 1996a).

Added to the uncertainty in estimating average slip along the fault is uncertainty in determining net slip, often from vertical slip data. The differences, however, are usually not significant for most normal faults in the Basin and Range Province. The dip slip is 10 to 41 percent greater than the vertical slip for typical fault dips (i.e., 45° to 65°). Similarly, lateral slip components are often small (<30 percent) for most faults in the Basin and Range, however, they can be significant in some areas (e.g., Walker Lane) and do need to be explicitly considered.

Both slip rates and recurrence intervals are usually the result of paleoseismic investigations, but recurrence intervals are usually limited to trench investigations whereas slip rates can come from both trench and surficial (such as scarp morphology) studies. Slip rates, similar to recurrence intervals, are best determined for well-defined, complete seismic cycles (see Machette and others, 1992 for further discussion), that is, by dividing displacements per event into recurrence intervals. This type of data are usually only available from trench investigations, whereas

slip rates from surficial studies include unknown open-ended time periods that can bias results. These open-ended periods include (1) the time since the most recent event and (2) the time between the age of the surface that the displacement is measured on and the time of the first event to offset the surface. The length of these open-ended periods can significantly affect slip-rate estimates. An example is provided by the Arco segment of the Lost River fault, where surficial data indicate a slip rate of 0.05 ± 0.01 mm/yr since 100,000 to 130,000 years ago, in contrast to trench data, which reveal that the slip rate for the past three or four *complete* seismic cycles is actually about 0.12 mm/yr (Olig and others, 1995). The difference is a result of the large open-ended time periods (about 20,000 years since the most recent event and about 40,000 to 70,000 years until the first event offsets the alluvial-fan surface). Inclusion of large open-ended periods in long-term slip-rate data from surficial studies may, in part, explain why McCalpin (1995) observed much higher short-term slip rates than long-term rates in his data compilation for the Basin and Range Province and the Rio Grande rift. Although the data may not always be available to assess the effects of including open-ended intervals in slip-rates, one can attempt to estimate uncertainties that may result from such intervals and incorporate them into the source characterization for the hazard assessment.

Finally, and probably most significantly, recurrence rates of surface-rupturing earthquakes on faults can vary significantly through time (e.g., Wallace, 1984; Machette and others, 1992). Temporal clustering of earthquakes results in large variations in recurrence parameters and adequately incorporating these variations is very important to hazard assessments. Detailed paleoseismic investigations indicate temporal clustering of surface-faulting earthquakes on both the Lemhi and Lost River faults (Schwartz, 1989; Hemphill-Haley and others, 1994; Olig and others, 1996b). For example, intervals for the Lost River fault have varied by more than an order of magnitude during the past 100,000 to 200,000 years, ranging from hundreds to a few thousand years during cluster periods, compared to many tens of thousands of years between cluster-periods (Olig and others, 1995; 1996b).

In the probabilistic seismic-hazard analysis for the INEL, we attempted for the first time to incorporate temporal clustering into the recurrence modeling of both the Lost River and Lemhi faults (WCFS and others, 1996). For the Lost River fault, the intercluster recurrence intervals ranged from 10,000 to 50,000 years. The intracluster recurrence intervals were significantly less ranging from a few hundred to 9,000 years. Determining that a fault is in an intracluster interval obviously can significantly raise the probabilistic hazard at a site. Conversely, the hazard can be significantly lower during an intercluster period. To some degree, this modeling of temporal clustering incorporates a real time element.

With regard to using slip rates or recurrence intervals, the approach taken to model faults that exhibit temporal clustering can be important in probabilistic-hazard analysis. For example, in the hazard analysis of the INEL, recurrence for both the Lost River and Lemhi faults were modeled using slip rates and recurrence intervals. Both

approaches resulted in very similar rates for the maximum events on the Lemhi fault, but significantly higher rates for the Lost River fault when using recurrence intervals due to its greater temporal clustering. Because the Lost River fault is the dominant fault contributing to the hazard at the INEL, the hazard is higher when using recurrence intervals and this is true at peak horizontal accelerations as well as at 0.1 and 1.0 sec spectral accelerations (figure 4).

As slip rates are usually measured over longer time periods than recurrence intervals, they may not reflect the most recent paleoseismic behavior of a fault or its short-term variations. Because in performing probabilistic seismic-hazard analysis, the intent is usually to assess the hazard in the near future for engineering applications, a characterization of the most recent behavior of seismic sources is often desired. Unfortunately, detailed slip-rate data to characterize possible short-term variations in activity is lacking for most faults. To address this problem in our southern Rio Grande rift study, we used an approach similar to that described by McCalpin (1995). As previously noted, he found that of the available slip-rate data for faults in the rift (34 vertical slip measurements on seven faults), short-term rates are generally higher than long-term rates, which may be due to both temporal clustering of earthquakes and inherent epistemic uncertainties due to large open-ended time periods in the long-term slip-rate data, as previously discussed.

Regardless of the source of the variations, one can address uncertainties in slip rates when data are lacking for a particular fault by assuming that variations for the fault can be characterized by variability of the local fault population as a whole for a particular tectonic regime. This ergodic substitution of space for time is the same in

principal as that used in defining areal source zones to characterize background earthquakes at a site. To do this, one normalizes the slip rates in the fault population to a common factor that is relevant to the fault of interest such as its long-term slip rate (see McCalpin, 1995 for details on normalizing). In our case (Wong and others, 1995), we normalized Rio Grande rift slip rates to 0.07 mm/yr, the long-term average vertical slip rate of the Pajarito fault. Figure 5 shows a cumulative frequency plot for these normalized rates, which reflects the expected variation or probability distribution in slip rate for the Pajarito fault, assuming it behaves similarly to the overall fault population in the rift. Slip-rate values and associated weights for hazard analysis can be determined directly from this curve, such as the 5th, 50th and 95th percentile values (0.01, 0.07, and 0.77 mm/yr). These values are then assigned probabilities of 0.185, 0.63, and 0.185, as recommended by Keefer and Bodily (1983) for a best three-point approximation of a continuous distribution. McCalpin (1995) also compiled slip-rate data for the Basin and Range Province which can be used to characterize slip-rate distributions for poorly understood faults throughout the region. Surely, it is a big assumption that a particular fault acts similarly to such a generalized distribution but when better data are lacking, this approach at least provides an objective and rational approach to characterizing uncertainties.

Fault Segmentation

Fault segmentation for nearby long faults (greater than about 50 km), such as the Wasatch or Lost River faults, is important to probabilistic hazard because there is often a significant correlation with recurrence. For exam-

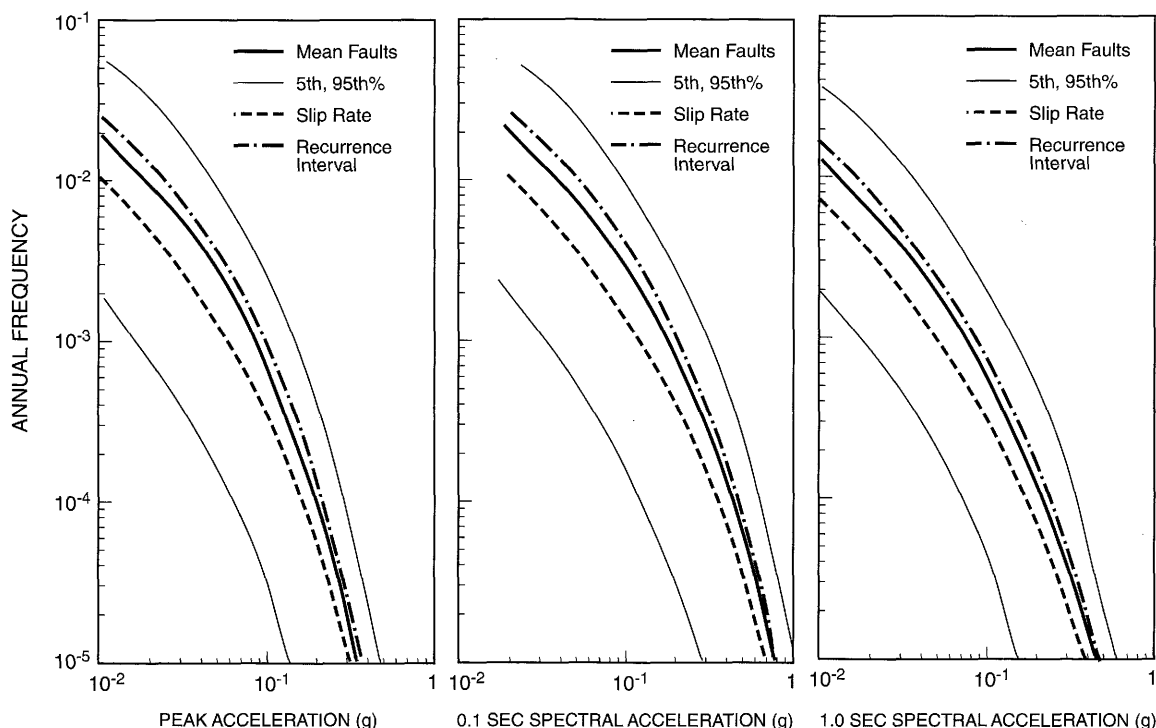


Figure 4. Effect of recurrence calculation method on seismic hazard from fault sources at the INEL.

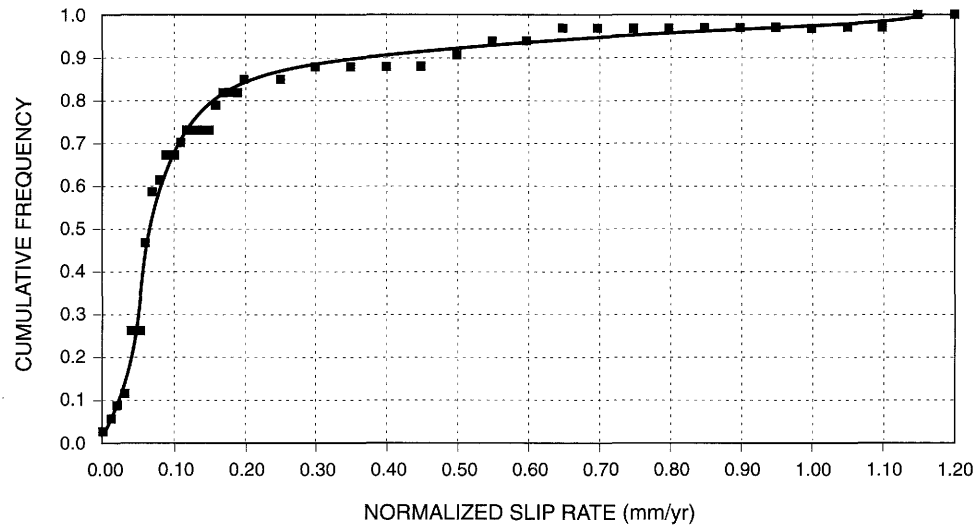


Figure 5. Slip rates normalized to 0.07 mm/yr for faults in the southern Rio Grande rift.

ple, for a site located near a long fault like the Wasatch, if the fault is assumed to be unsegmented and have a uniform along-strike slip rate (fixed seismic-moment rate), use of a single maximum earthquake will result in lower probabilistic hazard than smaller but more frequent maximum events which may characterize the fault if it were segmented. In other words, if the slip rate approach is used, lowering the maximum magnitude of a fault increases the frequency of moderate-sized events, which can result in increased hazard depending on the distance to the fault. This is a surprising consequence to many practitioners, although Youngs and Coppersmith (1985) discussed this observation more than a decade ago.

In the probabilistic analysis of the INEL, we considered both segmented and unsegmented models of the northern Basin and Range faults, weighted 0.70 and 0.30, respectively. The use of an unsegmented model recognizes the uncertainties in our segmentation model and the possibility of multiple segment ruptures. In the unsegmented model, continuous sections of the fault are allowed to rupture unconstrained by segment boundaries. To determine rupture lengths for this model, we calculated average segment lengths (from the segmented models) for each scenario on each fault. We then considered ruptures with this length (22 to 29 km), twice this length (44 to 58 km), and triple this length (66 to 87 km), weighted 0.185, 0.63, and 0.185, respectively. The greater weight for longer, "multiple segment" ruptures in the unsegmented model is primarily to account for uncertainty and the possibility of longer ruptures not accounted for in the segmented model. The segmented model produced the higher probabilistic hazard because it results in the higher estimate of earthquake recurrence (figure 6).

Background Seismicity

As previously discussed, background earthquakes are often the dominant contributor to probabilistic hazard.

Thus the calculation of the recurrence parameters a and b based on the historical seismicity record is crucial in probabilistic seismic-hazard analysis. Unfortunately, the historical record in the Basin and Range Province and many other regions in the western U.S. interior offers some difficult challenges in estimating earthquake recurrence. Because of the shortness of the historical period, it is often the case that the earthquake record contains a small number of events covering a narrow range of magnitudes with too few at the higher magnitudes. Many issues raised during the past few decades can also result in large uncertainties in recurrence parameters. They include for example, the uncertainties in magnitude values (particularly for pre-instrumental events and in converting from different magnitude scales), the issues regarding the definition of a seismotectonically uniform area in which recurrence is to be calculated, the adequacy of current techniques to remove all dependent events whose behavior appears to vary from region to region, and the removal of seismicity associated with faults to avoid double-counting. Finally, the ultimate question always remains, whether the historical record is adequately sampling the long-term behavior of the region.

Almost all of these issues are not only important for assessing the recurrence of background seismicity, but they also play a role in defining the recurrence of earthquakes along faults smaller than the maximum, usually surface-faulting, earthquakes. It is generally assumed that the slope of the recurrence curve for faults is the same as the b -value calculated for the surrounding region based on the historical record. This is the case regardless of the recurrence model (exponential or characteristic) assumed appropriate for the fault. Thus, great care must be taken in calculating the regional earthquake recurrence and the above issues need to be considered when incorporating uncertainties in the recurrence parameters in the probabilistic-hazard analysis. Simply inputting a range of b and a values, which account for the standard errors computed

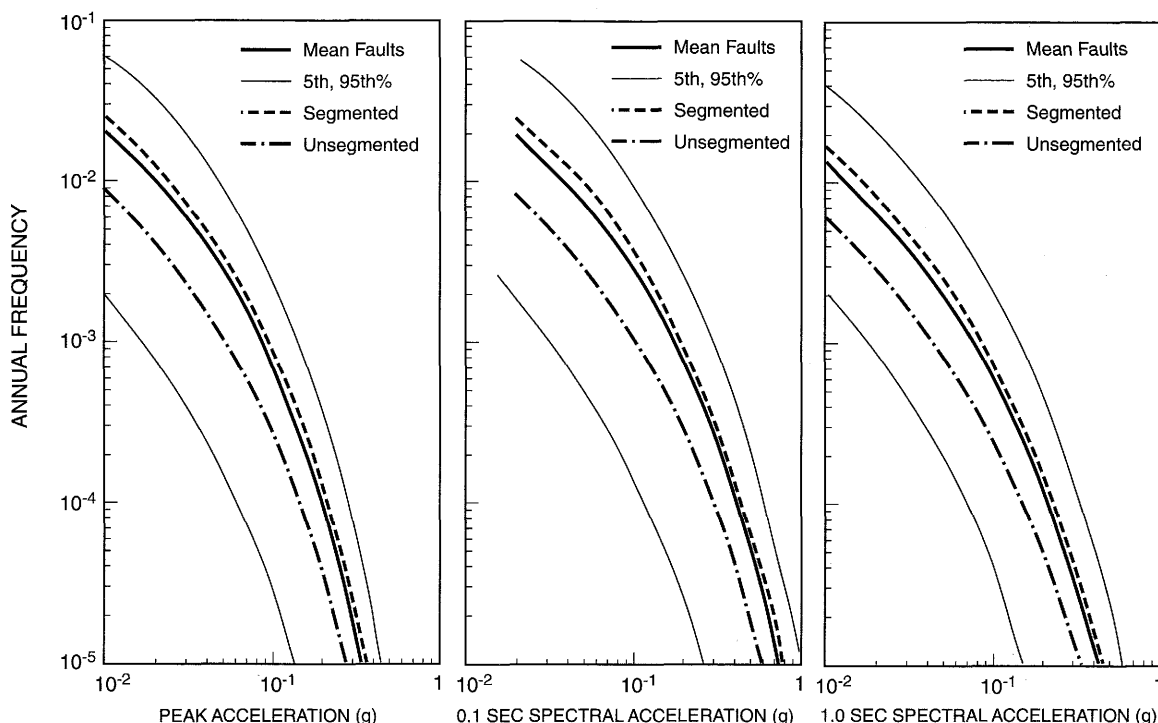


Figure 6. Effect of fault segmentation model on seismic hazard at the INEL.

in the regression analysis, is not adequate and in our opinion, underestimates the true uncertainties in the recurrence parameters. Systematic sensitivity analyses of the historical record by varying catalog parameters can provide a more realistic assessment of the uncertainties in earthquake recurrence and it is these estimated uncertainties that should be input into probabilistic-hazard analyses.

Another important issue is the non-stationarity of background seismicity. It has been the norm in probabilistic analyses to define areal seismic-source zones representing seismotectonic provinces domains. This was the case in each of the seven analyses described herein. In adopting this approach, the background seismicity is assumed to be distributed homogeneously and randomly within each source zone, thus displaying non-stationary behavior. This assumption is at least partially warranted because some areas in the Basin and Range Province have become seismically active after not exhibiting any previous seismicity, albeit over a short historical record. Areal seismic-source zones average or smooth out the seismicity throughout an area making it uniform in terms of its spatial and temporal occurrence. Thus the seismicity rates in areas of high historical seismicity are subdued and rates in low activity areas are enhanced. In general, the use of areal source zones has been effective in modeling seismic hazard for most engineering applications, particularly because information suggesting nonhomogeneous spatial distribution is often not available. Note that statistical techniques are available to test the assumption of homogeneity (e.g., EPRI, 1991).

There are areas of persistent historical seismicity in the Basin and Range Province and thus some background seismicity can be considered stationary. Hence, the de-

gree to which stationarity of background seismicity is incorporated into hazard analysis can be significant. In the recently developed U.S. Geological Survey (USGS) national ground-shaking maps, Frankel and others (1996) smoothed the historical seismicity using a set of Gaussian filters and calculated the hazard from this smoothed seismicity. (An alternative approach is to subdivide the areal source zones until more homogeneous zones are obtained.) This approach largely retains the stationarity of the historical record. The USGS also employs some areal source zones to account for potential nonstationarity of seismicity. In our view, this combination of approaches is the best way to address the uncertainty regarding the stationarity of historical seismicity.

Earthquake Stress Drops

To some degree, the results of the probabilistic analysis of Yucca Mountain cannot be directly compared with the results of the other six analyses described in this paper because of its use of the Spudich and others (1996) relationship. The use of this attenuation relationship can lower the spectral-acceleration hazard by up to 20 percent compared to other relationships which are largely based on California strong-motion data. Lower stress drop earthquakes in extensional regimes compared to compressional regimes have been suggested as the reason for lower ground motions in the former (McGarr, 1984). Analyses of earthquakes in the Basin and Range Province indicate that their stress drops tend to be lower on average, about 50 bars, than stress drops of earthquakes in California (Stark and others, 1992; Becker and Abrahamson, 1997). The average stress drop for California earthquakes

ranges from about 70 to 100 bars (Atkinson, 1995).

In our hazard analyses of the INEL and LANL, we incorporated this observation by using a lower range of stress drops when developing site-specific attenuation relationships. We used a best-estimate stress drop of 75 bars which, in retrospect, is still probably too high. Further research into this issue is important because of its significant impact on hazard, including the further development of attenuation relationships based solely on extensional earthquake strong-motion records.

Crustal Attenuation

Crustal attenuation of strong ground motions ($M \geq 5$) is not well constrained in the Basin and Range Province and other neighboring provinces due to a lack of strong-motion records. This path effect, which can be expressed in terms of the frequency(f)-dependent attenuation parameter $Q(f) = Q_0 f^\eta$, is particularly important at distances greater than 50 kilometers and for long-period ground motions. Studies by several researchers in the Basin and Range Province summarized in Benz and others (1997) indicate that crustal attenuation may be slightly less (higher Q) than in California. For example, Jackson and Boatwright (1987) observed that two free-field recordings of the 1983 M_w 6.8 Borah Peak earthquake are slightly higher in peak horizontal acceleration than what would be predicted by the Joyner and Boore (1981) attenuation relationship at a distance of about 90 kilometers. In adjacent tectonic provinces (e.g., Colorado Plateau), attenuation may be significantly less (Singh and Herrmann, 1983).

Thus, use of California-based empirical attenuation relationships may underestimate the seismic hazard in the western U.S. interior to varying degrees at longer dis-

tances, although this effect may be offset by the higher stress drops of California earthquakes compared to possibly lower stress drops in extensional regimes. We have incorporated region-specific Q_0 and η values from Singh and Herrmann (1983) in the development of site-specific stochastic attenuation relationships for the INEL and LANL and, as previously mentioned, a lower range of stress drops. The sensitivity of probabilistic hazard to Q_0 for the INEL is illustrated in figure 7 and the impact is particularly significant for long-period ground motions. Although large earthquakes have been relatively infrequent in the western U.S. interior in modern times, efforts to increase the number of strong-motion instruments will hopefully yield new data to characterize the attenuation of strong ground motions in this region.

Near-Surface Geologic Effects

Both site and basin response and near-surface rock attenuation (expressed by the parameter kappa) in alluvial basins and volcanic terrains can be important in modifying the levels of ground-shaking hazard. Although strong-motion records and hence, empirical attenuation relationships include, to some degree, soil amplification (and damping), basin effects, and a range of kappa values, these effects at significant levels can only be captured by using the higher fractiles of the relationships. In fact, based on our experience, using multiple empirical relationships results in only small differences between soil and rock sites for peak horizontal acceleration.

The increase in hazard due to soil amplification can be critically important in urbanized alluvial valleys in the Basin and Range Province such as the Salt Lake Valley (e.g., Wong and Silva, 1993) and the Rio Grande Valley in

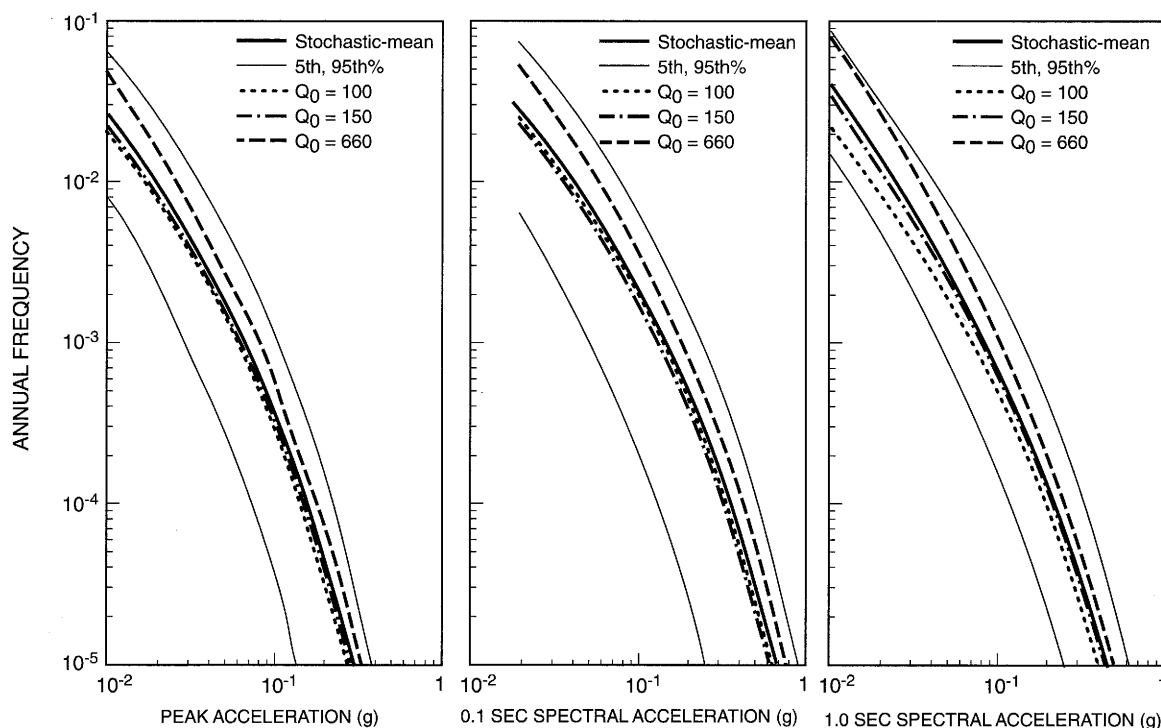


Figure 7. Effect of Q_0 on stochastic-based mean seismic hazard curve at the INEL.

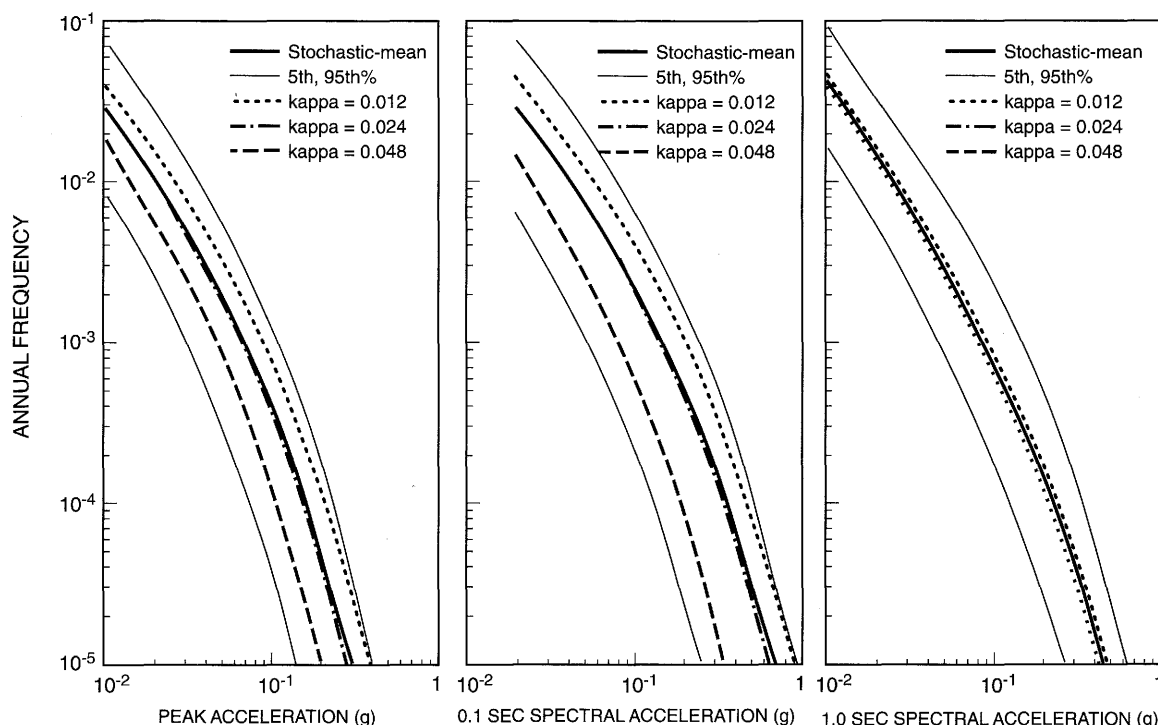


Figure 8. Effect of κ on stochastic-based mean seismic hazard curve at the INEL.

New Mexico. Basin effects, which are most prevalent at long periods (>1.0 sec), can pose significant hazard to tall and long structures.

Volcanic terrains (e.g., INEL and LANL) pose unique site response effects due to their distinctive highly variable velocity profiles as previously described. The effects of varying values of κ are particularly significant for high-frequency ground motions and this is illustrated in figure 8 for the INEL. For important and critical facilities and structures, analyses of site response, basin effects, and site-specific κ s should be performed if such frequency-dependent effects are considered to be important.

FINAL REMARKS

Probabilistic seismic-hazard analysis is well suited for sites in the Basin and Range Province and neighboring extensional tectonic regimes in the western U.S. interior where there can be large uncertainties in seismic-source and ground-motion characterization. Also these regions are characterized by large, infrequent earthquakes which

require engineering and societal decisions based on assessments of seismic risk. In particular, probabilistic analyses will be increasingly used due to the need for urban microzonation, probabilistic loss estimation, and seismic-risk evaluations for all manner of engineered structures including critical facilities.

ACKNOWLEDGMENTS

Our appreciation to many individuals who assisted in the probabilistic seismic-hazard analyses described in this paper including Bob Green, Jackie Bott, Doug Wright, Kevin Coppersmith, and Walt Silva. Our special thanks to Bob Youngs for performing the INEL calculations described in this paper. Thanks also to Sue Penn and Fumiko Goss for assisting in the preparation of this paper and the Professional Development Program of Woodward-Clyde for financial support. We appreciate the critical reviews by Jim Pechmann, Bob Youngs, and Bill Lund which greatly improved the paper.

REFERENCES

- Anderson, J.G., and Hough, S.E., 1984, A model for the shape of the Fourier amplitude spectrum of acceleration at high frequencies: *Bulletin of the Seismological Society of America*, v. 74, p. 1969-1994.
- Atkinson, G.M., 1995, Attenuation and source parameters of earthquakes in the Cascadia region: *Bulletin of the Seismological Society of America*, v. 85, p. 1327-1342.
- Becker, A.M., and Abrahamson, N.A., 1997, Stress drops in normal faulting earthquakes (abs.): *Seismological Research Letters*, v. 68, p. 322.
- Benz, H.M., Frankel, A., and Boore, D.M., 1997, Regional Lg attenuation for the continental United States: *Bulletin of the Seismological Society of America*, v. 87, p. 606-619.
- Black, B.D., Lund, W.R., and Mayes, B.H., 1995, Large earthquakes on the Salt Lake City segment of the Wasatch fault zone--Summary of new information from the South Fork Dry Creek site, Salt Lake County, Utah, in W.R. Lund (editor), *Environmental and engineering geology of the Wasatch Front region*: Utah Geological Association Publication 24, p. 11-30.
- Cornell, C.A., 1968, Engineering seismic risk analysis: *Bulletin of the Seismological Society of America*, v. 58, p. 1583-1606.
- Crone, A.J., Machette, M.N., Bonilla, M.G., Lienkaemper, J.J., Pierce, K.L., Scott, W.E., and Bucknam, R.C., 1987, Surface faulting accompanying the Borah Peak earthquake and segmentation of the Lost River fault, central Idaho: *Bulletin of the Seismological Society of America*, v. 77, p. 739-770.
- EPRI, 1991, Seismic hazard methodology for the central and eastern United States: Report No. NP-4726, v. 4, 367 p.
- Frankel, A., Mueller, C., Barnhard, T., Perkins, D., Leyendecker, E.V., Dickman, N., Hanson, S., and Hopper, M., 1996, National seismic-hazard maps: Documentation June 1996: U.S. Geological Survey Open-File Report 96-532, 68 p.
- Hemphill-Haley, M.A., Sawyer, T.L., Knuepfer, P.L.K., Forman, S.L., and Wong, I.G., 1994, Late Quaternary paleoseismicity and segmentation along the southern Lemhi fault, southeastern Idaho, *Proceedings of the Workshop on Paleoseismology*: U.S. Geological Survey Open-File Report 94-568, p. 81-83.
- Jackson, S.M., and Boatwright, J., 1987, Strong ground motion in the 1983 Borah Peak, Idaho, earthquake and its aftershocks: *Bulletin of the Seismological Society of America*, v. 77, p. 724-738.
- Joyner, W.B., and Boore, D.M., 1981, Peak horizontal acceleration and velocity from strong-motion records including records from the 1979 Imperial Valley, California earthquake: *Bulletin of the Seismological Society of America*, v. 71, p. 2011-2038.
- Keefer, D.I., and Bodily, S.E., 1983, Three-point approximations for continuous random variables: *Management Science*, v. 26, p. 595-609.
- Machette, M.N., Personius, S.F., and Nelson, A.R., 1992, Paleoseismology of the Wasatch fault zone: A summary of recent investigations, conclusions and interpretations, Chapter A, in P.L. Gori and W.W. Hays, editors, *Assessment of regional earthquake hazards and risk along the Wasatch Front area*, Utah: U.S. Geological Survey Professional Paper 1500, p. A1-A71.
- McCalpin, J.P., 1995, Frequency distribution of geologically determined slip rates for normal faults in the western United States: *Bulletin of the Seismological Society of America*, v. 85, p. 1867-1872.
- McGarr, A., 1984, Scaling of ground motion parameters, state of stress, and focal depth: *Journal of Geophysical Research*, v. 89, p. 6969-6979.
- Olig, S.S., Gorton, A.E., Bott, J.D., Knuepfer, P.K.L., Smith, R.P., and Forman, S.L., 1995, Temporal clustering of large earthquakes during the latest Pleistocene on the southern Lost River fault zone, Idaho (abs.): *Geological Society of America Abstracts with Programs*, v. 27, p. A395.
- Olig, S.S., Kelson, K.I., Gardner, J.N., Reneau, S.L., and Hemphill-Haley, M.A., 1996a, The earthquake potential of the Pajarito fault system, New Mexico: *New Mexico Geological Society Guidebook* 47, p. 143-151.
- Olig, S.S., Gorton, A.E., Bott, J.D., Knuepfer, P.L.K., Smith, R.P., Forman, S.L., and Wong, I.G., 1996b, Implications for seismic hazards at the Idaho National Engineering Laboratory from paleoseismic studies along the southern Lost River fault zone, in *Fifth DOE National Phenomena Hazards Mitigation Conference Proceedings*, p. 221-230.
- Schwartz, D.P., 1989, Paleoseismicity, persistence of segments, and temporal clustering of large earthquakes-examples from the San Andreas, Wasatch, and Lost River fault zones in D.P. Schwartz and R.H. Sibson, editors, *Proceedings of Conference XLV on fault segmentation and controls of rupture initiation and termination*: U.S. Geological Survey Open-File Report 89-315, p. 361-375.
- Schwartz, D.P., and Coppersmith, K.J., 1984, Fault behavior and characteristic earthquakes: Examples from the Wasatch and San Andreas fault zones: *Journal of Geophysical Research*, v. 89, p. 5681-5698.
- Schwartz, D.P., and Crone, A.J., 1985, The 1983 Borah Peak earthquake: A calibration event for quantifying earthquake recurrence and fault behavior on Great Basin normal faults, in R.S. Stein and R.C. Bucknam, editors, *Proceedings of Workshop XXVIII, on the Borah Peak, Idaho, Earthquake*: U.S. Geological Survey Open-File Report 85-290, p. 153-160.
- Silva, W., 1992, Factors controlling strong ground motion and their associated uncertainties, in Q.A. Hossain, editor, *Dynamic analysis and design considerations for high-level nuclear waste repositories*: American Society of Civil Engineers, p. 132-161.
- Silva, W.J., and Darragh, R.B., 1995, Engineering characterization of strong ground motion recorded at rock sites: Electric Power Research Institute, EPRI TR-102262, 415 p.
- Singh, S., and Herrmann, R.B., 1983, Regionalization of crustal coda Q in the continental U.S.: *Journal of Geophysical Research*, v. 88, p. 527-538.
- Spudich, P., Fletcher, J.B., Hellweg, M., Boatwright, J., Sullivan, C., Joyner, W.B., Hanks, T.C., Boore, D.M., McGarr, A., Baker, L.M., and Lindh, A.G., 1996, Earthquake ground motions in extensional tectonic regimes: U.S. Geological Survey Open-File Report 96-292, 351 p.
- Stark, C.L., Silva, W.J., Wong, I.G., and Jackson, S.M., 1992, Assessment of stress drops of normal faulting earthquakes in the Basin and Range Province (abs.): *Seismological Research Letters*, v. 63, p. 39.
- Wallace, R.E., 1984, Fault scarps formed during the earthquakes of October 2, 1915, Pleasant Valley, Nevada and some tectonic implications: U.S. Geological Survey Professional Paper, 1274-A, 33 p.

- Wong, I.G., Bott, J.D., Ake, J., and Unruh, J.R., 1996a, Earthquake hazard in central Colorado (abs.): Geological Society of America Abstracts with Programs, v. 28, p. A-283.
- Wong, I.G., Green, R.K., Sawyer, T.L., and Wright, D.H., 1994, Probabilistic seismic hazard analysis, Mormon Island Auxiliary Dam: Unpublished final report prepared for the U.S. Bureau of Reclamation by Woodward-Clyde Federal Services, 41 p.
- Wong, I., Kelson, K., Olig, S., Bott, J., Green, R., Kolbe, T., Hemphill-Haley, M., Gardner, J., Reneau, S., and Silva, W., 1996b, Earthquake potential and ground shaking hazard at the Los Alamos National Laboratory, in F. Goff, B. Kues, M.A. Rogers, L.D. McFadden, and J. Gardner, editors, The Jemez Mountains Region: New Mexico Geological Society Guidebook 47, p. 143-151.
- Wong, I.G., Olig, S.S., and Bott, J.D.J., 1996c, Earthquake potential and seismic hazards in the Paradox Basin, southeastern Utah, in A.C. Huffman, Jr., W.R. Lund, and L.H. Godwin, editors, Geology and resources of the Paradox Basin: Utah Geological Association Guidebook 25, p. 241-250.
- Wong, I.G., Olig, S.S., and Bott, J.D.J., 1997c, Characterizing active faults for seismic hazards: What's important, what's not, what's next (abs.): Geological Society of America Abstracts With Programs, v. 29, p. A-71.
- Wong, I., Olig, S., Green, R., Moriawaki, Y., Abrahamson, N., Baures, D., Silva, W., Somerville, P., Davidson, D., Pilz, J., and Dunne, B., 1995, Seismic hazard evaluation of the Magna tailings impoundment, in W.R. Lund, editor, Environmental and engineering geology of the Wasatch Front region: Utah Geological Association Publication 24, p. 95-110.
- Wong, I.G., Pezzopane, S.K., Abrahamson, N.A., Green, R.K., Sun, J.I., and Quittmeyer, R.C., 1997a, A preliminary assessment of earthquake ground shaking hazard at Yucca Mountain, Nevada, and implications to the Las Vegas region, in Seismic Hazards in the Las Vegas Conference Proceedings: Nevada Bureau of Mines and Geology (in press).
- Wong, I.G., Olig, S.S., Hassinger, B.W., and Blubaugh, R.E., 1997b, Earthquake hazards in the Intermountain U.S.: Issues relevant to uranium mill tailings disposal: Tailings and Mine Waste '97, A.A. Balkema Publishers, p. 203-212.
- Wong, I.G., and Silva, W.J., 1993, Site-specific strong ground motion estimates for the Salt Lake Valley, Utah: Utah Geological Survey Miscellaneous Publication 93-9, 34 p.
- Woodward-Clyde Federal Services, Geomatrix Consultants, and Pacific Engineering & Analysis, 1996, Site-specific probabilistic seismic hazard analyses for the Idaho National Engineering Laboratory: Unpublished final report prepared for Lockheed Martin Idaho Technologies, INEL-95/0536.
- Youngs, R.R., and Coppersmith, K.J., 1985, Implications of fault slip rates and earthquake recurrence models to probabilistic seismic hazard estimates: Bulletin of the Seismological Society of America, v. 75, p. 939-964.

POTENTIAL FOR TECTONICALLY INDUCED TILTING AND FLOODING BY THE GREAT SALT LAKE, UTAH, FROM LARGE EARTHQUAKES ON THE WASATCH FAULT

Wu-Lung Chang and Robert B. Smith
Department of Geology and Geophysics
University of Utah, Salt Lake City, UT, 84112

ABSTRACT

Flooding from the Great Salt Lake due to ground tilt accompanying large earthquakes on the Wasatch fault is shown to be an unusual and largely unrecognized hazard for the Wasatch Front, Utah, including parts of Salt Lake City, Salt Lake County, and Davis County. Following a large normal-faulting earthquake on the Wasatch fault, lake water could flow into hanging-wall subsidence troughs depending on pre-existing topography, location, size, and geometry of the fault, and the lake level. In this study, we investigated the earthquake-induced flooding problem by subtracting earthquake induced topography changes from ground elevations to determine the deformed topography and new lake shoreline locations and therefore potential for flooding and shoreline migration of the nearby Great Salt Lake. We first developed a high-resolution digital topographic data set from orthophoto maps with a horizontal interval of 500 feet and a vertical interval of 2 feet. Two methods were used to simulate ground deformation accompanying plausible earthquake scenarios for the Wasatch fault: 1) applying a three-dimensional boundary element modeling method with normal-fault earthquake scaling relationships between magnitude and fault parameters (length and displacement), and 2) by using the observed hanging-wall deformation accompanying the largest historic earthquake in the Intermountain seismic belt, the 1959 (M_s 7.5) Hebgen Lake, Montana, earthquake as an empirical model. Because of the proximity of the Wasatch fault to the Great Salt Lake, we demonstrate that earthquake induced ground tilt could displace the lake shoreline southward up to 3.5 miles (5.6 kilometers) into areas around Salt Lake City not now covered by the lake, and in turn produce flooding of places occupied by transportation corridors, commercial developments, etc. We stress that the tectonically induced flood hazard for the Wasatch Front requires much more information for site-specific analyses, including development of a higher resolution topographic data and more refined earthquake scenarios. This information is important for engineering analyses, emergency response preparation, and as a guide to long-term land use.

INTRODUCTION

Tectonically induced flooding and ground tilt associated with large normal-faulting earthquakes is an important and unappreciated hazard for parts of the Wasatch fault zone, Utah. The area potentially affected by such a hazard contains parts of Utah's growing population centers, including commercial zones and transportation corridors.

Motivation for this study came from observations of significant hanging-wall deformation accompanying large basin and range-style normal-faulting earthquakes (figure 1): (1) the M_s 7.1 1954 Dixie Valley earthquake, Nevada (Savage and Hastie, 1969); (2) the M_s 7.5 1959 Hebgen Lake earthquake, Montana (Myers and Hamilton, 1964; Barrientos and others, 1987); and (3) the M_s 7.3 1983 Borah Peak earthquake, Idaho (Barrientos and others, 1987). These events provide a working model for large, normal-faulting earthquakes for the Wasatch Front that are hypothesized to occur on planar faults that dip from $\sim 45^\circ$ to 60° and nucleate at mid-crustal depths of ~ 15 to 20 kilometers near the brittle-ductile transition (Smith and Bruhn, 1984; Smith and Arabasz, 1991).

Figure 1 shows the theoretical ground response produced by a large normal-faulting earthquakes (King and others, 1988). The model reveals an asymmetric pattern of greater hanging-wall subsidence than footwall uplift, an

important consideration along the Wasatch Front where the southeast part of the Great Salt Lake is in the hanging wall of the Wasatch fault. We assumed that scenario earthquakes can be applied to the Wasatch fault using models from the above historical normal-faulting ruptures in the Basin and Range Province.

Although the Wasatch fault has not experienced a scarp-forming earthquake in historic time, paleoearthquake studies reveal that several large events, magnitude 6.8 to 7.3, have occurred in the past 6,000 years (McCalpin and Nishenko, 1996). This of course implies the potential for future earthquakes of similar size. The flooding hazard of such large events is based on the premise that the nearby flat shoreline topography of the Great Salt Lake can be altered by tilting due to hanging-wall subsidence. This will cause faultward migration of the shoreline, allowing water from the lake to inundate adjacent lands.

The tectonically induced flooding hazard of the Wasatch Front was first recognized by Smith and Richins (1984). They estimated potential flooding areas by subtracting observed crustal deformation of the M_s 7.5 Hebgen Lake earthquake from ground elevations in the Great Salt Lake and Utah Lake areas. However their study, as well as the follow-up analysis by Keaton (1987) using a dislocation method to model the faulting, demonstrated that existing topographic data from U. S. Geological Survey (USGS) topography maps were not of sufficient reso-

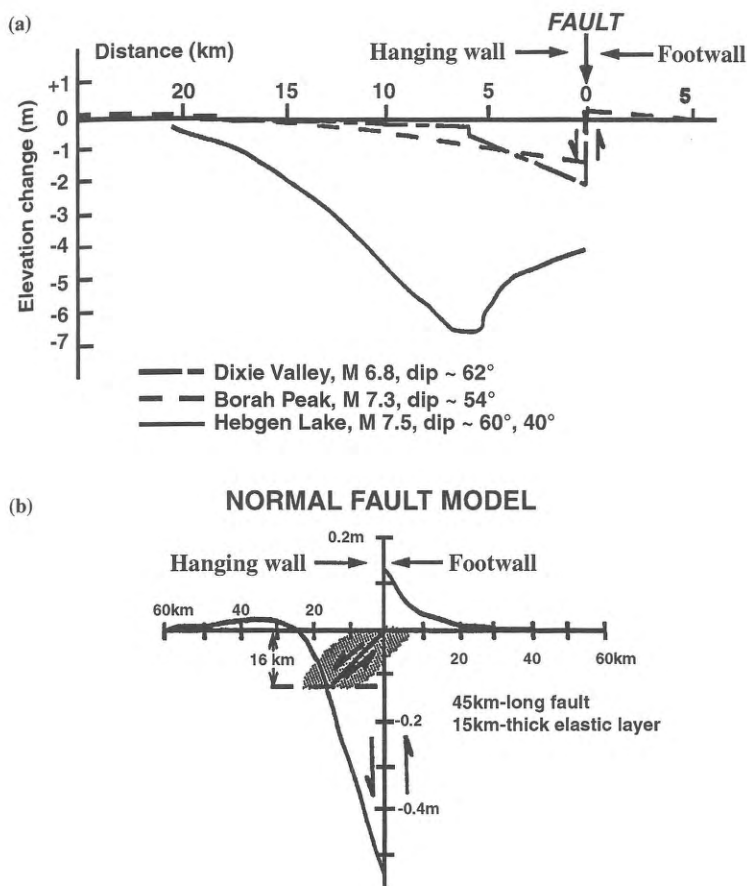


Figure 1. (a) Coseismic and postseismic deformation accompanying large normal-faulting earthquakes of the Basin and Range, including the $M_S = 7.1$, 1954 Dixie Valley, Nevada; the $M_S = 7.5$, 1959 Hebgen Lake, Montana; and the $M_S = 7.3$, 1983 Borah Peak, Idaho earthquakes (from Smith and Arabasz, 1991); and (b) theoretical surface deformation profile by 1 meter of normal displacement distributed from 0 to 16 kilometers, on a 45 degree dipping normal fault (from King and others, 1988).

lution and accuracy for detailed assessments. Furthermore, analytic modeling methods were not as flexible or refined as those now provided by the boundary-element methods (Okada, 1992; Simpson and Reasenberg, 1994) and a detailed paleoearthquake history for the Wasatch fault had not yet been worked out to better assess the large earthquake potential for the Wasatch fault.

Objectives for this study were to develop a numerical method to calculate the hanging-wall deformation accompanying geologically plausible earthquakes and to acquire the most accurate topographic data for meaningful analyses of the flooding hazard. Scenario earthquakes were hypothesized that reflect the seismic potential for the Wasatch fault. For example, we used magnitudes and extent of faulting commensurate with our knowledge of Basin and Range seismotectonics to characterize the Wasatch fault (Smith and Arabasz, 1991). Further, we employed scenario earthquakes from the maximum historic event in the Intermountain region, at locations on the Wasatch fault that best fit mapped fault lengths, fault alignments, and the late Quaternary earthquake history (see McCalpin and Nishenko, 1996 for a summary of Wasatch fault paleoseismicity information).

Our analysis shows that tectonically induced flooding is a noteworthy earthquake hazard for population centers that are adjacent both to large bodies of water and faults that are capable of producing hanging-wall subsidence accompanying large, normal-faulting earthquakes. This study also examined the effect of earthquake-induced ground tilt on gravity-fed sewer and water lines to determine if hanging-wall deformation could affect flow performance.

We note a limitation of our analyses for the Wasatch fault: while one of the best studied in the U.S., there is little data on the geometry and depth extent of the fault beneath the alluvial filled valleys of the Wasatch Front. This restricted our simulations to those typified by the large historic Basin and Range earthquakes.

Data And Methodology

For the purpose of this study, we developed topographic data at the highest resolution available to represent ground elevations. An elastic, three-dimensional boundary element model (Okada, 1992; Simpson and Reasenberg, 1994) was used to simulate surface deformation associated with scarp-forming scenario earthquakes on the Weber and the Salt Lake City segments of the Wasatch fault (Hecker, 1993; Mason, 1996). We also used observed hanging-wall ground deformation accompanying the largest normal-faulting earthquake in the Intermountain region, the 1959 M_S 7.5 Hebgen Lake, Montana earthquake (Myers and Hamilton, 1964), as an empirical example that we consider a reasonable maximum earthquake for the Wasatch fault.

Figure 2 shows our study area for the central Wasatch Front, Utah. It extends about 37 miles (60 kilometers) north-south, and 18 miles (30 kilometers) east-west, from Bountiful to the southern end of Salt Lake City, and including the southern Weber and the northern Salt Lake City segments of the Wasatch fault. See Machette and others (1992) for a definition of segment boundaries used in this study.

TOPOGRAPHIC DATA

Our study used orthophoto quadrangle contour maps that were produced for Salt Lake and Davis County authorities primarily for flood-management purposes. The accuracy of these maps is estimated to be ± 20 feet (± 6.1 meters) horizontal, and ± 2 feet (± 0.6 meters) vertical. We digitized 210 of these maps covering the study area that were obtained from the Davis County Surveyors Office, the Salt Lake City Corporation Engineering Department, and the Salt Lake County Flooding Control Office. The horizontal digitization interval was 500 feet (152.4 meters) with elevations of the digitized points forming a three-dimensional data base.

Because different datums and projections were used in the original orthophoto maps, for example, NAD-27 for Davis County (Northern Utah Zone) and NAD-83 for Salt

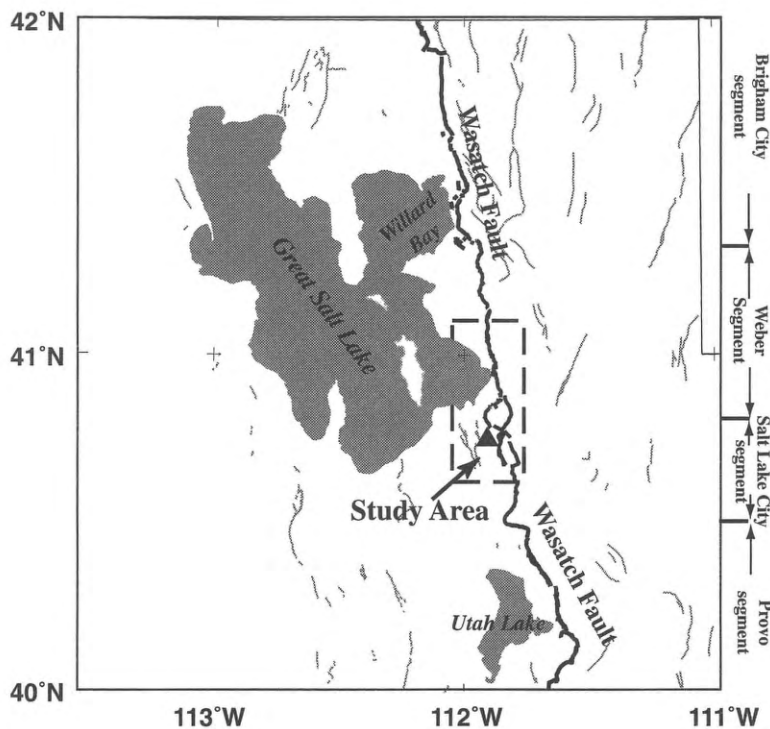


Figure 2. Map shows the study area (black dashed block) in northern Utah, including the Weber and Salt Lake City segments of the Wasatch fault (bold black lines). Light gray lines represent other late-Quaternary faults and the triangle is the location of Salt Lake City.

Lake City and County (Central Utah Zone), we employed the USGS program "TRALANE" to transform data coordinates into latitude, longitude, and elevation. A minimum curvature method (Webring, 1981) was then used to interpolate the data points into high-resolution topographic grids for the study area.

Figure 3a shows the location of our newly compiled topographic data, where "+" symbols in the polygon are the digitized points from orthophoto maps. The irregular outline of the polygon is the result of our decision to include only possible flooding regions with elevations lower than 4,240 feet (1,292.3 meters) and higher than the minimum elevation contour of the orthophoto maps (4,200 feet, or 1,280 meters). Areas outside the polygon are not included in our calculations. Figure 3b shows the location of the topographic data polygon with some important features or landmarks such as highways (I-15, I-80 and I-215), the Salt Lake City International Airport, and the mapped exposures of the Wasatch fault.

Methodology

Figure 4 illustrates how the numerical modeling method was used to calculate hanging-wall subsidence accompanying a typical normal-faulting earthquake. Figure 4b and 4c show respectively the horizontal and vertical components of the theoretically calculated ground displacements. The hanging wall in this example has dropped while the footwall has risen by a smaller amount.

Areas of potential flooding can then be estimated by subtracting the calculated vertical displacement from the undeformed topographic data. For the Salt Lake Valley normal-faulting scenario, the Great Salt Lake shoreline migrates toward the fault, allowing the lake to flood into depressed areas where the original shoreline is dropped below its undeformed dammed level.

Figure 5 shows how the hanging wall, such as for the northern Salt Lake Valley, could subside during a normal-faulting earthquake (figure 5a) with the amount of deformation depending on the distance from fault (figure 5b), fault displacement, and fault dip angle. Figure 5c illustrates locations with post-event elevations lower than the original height of the Great Salt Lake that could be flooded if the original shoreline is lowered. We caution that the amount of the ground subsidence would be only a few inches to a maximum of 1 or 2 feet (0.3 to 0.6 meters) in the deformed basin, and that man-made features could impede or enhance flooding.

Figure 5 reveals that lake elevation is a critical factor in assessing hazard scenarios. Because it varies annually and with long-term climate variations, we considered its extreme and average historic levels. Figure 6 shows the fluctuations of the Great Salt Lake measured at its south end since 1845 (Currey and others, 1983; Arnow and Stephens, 1990). In historic time, the maximum difference was as large as 20 feet (6.1 meters).

The elevations ranged from the lowest value of 4,192 feet (1,278 meters) in 1965 to its highest level of 4,212 feet (1,284 meters) in 1985, both notably within the past 20 years. In 1997, the lake level was near its long-term average of 4,200 feet (1,280 meters). The maximum (4,212 feet), long-term average (4,200 feet), and minimum (4,192 feet) height of lake water were used in the following analyses.

SCENARIO EARTHQUAKE MODELING

Scaling From Late Quaternary Paleoseismic Data

We developed deformation models from plausible earthquake scenarios based on paleoseismological data and postulated geometry of the Wasatch fault (Schwartz and Coppersmith, 1984; Smith and Arabasz, 1991; Machette and others, 1992; Mason, 1996; McCalpin and Nishenko, 1996). For example, prehistoric fault histories and displacements taken from a trench on the Salt Lake City segment of the Wasatch fault at the mouth of Little Cottonwood Canyon, about 12 miles (19.3 kilometers) southeast of Salt Lake City, revealed a 13 foot (4 meter) tectonic displacement for two scarp-forming earthquakes (Swan and others, 1981). Moreover, studies of Basin and Range normal-faulting earthquakes by Smith and Bruhn (1984) suggested that the fault dip angle ranges from 40° to 60° based on seismic modeling and other geophysical data. On the basis of these data, we postulated a normal-

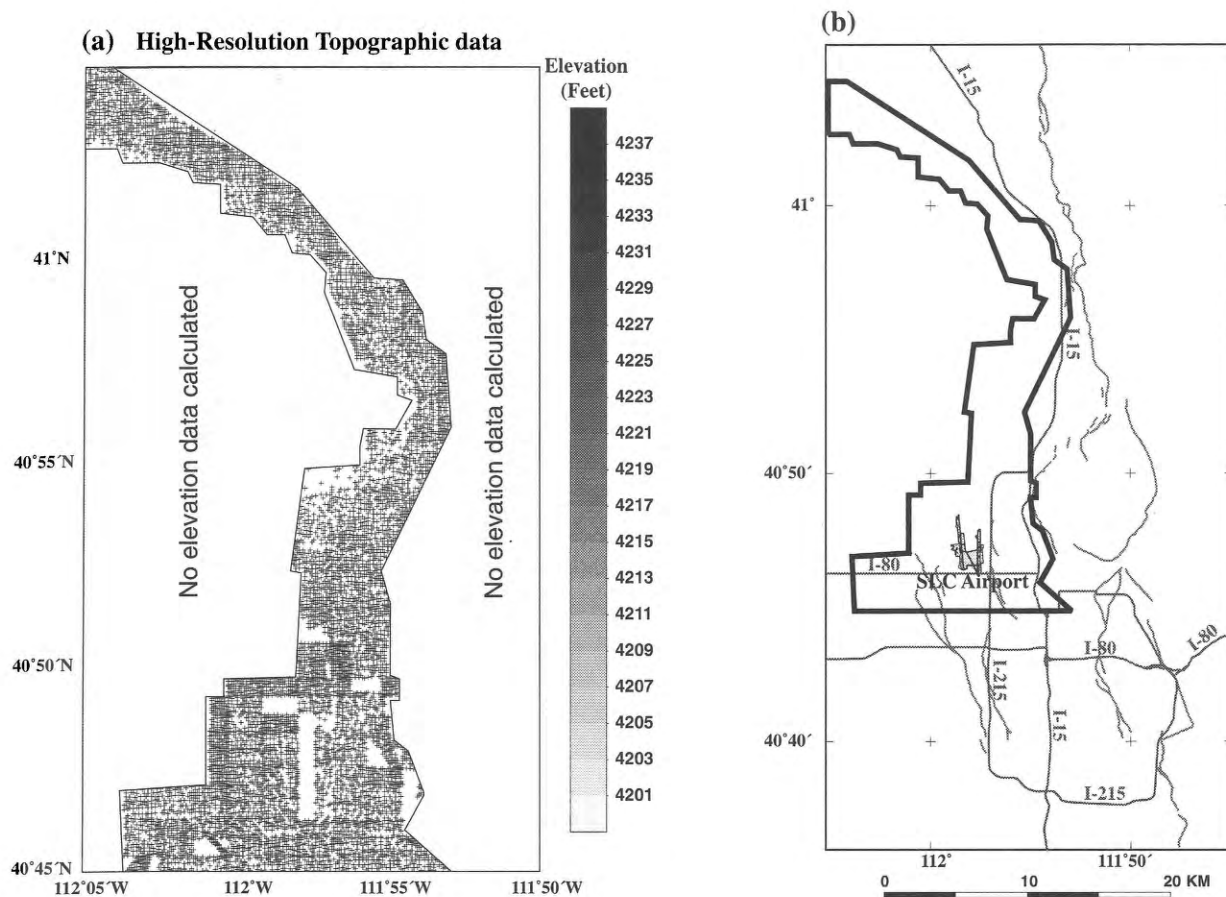


Figure 3. (a) Area of digital topographic data. Small crosses in the white polygon show data points that were digitized from photomaps. (b) Location of data polygon (bold black bounded, same as the white one at (a) in the study area. Also shown are late Quaternary faults (gray lines), main roads, airport, etc.

faulting earthquake scenario with 6.5 feet (2 meters) of displacement, a 45°W dip, and 28 miles (45 kilometers) of rupture length (corresponding to magnitude 7.0) for the Salt Lake City segment.

The inundation resulting from this scenario earthquake is shown in figure 7. The thick black lines represent the scenario fault segment and gray lines show surface traces of mapped Quaternary faults. Shaded patterns show areas potentially inundated by water at the three different lake elevations. Because of the close proximity of the Great Salt Lake to the modeled fault, at a lake elevation of 4,212 feet, water could flood approximately 1 mile (1.6 kilometers) southward and 2 miles (3.2 kilometers) westward into areas near highway I-215 and part of the Salt Lake City International Airport.

Another scenario earthquake model was developed for the Weber segment of the Wasatch fault (figure 2). This part of the fault has experienced a net vertical tectonic displacement of 5.9 feet (1.8 meters) in the past 600-800 years according to paleoearthquake data from a trench site (Swan and others, 1980; McCalpin and others, 1994) near Kaysville, Utah (figure 7b). Therefore a 5.9-foot (1.8-meter) displacement on a 45°W dipping fault plane with a rupture length of 35.4 miles (57 kilometers) was

assumed as the scenario earthquake rupture (magnitude 7.1). Figure 7b shows plausible inundation produced by this model. Due to the relatively steeper topographic gradient east of the lake shore in Davis County, the 4,212-foot (1,284-meter) contour line shifts less than 1,000 feet (305 meters) toward the fault (eastward). The 4,200-foot (1,280-meter) shoreline, on the other hand, is shifted to the southeast about 1 mile (1.6 kilometers).

Scaled Earthquake Modeling

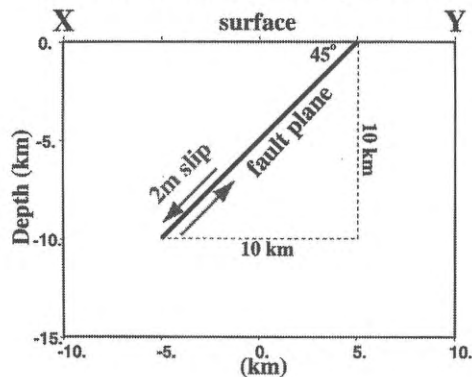
Mason (1996) developed an updated, worldwide set of historical, normal-faulting earthquakes to scale surface-faulting parameters to magnitude. He applied linear least-squares regressions between surface-wave magnitude (M_s) and maximum surface displacement, D_{\max} , as well as the product of D_{\max} and surface rupture length (L), $D_{\max}L$ as follows:

$$M_s = 0.74 \log(D_{\max}) + 6.81 \quad (1)$$

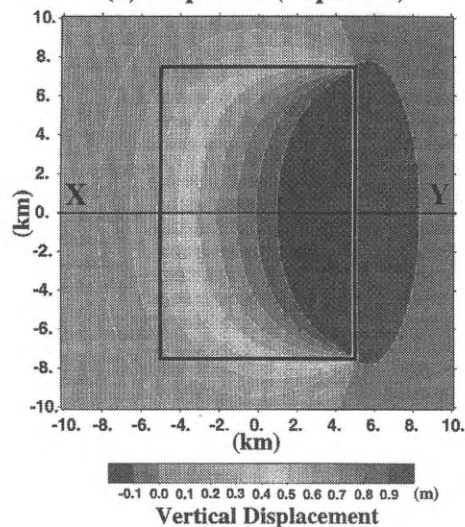
$$M_s = 0.55 \log(D_{\max}L) + 5.95 \quad (2)$$

Using these relations on the Salt Lake City segment would produce a $M_s = 7.0$ scenario earthquake, with 28 miles (45 kilometers) of surface rupture and a maximum

(a) Normal-Faulting Earthquake Model



(b) Map View (Depth = 0)



(c) Vertical Cross Section

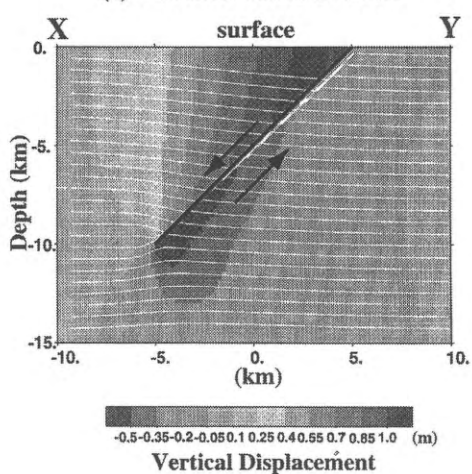
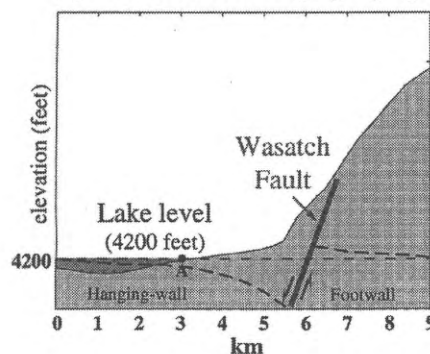
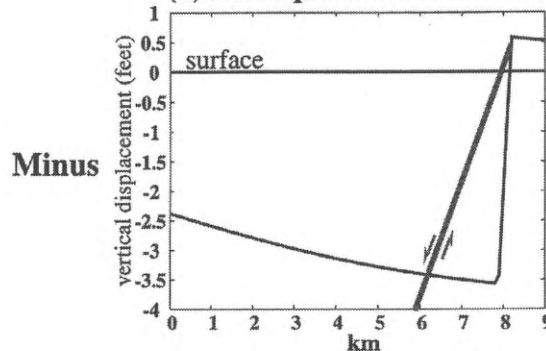


Figure 4. Example of the three-dimensional fault model used in this study; (a) cross section of a normal-faulting earthquake with 2 meter slip, (b) map view of the vertical displacement field on the surface, and (c) displacement cross section. Bold black lines represent projection of the fault plane boundary and white lines show contours of ground subsidences.

(a) Undeformed Topography



(b) Earthquake Deformation



(c) Deformed Topography

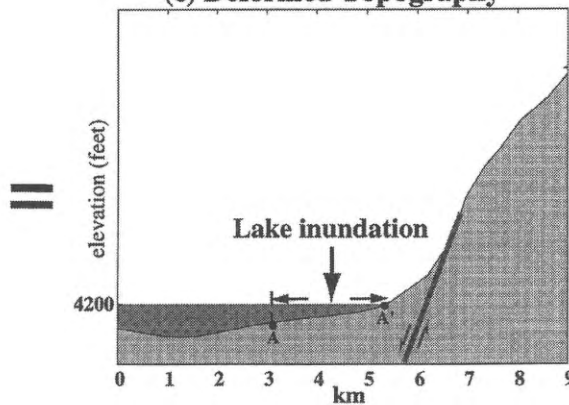


Figure 5. Example showing tectonically induced lake inundation by a normal faulting earthquake. Deformed topography is obtained by subtracting undeformed elevation (a) from the co-seismic vertical displacement (b). Following the earthquake, areas with elevations lower than the lake level (4200 feet in this figure) can be flooded by lake water, and the shoreline at point A moves toward the fault, A', (c). Dashed lines show the shape of the hanging-wall and foot-wall deformation pattern.

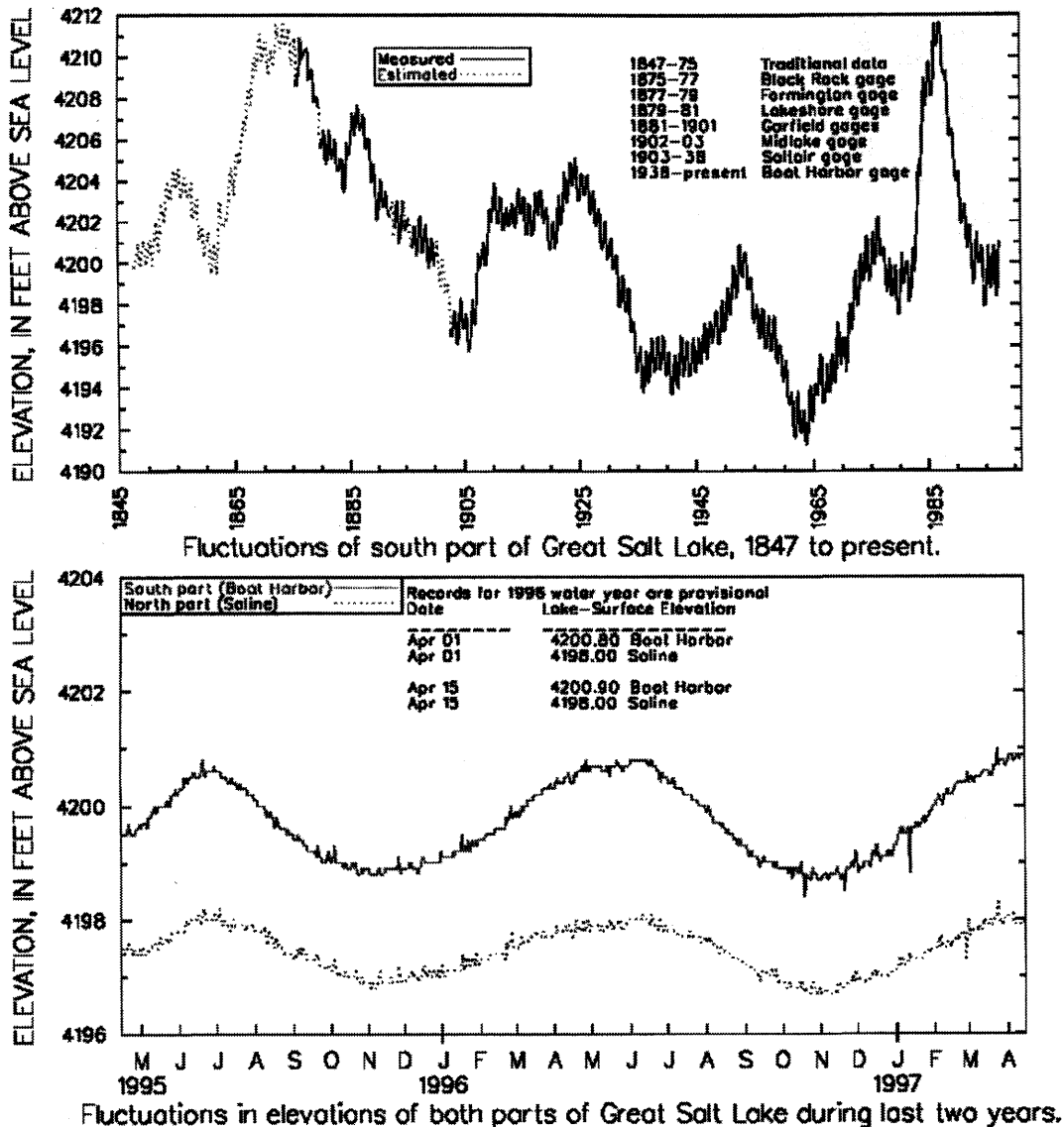


Figure 6. Fluctuations of Great Salt Lake levels, 1845-1997. The highest (4212 feet), average (and approximately the current, 4200 feet) and the lowest (4192 feet) level have been used as three scenarios in the modeling (data from Currey and others (1983) and U.S. Geological Survey web page: <http://www.dutslc.wr.usgs.gov/gsl.gif>)

surface displacement of 5.9 feet (1.8 meters). These parameters are similar to those from paleoearthquake data for the Salt Lake City segment, discussed above. However, for the 35.4-mile (57-kilometer)-long Weber segment, a corresponding D_{\max} of 11.8 feet (3.6 meters), $M_s = 7.2$ are significantly larger than the 5.9-foot (1.8-meter) fault slip inferred by paleoearthquakes. Hence, for the Weber segment, the scaled earthquake models would produce a larger area of hanging-wall subsidence and potential flooding compared with paleoearthquake models.

Multiple segment rupture scenarios were also considered in this study. For example, Mason (1996) noted several multiple-segment rupture scenarios, i.e., rupture on one or more contiguous segments in a single event. These included the two largest historic earthquakes of the Inter-

mountain region, the 1959 M_s 7.5 Hebgen Lake (Myers and Hamilton, 1964) and the 1983 M_s 7.3 Borah Peak earthquakes (Richins and others, 1987), that had surface offsets on two or more fault segments. Jackson and others (1995) also proposed multiple segment ruptures for earthquakes on the San Andreas fault, California, and that a cascade or multi-segment model was more appropriate to estimate earthquake recurrence rate for equivalent characteristic earthquakes. Further, fault-stress interaction studies of paleoearthquakes also suggests that the Wasatch fault can rupture in multiple segments (Chang and Smith, 1996).

Our first scenario is for a multi-segment rupture along most of the Salt Lake City segment (25 miles, 40 kilometers) and the southern part of the Weber segment (10.6

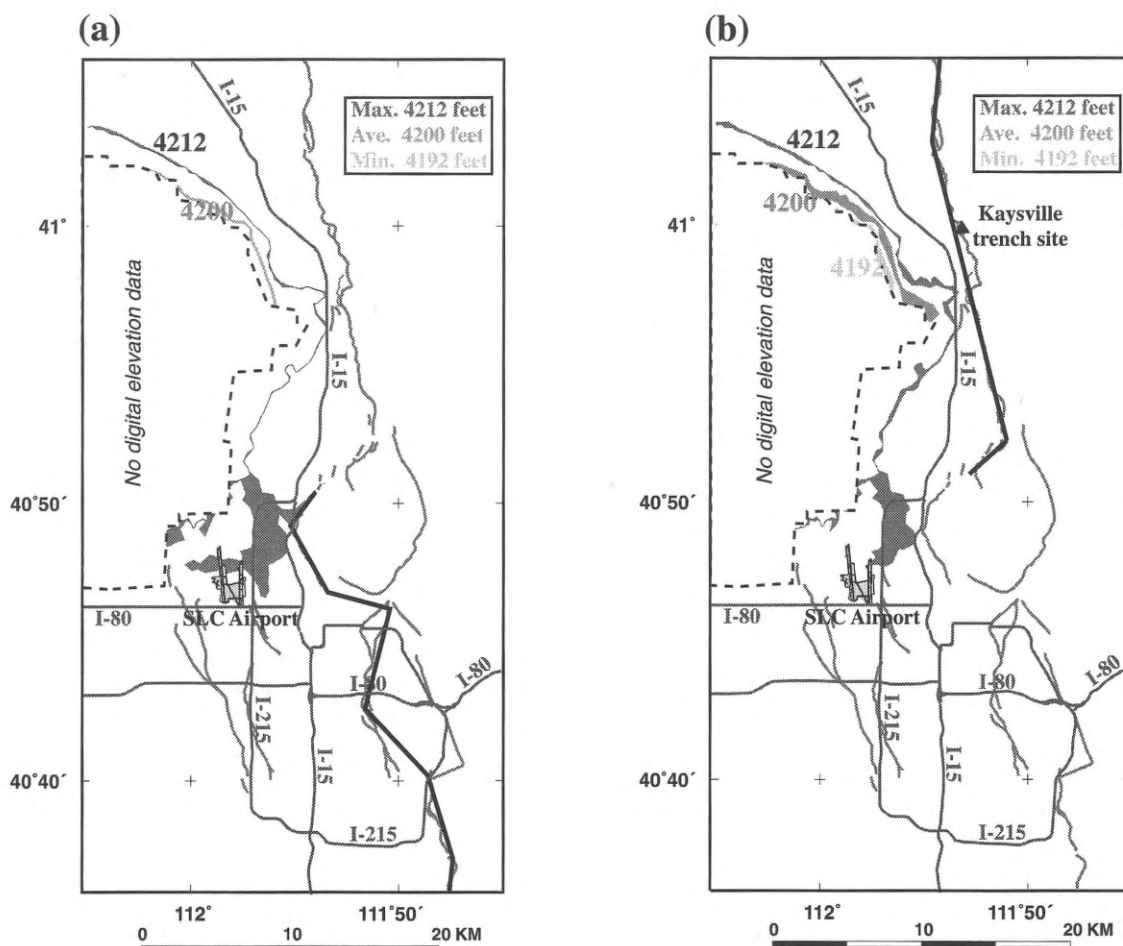


Figure 7. Paleoearthquake scenario modeling: (a) 2 meter slip on the Salt Lake City segment, and (b) 1.8 meter slip on the Weber segment. Gray shading represents potential inundation areas corresponding to selected lake elevations (4192, 4200, and 4212-foot). Bold black lines show surface traces of fault-segment model, and gray lines represent late Quaternary faults. Notice that the digital elevation data are not available inside the dash-line polygon.

miles, 17 kilometers). This corresponds to an event of $M_s = 7.2$ and $D_{max} = 11.8$ feet (3.6 meters) according to equations (1) and (2). Assuming a $45^\circ W$ dipping fault plane, figure 8a shows that the larger hanging-wall subsidence compared with a single-segment rupture would allow inundation at the 4,212-foot (1,284-meter) lake elevation into areas northwest of Salt Lake City.

Normal-faulting earthquakes with dips greater than 45° have been observed in the Basin and Range Province; for example, 62° for the 1954 Dixie Valley, Nevada, earthquake (Okaya and Thompson, 1985; Doser, 1986) and multiple, 40° to 60° , dipping ruptures for the 1959 Hebgen Lake, Montana, earthquake (Doser, 1985). We note that a fault with a larger dip angle would reduce the area of flooding because the hanging wall would have a narrower subsidence trough. On the other hand, a more precipitous fault plane could increase the amount of subsidence near the fault (figure 1). For example, a 60° dipping fault could produce a deformation zone with vertical displacements larger than 3 feet (0.9 meter), and it would be 0.5 mile (0.8 km) narrower than what a 45° dipping fault could produce. The 60° dip could also increase the maxi-

mum hanging-wall subsidence about 2.5 inches (6.35 centimeter) compared with a 45° dip for a 6.6-foot (2-meter) normal-faulting earthquake.

Assuming a 60° dip, figure 8b shows the area of potential flooding caused by the multi-segment scenario rupture described above. The ground elevation gradient in the hanging wall decreases faster away from the fault and could therefore mitigate the inundation effects compared with the shallower 45° dip model. Distinctions between the 45° and 60° fault dip models point out that fault geometry is an important factor in analyzing earthquake-induced flooding and is a poorly understood property for the Wasatch fault.

Maximum Normal-Faulting Earthquake Scenario

The largest historic earthquake in the Rocky Mountains, the M_s 7.5 August 17, 1959, Hebgen Lake earthquake occurred in southwestern Montana. This event is commonly taken as the maximum magnitude earthquake for the Intermountain region and we chose it as an upper-bound scenario model for the Wasatch fault.

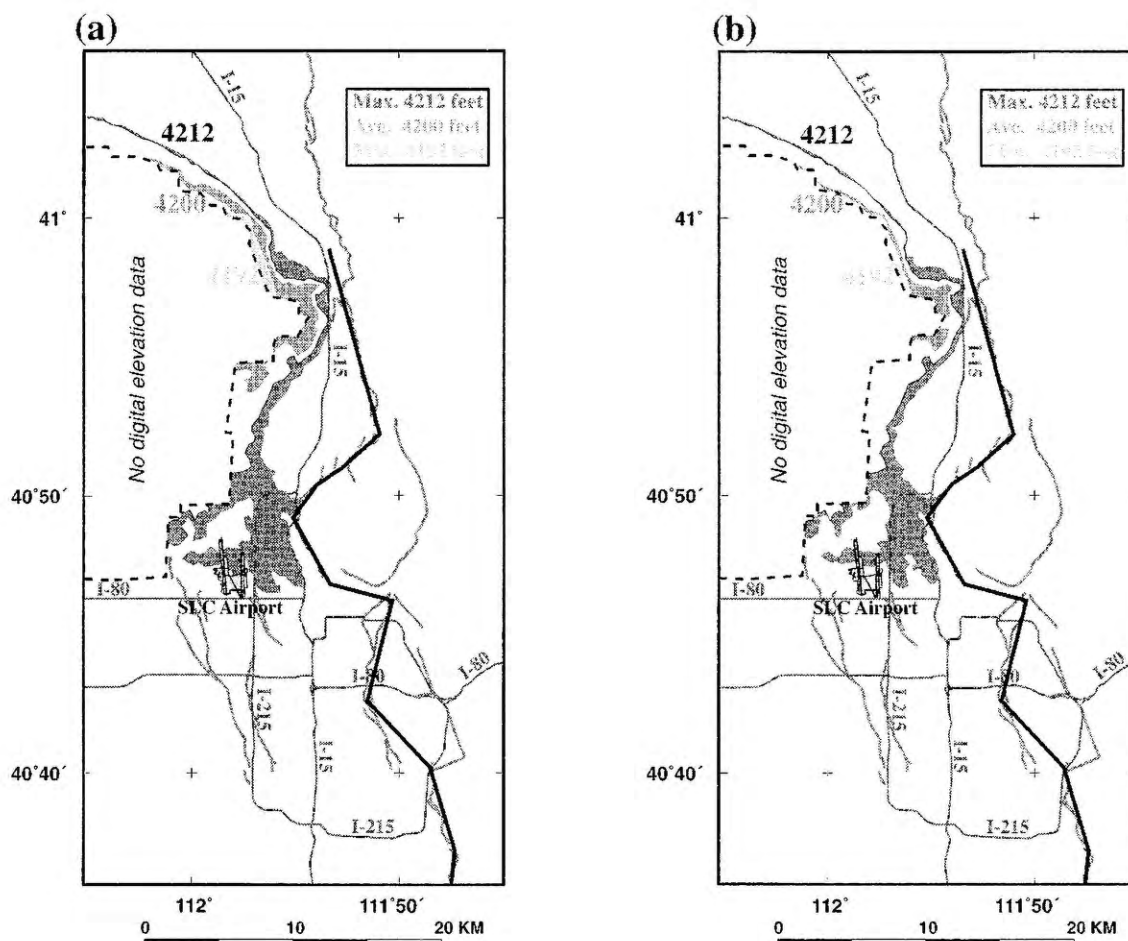


Figure 8. Scaled earthquake modeling shows multiple segment rupture corresponding to a $M_s = 7.2$ earthquake. The rupture includes the Salt Lake City segment and the southern part of the Weber segment (total rupture length is 57 kilometers). Fault dip angle is (a) 45° W, and (b) 60° W, respectively.

Changes in ground elevation based on extrapolated observations of bench marks along highways and profiles of topography on roads were surveyed by the U. S. Coast and Geodetic Survey shortly after the Hebgen Lake earthquake (Myers and Hamilton, 1964). These data provided an estimate of fault offset (in feet) and contours of subsidence with 2-foot (0.6-meter) intervals between 1 foot (0.3 meter) and 21 feet (6.4 meters). They were used to interpolate the hanging-wall subsidence for the postulated Hebgen Lake fault rupture that included an area 43 miles (69.2 kilometers) long and 14 miles (22.5 kilometers) wide with maximum subsidence up to 22 feet (6.7 meters). More than 60 square miles (155.4 square kilometers) subsided greater than 10 feet (3.05 meters). To model the Hebgen Lake earthquake scenario, we digitized both the fault scarp traces and deformation contours for the event (Myers and Hamilton, 1964) and then transformed the coordinates to the scale of the Wasatch Front study area.

Because of its length and geometry, a scenario Hebgen Lake fault was first placed on the southern part of the Weber segment. Its possible inundation aspects are shown

in figure 9. Due to the large hanging-wall subsidence, not only the 4,212-foot (1,284-meter), but also the 4,200-foot (1,280-meter) and 4,192-foot (1,278-meter) shorelines would be shifted to the east. This could result in flooding of areas around parts of I-15 and low-lying areas in Davis County near the Great Salt Lake shoreline.

A Hebgen Lake-type event was then placed on the Salt Lake City segment of the Wasatch fault. This simulation presents a realistic scenario because of the similarity between the geometry of the Hebgen Lake fault bounding the adjacent mountain, the Kirkwood Ridge, and the relation of the Wasatch fault to the nearby Wasatch Range (figure 10). Furthermore, paleoearthquake data on the northeastward extension of the Wasatch fault, the East Bench fault in Salt Lake City, show that it has experienced at least two large earthquakes in the past 26,000 years (Hecker, 1993). Figure 10 reveals an area up to 3.5 miles (5.6 kilometers) long that could be flooded compared with single- and multi-segment analytic models. This effect is due to larger and steeper tectonic tilts associated with this Hebgen Lake type earthquake.

Maximum Normal-Faulting Earthquake Model For Southern Weber Segment

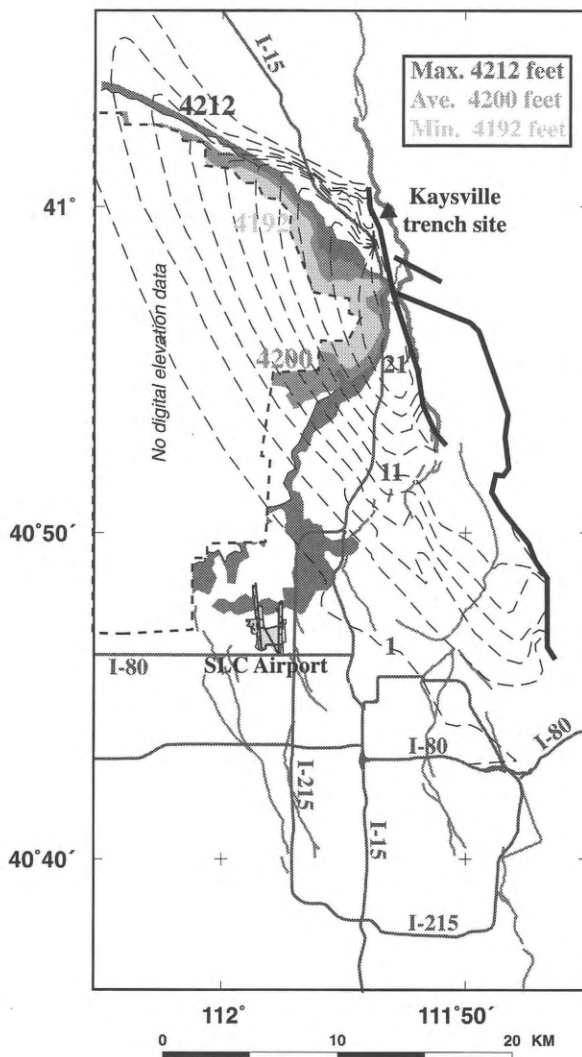


Figure 9. Maximum normal-faulting earthquake scenario for the 1959 $M_s = 7.5$, Hebgen Lake, Montana, earthquake applied to the south Weber segment (bold gray lines). Bold black lines show traces of surface rupture of the Hebgen Lake earthquake, and black dashed curves are measured surface subsidence contours from 1 foot to 21 feet at a 2-foot interval.

TECTONIC TILT EFFECTS ON SEWER AND WATER LINES

Another possible hazard from large earthquakes is the effect of hanging-wall backtilt on gravity-driven sewer lines. In Salt Lake Valley, sewers drain generally westward toward water treatment plants with appropriate slopes that depend on such factors as pipe diameter and required flow velocity. For sewer pipes of various diameters, engineering requirements list minimum slopes that provide an adequate velocity for keeping solids in suspension. An example from McGhee (1991) shows that mini-

Maximum Normal-Faulting Earthquake Model For Salt Lake City Segment

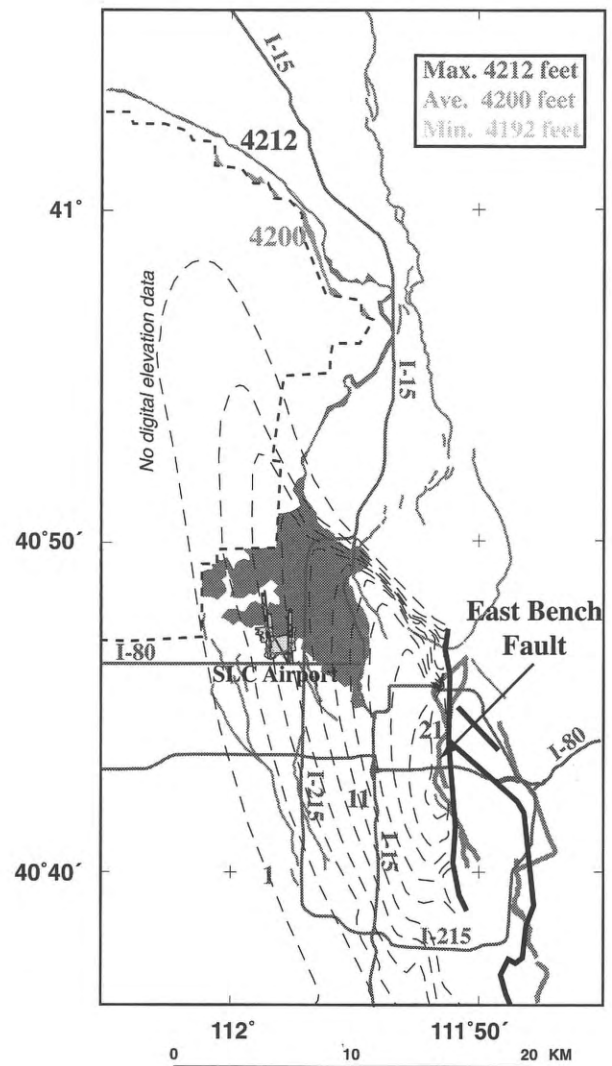


Figure 10. Maximum normal-faulting earthquake scenario for the 1959 $M_s = 7.5$, Hebgen Lake, Montana, earthquake applied to the north Salt Lake City segment. Notice the similar geometry between the surface rupture of Hebgen Lake earthquake (bold black lines) and the Wasatch fault (including the East Bench fault, bold gray lines). Black dashed curves are measured surface subsidence contours from 1 foot to 21 feet at a 2-foot interval.

um slopes are 0.43% (0.25°), 0.19% (0.11°), and 0.077% (0.04°) corresponding to sewer diameters of 6, 12, and 24 inches (15.2, 30.5, and 61 centimeters). Notice that, in this study, the elevations of the sewer lines are assumed to be the same as the ground surface.

We first examined the 1959 Hebgen Lake earthquake. With only sparse data on ground deformation (Myers and Hamilton, 1964), a coseismic hanging-wall displacement gradient of about 0.064% was exhibited perpendicular and within 6.2 miles (10 kilometers) of the Hebgen Lake fault. This slope would be eastward if a Hebgen Lake-style earthquake occurred on the Salt Lake City segment (figure

10), but the tilt does not appear to be sufficient to reverse the westward draining sewers in Salt Lake Valley or to cause stoppage of flow for pipes having diameters smaller than 24 inches (61 centimeters).

However, when we considered deformation near the ends of the Hebgen Lake fault, contours mapped by Myers and Hamilton (1964) showed a steeper slope of about 0.14% because of the end stress concentrations in the direction parallel to the fault. Therefore, if a Hebgen Lake-type earthquake shown in figure 10 occurred about 6.2 miles (10 kilometers) toward the southeast end of the Salt Lake City segment, it could produce southward ground tilt sufficient to influence the performance of northward-draining sewers in Salt Lake City with diameters larger than 12 inches (30.5 centimeters). We note that this effect only covers a small area compared to that of the entire hanging-wall subsidence (see figure 8 for example).

A second illustration considered was for a scenario earthquake with 6.5 feet (2 meters) of normal-fault slip ($M_s = 6.8$; figure 4). In this model, the ground would tilt with an average fault-perpendicular gradient up to 0.007% within 6.2 miles (10 kilometers) of the fault, whereas near the ends of the rupture, the fault-parallel slope is about 0.026%. Neither gradient appears sufficient to impede sewer flow for pipe diameters smaller than 24 inches (61 centimeters). We therefore conclude that, for most of the situations discussed above, sewer flow would not be seriously affected by tectonically induced backtilt. However site-specific studies for sewer lines in Salt Lake Valley require more detailed analysis.

The ground-tilting hazard associated with thrust earthquakes has also been recognized. The M_w 6.9 1997 Northridge, California earthquake was studied to evaluate the potential effects from ground tilt on water delivery systems such as aqueducts that feed the Los Angeles basin (Hodgkinson and others, 1996).

Ground deformation accompanying thrust earthquakes, however, is quite different from that caused by normal-faulting earthquakes. The Northridge earthquake produced an elongated uplift or bulge over the part of the fault that experienced the most slip in the earthquake. For the Northridge event, ground tilts were about 0.005%, which is the normal engineering grade for aqueduct design. Thus, the existing water systems were tilted back against their design grade by an amount about equal to it. In this study, we did not conduct analysis of the Wasatch Front water delivery systems, but the California example points out that it should be examined.

CONCLUSIONS

The results presented here show the potential for tectonically induced flooding of the Great Salt Lake from large earthquakes on the Wasatch fault. However, because of the lack of site-specific data on the subsurface geometry of the fault, such as along-strike structure, dip angle, and depth extent, our results should be considered as guidelines for future geological and engineering research rather than as specific information for management decisions. Moreover, additional studies of the Wasatch fault are necessary to clarify the model parameters. Our results

should therefore be used with caution until more knowledge about the actual configuration of the fault and secondary structures is known.

Although we used the high-resolution topographic data from orthophoto quadrangle maps for most of the study area, this type of information is generally not complete for other regions along the Wasatch Front with potential for earthquake induced flooding. This demonstrates the need for more well-covered, high-resolution topographic data, which should be acquired in the future, before our methodology can be widely used. We further point out that the high-resolution elevation data must also be evaluated to determine if man-made structures, such as roads, bridges, roadways, dikes, man-made mounds, and channels, etc., can alter flood potential.

Nonetheless, flooding of the Great Salt Lake into adjacent areas of the Wasatch Front induced by coseismic, hanging-wall subsidence of the Wasatch fault should be considered an important earthquake hazard. We demonstrate that the shoreline of the southeast Great Salt Lake could be generally shifted south and east and cause inundation in areas now occupied by man-made facilities. Not only could inundation potentially cause property and infrastructure damage, but emergency response efforts may be prevented by flood-affected transportation corridors. Several factors, including topography, lake level, earthquake size and location, fault geometry, and rupture length are key elements affecting the magnitude and distribution of water inundation. Note that scenarios considered in this paper are deterministic because their effects were assumed without respect to time dependence. Therefore, no likelihood of risk is assigned for a particular occurrence.

In conclusion, we point out that earthquake induced flooding is not restricted to the Great Salt Lake. Other regions of the state with a similar potential include Utah Lake and Willard Bay in northern Utah. Areas of the western U. S. that also may be susceptible to tectonic inundation or tilt-induced damage by normal faults near lakes include Bear Lake, Utah; Jackson Lake, Wyoming; Palisades and Henry's Fork Lakes, Idaho; Flathead and Hebgen Lakes, Montana; Walker and Pyramid Lakes, Nevada; and Lake Tahoe, California-Nevada.

ACKNOWLEDGMENTS

We gratefully acknowledge contributions and assistance to this study by Robert W. Simpson of the U. S. Geological Survey, who kindly provided his boundary element program. Max Elliot of the Davis County Surveyors Office and members of the Salt Lake City Corporation Engineering Department and Salt Lake County Flood Control Center loaned us their orthophoto maps. James P. McCalpin shared his insights on the Wasatch fault paleoearthquake studies. Catherine Lee and Yang-Show Chen assisted in the topographic digitization. Charles Martens and Craig dePollo provided reviews of our paper. This research was funded by the University of Utah Mineral Leasing Funds, College of Mines and Earth Sciences and the USGS, NEHRU (National Earthquake Hazard Reduction Program), Grant no. 1434-HQ-96-GO-02746.

REFERENCES

- Arnou, T., and Stephens, D.W., 1990, Hydrologic characteristics of the Great Salt Lake, Utah: 1847-1986: U. S. Geological Survey Water-Supply Paper 2332, 32 p.
- Barrientos, S.E., Stein, R.S., and Ward, S.N., 1987, Comparison of the 1959 Hebgen Lake, Montana and the 1983 Borah Peak, Idaho, earthquakes from geodetic observations: *Bulletin of the Seismological Society of America*, v. 77, no. 3, p. 784-808.
- Chang, W.L., and Smith, R.B., 1996, Earthquake hazard on the Wasatch Front, Utah, from fault interaction and possible flood inundation by the Great Salt Lake: EOS, (Transactions, American Geophysical Union), v. 77, no. 46, p. F507.
- Currey, D.R., Atwood, G., and Mabey, D., 1983, Major levels of Great Salt Lake and Lake Bonneville: Utah Geological Survey Map 73, scale 1:500,000.
- Doser, D.I., 1985, Source parameters and faulting processes of the 1959 Hebgen Lake, Montana, earthquake sequence: *Journal of Geophysical Research*, v. 90, no. B6, p. 4537-4555.
- Doser, D.I., 1986, Earthquake processes in the Rainbow Mountain-Fairview Peak-Dixie Valley, Nevada region, 1954-1959: *Journal of Geophysical Research*, v. 91, no. B12, p. 12572-12586.
- Hecker, S., 1993, Quaternary tectonics of Utah with emphasis on earthquake-hazard characterization: Utah Geological Survey Bulletin 127, 157 p., 2 plates.
- Hodgkinson, K.M., Stein, R.S., Hudnut, K.W., Satalich, J., and Richards, J.H., 1996, Damage and restoration of geodetic infrastructure caused by the 1994 Northridge, Calif. earthquake: U.S. Geological Survey Open-File Report 96-517, 70 p.
- Jackson, D., Aki, K., Cornell, A., Dieterich, J., Henyey, T., Mahdyiar, D., Schwartz, D., and Ward, S., 1995, Seismic hazards in southern California: Probable earthquakes, 1994 to 2024: *Bulletin of the Seismological Society of America*, v. 85, no. 2, p. 379-439.
- Keaton, J.R., 1987, Potential consequences of earthquake-induced regional tectonic deformation along the Wasatch Front, north-central Utah: Unpublished report by the Civil Engineering Department, Utah State University, 23 p., 6 plates.
- King, G.C.P., Stein, R.S., and Rundle, J.B., 1988, The growth of geological structures by repeated earthquakes, 1. Conceptual framework: *Journal of Geophysical Research*, v. 93, p. 307-318.
- Machette, M.N., Personius, S.F., and Nelson, A.R., 1992, Paleoseismology of the Wasatch fault zone: A summary of recent investigations, interpretations, and conclusions: U. S. Geological Survey Professional Paper 1500-A, 71 p.
- Mason, D.B., 1996, Earthquake magnitude potential of the Intermountain seismic belt, USA, from surface-parameter scaling of late Quaternary faults: *Bulletin of the Seismological Society of America*, v. 86, no. 5, p. 1487-1506.
- McCalpin, J.P., Forman, S.L., and Lowe, M., 1994, Reevaluation of Holocene faulting at the Kaysville site, Weber segment of the Wasatch fault zone, Utah: *Tectonics*, v. 13, no. 1, p. 1-16.
- McCalpin, J.P., and Nishenko, S.P., 1996, Holocene paleoseismicity, temporal clustering, and probabilities of future large ($M > 7$) earthquakes on the Wasatch fault zone, Utah: *Journal of Geophysical Research*, v. 101, no. B3, p. 6233-6253.
- McGhee, T.J., 1991, Water supply and sewerage (sixth edition), McGraw-Hill, Inc., New York, 602 p.
- Myers, W.B., and Hamilton, W., 1964, Deformation accompanying the Hebgen Lake earthquake of August 17, 1959: U. S. Geological Survey Professional Paper 435, p. 55-98.
- Okada, Y., 1992, Internal deformation due to shear and tensile faults in a half space: *Bulletin of the Seismological Society of America*, v. 82, no. 2, p. 1018-1040.
- Okaya, D.A., and Thompson, G.A., 1985, Geometry of Cenozoic extensional faulting: Dixie Valley, Nevada: *Tectonics*, v. 4, p. 107-126.
- Richins, W.D., Pechmann, J.C., Smith, R.B., Langer, C.J., Goter, S.K., Zollweg, J.E., and King, J.J., 1987, The 1983 Borah Peak, Idaho, earthquake and its aftershocks: *Bulletin of the Seismological Society of America*, v. 77, no. 3, p. 694-723.
- Savage, J.C., and Hastie, L.M., 1969, A dislocation model for the Fairview Peak, Nevada, earthquake: *Bulletin of the Seismological Society of America*, v. 59, p. 1937-1948.
- Schwartz, D.P., and Coppersmith, K.J., 1984, Fault behavior and characteristic earthquakes: Examples from the Wasatch and San Andreas fault zone: *Journal of Geophysical Research*, v. 89, no. B7, p. 5681-5698.
- Simpson, R.W., and Reasenber, P.A., 1994, Earthquake-induced static-stress changes on central California faults, in *The Loma Prieta, California, earthquake of October 17, 1989*: U. S. Geological Survey Professional Paper 1550-F, p. F55-F89.
- Smith, R.B., and Arabasz, W.J., 1991, Seismicity of the Intermountain seismic belt, in D. B. Slemmons, E. R. Engdahl, M.L. Zoback, and D.D. Blackwell, editors, *Neotectonics of North America*: Geological Society of America, SMV V-1, Decade Map Volume 1, p. 185-228.
- Smith, R.B., and Bruhn, R.L., 1984, Intraplate extensional tectonics of the eastern Basin-Range: inferences on structural style from seismic reflection data, regional tectonics, and thermal-mechanical models of brittle-ductile deformation: *Journal of Geophysical Research*, v. 89, p. 5733-5762.
- Smith, R.B., and Richins, W.D., 1984, Seismicity and earthquake hazards of Utah and the Wasatch Front: Paradigm and Paradox: U. S. Geological Survey Open-File Report 84-763, 27 p.
- Swan, F.H., III, Schwartz, D.P., and Cluff, L.S., 1980, Recurrence of moderate to large magnitude earthquakes produced by surface faulting on the Wasatch fault, Utah: *Bulletin of the Seismological Society of America*, v. 70, p. 1431-1462.
- Swan, F.H., III, Hanson, K.L., Schwartz, D.P., and Knuepfer, P.L., 1981, Study of earthquake recurrence intervals on the Wasatch fault at the Little Cottonwood Canyon site, Utah: U. S. Geological Survey Open-File Report 81-4550, 30 p.
- Webring, M., 1981, Minc: A gridding program based on minimum curvature: U.S. Geological Survey Open-File Report 81-1224, 11 p.

SHALLOW GEOPHYSICAL CONSTRAINTS ON DISPLACEMENT AND SEGMENTATION OF THE PAHRUMP VALLEY FAULT ZONE, CALIFORNIA-NEVADA BORDER

John Louie, Gordon Shields, Gene Ichinose, Michael Hasting, Gabriel Plank, and Steve Bowman
Seismological Lab (174), University of Nevada, Reno, NV 89557-0141
(702) 784-4219; fax (702) 784-1833; louie@seismo.unr.edu

ABSTRACT

The Pahrump Valley fault zone (PVFZ) is active and represents a potential seismic hazard for Las Vegas. Combining as many as six segments over a total length of more than 100 kilometers, the PVFZ may be able to produce a magnitude 7 event only 50 kilometers from the metropolitan area. We employ the seismic reflection, gravity, magnetic, and electromagnetic geophysical techniques to locate segments of the PVFZ and examine their subsurface geometry. Geophysical techniques can provide clues to segmentation and rates of activity in advance of detailed trench studies, and can uncover deeper and older displacements. On the PVFZ segment in southern Pahrump Valley we can locate fault strands near three Holocene scarps from pronounced magnetic and soil conductivity anomalies. We also observe truncations and limit the vertical offsets of reflective ash beds in shallow seismic profiles across two of these scarps. The sharpness of the magnetic and soil conductivity anomalies appears to correlate with the relative geomorphic youth of the scarps. These three geophysical techniques in combination can locate faults that lack clear surface expressions. A similar study of PVFZ strands in southern Stewart Valley shows clear evidence for more than 18 meters of Holocene dextral displacement in a 3-D seismic survey, but without any vertical component of displacement. The Pahrump Valley fault zone appears to have little evidence for segmentation that could limit earthquake rupture length to less than 60 kilometers anywhere in Pahrump Valley. The 18-meter minimum displacement of Wisconsin and pre-Wisconsin age lacustrine deposits likely results from a Holocene dextral slip rate above 0.1 mm/yr; the rate is certainly larger than 0.03 mm/yr, and probably less than 2 mm/yr.

PAHRUMP VALLEY FAULT ZONE

Although hidden on many maps by its location usually within 1 kilometer of the California-Nevada state line, the Pahrump Valley fault zone (PVFZ) is the longest seismogenic structure within 100 kilometers of the Las Vegas metropolitan area (figure 1). Only 50 kilometers distant at its closest reach, it extends at least 60 kilometers from Stewart Valley to southern Pahrump Valley (Hoffard, 1991), equal in length to any one of the four segments of the Death Valley fault system proposed by Sawyer and others (1996). Additional segments of the PVFZ may well extend north of Stewart Valley into Ash Meadows and Amargosa Valley as proposed by Donovan (1991) and Schweickert and Lahren (1994). To the south, it extends through Mesquite Valley (MIT Field Geophysics Course, 1985) and possibly into Sandy and even Ivanpah Valleys (Burt Slemmons, personal communication 1997). Thus, possible rupture lengths range from 60 to 150 kilometers, implying the potential for events with M_W magnitudes between 6.9 and 7.2. Such an event on the PVFZ could produce rock-site accelerations in the Las Vegas metropolitan area of up to 20 percent g, and possibly larger spectral accelerations at frequencies of two hertz or below (Su and Anderson, 1996).

Given the 12 mm/yr of the 56 mm/yr of Pacific-North America plate motion that diverts into the Eastern Mojave shear zone (Dokka and Travis, 1990) and the Walker Lane, Slemmons (1996) accounts for 2 mm/yr on the Owens Valley fault system, 2 mm/yr in Panamint Valley,

and now 4 mm/yr on the Death Valley fault system (Sawyer and others, 1996). This leaves 4 mm/yr for all Basin and Range motions east of Death Valley. Structures such as the Eglington scarp and the Frenchman Mountain fault in Las Vegas Valley show inconclusive evidence of rates as high as 1 mm/yr. However, the PVFZ may be the only candidate for a structure east of Death Valley long enough to show a rate as high as 1 mm/yr.

dePolo and Ramelli (1996) find rates in southern Nevada to average near 0.01 mm/yr, largely a result of the concentration of neotectonic studies around Yucca Mountain, an order of magnitude below the 0.1 mm/yr average deformation rates for Great Basin faults. Seismicity rates presented by Smith and others (1996) support such lower rates in southern Nevada; except in association with Lake Mead reservoir induced seismicity, activity associated with the 1992 Little Skull Mountain and Rock Valley sequences, and a cluster of seismicity in southern Pahrump Valley. Anderson and others (1996) examined a segment of the PVFZ that extends from the main segment in southern Pahrump Valley on a more northerly path past the west side of the Spring Mountains, perhaps following Nevada Highway 160 as far as U.S. Highway 95 (figure 1). They measured scarp profiles in alluvium to estimate that two large $M_W = 7$ earthquakes had occurred in approximately the past 128 thousand years. They did not find any Holocene scarps on that segment, however.

We will examine the main segments of the PVFZ at two locations, in Southern Pahrump Valley at the Old Spanish Trail Highway, and in Stewart Valley near Cali-

California Highway 178 and Nevada Highway 372 (figure 1). Each of these localities crosses a section of the PVFZ that appears to differ from the other in its apparent style of faulting, and type of scarp exposure. The authors all contributed to a University of Nevada, Reno (UNR) course in Geophysical Applications that performs field exercises in the area every two years. Our objective is to investigate how inexpensive shallow geophysical exploration methods may allow some characterization of fault displacement amounts and styles on these two parts of the PVFZ, and describe localities most appropriate for more detailed paleoseismic investigations.

SOUTHERN PAHRUMP VALLEY

In southern Pahrump Valley, the PVFZ divides into three fault-line scarps, each dissected by headward erosion of the uplifted playa and alluvial surfaces (Hoffard, 1991). The scarp closest to the California-Nevada state line, which appears geomorphically youngest and sharpest, with about 10 meters of relief, we call scarp 1. The scarps further from the state line, scarps 2 and 3, while about twice as high, have gentler slopes and appear more eroded (figure 2). Piety (1996) presents a map suggesting scarp 1 may belong to the main fault segment that

continues 60 kilometers northwestward to Stewart Valley. Scarps 2 and 3 may instead be related to the more northerly striking zone skirting the west side of the Spring Mountains examined by Anderson and others (1995).

Shields and others (1996) discuss the collection of geophysical profiles across the scarps (figure 2), and establish the repeatability of both the conductivity and magnetic measurements, including the fact that the strike of the anomaly at scarp 1 follows the strike of the scarp. Note on figure 2 that both types of anomaly suggest that all three scarps are fault-line scarps, with the topographic scarps having eroded back between 50 and 300 meters from the fault-break locations suggested by the anomalies.

At scarp 1, a tephra bed has been exposed by headward erosion, appearing to slump about a meter into the fault zone. We have not yet identified this tephra, nor its age. Based on work by Hillhouse (1987) and Morrison (1991) in the Tecopa and Chicago Valleys immediately to the west of Pahrump Valley, active lacustrine deposition ended no earlier than 0.16 million years ago, with prominent tephras deposited at 0.76 Ma (Bishop), 0.9 Ma, and 2.01 Ma (Huckleberry Ridge). The pluvial lake in Pahrump Valley drained north to or was contiguous with a lake in Stewart Valley, which drained north in turn to Ash Meadows and the Amargosa River; and so was at least occasionally tributary to pluvial Tecopa Lake.

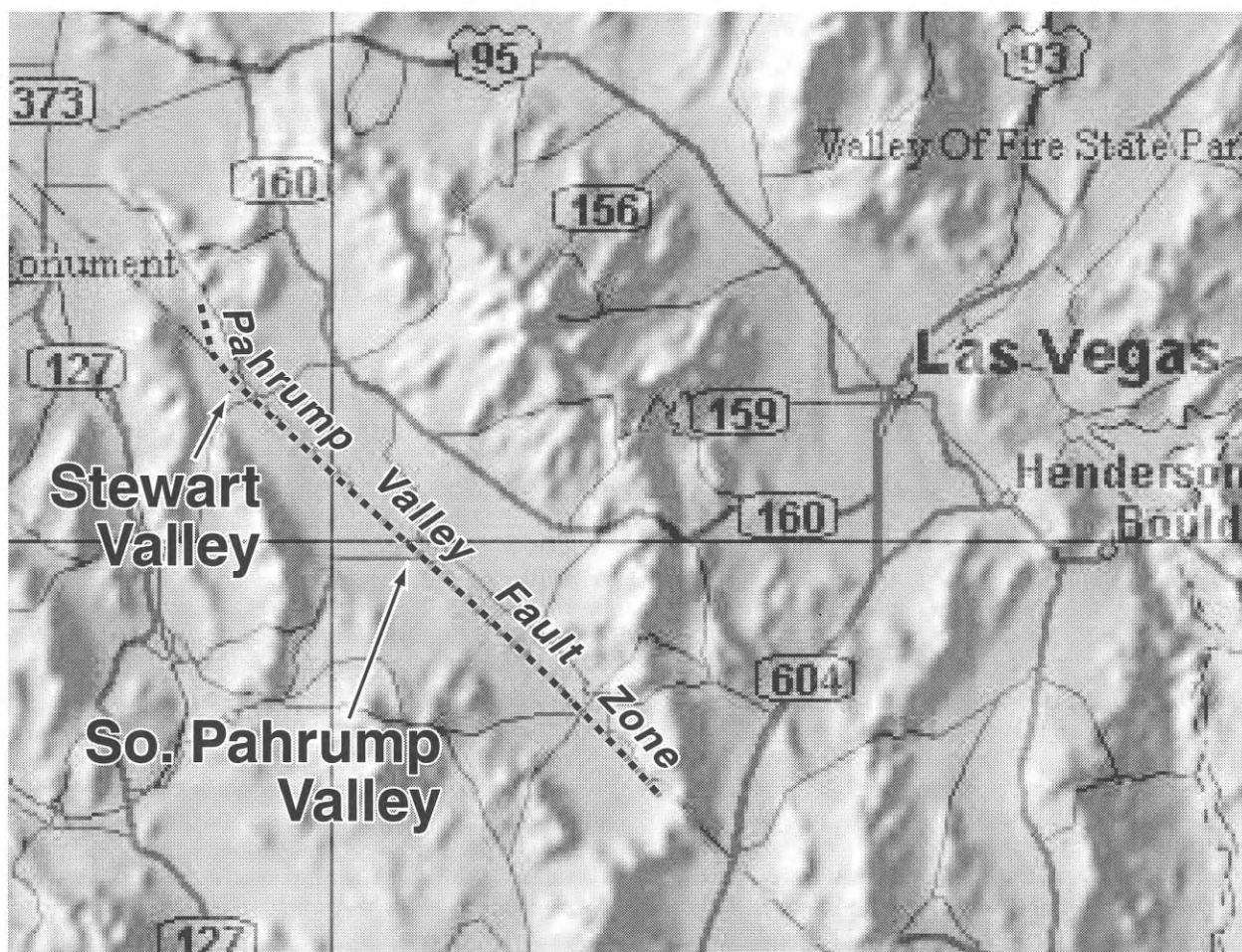


Figure 1. Map showing our two geophysical study areas along the Pahrump Valley fault zone (PVFC) 50 kilometers west of Las Vegas.

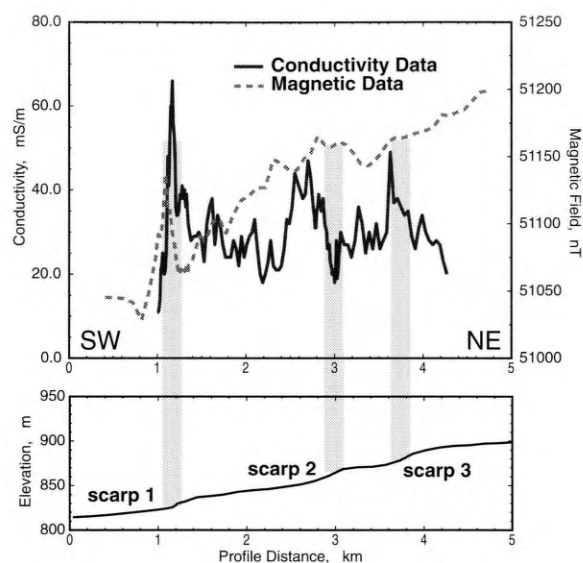


Figure 2. Elevation profile (bottom) along the Old Spanish Trail Highway showing the three scarps, with the state border at 700 meters profile distance. Above are the results of shallow (<3 m) ground conductivity measurements (solid line) made with a Geonics EM-31 instrument along the road, together with total-field magnetometer measurements (dashed line). The magnetic survey extended completely across Pahrump Valley; only the section crossing the fault zone is shown here. The overall increase in magnetic field toward the east is due to a large regional magnetic anomaly centered at the Spring Mountains.

Despite the evidence at scarp 1 for vertical offset of tephra layers and other lacustrine beds, our attempts to model the magnetic anomaly at the scarp with a vertical fault displacement of a magnetic layer (figure 3, lower) were not successful. Given the orientation of our survey with respect to Earth's magnetic field, the displacement anomaly cannot match the symmetry of the magnetic high in the data. A model placing a magnetic body as an inclusion within the steeply dipping fault plane (figure 3, upper) fits the symmetry better.

Shields and others (1996) propose that pluvial spring activity (as discussed by Quade and others, 1995) produced mineralization of the fault plane allowing the conductivity and magnetic observations. Under this mineralization hypothesis, scarp 1 appears to have the most recent motion and best preserved mineralization, with the largest anomalies, while scarps 2 and 3 appear to be associated with older and more degraded fault mineralization.

In addition to the shallow conductivity and magnetic measurements, we conducted more deeply penetrating transient electromagnetic (TEM) soundings. Analysis of the three TEM soundings (figure 4) shows distinct high-conductivity layers at about 10 meters depth away from the fault zone, with only evidence of a very shallow conductivity high at scarp 1. The TEM soundings average over the 40 meters squared area of the transmitter loops above 20 meter depths, and over larger areas at deeper depths. The sounding 200 meters northeast of scarp 1 shows the apparently conductive tephra layer at the same absolute elevation as the layer exposed at scarp 1, since the ground surface at the sounding to the northeast is about 10 meters higher in elevation than the surface at the

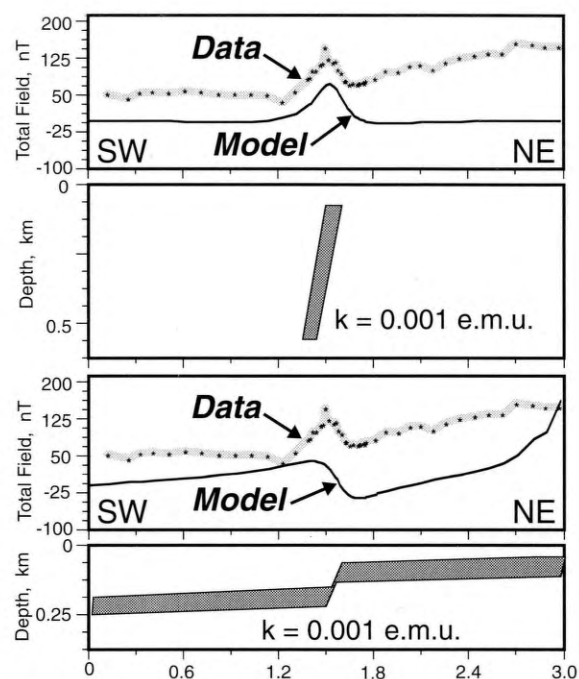


Figure 3. Trial magnetic models for the southern Pahrump Valley scarp 1. This section shows just the scarp 1 anomaly seen on the left side of figure 2. Edge effects of the faulted, near-horizontal-layer model create an asymmetry that matches the data poorly, while the steeply dipping fault-zone-inclusion model creates a more symmetric fit. Vertical exaggeration of cross sections is 1.8 times.

scarp 1 sounding (figure 4). The surface elevation at the sounding 200 meters southwest of scarp 1 is at about the same elevation as the scarp 1 sounding. The exposed, conductive tephra at the scarp agrees well with the coincident shallow ground conductivity high shown in figure 2. The TEM technique and the time-domain depth inversion we use is not, however, expected to be sensitive to any layers below the uppermost conductive layer.

Two-dimensional seismic-reflection profiles confirmed the lack of absolute vertical offset of the lake beds and tephra layers by the PVFZ at scarp 1 (figure 5, upper). The reflection at 40 ms two-way travel time in the unmigrated section at left shows an approximately constant subsurface elevation after correction for surface elevation statics, with some slumping and disruption within a 70-meter-wide zone on the southwest edge of the surface fault-line scarp. The slumping may be part of a negative flower structure along an almost purely strike slip PVFZ at scarp 1, or it may originate as a fault-trace graben due to a small extensional component of fault motion. This reflective bed thus cannot be the tephra layer exposed at scarp 1 and buried at 10 meters away from the scarp; it is likely to be an older tephra buried about 20 meters deeper.

The seismic section at scarp 2 (figure 5, lower) also suggests a slumped tephra layer at about 60 meters depth, more centered on the topographic scarp, with at least twice the vertical displacement. The image cannot rule out an absolute offset of the tephra layer of 40 meters at scarp 2, and may instead suggest that scarp 2, and by inference scarp 3, have a much higher proportion of normal slip than does scarp 1. If scarps 2 and 3 belong to the

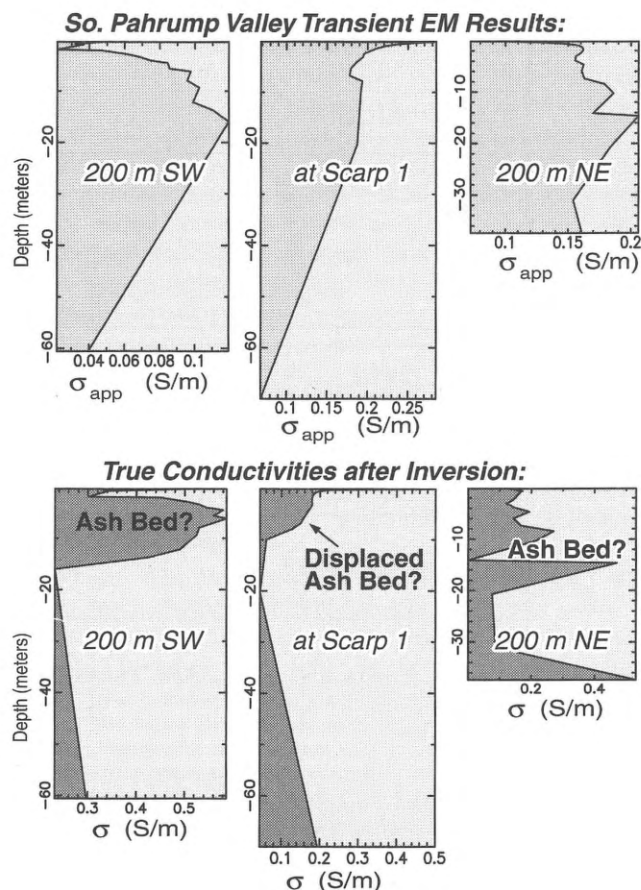


Figure 4. Analysis of the three TEM soundings in southern Pahrump Valley at three locations: at scarp 1, and 200 meters southwest, and 200 meters northeast of scarp 1. The upper columns depict raw apparent conductivity measurements plotted against the transient time-depth. The lower columns plot interval conductivities against true depth.

north-trending segment of the PVFZ that defines the western edge of the Spring Mountains, then a larger proportion of dip slip would not be surprising.

The geophysical investigations in southern Pahrump Valley suggest the PVFZ has its most recent, and almost purely strike-slip, motion at scarp 1, closest to the California-Nevada border. The other two scarps show older motions, possibly with larger proportions of dip slip.

STEWART VALLEY

Low-sun-angle aerial photography shows the PVFZ as a series of continuous scarps that follow within 1 kilometer of the state line from southern Pahrump Valley to the southern end of Stewart Valley, directly west of the town of Pahrump (Hoffard, 1991). The highway running across the middle of figure 6 is California 178/Nevada 372, and Ash Meadows Road extends to the north along the east side of the PVFZ. The intersecting east-west road is part of a residential development, and has been paved since the photo was taken about 1987. Several homes are now occupied within the development.

As the PVFZ enters southern Stewart Valley, it turns

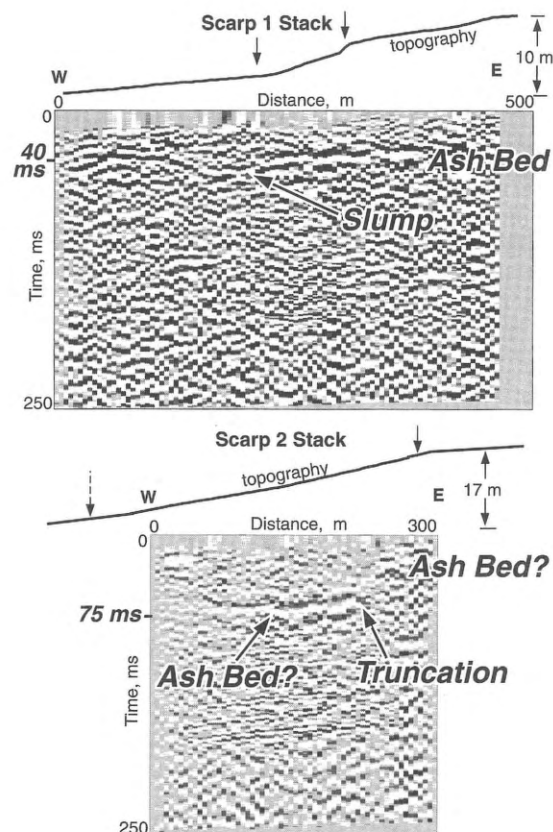


Figure 5. Two-dimensional, high-resolution, seismic stacked sections across PVFZ scarps 1 and 2 in southern Pahrump Valley. Note that the vertical scale bars apply only to the scarp profiles. The 40 ms two-way travel time implies a depth of the relective bed of about 30 m, and the 75 ms time about twice that depth, yielding an approximately 1.3 times vertical exaggeration of the sections.

to a more northerly strike, and may become the basin-bounding fault between Stewart Valley and the Montgomery Mountains to the east. Landowners along the PVFZ in central Stewart Valley report the water table at 9 or 10 meters depth, and the fault is marked there by groves of tamarisk and other phreatophytes. The main trace of the PVFZ in southern Stewart Valley is visible near the left edge of figure 6 as a continuous vegetation lineament. Additional traces to the right follow a series of spring mounds (Quade and others, 1995), or possibly terraces in the lake beds cut by wave action in the pluvial lake. We targeted our work in Stewart Valley to a relatively simple stretch of the fault at the northward bend, between more complex sets of traces to the north and south. This location appears about midway along the fault trace between the highway and the development road (figure 6).

Although the surface at this locality (figure 7) exposes pluvial lacustrine sediments and/or spring deposits, it is covered with a desert pavement of volcanic float washed from the hills to the east. The volcanic cobbles and rubble rendered no useful magnetic signal from the fault scarps at this locality; the rapidly varying field from surface float blocks swamped any anomalies from subsurface structures.

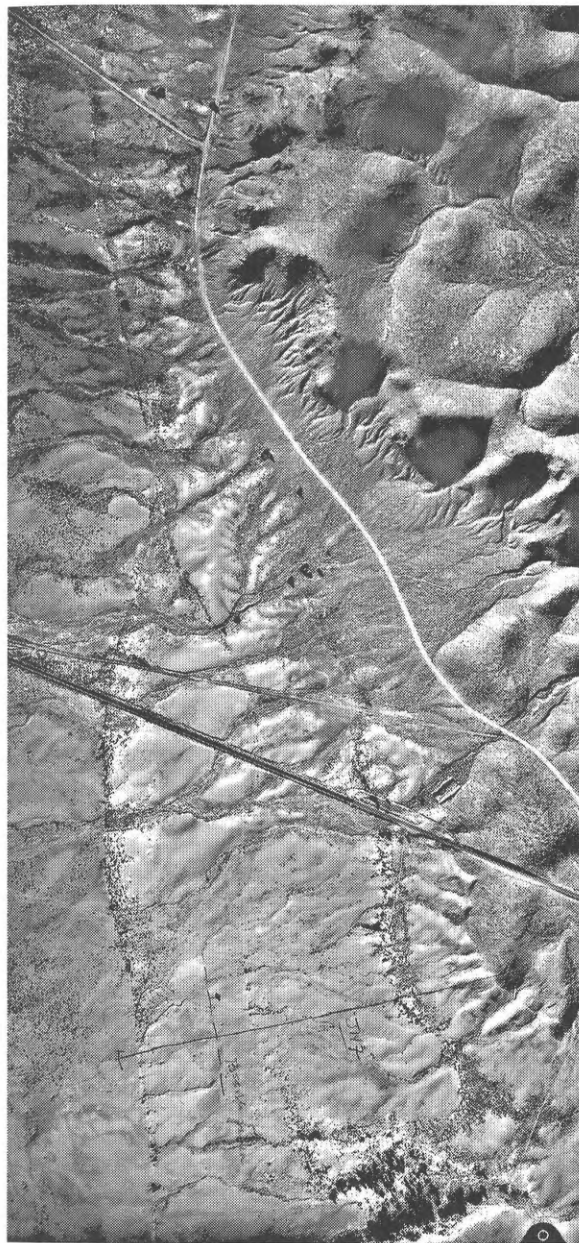


Figure 6. Enhanced low-sun-angle air photo of PVFZ traces in southern Stewart Valley. North is toward the upper right. Our study area is located along the fault about midway between the two east-west roads.

The gravity results of figure 8 (top, triangles) can match a synthetic model (figure 8, top, solid line) putting a small, approximately 50-meter-deep basin or shelf between the air-photo lineaments we call fault 1 and fault 2 (figure 7). These possible fault locations are noted on the topographic profiles (figure 8, bottom; figure 9, top). As in southern Pahrump Valley, the EM-31 shallow conductivity measurements (figure 8, center) produced clear anomalies centered on the surface lineaments and continuous along their strike. However, anomalies also appear that we have not been able to associate with any fault break on the ground or in the low-sun-angle aerial photography.

Unlike in southern Pahrump Valley, TEM surveys in Stewart Valley (figure 9) did not identify discrete conductive layers, possibly because of the relatively shallow water table. Combining the eight TEM soundings into the pseudosection of figure 9 (bottom), fault 1 appears to mark the edge of conductive lacustrine sediment filling the basin to the west. At fault 2, a low-conductivity anomaly near the surface suggests abundant silica cementation within the spring mound. The apparent very high conductivity below may be an artifact of the low-conductivity anomaly. The EM-31 shallow conductivity measurements only cover the very top layers of the pseudosection, and there does appear to be some correspondence between higher conductivities in the TEM results (figure 9) and in the EM-31 profiles (figure 8) at fault 1.

Ultra high-resolution, three-dimensional, seismic reflection surveying we carried out across fault 1 in Stewart Valley reveals the details of fault geometry and displacement. We laid out 11 lines across the fault (figure 7) spaced at 3.05 meters, and recorded each line individually. Each line consisted of 48 fixed 100 Hz single-phone receivers, buried about 20 centimeters and tamped with soil. A 5 kilogram sledgehammer hit against a 30-centimeter-squared, 2-centimeter-thick steel plate provided the most effective source for this survey, and was set on the surface at each receiver point on each line. The 10 hits at each point were stacked by a Bison Galileo-21 seismic recorder, generously donated to the UNR Mackay School of Mines by the W. M. Keck Foundation.

Data reduction consisted of minimal bandpass filtering followed by true three-dimensional imaging using an interval velocity profile derived from analysis of a suite of constant-velocity stacked sections. The 3-D prestack depth imaging technique is almost identical to the Kirchhoff-sum migration of Louie and others (1988), with operator aliasing controls as described by Lumley and others (1994), but using boxcar instead of triangle antialias filters.

The front face of the image volume (figure 10) shows interruptions in flat reflectors between 24 and 48 meters depth that locate the subsurface fault break with a near-vertical dip, surfacing at the center of the volume (figure 10, PVF). The upward curving of deeper reflectors near the sides of the volume is an artifact of low fold coverage near the ends of the survey lines. No measurable vertical offset of any of the layers is apparent, limiting the dip slip of PVFZ fault 1 in Stewart Valley to less than one meter. The depth slice at 48 meters (figure 10, right) shows the interruption of a layer by the fault trace at that depth, without vertical displacement.

The depth slice at 24 meters (figure 10, center) shows a lateral discontinuity on the northeast side of fault 1 that could arise at a fluvial channel wall, a facies change, or the side of a spring mound structure. The layer on the southwest side of the PVFZ fault 1 shows no similar lateral discontinuity within the image volume, proving that the discontinuity was dextrally displaced a minimum of 18 meters into the image volume by PVFZ fault motion.

The image in figure 10 establishes a minimum fault displacement on a sedimentary structure of unknown age. This structure, at 24 meters depth, is likely much older

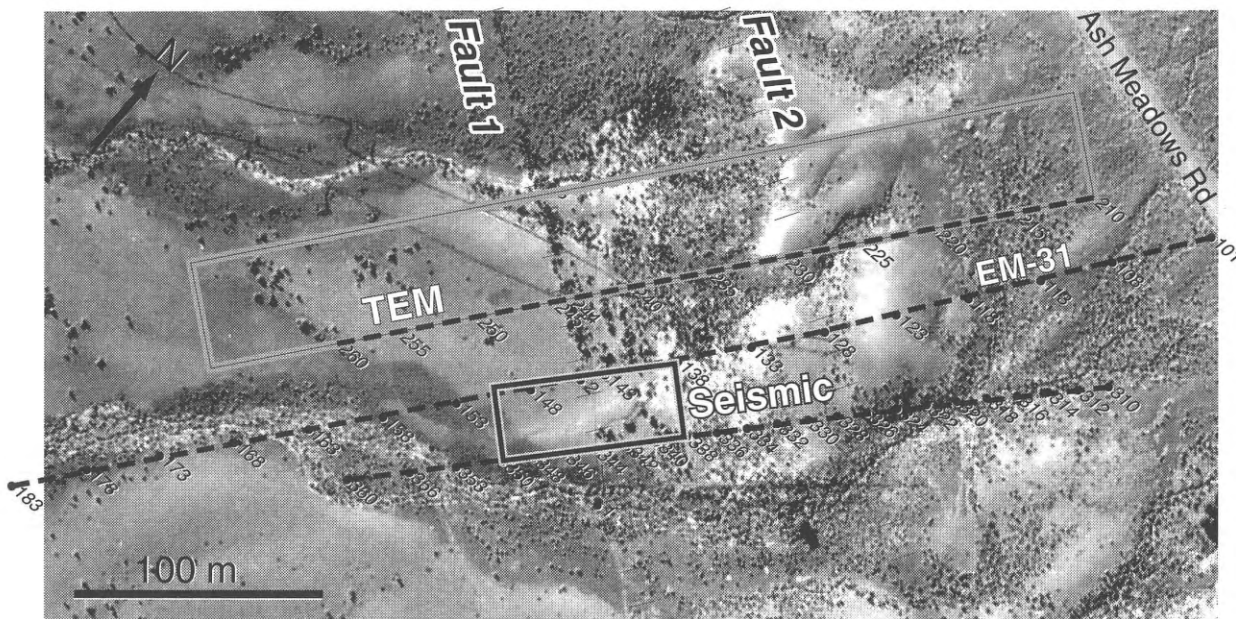


Figure 7. Section of air photo in figure 6 showing the locations of our geophysical surveys in Stewart Valley. Station EM344, on the south side of our 3-D seismic reflection survey area, is on the most continuous vegetation lineament and in the middle of the gravity line, and on one of the three lines where we took Geonics EM-31 shallow ground conductivity and magnetic measurements. The northern of the three lines was the basis for our layout of eight adjacent TEM transmitter loops, each 40 meters square on a side. The main trace of the PVFZ at the most continuous lineament is the finely hatched line at left (fault 1); while the hatched line to the right denotes a topographic scarp and second trace cutting the spring mounds, or possibly a pluvial lake terrace (fault 2).

than the most recent rupture, which figure 7 shows as breaking the surface. Quade and others (1995) establish a pre-Wisconsin Rancholabrean age range of 10 thousand years to less than 450 thousand years for spring mounds in Stewart and Pahrump Valleys. Since the pluvial lake in Stewart Valley served as an outlet for all discharge from the western Spring Mountains certainly as late as the Wisconsin pluvial period, near-surface lacustrine deposits in Stewart Valley could be as young as 5-10 thousand years. The lateral offset at 24 meters depth may well represent fault displacement of the top of a pre-Wisconsin age spring mound, within Wisconsin-age lake deposits.

Thus the 18 meter minimum offset could represent a cumulative displacement rate as high as 1.8 mm/yr, if the spring mound has the 10 thousand year minimum age. Spring activity may have peaked earlier in southern Nevada, at 100-150 thousand years, suggesting that the displacement rate is likely above 0.1 mm/yr, about average for faults in the Great Basin (dePolo and Ramelli, 1996). Putting the spring mound at the earliest possible Rancholabrean age, we see that the Quaternary displacement rate on the PVFZ cannot be less than 0.03 mm/yr, well above the rate for smaller faults in southern Nevada.

CONCLUSIONS

Geophysical surveys across two sections of a major right-lateral, strike-slip fault zone on the California-southern Nevada border have established that the Pahrump Valley fault zone maintains an almost completely strike-slip

character from southern Pahrump Valley to southern Stewart Valley. Despite apparent changes in tectonic setting that suggested segmentation, the PVFZ is straight, continuous, purely strike slip, and shows Holocene activity over a distance of more than 60 kilometers. While this length of the fault may be a segment of a longer system possibly extending south into Mesquite Valley and north into Ash Meadows, segmentation hypotheses would propose that the main 60 kilometers length in Pahrump Valley could rupture completely, producing an earthquake having a moment magnitude M_w as large as 7.2. Contrary to current assessments of regional seismic hazards to the Las Vegas metropolitan area, the 18 meter minimum Holocene dextral displacement found by high-resolution 3-D seismic surveying in Stewart Valley (figure 10) establishes a displacement rate much greater than the average for faults in southern Nevada. The PVFZ may have a displacement rate above the 0.1 mm/yr average for faults in the Great Basin overall. As little as 50 kilometers from the metropolitan area, the Pahrump Valley Fault Zone could pose the most significant seismic hazard to Las Vegas after the very active 4 mm/yr Death Valley fault system.

ACKNOWLEDGMENTS

This research was generously supported by the National Science Foundation under grant EAR-9405534, by the S. F. Hunt Fund of the UNR Mackay School of Mines, and by the W. M. Keck Foundation. Electromagnetic instruments were provided by Dr. Ken Taylor of the

Desert Research Institute, and by Chet Lide of Zonge Geoscience Inc. The authors thank Chet Lide and D. Burt Slemmons for helpful reviews of the manuscript; and acknowledge the kind assistance of the California Dept. of Transportation, Inyo County, the Nevada Dept. of Transportation, Clark County, and Nye County. Students participating in the 1994 and 1996 field exercises were David Aglietti, Kip Allander, Steve Bowman, Russell Brigham,

Ryan Crosbie, Michael Hasting, Andrew Hessel, Gene Ichinose, Zakir Kanbur, Sheander Ni, Jim Ollerton, Gordon Shields, Mike Sleeman, Lorenzo Trimble, Richard Tucker, and Hongbin Zhan.

An electronic version of this document is available at the location: <http://www.seismo.unr.edu/ftp/pub/louie/talks/lvsh/gbshs.html>.

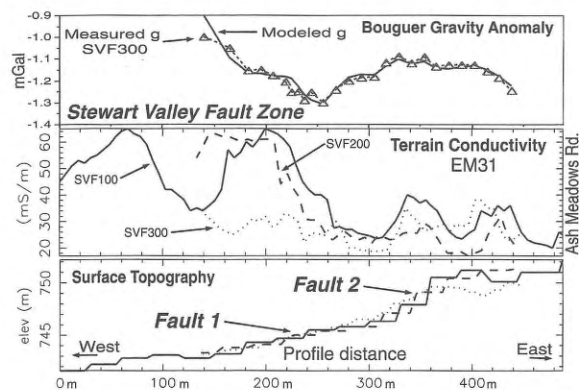


Figure 8. Gravity, EM-31 shallow conductivity, and elevation profiles across faults 1 and 2 on the PVFZ in Stewart Valley.

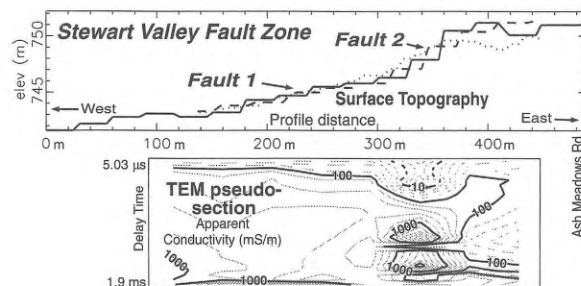


Figure 9. Elevation profiles and TEM pseudosection across the PVFZ in Stewart Valley.

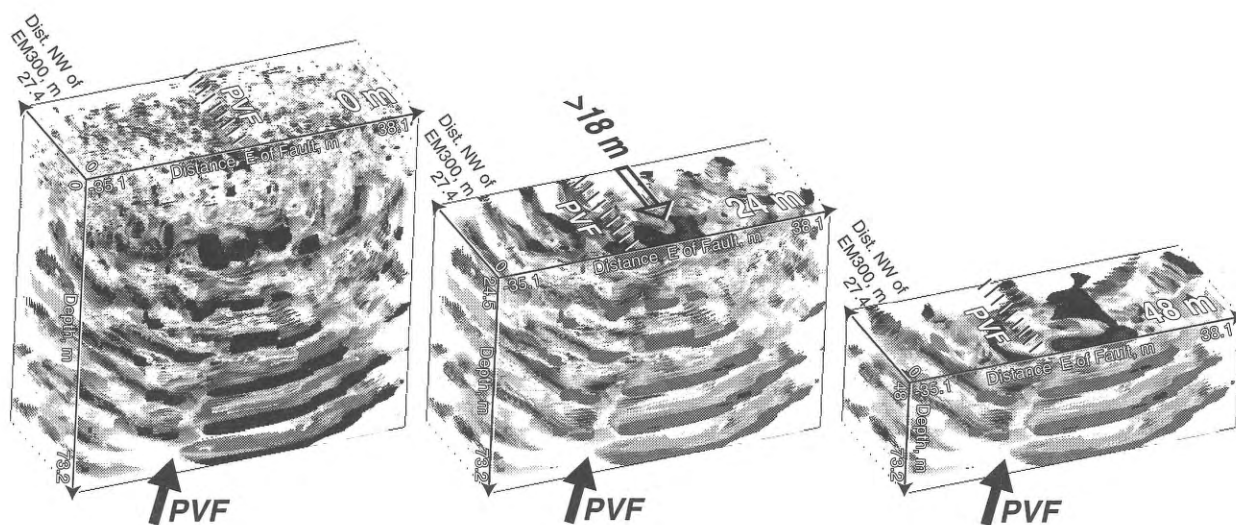


Figure 10. Three-dimensional seismic image volume 73 meters wide, 27 meters thick, and 73 meters deep across PVFZ fault 1 in Stewart Valley (figure 7), rendered to emphasize the positive reflectivities of greatest amplitude as darkly shaded, opaque 3-D objects. Near-zero reflectivities are rendered transparent. The whole volume is at left, and the two at center and right show depth slices at 24 and 48 m, respectively. The upward curving of the reflectors at the volume edges is a migration artifact; note the gaps in the layers where fault 1 passes through (PVF).

REFERENCES

- Anderson, R.E., Bucknam, R.C., Crone, A.J., Haller, K.M., Machette, M.N., Personius, S.F., Barnhard, T.P., Cecil, M.J., Dart, R.L., 1996, Characterization of Quaternary and suspected Quaternary faults, regional studies, Nevada and California: U. S. Geological Survey, Open-File Report 95-0599.
- dePolo, C. M., and Ramelli, A.R., in press, Quaternary and suspected Quaternary faults in Nevada south of 37 N. latitude: Seismic Hazards in the Las Vegas Region conference, Las Vegas, 1996.
- Dokka, R. K., and Travis, C.J., 1990, Role of the eastern California shear zone in accommodating Pacific-North American plate motion: *Geophysical Research Letters*, 17, p. 1323-1326.
- Donovan, D.E., 1991, Neotectonics of the southern Amargosa Desert, Nye County, Nevada and Inyo County, California: Reno, University of Nevada, M.S. thesis 2755, 151 p.
- Hillhouse, J.W., 1987, Late Tertiary and Quaternary geology of the Tecopa basin, southeastern California: U.S. Geological Survey Miscellaneous Investigations Map I-1728, 1:48,000, 1 sheet, 16 p.
- Hoffard, J. L., 1991, Quaternary tectonics and basin history of Pahrump and Stewart Valleys, Nevada and California: Reno, University of Nevada, M.S. thesis 2747, 138 p.
- Louie, J. N., Clayton, R.W., and Le Bras, R.J., 1988, Three-dimensional imaging of steeply dipping structure near the San Andreas fault, Parkfield, California: *Geophysics*, 53, p. 176-185.
- Lumley, D. E., Claerbout, J.F., and Bevc, D., 1994, Anti-aliased Kirchhoff 3-D migration: Society of Exploration Geophysicists Annual International Meeting, Los Angeles, 1994, Expanded Abstracts, p. 1282-1285.
- MIT Field Geophysics Course, 1985, A Geophysical Study of Mesquite Valley, Nevada-California Border: *Journal of Geophysical Research*, 90, p. 8685-8690.
- Morrison, R. B., 1991, Quaternary stratigraphic, hydrologic, and climatic history of the Great Basin, with emphasis on Lakes Lahontan, Bonneville, and Tecopa, in Morrison, R. B., editor, Quaternary Non-Glacial Geology, Conterminous U.S.: Boulder, Colorado, Geological Society of America, *Geology of North America*, K-2, p. 283-320.
- Piety, L. A., 1996, Compilation of known or suspected Quaternary faults within 100 km of Yucca Mountain: U. S. Geological Survey, Open-File Report 94-0112, 1:250,000.
- Quade, J., Mifflin, M.D., Pratt, W.L., McCoy, W., and Burckle, L., 1995, Fossil spring deposits in the southern Great Basin and their implications for changes in water-table levels near Yucca Mountain, Nevada, during Quaternary time: *Geological Society of America Bulletin*, 107, p. 213-230.
- Sawyer, T. L., Klinger, R.E., dePolo, C.M., and Reheis, M.C., in press, Death Valley fault system: Significant ground motion sources for southern Nevada: Seismic Hazards in the Las Vegas Region conference, Las Vegas, 1996.
- Schweickert, R. A., and Lahren, M.M., 1994, Amargosa fault system near Yucca Mountain, Nevada (abs.): Geological Society of America, Abstracts with Programs, v. 26, no. 7, p. 250.
- Shields, G., Allander, K., Brigham, R., Crosbie, R., Trimble, L., Sleeman, M., Tucker, R., Zhan, H., and Louie, J.N., in press, Geophysical surveys of an active fault: Results from southern Pahrump Valley, California-Nevada border: *Bulletin of the Seismological Society of America*, 88, Feb. 1998.
- Slemmons, D. B., in press, Seismotectonic setting for the Las Vegas basin, Nevada: Seismic Hazards in the Las Vegas Region conference, Las Vegas, 1996.
- Smith, K., dePolo, D., Gross, S., Von Seggern, D., Biasi, G., Anderson, J.G., Brune, J.N., and dePolo, C., in press, Historical earthquakes and recorded seismicity of the southern Great Basin in the vicinity of Las Vegas, Nevada: Seismic Hazards in the Las Vegas Region conference, Las Vegas, 1996.
- Su, F., and Anderson, J.G., in press, Basin effects on strong motion in Las Vegas: Seismic Hazards in the Las Vegas Region conference, Las Vegas, 1996.

NONLINEAR AMPLIFICATION STUDIES OF DEEP DEPOSITS IN RENO, NEVADA

Raj V. Siddharthan
Department of Civil Engineering, University of Nevada,
Reno, Nevada 89557

Shen-Der Ni
Graduate Student, Seismology Laboratory,
University of Nevada, Reno, Nevada 89557

John G. Anderson
Seismological Laboratory, University of Nevada,
Reno, Nevada, 89557

ABSTRACT

Recent design recommendations call for dynamic soil properties (shear modulus ratio and damping) and liquefaction strength curves to be characterized as a function of the effective vertical stress (or depth). A modified version of DESRA2 computational model for saturated soil has been developed to study the nonlinear seismic response including liquefaction of a medium-dense, deep soil deposit. The study gives responses in terms of acceleration and residual porewater pressure for a deep soil site near Reno, when subjected to a strong synthetic base excitation. The field case study reveals that the response predicted from a conventionally used stress-independent soil properties model is unconservative for deep deposits.

INTRODUCTION

Laboratory model studies and field observations have clearly shown that identical structures founded on different types of soil but subjected to the same base (or bedrock) excitation will exhibit different responses. This means that the influence of the foundation soil on the response of the structures is a critical component in the assessment of earthquake resistant design. The first step in many earthquake response studies is to evaluate the free-field (soil response) to a suite of base excitations that may be expected at the site. The earthquake response of a soil deposit subjected to base (or bedrock) excitation is heavily dependent upon an accurate assessment of the dynamic behavior of the soil deposit.

Among the important response parameters that can be obtained from dynamic soil response studies, permanent deformation, acceleration, and residual porewater pressure response are the most critical. Deformation in soils adjacent to the structure can be directly used to interpret the performance of the structure. While deformation of a few inches to a foot may be critical to nuclear power plants and bridge abutments, a few feet may be acceptable for earth dams. The assessment of seismic performance based upon permanent displacement has been the norm in geotechnical practice since the pioneering work of Newmark (Newmark, 1965).

The study of soil response to base excitation is a difficult task. It is further complicated by the presence of soils that can generate residual porewater pressure under cyclic loading. Porewater pressure buildup reduces effective stress and thus the stiffness and strength of soil. An extreme case is the phenomenon of "liquefaction" where

residual porewater pressure becomes equal to the initial vertical effective stress, resulting in "zero" effective stress. Since residual porewater pressure can substantially affect soil behavior, a realistic dynamic soil-response evaluation should incorporate the influence of residual porewater pressure in the analysis procedure. In such cases, an "effective stress based" approach becomes an important tool in response evaluations.

Soil response studies have been evolving since researchers initiated studies to explain the massive ground deformation and liquefaction that occurred during major earthquakes in Alaska and Japan in 1964. Significant achievements in this important field have been reported in many national and international conferences. This paper focuses on those cases where the soil deposit consists of saturated cohesionless soils. The intent of the dynamic soil-response evaluation studies reported here is to simulate the expected performance of the deposit so that an optimum design can be achieved. This enables practicing engineers to use dynamic soil-response information to carry out a cost-effective design.

SUMMARY OF PAST SOIL RESPONSE STUDIES

The nonlinear behavior of soil when subjected to strong ground shaking plays an important role in altering the characteristics of ground motions. Numerical approaches to predict the nonlinear response of soil can be classified as either a equivalent secant approach (e.g., SHAKE program by Schnabel and others, 1972) or a direct nonlinear approach (e.g., CHARSOIL program by

Streeter and others, 1974; DESRA2 program by Lee and Finn, 1978). Many studies have compared the responses computed by both of these methods. Such studies have concluded that the secant approach cannot reproduce some of the important characteristics of the ground motion, especially for the case of strong ground shaking (e.g., Constantopoulos and others, 1973; Streeter and others, 1974; Finn and others, 1978). Recently, Yu and others (1993) used DESRA2 to examine the differences between linear and nonlinear soil response with various levels of base excitations. By using this direct nonlinear program, they showed that in strong excitations soil nonlinearity causes deamplification and also a shift in peak frequencies to lower values. They based their conclusions on the computed dynamic soil responses of an unsaturated, 20-meter-thick, shallow soil deposit.

Response evaluation of deep saturated deposits, which is the topic of this paper, differs in many ways from that of shallow unsaturated deposits. The term saturated is used here to refer to a soil column with a shallow (usually 3 m or less) water table. The soil properties and characteristic behavior of deep deposits are quite different from those of shallow deposits as noted by the Electric Power Research Institute (EPRI, 1993). The material properties are a function of effective stress and, consequently, a function of depth. Thus, the hysteretic nonlinear soil behavior of a deep strata should be characterized using many sublayers, with each sublayer assigned a set of uniform properties. The sublayer properties, as will be pointed out later, should account for a stress (or depth) dependent shear modulus ratio (G/G_{\max}) and damping ratio variations with shear strain (EPRI, 1993). In addition, the coupling of residual porewater pressure and ground shaking substantially affect the soil response. The influence of residual porewater pressure becomes significant when the strength of excitation is large. The generation of residual porewater pressure reduces the effective stress during excitation and, as the input excitation becomes larger, can result in liquefaction. These factors are vital to the dynamic response of deep soil columns subject to base excitation. This study extends the work of Yu and others (1993) to deep soil deposits and accounts for the aforementioned factors.

BRIEF OUTLINE OF PROPOSED MODEL

This study uses a numerical code to evaluate nonlinear soil response, including porewater pressure generation and dissipation. The numerical model used here is a modified version of the DESRA2 program developed by Lee and Finn (1978). The model is based on the finite element method and is capable of evaluating motions within a soil column subjected to vertically propagating shear waves. Dynamic equations of motions are numerically integrated in the time domain (direct method) using the tangent approach. It is an effective stress based approach in which soil shear stiffness is modified as residual porewater pressure is generated.

Each finite element in the physical model follows a nonlinear shear stress-strain relationship and the hys-

teretic behavior of the soil is modeled using Masing criteria as described by Finn and others (1977). The program DESRA2 is widely used by many researchers and practicing engineers to compute soil response (Finn, 1981, 1988; Hushmand and others, 1987).

Modifications to the original program were made so that recently available nonlinear soil behavior data can be readily incorporated. The main changes made to the original DESRA2 include new characterization for stress-strain and volumetric strain relationships since better characterizations have been proposed recently (Byrne, 1991; EPRI, 1993). The modifications have been incorporated such that only a minimum number of soil parameters are used in the model, while retaining many convenient features of the original model.

The new shear stress-strain equation for initial loading is defined as:

$$\tau = \frac{G_{\max} \gamma}{1 + \left| \frac{\gamma}{\gamma_y} \right|^a} \quad (1)$$

in which τ and γ are shear stress and strain; G_{\max} is the shear modulus at a very low strain level; γ_y is the reference strain; and a is a constant. In the original DESRA2 model, a equals unity. Recently, based on a large database of laboratory soil behavior, Nakagawa and Soga (1995) also proposed the variation of the type given in equation 1.

The subsequent unloading and reloading are given by Masing-type stress-strain curves (Masing, 1926). During the strong shaking, the effective vertical stress decreases because of residual porewater pressure generation. The increment in residual (excess) porewater pressure, is evaluated using the porewater pressure model of Martin and others (1975), given by:

$$\Delta u = E_r \Delta \epsilon_{vd} \quad (2)$$

in which $\Delta \epsilon_{vd}$ is the increment in plastic (or permanent) volumetric compaction strain, and E_r is the one-dimensional rebound modulus. The $\Delta \epsilon_{vd}$ is a function of accumulated volumetric strain ϵ_{vd} and shear strain γ . Martin and others (1975) used four coefficients to evaluate $\Delta \epsilon_{vd}$. Byrne (1991) provided a new, much simpler relation,

$$\frac{\Delta \epsilon_{vd}}{\gamma} = c_1 \exp \left(-c_2 \frac{\epsilon_{vd}}{\gamma} \right) \quad (3)$$

in which c_1 and c_2 are constants that depend on the relative density of sand.

The rebound modulus E_r is a function of effective stress level. The relation given by Martin and others (1975) is:

$$E_r = \frac{(\sigma'_v)^{1-m}}{mK_r (\sigma'_{v0})^{n-m}} \quad (4)$$

in which σ'_{vo} is the initial value of the effective stress and K_r , m , and n are experimental constants for a given sand. The equations (1) through (4) form the basis of the modified DESRA2 program used in this study. These equations are solved numerically in conjunction with the dynamic equations of motion of the sand layer using a step by step integration procedure in the time domain.

Since soil behavior is governed by effective stress, soil stiffness decreases as residual porewater pressure increases. The reduction in soil stiffness (shear modulus) is handled the same way as in the original program. Redistribution of residual porewater pressure can take place during excitation, and the net effects of contemporary generation and dissipation are also considered by the program. In such cases, the permeability of the soil layers must be known. More details on the procedure may be found in Finn and others (1977), Lee and Finn (1978), and Ni and others (1997).

SELECTION OF SOIL PARAMETERS

Consider a deep stratum of medium-dense sandy deposits (relative density, $D_r = 60\%$) with a water table 3 meters below the surface (figure 1). The properties of the sand vary only in the vertical direction. The sand deposit is assumed to rest on an impermeable rock with a shear wave velocity of 2,500 m/sec. The input motion is present at the interface between the soil and rock.

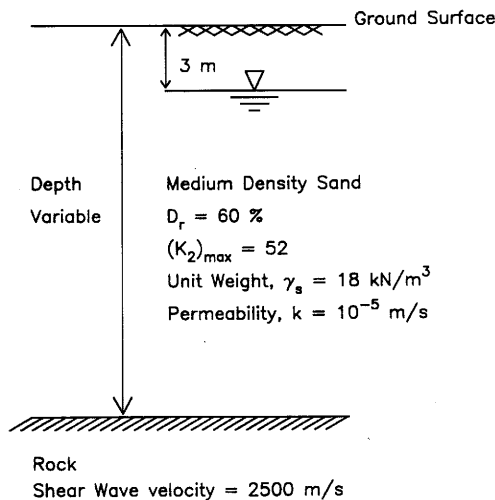


Figure 1. Soil deposit used in the study.

The deposit is divided into sublayers each 1 meter thick and with approximately uniform properties. The maximum shear modulus, G_{\max} , in any sublayer is computed as:

$$G_{\max} = 218.8 (K_2)_{\max} (\sigma'_m)^{1/2} \quad (5)$$

in which $(K_2)_{\max}$ is a constant that depends on the relative density of soil and σ'_m is the effective mean normal stress of the layer (Seed and Idriss, 1970). Here G_{\max} and σ'_m are given in kPa.

Traditionally, the nonlinear behavior of soil is defined by two strain-dependent soil parameters: normalized shear modulus ratio, G/G_{\max} , and damping ratio, ζ (Seed and Idriss, 1970; Hardin and Drnevich, 1972). There is a large database for these parameters for many types of soil. However, a vast majority of the data used to estimate these parameters were obtained from tests conducted at a confining pressure range of 100-300 kPa. Therefore, the applicability of these parameters is limited to shallow deposits of depths of 20 to 30 meters or so.

The EPRI recently recommended the use of depth (or stress level) dependent soil properties (G/G_{\max} and ζ) in the evaluation of deep soil response (EPRI, 1993). This recommendation is based on many laboratory tests under low and high confining pressures. Figure 2 shows the EPRI recommendation for normalized shear modulus ratios, G/G_{\max} and damping ratios, ζ for sand at different depths as a function of shear strain (EPRI, 1993). As soil depth increases, the values of G/G_{\max} and ζ for a given strain level increases and decreases respectively. In other words, soil elements under large confining pressures have lower damping and do not exhibit a strong nonlinear behavior compared with elements under lower confining pressures.

The shear stress-strain relationship (equation 1) can be re-written as:

$$\frac{G}{G_{\max}} = \frac{1}{1 + \left| \frac{\gamma}{\gamma_y} \right|^a} \quad (6)$$

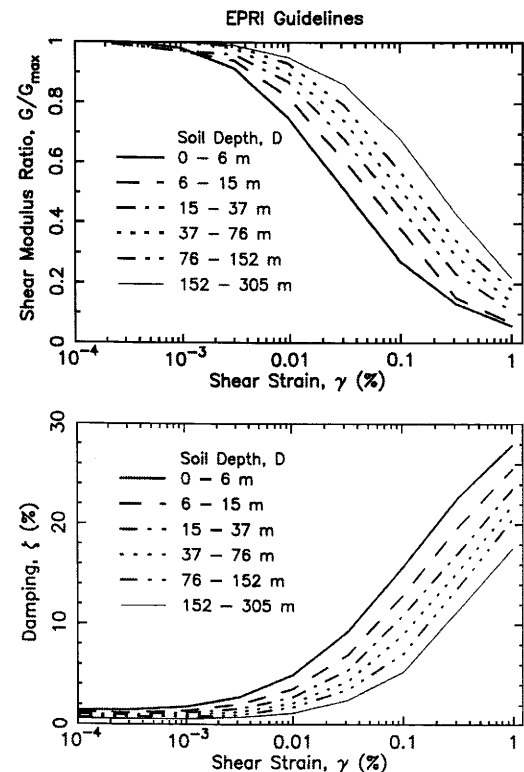


Figure 2. Characteristic behavior of sand (after EPRI, 1993).

The soil parameters γ_y and α in the above equation have been evaluated such that equation (6) provides a best fit to the G/G_{\max} and ζ given in figure 2. The Masing criteria, which defines the unloading and reloading, gives the area enclosed by a strain cycle, which is proportional to ζ . An optimization technique was utilized to estimate different sets of γ_y and ζ values for each depth (or stress level). Figure 2 shows that there is a certain damping, ζ_0 at the low ($10^{-4}\%$) strain level. This damping amount is not considered to be due to hysteretic soil behavior and therefore, was subtracted from EPRI data in the optimization. Table 1 gives the optimum values of γ_y and α for all the EPRI recommended relations shown in figure 2.

The EPRI data and the soil properties G/G_{\max} and ζ computed from the proposed stress-strain model are shown in figure 3. The ζ_0 values have been subsequently

Table 1. Soil Properties.

Depth of Soil	Average Stress Level σ'_{vo} kPa	Reference Strain γ_y	Model Constant α	Model Constant K_r
0-6 m	26.0	0.0004	0.72	0.0085
6-15 m	92.0	0.0007	0.73	0.0080
15-37 m	224.0	0.0010	0.75	0.0060
37-76 m	487.0	0.0014	0.77	0.0030
76-152 m	988.0	0.0020	0.81	0.0016
152-305 m	1976.0	0.0032	0.84	0.0014

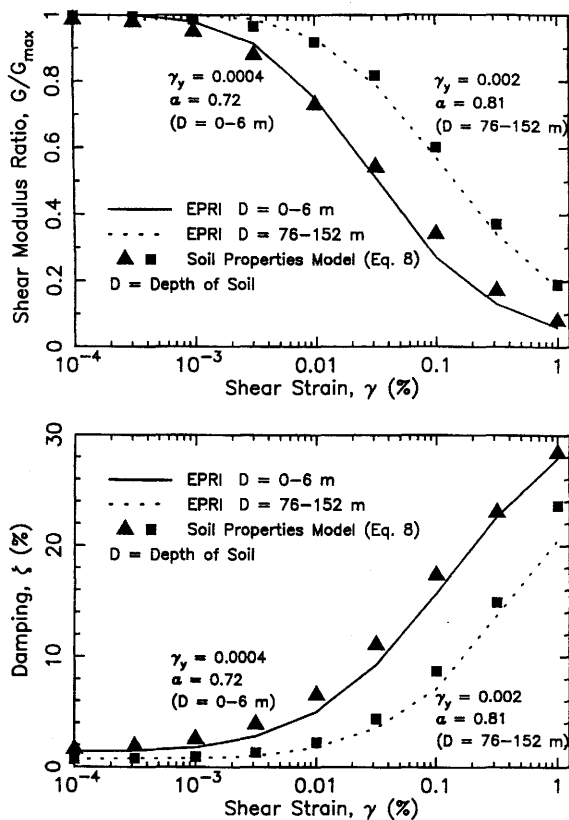


Figure 3. Calibration of model constants using EPRI guidelines.

added to the computed damping values when plotted in the figure. Only two sets of data (depths 0-6 m and 76-152 m) are shown. The figure reveals that the predicted values provide a good fit to the EPRI data.

Other important model parameters are those that define the volume change and porewater-pressure generation behavior. Volume change behavior (constants c_1 and c_2) has been extensively studied by Byrne (1991), who recommends values as a function of the relative density of sand. Recommended values for c_1 and c_2 are 0.24 and 1.66 respectively for a sand with $D_r = 60\%$.

A convenient way to obtain porewater-pressure model parameters is to match a specified liquefaction potential curve with the one predicted by the porewater-pressure generation model used in the proposed approach (Finn and others, 1982). When using the DESRA2 model, it is customary to select model constant K_r (equation 4) such that there is a close match between the predicted and specified liquefaction potential curves. The liquefaction curve for any given D_r (or SPT value, N_1) can be obtained from an extensive field database compiled by Seed and Idriss (1982). This database is applicable for shallow deposits (stress level 100 kPa) and should be modified when using it for a deep deposit. Guidelines reported by Marcuson and others (1990) can be used to obtain the liquefaction potential curves relevant for higher confining pressures by scaling the curve obtained from Seed's data.

Figure 4 shows the three predicted and target liquefaction potential curves; note that liquefaction resistance when specified as a ratio (τ/σ'_{vo}) is higher for low confin-

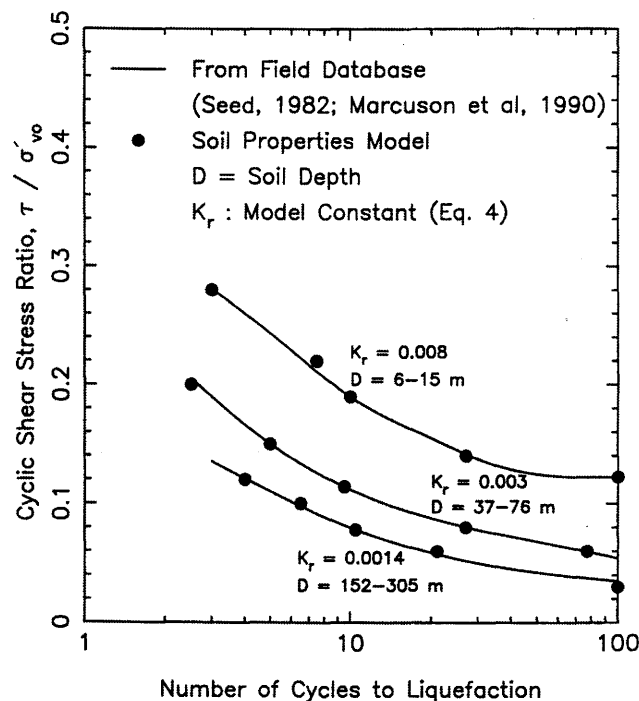


Figure 4. Calibration of porewater pressure model using liquefaction potential curves.

ing stress case. Figure 4 shows that by selecting an appropriate value for K_r , it is possible to closely match a given liquefaction potential curve. The K_r values vary between 0.0085 and 0.0014 when the stress level changes from 30 to 1,980 kPa. Table 1 lists the optimum value of K_r for all the stress levels reported in the EPRI study.

APPLICATION: RENO SITE

The Reno-Carson City urban corridor, the second most populated region in Nevada, is in one of the most seismically active parts of the state. This area is at the western margin of the Basin and Range Province. Based on the historical earthquake record and geological evidence of numerous active faults, chances of having earthquakes with magnitudes more than 6 are quite high in the area. Twelve earthquakes of magnitude 6 or greater, two of which were greater than magnitude 7, have occurred in western Nevada since the 1850s. One fault system that could generate destructive motion in the Reno-Carson City area is the Carson Range fault system. This system bounds the Carson Range on the east and extends from Reno to south of Woodfords, California. It is one of the largest and most active fault system in Nevada. There is evidence preserved in the geologic record that an earthquake of magnitude larger than 7.5 occurred on this fault system about 500 to 650 years ago. The northern part of the system, which extends into southern Reno, is somewhat less active, with activity distributed on multiple fault traces. Shorter fault lengths in the north segment suggest an earthquake with magnitude 7.1 may be a more likely event in the Reno area. This magnitude has been selected as the "scenario earthquake event magnitude" in a recent planning scenario study undertaken by Nevada Bureau of Mines and Geology (de Polo and others, 1996).

Unfortunately there are no accelerograms available in the Reno-Carson City area from a large earthquake. The results presented below employ a synthetic accelerogram as input and gives the soil response for a large earthquake that could affect the Reno area. The synthetic accelerogram, which represents "earthquake-like" excitation, provides a flexible way for performing seismic-hazard assessments because they can be generated from a specific fault plane and propagated to an assumed site using different substructure (earth) models. The segments of the Carson Range fault system close to Reno are the Washoe Valley segment, the Mt. Rose segment, and the Reno segment. These three fault segments are assumed to rupture together to generate the Reno scenario earthquake (dePolo and others, 1996) with a magnitude of 7.1. The locations of these three fault segments, the epicenter, and the site of interest are shown on figure 5. A synthetic accelerogram for a Reno scenario earthquake has been generated from a composite source model (Yu, 1994; Zeng and others, 1994; Anderson and Yu, 1996).

Several studies show that synthetic seismograms from a composite source model can provide realistic estimations of ground motions of future large earthquakes (Su and others, 1994a, 1994b; Zeng and others, 1994; Anderson and Yu, 1996). Fault parameters, such as extent of

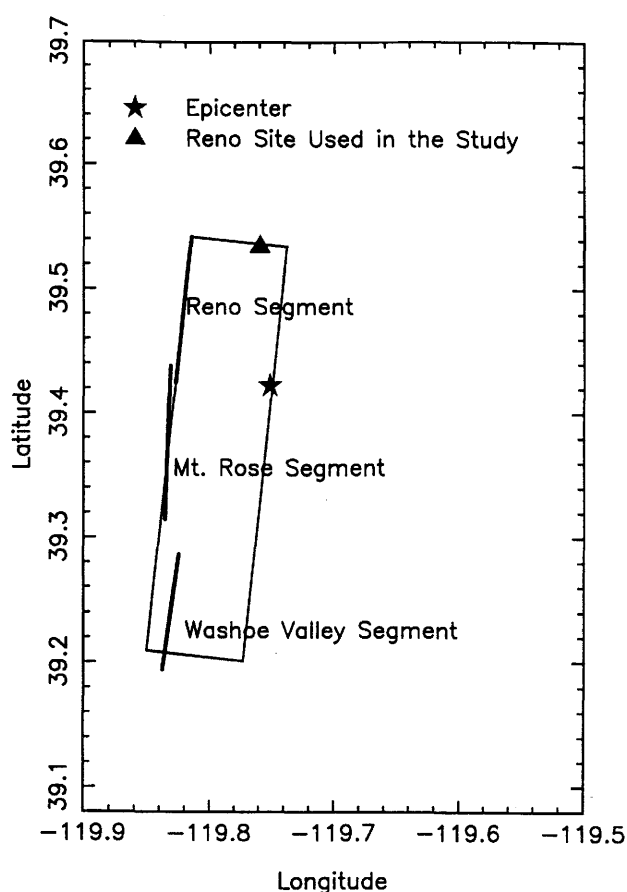


Figure 5. Surface projection of the fault plane, epicenter, and the site used in the development of the Reno scenario seismogram.

fault rupture and displacements which are required to produce the synthetic accelerogram, were obtained from geological descriptions of the faults or from prior experience. The values selected are consistent with the Carson Range fault system and with the historical earthquakes in the Basin and Range Province. The NS component of the corresponding synthetic motion is applied at the base of the soil deposit.

Beeston and others (1992) provided a soil profile and field measured shear-wave velocity for a site near Reno (figure 6). The soil consists of various layers of clay, fine to coarse sand, and gravel. The water table varies at this location, depending on the season, and is assumed to be 3 meters below the surface for this study. Clay layers at 30 to 38 and 60 to 83 meter depths are impervious and incapable of generating porewater pressure. The sand and silty sand layers have a permeability of 10^{-5} m/sec, and are capable of generating porewater pressure when subject to strong shaking.

The soil parameters, γ_v , a , volume change, and porewater-pressure generation parameters of the sand and silty sand layers, have been selected from table 1 ($D_r = 60\%$). The shear modulus reduction and damping properties of the clay strata were assumed to be those given by Vucetic and Dobry (1991). There is no data for shear velocity below 120 meters at this site. It is assumed that bedrock is immediately below the 120 meter soil deposit, and that the shear wave velocity of the rock is 2,500 m/sec as assumed

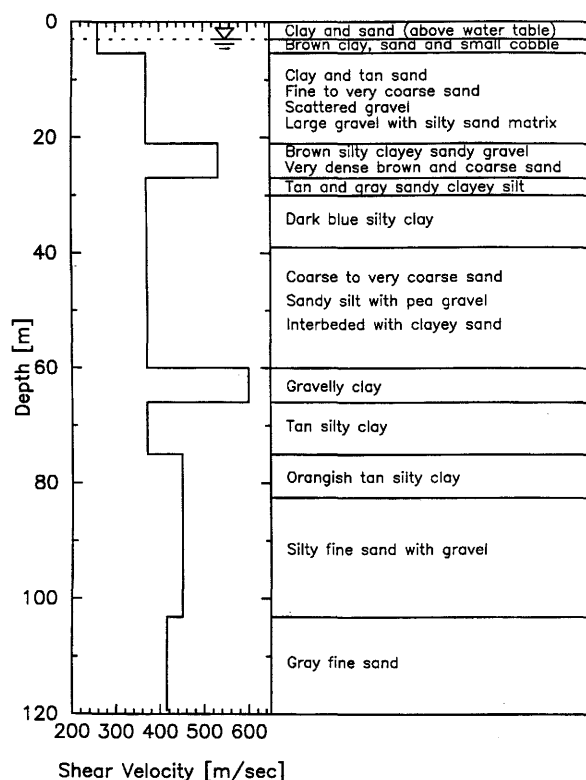


Figure 6. The soil profile at the selected Reno site (after Beeston and others, 1992).

in the composite source model. Recently Ni and others (1997) reported that deep soil deposits (thickness >100 m) showed similar surface amplification and maximum pore-water pressure ratio; and among deep deposits, the deeper the soil deposit the lower the amplification ratio and residual porewater pressure. Therefore, using a 120 meter soil deposit model should give a conservative estimation of soil response.

Figure 7 shows the input seismogram obtained from the composite source model at a depth of 120 meters along with the nonlinear soil response. The base excitation history is shown in figure 7a and has a maximum value of 0.41g. Two types of soil behavior models were used in the response study: a depth- (or stress) dependent properties model and a stress-independent soil behavior model. The properties presented in table 1 are assigned for the stress-dependent soil behavior model. In the case of stress-independent soil behavior model, the soil properties relevant for 100 kPa (second row in table 1) were selected for the entire deposit. The stress-independent soil model has been used routinely in response analysis in the past. Though both soil behavior models show deamplification at the surface, the stress-dependent soil behavior model predicts larger response, i.e., lower attenuation of the input excitation. The surface deamplification ratio in the case of stress-dependant (figure 7b) and stress-independent (figure 7c) soil behavior models are 0.45 and 0.34 respectively.

Many factors influence the response differences between the two soil models. The stress-dependent model is initially stiffer, has lower damping (figure 2), but lower

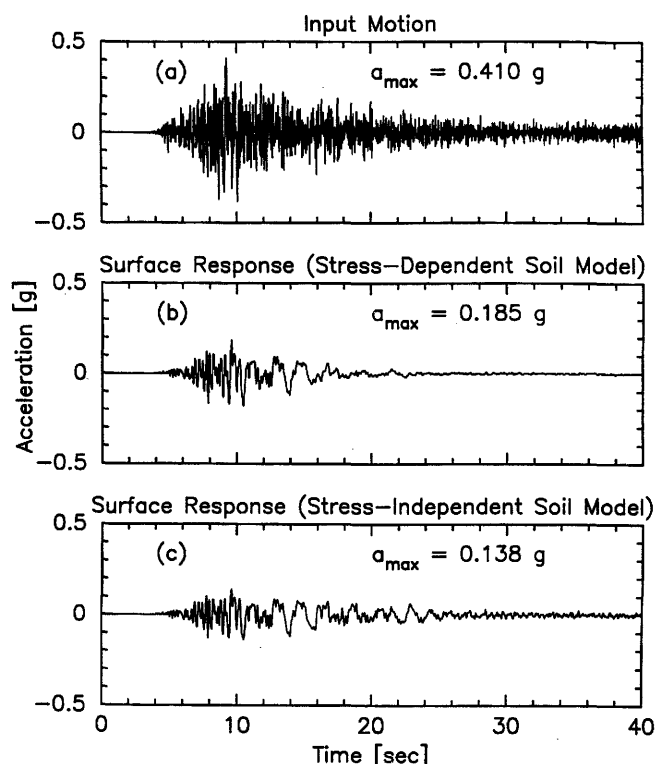


Figure 7. The input synthetic strong motion and the surface soil response at the Reno site.

liquefaction strength (figure 4). Therefore, it is not straightforward to ascertain that the stress-dependent soil properties model will exhibit higher acceleration response. It is clear from this figure that for the field case being studied, the conventionally used soil properties model (stress-independent) will underestimate the surface amplitudes and thus can give rise to unconservative soil amplification response.

Figure 8 shows the maximum porewater-pressure ratios for stress-dependent and stress-independent soil properties models. The difference between these two models is significant for porewater generation. The stress-independent model substantially underestimates the residual porewater pressure. The stress-dependent model predicts liquefaction at depths below 107 meters, and the stress-independent model does not. This deep liquefaction is a consequence of the lower normalized liquefaction resistance for high confining stress (figure 4). It causes additional filtering of high frequencies later in the seismogram as seen in figure 7b. Although consistent with the reported shear velocity profile (figure 6), the assumption that the relative density is constant (60%) is significant for this result. From an engineering perspective, liquefaction at such depths may not be detrimental to structures at the surface.

Thus far, response calculations have been limited to one level of base excitation ($a_{\max} = 0.41g$) caused by the scenario earthquake. Variation of acceleration and porewater pressure response with depth, for excitations from three levels of earthquakes are shown in figures 9 and 10. The synthetic accelerogram (figure 7a) has been scaled to yield three levels of maximum base acceleration of $a_{\max} = 0.2g, 0.4g$ and $0.6g$. Only responses computed within the

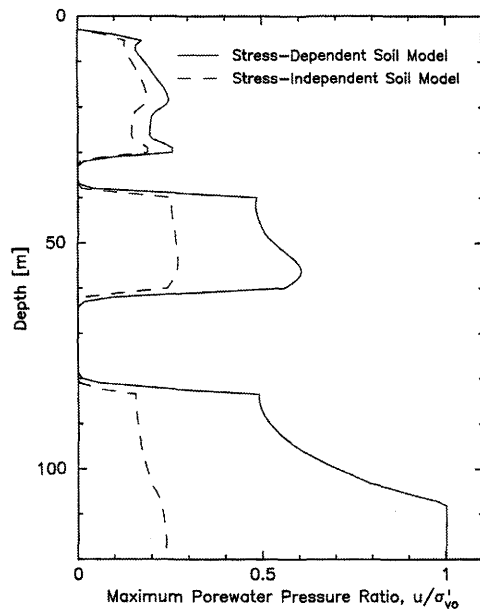


Figure 8. The porewater pressure response at the Reno site.

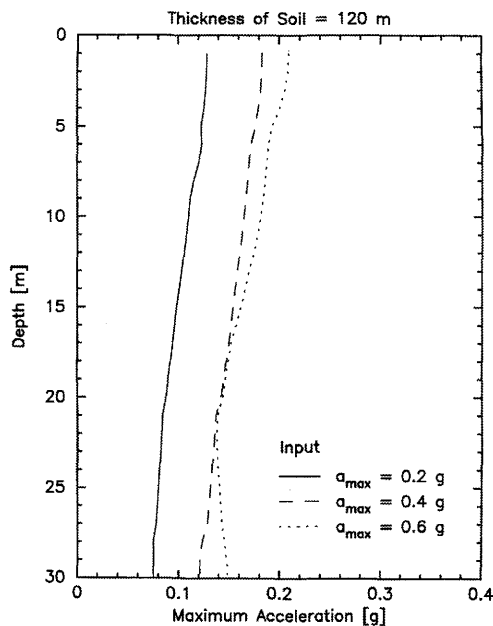


Figure 9. Acceleration response for different excitation levels at the Reno site.

first 30 meters using the stress-dependant soil behavior model are presented. The acceleration variation (figure 9) indicates that the responses are similar above an acceleration level of 0.4g. However, for the porewater-pressure response, there is appreciable difference between the excitation levels $a_{\max} = 0.4g$ and $0.6g$ (figure 10).

CONCLUSIONS

The study presented here used a direct nonlinear approach to investigate the soil response of a deep deposit. The program DESRA2 (Lee and Finn, 1978) has been

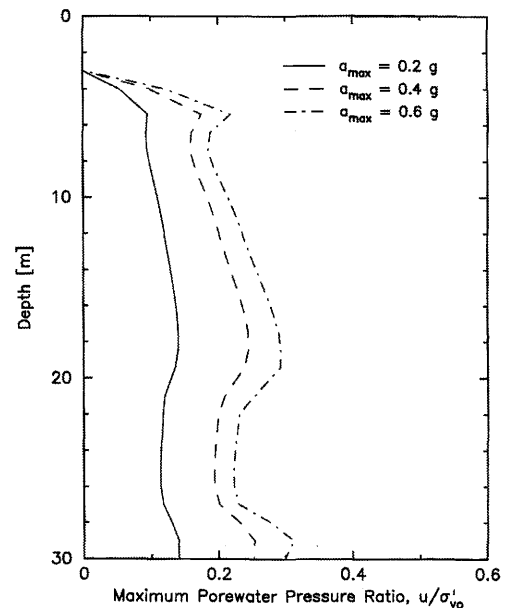


Figure 10. Residual porewater pressure response for different excitation levels at the Reno site.

modified to account for recently developed nonlinear soil property guidelines provided by EPRI. These recent guidelines propose to use depth- (or stress) dependent shear modulus (G/G_{\max}) and damping ζ ratios. The stress-dependent behavior of the liquefaction potential curves (Marcuson and Hynes, 1990) also have been incorporated in the DESRA2 computations. This was achieved by calibrating the porewater-pressure generation model of DESRA2 against the stress-dependent liquefaction potential curves.

"Earthquake-like" excitation was generated using a recently developed composite source model. Since the stress-independent soil properties model has been used routinely in the past, comparisons between the stress-dependent and stress-independent soil properties model responses have been highlighted in the paper. A synthetic strong motion from a magnitude 7.1 earthquake was applied at the base of the deep soil deposit in Reno for which a field measured shear-wave velocity profile is available. The maximum input base acceleration was 0.41 g. Though the stress-dependent and stress-independent soil properties models predict deamplification, the acceleration response computed with the stress-dependent model is much larger. Similarly, the residual porewater pressures generated in the stress-dependent model was higher. The field case study considered here clearly reveals that the soil response computed using a conventional stress-independent soil properties model is unconservative for deep deposits.

ACKNOWLEDGMENTS

We would like to thank the reviewers for an excellent job. This research was supported by the Southern California Earthquake Center (SCEC), whose support is gratefully acknowledged.

REFERENCES

- Anderson, J.G., and Yu, G., 1996, Predictability of strong motions from the Northridge, California earthquake: *Bulletin of the Seismological Society of America*, Vol. 86, p. S100-S125.
- Beeston, H.E., Soltani, A.M., and Cochran, D.G., 1992, Seismic characterization of the Sparks viaduct site for seismic retrofit bridge numbers H866E & H866W: *Geotechnical Report*, State of Nevada, Department of Transportation, Materials and Testing Division, Geotechnical Section.
- Byrne, P.M., 1991, A cyclic shear-volume coupling and pore pressure model for sand: *Proceedings, 2nd International Conference on Recent Advances in Geotechnical Engineering and Soil Dynamics*, St. Louis, Missouri, March, p. 47-55.
- Constantopoulos, I.V., Roesset, J.M., and Christian, J.T., 1973, A comparison of linear and exact nonlinear analysis of soil amplification: *Proceedings, 5th World Conference on Earthquake Engineering*, Rome, p. 1806-1815.
- dePolo, C.M., Rigby, J.G., Johnson, G.L., Jacobson, S.L., Anderson, J.G., and Wythes, T.J., 1996, Planning scenario for a major earthquake in Western Nevada: *Nevada Bureau of Mines and Geology Special Publication No. 20*.
- Electric Power Research Institute, 1993, Guidelines for determining design basic ground motions - Volume 1: Method and guidelines for estimating earthquake ground motion in Eastern North America: *Report EPRI TR-102293*, November, 1993.
- Finn, W.D.L., Lee, M.K.W., and Martin, G.R., 1977, An effective stress model for liquefaction: *Journal Geotechnical Engineering*, ASCE, v. 103, p. 517-533.
- Finn, W.D.L., Martin, G.R., and Lee, M.K.W., 1978, Comparison of dynamic analysis of saturated sand: *Proceedings, ASCE Geotechnical Engineering Division Specialty Conference on Earthquake Engineering and Soil Dynamics*, Pasadena, June, p. 472-491.
- Finn, W.D.L., 1981, Liquefaction potential development since 1976: *Proceedings International Conference on Recent Advances in Geotechnical. Earthquake Engineering and Soil Dynamics*, St. Louis, Missouri, p. 655-681.
- Finn, W.D.L., Iai, S., and Ishihara, K., 1982, Performance of artificial offshore island under water and earthquake loading: *Offshore Technology Conference*, v. I, OTC paper no. 4220, p. 661-672.
- Finn, W.D.L., 1988, Dynamic analysis in geotechnical engineering: *State-of-the-art Report: Earthquake Engineering and Soil Dynamics 2*, ASCE Special Publication, No. 20, p. 523-591.
- Hardin, B.O., and Drnevich, V.P., 1972, Shear modulus and damping in soil: design equations and curves: *Journal of Soil Mechanics and Foundations Division*, ASCE, v. 98, p. 667-692.
- Hushmand, B., Crouse, C.B., Martin, G.R., and Scott, R.F., 1987, Site response and liquefaction studies involving the centrifuge - *Structures and stochastic methods: Elsevier/Computational Mechanics Publication No. 45*, p. 3-24.
- Lee, K.W., and Finn, W.D.L., 1978, DESRA-2: Dynamic effective stress response analysis of soil deposit with energy transmitting boundary including assessment of liquefaction potential: *Soil Mechanics Series*, University of British Columbia, Vancouver, Canada.
- Marcuson, W.F., Hynes, M.E., and Franklin, A.G., 1990, Evaluation and use of residual strength in seismic safety analysis of embankments: *Earthquake Spectra*, v. 6, p. 529-572.
- Martin, G.R., Finn, W.D.L., and Seed, H.B., 1975, Fundamentals of liquefaction under cyclic loading: *Journal of Geotechnical Engineering Division*, ASCE, v. 101, p. 422-438.
- Masing, G., 1926, *Eigenspannungen und Verfestigung beim Messing: Proceedings, 2nd International Congress of Applied Mechanics*, p. 323-335.
- Nakagawa, K., and Soga, K., 1995, Nonlinear cyclic stress-strain relation: *Proceedings, 3rd International Conference on Recent Advances in Geotechnical Earthquake Engineering and Soil Dynamics*, vol. I, St. Louis, p. 57-60.
- Newmark, N.M., 1965, Effects of earthquakes on dams and embankments: *Geotechnique*, v. 15(2), p. 139-160.
- Ni, S.D., Siddharthan, R.V., and Anderson, J.G., 1997, Characteristics of nonlinear response of deep saturated soil deposits: *Bulletin of the Seismological Society of America*, v. 82(2), p. 342-355.
- Schnabel, P.B., Lysmer, J., and Seed, H.B., 1972, SHAKE: A computer program for earthquake response analysis of horizontally layered sites: *Berkeley, University of California, Earthquake Engineering Research Center Report No. EERC 72-12*.
- Seed, H.B., and Idriss, I.M., 1970, Soil moduli and damping factors for dynamic response analysis: *Berkeley, University of California, Earthquake Engineering Research Center, Report EERC 70-10*.
- Seed, H.B., and Idriss, I.M., 1982, Ground motions and soil liquefaction during earthquakes: *Berkeley, California, Earthquake Engineering Research Institute Publication*.
- Streeter, V.L., Wylie, E.B., and Richart, F.E., 1974, Soil motion computation by characteristic method: *Journal of Geotechnical Engineering Division*, ASCE, v. 100, p. 247-263.
- Su, F., Zeng, Y., and Anderson, J.G., 1994a, Simulation of Landers earthquake strong motion using a composite source model: *Seismological Research Letters*, v. 65, p. 52-65.
- Su, F., Zeng, Y., and Anderson, J.G., 1994b, Simulation of Loma Prieta earthquake strong motion using a composite source model: *EOS*, v. 75, p. 448.
- Vucetic, M., and Dobry, R., 1991, Effect of soil plasticity on cyclic response: *Journal of Geotechnical Engineering Division*, ASCE, v. 117, p. 89-107.
- Yu, G., Anderson, J.G., and Siddharthan, R.V., 1993, On the characteristics of nonlinear soil response: *Bulletin of the Seismological Society of America*, v. 83, p. 218-244.
- Yu, G. 1994, Some aspects of earthquake seismology: Slip partitioning along major convergent plate boundary; composite source model for estimation of strong motion and nonlinear soil response modeling: *Reno, University of Nevada, Ph.D. Thesis*.
- Zeng, Y., Anderson, J.G., and Yu, G., 1994, A composite source model for computing realistic synthetic strong ground motions: *Geophysical Research Letters*, v. 21, p. 725-728.

MAGMA INTRUSION AND SEISMIC-HAZARDS ASSESSMENT IN THE BASIN AND RANGE PROVINCE

R.P. Smith

*Idaho National Engineering and Environmental Laboratory, Lockheed-Martin
Idaho Technologies Company, P.O. Box 1625, Mail Stop 2107, Idaho Falls, ID 83415
E-mail: rps3@inel.gov*

S.M. Jackson

*Idaho National Engineering and Environmental Laboratory, Lockheed-Martin
Idaho Technologies Company, P.O. Box 1625, Mail Stop 2107, Idaho Falls, ID 83415
E-mail: smj@inel.gov*

W.R. Hackett

*WRH Associates, 2880 Nonoly Circle, Salt Lake City, UT 82117
E-mail: wrhackett@aol.com*

ABSTRACT

In Basin and Range Province seismic-hazards assessments it is often appropriate to consider the influence of magmatic processes on tectonic faulting. Magma intrusion into the seismogenic crust tends to supplant single, large tectonic earthquakes with swarms of low to moderate magnitude earthquakes. If magma intrusion is not considered, both maximum magnitude and frequency of large earthquakes can be overestimated.

Magma intrusion and normal faulting are fundamental processes of crustal extension. In areas with sufficient magma output rates, extension is accommodated in the upper crust by intrusion of vertical dikes perpendicular to the extension direction and tectonic normal faulting is suppressed or replaced. This is because the dike intrusion process prevents differential stresses from building to levels necessary for normal faulting. Dike intrusion commonly induces surface deformation in extensional volcanic terrains. Surface deformation includes open fissures, monoclines, normal faults, and graben. They are caused by extensional stresses above and ahead of dikes propagating in the shallow subsurface.

The mechanism of dike intrusion and the nature of co-intrusive seismicity have important implications for determination of the maximum magnitude and recurrence of earthquakes. Observational seismicity from volcanic rift zones worldwide suggests the maximum magnitudes of dike-induced earthquakes are 3.8 ± 0.8 . Earthquakes are generally small to moderate because the downdip extent of dike-induced faults and fissures are controlled by the depth to the top of the associated dike (usually < 5 km), permitting only small rupture areas. Also, rupture and displacement on faults and fissures migrate incrementally at about the velocity of propagating dikes (0.5 m/s) as dike dilation stresses the zone above and ahead of the dike. Earthquake recurrence is tied to recurrence of volcanic cycles based on the geochronology of the associated volcanic materials. The volcanic recurrence data must be interpreted as representing recurring periods of co-intrusive seismicity, not the recurrence of individual earthquakes as are typically used for estimating slip rates in normal faults.

Areas where magmatism has affected the activity of Basin and Range normal faults include the eastern Snake River Plain (ESRP) of Idaho, the Mono Basin of eastern California, the Northern Nevada Rift in the central Great Basin, and possibly the Yucca Mountain area of southern Nevada, and the Modoc Plateau-Lassen volcanic highland of northern California. The distribution of Quaternary igneous rocks in the Basin and Range Province shows that magma intrusion may be important over large areas of eastern California, western Nevada, and southwestern Utah.

In the ESRP, Quaternary basaltic magmatism has completely replaced normal faulting as the primary extension mechanism. Northwest-trending volcanic rift zones with both volcanoes and dike-induced extensional structures are the surficial manifestations of magmatic accommodation of northeast-directed extension. In the Mono Basin, volcanism and dike intrusion in the Mono Craters and Inyo Domes, beginning at about 40 thousand years ago, caused shutdown of normal fault slip on the adjacent portions of the Sierra Nevada range-front normal fault. Recognition of magma intrusion as the source of seismicity in place of large, normal-faulting earthquakes can greatly affect seismic-hazards assessments. Because of low magnitudes and long recurrence intervals, the seismic hazard associated with magma intrusion is commonly less than that posed by background (non-surface rupturing) tectonic seismicity.

INTRODUCTION

Special problems sometimes exist for paleoseismology in extensional volcanic environments. The genetic relationship of structures found there to subsurface dike swarms and their formation in cogenetic volcanic rocks, typically lavas, makes them difficult to analyze with conventional paleoseismic field methods (Hackett and others, 1996; Smith and others, 1996).

In extensional volcanic regions worldwide, linear belts of eruptive fissures, tensile fissures, normal faults, flexural monoclines, and graben are developed. These structures commonly develop solely as a consequence of magma intrusion, and magma-induced surface faults with co-intrusive displacements of several meters can form aseismically or be accompanied only by shallow, low-magnitude earthquake swarms (Brandsdottir and Einarsson, 1979). Seismicity, surface faulting, magma intrusion, and volcanism are expressed within many tectonic settings, and extension of the brittle crust is accommodated by a combination of normal faulting and magmatic (dike injection) processes (Bursik and Sieh, 1989; Forslund and Gudmundsson, 1991; Parsons and Thompson, 1991, 1993). The dike intrusion process is emphasized because dike intrusion is a widespread process within the upper crust, regardless of magma type or tectonic setting (Emery and Marrett, 1990; McKenzie and others, 1992).

If traditional methods of determining slip rates and maximum magnitude are applied without consideration of the volcanic record or of the mechanics of magma intrusion, then the estimated frequencies and magnitudes of past seismic events may be overestimated. Recognition of volcanic rift zone structures as the surface expression of intrusion of dikes into the shallow subsurface and application of suitable approaches to the analysis of their seismic potential can prevent such exaggeration. Several areas of the Basin and Range Province, specifically the eastern Snake River Plain of Idaho, the Mono Basin area of California, and the Northern Nevada Rift each illustrate a unique response to coeval extension and magma intrusion into the upper crust.

DIKE-INDUCED STRUCTURES

Structures occurring above shallowly intruding dikes include fissures, fissure swarms, monoclinical flexures, normal faults, and graben. In addition to structural deformation, volcanic constructs also commonly occur. These consist of eruptive fissures, cinder/spatter cones, shield volcanoes, obsidian domes, and tuff rings. They typically occur in linear belts (figure 1), whose orientation is controlled by regional tectonic stress conditions. For example, those in Iceland occur along and parallel to the mid-Atlantic ridge. Those in the Basin and Range Province trend perpendicular to the regional extension direction and thus are parallel or subparallel to normal faults.

MECHANISM OF DIKE-INDUCED SURFACE DEFORMATION

Numerical and scaled empirical experiments on dike intrusion provide a foundation for understanding the origins of dike-induced deformational structures (figures 2 and 3). Numerical modeling of elastic media gives information on the relations between dike geometry, stress and strain distribution, and surface deformation (Pollard and others, 1983; Marquart and Jacoby, 1985; Mastin and Pollard, 1988; Rubin and Pollard, 1988; Rubin, 1992; Roth, 1993; Rubin, 1993). In numerical elastic experiments, dike intrusion produces a broad zone of uplift, with a narrow subsidence zone centered above the propagating dike (figure 2b). The locations of displacement (or strain) maxima are a function of the ratio of dike height (vertical dimension of the dike) to dike depth (distance of dike top below surface). Displacement or strain maxima are symmetrical for vertical dikes, but are asymmetrical for non-vertical dikes (Pollard and others, 1983). The calculated stress field around the dike (Pollard and others, 1983; figure 2b) is generally consistent with field and geodetic observations of strain along active volcanic rift zones undergoing dike intrusion, such as those of Iceland, Hawaii, and Afar (Rubin and Pollard, 1987; Rubin, 1992).

Because real earth deformation is inelastic, normal faults and fissures develop where the tensile zone above the dike top interacts with the earth's surface (Rubin, 1992). Although the regions alongside the propagating dike are under compression (figure 2b), compressional structures are rarely observed in nature (Pollard and others, 1983) because the magnitude of the compressive stress change is small in relation to the compressive strength of the rocks. In contrast, tensile stress often exceeds tensile strength, because rocks are inherently weaker in tension than in compression. The investigation of surface faulting and the formation of other inelastic structures using physical analog models of dike injection (Mastin and Pollard, 1988) allow visualization of the extent and nature of deformation at various stages in the process (figure 3).

CRITERIA FOR FIELD RECOGNITION

Although discrete, dike-induced structures are morphologically similar to non-magmatic extensional structures, several criteria can be used to recognize them in the field.

1. The best criterion is the inferred or demonstrated relationship to cogenetic volcanic materials. In fact, structures formed by dike intrusion are sometimes partially to completely buried by cogenetic volcanic products (usually lavas) that erupt when the dike reaches the surface.

2. Extensional volcanic structures occur in diffuse belts several kilometers wide instead of a narrow zone associated with the surface expression of a normal fault (figure 1).

3. A graben or two zones of non-eruptive fissures commonly occur symmetrically disposed about an eruptive fissure (figure 2a).

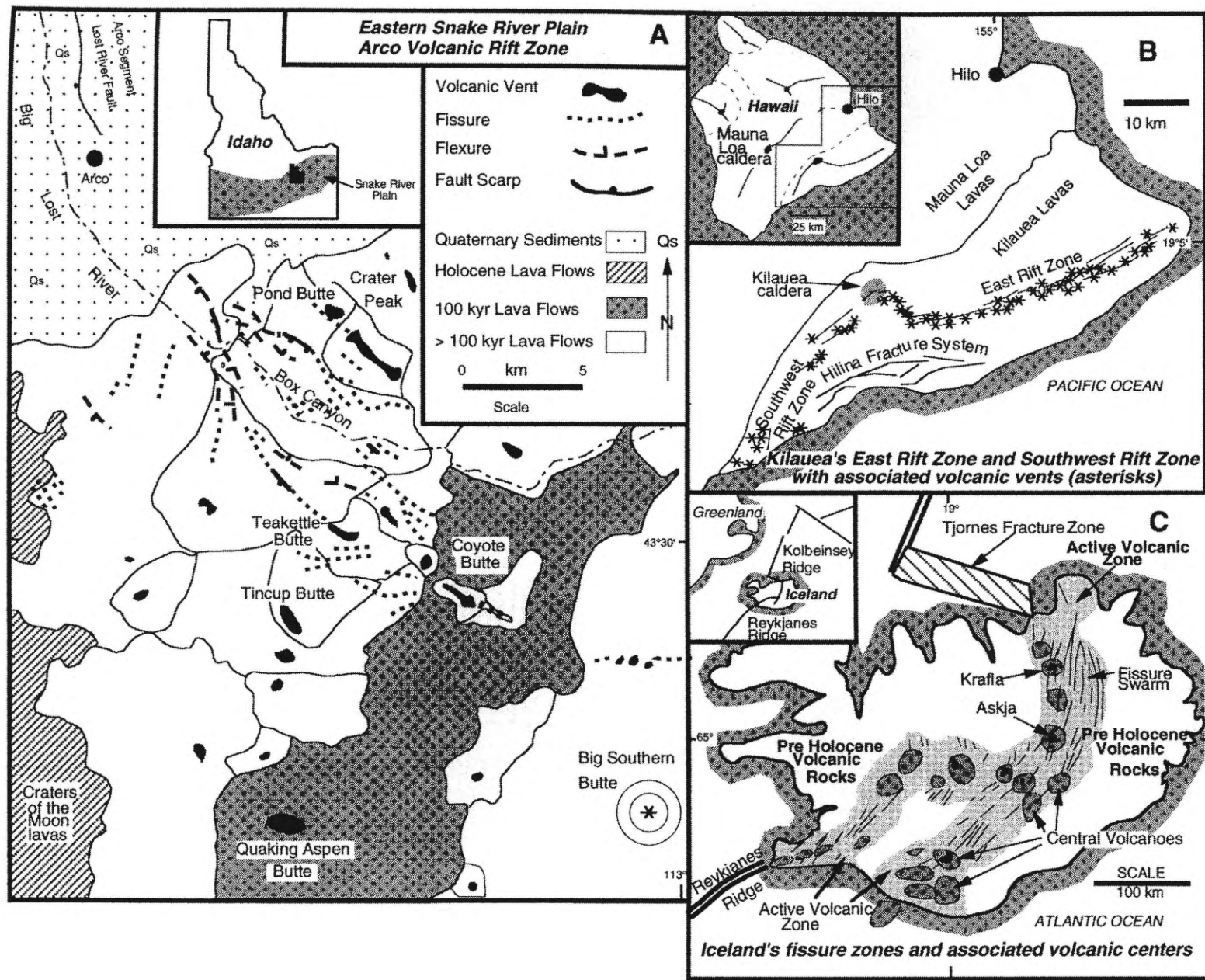


Figure 1. Maps of dike-induced features in the eastern Snake River Plain (A), the island of Hawaii (B), and Iceland (C). Modified from Smith and others, 1996.

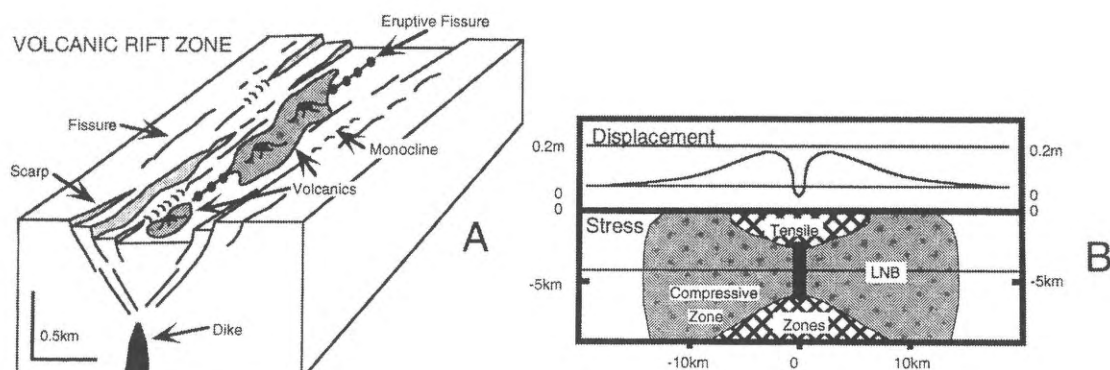


Figure 2. (A) Block diagram showing the relationship between shallow dikes and their surface manifestations. (B) Results of numerical elastic deformation model of dike intrusion (Rubin, 1992) are comparable to observed brittle deformation features. The upper part of the diagram shows a vertical displacement profile above a dike of 1 meter thickness, extending from 1 to 6 kilometer depth. Lower part of the diagram shows the zones of compressive and tensile stress that develop around a dike as a result of magma pressure.

4. Tensional fissures are most abundant (figures 1 and 3), indicating that most of the deformation is purely dilatational.

5. Most vertical offsets are less than 1 meter, but may reach several tens of meters with thick (silicic) dikes or with repeated injection of closely spaced dikes.

6. Vertical displacements typically vary abruptly along strike, and individual faults are short (hundreds of meters to about 10 kilometers), commonly grading into monoclines or purely tensional fissures.

7. On a regional scale, extensional magmatism produces diffuse belts of volcanism, fissuring, and subdued normal-fault scarps. Even after millions of years of extension accompanied by basaltic volcanism and dike intrusion as in Iceland and the eastern Snake River Plain, the terrain is topographically subdued. This is in contrast to extensional provinces that lack substantial magma flux into the upper crust (Parsons and Thompson, 1991), where recurrent faulting is a primary mountain-building process that produces several kilometers of vertical offset, substantial topographic relief, and significant rotation of crustal blocks.

IMPLICATIONS FOR PALEOSEISMIC ANALYSIS

Maximum Magnitudes

There are two approaches for estimation of the maximum magnitude of seismicity in volcanic rift zones. One is to estimate the magnitude from the rupture surface area of fissures and faults, and the other is to use recorded seismicity during dike injection events in active volcanic rift zones as an analogy.

The mechanism of formation of faults and fissures in volcanic rift zones (figures 2 and 3) limits the down-dip extent to a shallow zone above the associated dike top. This zone is commonly only a few hundred meters to about 2 kilometers deep and is not likely to exceed about 5 kilometers, consistent with the depth to the level of neutral buoyancy (Ryan 1987; Rubin, 1992). Even so, estimation of the maximum magnitude from rupture surface area is

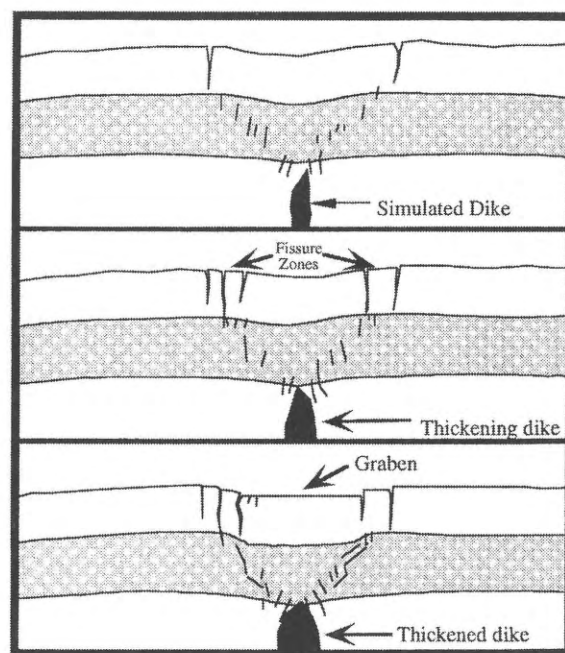


Figure 3. Sketch of results of physical analog experiments of Mastin and Pollard (1988).

an extremely conservative approach because slip typically does not occur instantaneously across an entire fault or fissure surface during a dike injection event. Instead, movement gradually (about 0.5 m/s, the velocity of dike propagation) traverses the shallow subsurface as a migrating swarm of low-magnitude earthquakes around and above the propagating dike.

Geochronology and Recurrence

In contrast to the poorly consolidated sedimentary materials that are shed from rising normal faults and that are typically sought for paleoseismic analysis, volcanogenic structures are commonly developed in volcanic bedrock which is composed of strongly lithified materials that do not produce well-developed colluvial wedges. Therefore, magma-induced structures should be carefully

chosen for analysis and geochronometry. It is often more productive to demonstrate cogenetic or relative relations with volcanic deposits, rather than to attempt excavation and dating of the deformational features themselves.

Since dike-induced faults may lack sufficient displacement or suitable materials for the development of colluvial wedges, it is often more productive, as an alternative to the excavation and direct dating of dike-induced faults and fissures, to focus on mapping and dating the associated volcanic materials. Because earthquakes occur as a consequence of dike injection during magmatic cycles, earthquake recurrence can be estimated by establishing the recurrence interval of volcanic cycles. This requires thorough knowledge of volcanic processes and the regional patterns of volcanism, and should take into account the nature of vent clusters (single dikes can produce several aligned vents).

Even when precise and sufficient age determinations are available from volcanic rocks to confidently establish volcanic recurrence intervals, the information is not analogous to that established by paleoseismic studies of individual normal faults. Each cycle of recurrent volcanism may involve several dike-injection events, and each event in turn may or may not generate earthquake swarms. Conservatism is introduced by assuming only one vent per dike-injection episode, and by adopting a maximum magnitude that is consistent with the largest measured fault dimensions. Added conservatism is introduced by assuming that each dike-intrusion episode produces a maximum magnitude earthquake, even though observed seismicity of numerous dike-intrusion episodes indicates substantial variation in maximum magnitude (tables 1 and 2).

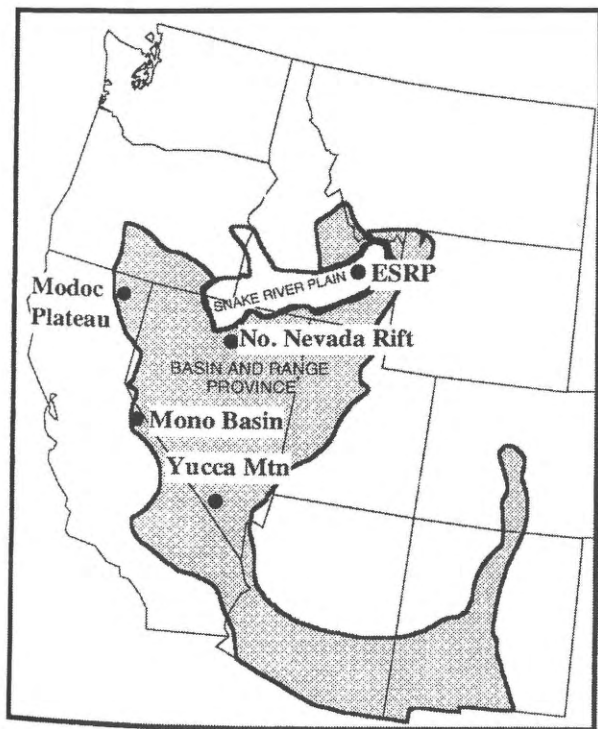


Figure 4. Location of example areas discussed in text. Physiographic provinces of the western United States for reference.

EXAMPLES FROM THE BASIN AND RANGE PROVINCE

Eastern Snake River Plain, Idaho

The eastern Snake River Plain (ESRP) volcanic province transects the northeastern part of the Basin and Range Province (figure 4). Active basin-and-range normal faults die out near the margin of the ESRP (figure 5) and dike-induced faults within volcanic rift zones occur on the ESRP. Seismic-hazards assessments for the INEEL, which occurs near the northeastern boundary of the ESRP, must consider both tectonic normal faults and dike-induced fractures as seismic sources. Additional sources are also considered, including background seismicity in both the Basin and Range Province and the ESRP. The seismic hazard from the tectonic normal faults have been addressed by trenching investigations, mapping of Quaternary deposits along the faults, and detailed structural mapping of the faults.

In order to assess the seismic hazard from volcanic rift zones, we have developed and applied the approaches described in this paper. The approaches facilitate estimation of both the maximum magnitude and recurrence for dike-induced seismicity.

Maximum Magnitude

The upper-bound maximum magnitude for seismicity in the eastern Snake River Plain volcanic rift zones is assessed to be M_w 5.5 (tables 1 and 2, and figure 6).

Recurrence

Recurrence intervals of seismicity were determined from estimated recurrence intervals of volcanic cycles (table 3). Existing whole rock K/Ar age determinations of ESRP basalts (Kuntz and others, 1994) and an independent TL age (Forman and others, 1993, 1994) of the Quaking Aspen Butte lava flow in the Arco volcanic rift zone (figure 1) were used to determine the time period during which each of the volcanic rift zones was active. This information was augmented by existing whole rock K/Ar and paleomagnetic age determinations from two drill holes (Champion and others, 1988). The drill-hole information serves as an independent check for volcanic recurrence intervals determined for volcanic rift zones.

Counting of individual volcanic vents or groups of vents within each of the volcanic rift zones allows estimation of the average time between volcanic cycles and the annual probabilities of recurrence (table 3). Since the injection of a single dike can produce several volcanic vents along or near its trace, there is some judgment involved in estimating the number of volcanic cycles. Criteria for grouping vents into individual dike intrusion events include spatial proximity, geometric alignment, and petrographic and chemical similarities.

Recurrence intervals for volcanic zones on or sufficiently near INEEL to pose a seismic hazard to facilities range from about 16 thousand to 100 thousand years (table 3). The estimation of these numbers is similar to

Table 1. Maximum magnitudes and focal depths of earthquakes associated with dike intrusion^a.

LOCATION ^b	MAGMATIC EVENT ^c (Year)	MAXIMUM MAGNITUDE ^d	FOCAL DEPTH(S) ^e (km)	REFERENCES
Iceland				
Krafla	1975-76	5.0 ^f	0-4	1,2
Krafla	1977	3.8 ^f	0-6	3
Krafla	1978	4.1 ^f	1-4	4
Hawaii, USA				
Kilauea Rift Zones				
East	1965	4.4 (M _L)	0-8	5
East	1968, Aug.	3.3	<5	6
East	1968, Oct.	3.1	<6	6
East	1969	4.7	<7	7
Southwest	1975	3.0	nd	8
East	1976-77	4.0	<10	8
East	1980, Aug.	3.0 (M _c) ^g	0.5-3	9
East	1980, Nov.	3.1 (M _c) ^g	0.7-4	9
Southwest	1981	3.4 (M _c) ^g	1-2	9
East	1982	3.0 (M _c) ^g	0.5-3	9
Africa				
Asal, Afar	1978	5.3(m _b)	0-6	10, 11
New Zealand				
Taupa Volcanic Zone ^h	1964-65	4.6	4-8	12
Taupa Volcanic Zone ^h	1983	4.3	6-10	12
Italy				
Mt. Etna	1989	3.3(M _L)	<4	13,14
Mt. Etna	1991	3.3(M _L)	<6	15
Mean ± sigma; n=18 ⁱ		3.8 ± 0.8		

a - Modified from Hackett and others, (1996).

b - Worldwide dike-injection events associated with mafic magma except for Mono craters which is associated with silicic magma and Mt. Etna which is associated with intermediate magma. Composition of magma for New Zealand episodes are unknown.

c - An episode of dike-injection as defined in text under Section 3.3.

d - Maximum magnitude reported for the dike-injection event. Magnitudes: M_L - Local or Richter; M_c - Coda; m_b - Body-wave; M_s - Surface-wave. No definition of magnitude scale was reported for values without magnitude designation.

e - Depth range of seismicity and maximum magnitude earthquake associated with the dike-intrusion event.

f - Einarsson (1991) reports earthquakes of magnitude ≥ 5.0 are usually associated with caldera deflation events and magnitude ≤ 4.0 with dike injection at Krafla.

g - Coda magnitudes greater than amplitude magnitudes for these events (Nakata and others, 1982; Tanigawa and others, 1981, 1983).

h - This earthquake is interpreted to have triggered magma movement, but was part of an earthquake swarm that began about 10 days prior to a dike-fed submarine eruption (10, 11, 12).

j - Associated with or triggered by dike intrusion, or possibly associated with tectonic subsidence of the basin (15).

k - Minimum estimate of the largest of five historic earthquakes based on liquefaction deposits produced by earthquakes equivocally associated with dike intrusion or tectonic faults (16).

l - Mean and one standard deviation computed based on magnitudes as presented without Mono Craters because its a minimum estimate.

nd - No data obtained.

References: (1) Einarsson & Björnsson, 1979; (2) Björnsson and others, 1977; (3) Brandsdóttir and Einarsson, 1979; (4) Einarsson and Brandsdóttir, 1980; (5) Bosher and Duennbier, 1985; (6) Jackson and others, 1975; (7) Swanson and others, 1976; (8) Dzurišin and others, 1980; (9) Karpin and Thurber, 1987; (10) Okada and Yamamoto, 1991; (11) Takeo, 1992; (12) Oura and others, 1992; (13) Abdallah and others, 1979; (14) Lepine and Hirn, 1992; (15) Grindley and Hull, 1986; (16) Sieh and Bursik, 1986; (17) Bonaccorso and Davis, 1993; (18) Barberi and others, 1990; (19) Ferrucci and Patane, 1993.

Table 2. Maximum magnitudes calculated from normal fault and fissure dimensions in volcanic rift zones.

Eastern Snake River Plain, Idaho Volcanic Rift Zone	Normal Faults or Fissures	Moment Magnitudes (M) ^a			
		Surface Length (km)	Fault Width (km) ^b	Rupture Area SL X DDT	Rupture Area SL X LNB ^c
Great Rift	Fissure	6.4	3.6	5.0	5.8
	Fissure	6.6	4.1	5.4	6.0
	Fissure	6.3	4.1	5.1	5.7
Arco	Fault	5.9	2.5	4.1	5.3
	Fault	5.7	nc	nc	6.4
	Fault	5.6	2.5	4.8	5.6
	Fault	4.9	nc	nc	5.6
	Fissure	4.9	nc	nc	5.6
	Fissure	5.5	nc	nc	6.2
	Fissure	5.2	nc	nc	5.9
	Fissure	4.5	nc	nc	5.2
	Fissure	4.7	nc	nc	5.4
	Fissure	5.1	nc	nc	5.8
	Fissure	4.8	nc	nc	5.5
	Fissure	5.3	nc	nc	6.0
Lava Ridge- Hells Half Acre	Fissure	6.4	3.8	5.1	5.8
	Fissure	5.2	nc	nc	5.9
Spencer- High Point	Fault	6.3	3.4	4.8	5.7
	Fault	6.2	4.3	5.1	5.6
	Fault	6.2	4.1	5.1	5.6
	Fault	6.3	4.6	5.3	5.7
	Fault	5.7	2.9	4.1	5.2
	Fault	5.7	2.9	4.1	5.2
LNB ^c		na	5.4	na	na
Mean ± sigma		5.6 ± 0.7	3.8 ± 0.9	4.9 ± 0.4	5.7 ± 0.3
Range of Values		4.5 - 6.6	2.5 - 4.6	4.1 - 5.4	5.2 - 6.4

SL - Surface length; FW - Fault width; DDT- Depth to the dike top; LNB- Level of neutral buoyancy.

nc - Not calculated because only on fissure of fault exposed and therefore the depth to the dike top could not be estimated (Jackson, 1994).

na - Not applicable.

a - Maximum magnitudes calculated by Jackson (1994) using empirical relationships of Wells and Coppersmith (1994) for surface length, fault width, and rupture area.

b - Fault widths were calculated using graben widths to estimate the depths to the dike top (Jackson, 1994).

c - A fault width of 4.0 km (Jackson, 1994) was used for the level of neutral buoyancy (Ryan, 1987) or depth extent of low tensile strength where dikes propagate within the upper crust (Gudmundsson, 1984).

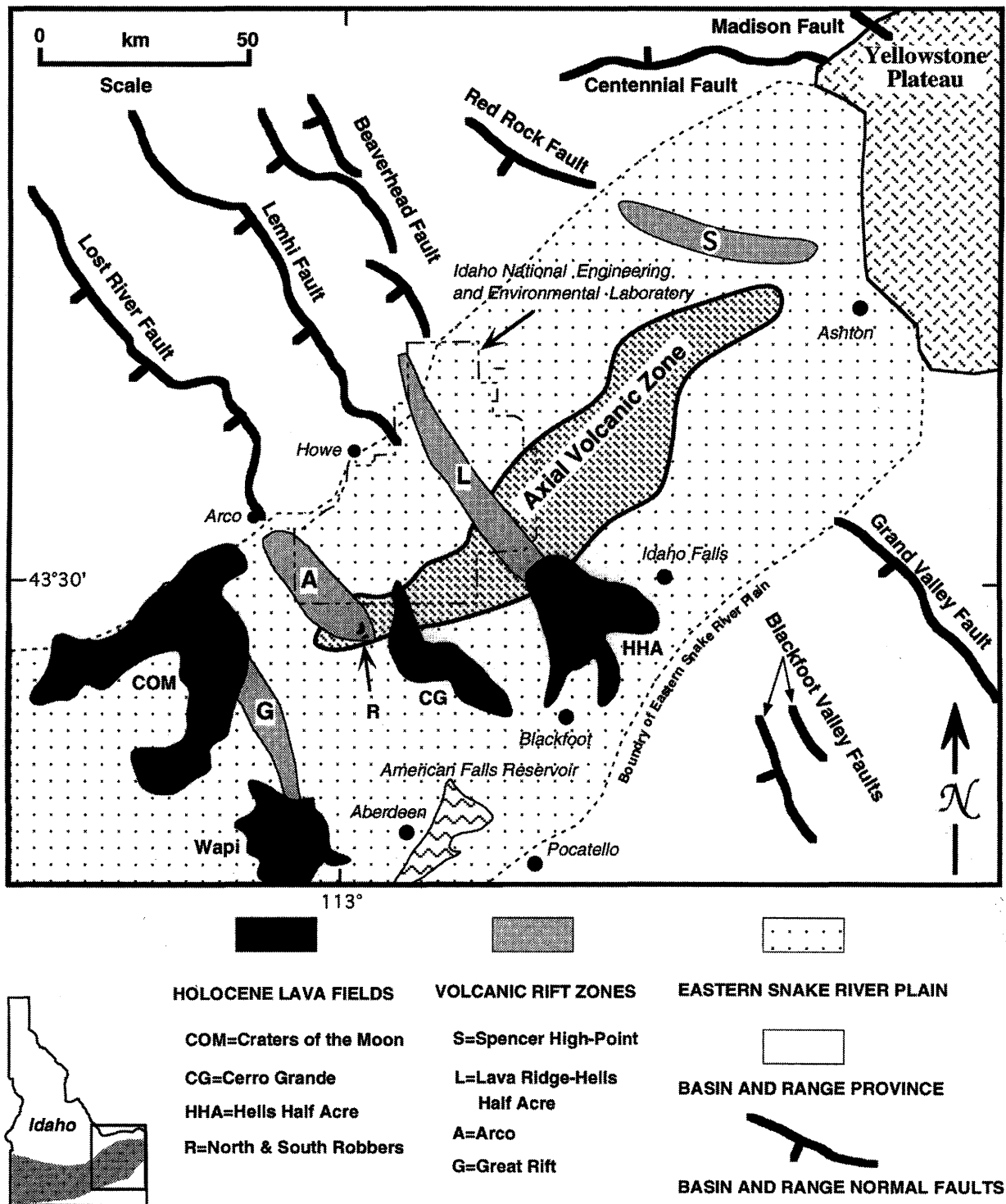


Figure 5. Map of the eastern Snake River Plain showing locations of volcanic rift zones, Holocene volcanic fields, and Basin and Range normal faults.

Table 3. Estimated volcanic recurrence intervals for volcanic rift zones and borehole sites in the INEL area.

VOLCANIC ZONE OR BOREHOLE	DATA SOURCES	TIME INTERVAL OF VOLCANISM [yrs before present]	NUMBER OF VENTS, FISSURES, OR FLOW GROUPS	COMMENTS	ESTIMATED RECURRENCE INTERVAL
Great Rift (25 km southwest of INEL)	Kuntz and others, 1986, 1988	2,100 - 15,000 yrs (radiocarbon dating)	> 100 vents 8 Holocene eruptive periods (each lasting a few decades or centuries, and each including multiple flows and cones).	No impact on INEL; most recently and frequently active of all ESRP rift zones; thus provides minimum-recurrence for entire ESRP; most probable area of future ESRP volcanism	2000 yrs (5×10^{-4} / yr)*
Axial Volcanic Zone (southern INEL)	Kuntz and others, 1986, 1994	5,000 - 730,000 yrs (K-Ar dating; radiocarbon; paleomagnetic data)	73 vents and fissure sets; 4 Holocene lava fields, 3 of them shared by volcanic rift zones. 45 cogenetic vent/fiss gps	Could affect much of southern INEL; most recently and frequently active of all volcanic zones that could impact INEL	16,000 yrs (6.2×10^{-5} / yr)
Arco Volcanic Rift Zone (southwestern INEL)	Kuntz, 1978; Smith and others, 1989; Kuntz and others, 1994	10,000 - 600,000 yrs (radiocarbon, K-Ar, and TL dating; paleomagnetic data)	83 vents & fissure sets; 2 Holocene lava fields. 35 cogenetic vent/fiss gps	Volcanism could affect southwestern INEL	17,000 yrs (5.9×10^{-5} / yr)
Lava Ridge-Hells Half Acre Volcanic Rift Zone (Includes Circle Butte/Kettle Butte Volcanic Rift Zone) (north & east INEL)	Kuntz and others, 1986, 1994	5,000 - 1,200,000 yrs (K-Ar dating; radiocarbon; paleomagnetic data)	48 vents & fissure sets; 1 Holocene lava field: Hells Half Acre. 30 cogenetic vent/fiss gps	Could affect northern & eastern INEL; extremely long eruptive history; includes oldest and youngest basalts in the INEL area	40,000 yrs (2.5×10^{-5} / yr)
Howe-East Butte Volcanic Rift Zone (central INEL)	Kuntz, 1978, 1992; Golder Associates, 1992	230,000 - 730,000 yrs (K-Ar dating; paleomagnetic data)	7 vents & fissure sets. no Holocene features. 5 cogenetic vent/fissure groups	Old, poorly exposed and sediment-covered; identified in part by subsurface geophysical anomalies	100,000 yrs (1×10^{-5} / yr)
Borehole NPR SITE E (south-central INEL)	Champion and others, 1988	230,000 - 640,000 yrs (K-Ar dating; paleomagnetic data)	9 lava-flow groups (each group contains multiple flows, erupted over a short time)	Dates from 600-foot interval of subsurface lavas give recurrence estimate consistent with surficial geology of the area	45,000 yrs (2.2×10^{-5} / yr)
Borehole RWMC 77-1 (southwestern INEL)	Kuntz, 1978; Anderson and Lewis, 1989	100,000 - 565,000 yrs (K-Ar and TL dating; paleomagnetic data)	11 lava-flow groups (each group contains multiple flows, erupted over a short time)	Dates from 600-foot interval of subsurface lavas give longer recurrence interval than nearby Arco and Axial zones, reflecting flow-group (sub-surface) vs. vent-counting (surface geology) approaches	45000 yrs (2.2×10^{-5} / yr)

*annual probabilities of occurrence given in parentheses

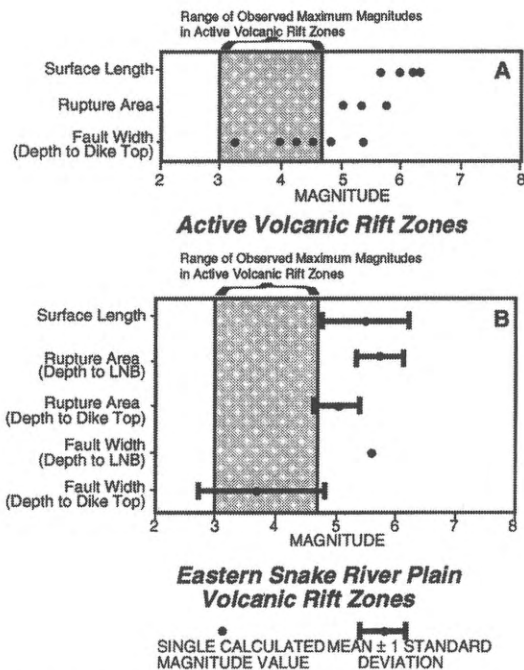


Figure 6. Graphical representation of maximum magnitudes calculated using Wells and Coppersmith's (1994) empirical relationships and dimensions of dike-induced normal faults and fissures in (A) active volcanic rift zones and (B) eastern Snake River Plain volcanic rift zones. Shaded band represents the range of the mean and one standard deviation of maximum magnitudes. ($M = 3.8 \pm 0.8$) observed for dike intrusion episodes worldwide. Adapted from Jackson (1994).

the estimation of slip rate for certain time periods on tectonic faults, but is different in one important aspect. The average recurrence intervals resulting from the analysis of separate volcanic cycles, each of which lasted several years to several hundred years (Kuntz and others, 1992). During those times, one to many dike intrusion events occurred and each was accompanied by a migrating swarm of seismicity.

Mono Basin, California

Bursik and Sieh (1989) used dated glacial deposits in the Sierran range-front fault system and radiocarbon dating of volcanic activity in Mono Basin (figure 4) to show that tectonic faulting in the range-front ceased in the latest Pleistocene and Holocene when dike intrusion began to accommodate extension. As volcanism began in Mono Craters at about 40 thousand years ago those tectonic normal faults directly to the west of the area of volcanism ceased movement. As the volcanism spread southward into the Inyo Domes area and northward into the Mono Lake area during the latest Pleistocene and Holocene time, the shutdown of fault activity also spread to the south and to the north.

Northern Nevada Rift

The Miocene Northern Nevada Rift (figure 4) is characterized by large swarms of mafic dikes that are apparent in magnetic anomalies and in outcrop (Zoback and others, 1994). Scores of dikes ranging in thickness up to 250

meters are exposed in swarms in the Cortez Range and in the Roberts Mountains. They were emplaced about 14 to 17 million years ago, coincident with the eruption of Columbia Plateau basalts, and must have accommodated a large portion of early basin-and-range extension.

Modoc Plateau, California

The northwestern part of the Basin and Range Province encroaches upon the southern end of the Cascade volcanic arc in the Modoc Plateau area of northeastern California (figure 4). Late Tertiary through Holocene volcanic rocks erupted from numerous vents cover the plateau and normal faulting extends westward across the plateau to the eastern foot of the Cascades. Pleistocene to Holocene volcanic centers, such as Lassen Peak and Medicine Lake, contain numerous volcanic vents, often aligned parallel to normal faults in the region. The decreased abundance of basin-and-range faults in the vicinity of these volcanic centers invites speculation. On a regional scale, Guffanti and others (1990) suggest that onset of extension triggered widespread volcanism. At Medicine Lake, Dzurisin and others (1991) propose that recent seismicity and faulting are caused by a combination of volcanic loading of the crust and basin-and-range extension. Our suggestion is that vertical feeder dikes accommodate extension in the vicinity of the volcanic centers, while normal faulting is the extensional mechanism elsewhere.

Yucca Mountain, Nevada

Quaternary extension in the Yucca Mountain area (figure 4) has been accommodated by a combination of normal faulting and basaltic dike intrusion. The intrusion of basaltic feeder dikes for two north- to northeast-trending volcanic alignments in Crater Flat (one at ~4 Myr and one at ~1 Myr; Faulds and others, 1994; Perry, 1994) and for the Lathrop Wells volcano (~100 kyr; Turrin and others, 1991) may help to explain the relatively low slip rates (0.01 to 0.02 mm/year; Menges and others, 1994) of faults in and near the Yucca Mountain block.

CONCLUSIONS AND SUMMARY

The potential for seismicity associated with structures in extensional volcanic terrains can be assessed using an approach that recognizes their genetic relationship to intrusion of dikes in the shallow subsurface and to cogenetic volcanic products. The most successful approaches are not typical of paleoseismic assessments of tectonic faults. Recurrence relationships of volcanic cycles determined from dating the volcanic products are used in place of recurrence intervals for individual earthquakes determined from investigations of colluvial wedges and fault-scarp morphology in unconsolidated deposits. Procedures for dating of individual fissures and scarps in volcanic rift zones are proposed but not yet tested; they have potential problems involving complexities of sediment accumulation and fissure/fault development.

Maximum magnitudes of intrusion-related seismicity can be conservatively estimated by determination of fault/fissure surface areas based on limitation of down-dip extent to the region between the dike top and the surface (usually < 5 km). Such magnitude estimations are usually greater than those instrumentally observed during dike intrusion events in active volcanic rift zones.

Application of the approaches discussed in this paper to dike-induced faults and fissures of the ESRP have been used to assess their seismic potential. In probabilistic seismic-hazards assessments, dike-induced seismicity in the INEEL area is shown to be a minor contributor to the total hazard because of the long recurrence intervals and low to moderate magnitudes.

The distribution of late Quaternary and Holocene volcanic rocks in the Basin and Range Province (Leudke and Smith, 1991) indicates that magma intrusion may have a significant influence on fault movement and seismic hazards in many areas of the Basin and Range Province. Places where dike intrusion has been demonstrated to affect tectonic activity and seismic hazards include the eastern Snake River Plain and the Sierra range front near Mono Basin. We speculate that dike intrusion in several other areas of the Basin and Range Province will eventually be shown to have a significant effect on seismicity and seismic hazards.

REFERENCES

- Abdallah, A., Courtillot, V., Kasser, M., Le Dain, A. Y., Lepine, J. C., Robineau, B., Ruegg, J. C., Tapponnier, P., and Tarantola, A., 1979, Relevance of Afar seismicity and volcanism to the mechanics of accreting plate boundaries: *Nature*, v. 282, p. 17-23.
- Anderson, S.R., and Lewis, B.D., 1989, Stratigraphy of the unsaturated zone at the Radioactive Waste Management Complex, Idaho National Engineering Laboratory, Idaho: U.S. Geological Survey Water Resources Investigations Report 89-4065, IDO-22080, 54 p.
- Barberi, F., Bertagnini, A., and Landi, A., editors, 1990, Mt. Etna: The 1989 eruption: Giannini, Pisa, 75 p.
- Bjornsson, A., Saemundsson, K., Einarsson, P., Tryggvason, E., and Gronvald, K., 1977, Current rifting episode in north Iceland: *Nature*, v. 266, p. 318-323.
- Bonaccorso, A., and Davis, P.M., 1993, Dislocation modeling of the 1989 dike intrusion into the flank of Mount Etna, Sicily: *Journal of Geophysical Research*, v. 98, p. 4,261-4,268.
- Bosher, R., and Duennebie, F. K., 1985, Seismicity associated with the Christmas 1965 event at Kilauea volcano: *Journal of Geophysical Research*, v. 90, p. 4529-4536.
- Brandtsdottir, B., and Einarsson, P., 1979, Seismic activity associated with the September 1977 deflation of the Krafla central volcano in northeastern Iceland: *Journal of Volcanology and Geothermal Research*, v. 6, p. 197-212.
- Bursik, M., and Sieh, P., 1989, Range front faulting and volcanism in the Mono Basin, eastern California: *Journal of Geophysical Research*, v. 94, p. 15,587-15,609.
- Champion, D. E., Lanphere, M. A., and Kuntz, M. A., 1988, Evidence for a new geomagnetic reversal from lava flows in Idaho - discussion of short polarity reversals in the Brunhes and late Matuyama polarity chrons: *Journal of Geophysical Research*, v. 93, no. B10, p. 11,667-11,680.
- Dzurisin, D., Anderson, L.A., Eaton, G.P., Koyanagi, R.Y., Lipman, P.W., Lockwood, J.P., Okamura, R.T., Puniwai, G.S., Sato, M.K., and Yamashita, K.M., 1980, Geophysical observations of Kilauea volcano, Hawaii -- 2. Constraints on the magma supply during November 1975-September 1977: *Journal of Volcanology and Geothermal Research*, v. 7, p. 241-269.
- Dzurisin, D., Donnelly-Nolan, J.M., Evans, J.R., and Walter, S.R., 1991, Crustal subsidence, seismicity and structure near Medicine Lake volcano, California: *Journal of Geophysical Research*, v. 96, p. 16,331-16,333.
- Einarsson, P., 1991, Earthquakes and present-day tectonism in Iceland: *Tectonophysics*, v. 189, p. 261-279.
- Einarsson, P., and Bjornsson, A., 1979, Earthquakes in Iceland: *Jokull*, v. 29, p. 37-43.
- Einarsson, P., and Brandtsdottir, B., 1980, Seismological evidence for lateral magma intrusion during the July 1978 deflation of the Krafla volcano in NE-Iceland: *Journal of Geophysics*, v. 47, p. 160-165.
- Emerman, S.H., and Marrett, R., 1990, Why dikes?: *Geology*, v. 18, p. 231-233.
- Faulds, J.E., Bell, J.W., Feuerbach, D.L., and Ramelli, A.R., 1994, Geologic map of Crater Flat area, Nevada: Nevada Bureau of Mines Geologic Map, 101.
- Ferrucci, F., and Patane', D., 1993, Seismic activity accompanying the outbreak of the 1991-1993 eruption of Mt. Etna (Italy): *Journal of Volcanology and Geothermal Research*, v. 57, p. 125-135.
- Forman, S.L., Smith, R.P., Hackett, W.R., Tullis, J.A., and McDaniel, P.A., 1993, Timing of late Quaternary glaciations in the western United States based on age of loess on the eastern Snake River Plain, Idaho: *Quaternary Research*, v. 40, p. 30-37.
- Forman, S.L., Pierson, J., Smith, R.P., Hackett, W.R., and Valentine, G., 1994, Assessing the accuracy of thermoluminescence for dating baked sediments beneath late Quaternary lava flows, Snake River Plain, Idaho: *Journal of Geophysical Research*, v. 99, no. B8, p. 15,569-15,576.
- Forslund, T., and Gudmundsson, A., 1991, Crustal spreading due to dikes and faults in southwest Iceland: *Journal of Structural Geology*, v. 13, p. 443-457.
- Golder Associates, 1992, New Production Reactor Site Characterization, Volume I: Volcanic Zones Mapping Report, Volume II: Regional Geomorphic Study, and Volume III: NPR Site Geologic Report: EG&G Informal Report EGG-NPR-10625.
- Grindley, G.W., and Hull, A.G., 1986, Historical Taupo earthquakes and earth deformation: *Royal Society of New Zealand Bulletin*, v. 24, p. 173-186.
- Gudmundsson, A., 1984, Tectonic aspects of dykes in northwestern Iceland: *Jokull*, v. 34, p. 81-96.
- Guffanti, M., Clynne, M.A., Smith, J.G., Muffler, L.J.P., and Bullen, T.D., 1990, Late Cenozoic volcanism, subduction, and extension in the Lassen region of California, southern Cascade Range: *Journal of Geophysical Research*, v. 95, p. 19,452-19,464.
- Hackett, W.R., Jackson, S.M., and Smith, R.P., 1996, Paleoseismology of volcanic environments, in McCaig, J.P., editor, *Techniques in Paleoseismology*: Academic Press, San Diego.
- Jackson, D.B., Swanson, D.A., Koyanagi, R.Y., and Wright, T.L., 1975, The August and October 1968 East Rift eruptions of Kilauea vol-

- cano, Hawaii: U.S. Geological Survey Professional Paper 890, 33 p.
- Jackson, S.M., 1994, Magnitudes of earthquakes associated with basalt dike-injection for use in INEL seismic hazards evaluations: EG&G Informal Report EGG-EES-11375, 40 p.
- Karpin, T. L., and Thurber, C. H., 1987, The relationship between earthquakes swarms and magma transport -- Kilauea Volcano, Hawaii: *Pure and Applied Geophysics*, v. 125, p. 971-991.
- Kuntz, M.A., 1978, Geology of the Arco-Big Southern Butte area, eastern Snake River Plain, and potential volcanic hazards to the Radioactive Waste Management Complex and other waste storage and reactor facilities at the Idaho National Engineering Laboratory, Idaho: U. S. Geological Survey Open-File Report 78-691, 70 p.
- Kuntz, M. A., Spiker, E. C., Rubin, M., Champion, D. E., and Lefebvre, R. H., 1986, Radiocarbon studies of latest Pleistocene and Holocene lava flows of the Snake River Plain, Idaho - Data, lessons, interpretations: *Quaternary Research*, v. 25, p. 163-176.
- Kuntz, M. A., Champion, D. E., Lefebvre, R. H., and Covington, H. R., 1988, Geologic map of the Craters of the Moon, Kings Bowl, Wapi lava fields and the Great Rift volcanic rift zone, south-central Idaho: U.S. Geological Survey Miscellaneous Investigations Series Map I-1632, scale 1:100,000.
- Kuntz, M. A., Covington, H. R., and Schorr, L. J., 1992, An overview of basaltic volcanism of the eastern Snake River Plain, Idaho, in Link, P. K., Kuntz, M. A., and Platt, L. B., editors, *Regional geology of eastern Idaho and western Wyoming*: Geological Society of America Memoir 179, p. 227-267.
- Kuntz, M. A., Skipp, B., Lanphere, M. A., Scott, W. E., Pierce, K. L., Dalrymple, G. B., Morgan, L. A., Champion, D. E., Embree, G. F., Smith, R. P., Hackett, W. R., and Rodgers, D. W., 1994, Geologic map of the INEL and adjoining areas, eastern Idaho: U.S. Geological Survey Miscellaneous Investigation Map I-2330, scale 1:100,000.
- Lepine, J.C., and Hirn, D. W., 1992, Seismotectonics in the Republic of Djibouti, linking the Afar Depression and the Gulf of Aden: *Tectonophysics*, v. 209, p. 65-86.
- Leudke, R.G., and Smith, R.L., 1991, Quaternary volcanism in the western conterminous United States, in Morrison R.B., editor, *Quaternary nonglacial geology - conterminous U.S.*: Geological Society of America, *The Geology of North America*, v. K-2, p.75-92.
- Marquart, G., and Jacoby, W., 1985, On the mechanism of magma injection and plate divergence during the Krafla rifting episode in northeast Iceland: *Journal of Geophysical Research*, v. 90, p. 10,178-10,192.
- Mastin, L. G., and Pollard, D. D., 1988, Surface deformation and shallow dike intrusion processes at Inyo Craters, Long Valley, California: *Journal of Geophysical Research*, v. 93, p. 13,221-13,235.
- McKenzie, D., McKenzie, J.M., and Saunders, R.S., 1992, Dike emplacement on Venus and Earth: *Journal of Geophysical Research*, v. 97, p. 15,977-15,990.
- Menges, C.M., Wesling, J.R., Whitney, J.W., Swan, F.H., Coe, J.A., Thomas, A.P., and Oswald, J.A., 1994, Preliminary results of paleoseismic investigations of Quaternary faults on eastern Yucca Mountain, Nye County, Nevada: *High Level Radioactive Waste Management, 5th Annual International Conference Proceedings*, v. 4, p. 2372-2390.
- Nakata, J.S., Tanigawa, W.R., and Klein, F.W., 1982, Hawaiian Volcano Observatory Summary 81, Part 1, Seismic data, January to December, 1981: U.S. Geological Survey Report.
- Parsons, T., and Thompson, G.A., 1991, The role of magma overpressure in suppressing earthquakes and topography -- Worldwide examples: *Science*, v. 253, p. 1399-1402.
- Perry, F.M., 1994, Update on characterization of volcanic features: Presentation to the Advisory Committee on Nuclear Waste, Bethesda, Md. Pollard, D. D., Delaney, P. T., Duffield, W. A., Endo, E. T., and Okamura, A. T., 1983, Surface deformation in volcanic rift zones: *Tectonophysics*, v. 94, p. 541-584.
- Roth, F., 1993, Deformation in a layered crust due to a system of cracks -- Modeling the effect of dike injections or dilatancy: *Journal Geophysical Research*, v. 98, p. 4543-4551.
- Rubin, A. M., 1992, Dike-induced faulting and graben subsidence in volcanic rift zones: *Journal of Geophysical Research*, v. 97, p. 1839-1858.
- Rubin, A. M., 1993, Tensile fracture of rock at high confining pressure: Implications for dike propagation: *Journal of Geophysical Research*, v. 98, p. 15,919-15,936.
- Rubin, A.M., and Pollard, D.D., 1987, Origins of blade-like dikes in volcanic rift zones, in *Volcanism in Hawaii*: U.S. Geological Survey Professional Paper 1350, p.1449-1470.
- Rubin, A. M., and Pollard, D. D., 1988, Dike-induced faulting in rift zones of Iceland and Afar: *Geology*, v. 16, p. 413-417.
- Ryan, M. P., 1987, Neutral buoyancy and the mechanical evolution of magmatic systems, in Mysen, B.O., editor, *Magmatic processes -- Physiochemical principles*: The Geochemical Society Special Publication No. 1, p. 259-287.
- Smith, R. P., Hackett, W. R., and Rodgers, D. W., 1989, Geological aspects of seismic hazards assessments at the INEL, southeastern Idaho: *Proceedings of the Second DOE Natural Hazards Mitigation Conference*: Knoxville, Tennessee, p. 282-289.
- Smith, R.P., Jackson, S.M., and Hackett, W.R., 1996, Paleoseismology and seismic hazards evaluations in extensional volcanic terrains: *Journal of Geophysical Research*, v. 101, no. B3, p. 6277-6292.
- Swanson, D.A., Jackson, D.B., Koyanagi, R.Y., and Wright, T.L., 1976, The February 1969 East Rift eruption of Kilauea volcano, Hawaii: U.S. Geological Survey Professional Paper 891, 30 p.
- Tanigawa, W.R., Nakata, J.S., and Klein, F.W., 1981, Hawaiian Volcano Observatory Summary 80, part 1, Seismic Data, January to December 1980: U.S. Geological Survey Report.
- Tanigawa, W.R., Nakata, J.S., and Klein, F.W., 1983, Hawaiian Volcano Observatory Summary 82, part 1, Seismic Data, January to December 1980: U.S. Geological Survey Report.
- Turrin, B.D., Champion, D., and Fleck, R.J., 1991, $^{40}\text{Ar}/^{39}\text{Ar}$ age of the Lathrop Wells volcanic center, Yucca Mountain, Nevada: *Science*, v. 253, p. 654-657.
- Wells, D.L., and Coppersmith, K.J., 1994, New empirical relationships among magnitude, rupture length, rupture area, and surface displacement: *Bulletin of the Seismological Society of America*, v. 84, p. 974-1002.
- Zoback, M.L., McKee, E.H., Blakely, R.J., and Thompson, G.A., 1994, The northern Nevada rift -- Regional tectono-magmatic relations and middle Miocene stress direction: *Geological Society of America Bulletin*, v. 106, p. 371-382.

RELATION OF GRAVITATIONALLY DRIVEN LITHOSPHERIC EXTENSION TO LOW SLIP-RATE FAULTS AND REGIONAL SEISMIC HAZARDS IN THE WESTERN UNITED STATES

Jeffrey R. Unruh

*William Lettis & Associates, Inc., 1777 Botelho Drive, Suite 262,
Walnut Creek, California 94596*

Leslie J. Sonder

*Department of Earth Sciences, 6105 Fairchild Science Center,
Dartmouth College, Hanover, New Hampshire 03755*

Craig H. Jones

*Cooperative Institute For Research in the Environmental Sciences (CIRES),
Campus Box 216, University of Colorado, Boulder 80309-0216*

ABSTRACT

Quaternary normal faults with very low slip rates (i.e., 10^{-1} mm/yr to 10^{-4} mm/yr) and long recurrence intervals for surface-rupturing events have been documented in the Basin and Range Province, Rio Grande rift, Sierra Nevada, and southern Rocky Mountains. We propose that the slow extension represented by these faults primarily is driven by lithospheric gravitational potential energy (PE). Previous work has shown that over much of the Basin and Range, estimated magnitudes of PE are capable of driving extensional strain rates of 10^{-16} /s to 10^{-15} /s, similar to province-wide average extension rates measured by geodetic and geologic techniques. The Sierra Nevada and southern Rocky Mountains are characterized by high values of PE similar to the Basin and Range, which should give rise to comparable horizontal deviatoric tensile stresses. However, the lithosphere in these regions is significantly thicker, colder, and stronger than in the Basin and Range, and thus is able to support large tensile forces without deforming at equally high rates. Based on our estimates of the average strength of the Sierra Nevada and southern Rocky Mountains lithosphere, the PE available to drive deformation in these regions is sufficient to produce average extension rates of 10^{-18} /s to 10^{-17} /s, at least an order of magnitude less than the average extension rates across the Basin and Range. Local estimates of long-term average late Cenozoic extension rates across these regions, from available geologic and paleoseismic data, are also about 10^{-18} /s to 10^{-17} /s, which is similar to the model predictions at the order-of-magnitude level. Implications of this model for seismic hazards include the following: (1) large areas of the southwestern United States are subject to intrinsic, gravitationally derived tensile forces that are available to drive deformation; (2) average strain rates driven by buoyancy forces are strongly influenced by lithospheric strength; and (3) very slow, gravity-driven lithospheric extension can be accommodated by moderate to large magnitude earthquakes with return periods of 10^4 to 10^5 years.

INTRODUCTION

In this paper we discuss the significance of active, low slip-rate normal faults in mountainous areas of the western United States. In contrast to plate boundary structures (e.g., the San Andreas fault system in western California) and zones of localized deformation in the interior of the Cordillera (e.g., the Wasatch fault system in Utah), where active faults exhibit slip rates on the order of mm/yr to tens of mm/yr, low slip-rate faults in some regions of the western United States exhibit slip rates on the order of 10^{-1} to 10^{-4} mm/yr. Such structures have been recognized and documented by numerous seismic-hazard studies in the mountains of California and Colorado (e.g., Woodward-Clyde Consultants, 1977a, 1977b; Dames and Moore, 1981; Denver Water Department, 1986; Page and others, 1995; William Lettis & Associates and Pacific Gas and Electric Company, 1996), and locally they are recog-

nized as potentially significant seismic sources for engineered and critical facilities. To date, however, low slip-rate normal faults have not been the subject of focused research to place them in a regional tectonic context, or to evaluate quantitatively the forces driving the active - but very slow - extensional deformation of the lithosphere.

We propose that low slip-rate normal faults in the southwestern United States primarily are driven by tensile forces arising from horizontal variations in gravitational potential energy (ΔPE) in the lithosphere. These forces (commonly referred to as buoyancy forces) are intrinsic to the lithosphere, and are distinct from stresses that arise from tractions acting on the margins or base of a lithospheric plate. In the following sections, we first summarize previous work by Jones and others (1996) that evaluates the magnitude of buoyancy forces available to drive deformation in the southwestern United States, and relates those forces to average strain rates through esti-

mates of lithospheric strength. We discuss the implications of relatively strong lithosphere for limiting the rate of gravity-driven extension in the Cordilleran interior. We then describe characteristics of very low slip-rate faults in the Sierra Nevada and southern Rocky Mountains, and compare local geologic estimates of strain rates in these regions with the predictions of our model. Finally, we discuss implications of this model for seismic hazards in areas of slow lithospheric extension.

DRIVING FORCES FOR ACTIVE DEFORMATION OF THE CORDILLERAN INTERIOR

It has long been recognized that gravitational body forces acting on the lithosphere can give rise to large horizontal forces (i.e., buoyancy forces) that are capable of driving deformation in continental interiors (Artyushkov, 1973; Fleitout and Froidevaux, 1982; Molnar and Lyon-Caen, 1988; England and Jackson, 1989). Under the assumption of isostatic compensation of topography, it can be shown that these forces arise from lateral variations in the gravitational potential energy (ΔPE) of the lithosphere. The primary effect of these forces is to thicken or thin the lithosphere (i.e., drive horizontal extension or contraction). In two dimensions, horizontal gradients in the rate of PE-driven extension or contraction may be accommodated by strike-slip faulting, but this is likely to be a local effect subordinate to regional lithospheric thickening or thinning. Buoyancy forces have been invoked by many workers to explain the Tertiary extensional "collapse" of the hinterland of the Mesozoic-early Tertiary Cordilleran orogen (Molnar and Chen, 1983; Coney and Harms, 1984; Sonder and others, 1987).

Jones and others (1996) developed a method for calculating buoyancy forces from seismic observations of lithospheric structure. Their approach consists of the following steps:

- (1) Derive vertical density profiles of the crust from seismic velocity models by using empirical relations between seismic P-wave velocity and rock density (Christensen and Mooney, 1995);
- (2) Use the vertical crustal density profile to calculate the crustal contribution to PE relative to a reference asthenospheric column;
- (3) Use the crustal density distribution to solve for the mass excess in the mantle that contributes to mean buoyant elevation of the region relative to a reference asthenospheric column;
- (4) Using a reasonable model for the distribution of the excess mass in the upper mantle, calculate the mantle contribution to PE relative to the reference asthenospheric column;
- (5) Sum the crustal and mantle contributions to ΔPE to calculate the buoyancy force available to drive deformation.

Using this approach, Jones and others (1996) mapped the present distribution and magnitude of these forces in the southwestern United States (figure 1). They showed

that areas associated with large positive buoyancy forces like the Basin and Range Province and Rio Grande rift correlate with areas of active extension or areas in a state of horizontal deviatoric tension but not extending significantly (Zoback and Zoback, 1989). Similarly, areas associated with negative buoyancy forces like the Transverse Ranges of southern California and the western Great Plains are actively shortening or are in a state of horizontal compressive deviatoric stress.

As an additional test of this hypothesis, Jones and others (1996) presented simple calculations showing that observed strain rates in the southwestern United States are compatible with strain rates that are predicted by applying the calculated buoyancy forces to a lithospheric column with vertically averaged rheology. For example, the mean calculated tensile buoyancy force in the northern Basin and Range is approximately 1.5×10^{12} N/m (Jones and others, 1996; figures 1 and 2). Although the predicted horizontal strain rate is highly dependent on assumptions about the strength of the lithosphere, which in turn depends on rheology, thermal state, and pore fluid pressure, most models of the lithospheric strength of the Basin and Range predict that tensile buoyancy forces of about 10^{12} N/m are sufficient to produce extensional strain rates ranging between 10^{-14} /s and 10^{-16} /s (Sonder and England, 1986; Kuszniir and Park, 1987; Lynch and Morgan, 1987; Jones and others, 1996) (figure 2). These rates are consistent with observed strain rates of 10^{-15} /s to 10^{-16} /s across the Basin and Range determined by analysis of seismicity and geodetic data (Eddington and others, 1987; Ward, 1990; Argus and Gordon, 1991), and thus are consistent with the hypothesis that buoyancy-driven deformation is an important factor in modern Cordilleran tectonics (Jones and others, 1996).

THE ROLE OF LITHOSPHERIC STRENGTH IN GOVERNING REGIONAL STRAIN RATES

In addition to explaining the style and rate of active deformation in the Basin and Range, the PE-based approach can explain the *lack* of geologically significant deformation in other regions of the Cordillera subjected to large tensile buoyancy forces. For example, the southern Rocky Mountains and Colorado Plateau are regions of high positive ΔPE (figure 1), implying the presence of tensile buoyancy forces similar to those of the Basin and Range. Unlike the Basin and Range, however, the southern Rockies and the Colorado Plateau are not regions of significant active extension (here defined as rates $\geq 10^{-16}$ /s), nor have they been subjected to large extensional strains during the Tertiary. Jones and others (1996) suggested that these regions are deforming more slowly than the Great Basin because the underlying lithosphere is stronger and able to support high buoyancy forces without deforming at rates that are high enough to result in significant geomorphic expression of active faulting. For example, estimates of the vertically averaged lithospheric strength in the Colorado Plateau (figure 2) show that the calculated buoyancy force is not sufficient to produce geologically significant deformation. In the case of the southern Rocky Mountains, the predicted extensional strain rates for the

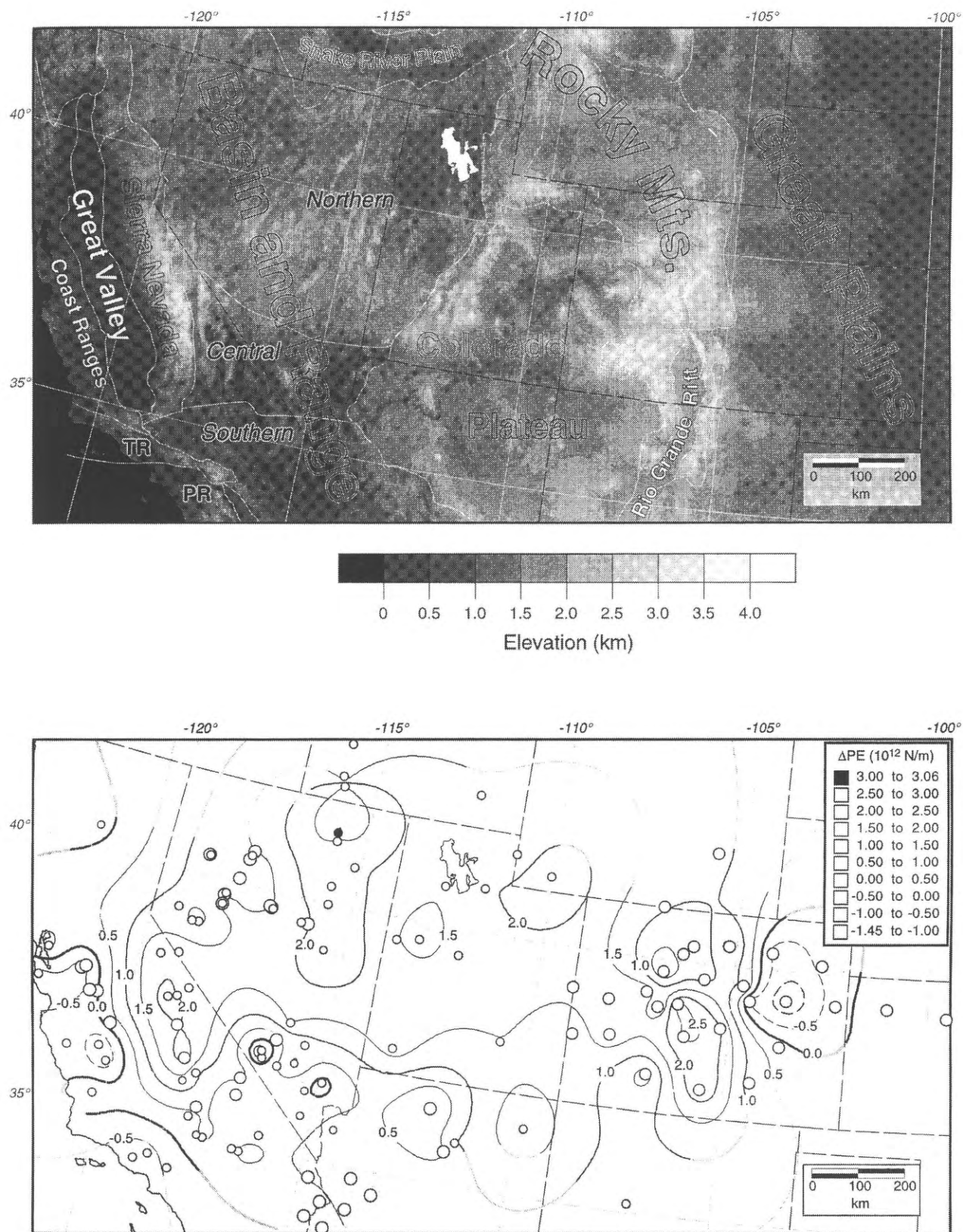


Figure 1. a) Topographic map of the southwestern United States with physiographic province boundaries (modified from color version in Jones and others, 1996); b) Contour plot of buoyancy force (ΔPE) for the southwestern United States (modified from color version in Jones and others, 1996). Contours grayed outside area of some control to show extrapolated ΔPE values.

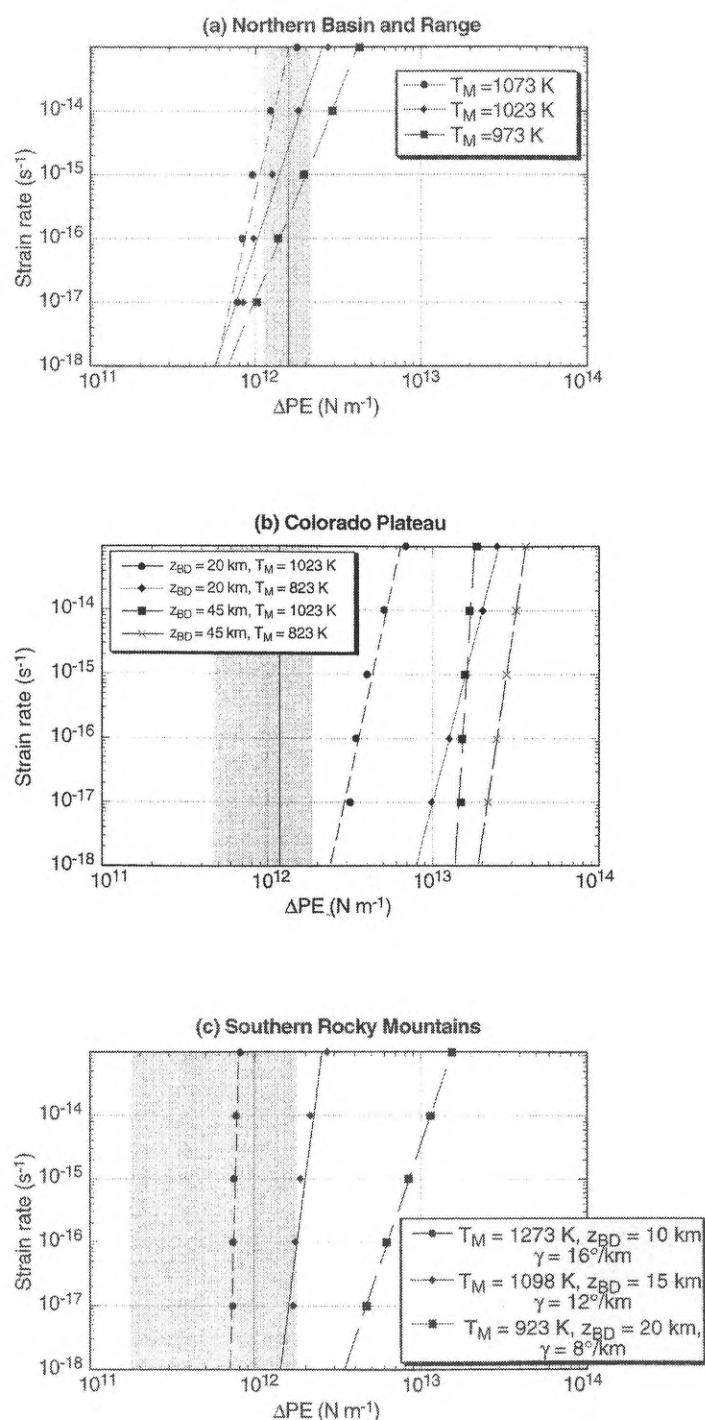


Figure 2. Strength plots for various regions of the western Cordillera that show the magnitude of buoyancy force (ΔPE) necessary to deform a unit column of lithosphere at a given horizontal extensional strain rate. Shaded regions indicate the range of gravitational potential energy available to drive deformation (from figure 1; see also Jones and others, 1996). Strain rates were calculated for given magnitudes of buoyancy force, following Sonder and England (1986), by assuming a brittle upper crustal rheology governed by Byerlee's law with hydrostatic pore fluid pressure, and a ductile lower crust and upper mantle governed by creep mechanisms. Free parameters include crustal thickness (L_c), lithospheric stress state (compressional or extensional), Moho temperature (T_M), depth to the brittle/ductile transition (z_{BD}), and mantle thermal gradient (γ).

calculated tensile buoyancy force is approximately 10^{-18} /s to 10^{-17} /s (figure 2), which is at least one order of magnitude lower than the predicted and observed extensional strain rates in the Basin and Range Province.

Regions that are deforming at such low rates most likely will exhibit low or negligible rates of seismicity and surface faulting. To illustrate the relationship between very slow tectonic deformation and rates of seismicity, consider the following scenario. An average lithospheric strain rate of 10^{-16} /s across a 100-kilometer-wide region is equivalent to an integrated extensional velocity of about 0.3 mm/yr. If there are no vertical gradients in horizontal velocity through the lithosphere, and if this extension rate is accommodated along a given transect across the region by seismic slip on a single normal fault that typically ruptures in M_w 7 events (i.e., average coseismic displacement of about one meter; Wells and Coppersmith, 1994), then the implied average return period for such events is about 2,400 years. If the average extensional strain rate across the region is an order of magnitude lower (i.e., 10^{-17} /s), then the predicted return period for M_w 7 events is at least 20,000 years. Longer return periods are possible if the extension is distributed among several faults; if the average slip per event is greater than one meter; and/or if the average regional strain rate is lower than 10^{-17} /s.

SLOW LITHOSPHERIC EXTENSION IN THE SIERRA NEVADA AND SOUTHERN ROCKY MOUNTAINS

The hypothetical example discussed above suggests that very slow, gravity-driven lithospheric extension at rates of 10^{-16} /s (or lower) can be accommodated by infrequent earthquakes with return periods of thousands of years (or longer). This scenario is consistent with geologic and paleoseismic observations of late Cenozoic normal fault activity in many areas of the Cordillera east of the Central Valley in California. In the following section, we evaluate the hypothesis that low slip-rate normal faults accommodate gravity-driven extension with geologic data from the northern Sierra Nevada in California and the Front Range in central Colorado. We first describe characteristics of Quaternary faulting and seismicity in these regions, then estimate long-term average horizontal extension rates accommodated by low slip-rate normal faults. Finally, we compare the estimated extension rates with predictions from the PE model (Jones and others, 1996).

Characteristics of Low Slip-Rate Normal Faults

Examples From the Sierra Nevada, California

Some of the best-documented examples of low slip-rate normal faults are located in the Sierra Nevada range, eastern California. Although the Sierra Nevada is interpreted to be a relatively rigid, tectonically stable block that is translating northwestward with respect to stable North American as a discrete microplate (Ward, 1990; Argus and Gordon, 1991), regional seismic-hazard studies

have identified numerous faults within the range that have been active since the late Neogene, and which have accommodated minor distributed extension (Woodward-Clyde Consultants, 1977a, 1977b; William Lettis & Associates and Pacific Gas and Electric Company, 1996). A recent compilation that draws on unpublished consulting studies to document these structures is provided by Jennings (1994).

Late Cenozoic normal faults within the Sierra Nevada are commonly, though not exclusively, located along the traces of Mesozoic contractional faults (Woodward-Clyde Consultants, 1977a, 1977b; Bartow, 1980). Several late Cenozoic faults have been identified along the Foothills fault system (Jennings, 1994), a northwest-trending belt of Mesozoic faults that can be traced for approximately 300 kilometers along the central and northern foothills of the western Sierran slope (Clark, 1960). Other examples of late Cenozoic activity have been recognized along the trends of faults at higher elevations on the western Sierran slope (Jennings, 1994) that formed during the late Jurassic Nevadan orogeny (Day and others, 1988). In many cases, cumulative late Cenozoic vertical separation on the faults within the Sierran block is well constrained by displacements of dated Neogene volcanic flows (e.g., Woodward-Clyde Consultants, 1977a, 1977b; Page and others, 1995). These data indicate long-term average slip rates ranging from 10^{-4} mm/yr to 10^{-1} mm/yr, with the lower slip rates generally associated with faults to the west in the Sierran foothills. Detailed geomorphic, stratigraphic, and paleoseismic investigations provide evidence for Quaternary surface-faulting activity on many of these structures (Woodward-Clyde Consultants, 1977a, 1977b; Page and others, 1995; William Lettis & Associates and Pacific Gas and Electric Company, 1996).

Seismologic studies show that the Sierran block is a persistent source of low-level seismicity (Hill and others, 1991; Uhrhammer, 1991; William Lettis & Associates and Pacific Gas and Electric Company, 1996). Focal mechanisms from microearthquakes and small to moderate magnitude events generally indicate normal faulting. The 1975 Oroville earthquake (M 5.7) produced west-side-down normal displacement on a north-striking fault in the northern Sierra foothills and minor surface rupture along one of the strands of the Foothills fault system (Bufe and others, 1976; Clarke and others, 1976; Marks and Lindh, 1978). South of Oroville, Cramer and others (1978) described small earthquakes in the Sierran foothills. Swarms of events with normal faulting focal mechanisms also have been recorded in the Soda Springs area west of Truckee, California (Martinelli, 1989; William Lettis & Associates and Pacific Gas and Electric Company, 1996). A very well-documented example of seismogenic normal faulting in the higher parts of the southern Sierra Nevada is the 1983-84 Durrwood Meadows swarm (Jones and Dollar, 1986). Although the Oroville, Soda Springs, and Durrwood Meadows events generally accommodate normal faulting and crustal extension at seismogenic depths, it should be noted that limited paleoseismic studies of late Cenozoic faults in the Sierra indicate the sense of slip observed at the surface is commonly oblique slip or strike slip (T. Sawyer, personal communication, 1997).

Examples From the Southern Rocky Mountains, Colorado

Late Cenozoic low slip-rate faults also have been documented in the southern Rocky Mountains, where they commonly are associated with contractional structures of the Mesozoic Sevier orogeny (Royse and others, 1975; West, 1993), and the latest Cretaceous-early Tertiary Laramide orogeny (Sales, 1983; Dickson, 1986; Shaffer and Williamson, 1986). In many cases, extensional reactivation of the older thrust faults has led to the development of Neogene and Quaternary basins (Izett, 1975), and in more extreme cases, the "collapse" or "foundering" of basement-cored structural uplifts (Sales, 1983). Examples include development of the Rocky Mountain trench (Royse and others, 1975) and late Cenozoic normal faulting in the Uinta Mountains (Hansen, 1986).

Geologic studies (Witkind, 1976; Kirkham and Rogers, 1981; Colman, 1985), and in particular detailed seismic-hazard assessments conducted during the mid-1980s (e.g., Denver Water Department, 1986), have documented Quaternary extensional reactivation of several Laramide thrust and reverse faults in the Front Range of northern and central Colorado, including: the Golden fault (Kirkham, 1977), the Rampart Range fault (Scott, 1970; Dickson, 1986), and the Chase Gulch fault (Shaffer and Williamson, 1986). Vertical separation rates on these structures estimated from displaced Quaternary strata range from 10^{-1} to 10^{-3} mm/yr (calculated from data in references cited above).

In addition to Quaternary fault studies, investigations of the Front Range included operation of a seismic network to monitor seismicity during the period 1983-1993 (data collected by Microgeophysics Corp.; summarized in Bott and others, 1996, and Unruh and others, 1996). Data collected by this network show persistent levels of seismicity within the Front Range. Seismicity cross-sections across the Front Range in the vicinity of Colorado Springs show subvertical to steeply dipping alignments or clusters of hypocenters extending to depths of about 15 to 17 kilometers (Bott and others, 1996). Upward projections of these alignments suggest that they may be spatially associated with some Laramide faults within the range, although the resolution of the data is not sufficient to confidently associate the seismicity with specific structures (Bott and others, 1996). Regardless of whether the seismicity can be unequivocally associated with mapped surface faults, the data from the Front Range network indicate that discrete seismogenic structures are present within the Front Range that have produced detectable levels of seismicity during the 10-year period of network operation.

The geomorphic expression of low slip-rate normal faults in the Colorado Front Range is significantly different from that of active structures of the northern Rio Grande rift, which borders the southwestern margin of the Front Range. Quaternary faults of the Rio Grande rift generally bound actively subsiding, asymmetric half-graben such as the San Luis Basin in south-central Colorado. The faults form major escarpments along range fronts (e.g., the Sangre de Cristo fault bounding the west-

ern Sangre de Cristo Mountains, southern Colorado); the morphology of scarps formed in Quaternary deposits or geomorphic surfaces suggest multiple late Quaternary surface faulting events; and slip rates calculated from displaced moraines are on the order of several tenths of mm/yr (e.g., McCalpin, 1981). In contrast, the low-slip rate faults in the Front Range to the northeast are not associated with large Quaternary basins; available paleoseismic evidence suggests recurrence intervals for surface-faulting events up to 10^5 years (Kirkham, 1977; Dickson, 1986); and the geomorphic expression of the faults is markedly subdued compared to the active structures of the Rio Grande rift, consistent with a much lower average rate of activity.

Summary

Based on this review of the literature, low slip-rate faults in the Sierra Nevada and Colorado Rocky Mountains exhibit the following characteristics:

- (1) The faults are located outside of zones of concentrated late Cenozoic activity (e.g., the San Andreas fault system in western California; the Walker Lane belt in eastern California and western Nevada);
- (2) The faults are located in areas that have low rates of moderate to large magnitude historical seismicity;
- (3) Late Cenozoic vertical separation rates determined from displacement of Neogene and Quaternary strata generally are 10^{-1} mm/yr or less, with some faults exhibiting long-term average separation rates as low as 10^{-4} mm/yr;
- (4) The late Cenozoic normal-fault traces commonly coincide with or are subparallel to contractional faults that formed during an earlier orogeny;
- (5) The high mountains in which the low slip-rate faults are located exhibit persistent low-level seismicity; and
- (6) In many cases, the faults are apparent only from displacement of Quaternary and/or Neogene strata. The surface expression of late Cenozoic faulting typically is poorly preserved and is discontinuous at best, which suggests that geomorphic features such as scarps formed by coseismic slip on the faults are degraded by weathering and erosion faster than they are renewed by tectonic activity.

Estimated and Predicted Strain Rates

Late Cenozoic Extension of the Northern Sierra Nevada

At the latitude of the Feather River, the northern Sierra Nevada is crossed by flows of the 16 Ma Lovejoy basalt. Detailed mapping and profiling of these flows by Page and others (1995) provide constraints on the total late Cenozoic separation across low slip-rate normal faults in the interior of the range. Based on stratigraphic relations, Sawyer and others (1993) and Page and others (1995) concluded that regional extension of the Sierran block began approximately 5 million years ago, and they used this age constraint on the timing of deformation to estimate average vertical separation rates for faults that displace the Lovejoy basalt (table 1).

The separation rates calculated by Page and others (1995) can be used to estimate average late Cenozoic extension and strain rates of the Sierran block along a north-east-southwest profile approximately at the latitude of the town of Oroville, California (figure 3). To estimate horizontal extension rates from vertical separation rates, we assume that the average dip of the faults extending to seismogenic depths ranges between 45° (the world-wide mean dip of seismogenic normal faults; Thatcher and Hill,

Table 1. Low slip-rate faults west of the northern Sierra crest.

Fault Name	Separation Measured on the 16 Ma Lovejoy Basalt ¹	Long-Term Average Separation Rate ¹ (mm/yr)	Contribution to Long-Term Average Horizontal Extension Rate ² (mm/yr)
Prairie Creek Fault	30 m	0.005	0.003-0.005
Oroville Table Mountain Faults	≤15 m	0.0008	0.0005-0.0008
Sucker Run Fault	20 m	0.0025	0.0014-0.0025
Maynards Fault	20-50 m	0.0083	0.0048-0.0083
Sandborn Mine Fault	60 m	0.012	0.007-0.012
Little Grass Valley Fault ³	240 m	0.04	0.02-0.04
Bottle Springs Fault ³	100 m	0.02	0.01-0.02

Notes:

¹Data taken from table 4 in Page and others (1995).

²Range in extension rate assumes that fault dips range from 60° to 45° .

³Tectonic affinity of faults uncertain. May accommodate a component of Walker Lane deformation.

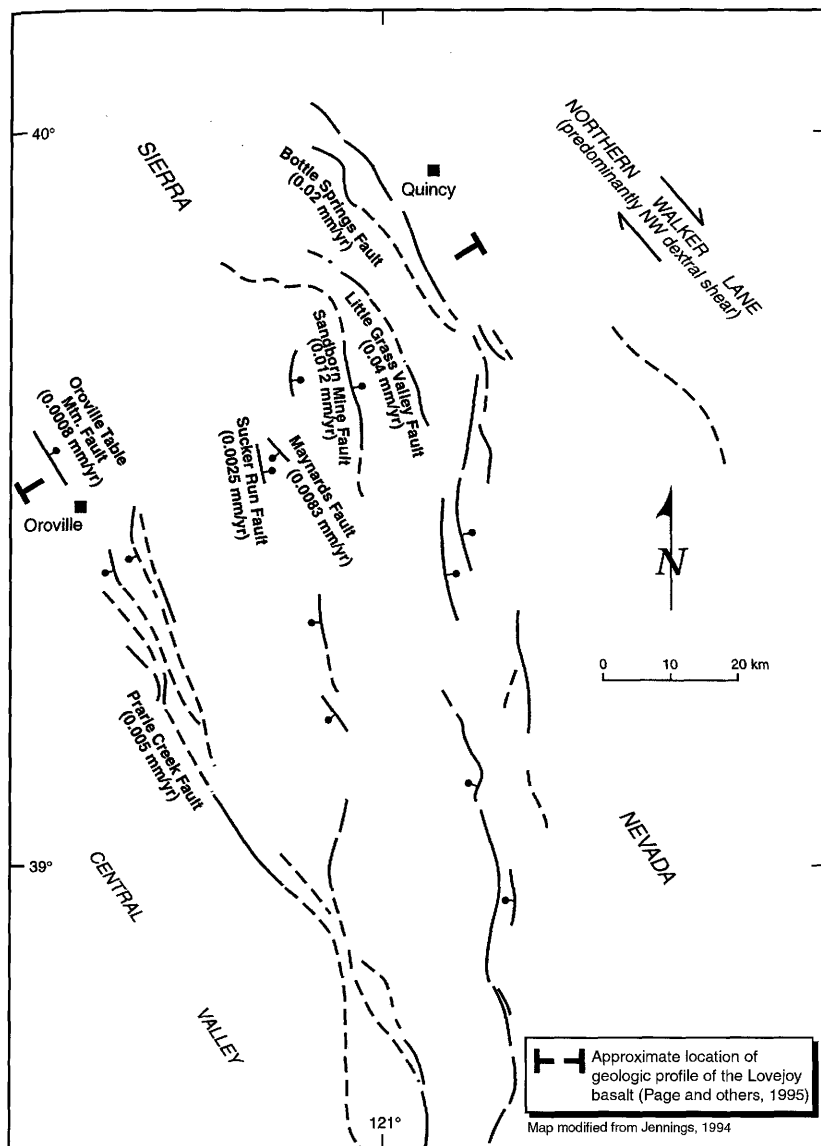


Figure 3. Map of late Cenozoic faults in the northern Sierra Nevada (modified from Jennings, 1994). Many of these structures are parallel to or coincident with the traces of Mesozoic basement faults. Barbs show the location of the traverse used to estimate the late Cenozoic extensional strain rate across the northern Sierra Nevada (see text for discussion).

1991; also see Jackson, 1987) and 60° (the orientation predicted by Coulomb fracture criteria). We sum the extension rates for all faults along the transect and express the cumulative horizontal velocity (in mm/yr) as an average extensional strain rate.

To exclude structures probably belonging to the dextral Walker Lane belt along the eastern margin of the Sierra Nevada, we only consider faults along the western Sierran slope approximately between latitudes 39° and 40° in this analysis (figure 3). The faults that we confidently assign to the Sierran block are listed in table 1, along with the total separation of the Lovejoy basalt across each fault, the long-term average separation rate, and the calculated horizontal extension rate (data from Page and others, 1995).

Also shown in table 1 are data for the Little Grass Valley and Bottle Springs faults, which are located in the

northern Sierran crest but may accommodate a component of strike-slip deformation associated with the Walker Lane belt along the eastern margin of the Sierra Nevada (T.L. Sawyer, personal communication, 1997). Because the tectonic role of these faults is uncertain, we calculate values of long-term average extensional strain rates across the northern Sierra Nevada that both include and exclude these structures, with the caveat that the strain rate that includes the contribution of these faults may over-estimate the internal deformation rate of the Sierran block west of the Walker Lane belt.

The vertical separation rates for faults west of the Little Grass Valley fault contribute to a cumulative horizontal extension rate of approximately 0.017 to 0.029 mm/yr. This corresponds to a range of strain rates from about $8 \times 10^{-18}/s$ to $1 \times 10^{-17}/s$ across the 67 kilometer length of the traverse west of the Little Grass Valley fault. The cumulative horizontal extension rate is 0.05 to 0.09 mm/yr if the Little Grass Valley and Bottle Springs faults are included, which results in an average horizontal strain rate of about $2 \times 10^{-17}/s$ to $4 \times 10^{-17}/s$ along the total 75 kilometer length of the profile. Given the uncertainties involved in the estimates (discussed below), we consider the rates valid at the order-of-magnitude level only, and hence adopt a range of strain rates from $10^{-18}/s$ to $10^{-17}/s$ for the Sierran block at the latitude of Oroville.

Calculated values of the tensile buoyancy force in the Sierra Nevada range from about $1.5\text{--}2.5 \times 10^{12}$ N/m (Jones and others, 1996). For an appropriate range of parameters that affect the strength of the northern Sierra Nevada lithosphere, buoyancy forces of this magnitude can drive extensional strain rates of approximately $10^{-18}/s$ in the region along the traverse (figure 4). Higher strain rates (i.e., $10^{-17}/s$) appear to be possible if the depth to the base of seismicity is relatively shallow (about 15 km) and the upper mantle is relatively warm (Moho temperature at least $\sim 900^\circ\text{C} \pm 100^\circ$), or if pore fluid pressure approaches hydrostatic levels in the upper crust, thereby reducing the brittle strength of the crust.

Strength plots for the Sierran lithosphere (figure 4) indicate that the predicted strain rate is especially sensitive to upper mantle temperatures and the depth to the brittle-ductile transition. Cross-sections of seismicity show that most earthquakes in the northern Sierra at the latitude of the traverse occur above 10–15 kilometers near the crest of the range, with the average base of seismicity deepening to about 20 kilometers beneath the western slope of the range (e.g., cross-section A-A' in figure 11 of Hill and others, 1991; figure 5-14 in William Lettis & Associates and Pacific Gas and Electric Company, 1996). Virtually all of the aftershocks of the 1975 Oroville earthquake sequence in the northern Sierran foothills occurred in the upper 15 kilometers of the crust (Bufe and others,

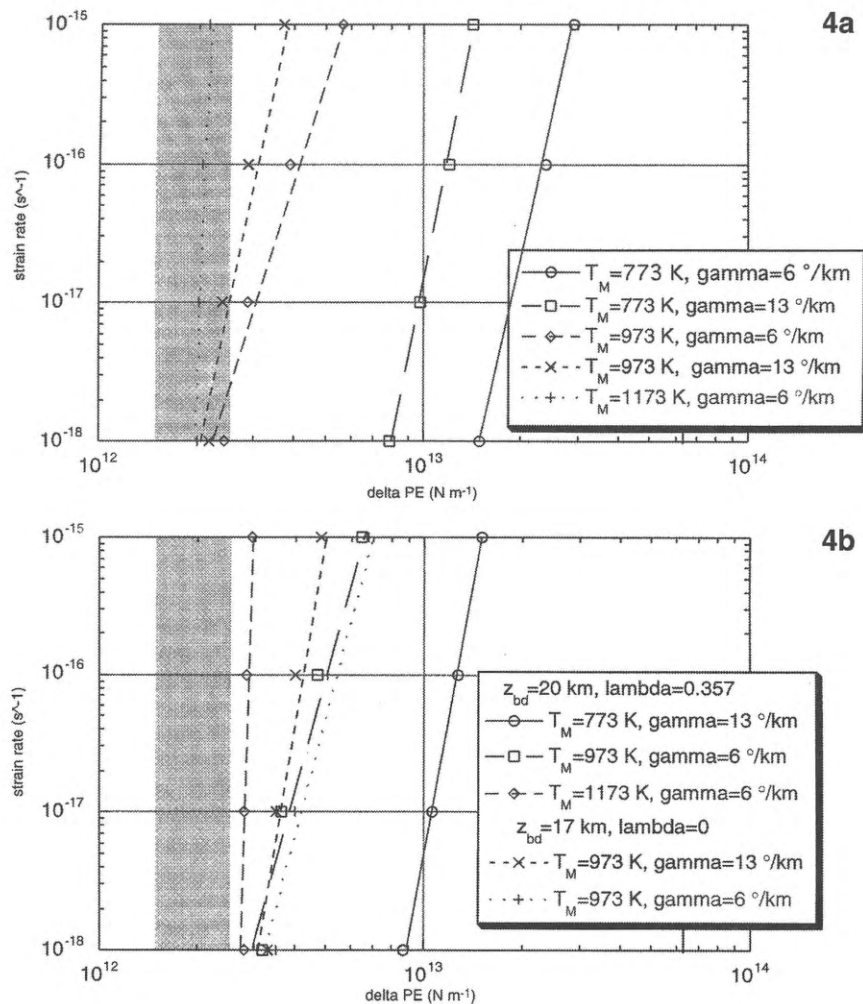


Figure 4. Strength plots for the northern Sierra Nevada showing predicted extensional strain rate for a given magnitude of tensile buoyancy force (see figure 2 for description of parameters shown on the plots). Shaded regions indicate the range of gravitational potential energy available to drive deformation.

4a: Strength of a lithospheric column with a 38-kilometer-thick crust, 17 kilometer depth to the brittle-ductile transition, and hydrostatic pore pressure. Grey region shows range of buoyancy forces calculated for the Sierra Nevada by Jones and others (1996). Plot shows that the available buoyancy force is sufficient to drive strain rates of about 10^{-18} to 10^{-17} /s, provided that upper mantle temperatures are about 900° K or greater.

4b: Strength of a lithospheric column with a 38-kilometer-thick crust with variable depth to the brittle-ductile transition (Z_{bd}), upper mantle temperatures (T_M), upper mantle temperature gradients (γ), hydrostatic pore pressure ($\lambda=0.357$), and dry crust (i.e., zero pore pressure, or $\lambda=0$). Grey region shows range of buoyancy forces calculated for the Sierra Nevada by Jones and others (1996). Note that for this range of parameters the available buoyancy force is not sufficient to produce strain rates of 10^{-18} /s or higher.

1976; Clarke and others, 1976; Marks and Lindh, 1978). These relations suggest that the depth to the brittle-ductile transition at the latitude of the traverse in figure 3 is not anomalously deep and that temperatures are not so low as to permit brittle failure in the uppermost mantle. If so, this would favor slow, gravity-driven extension and low slip-rate normal faulting along the western slope of the northern Sierra Nevada. It should be noted that significant seismicity in the central Sierra Nevada south of figure 1 extends to depths of 30 kilometers or greater (Hill and others, 1991). Also, upper mantle temperatures in the central Sierra Nevada are estimated to be significantly lower

than 900° C (Wong and Chapman, 1990) consistent with the occurrence of deep earthquakes in this region. These data indicate that the profiles in figure 4 cannot be assumed to reflect the strength of the Sierra Nevada as a whole.

In addition to buoyancy forces, a potential source of tectonic stress within the Sierran block is elastic flexure associated with the inferred late Cenozoic uplift and westward tilting of the range. If it is assumed that the Sierra can be modeled as a flexed elastic plate with a free eastern boundary then the simple physical analog for interpreting the distribution of stress in the upper crust is a cantilever beam (Johnson, 1970). The distribution of elastic stresses in such a beam would require horizontal compressive stresses in the vicinity of the hinge of the flexure above a neutral surface, which presumably is somewhere in the middle of the elastic plate. The analogous hinge in the Sierran block is along the western Sierra foothills/Central Valley boundary, and thus the flexed elastic-beam model suggests that this region should be subject to horizontal east-west compressive elastic stresses in the upper crust. The 1975 Oroville earthquake, however, demonstrated that the state of stress in the upper crust is characterized by horizontal east-west tension, not compression, which is not consistent with the predictions of the cantilever beam model. We thus conclude that elastic stresses resulting from the interpreted uplift and tilting of the Sierra Nevada do not provide a good explanation for the distribution or style of faulting along the traverse shown in figure 3.

The major sources of uncertainty in the strain rate estimate are: (1) uncertainty in calculation of vertical separation, (2) errors in assumed fault dip, (3) uncertainty in timing of the onset of extensional deformation, and (4) omission of unmapped or unrecognized faults. The first three of these potential error sources are related to uncertainties in the geologic data about known faults and assumptions used in obtaining extension rates from separation rates. Because the separation values were calculated by projecting the elevations of Lovejoy basalt remnants on topographic maps, the precision is controlled in part by the contour intervals of topographic maps along the profile. Page and others (1995) estimated an uncertainty of about ± 7 to 13 meters for the separation values, depending on the contour interval of the map. If we conservatively adopt a maximum uncertainty of ± 13 meters in the separation for all six faults in table 1, the total contribution to uncertainty in average strain rate along the 75 kilometer length of the profile is $\pm 7 \times 10^{-18}$ /s. Additional uncertainty is associated with correlation of individual flows within the basalt

across erosional gaps in the unit along the length of the traverse (T. Sawyer, personal communication, 1997).

Although the range of fault dips we have adopted for calculating horizontal extension from separation (i.e., 45° to 60°) is supported by empirical data on seismogenic faults (Thatcher and Hill, 1991) and laboratory studies of rock strength, it is possible that the bedrock faults within the northern Sierra Nevada may be very steeply dipping to subvertical, based on analysis of seismic-reflection profiles across bedrock shear zones in the southern Sierran foothills (Miller and Mooney, 1994), and the linearity of fault traces across canyons as deep as 750 meters (T. Sawyer, personal communication, 1997). If so, then the range of fault dips we use overestimates the extension rate. Also, it is possible that slow extensional deformation of the Sierran block has occurred throughout the Neogene, rather than starting about 5 million years ago as inferred by Sawyer and others (1993). If so, separation rates should be calculated over a period of 16 million years rather than 5 million years, which would reduce our estimates of the long-term average horizontal strain rate by a factor of three.

The presence of an unrecognized late Cenozoic fault or faults along the traverse would contribute to an underestimate of the strain rate. The technique of Page and others (1995) is limited by the discontinuous distribution of the Lovejoy basalt along the traverse in figure 3. Geomorphically prominent and laterally continuous lineaments

have been observed along the length of the traverse, but cannot be evaluated because the basalt is locally missing (T. Sawyer, personal communication, 1997). At the order-of-magnitude level, however, only undetected faults with a slip rate that is comparable to or greater than the *combined* slip rate of all of the structures along the traverse would significantly affect the integrated strain-rate estimate. Although we cannot preclude the possibility such faults exist, they should have correspondingly greater geomorphic expression, and thus are at least as likely to be recognized by existing reconnaissance studies of the Sierra Nevada (Woodward-Clyde Consultants, 1977a, 1977b; Page and others, 1995) as the faults shown in table 1.

To summarize, we believe that expressing the horizontal strain rates at the order-of-magnitude level (i.e., $10^{-18}/s$ to $10^{-17}/s$) captures most of the uncertainty, and that the rates used in the analysis above more likely err on the side of overestimating, rather than underestimating, the average late Cenozoic extensional strain rate of the northern Sierra Nevada.

Late Cenozoic Extension of the Southern Front Range, Colorado

We use a similar approach to estimate the average late Cenozoic extensional strain rate across the Front Range at the approximate latitude of Colorado Springs. The two

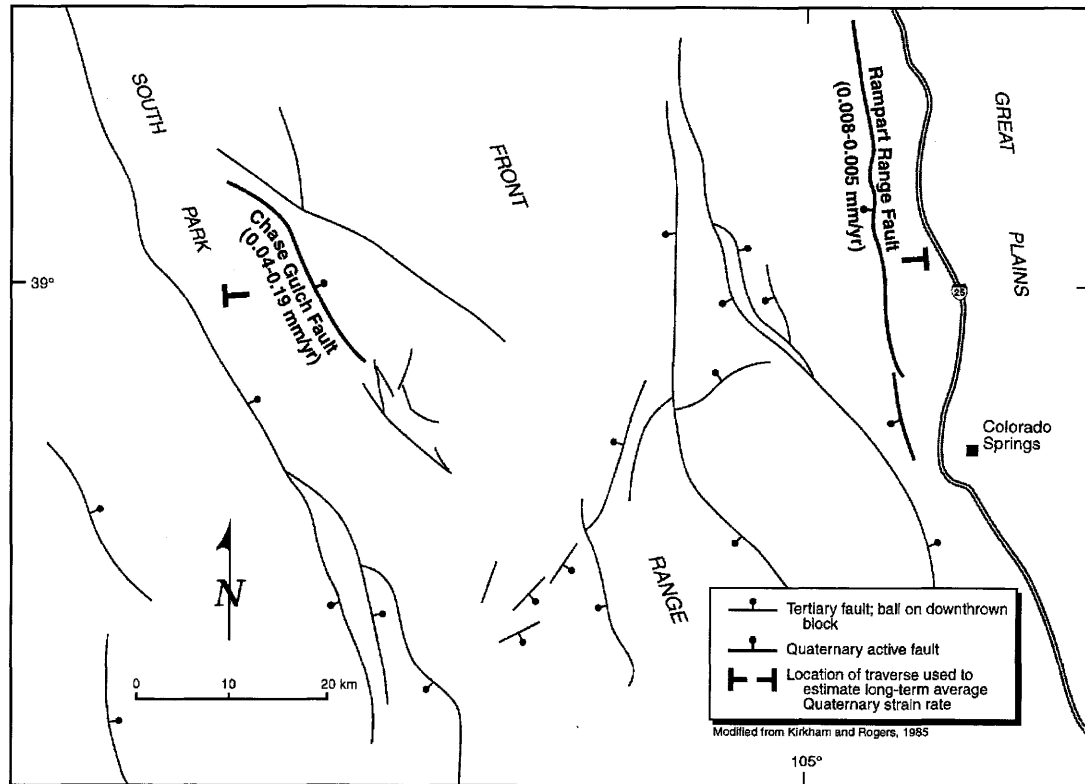


Figure 5. Map of Tertiary and Quaternary faults in the southern Front Range at the latitude of Colorado Springs, Colorado (modified from Kirkham and Rogers, 1981).

Quaternary faults identified along a 70-kilometer-wide transect across the southern Front Range are the Rampart Range and the Chase Gulch faults (figure 5). Long-term Quaternary slip rates and horizontal extension rates for each fault are listed in table 2. The cumulative horizontal extension rate ranges between 0.05 and 0.24 mm/yr. At the order-of-magnitude level, this extension rate corresponds to an average strain rate of about $10^{-17}/s$ along the transect.

The southern Rocky Mountains are characterized by buoyancy forces of approximately 1×10^{12} N/m (Jones and others, 1996). Based on estimates of vertically averaged lithospheric strength in the Colorado Rocky Mountains (figure 2), buoyancy forces of this magnitude should drive extensional strain rates of approximately $10^{-17}/s$. This prediction agrees at the order-of-magnitude level with the long-term average rate across the southern Front Range estimated from geologic data (table 2).

The uncertainties in our estimate of late Cenozoic strain rate across the southern Front Range are similar to those discussed for the northern Sierra Nevada above. Given the order-of-magnitude level of the analysis, the greatest potential source of error is one or more unrecognized Quaternary normal faults with slip rates comparable to or greater than the combined slip rates of the structures listed in table 2. Although we cannot preclude the possibility that such faults are present, we assume that they would have geomorphic expression comparable to or better than the faults listed in table 2. For example, normal faults with slip rates on the order of tenths of mm/yr in the northern Rio Grande rift are associated with well-defined range-front escarpments and graben (e.g., the Sawatch fault in the upper Arkansas basin; Ostenaa and others, 1981). We believe such faults in the Front Range would be recognized by the reconnaissance-level investigations that identified the structures in table 2, and thus we conclude that the average strain-rate estimated for the southern Front Range is robust at the order-of-magnitude level.

DISCUSSION

The examples presented above suggest that long-term average strain rates accommodated by low slip-rate faults in the northern Sierra Nevada and southern Rocky Moun-

tains are consistent with the order-of-magnitude predictions of our model for slow lithospheric extension under the influence of gravitational buoyancy forces. Clearly, additional tests of the hypothesis need to be performed. Geologic data on long-term slip rates in other regions of the Cordillera can be used to estimate strain rates for comparison with the model predictions. Also, focal mechanisms from earthquakes in the Sierra Nevada and southern Rocky Mountains can be analyzed to evaluate the kinematics of active deformation. This approach could be used to distinguish primarily horizontal extension and vertical crustal thinning within the Sierran block from strike-slip faulting and dextral shearing in the Walker Lane belt to the east, and evaluate the contribution of Walker Lane deformation, if any, to the internal deformation of the Sierran block.

Slow extensional deformation of the Sierra Nevada and southern Rocky Mountains is accommodated at least locally by reactivation of pre-existing crustal faults. Because the basement structure in mountain belts almost universally reflects old contractional orogenies, the pre-existing faults typically are thrust or reverse faults. When reactivated to accommodate extension, the observed sense of late Cenozoic slip is opposite from the older sense of slip (e.g., West, 1993). The PE model thus is consistent with observations that Laramide-age basement uplifts in the southern Rocky Mountains have "foundered" or "collapsed" during Tertiary and late Cenozoic extension (e.g., Royse and others, 1975; Sales, 1983).

The identification and characterization of low slip-rate faults for seismic-hazard assessment is problematic because the rates of erosional processes in mountainous regions are comparable to or greater than the deformation rates, leaving a poor stratigraphic or geomorphic record with which to confidently evaluate slip-rate, recurrence intervals, and other measures of neotectonic fault activity. Because most areas of the Cordillera lie outside zones of concentrated tectonism and high deformation rates, this situation tends to be the rule rather than the exception. Also, some deterministic analyses that evaluate strong ground motions resulting from the "maximum credible earthquake" tend to ignore low-slip rate faults because the recurrence intervals for large events may be greater than the cut-off criterion for what constitutes an "active" fault. Thus, the best approach to assess and evaluate the hazard

Table 2. Low slip-rate faults in the southern Front Range, Colorado.

Fault Name	Slip or Separation	Age of Deformed Deposits	Horizontal Extension Rate ³
Rampart Range Fault ¹	8-30 m on the Douglas Mesa gravel	about 600 ka	0.008-0.05 mm/yr
Chase Gulch Fault ²	2.5 m	Late Pinedale (13-35 ka)	0.04-0.19 mm/yr
Notes: ¹ Data from Scott (1970) and Dickson (1986). ² Data from Shaffer and Williamson (1986). ³ Range in extension rate represents assumed range of fault dips from 60° to 45°.			

due to low slip-rate faults probably is through a probabilistic seismic hazard analysis that considers the contribution of these structures to total ground-motion hazard at a site. The PE model provides a theoretical basis for confidently assigning very low rates of activity to normal faults in mountainous regions that lie outside of well-defined zones of active tectonism.

CONCLUSIONS

Our model provides a simple explanation for the occurrence of low slip-rate normal faults in areas of the southwestern United States that arguably lie outside the mechanical influence of the Pacific/North American plate boundary (Sonder and others, 1986). The model implies that some areas of the Cordillera not considered to be regions of significant tectonic activity nonetheless are subject to intrinsic tensile buoyancy forces that are capable of driving deformation and generating rare but potentially significant large earthquakes. The strain rate for a given magnitude of buoyancy force is controlled by the

strength of the lithosphere, and our analysis suggests that the slow rate of extension of the Sierra Nevada and Rocky Mountains is not due to the absence of driving forces, but rather to the intrinsic strength and ability of the lithosphere to support the large buoyancy forces estimated for these regions. The slow extension of such regions under the force of gravity gives rise to very low levels of tectonic activity and seismicity, which can be incorporated in seismic-hazards studies using probabilistic approaches.

ACKNOWLEDGMENTS

We are grateful for critical reviews by Roland Bürgmann (University of California, Davis), Ivan Wong (Woodward-Clyde Consultants), and Tom Sawyer (Piedmont Geosciences), which significantly improved the paper. J.R.U. acknowledges support from the National Science Foundation (grant EAR-9526105), and from the William Lettis & Associates Professional Development Program.

REFERENCES

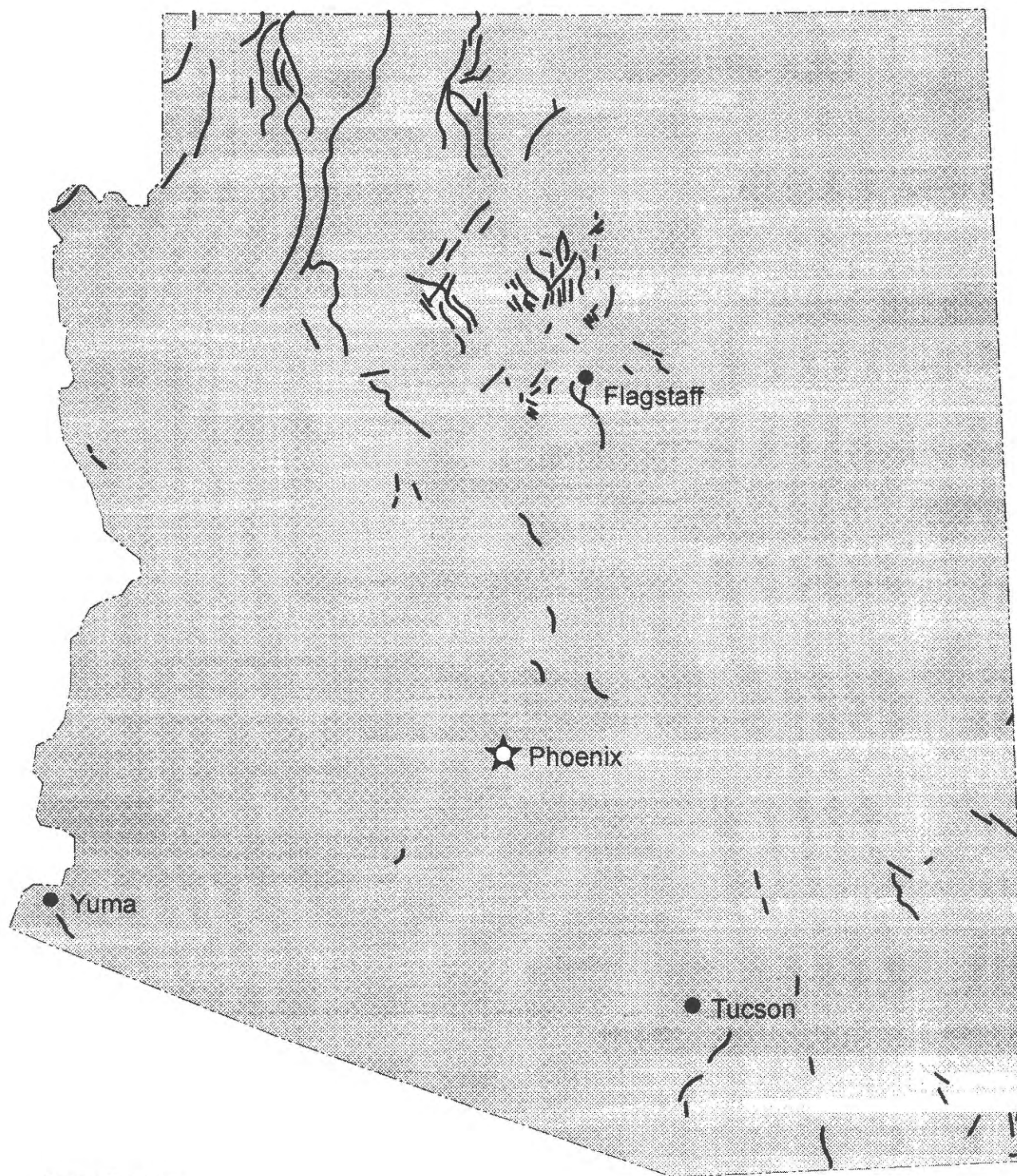
- Argus, D.F., and Gordon, R.G., 1991, Current Sierra Nevada-North American motion from very long baseline interferometry: Implications for the kinematics of the western United States: *Geology*, v. 19, p. 1085-1088.
- Artyushkov, E.V., 1973, Stresses in the lithosphere caused by crustal thickness inhomogeneities: *Journal of Geophysical Research*, v. 78, p. 7675-7708.
- Bartow, J.A., 1980, Constraints on the latest movements of the Melones fault zone, Sierra Nevada foothills, California: United States Geological Survey Professional Paper 1126-J, p. J1-J4.
- Bott, J.D.J., Wong, I.G., Ake, J., Unruh, J., Nicholl, J., and Butler, D., 1996, Contemporary seismicity of the central Front Range, Colorado (abs): Geological Society of America Abstracts with Programs, v. 28, p. A-283.
- Bufe, C.G., Lester, F.W., Lahr, K.M., Lahr, J.C., Seekins, L.C., and Hanks, T.C., 1976, Oroville earthquakes: Normal faulting in the Sierra Nevada foothills: *Science*, v. 192, p. 72-74.
- Christensen, N.I., and Mooney, W.D., 1995, Seismic velocity structure and composition of the continental crust: A global view: *Journal of Geophysical Research*, v. 100, p. 9761-9788.
- Clark, L.D., 1960, The Foothills fault system, western Sierra Nevada, California: Geological Society of America Bulletin, v. 71, p. 483-496.
- Clark, M.M., Sharp, R.V., Castle, R.O., and Harsh, P.W., 1976, Surface faulting near Lake Oroville, California: Bulletin of the Seismological Society of America: v. 66, p. 1101-1110.
- Colman, S.M., 1985, Map showing tectonic features of late Cenozoic origin in Colorado: United States Geological Survey Miscellaneous Investigations Map I-1566, scale 1:1,000,000.
- Coney, P.J., and Harms, T.A., 1984, Cordilleran metamorphic core complexes: Cenozoic extensional relics of Mesozoic compression: *Geology*, v. 12, p. 550-554.
- Cramer, C.H., Toppozada, T.R., and Parke, D.L., 1978, Seismicity in the Foothills fault system between Folsom and Oroville, California: *California Geology*, v. 31, p. 183-185.
- Dames and Moore, 1981, Geologic and seismologic investigation for Rocky Flats plant: Unpublished report for the United States Department of Energy, Contract DE-AC04-80AL10890.
- Day, H.W., Schiffman, P., and Moores, E., 1988, Metamorphism and tectonics of the northern Sierra Nevada, in Ernst, W.G., editor, Metamorphism and crustal evolution, western coterminal United States, Rubey Volume VII: Prentice-Hall, Englewood Cliffs, New Jersey, p. 737-763.
- Denver Water Department, 1986, Geologic and seismotectonic investigations, central Front Range, Colorado: Unpublished summary report, Geotechnical Advisory Committee, Denver, Colorado, 89 p.
- Dickson, P.A., 1986, Investigation of the Rampart Range fault at the Air Force Academy trench site, Colorado Springs, Colorado, in Rogers, W.P., and Kirkham, R.M., editors, Contributions to Colorado seismicity and tectonics--a 1986 update: Colorado Geological Survey Special Publication 28, p. 211-227.
- Eddington, P.K., Smith, R.B., and Renggli, C., 1987, Kinematics of Basin-Range intraplate extension, in Coward, M.P., Dewey, J.F., and Hancock, P.L., editors, Continental extensional tectonics: Geological Society of London Special Publication, no. 28, p. 371-392.
- England, P., and Jackson, J., 1989, Active deformation of the continents: *Annual Review of Earth Planetary Science*, v. 17, p. 197-226.
- Fleitout, L., and Froidevaux, C., 1982, Tectonics and topography for a lithosphere containing density heterogeneities: *Tectonics*, v. 1, p. 21-56.
- Hansen, W.R., 1986, Neogene tectonics and geomorphology of the eastern Uinta Mountains in Utah, Colorado, and Wyoming: United States Geological Survey Professional Paper 1356, 78 p.

- Hill, D.P., Eaton, J.P., Ellsworth, W.L., Cockerham, R.S., Lester, F.W., and Corbett, E.J., 1991, The seismotectonic fabric of central California, in Slemmons, D.B., Engdahl, E.R., Zoback, M.D., and Blackwell, D.D., editors, *Neotectonics of North America: Geological Society of America, Decade Map Volume 1*, p. 107-132.
- Izett, G.A., 1975, Late Cenozoic sedimentation and deformation in northern Colorado and adjoining areas, in Curtis, B.F., editor, *Cenozoic history of the southern Rocky Mountains: Geological Society of America Memoir 144*, p. 197-209.
- Jackson, J. A., 1987, Active normal faulting and crustal extension, in Coward, M.P., and Hancock, P.L., editors, *Continental extensional tectonics: Geological Society of London Special Publication*, no. 28, p. 3-17.
- Jennings, C.W., 1994, Fault activity map of California and adjacent areas, with locations and ages of recent volcanic eruptions: California Division of Mines and Geology, *Geologic Data Map No. 6*, scale 1:750,000.
- Johnson, A.M., 1970, *Physical processes in geology*: Freeman, Cooper and Company, San Francisco, 576 p.
- Jones, L.M., and Dollar, R.S., 1986, Evidence of basin-and-range extensional tectonics in the Sierra Nevada; the Durrwood Meadows swarm, Tulare County, California: *Bulletin of the Seismological Society of America*, v. 76, p. 439-461.
- Jones, C.H., Unruh, J.R., and Sonder, L.J., 1996, The role of gravitational potential energy in active deformation in the southwestern United States: *Nature*, v. 381, p. 37-41.
- Kirkham, R.M., 1977, Quaternary movements on the Golden fault, Colorado: *Geology*, v. 5, p. 689-692.
- Kirkham, R.M., and Rogers, W.P., 1981, Earthquake potential in Colorado: A preliminary evaluation: *Colorado Geological Survey Bulletin 43*, 171 p.
- Kusznir, N.J., and Park, R.G., 1987, The extensional strength of the continental lithosphere: Its dependence on geothermal gradient, crustal composition and thickness, in Coward, M.P., Dewey, J.F., and Hancock, P.L., editors, *Continental extensional tectonics: Geological Society of London Special Publication*, no. 28, p. 35-52.
- Lynch, H.D., and Morgan, P., 1987, The tensile strength of the lithosphere and the localization of extension, in Coward, M.P., Dewey, J.F., and Hancock, P.L., editors, *Continental extensional tectonics: Geological Society of London Special Publication*, no. 28, p. 53-65.
- Marks, S.M., and Lindh, A.G., 1978, Regional seismicity of the Sierra foothills in the vicinity of Oroville, California: *Bulletin of the Seismological Society of America*, v. 58, p. 1725-1767.
- Martinelli, D.M., 1989, *Geophysical investigations of the northern Sierra Nevada-Basin and Range boundary, west-central Nevada and east-central California*: Reno, unpublished M.S. thesis, University of Nevada, 172 p.
- McCalpin, J., 1981, Quaternary geology and neotectonics of the west flank of the northern Sangre de Cristo Mountains, south-central Colorado: Golden, Colorado School of Mines, Ph.D. Dissertation, 287 p. with maps.
- Miller, K.C., and Mooney, W.D., 1994, Crustal structure and composition of the southern Foothills metamorphic belt, Sierra Nevada, California, from seismic data: *Journal of Geophysical Research*, v. 99, p. 6865-6880.
- Molnar, P., and Chen, W.-P., 1983, Focal depths and fault plane solutions of earthquakes under the Tibetan plateau: *Journal of Geophysical Research*, v. 88, p. 1180-1196.
- Molnar, P., and Lyon-Caen, H., 1988, Some simple physical aspects of the support, structure, and evolution of mountain belts, in Clark, S.P., Jr., Burchfield, B.C., and Suppe, J., editors, *Processes in continental lithospheric deformation: Geological Society of America Special Paper 218*, p. 179-207.
- Ostenaar, D.A., Losh, S.L., and Nelson, A.R., 1981, Evidence for recurrent late Quaternary faulting, Sawatch fault, upper Arkansas River Valley, Colorado (abs.): *Seismic Hazards in Colorado: A Symposium: Association of Engineering Geologists*.
- Page, W.D., Sawyer, T.L., and Renne, P.R., 1995, Tectonic deformation of the Lovejoy basalt, a late Cenozoic strain gauge across the northern Sierra Nevada and Diamond Mountains, California, in Page, W.D., editor, *Quaternary geology along the boundary between Modoc Plateau, southern Cascade Mountains and northern Sierra Nevada: Guidebook, Friends of the Pleistocene-1995 Pacific Cell Field Trip*, Appendix 3-3A.
- Royse, F., Warner, M.A., and Reese, D.L., 1975, Thrust belt structural geometry and related stratigraphic problems, Wyoming-Idaho-northern Utah, in Bolyard, D.W., editors, *Deep drilling frontiers of the central Rocky Mountains: Rocky Mountain Association of Geologists*, p. 41-54.
- Sales, J.K., 1983, Collapse of Rocky Mountain basement uplifts, in Lowell, J.D., and Gries, R., editors, *Rocky Mountain foreland basins and uplifts: Rocky Mountain Association of Geologists*, p. 79-97.
- Sawyer, T.L., Wakabayashi, J., Page, W.D., Thompson, S.C., and Ely, R.W., 1993, Late Cenozoic internal deformation of the northern and central Sierra Nevada, California: A new perspective: EOS (Transactions, American Geophysical Union), Fall meeting supplement, p. 609.
- Scott, G.R., 1970, Quaternary faulting and potential earthquakes in east-central Colorado: U. S. Geological Survey Professional Paper 700-C, p. C11-C18.
- Shaffer, M.E., and Williamson, J.V., 1986, Seismic evaluation of Spinney Mountain dam, in Rogers, W.P., and Kirkham, R.M., editors, *Contributions to Colorado seismicity and tectonics--a 1986 update: Colorado Geological Survey Special Publication 28*, p. 104-121.
- Sonder, L.J., and England, P.C., 1986, Vertical averages of rheology of the continental lithosphere: Relation to thin sheet parameters: *Earth and Planetary Science Letters*, v. 77, p. 81-90.
- Sonder, L.J., England, P.C., and Houseman, G.A., 1986, Continuum calculations of continental deformation in transcurrent environments: *Journal of Geophysical Research*, v. 91, p. 4797-4810.
- Sonder, L.J., England, P.C., Wernicke, B.P., and Christiansen, R.L., 1987, A physical model for the Cenozoic extension of western North America, in Coward, M.P., Dewey, J.F., and Hancock, P.L., editors, *Continental extensional tectonics: Geological Society of London Special Publication 28*, p. 187-201.
- Thatcher, W., and Hill, D.P., 1991, Fault orientations in extensional and conjugate strike-slip environments and their implications: *Geology*, v. 19, p. 1116-1120.
- Uhrhammer, R.A., 1991, Northern California seismicity, in Slemmons, D.B., Engdahl, E.R., Zoback, M.D., and Blackwell, D.D., editors, *Neotectonics of North America: Geological Society of America, Decade Map Volume 1*, p. 99-106.
- Unruh, J.R., Wong, I.G., Knudsen, K.L., Bott, J.D.J., Becker, A., Silva, W., and Lettis, W.R., 1996, *Seismotectonic evaluation: Rattlesnake and Flatiron dams, Colorado-Big Thompson Project: Unpublished Final Seismotectonic Report prepared for the United States Bureau of Reclamation, Denver, Colorado, by William Lettis & Associates*, 174

- p. with appendices.
- VanWormer, J., and Ryall, A., 1980, Sierra Nevada-Great Basin boundary zone: Earthquake hazard related to structure, active tectonic processes, and anomalous patterns of earthquake occurrence: *Bulletin of the Seismological Society of America*, v. 70, p. 1557-1572.
- Ward, S.N., 1990, Pacific-North American plate motions: New results from very-long baseline interferometry: *Journal of Geophysical Research*, v. 95, p. 21,965-21,981.
- Wells, D.L., and Coppersmith, K.J., 1994, New empirical relationships among magnitude, rupture length, rupture width, rupture area, and surface displacement: *Bulletin of the Seismological Society of America*, v. 84, p. 974-1002.
- West, M.W., 1993, Extensional reactivation of thrust faults accompanied by coseismic surface rupture, southwestern Wyoming and north-central Utah: *Geological Society of America Bulletin*, v. 105, p. 1137-1150.
- William Lettis & Associates and Pacific Gas and Electric Company, 1996, Lake Almanor and Butt Valley dams seismic-stability assessment, volume 1: Seismic source characterization and estimated ground motions: Unpublished report prepared for Pacific Gas and Electric Company, 272 p. with figures, maps and appendices.
- Witkind, I.J., 1976, Preliminary map showing known and suspected active faults in Colorado: United States Geological Survey Open-File report 76-0154, scale 1:500,000.
- Wong, I.G., and Chapman, D.S., 1990, Deep intraplate earthquakes in the western United States and their relationship to lithospheric temperatures: *Bulletin of the Seismological Society of America*, v. 80, p. 589-599.
- Woodward-Clyde Consultants, 1977a, Earthquake evaluation studies of the Auburn Dam area, 8 vols.
- Woodward-Clyde Consultants, 1977b, Site geology, in Early site review report for the Stanislaus Nuclear project, section 2.5.1: Unpublished report prepared for Pacific Gas and Electric Company, San Francisco, California.
- Zoback, M.D., and Zoback, M.L., 1989, Tectonic stress field of the continental United States, in Pakiser, L.C., and Mooney, W.D., editors, *Geophysical framework of the continental United States: Geological Society of America Memoir 172*, p. 523-540.

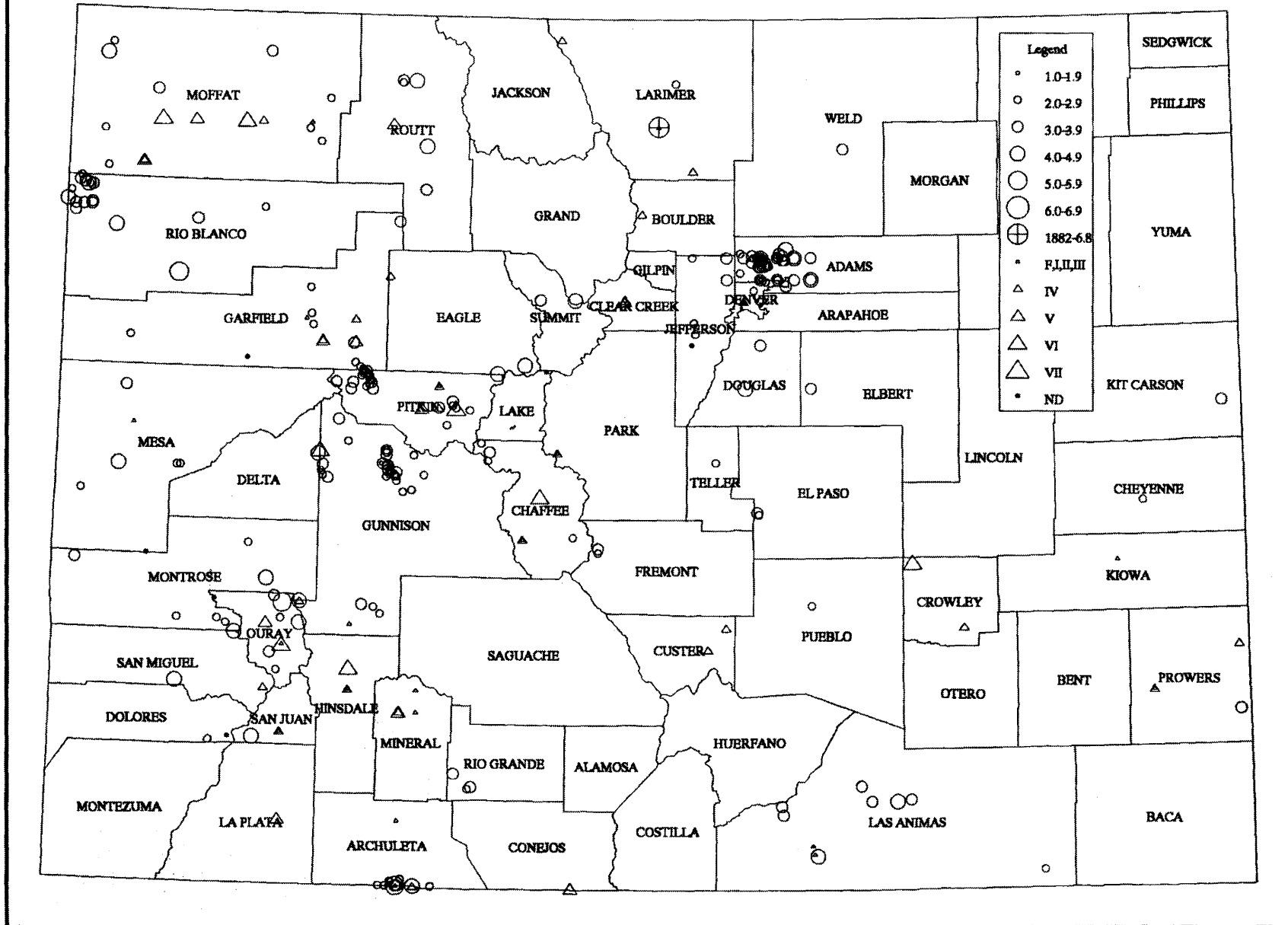
STATE SEISMICITY AND PROBABILISTIC MAPS

YOUNG FAULTS IN ARIZONA



Compiled by
P.A. Pearthree, Arizona Geological Survey
4/15/97

Colorado Earthquake Map, 1867 through 1996



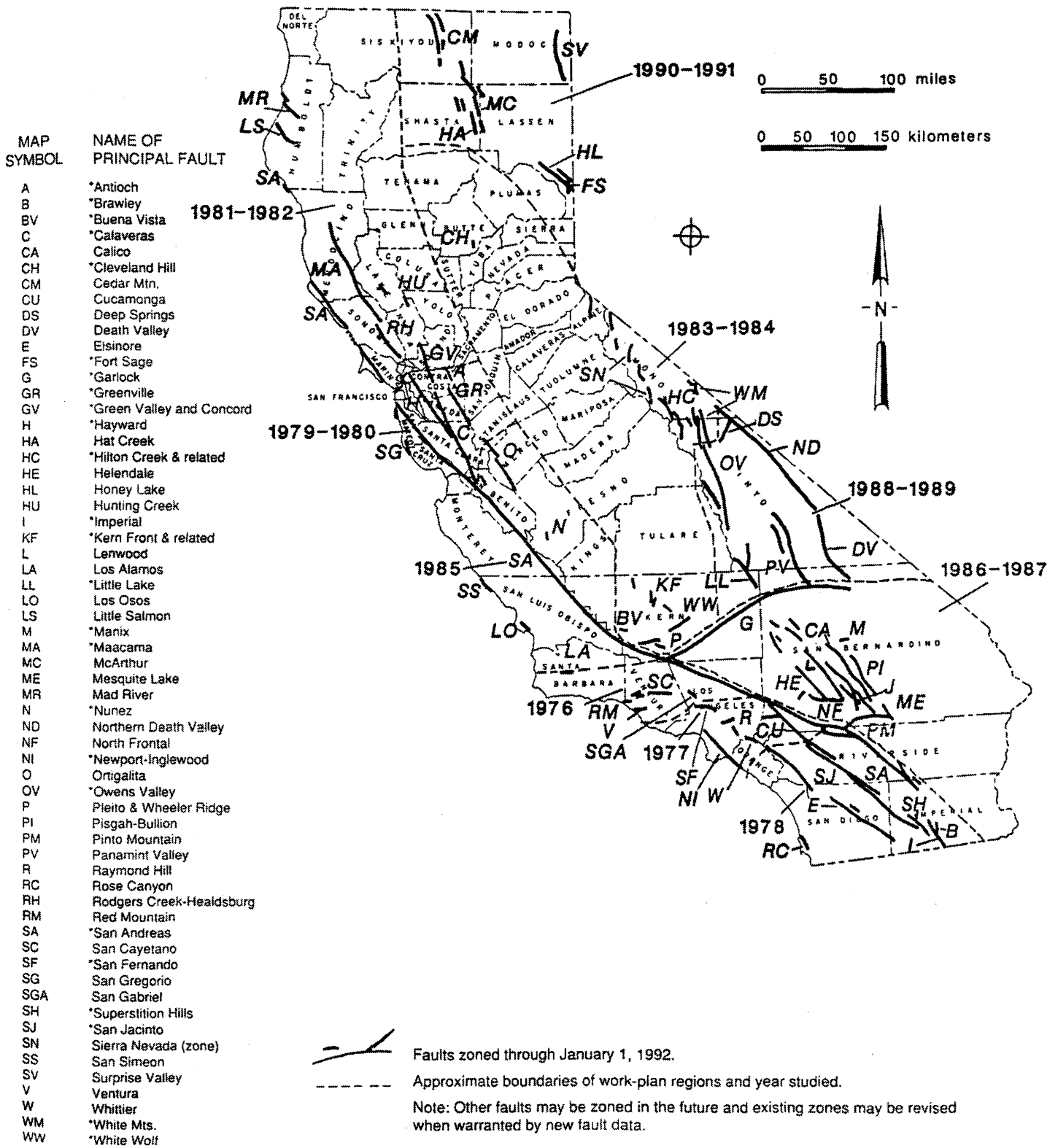
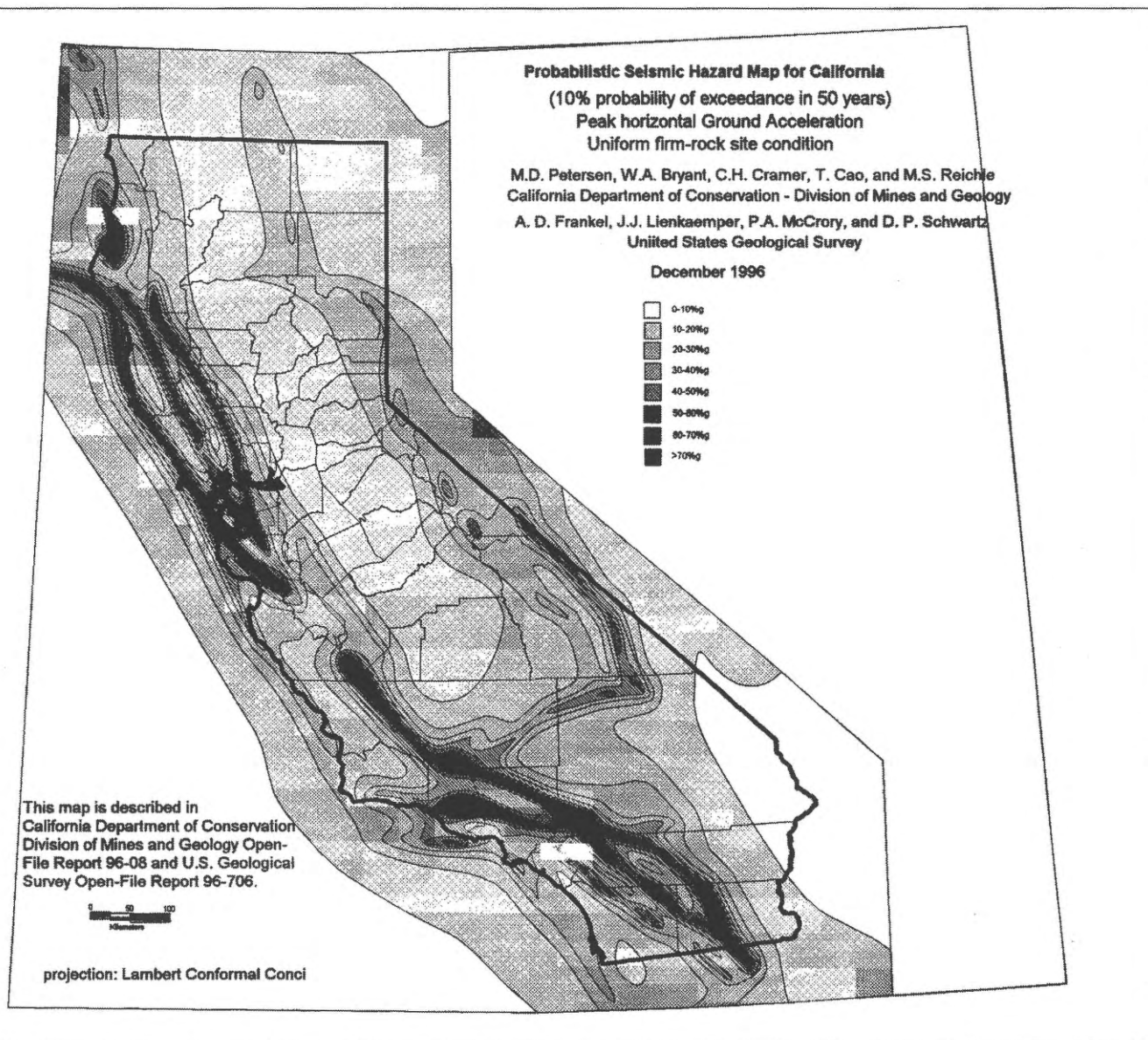
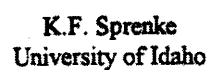


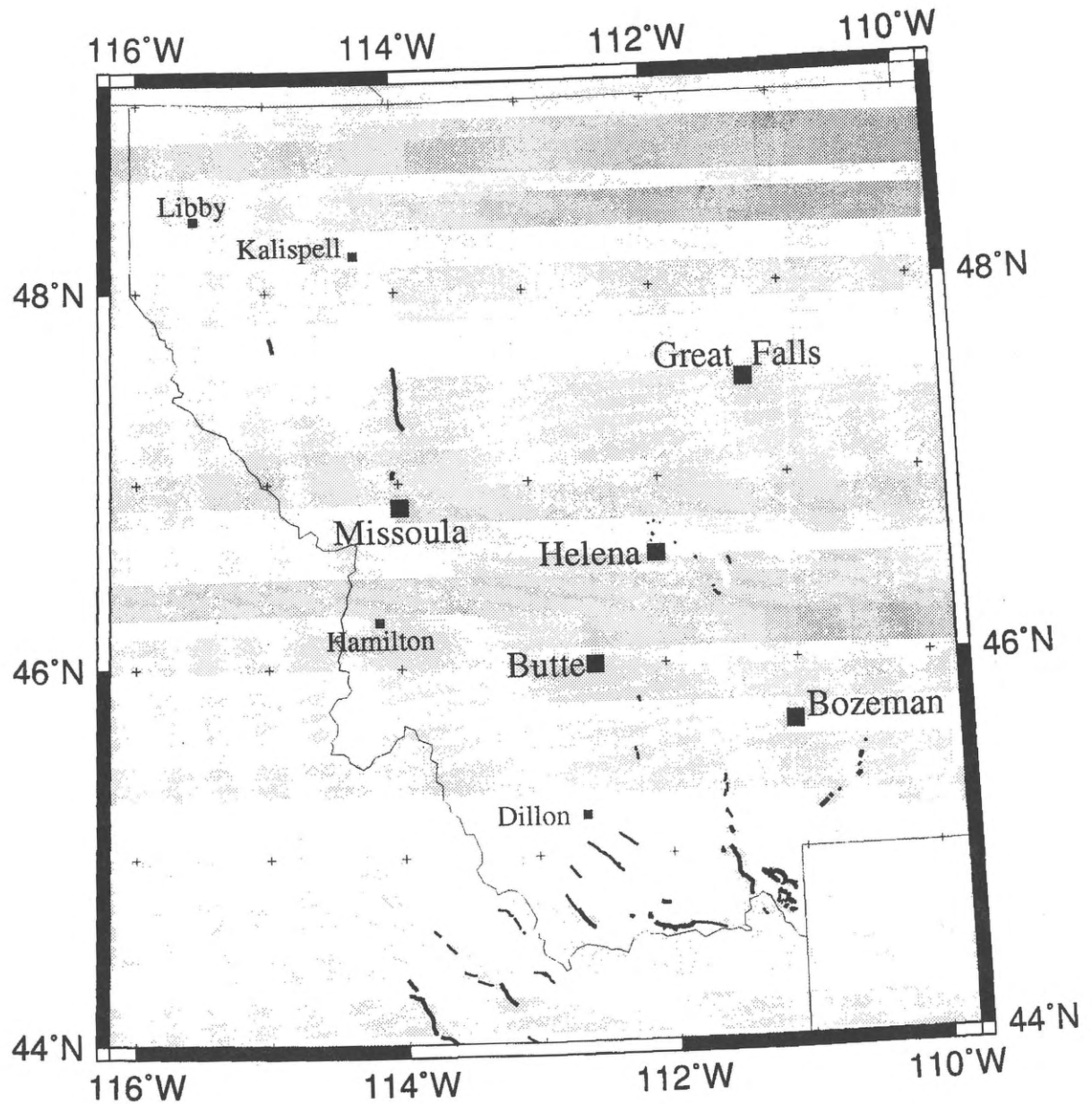
Figure 1. Principal active faults in California zoned for special studies under the Alquist-Priolo Special Studies Zones Act of 1972. Dashed lines and dates identify recently completed work-plan for 10 regions and when studied.





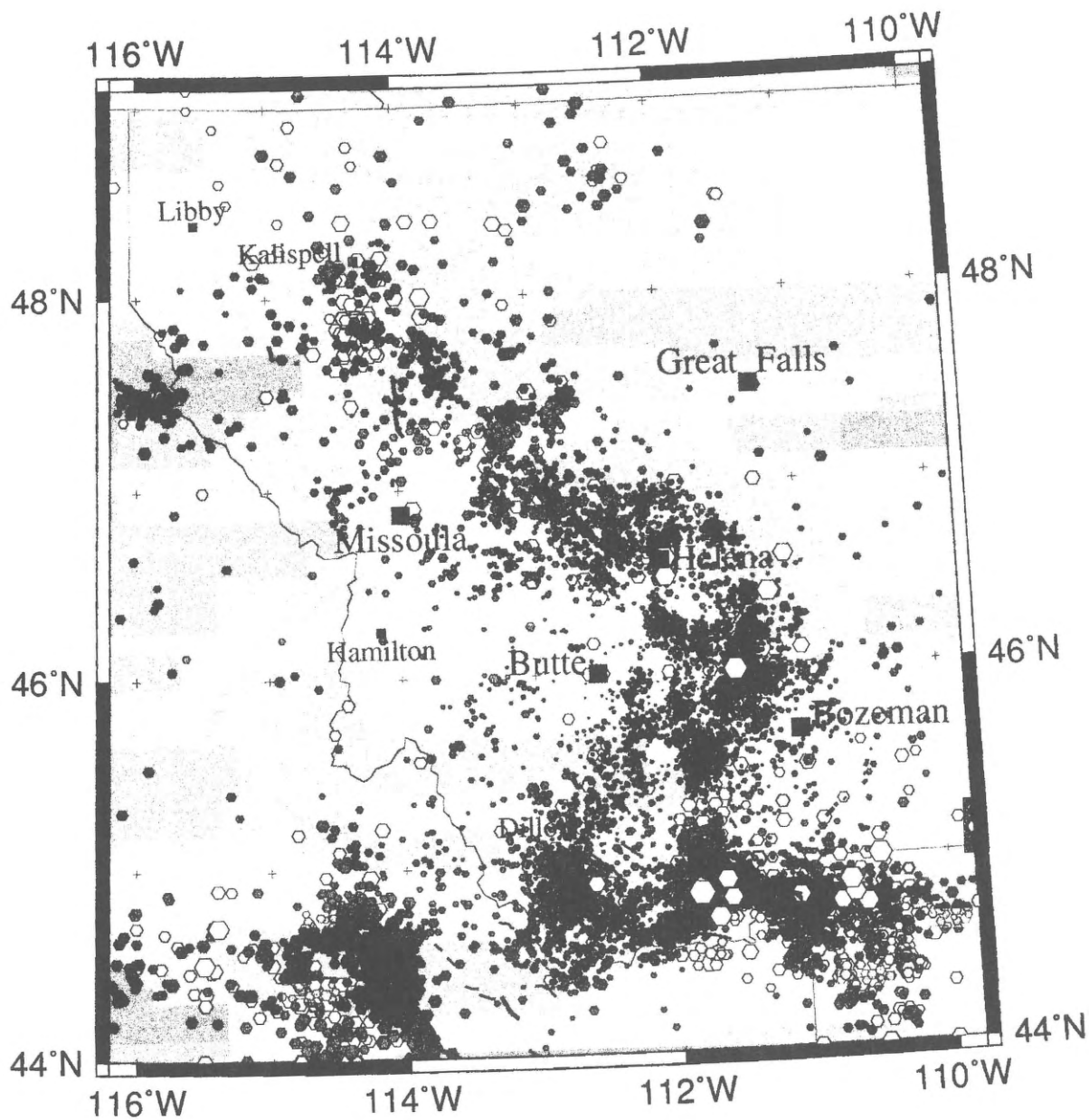
This map is a simplified version of the 1:500,000 scale version of the Fault Map of Idaho - 1997 Update, which shows all known and suspected late Cenozoic faults Update in Idaho. Many Miocene-Pliocene faults remain on the map because Miocene volcanism was widespread in Idaho and there has been little mapping of Quaternary units. The older structures may represent planes of weakness and zones of stress transfer between tectonic provinces.

MONTANA

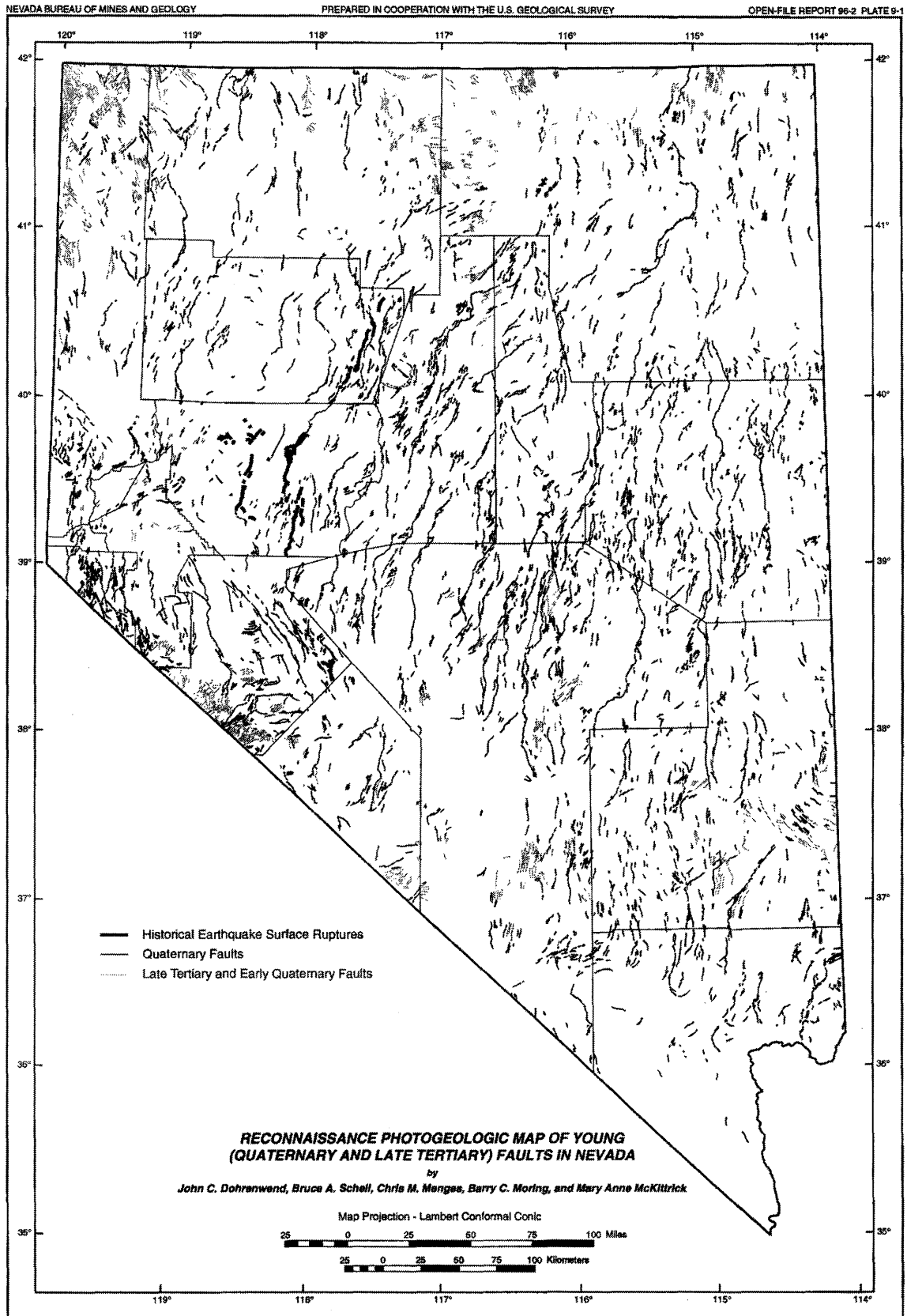


GMT Apr 21 16:26 Active faults with post-Bull Lake age (150,000 yrs) and post-Pinedale (12,000 yrs-bold traces) offset

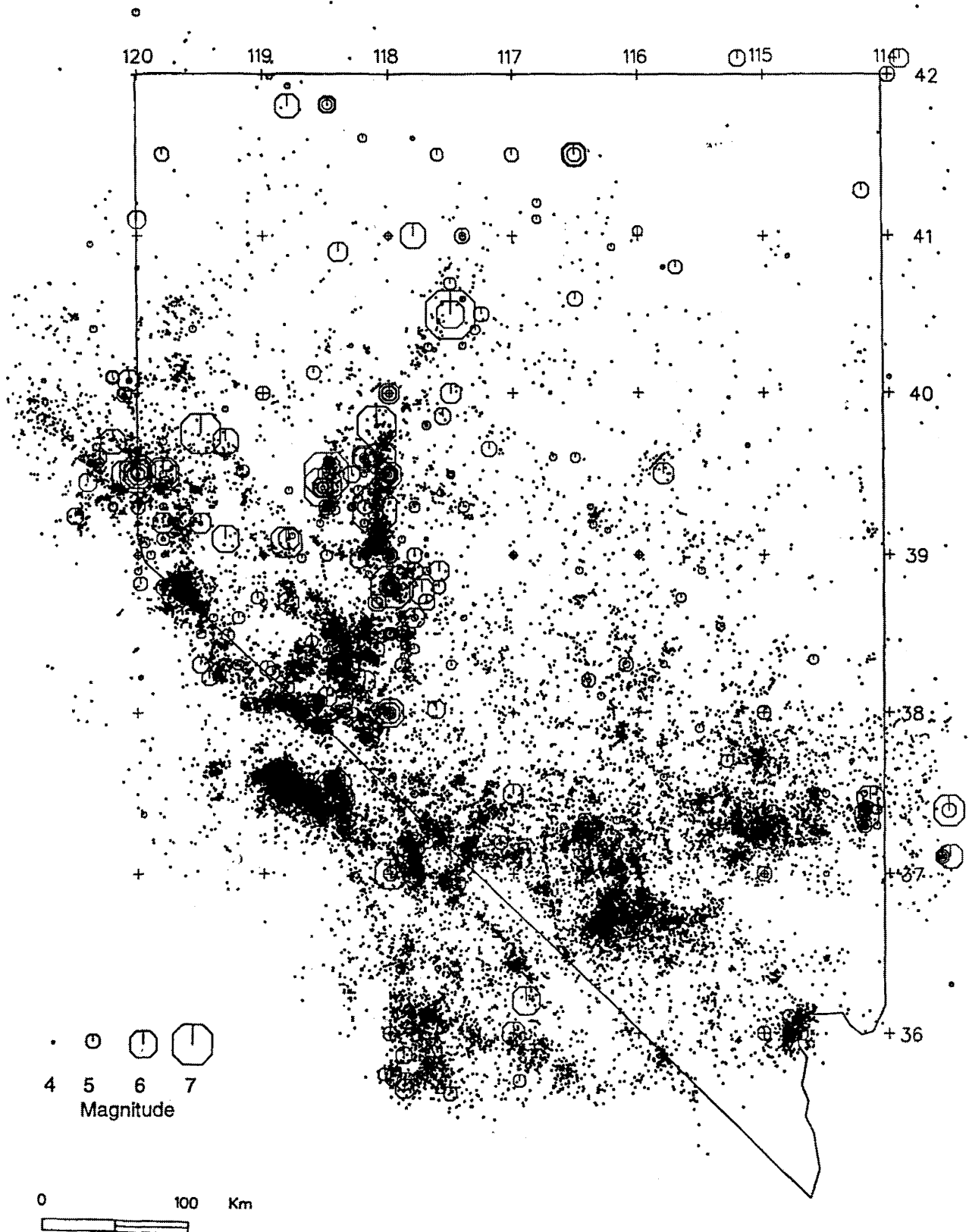
MONTANA

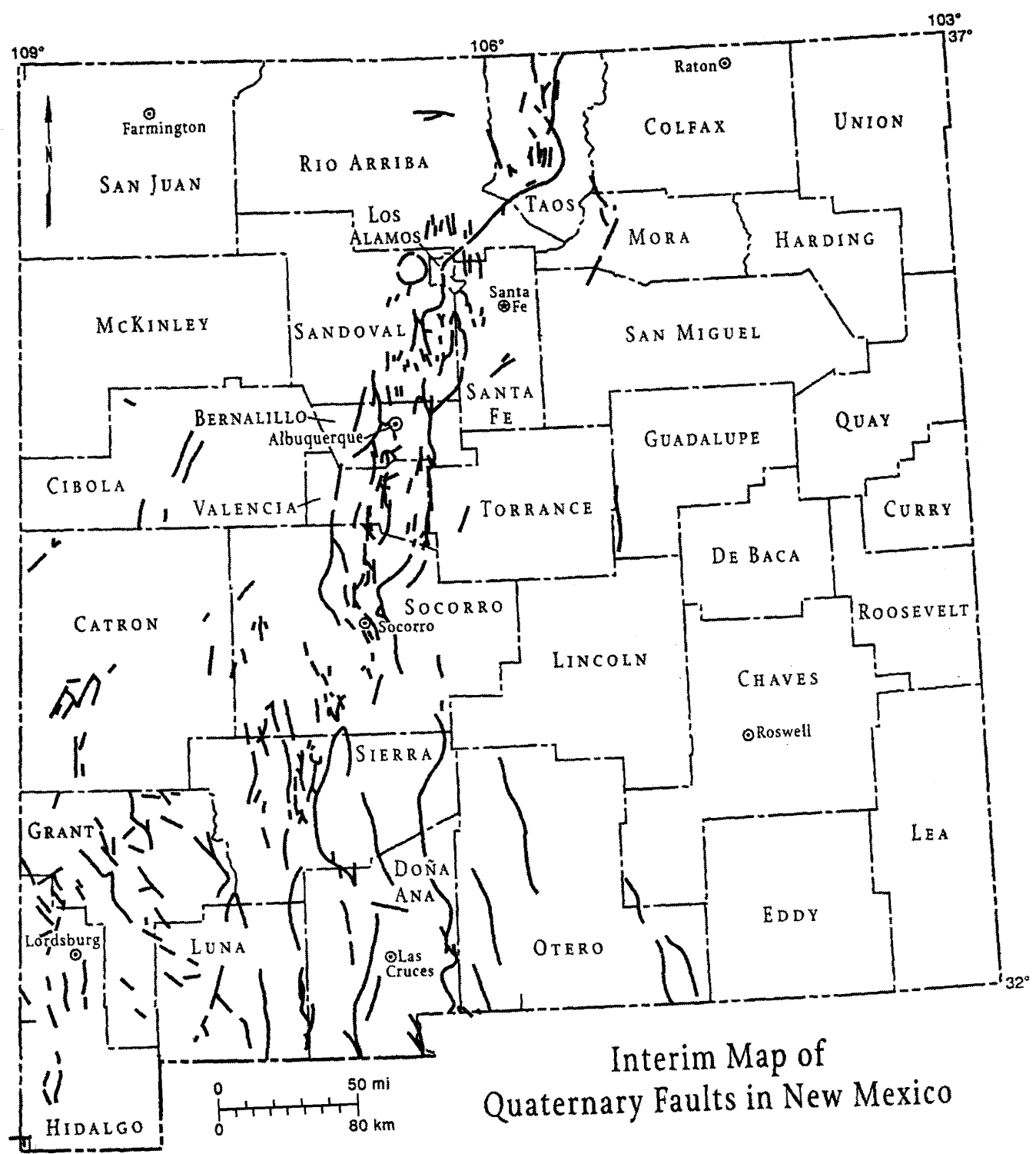


GMT Apr 21 16:02 Historic (1864-1981, unshaded hexagons) and recent (1982-1997, shaded hexagons) epicenters



Earthquakes in Nevada 1852 - 1996





Interim Map of
Quaternary Faults in New Mexico

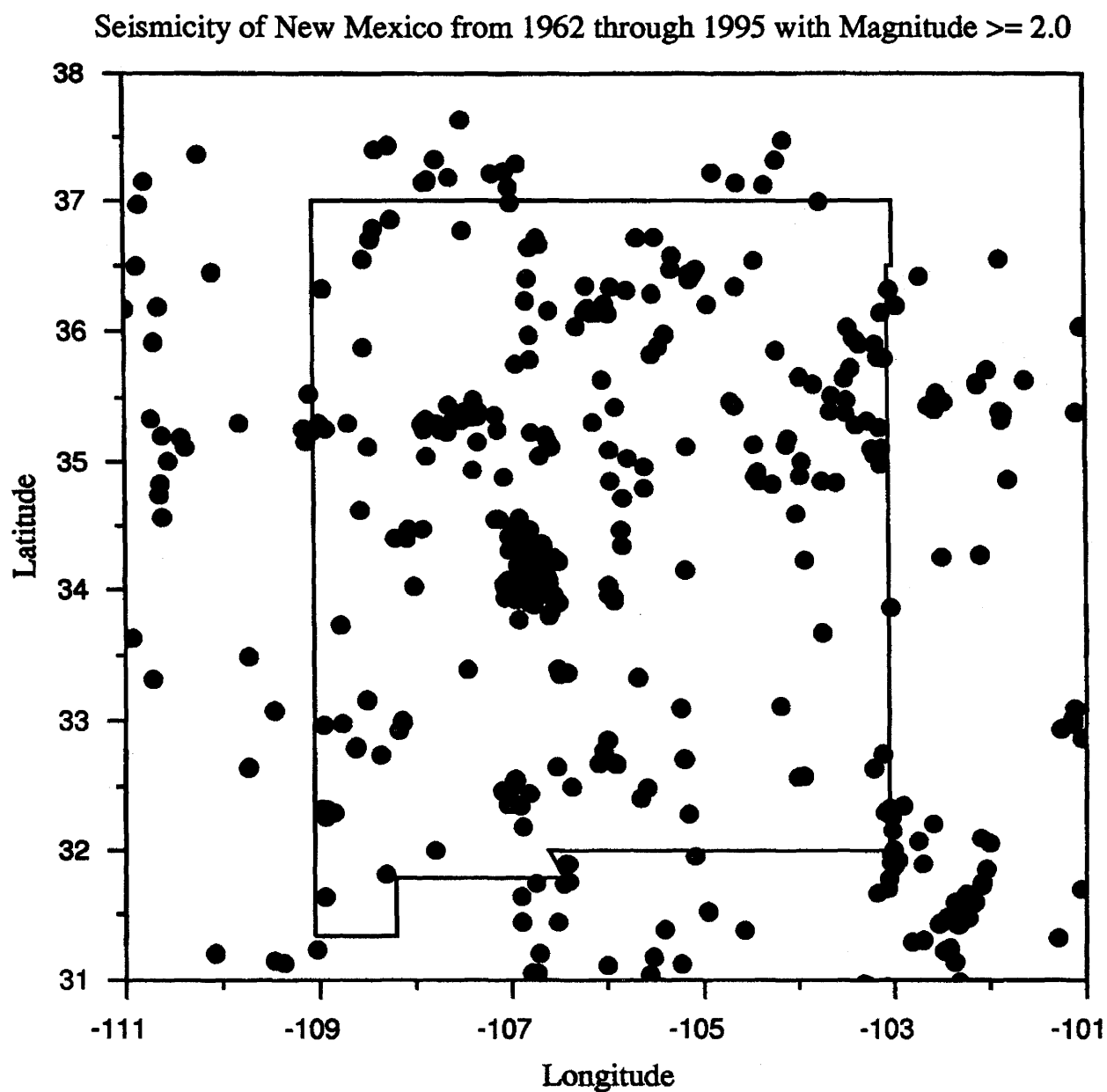


Figure 1. Preliminary seismicity map for New Mexico and bordering areas. See text for details on extent and limitations of the data set.

We are in the process of preparing an earthquake catalog for New Mexico and bordering areas (31° N to 38° N and 101° W to 111° W) for earthquakes with duration magnitudes of 1.3 or greater for the time period of 1962 through 1995. We anticipate completion of the catalog by September 1997. However, at the request of the Western States Seismic Policy Council (WSSPC) we are releasing a preliminary epicenter map from this study (figure 1). The distribution of activity presented is for instrumentally located earthquakes of magnitude 1.3 or greater regardless of quality of the epicenter or the strength of the events. Work in progress is to classify quality of the epicenter locations and to reconcile any differences in computed magnitudes over the 34-year period.

As far as we know most explosions have been excluded from our catalog but some further checking will be required. We have not excluded induced seismicity. It is our opinion that the clusters of activity in SE New Mexico and adjacent areas of West Texas are earthquakes induced by oil and natural gas production and/or enhanced recovery procedures.

Some important characteristics of the distribution of natural earthquakes within the region are:

1. Earthquake activity occurs almost as frequently in stable tectonic provinces (the Colorado Plateau and the Great Plains) as in the less stable provinces (the Rio Grande rift and the Southern Basin and Range). As a result the Rio Grande rift is not a clearly defined feature on the basis of seismicity.
2. Centered at 34° N and 107° W is a tight cluster of activity surrounded by an aseismic halo. The active region covers less than 2% of the area of New Mexico but contributes over one-third of the earthquake activity. We have designated this concentration of earthquake activity, the Socorro Seismic Anomaly (SSA). A probabilistic seismic-hazard map for SSA has been generated.

Most of the data for this map comes from files at New Mexico Tech; however, some contributions to the catalog have come from investigators at Los Alamos National Laboratory, University of Texas at El Paso, and the U.S. Geological Survey. A remaining task in preparing a com-

prehensive catalog for the region is to incorporate data from the above organizations on earthquakes that were not detected by New Mexico Tech. We will be collaborating with these organizations in the preparation of the final catalog.

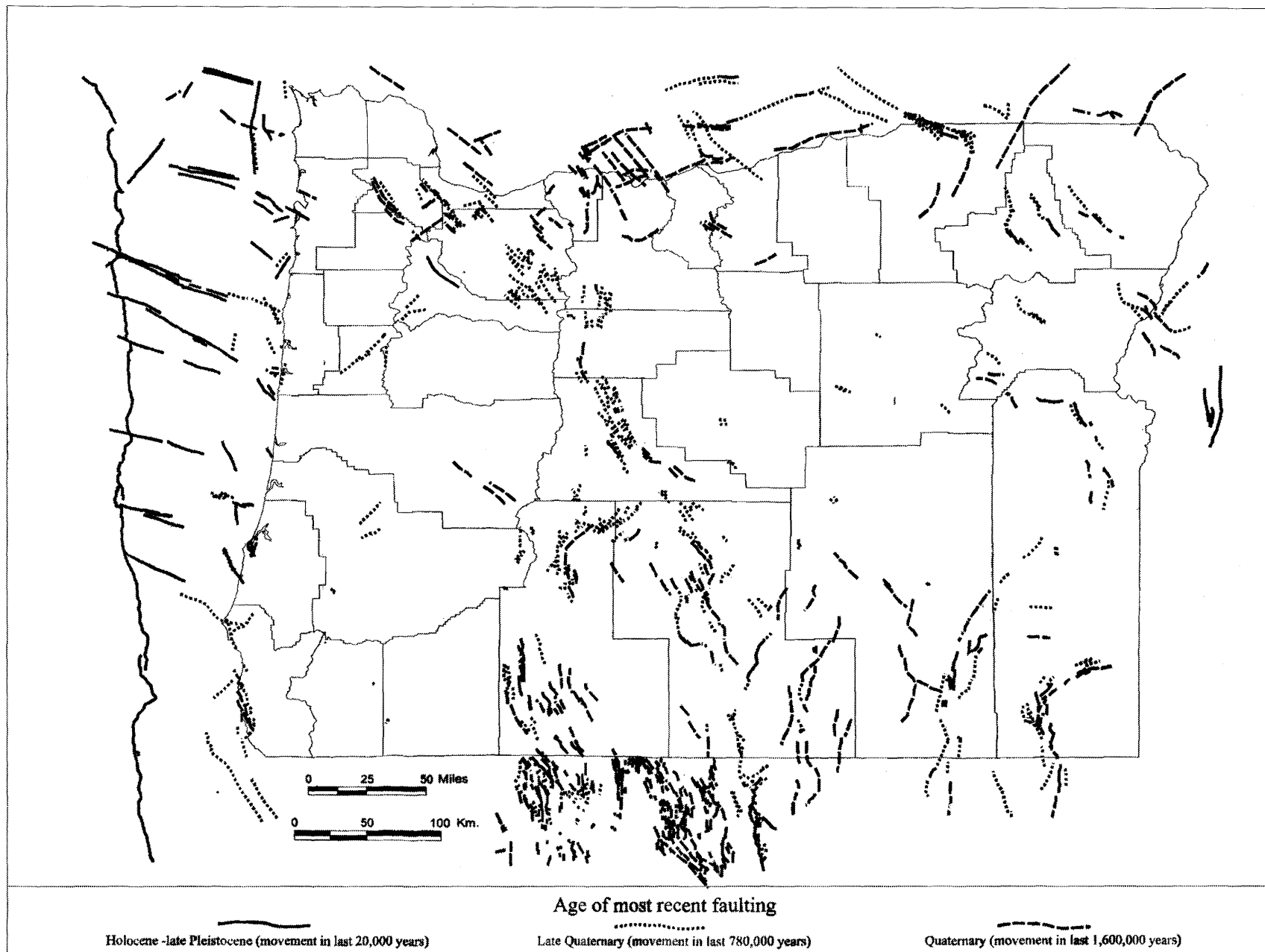
For anyone interested in obtaining further information on earthquake studies by New Mexico Tech investigators, we have placed our Geophysics Open-File reports (including this one) on the Internet at the following URL: <http://krach.nmt.edu/>

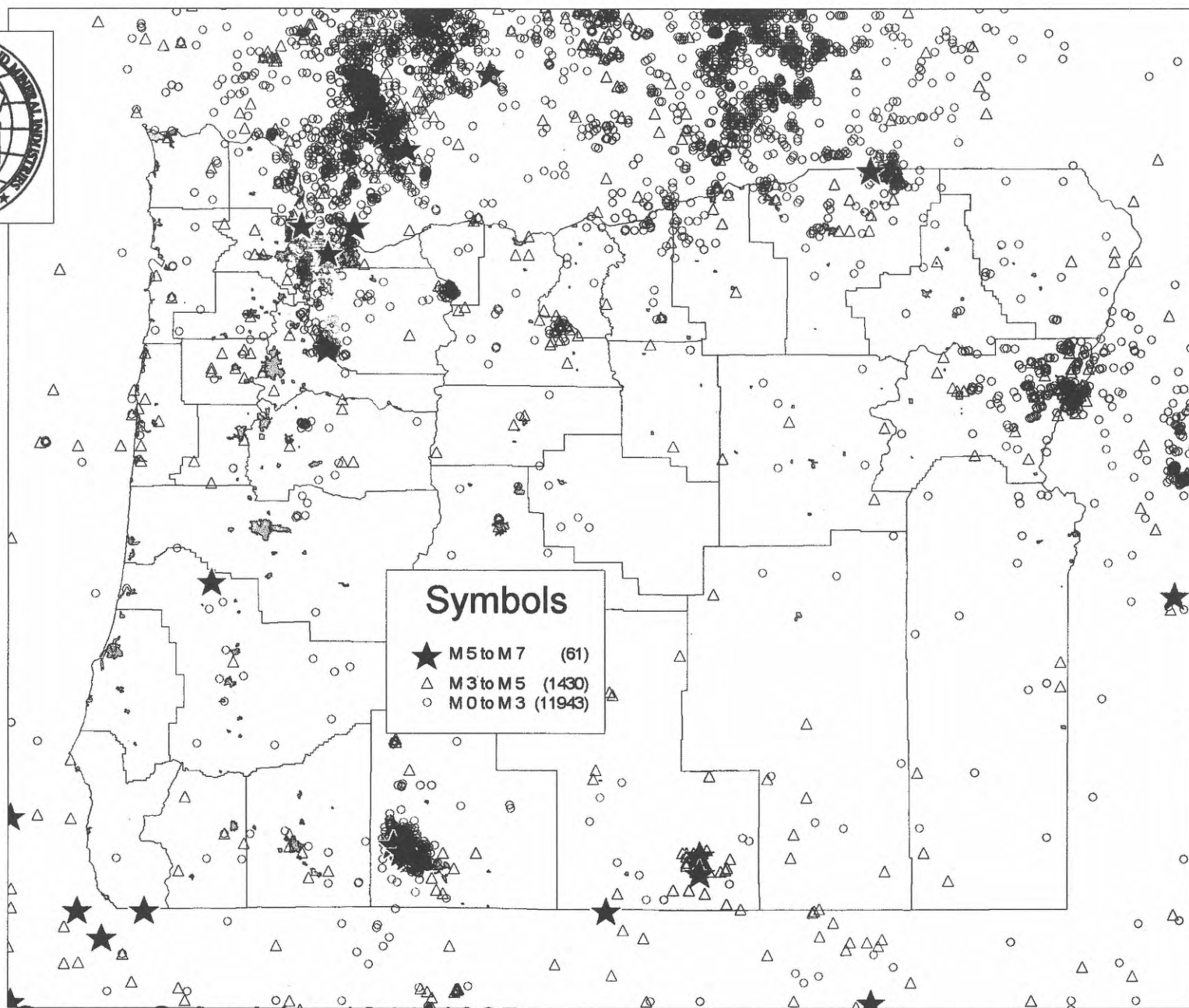
This interim map of Quaternary faults in New Mexico was produced as a temporary substitute for the more accurate and comprehensive map of Quaternary faults being compiled by Michael Machette of the U.S. Geological Survey. The U.S. Geological Survey map should be available soon. The primary sources of this map are listed below.

- Callender, J.F., 1986, Young faults and geothermal areas, in Williams, J.L., editor, *New Mexico in maps*: University of New Mexico Press, p. 14-16.
- Johnpeer, G.D., Love, D.W., and Hemingway, M., 1986, Assessment of earthquake hazards in New Mexico: Third U.S. National Conference on Earthquake Engineering, Charleston, South Carolina, August 24-28, 1986, *Proceedings*, v. 1, p. 233-244.
- Machette, M.N., and McGimsey, R.G., 1983, Map of Quaternary and Pliocene faults in the Socorro and western part of the Fort Sumner 1 x 2 quadrangles, central New Mexico: U.S. Geological Survey, *Miscellaneous Field Studies Map*, MF-1465-A, 1:250,000 scale.
- Machette, M.N., and Personius, S.F., 1984, Map of Quaternary and Pliocene faults in the eastern part of the Axtec 1 x 2 quadrangle, and the western part of the Raton 1 x 2 quadrangle, northern New Mexico: U.S. Geological Survey, *Miscellaneous Field Studies Map*, MF-1465-B, 1:250,000 scale.
- Machette, M.N., Personius, S.F., Menges, C.M., Peartree, P.A., and Arizona Bureau of Mines and Mineral Technology, 1986, Map showing Quaternary and Pliocene faults in the Silver City 1 x 2 quadrangle and Douglas 1 x 2 quadrangle, southeastern Arizona and southwestern New Mexico: U.S. Geological Survey, *Miscellaneous Field Studies Map*, MF-1465-C, 1:250,000 scale.
- Salyards, S.L., 1991, A preliminary assessment of the seismic hazard of the southern Rio Grande rift, New Mexico: *New Mexico Geological Society, 42nd Field Conference Guidebook*, p. 199-202.

Map of Oregon Earthquake Faults

Oregon Department of Geology and Mineral Industries
Data from Geomatrix, 1995, Design for Oregon, and Pezzopane, 1993



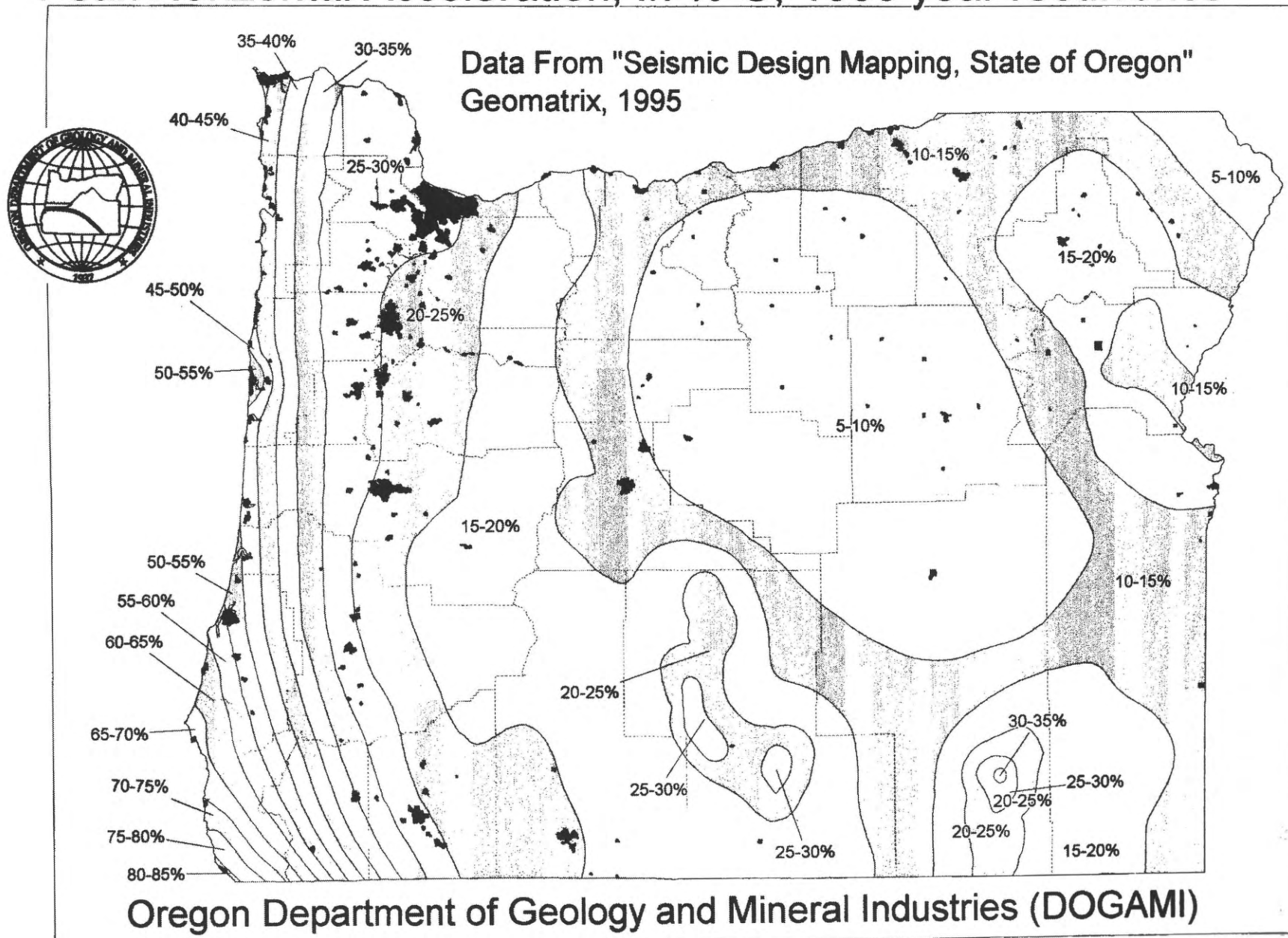


Oregon Seismicity, 1841-1995.

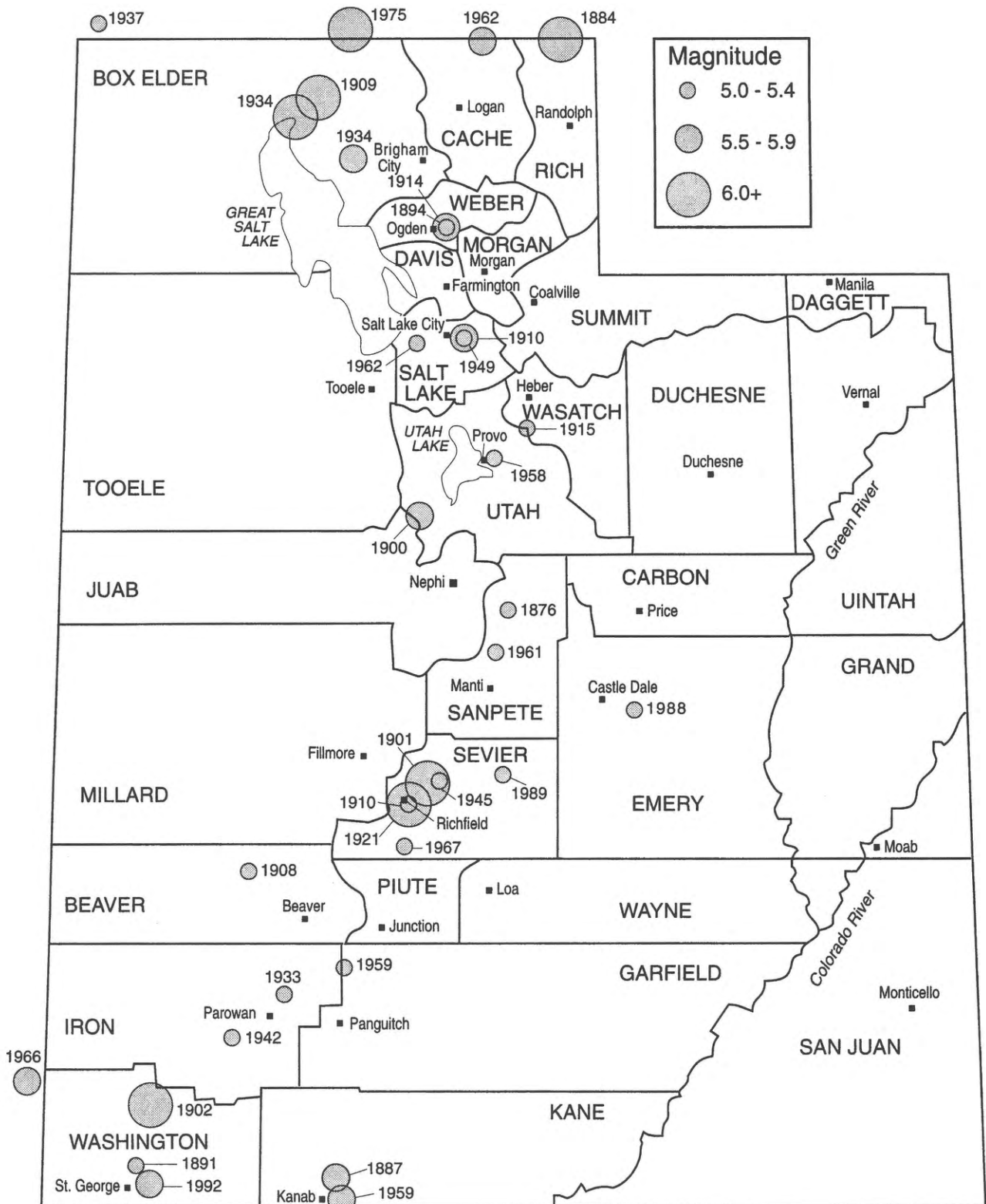
Oregon Department of Geology and Mineral Industries (DOGAMI)

Data from DOGAMI OFR-94-01, University of Washington Catalog and Boise State University Catalog.

Peak Horizontal Acceleration, In % G, 1000 year recurrence

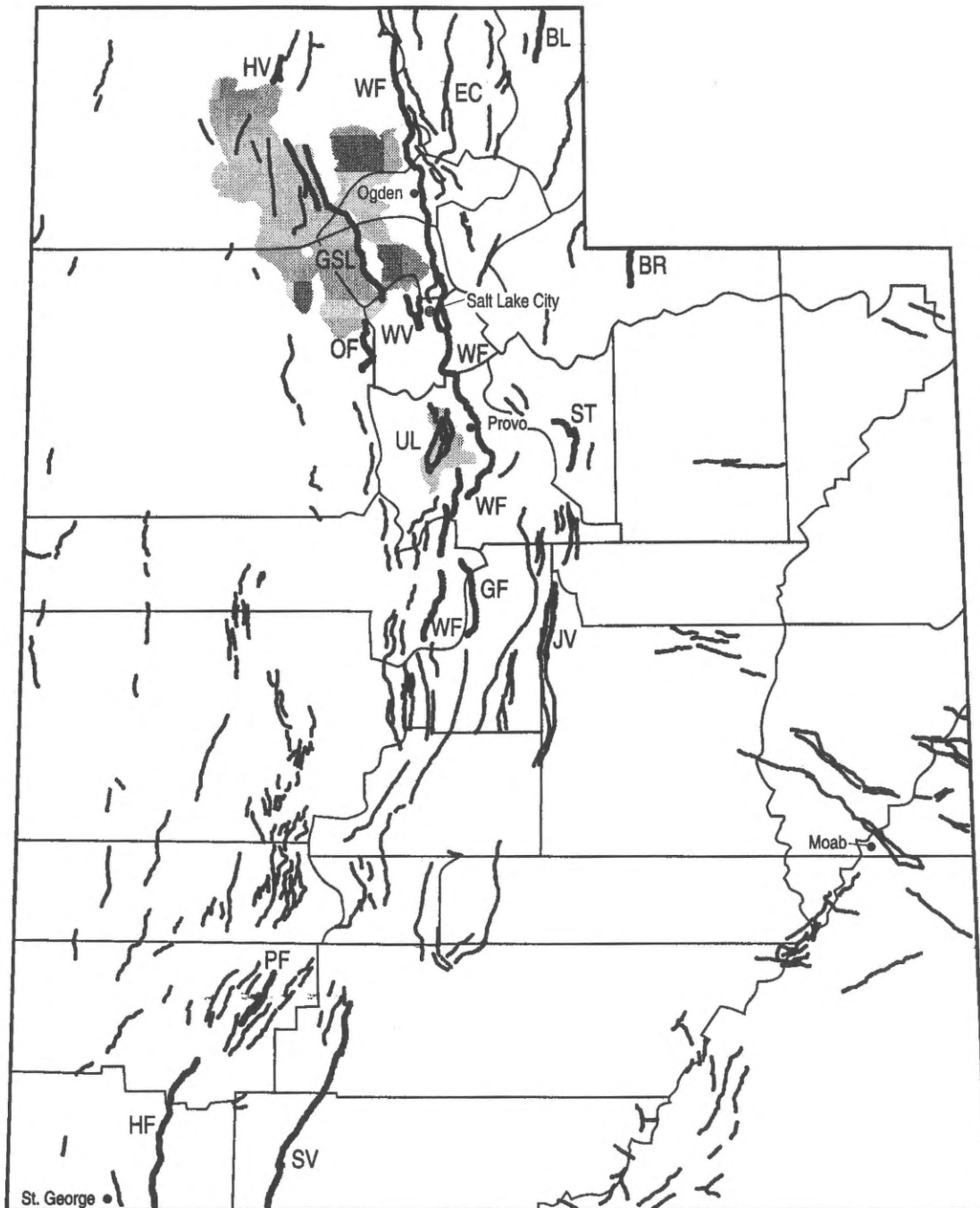


Magnitude 5.0 and Larger Earthquakes from 1850 - 1996, Utah Region (University of Utah Seismograph Stations Catalog)



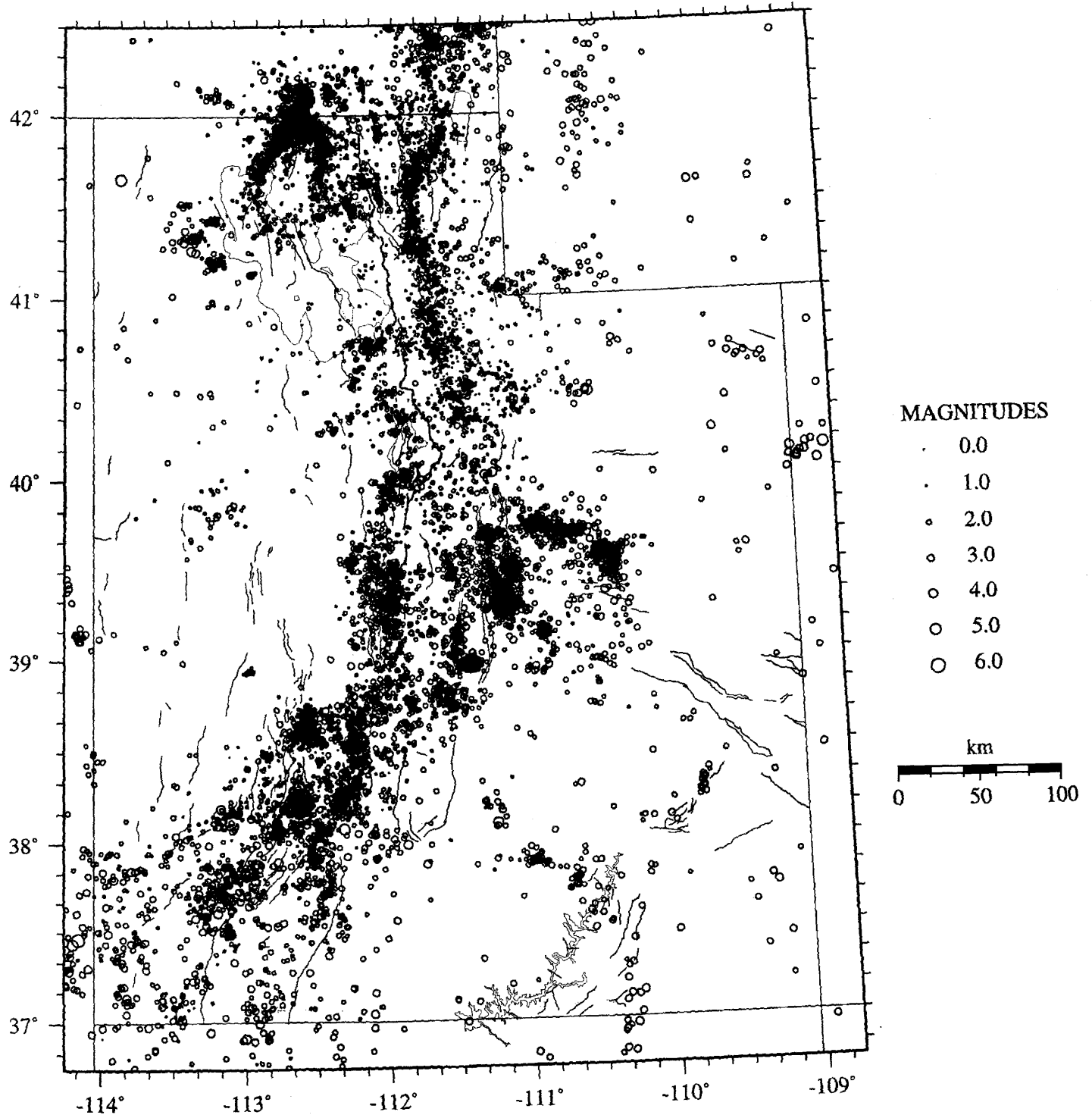
Quaternary Fault Map of Utah (modified from Hecker, 1993)
Highlighting the Most Active Faults (heavier lines)

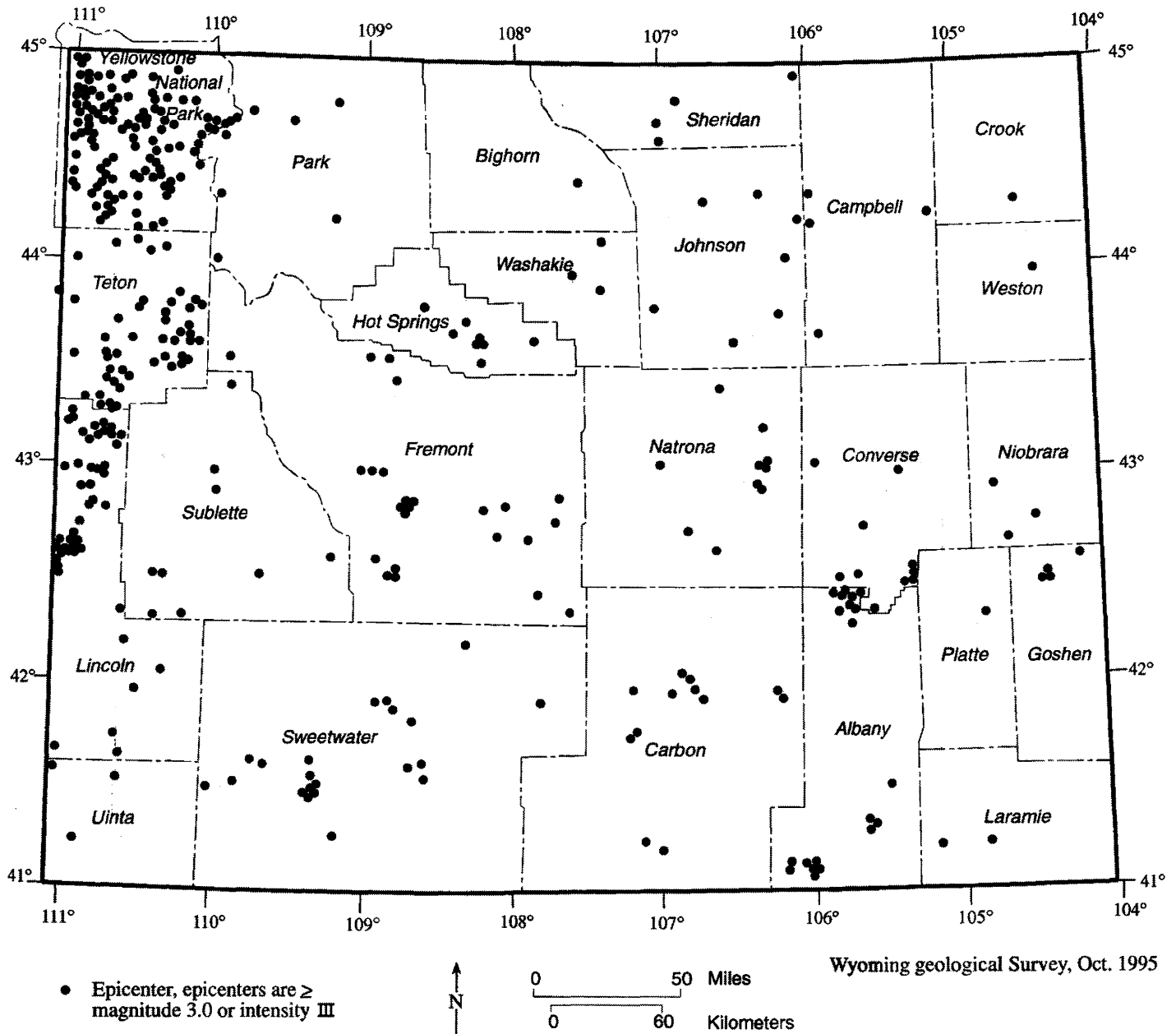
(Wasatch, WF; Bear River, BR; East Cache, EC; East Bear Lake, BL; Hansel Valley, HV; Oquirrh, OF; West Valley, WV; East Great Salt Lake, GSL; Utah Lake, UL; Strawberry, ST; Joes Valley, JV; Gunnison, GF; Paragonah, PF; Hurricane, HF; and Sevier, SV)



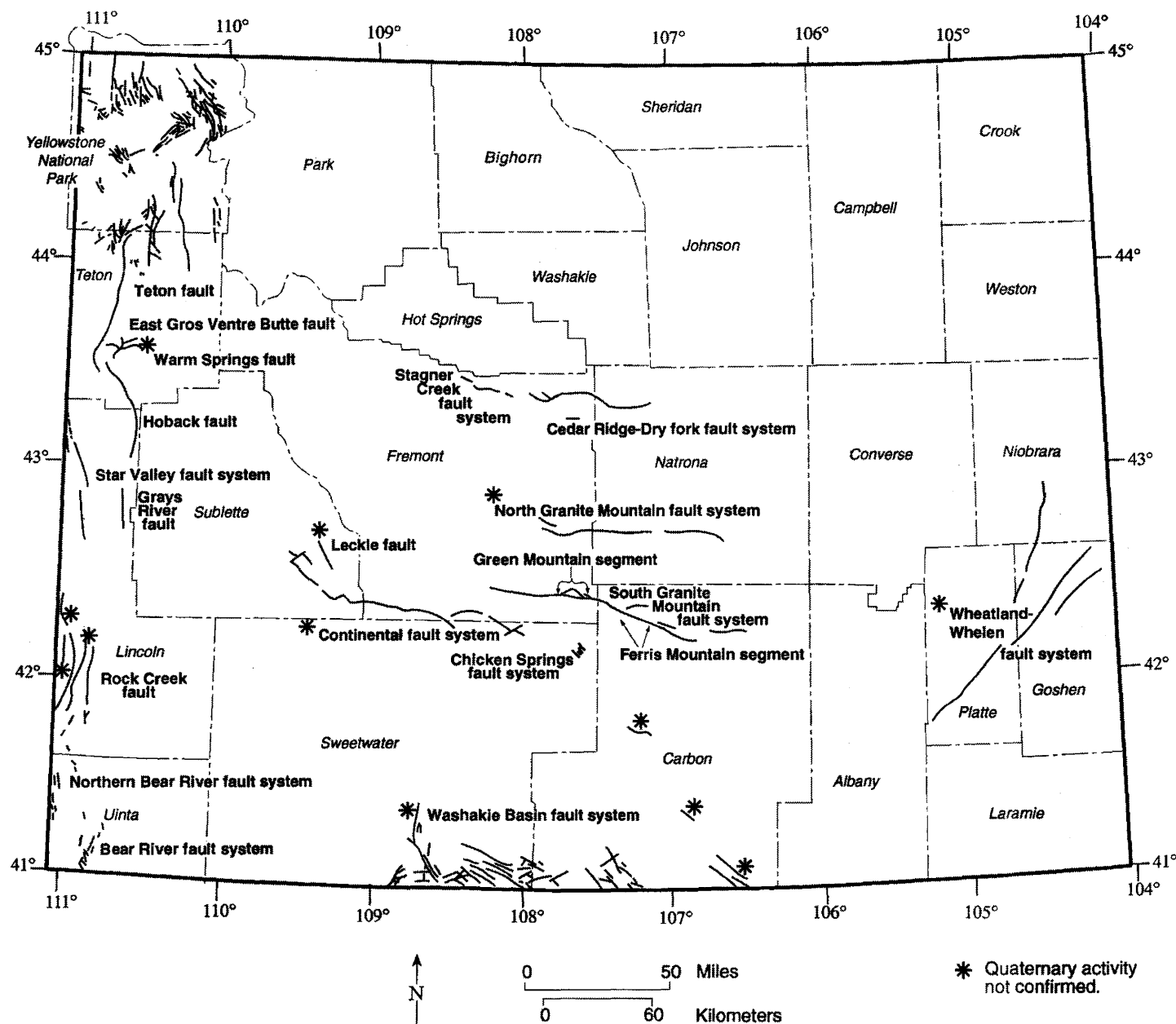
Seismicity of Utah

July 1962 - December 1996





GENERALIZED HISTORIC EARTHQUAKE EPICENTER MAP FOR WYOMING



SUSPECTED ACTIVE FAULTS IN WYOMING

AUTHOR INDEX

- Abrahamson, Norman *Yucca Mountain Ground-Motion Panel* (abs)
 Allen, Clarence R. *Challenges of Characterizing Seismic Hazards in The Basin and Range Province* (abs)
 Allen, Clarence R. *Challenges of Characterizing Seismic Hazards in The Basin and Range Province* (paper)
 Anderson, J. G. See SU, Feng
 Anderson, J. G. See dePOLO, Craig M. (2)
 Anderson, J. G. See dePOLO, Diane M.
 Anderson, J. G. See ICHINOSE, Gene A.
 Anderson, J. G. See SIDDHARTHAN, Raj V.
 Anderson, R. Ernest *Detachment Faults: Superstars or Bit Players in Seismic Hazards of the Great Basin* (abs)
 Anooshehpour, A. See BRUNE, James N.
 Arabasz, Walter J. *Earthquake Database Issues for Seismic-Hazard Analysis in the Utah Region* (abs)
 Bachman, Robert E. *1997 Uniform Building Code Ground-Shaking Criteria* (abs)
 Bachman, Robert E. *1997 Uniform Building Code Ground-Shaking Criteria* (paper)
 Baker, L.M. See SPUDICH, Paul
 Bao, Hesheng *Characterizing Basin Effects* (abs)
 Barnhard, T. See Frankel, Arthur
 Barnhard, Ted *Quaternary Faults Used for the 1996 National Seismic-Hazard Maps* (abs)
 Bell, J. W. See RAMELLI, Alan R.
 Berger, G.W. *Paleoseismology from Luminescence Dating: Tests and Application Near Landers, California* (abs)
 Beukelman, G. S. See ZOLLWEG, J. E.
 Biasi, G. P. See SMITH, Kenneth D.
 Bielak, J. See BAO, Hesheng
 Blakely, Mike D. *Engineering Infrastructure Needs* (abs)
 Boatwright, J. See SPUDICH, Paul
 Boore, D.M. See SPUDICH, Paul
 Bowman, S. See LOUIE, John (2)
 Brune, J. N. See ICHINOSE, Gene A.
 Brune, J. N. See Von Seggern, D. H.
 Brune, James N. *Strong Ground Motion Expected from Large Normal-Fault Earthquakes Based on Evidence from Precarious Rocks and Source Modeling* (abs)
 Bryant, B.A. See Chrisenson, G.E. (1) (2)
 Chang, W. L. See SMITH, Richard
 Chang, W. L. (1) *Earthquake Hazard on the Wasatch Front, Utah, from Fault Interaction and Tectonic Induced Flood Inundation Associated with the Wasatch Fault* (abs)
 Chang, W.L. (2) *Potential for Tectonically Induced Tilting and Flooding by the Great Salt Lake, Utah From Large Earthquakes on the Wasatch Fault* (paper)
 Christenson, Gary E. (1) *Surface-Faulting Hazards and Land-Use Planning, Utah* (abs)
 Christenson, Gary E. (2) *Surface-Faulting Hazards and Land-Use Planning in Utah* (paper)
 dePolo, C. M. See dePOLO, Diane M.
 dePolo, C. M. See RAMELLI, Alan R.
 dePolo, Craig M. (1) *130,000 Year vs. 10,000 Year (Holocene) Classification of "Active" Faults in the Basin and Range Province* (abs)
 dePolo, Craig M. (2) *Planning Scenario for a Major Earthquake in Western Nevada* (abs)
 dePolo, Craig M. (3) *Age Criteria for Active Faults in the Basin and Range Province* (paper)
 dePolo, Diane M. *Historical Earthquakes, and Patterns and Behavior of Seismicity in Western Nevada and Eastern California* (abs)
 Dickman, N. See Frankel, Arthur
 Diehl, S. F. See ANDERSON, R. Ernest
 Durukal, E. See ERDIK, Mustafa
 Eguchi, Ronald T. *Sensitivity of Loss Estimates to Different Source-Zone Maps and Parameters* (abs)
 Erdik, Mustafa *Analysis of the Strong-Motion Data Associated with the 1995 Dinar (Turkey) Earthquake* (abs)
 Fletcher, J.B. See SPUDICH, Paul
 Frankel, Arthur. *New Seismic-Hazard Maps for the Western U.S.* (abs)
 Ghattas, O. See BAO, Hesheng
 Hackett, W.R. See SMITH, R. P.
 Haller, Kathleen M. *Geologic Input for Seismic-Hazards Maps- Examples from the Database of Quaternary Faults in Montana* (abs)
 Hammond, K. J. See TAYLOR, Wanda J.
 Hanks, T.C. See SPUDICH, Paul
 Hanson, S. See Frankel, Arthur
 Harmsen, S. See Frankel, Arthur

- Hasting, M. See LOUIE, John (2)
 Hellweg, M. See SPUDICH, Paul
 Huntley, D.J. See BERGER, G.W.
 Ichinose, G. See LOUIE, John (2)
 Ichinose, Gene A. *The Seismotectonics and Source Parameters of Recent Earthquake Near Reno, Nevada* (abs)
 Jackson, S.M. See SMITH, R. P.
 Jacobson, S. L. See dePOLO, Craig M. (2)
 Jamieson, Gil *HAZUS: The FEMA Tool for Estimating Earthquake Losses* (abs)
 Ji, Xu *Numerical Prediction of Seismic-Wave Amplification in the Salt Lake Basin, Utah* (abs)
 Johnson, G. L. See dePOLO, Craig M. (2)
 Jones, C.H. See UNRUH, J. R.
 Joyner, W.B. See SPUDICH, Paul
 Kallivokast, L. See BAO, Hesheng
 Keaton, Jeffrey R. *Implications of Variable Late-Quaternary Recurrence Intervals for Probabilistic Seismic-Hazard Assessments; Examples from Utah and west Texas* (abs)
 Kirkham, Robert M. *Recognition of Active But Non-Seismogenic Salt-Related Deformation within an Extensional Environment, West-Central Colorado* (abs)
 Leyendecker, E. See Frankel, Arthur
 Lindh, A.G. See SPUDICH, Paul
 Louie, John (1) *Geophysical Characterization of Active Faults in the Basin And Range, and the Earthquake Hazard of the Pahrump Valley Fault Zone* (abs)
 Louie, John (2) *Shallow Geophysical Constraints on displacement and Segmentaion of the Pahrump Valley Fault Zone, California-Nevada Border* (paper)
 Lynn, Ron L. *A Practical Approach to Implementing Fault Criteria in Community Planning* (abs)
 Machette, Michael N. *Contrasts Between and Short- and Long-Term Records of Seismicity in the Rio Grande Rift-Important Implications for Seismic-Hazards Analysis* (abs)
 Machette, Michael N. *Contrasts Between and Short- and Long-Term Records of Seismicity in the Rio Grande Rift-Important Implications for Seismic-Hazard Assessments in Areas of Slow Extension* (paper)
 McGarr, A. See SPUDICH, Paul
 Meertens, C. M. See SMITH, Richard
 Mueller, C. See Frankel, Arthur
 Olig, S. S. See WONG, Ivan G.
 Olsen, K. B. See JI, Xu
 Oswald, John A. *Character of Faulting Along the Hunter Mountain Fault Zone and Evidence for Active Dextral Slip Transfer Across Saline Valley Rhombochasm, Eastern California* (abs)
 Pechmann, J. C. See JI, Xu
 Pechmann, J. C. See ARABASZ, Walter J.
 Perkins, D. See Frankel, Arthur
 Pezzopane, Silvio *Impact of Distributed Faulting to Seismic-Hazard Assessments in the Basin and Range Province – Examples from Yucca Mountain, Nevada* (abs)
 Plank, G. See LOUIE, John (2)
 Ramelli, Alan R. *Recent Large-Magnitude Events Along the Carson Range Fault System, A Principal Frontal Fault of the Northern Sierra Nevada* (abs)
 Redden, Robert *Emergency Management Needs in the Basin & Range Province* (abs)
 Reheis, M.C. See SAWYER, Tom L.
 Rigby, J. G. See dePOLO, Craig M. (2)
 Rockwell, T.K. See BERGER, G.W.
 Sawyer, Tom L. *Holocene Paleoseismicity, Segmentation, and Seismic Potential of the Fish Lake Valley Fault Zone, Nevada and California* (abs)
 Schuster, G. T. See JI, Xu
 Schwartz, David P. *Earthquake Recurrence Models* (abs)
 Shen-Der, Ni See SIDDHARTHAN, Raj V.
 Shields, G. See LOUIE, John (2)
 Siddharthan, Raj V. *Nonlinear Amplification Studies on Deep Soil Deposits in Reno, Nevada* (abs)
 Siddharthan, Raj V. *Nonlinear Amplification Studies of Deep Deposits in Reno, Nevada* (paper)
 Simpson, R. W. Jr. See CHANG, W.L.
 Slemmons, D. B. See dePOLO, Craig M. (1) (3)
 Smith, K. D. See deDPOLO, Diane M.
 Smith, K. D. See ICHINOSE, Gene A.
 Smith, Kenneth D. *Attenuation and Site Effects in Northern and Southern Nevada from Three-Component Digital Seismograms* (abs)

- Smith, Richard P.
Smith, Richard P.
Smith, Robert B.
- Smith, Robert B.
Somerville, Paul
Somerville, Paul
- Sonder, L.J.
Spudich, Paul
Stirling, Mark W.
Streufert, R. K.
Su, Feng
Switzer, D. D.
Taylor, Wanda J.
- Unruh, J.R.
- Unruh, J.R.
- Von Seggern, D. H.
Waag, C. J.
Watson, Charles P.
- Weiser, Stephen
Weiser, Stephen
Wesnousky, S. G.
Wesnousky, S. G.
Wesnousky, S.G.
Whitney, J. W.
Willoughby, C.H.
- Wong, Ivan G.
Wong, Ivan G.
Wythes, T. J.
Xu, J.
Xu, J.
Zollweg, J. E.
- Magma Intrusion and Seismic-Hazards Assessment in the Basin and Range Province* (abs)
Magma Intrusions and Seismic-Hazards Assessment in the Basin and Range Province (paper)
Earthquake Risk Assessment for Seismically Dormant Normal Faults: An Example from the Wasatch Front, Utah, Using GPS Measurements, Quaternary Faults, and Seismicity (abs)
See CHANG, W.L. (2)
Rupture-Directivity Effects and Strong Fault-Normal Pulses Near Normal Faults (abs)
The Characteristics and Quantification of Near-Fault Ground Motion With Implications for the Basin and Range Province (paper)
See UNRUH, J. R.
Earthquake Ground Motions in Extensional Tectonic Regimes (abs)
Shape of the Magnitude-Frequency Distribution for Individual Faults (abs)
See KIRKHAM, Robert M.
Site Effects on Strong Motion in Las Vegas (abs)
See TAYLOR, Wanda J.
Definition of Fault Segments on Young Normal Faults: Geometry, Offset, and Scarps of the Hurricane Fault, Utah and Hiko Fault, Nevada (abs)
Relation of Gravitationally Driven Lithospheric Extension to Low Slip-Rate Faults and Regional Seismic Hazards in the Western U.S. (abs)
Relation of Gravitationally Driven Lithospheric Extension to Low Slip-Rate Faults and Regional Seismic Hazards in the Western United States (paper)
Seismicity in the SGB: What Do Earthquake Catalogs Accurately Indicate? (abs)
See ZOLLWEG, J. E.
The Seismo-Watch Weekly Earthquake Report, A Weekly Broadcast of Global and Regional Earthquake Information on Community Access Television (abs)
(1) Emergency Management Needs in the Basin and Range Province (abs)
(2) What Emergency Managers Need From Geoscientists (paper)
See STIRLING, Mark W.
See OSWALD, John A.
See Willoughby, C.H.
See PEZZOPANE, Silvio
Character of Late Quaternary Low-Angle(?) Normal Faulting on the Northwestern Side of the Ruby Mountains / East Humboldt Range, Northeastern Nevada (abs)
Seismic Hazards in the Basin and Range Province: Perspectives from Probabilistic Analyses (abs)
Seismic Hazards in the Basin and Range Province: Perspectives from Probabilistic Analyses (paper)
See dePOLO, Craig M. (2)
See JI, Xu
See BAO, Hesheng
Recent Microseismicity in the Western Snake River Plain, Idaho, and Trench Evidence for Recurrent Late Quaternary Faulting Near the WSRP Southern Margin (abs)

